Ministry for Primary Industries
Manatū Ahu Matua

Modelling the effect of climate change on land suitability for growing perennial crops

MPI Technical Paper No: 2022/06

Prepared for Ministry for Primary Industries By Vetharaniam I, Müller K, Stanley J, Van den Dijssel C, Timar L, Cummins M, Plant and Food Research

ISBN No: 978-1-99-102652-1(online)
ISSN No: 2253-3923 (online)

June 2022

Te Kāwanatanga o Aotearoa
New Zealand Government

Disclaimer

PFR SPTS No. 20712

Modelling the effect of climate change on land suitability for growing perennial crops

Vetharaniam I, Müller K, Stanley J, van den Dijssel C, Timar L, Cummins M

October 2021

Confidential report for:

Ministry for Primary Industries
405421

PUBLICATION DATA

Vetharaniam I, Müller K, Stanley J, van den Dijssel C, Timar L, Cummins M. April 2021. Modelling the effect of climate change on land suitability for growing perennial crops. A Plant & Food Research report prepared for: Ministry for Primary Industries. Milestone No. 87023 & 73685. Contract No. 34671. Job code: P/405421/01. PFR SPTS No. 20712.

Report prepared by:

Kumar Vetharaniam
Scientist, Land Use Impacts
October 2021

Report approved by:

Paul Johnstone
Science Group Leader, Cropping Systems & Environment – Sustainable Production
March 2021

Contents

Executive summary

Modelling the effect of climate change on land suitability for growing perennial crops

Vetharaniam I[1], Müller K[1], Stanley J[2], van den Dijssel C[3], Timar L[4], Cummins M[1]
Plant & Food Research: [1]Ruakura, [2]Clyde, [3]Palmerston North
[4]Motu Economic and Public Policy Research Trust, Wellington

October 2021

Under climate change, land-use suitability for horticultural production, and other primary industry production, will change. In this Sustainable Land Management and Climate Change (SLMACC) project we estimated potential impacts of climate change on the spatial footprint (location and extent) of New Zealand horticulture under a range of climate-change scenarios. The focus was on New Zealand's three major horticultural export industries, viticulture, kiwifruit and apple, as well as avocado, berryfruit and summerfruit.

This report addresses climate-change impacts on kiwifruit and apple, avocado, blueberry, cherry and wine grape (Pinot noir and Sauvignon blanc) through:

- Development of a suitability assessment model plus the reasoning for changes made in the approach chosen.
- Description and discussion of criteria that express climate-, land- and soil-related requirements for growing kiwifruit and apple, avocado, blueberry, cherry and wine grape (Pinot noir and Sauvignon blanc).
- Development of phenological modelling for avocado, blueberry, cherry and wine grape.
- Adjustment of simulated climate model datasets used for projecting climate-change impacts, to provide better baselining of suitability maps used for comparing future change.
- Outputs of suitability assessments using our model with current and projected climate data until the end of the century for kiwifruit and apple, avocado, blueberry, cherry and wine grape (Pinot noir and Sauvignon blanc) across New Zealand.
- Economic assessment of land-use change for apple and kiwifruit performed using the Land Use in Rural New Zealand (LURNZ) model.

Continuous suitability models

We have developed a new nonlinear method for assessing land-use suitability criteria, to replace the commonly used binary assessment of 'suitable' and 'unsuitable'. Our modelling approach uses sliding-scale scoring functions that express how well locations meet growing requirements on a continuous scale of 0 (totally unsuitable) to 1.0 (no limitations to suitability), allowing a more nuanced appraisal of assessment criteria. Weighted geometric averaging of scores is used to combine suitability scores for multiple criteria in a manner that reflects the importance of each criterion. This approach enables us to develop maps that show the suitability of different locations for different perennial crops based on a

weighted appraisal of criteria, to provide relative rankings of locations for horticultural use, and to identify optimal areas. The assessment scores could be adapted for interpretation in terms of risk, and in the future could be expressed in terms of potential yields or productivity. The sliding scale system can be categorised to facilitate discussion, and for convenience we (arbitrarily) refer to suitability scores in the 0.9 to 1.0 range as “excellent”, 0.8 to 0.9 as “very good”, 0.7 to 0.8 as “good”, and 0.6 to 0.7 as “acceptable”. Where the suitability scores are lower, it indicates lower suitability for a location to grow that crop and/or more mitigation strategies would be required to reduce risk and improve production.

We obtained feedback from industry representatives and expert researchers on our initial suitability maps constructed for growing perennial crops across New Zealand under current climatic conditions. Through this exercise we have ground-truthed our assumptions for our suitability assessment criteria, and extended the model by including additional criteria that were identified as important.

Data used

Input climate data for ground-truthing the suitability models were modelled historic weather data from the National Institute of Water and Atmospheric Research’s (NIWA’s) Virtual Climate Station Network (VCSN), and soil and topographical data from the Functional Soil Layers (FSL) and New Zealand Land Resource Information (NZLRI) databases.

At the start of the project it was envisaged that, for projecting climate impacts, we would use modelled climate data supplied by NIWA and derived from NIWA’s high-resolution Regional Climate Model (RCM). The RCM was run separately using inputs from six CMIP5 (Coupled Model Intercomparison Project (CMIP) Phase 5) global climate models (GCMs: BCC-CSM1.1, CESM1-CAM5, GFDL-CM3, GISS-EL-R, HadGEM2-ES and NorESM1-M). For each GCM, the same four climate-change scenarios, referred to as Representative Concentration Pathways (RCPs), were considered, giving 24 separate datasets.

New climate model datasets

However we identified that the RCM datasets were not suitable for our use, since the modelled RCP Past data did not sufficiently reflect the distributional patterns in the VCSN data. Thus we undertook a project variation in which we diagnosed differences in the datasets and developed adjusted future climate data series (one for each RCP and each GCM run) that were more suitable for our purpose. These 24 datasets were developed specifically for application in this project, and we refer to them as the “SLM RCP datasets”. The adjustments that we performed were designed to (and did) preserve the climate change signals from the original RCM datasets, and thus the essential information from the climate model studies contained in the RCM datasets was preserved.

We projected future change in crop suitability under all four RCPs using the SLM RCP datasets. For each RCP, we obtained a representative projection by averaging the individual projections from the six SLM RCP datasets corresponding to the six GCMs. For brevity we have focused on results for the extremes of the four RCP pathways: RCP 2.6, which represents a low greenhouse gas (GHG) concentration pathway consistent with significant emissions reductions, and RCP 8.5, which represents a high GHG concentration pathway consistent with unabated emissions.

Future projections for RCP 2.6 and RCP 8.5

Under RCP 2.6, for all crops of apple, kiwifruit, avocado, blueberry, cherry and wine grape, there is very little difference between the mid-century suitability maps and late-century maps, with most changes having occurred by mid-century. For each crop considered, the area of land with excellent suitability (0.9–1.0) is projected to increase modestly by mid-century compared with a historic period (1972-2005). For crops such as cherry and wine grape, starting with very small areas of land in this category, the relative increase ranged from 30 to 400%. Between the mid- and late-century, however, a small loss of excellent suitability land is projected to occur for all crops except avocado, with cherry dropping below its historic-period level.

Mid-century suitability maps projections under RCP 8.5 show similarities to the late-century maps projections under RCP 2.6. In comparison with the historic period, the total area of land with excellent cultivation suitability is projected to halve for apple by the late-century, remain more or less constant for kiwifruit, have a modest 24% increase for blueberry, double for Pinot noir and have several-fold increases for Sauvignon blanc, avocado and cherry.

Apple

Under RCP 2.6, climate change will reduce average suitability of Hawke’s Bay, Gisborne and the Waikato for apple, but favour other apple regions such as Central Otago and Nelson, and possibly open up areas of the Taranaki. Under the RCP 8.5 projections, a reduction in the footprint of apple in its main growing area of Hawke’s Bay is expected (as well as Waikato and Gisborne), but some new opportunities for orchard establishment could occur in Southland.

Kiwifruit

Under RCP 2.6, the kiwifruit heartland in the Bay of Plenty is projected to have an increase in suitability apart from coastal areas. However, areas from Northland down to the Waikato, the Coromandel and areas around the East Cape are projected to decrease in suitability, and given that Northland does not have a high suitability for winter chill, these changes would increasingly favour low-chill cultivars in this region.

Under RCP 8.5 decreasing suitability in kiwifruit strongholds, such as the Bay of Plenty and Northland, could see the kiwifruit footprint shift to new locations such as Taranaki and North Canterbury where suitability is expected to increase.

Avocado

A modest increase in suitability is expected across most of the country by mid-century under RCP 2.6. Areas with the highest suitability for avocado will be predominantly in the Northland region and suitability is projected to increase, some change in land use from kiwifruit to avocado could be expected in Northland. Areas of higher suitability will expand in Taranaki, Bay of Plenty, Hawke’s Bay and Waikato regions providing new opportunities.

Under RCP 8.5, suitability for avocado is projected to be very good or excellent in many scattered locations around the North Island away from the centre of the Central Plateau, offering the opportunity for a significantly increased footprint. Further and significant land-use change from kiwifruit to avocado could be expected.

Blueberry

Blueberry is expected to experience a small decrease in its main growing regions under RCP 2.6, but in the Waikato and Bay of Plenty suitability will remain high, as it is in many locations in both islands of the country. Thus footprints are unlikely to be significantly affected, with the possible exception of Northland where lower-chill varieties of blueberry would currently be required. Under RCP 8.5, the projected reduction in suitability for blueberry in Northland and coastal areas around the North Island and the increased appearance of highly suitable land across Canterbury, parts of Otago and Southland could result in a wider distribution of the blueberry production, especially in the South Island.

Cherry

Under RCP 2.6 most inland areas of the North Island and nearly the whole of the South Island will see improved suitability. This will benefit Otago cherry growers in particular. In contrast, Hawke's Bay is projected to reduce in suitability, and since lower-chill varieties of cherry are already required in that region, this could place further limitations on cherry cultivation there. However, significant areas of very good to excellent suitability land are expected to remain in Hawke's Bay. Under RCP 8.5, changes in suitability would show similar spatial patterns to those under RCP 2.6, but would be more pronounced.

Pinot noir and Sauvignon blanc

Both the Pinot noir and Sauvignon blanc industries would have the opportunity to substantially increase their growing footprint under RCP 2.6. Although suitability for Pinot noir decreases a fraction in parts of Marlborough and Nelson, suitability for Sauvignon blanc increases in the same regions. The overall suitability for both wine grape cultivars will remain excellent in many areas of the region. Thus there is little likelihood of a climate-driven change in land use between the cultivars in these areas or other wine-growing areas.

The warmer late-century temperatures under RCP 8.5 are projected to make most of the North Island unsuitable for Pinot noir, and greatly reduce the suitability of the Nelson and Marlborough regions, while opening up a few new areas of land in Canterbury and Otago with very good or excellent suitability. A similar situation is projected for Sauvignon blanc by late-century under RCP 8.5, with the North Island and Nelson becoming broadly unsuitable, while areas in Central Otago and South Canterbury developing excellent cultivation suitability. Although Marlborough (around the Blenheim area) is projected to experience widespread reductions in suitability, a few locations are expected to still have very good suitability (reducing from excellent suitability).

Econometric modelling

Model results from the LURNZ economics model gave projections that by late-century, the national area of apple orchards will increase slightly from a current value of 9425 ha to 9575 ha under RCP 2.6 but have a small decline to 9125 ha under RCP 8.5. The area of kiwifruit orchards was projected to have sizeable increases from a current value of 15,600 ha to 17,475 ha under RCP 2.6 and to 18,675 ha under RCP 8.5 over the same period.

Outlook

A common theme across all the crops studied apart from avocado is that in the future obtaining adequate winter chill will become more challenging in many areas where these crops are currently grown, and this will be critical if the future climates resemble those of RCP 8.5 than RCP 2.6. At the same time, climate change could improve the suitability many locations for other growing criteria (such as frost risk or warmth during the growing season). Thus there will be both threats and opportunities, and adaptation strategies will be needed to mitigate threats and capitalise on opportunities. For apple, some relocation of the industry footprint is likely, while the increased use of low-chill cultivars could be a suitable adaptation to warmer climates. For kiwifruit, a shift in the industry footprint is also likely with new areas opening up, and we also expect to see an increase in the cultivation of 'Zesy002' at the expense of the green 'Hayward' due to winter chill requirements. Selection of new low-chill cultivars might allow continued cultivation in current areas that become unsuitable for 'Hayward'. The avocado industry stands poised to benefit from the declining suitability of Northland for kiwifruit. An increased used of low-chill cultivars is expected for both the cherry and blueberry industries, especially in the North Island. Climate change could be problematic for growers of Pinot noir and Sauvignon blanc since, in addition to the need for winter chill, these grape varieties have relatively tight optimal bands in their warmth requirements during the growing season; increasing temperatures could push current locations with excellent suitability outside the optimal warmth band. However, new opportunities for the industry will arise as locations elsewhere come into scope.

For further information please contact:

Kumar Vetharaniam
Plant & Food Research Ruakura
Private Bag 3230
Waikato Mail Centre
Hamilton 3240
NEW ZEALAND

Tel: +64 7 959 4430
DDI: +64 7 959 4446
Email: kumar.vetharaniam@agresearch.co.nz

1 Introduction

New Zealand’s primary sector is vulnerable to a range of weather-related risks and this could be exacerbated by climate change, with prospects of declining yields and profitability and of adverse socio-economic impacts as a consequence of unfavourable changes to temperature and rainfall (Hopkins et al. 2015; Ausseil et al. 2016; Cradock-Henry et al. 2019). However, climate change could also provide new opportunities. While projected climate changes for New Zealand are less than the global average, they are expected to have significant impacts because of our mild climate (Manning et al. 2015). These changes could affect production systems by influencing the soil-based processes that support plant growth (Orwin et al. 2015), through altering rainfall patterns (Snyder 2017), more acutely by modulating the virulence of pests and disease (Jones 2016; Trębicki et al. 2017; Wakelin et al. 2018), and directly through temperature regulation of growth and development (Hatfield & Prueger 2015).

Climate change will affect New Zealand’s diverse range of climatic systems in different ways, with impacts on horticulture expected to vary with geographical location and the specific requirements of different horticultural systems (Warrick et al. 2001). Under climate change, some areas may become less suitable for certain crops, but new opportunities may arise elsewhere. New Zealand’s horticultural industries are easily capable of adaptation to overcome the challenges of future climate change, having already demonstrated a history of using a number of strategic adaptations to fight weather-related damage to crops (Clothier et al. 2012). Thus adaptation strategies are likely to become more prevalent in the future, in order to maintain horticultural industries, but must be adequately informed to ensure they provide optimal benefits.

Hall et al. (2018) discussed the importance of understanding the possible impacts and their implications for horticulture, and presented criteria for the suitability of climate and land for the production of viticulture, kiwifruit and apple, along with preliminary criteria for avocado, summerfruit and berries. These criteria were generally developed from a binary perspective of assigning binary categories of ‘suitable’ or ‘unsuitable’, or in some cases grading into the categories of ‘highly suitable’, ‘suitable’, ‘moderately suitable’ or ‘unsuitable’ as used by Kidd et al. (2015) and Thomas et al. (2019). Hall et al. (2018) proposed that simulated weather data from future climate change projections could be used to project how climate change might affect the potential for production in different areas, when used with soil and topographical information to further refine suitability.

This approach was applied to apple and kiwifruit production by Vetharaniam et al. (2019), who extended the binary suitability approach to a more flexible continuous scoring system, and modelled the potential suitability of geographical locations across New Zealand for growing kiwifruit and apple under future climate change scenarios. These authors additionally identified the need to ensure that projections of crop suitability under future climate projections are rigorously baselined with predictions for the contemporary period, in order that differences can be meaningfully compared.

2 Methodology

As part of good practice, crop models used for investigating climate change impacts should be evaluated using historical observed data (Challinor et al. 2018). For this purpose we used historical climate data from the National Institute of Water and Atmospheric Research's (NIWA's) Virtual Climate Station Network (VCSN) for the period 2006 to 2016 ("observed data"), to fine-tune and "ground-truth" these models in conjunction with crop experts, and to develop maps showing the suitability of different locations across New Zealand for each of the crops. Estimates of how climate change might affect the suitability of land for crop cultivation, 'suitability maps' are obtained by running the suitability models with modelled climate data that extends from a historic period and are projected into the future. For reasons of consistency, the impacts of climate change are estimated by comparing future suitability maps with reference suitability maps that are constructed using data from the historic period of the climate model simulations. In order that these comparisons have relevance, it was important to ensure that these reference maps have alignment with maps constructed from observed historical data. This is also a key requirement for assessing climate change impacts on crop suitability and adjustments to the climate-model data should be performed to achieve this (Challinor et al. 2018).

We developed a modelling framework implementing the climate- and soil/land-related criteria that were identified by Hall et al. (2018) as well as additional criteria identified through consultation with industry and expert researchers. The model was run using weather data from the VCSN, which is interpolated to a 0.05 x 0.05 degree grid defined in New Zealand Geodatum 1949 (NZGD49) and further soil and topographical data that we resampled to a finer 0.01 x 0.01 degree grid that matches the VCSN grid perfectly at 25 cells to 1. The 0.05 x 0.05 degree grid approaches a 5 x 5 km grid (and the 0.01 x 0.01 degree grid approaches a 1 x 1 km grid) so for readability throughout this report the term 5 x 5 km grid and its equivalents will be used. It is worth noting that the axes in all the maps represent latitude and longitude in NZGD49.

These model runs provided suitability assessments of each individual climate-related criterion and of the combined climate-related criteria at a 25-km^2 resolution. Suitability assessments of the individual and combined soil/land-related criteria were performed at a 1 x 1 km resolution. This resolution was preserved when combining the climate-related and soil/land-related criteria, with the results of the climate data for each 5 x 5 km grid-square being applied to these 1 km^2-grid-squares. Model outputs include suitability maps for growing apple or kiwifruit across all geographic locations in New Zealand.

This report describes the application of the continuous suitability score modelling methodology developed by Vetharaniam et al. (2019) and extended by Vetharaniam et al. (2020b) to determine the suitability of different locations in New Zealand for growing perennial crops, based on climate, soil and land-related criteria. A number of these criteria had been identified by Hall et al. (2018), and were supplemented by additional criteria identified through literature searches, industry feedback and consultation with expert researchers.

For each crop, functions and models were constructed to provide a suitability score for each climate and soil criterion related to that crop, and suitability scores were combined using weighted geometric means to provide multifactorial assessments. Models were run using historic weather data from the VCSN database together with soil and topographical data from the Functional Soil Layers (FSL) and New Zealand Land Resource Information (NZLRI) databases. These databases are described in more detail in Sections 2.1.1 and 2.1.3. Maps indicating suitability of locations across New Zealand were created for both individual criteria and combined criteria, and these were refined after review by research experts and then presented to industry for further feedback.

2.1 Data

2.1.1 Observed, historic climate data

NIWA's VCSN database provides estimates of historic values of daily climate variables for a grid with a resolution of approximately 5 x 5 km, covering the entire country. The VCSN data are estimates of daily climate variables based on spatial interpolation of actual observations made at climate stations spanning the country (Tait et al. 2006; Tait 2008). We used daily maximum and minimum temperatures, relative humidity (RH) and rainfall data, which were available from 1972 to early 2018. The maximum temperature for each day is the maximum recorded **from** 9 a.m. of that day; the minimum temperature corresponds to the minimum recorded **to** 9 a.m. of that day; RH is humidity at 9 a.m. The 46 years of data allowed us to assess the impacts of a changing climate by comparing our model simulations for different time periods.

2.1.2 Projected climate data

The modelled climate data were supplied by NIWA, and are derived from NIWA's high resolution Regional Climate Model (RCM), which is applied on a domain that encompasses all of New Zealand. When the RCM is run, it is constrained by conditions for the boundary of this domain. In alternative simulations, these 'boundary conditions' were provided by outputs from six CMIP5 (Coupled Model Intercomparison Project (CMIP) Phase 5) global climate models (GCMs): BCC-CSM1.1, CESM1-CAM5, GFDL-CM3, GISS-EL-R, HadGEM2-ES and NorESM1-M. Each was run under four Representative Concentration Pathways (RCPs). Each RCP represents a different scenario of future atmospheric greenhouse gas (GHG) concentrations, and thus four different levels of global and regional warming were considered.

The daily RCM data start in 1971 and extend until at least 2099, with the end date of simulations varying with climate model and RCP. Simulations for the period 1971–2005 are considered to be historical simulations and are referred to as 'RCP Past'; for each CMIP5 model, all four RCPs share the same RCP Past dataset. Simulations from 2006 onwards are considered to be future simulations.

2.1.3 Land and soil information

The soil- and land-related criteria were assessed using data from the FSL and NZLRI databases including data on the potential rooting depth (PRD, https://lris.scinfo.org.nz/layer/48110-fsl-potential-rooting-depth/) provided by the soil, soil drainage (https://lris.scinfo.org.nz/layer/48104-fsl-soil-drainage-class/), and land use capability (LUC) class (https://lris.scinfo.org.nz/layer/48076-nzlri-land-use-capability/). These related databases contain information for irregular polygons covering the country. This format is not readily compatible with the gridded climate data. We extracted the information from these databases with a grid resolution of approximately 1 x 1 km. Information on the location of urban areas, quarries, rivers and lakes were available in the NZLRI database. Slope information was obtained from Land Environments of New Zealand (LENZ, https://lris.scinfo.org.nz/layer/48081-lenz-slope/) and resampled to our 1 x 1 km grid. Locations of public conservation areas were obtained from the Department of Conservation (DOC) Public Conservation Areas database (https://koordinates.com/layer/754-doc-public-conservation-areas/) and extracted to our 1 x 1 km grid like the other polygon data.

2.1.4 Limitations of gridded data

Each grid cell in the VCSN database represents an area of approximately 25 km^2, and there could be significant variation in each weather variable in an area of this size, especially if it contains microclimates. For example, as we noted in our earlier report (Vetharaniam et al. 2019), Ellenwood (1941) found differences of 3 to 4°F (1.7 to 2.2°C) between places in neighbouring apple orchards that had no more than a 7.5 m difference in elevation. The VCSN database does not include estimates of such variation and provides a single daily value per grid cell for each weather variable in the database. We conservatively assumed a variation in temperature of ±2°C around the nominal maximum and minimum VCSN temperatures within each VCSN grid cell, which appeared reasonable in light of comparisons between VCSN data and measurements from independent weather stations reported by Mason et al. (2017). Similarly, there is likely to be significant variation in each 1 x 1 km grid cell for the in soil- and land-related databases. Such variation should be considered in land-use modelling.

2.1.5 Suitability scores

The criteria identified by Hall et al. (2018) were presented as threshold requirements for a typical (currently grown) cultivar of apple or kiwifruit, and with supporting equations that were obtained from experimental data, which correspond to the "average" kiwifruit or apple. Each of these criteria was associated with a nominal rule or requirement for satisfactory crop performance. These rules and requirements were either based on published information or on expert opinion. Growing criteria provide a useful basis for predicting how well a crop will perform in a particular location.

Triantafilis et al. (2001) described an approach to continuous modelling that provided suitability assessments on a sliding scale from 0 (unsuitable) to 1 (suitable). This approach allowed different factors to be assessed together in one score rather than by separate rules and scores. Continuous suitability approaches have been used for allocation of land use (Santé-Riveira et al. 2008) and in conjunction with neural networks to assess land suitability for soy (Bagherzadeh et al. 2016).

The continuous suitability approach provides an alternative to more common discrete suitability assessments, such as that of Kidd et al. (2015) who specified categories of 'highly suitable', 'suitable', 'moderately suitable' or 'unsuitable' to characterise the suitability of land for horticultural uses. Triantafilis et al. (2001) noted that categorical distinctions may not represent the continuity of the land. Categories also require thresholds for indicator values, which can result in misleading predictions. For example, similar locations whose indicator values fall either side of a threshold would be assigned different categories, while dissimilar sites with indicator values at opposite ends of the same range would be treated as having equal merit. A consequence of this is that very minor climate change impacts on a crop might be reflected as significant under a categorical approach, while large impacts may not be detected. However, a categorical approach does have the advantage of unambiguous delineation of good versus bad, whereas under a continuous scoring system, use or non-use is a management decision (Triantafilis et al. 2001).

We applied the continuous suitability score approach developed earlier in this project for evaluating climate and soil criteria of crops at each location (Vetharaniam et al. 2019). This method differs from that of (Triantafilis et al. 2001), and provides a novel approach to modelling continuous suitability scores. This approach can consider differences between cultivars and allow for spatial variations in climate and soil/land variables that occur within a grid cell but which are not reflected in input data from databases (Vetharaniam et al. 2019). This is an alternative approach to specifying growing criteria in terms of thresholds as was presented by Hall et al. (2018) who either considered an “average” cultivar to represent a crop or specified separate requirements for different cultivars of the same crop.

We developed a “suitability score” for each criterion. These suitability scores indicate how well a particular location satisfies the assessment criteria. This approach does not rule locations as suitable or unsuitable. Rather a lower suitability score indicates higher establishment and/or maintenance costs with respect to the corresponding criterion, or alternatively a lower potential yield if deficiencies are not mitigated. By combining the suitability scores for several criteria, we obtain a modular modelling framework that provides a more representative view of the suitability of a location for growing a crop, balancing the pros and cons of that location. This also allows a comparison and ranking between locations.

2.1.6 Ground-truthing the model

For each crop considered, VCSN data were used to calculate suitability scores for individual and combined climate criteria for each of the growing years from 2006 to 2016, using VCSN data from 2006 to 2017 as inputs along with relevant soil- and land-related data. Suitability scores for each climate-related criterion were calculated for each year and then averaged using an arithmetic mean over the 2006 to 2016 period for each location. Combining of climate-related suitability scores was performed by taking weighted geometric means of scores within each year, and then the yearly combined scores were averaged using an arithmetic mean to get the suitability score of the combined criteria for the 2006 to 2016 period. The weights used when taking geometric means were chosen to reflect the relative importance of the different criteria as assessed by horticultural experts.

Similarly, suitability scores for different land and soil criteria were combined with each other by taking weighted geometric means, to get an overall land/soil suitability score, and an overall cultivation suitability score was obtained by geometric averaging of the combined climate suitability scores and combined soil suitability scores.

Resulting maps were used to ground-truth our initial suitability criteria and parameterise the model, in consultation with experts and industry representatives. In an iterative process, we then ran the improved model to generate updated maps, until we obtained maps that were considered to realistically represent the current suitability of different locations across the country for growing crops.

2.1.7 Disease and pest risk

A recurrent theme in the industry consultations was the absence of an evaluation of the risk of pest and diseases. Hall et al. (2018) had suggested that this would be best handled qualitatively because of its complexity, noting that the risk factors for damage from pests and diseases vary among pathogens that damage fruit trees, and different pathogens may be favoured by contrasting conditions posing a complexity of interactions. However, in our previous report we responded to consultation feedback by developing a broad-brush approach to model a general risk profile and creating maps showing the variation in this risk profile across locations (Vetharaniam et al. 2019). At this stage we have not included the disease module in calculating overall suitability scores precisely because of its generality. However, we have developed a specific botrytis risk map for wine grape and included it in overall suitability calculations, since this was considered by our expert researcher to be one of the major risk factors for wine grape. Whilst control measures exist for botrytis, higher botrytis pressure and risk makes grape growing significantly more challenging and reduces sustainability.

3 Modelling climate criteria

3.1 Modelling phenology

Growing criteria related to climate or weather patterns are often specified with respect to a particular development stage, a common example being relating the flowering interval with respect to frost events, and another being the day of bud burst as a reference date for accumulation of heat units. Some approaches in the literature have assumed that different plant phenology events occur in fixed time periods of the year. Alternative approaches seek to predict development stages as a function of season and climate variables. The choice of approach varies with crop, development stage and phenological data available. In this project we have used both approaches. In this section we describe phenological modelling to predict the periods from day of bud burst to open cluster and from bud burst to fruit ripening in cherry, and also the period from bud burst to harvest in wine grape. Phenological modelling was used for these crops to correspond to literature-based suitability considerations around climate. For apple, kiwifruit, avocado and blueberry, suitability rules were formulated on a calendar basis.

3.1.1 Cherry: day of bud break and open cluster

Chmielewski & Götz (2016) compared different approaches for predicting the start of cherry blossom, assessing two growing degree days (GDD) forcing models (with fixed vs optimised starting date) and a chilling/forcing model, each with and without a day-length term. Hall et al. (2018) used the results of this work to estimate cherry flowering date based on an accumulation of 295 d°C GDD base 0.4° starting from 27 August. Chmielewski & Götz (2016) did not, however, predict the day of bud-burst, which we used as the start of the period for assessing GDD requirements for maturation. Although Miranda et al. (2012) calculated thermal time requirements to reach different phenophases including bud-burst, these authors worked in growing degree hours, which requires hourly temperature information, whereas we had daily maximum and minimum temperatures. While it is possible to estimate hourly temperatures from a daily maximum and minimum, this requires assuming how temperatures will vary over 24-hour periods; thus we chose to work with GDD. Cittadini et al. (2006) used GDD accumulation when modelling frost risk for sweet cherry in Patagonia, presented thermal time requirements for a range of cultivars (‘Bing’, ‘Burlat’, ‘Lapins’, ‘Stella’, ‘Sunburst’ and ‘Van’) to reach different phenological stages: using a reference date of 15 July and a base of 4.5°C, the range in mean GDD requirements across cultivars to reach the start of bud break and the start of open-cluster were, respectively, 162 to 186 d°C and 192 to 230 d°C.

Allowing for variation in temperature within a grid cell, we modelled the probability of having started bud break across cultivars as a sigmoidal function, assigning probabilities of 0.15, 0.5 and 0.85 to GDD base 4.5°C values of 162, 174 and 186 d°C, respectively, with a reference date of 15 July. The probability curve for having reached bud burst is used to weight daily GDD from the bud-burst period to calculate sufficient GDD for maturation before the end of April and hence suitability from a warmth perspective. Since early stages after bud break are significantly more frost resistant than open cluster to post-bloom stages (Ballard et al. 1997), we used the GDD requirements to reach open cluster that were presented by Cittadini et al. (2006). We modelled the probability of having reached open cluster across cultivars as a sigmoidal function, assigning probabilities of 0.1, 0.5 and 0.9 to GDD base 4.5°C values of 192, 211 and 230 d°C, respectively, with a reference date of 15 July. As an example, Figure 1 shows GDD accumulation in a warmer vs a cooler location, and the corresponding phenological development.

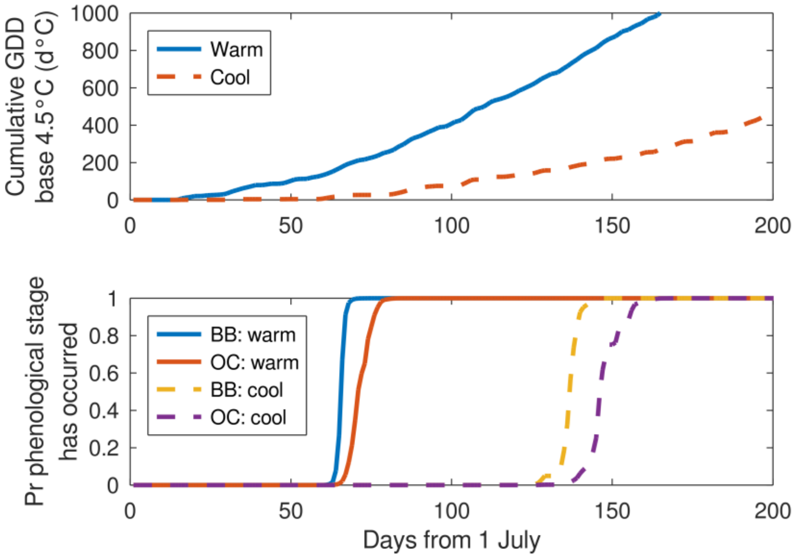

Figure 1. Cherry: growing degree days (GDD) accumulation and examples of probability (Pr) that bud break (BB) and open cluster (OC) have occurred over time from 1 July, shown for warm and cool locations.

The chill hour accumulation period used above (March to August) overlaps the forcing accumulation period starting on 15 July. While this may appear inconsistent, studies to determine chilling and forcing phases have found overlaps between the two phases for some cultivars of almond and apple (Díez-Palet et al. 2019). Dormancy-breaking models could be separated into "sequential" models involving a period of chilling followed by a period of forcing, and "parallel" models involving overlapping periods of chilling and forcing (Cesaraccio et al. 2004).

3.1.2 Cherry: period from bud burst to ripening

The post-bud-burst cumulative GDD base 4.5°C is used to develop a probability over time that fruit have not fully matured on that day. This was done by calculating for each day the cumulative GDD from the bud-burst period, with the daily GDD contribution weighted by the probability of bud break having occurred for that day. The GDD suitability function was applied to each daily cumulative GDD, giving a curve as a function of time that estimates the proportion of crops for each location that has reached maturity. We interpret 1 minus this proportion curve as a probability curve that fruit has not sufficiently matured. Multiplying this probability curve by the probability curve for having reached open-cluster gives a probability window that crops are between open-cluster and maturity and thus at risk of frost damage, over time from post-bud burst. Examples of a warmer and a cooler location are shown in Figure 2.

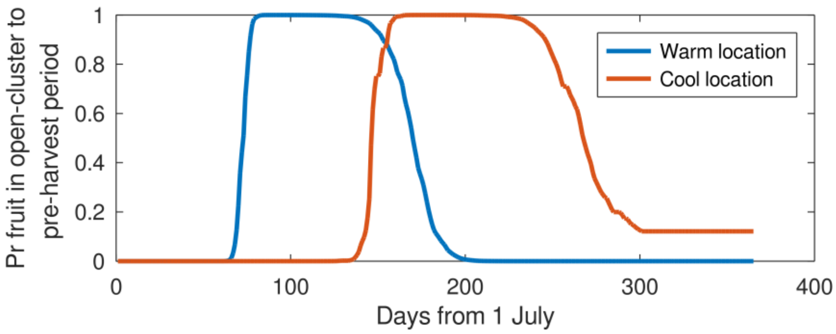

Figure 2. Cherry: probability (Pr) that fruit is between open cluster and the end of maturation, shown for warm and cool locations.

3.1.3 Grape: day of bud break

The 1 September reference date used by Hall et al. (2018);seems too late; a 1 July reference date would be preferable and would correspond to the 1 January reference date that is frequently used in the literature for northern hemisphere settings. McIntyre et al. (1982) found that bud break in Pinot noir occurred 4 days earlier on average than in Sauvignon blanc. Van Leeuwen et al. (2008) determined that on average, Pinot noir and Sauvignon blanc required 57 and 59 GDD (base 10), respectively, from 1 January to reach bud break. Zapata et al. (2017) found that the most appropriate GDD bases for Pinot noir and Sauvignon blanc were, respectively, 8.1 and 7.4°C, with respective GDD requirements of 79 and 101 from 1 January. For New Zealand conditions, Hall & Blackman (2019) used a GDD base of 4.5°C and GDD requirement of 450 from 1 July to predict bud break in three viticulture regions in Australia. Hall et al. (2018) specified rules that estimated date of bud break based on a GDD base 0°C (GDD0) requirement from 1 September of 380 for Pinot noir and 410 for Sauvignon blanc, citing unpublished work by A.K. Parker and others.

For calculating bud break in New Zealand situations, a suitable choice would be a 1 July reference and 4.5°C base, with GDD to bud break being 450 and 500 for Pinot noir and Sauvignon blanc (Damian Martin, pers. comm.). To reflect variation, we assumed bud break occurred within an interval of ±10% around these nominal GDD requirements, with 1% and 99% of bud break at the lower and higher range of the interval, respectively. The probability of the two varieties reaching bud break is plotted over time in Figure 3.

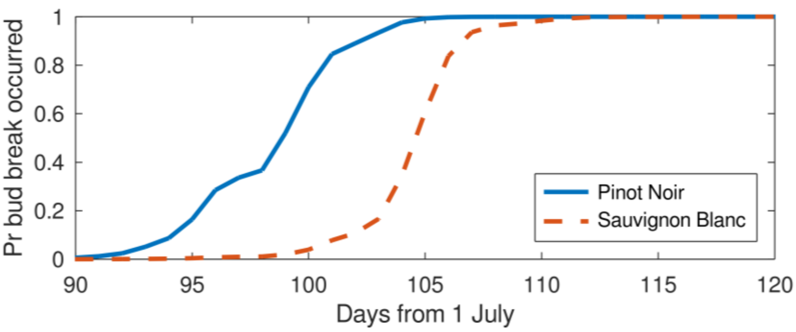

Figure 3. Grape: simulated probability of bud break having occurred on a particular day for Pinot noir and Sauvignon blanc compared for an example grid cell.

3.1.4 Grape: end of the growing season

A suitable rule for modelling the end of the growing season is that the average monthly temperatures drop to 13°C (Hall et al. 2018). Using a 14-day window, we performed a moving average of mean daily temperature for each grid cell, over the growing season (Figure 4, upper panel). To reflect variation within a grid cell we assumed that, when the moving average of mean daily temperature dropped below 13.5°C, 13°C and 12.5°C for the rest of the season, growth would stop in, respectively, 5, 50 and 95% of vines. This results in growth ceasing earlier in cool locations compared with warm ones (Figure 4, lower panel). We have assumed that, within a grid, variations in the 14-day averages of mean temperature are less than the variations in maximum or minimum temperature. With our probabilistic approach, in very cold regions where average temperatures are not sufficiently high, the probability that the growing season has not ended may be less than 1.0 on 1 July.

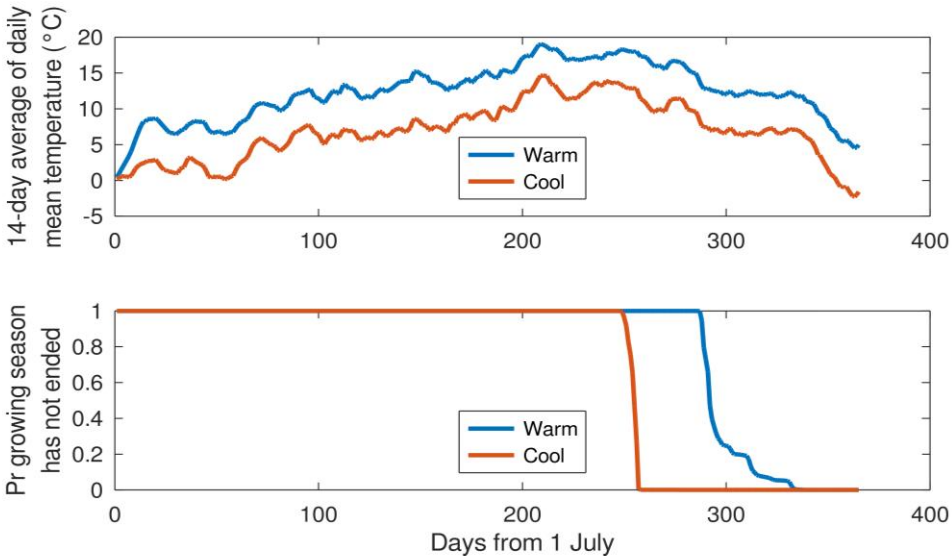

Figure 4. Grape: fortnightly average of daily mean temperature (upper panel) and the probability that the growing season has not ended (lower panel) for a warm region and a cool region.

3.1.5 Wine grape: bud burst to end of fruit ripening window

For each grid location, the daily probabilities of budburst and the daily probabilities of growing up to fruit ripening are multiplied. The non-zero values define the effective growing season on a probability basis (Figure 5).

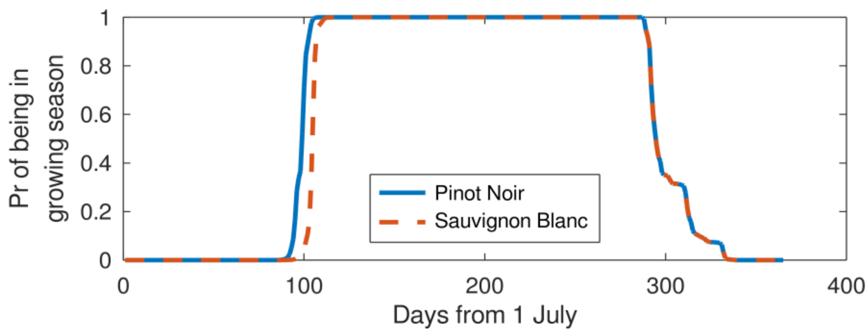

Figure 5. Wine grape: probability that Pinot noir and Sauvignon blanc are in the growing season (bud burst to completion of ripening) for an example cell.

3.2 Winter chill

Chilling requirements refer to the minimum period of cold weather needed for plants to break bud and flower adequately for crop production, after a dormant rest period.

3.2.1 Apple

Hall et al. (2018) placed a minimum chill requirement of 500 hours base 7.2°C during May to August for a mid-season apple. However, the literature reports a wide range of minimum chilling hours for apple. For example, Rai et al. (2015) considered a range of 1000–1500 (7°C base) as suitable. Guak and Nielson (2013) reported a mean chill requirement of 970 hours (7.2°C base) for the cultivar 'Gala'. Hauagge and Cummins (1991b) found that the mean chill requirement ranged from 218 to 1530 chill units (CU) depending on cultivar, with 'Gala' having a requirement of 1094 CU, and the majority of cultivars requiring 800 to 1200 CU. These authors used an unconventional calculation for CU (Hauagge & Cummins 1991a), which cannot be directly compared with 7.2°C base chill hours. Nevertheless, their results highlight the huge variation in chill requirement between cultivars, with the lowest chill requirement being 80% less and the highest chill requirement 40% more than the 'Gala' requirement, and the requirements for many cultivars ranging from 30% below to 10% above the 'Gala' requirement. Thus, a chilling suitability score that switches slowly over a large range of chill units would be appropriate to reflect this variation.

Table 1. Richardson chill units (RCU) assigned for different temperature ranges.

Temperature (°C)	RCU (per hour)
T < 1.5	0.0
1.5 ≤ T < 2.5	0.5
2.5 ≤ T < 9.2	1.0
9.2 ≤ T < 12.5	0.5
12.5 ≤ T < 16.0	0.0
16.0 ≤ T < 18.0	−0.5
T ≥ 18.0	−1.0

Furthermore, during our consultations, it was recommended that we consider chill in terms of Richardson chill units (RCU), which are more biologically based. They can be calculated using the values in Table 1, which were sourced from http://www.harvest.com/support/calculations/.

Calculation of either chill hours base 7.2°C or RCU require hourly temperatures, whereas our data provided a daily maximum and minimum temperature for each grid-square. To overcome this limitation, we assumed that temperature would vary sinusoidally over a 24-hour period, which allowed an estimation of hourly temperatures.

We compared RCU versus chill hours base 7.2°C over an 11-year period for the entire country, and found a marked difference between the two methods. Locations with the highest RCUs had only intermediate chill hours base 7.2°C, and locations with the lowest RCUs variously had either the highest or lowest chill hours base 7.2°C (Figure 6). This is because the chill hour system is binary, while the RCU system takes a more nuanced approach and allows reversal of chill when temperatures exceed 16°C. We therefore selected RCU as the preferred option. The calculation of CU used by Hauagge and Cummins (1991b, a) has a rough equivalence to RCU, which facilitated developing our chill curve for RCU (Figure 7). Maps in Figure 8 show mean May to August RCU accumulations across the country over the 2006–16 period and the corresponding suitability scores. These maps indicate most areas would provide good chill across a range of cultivars, except for Northland and upper Waikato and some areas of the Coromandel and East Cape, which would be suitable only for varieties of apple with low chill requirements. The suitability map shows no conflict with current apple growing regions.

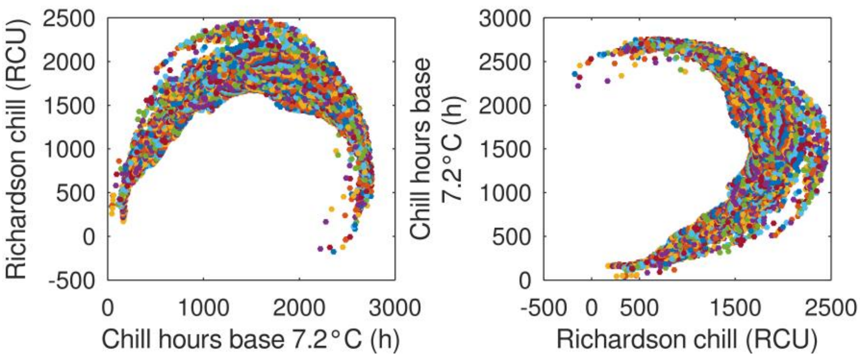

Figure 6. Comparison of Richardson chill units (left) and chill hours base 7.2°C (right) for May to July from 2006 to 2016 across the country.

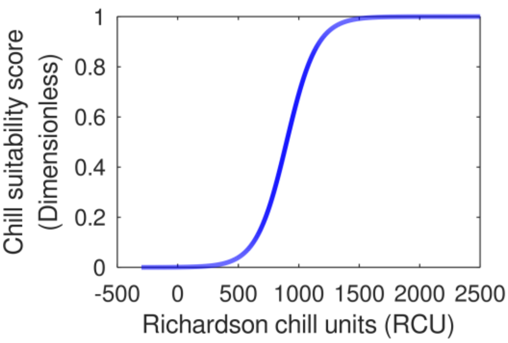

Figure 7. Chill score curve for apple as a function of Richardson chill units (RCU).

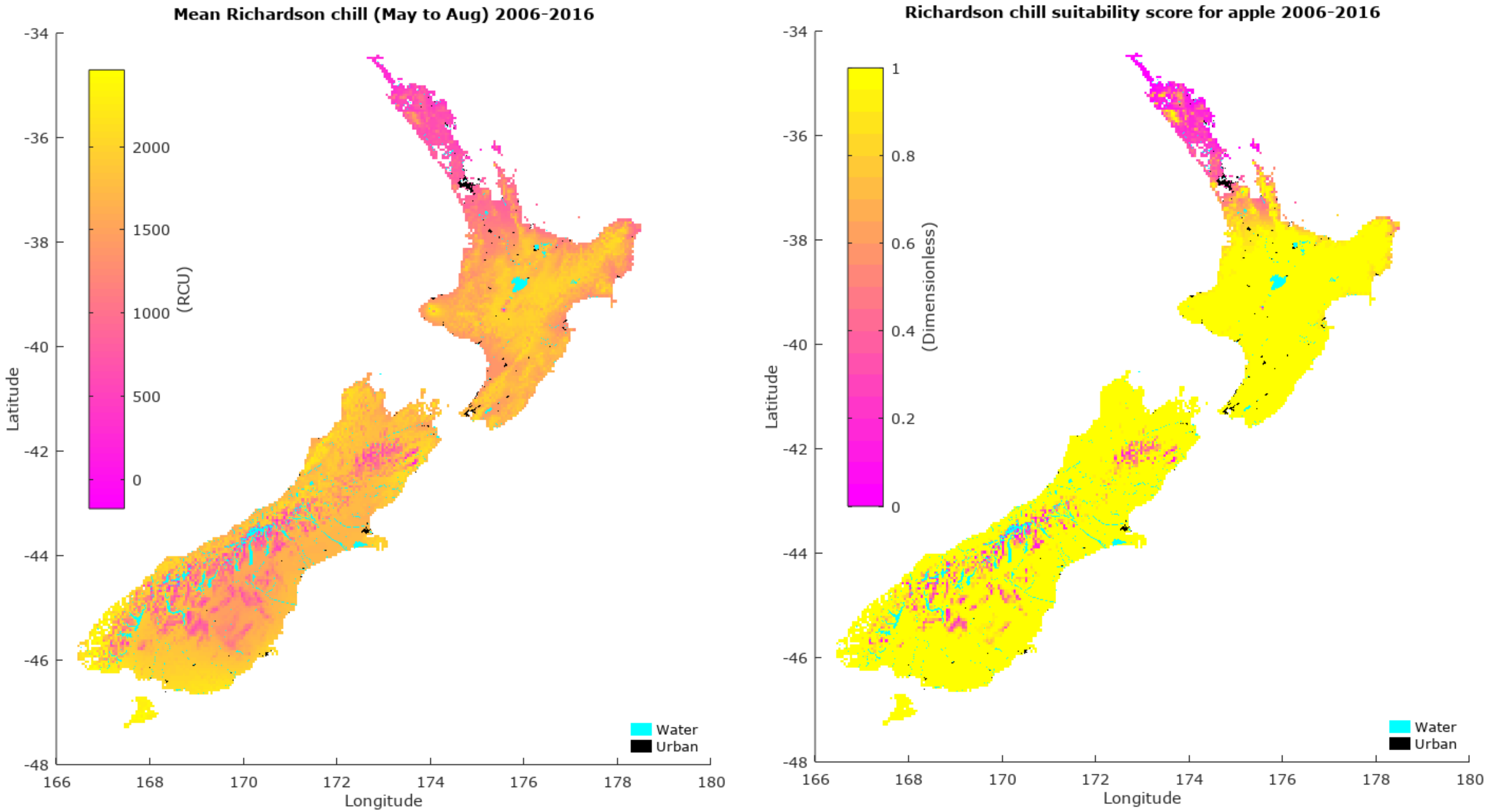

Figure 8. Accumulated Richardson chill units from May to August (left) and corresponding suitability score (right) for apple, mapped across New Zealand. Calculations used Virtual Climate Station Network (VCSN) data.

3.2.2 Kiwifruit

Winter chill requirements for having at least one king flower per winter bud are typically expressed in mean temperatures. Hall et al. (2018) gave chill requirements as average May to July temperatures being less than 11.7°C for *Actinidia chinensis* var. *deliciosa* 'Hayward' and 12.7°C for *A. chinensis* var. *chinensis* 'Zesy002' (commonly known as Gold3) (Snelgar et al. 2008; Hall & Snelgar 2014) with the use of Hi-Cane® raising this threshold by 2.3°C for 'Hayward', and by assumption, this would apply to 'Zesy002' also. Bearing in mind that these values are averages from experimental data, and the likely variable conditions across a 25-km^2 grid-square, we chose the chilling score to switch slowly with mean May to July temperatures to reflect the differences between green kiwifruit and gold kiwifruit, and to accommodate other (including future) cultivars (Figure 9).

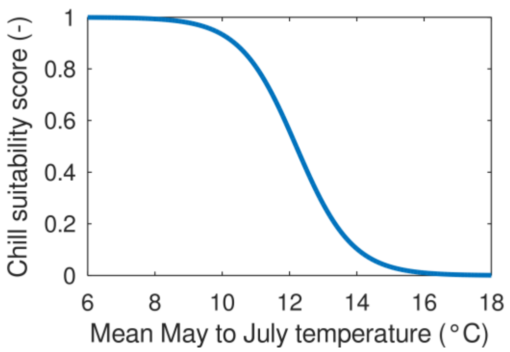

Figure 9. Chill score curve for kiwifruit as a function of mean May to July temperatures.

Mean May to July temperature is mapped across New Zealand in the left hand panel of Figure 10 and the resulting chill suitability score is mapped in the right-hand panel.

Most areas would provide good chill except for Northland, which generally would require Hi-Cane® in most areas, though there are some small areas with good chill. Certainly Hi-Cane® is extensively used in Northland kiwifruit orchards. The upper Waikato and some areas of the Coromandel are marginal from a chill perspective, and thus mitigation in the form of Hi-Cane® may be beneficial. New cultivars that require less chill for good bud break and flowering would also be suitable in these areas, and of current cultivars, 'Zesy002' would be preferable in these areas compared with 'Hayward'.

3.2.3 Avocado

Winter chill was not considered a requirement for avocado since it is a warm-climate crop.

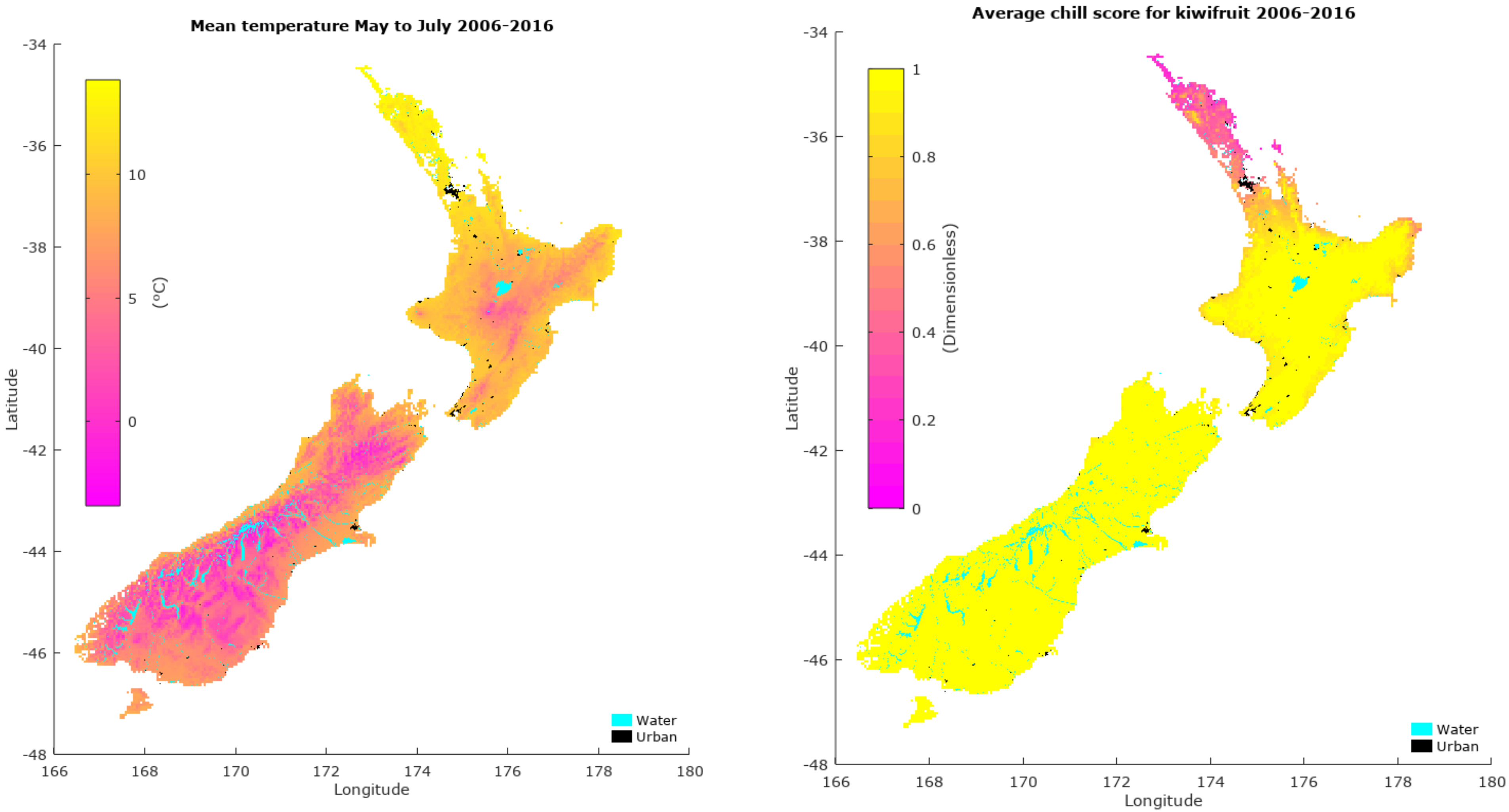

Figure 10. Mean May to July temperature for the period 2006 to 2016 for different locations across the country (left), which is used to estimate chill requirements for kiwifruit, and the corresponding chill suitability score for kiwifruit (right). Calculations used Virtual Climate Station Network (VCSN) data.

3.2.4 Blueberry

Lowbush varieties are highly sensitive to frost (Hicklenton et al. 2002) and are ignored here since commercial cultivation appears to centre on Rabbiteye and Highbush varieties. Requirements for Rabbiteye have been reported as 400–700 chill hours (threshold 6–7°C) (Spiers & Draper 1974), while Austin & Bondari (1987) found that the chilling requirements for eight Rabbiteye cultivars ranged from 250 to 650 hours <7°C. Overlapping chill requirements have been reported for Southern highbush varieties, with ranges of 100–450 hours <7°C (Lyrene & Sherman 2000) and 200–600 hours <7°C (Lang 1993). In contrast, Northern Highbush varieties that are adapted to cold mid-winter temperatures have a chill requirement of 800–1000 hours <7°C (Hancock 2006).

The Department of Primary Industries (DPI) Tasmania gave the chill requirements for blueberry as more than 800 hours between 0 and 7.2°C from May to August, but did not consider variation between cultivars (https://dpipwe.tas.gov.au/Documents/BLUEBERRIES.pdf). Blueberries NZ (https://www.blueberriesnz.co.nz/varieties/) gave chill requirements for a range of different cultivars, ranging from 500 to over 1000: with Rabbiteye and Southern Highbush varieties chill accumulations being in the lower part of the range, and Highbush varieties requiring chill accumulations at the higher end. However, no threshold temperatures for chill accumulation were given, which limited using these values in calculations. Hall et al. (2018) considered chill requirements in terms of low (some Rabbiteye and Southern Highbush varieties), moderate and high chill varieties of blueberry, with these groupings, respectively, requiring at least 200, 500 and 800 hours of chill below 7.2°C.

Following Lang (1993), we used daily chill hours below 7°C, and calculated these from daily maximum and minimum temperatures from May to August, and summed to obtain a total winter chill. Taking into account spatial variation in temperature within each 25-km^2 grid cell, along with the variation between bush type and cultivars, we used a sliding-scale suitability score for chill, with values 0.05, 0.5 and 0.95 for, respectively, 150, 550 and 950 accumulated chill hours (Figure 11). A lower chill score for a location can be interpreted as indicating unsatisfactory chill accumulation, or alternatively as indicating a reduction in the range of cultivars that will receive adequate chill.

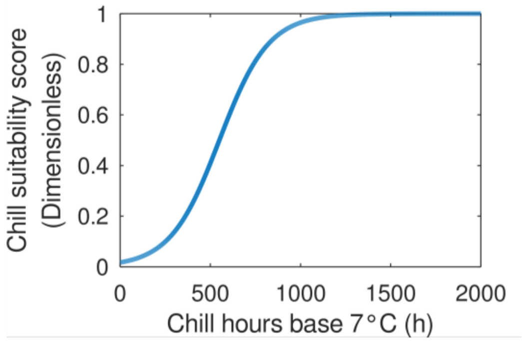

Figure 11. Blueberry: winter chill suitability curve as a function of chill hours below 7°C.

Figure 12 shows a map of average accumulations of May–July chill for blueberry over the growing seasons 2006 to 2016 for locations across New Zealand (left panel), and the corresponding chill suitability scores (right panel). These maps show good chill in most areas, with Northland and coastal areas of the East Cape down to Gisborne being a significant contrast, with average accumulations of up to 500 chill hours and thus being suitable for only the very low chill varieties. Although not highly suitable, other coastal areas of the North Island and the northern Waikato would support moderate chill varieties as well. This paints a picture of some of the main current growing regions such as Auckland and Waikato not being ideal from a chill perspective, with mitigation by using low and medium chill varieties being likely.

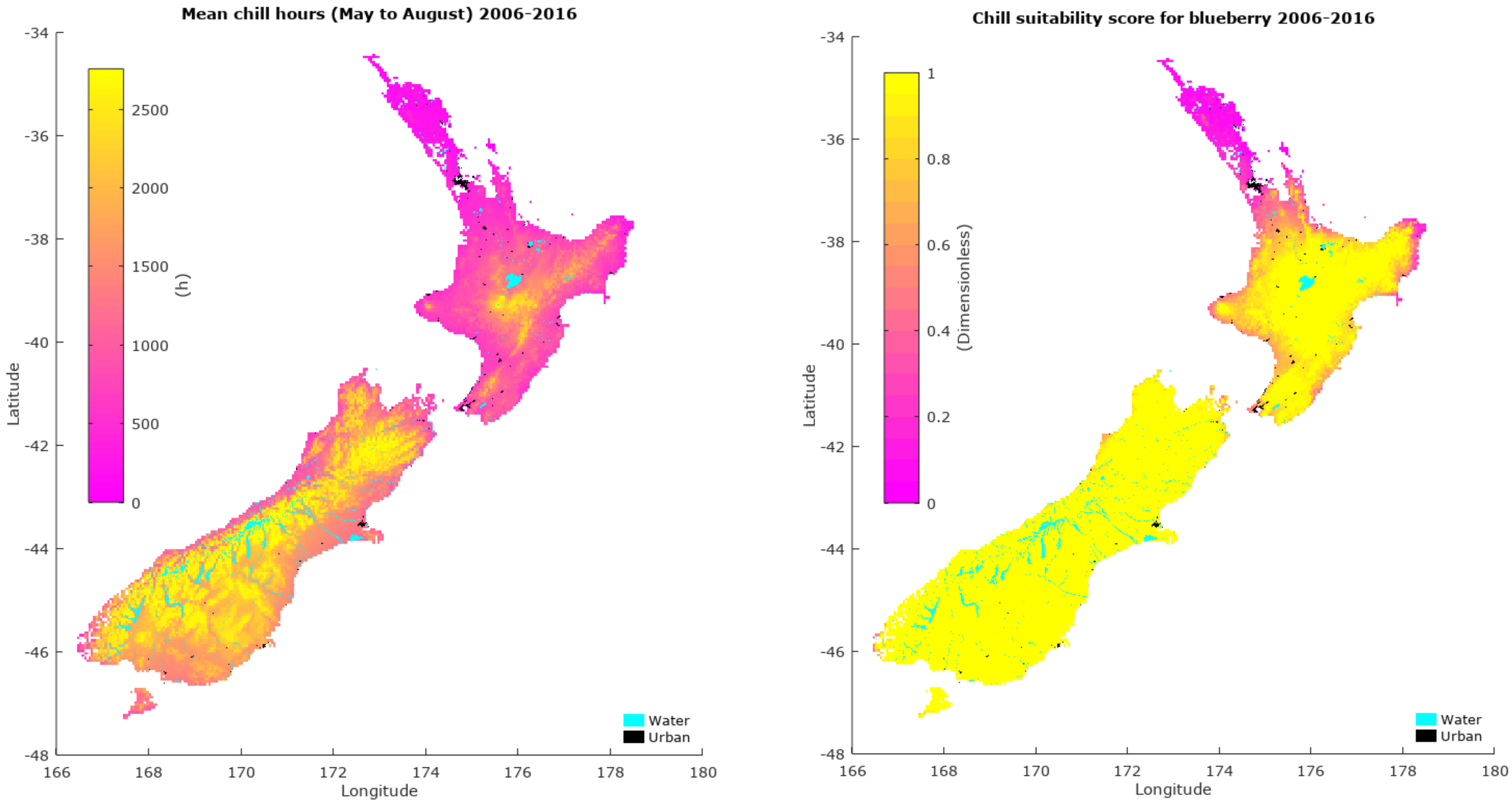

Figure 12. Average May to August chill hour accumulations (left) and corresponding chill suitability scores (right) for blueberry, for locations across the country. Calculations used Virtual Climate Station Network (VCSN) data.

3.2.5 Cherry

Common models for estimating winter chill are variations of the Utah (Richardson) model, the Dynamic model (Erez et al. 1990), and chill hours below 7°C (Alburquerque et al. 2008; Palasciano & Gaeta 2017). Chill hours between 0 and 7°C are also used, reflecting a view that sub-zero temperatures do not contribute to winter chill (Luedeling 2012), and for New Zealand conditions Hall et al. (2018) suggested that chill hours between 2 and 12°C be used, specifying a requirement of at least 700 hours accumulated from May to August. However, Kaufmann & Blanke (2019) found that temperatures from –5 to 0°C did contribute to winter chill. Although the process-based Dynamic model is based on speculation, it has been found to be more accurate than other models (Luedeling 2012; Palasciano & Gaeta 2017) but these results were not consistent between sites or years (Measham et al. 2017). Kaufmann & Blanke (2019) found that, irrespective of the chill model, up to 50% of the chill requirements (depending on cultivar) could be substituted by increased spring forcing.

Here we use hours below 7°C as the chill model, because there is more information in the literature regarding variation between cultivars for this metric and additionally it allows contributions from sub-zero temperatures. Seif & Gruppe (1984) found that in a region of Germany winter chill requirements varied between 733 and 1343 hours below 7°C for 30 sweet cherry cultivars, and between 1051 and 1889 for interspecific cherry hybrids. Those authors noted that winter chill requirements for sweet cherry reported in the literature varied between 1300 and 1700 hours below 7°C in Turkish studies and between 2007 and 2272 hours below 7°C in US studies. In an Argentinian study, average chill requirement between cultivars was 1615 hours at or below 7°C (Hochmaier 2014).

Hortinfo (2010) gave winter chill requirements as 1000–1300 hours below 7°C from 1 June to 31 August. Brunt et al. (2017) categorised Australian-grown cherry cultivars into five categories of chill requirements: 300–500; 500–750, 750–1000, 1000–1500 and >1500 chill hours accumulated from 1 March to 31 August, with the range in values reflecting variability between locations, rootstocks, management systems and research methodologies. Taking into account the variability between cultivars and the potential for new cultivars to be grown in New Zealand, we use a sigmoidal sliding scale with values of 0.05, 0.5 and 0.95 for, respectively, 500, 900 and 1300 chill hours below 7°C in the period 1 June to 31 August (Figure 13).

Mean annual chill hours and chill suitability scores for locations across the country are shown in Figure 14, indicating that most areas of the South Island would provide adequate chill across a range of cultivars, while the Hawke's Bay, which has a small but established cherry industry, shows lower suitability. While there are small pockets of land that would suit high-chill cultivars in the Hawke's Bay, in most areas the level of chill would be sufficient only for moderate- and low-chill cultivars, and it is likely that these are the predominant cultivars in that region. Areas north of central Waikato and major portions of coastal areas of the North Island would appear unsuitable for cherry from a commercial perspective.

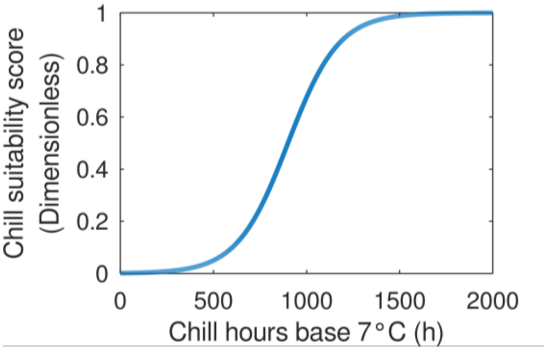

Figure 13. Cherry: chill suitability score as a function of chill hours.

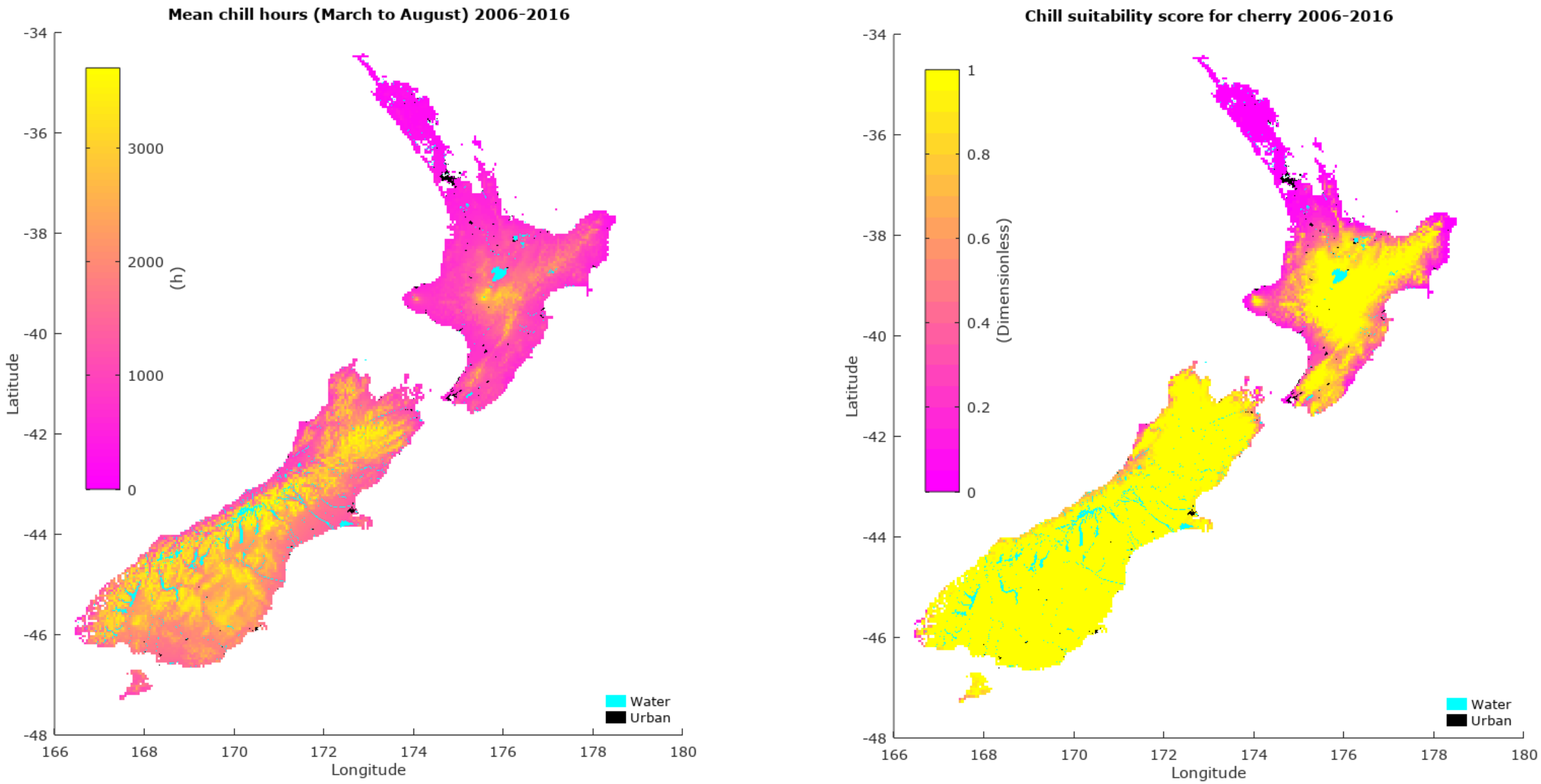

Figure 14. Mean March to August chill hours (left) and corresponding chill suitability score (right) for cherry, for locations across the country. Calculations used Virtual Climate Station Network (VCSN) data.

3.2.6 Wine grape

The literature was comparatively sparse on winter chill requirements for grape compared with cherry and blueberry. Hall et al. (2018) avoided chill hours and specified that the chill requirement for wine grape is a mean July temperature of below 12°C. (Hortinfo 2010) used chill hours for specifying winter chill requirements of 100–200 hours below 7°C from 1 June to 31 August. Londo & Johnson (2014) stated that the cultivated grapevine is adapted to Mediterranean conditions and has chill requirements of 50–400 hours between 0°C and 7°C, in contrast to wild *Vitis* species and hybrids, which can have much higher chill requirements. Although sub-zero temperatures may contribute towards chilling, as discussed above for cherry, we chose to use the chill hour specification of Londo & Johnson (2014). To calculate this, we assumed that temperature varies sinusoidally over the day between minimum and maximum temperature. We expressed the suitability score using a sigmoidal curve that was a function of chill hours between 0°C and 7°C with approximate values of 0, 0.03, 0.20, 0.8 and 1.0 at 0, 50, 100 200 and 400 hours of chill (Figure 15).

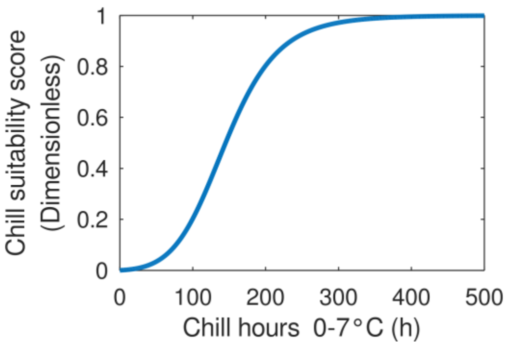

Figure 15. Grape: chill suitability score as a function of chill hours accumulated from 1 June to 31 August.

Chill hours and suitability scores are mapped at the national level in Figure 16, showing that most areas of NZ provide good chill for wine grape, although there are dispersed areas in Northland that provide less than ideal chill, as indicated by the mottling of the suitability map in that region. The main wine-growing regions, however, fall in the high chill suitability areas.

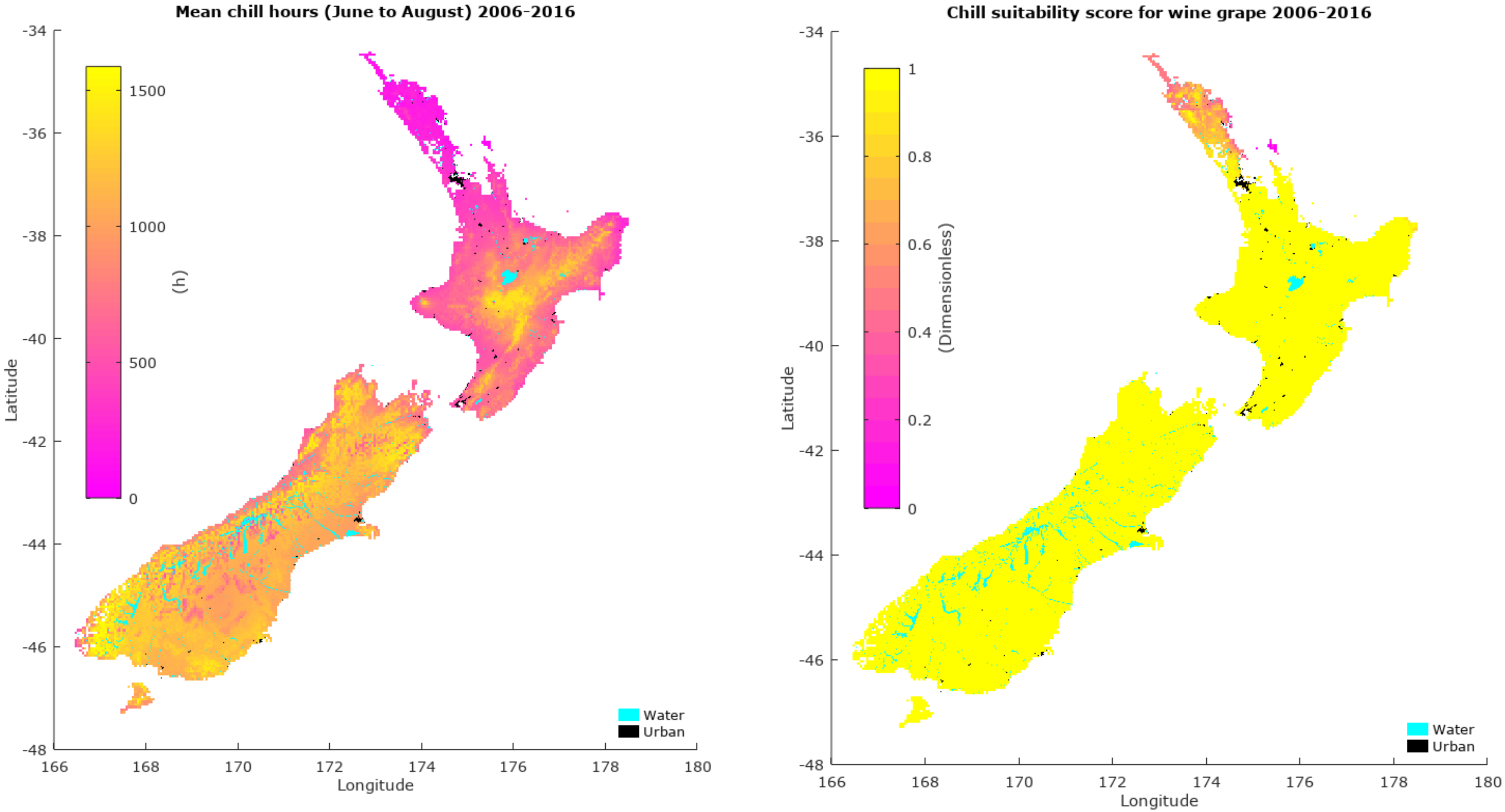

Figure 16. Grape: average winter chill hours from June to August (left) and chill scores (right) for locations across NZ for 2006–2016. Calculations used Virtual Climate Station Network (VCSN) data.

3.3 Frost risk

The effects of frosts occurring after flowering and before harvest need to be taken into account for horticultural production, bearing in mind that mitigation through frost protection including, for example, windmills, helicopters, frost fans and overhead irrigation is already being used.

3.3.1 Apple

For apple trees, Murray (2009) provides an overview of bud kill rates at different bud stages and temperatures: the most vulnerable stages are from open cluster to full bloom and post bloom, with a 10% loss at −2.2°C and 90% loss at −3.8°C (survival rates of 90% or 10% of fruit after a frost of −2.2°C or −3.8°C). Based on these data and considering a temperature variability of ±2°C around the VCSN temperature within each 25-km^2 grid-square, we chose a frost suitability curve corresponding to a fruit survival rate of approximately 12% at −5°C, and 88% at −1°C, with a 50% midpoint at −3°C (Figure 17).

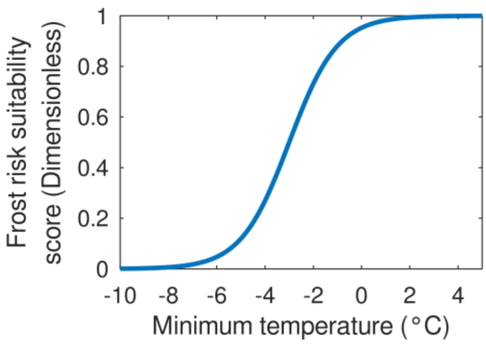

Figure 17. Frost risk score for daily minimum temperatures for apple. A higher score indicates a lower frost risk for that day. The frost risk score for a time period is obtained by multiplying daily scores.

Based on results published by Ellenwood (1941), we expect at least a 9-day spread between cultivars in the day of full bloom (DFB), and about a 3-day duration from the start of full bloom until the end, with about a 5-day period from first bloom to the start of full bloom. Hall et al. (2018) proposed that the equation published by Austin et al. (2002) be used to calculate DFB. This equation is for the end of full bloom for ‘Delicious’, which has a DFB roughly in the middle of the spread for cultivars studied by Ellenwood (1941), with the earliest being 4 days before.

We applied an equation from Austin et al. (2002) to calculate nominal DFB for each location based on average maximum temperature from August to September. To accommodate the variation between cultivars, and within a tree, we started the period of frost risk 21 days before nominal DFB. A down-weighting was applied to this period, in the manner described for kiwifruit, but only for the first week since frost might kill unopened flower buds. Since early maturing cultivars will be harvested before April, April poses less of a risk than preceding months. A decreasing weight was placed from April 1 to April 30, so that a frost on April 30 would have little impact. For the period from DFB until harvest (assumed 30 April the following year), the frost survival score was calculated for each daily minimum temperature and the values multiplied together to represent the cumulative effect of frosts.

Frost suitability scores calculated for apple are mapped across the country in Figure 18, showing that many areas in the North Island have good suitability scores for frost risk for apple, although some areas of the Hawke’s Bay are indicated as having a moderate frost risk. In the South Island, while large areas of Otago show a high frost risk, there are regions around well know apple-growing areas such as Alexandra that have moderate frost risks, indicating the potential for loss from frost in some years unless frost mitigation is sufficient. Some know central Otago production areas show poor suitability, most likely due to microclimatic pockets not showing in the 25-km grid, although frost mitigation in the form of overhead sprinklers, helicopters, and/or frost fans can be used.

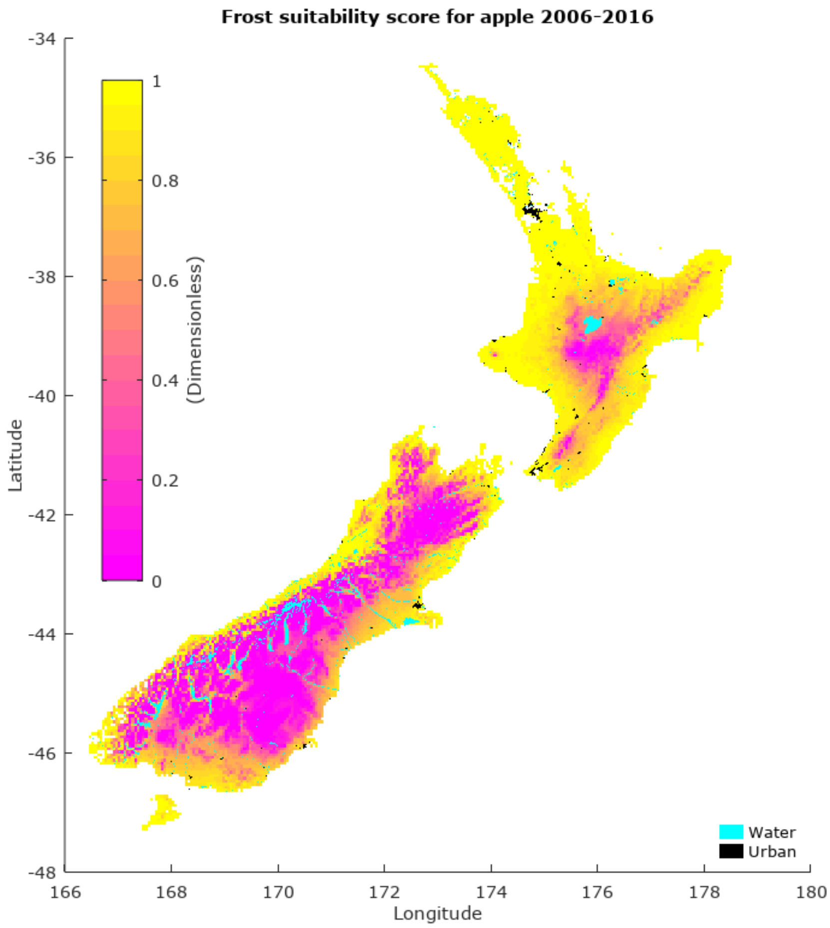

Figure 18. Frost suitability scores calculated for apple for locations across the country. Calculations used Virtual Climate Station Network (VCSN) data.

3.3.2 Kiwifruit

Hewett & Young (1981) found no frost damage to buds on newly formed kiwifruit vine shoots at −1°C, slight damage at −2°C, and 95% of buds were killed at −3°C. In contrast, dormant buds survived much colder temperatures. To reflect the large variation that can occur over short distances, we chose a frost suitability curve corresponding to bud/flower survival rates of approximately 12% at −4°C, and 88% at 0°C, with a 50% midpoint at −2°C (Figure 19).

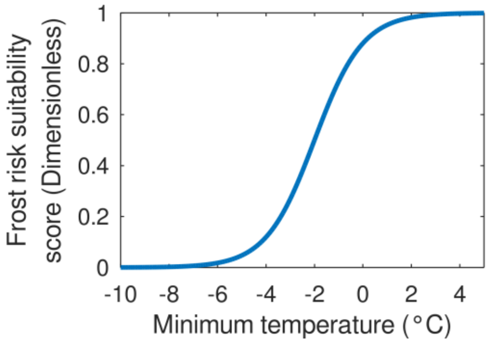

Figure 19. Frost risk score for daily minimum temperatures for kiwifruit. A higher score indicates a lower frost risk for that day. The frost risk score for a time period is obtained by multiplying daily scores.

Since fruit are at risk from autumn frost (or winter frosts if harvested late), we used the same approach as for spring frost, but with a lower weighting to represent that leaves will provide protection from the first frosts. For kiwifruit, the frost risk period for fruit yield was considered to be from day of bud break (DBB) to harvest.

Based on data for *A. chinensis* var. *chinensis* 'Hort16A', 'Zesy002' and 'Hayward' provided by Alistair Hall (pers. comm., June 2019) we estimated the time band from earliest DBB to "typical" DBB to cover current and future cultivars. For typical DBB we combined data for 'Zesy002' and 'Hayward' and constructed the following equation:

$$DBB = \min(335, 245 + \exp(0.267 * T_{MJJ})),$$

where T_{MJJ} is average temperature from May to July, and 335 is an arbitrary cut-off that prevents DBB occurring later that 1 December. We based the earliest DBB on data for the 'Hort16A' cultivar, which showed little sensitivity to T_{MJJ} or to site, and had a DBB ranging from 225 to 245 days from 1 January. Although the 'Hort16A' cultivar is no longer grown as a commercial variety, it is useful as a reference, and we used day 225 as the earliest DBB for any cultivar.

For each year, the frost survival scores were calculated for all days from the earliest DBB (day 225) until the end of harvest, the end of June in the following year, and a weighted multiplication was performed to get a survival score for the frost risk period for each growing year. For the period defined above, we progressively increased the weight from approximately zero at earliest DBB to one at typical DBB.

Since progressive harvesting from mid-March onwards would decrease the fruit at risk from frosts, the frost survival score for each day of the harvest period was progressively down-weighted, with a weight of 0.5 at mid-March decreasing to almost zero at the end of June. The weight of 0.5 instead of one for mid-March was chosen to reflect the protection that leaves will provide fruit during an autumn harvest. Frost suitability scores calculated for apple are mapped across the country in Figure 20. Apart from Northland and the East Cape/Gisborne areas, there is a moderate to high frost risk across the country. Notably, the current growing areas of Nelson and the Hawke's Bay have a moderate to high frost risk indicating growers there will need to engage in frost mitigation in a number of years.

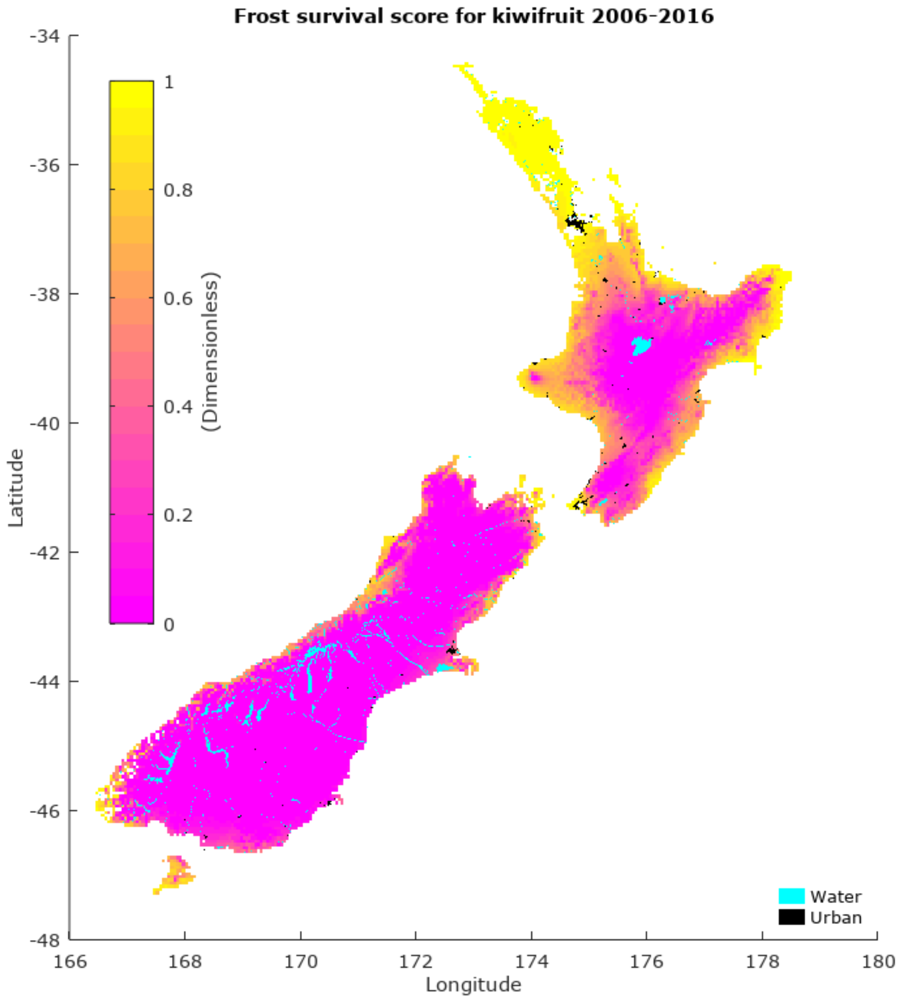

Figure 20. Frost suitability scores calculated for kiwifruit for locations across the country. Calculations used Virtual Climate Station Network (VCSN) data.

3.3.3 Avocado

Selim et al. (2018) noted that avocado frost resistance varied with variety, and considered that in general –5°C was a suitable minimum temperature cut-off. Dubrovina & Bautista (2014) give the frost resistance of ‘Hass’ as down to –1.1°C (Dubrovina & Bautista 2014). Damage to ‘Hass’ avocado exposed to temperatures varying between 0 and –3.3°C over 32 hours and 0 and –4.4°C over 51 hours was extensive, with up to 50% foliage killed within 3 weeks and over 80% of foliage killed after 2 months (Malo et al. 1977). We used a curve that took into account a possible 2°C variation around the nominal grid (e.g. for a nominal temperature of 0°C, the temperatures within the grid would range from –2 to 2°C). This had the following leaf survival rates: 21% at –4°C, 98% at 0°C, and a 50% midpoint at –3°C (Figure 21).

Scores were calculated for the years 2006 to 2016 for each location, and the average across years taken as an indication of location suitability (Figure 22). Northland, East Cape/Gisborne, and areas of Bay of Plenty and coastal Wairarapa have low frost risk. Other North Island coastal areas and a few in the South Island have moderate frost risk, whilst most other areas of New Zealand have high frost risk. This is in line with known growing regions and most regions requiring frost protection on young, establishing trees that then eventually outgrow the frost risk.

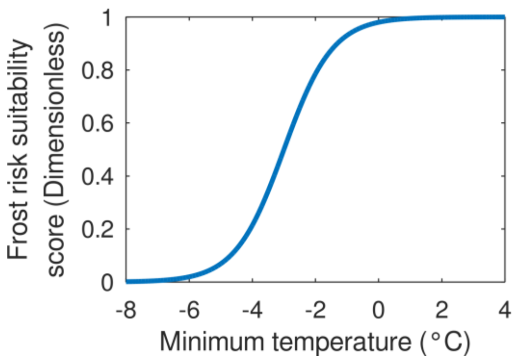

Figure 21. Avocado: frost survival score vs minimum daily temperature.

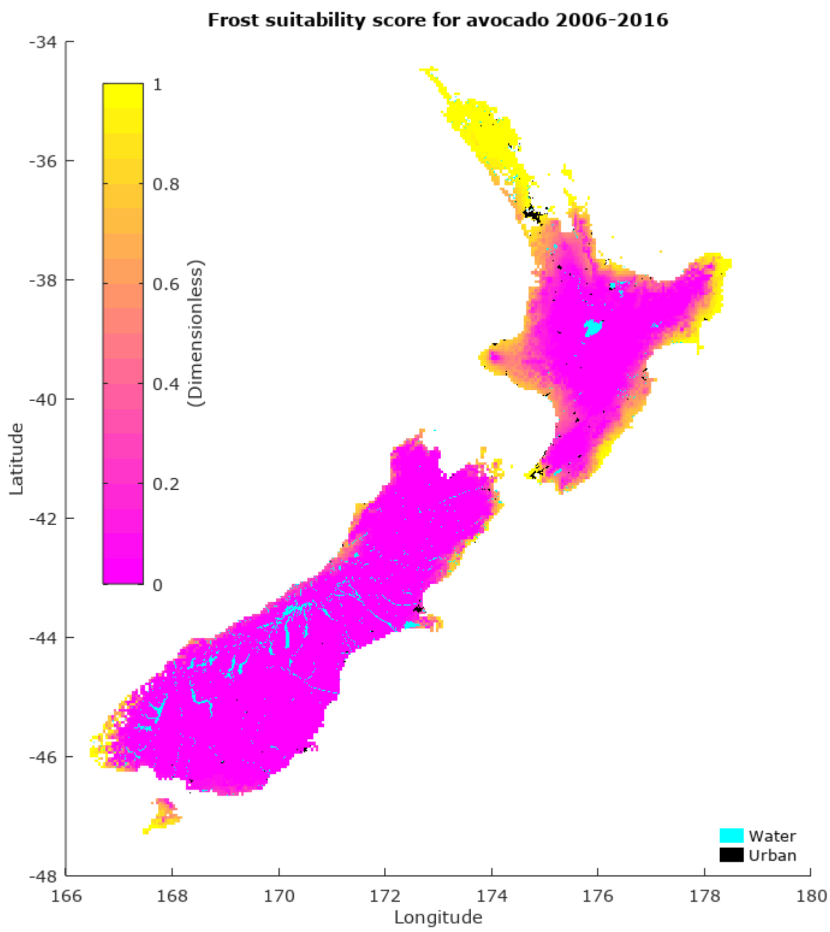

Figure 22. Avocado: map of location suitability for frost criteria throughout the year, based on data from 2006 to 2016. Calculations used Virtual Climate Station Network (VCSN) data.

3.3.4 Blueberry

Blueberry flower buds were considered the tissues most sensitive to frost damage with an LT_{50} (lethal temperature for 50% kill) of –7.5°C for some varieties of Highbush flowers (Zydlik et al. 2019). Patten et al. (1991) found Southern Highbush and Highbush cultivars to be more tolerant of frost than Rabbiteye. Rejman (1977) found that in a Polish winter young shoots of Highbush varieties were damaged only when temperatures dropped to –23.4°C, while a spring frost of –8.4°C killed only 9.9 and 6.8% of 'Blueray' and 'Darrow' flower buds, respectively. The corolla is the most sensitive part of the flower with the LT_{50} for five Highbush cultivars ranging from –2.1 to –3.3°C, and corolla damage is likely correlated with reduction in fruit set (Rowland et al. 2013). NeSmith et al. (1999) found that 0, 20% 75% and 100% of 'Brightwell' Rabbiteye flowers suffered corolla damage at temperatures of –2, –2.5, –3 and –3.5°C. The LT_{50} that corresponds to this response is approximately –2.8°C , which is in the range observed by Rowland et al. (2013). These last two studies were conducted in controlled environments with limited cultivars and are not necessarily indicative of outcomes across commercial enterprises involving different cultivars. For example, a –6°C frost in a warmer-than-usual Polish spring caused different yield losses in different Highbush cultivars, with reduction in numbers of final fruit set varying from 89% to 8%, with this variation related to the timing of the frost with the flowering periods of the cultivars (Lin & Pliszka 2003).

We used a frost survival curve to indicate how to represent how much of potential fruit yield is lost after a single day of frost, assuming a range of cultivars with different flowering times can be grown in the location. Assuming a temperature variability of ±2°C around the VCSN temperature within each 25-km^2 grid-square and considering the LT_{50} across studies, with more weight on field observations, we assigned survival rates of 50% at –4.5°C, 10% at –7.5°C, and 90% at –1.5°C (Figure 23).

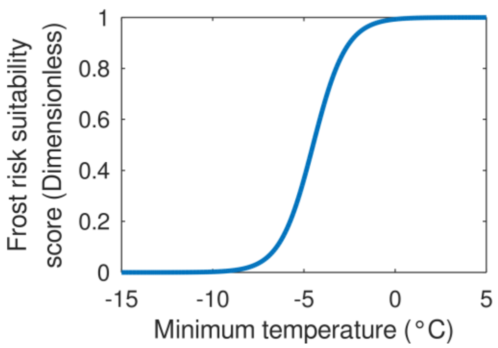

Figure 23. Blueberry frost survival score vs minimum daily temperature.

Given the spread in flowering time of different cultivars, we have taken the approach of DPI Tasmania (https://dpipwe.tas.gov.au/Documents/BLUEBERRIES.pdf) and characterised September and October as risk periods for frost, rather than trying to predict flowering times for each cultivar. The frost survival score was calculated using the minimum daily temperatures for each day in the frost risk period. The calculated loss was combined to get a cumulative damage calculation for the total period, which was used as a frost suitability score (Figure 24). Most of the North Island, except for mountainous and high elevation inland areas have high frost suitability scores, as well as most lowland areas of the South Island, and thus the map suggests that most current blueberry growing areas are not presently faced with high frost risk issues.

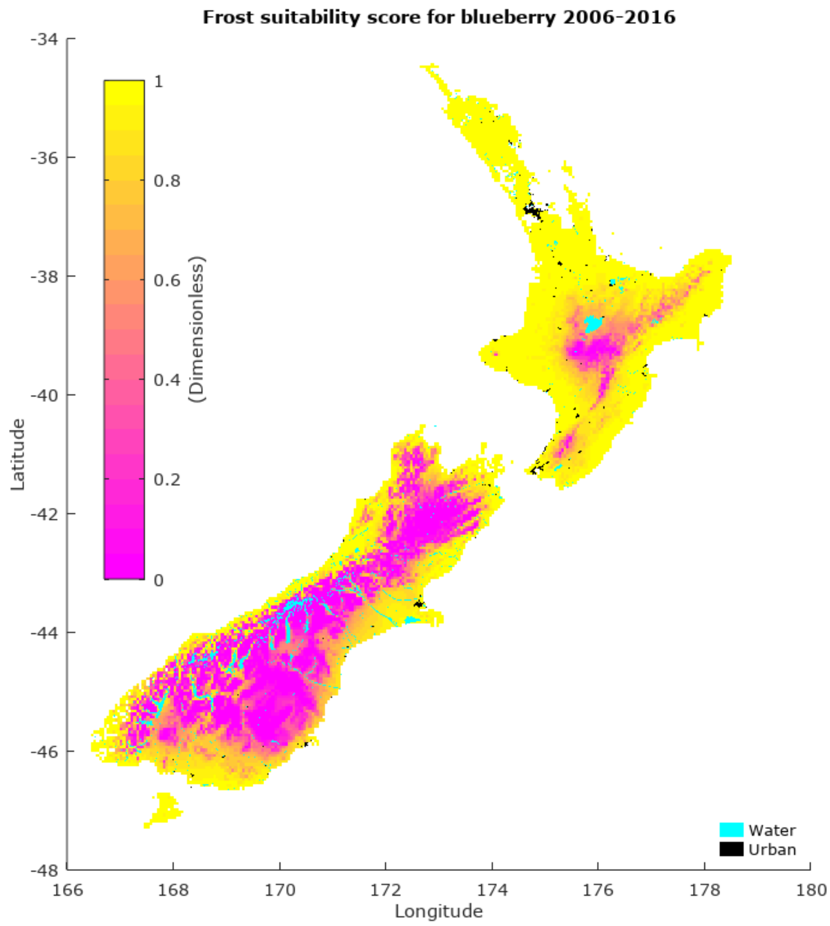

Figure 24. Blueberry: average frost suitability score for locations across the country. Calculations used Virtual Climate Station Network (VCSN) data.

3.3.5 Cherry

Spring frosts have varying effects on different sweet cherry cultivars and can be a limiting factor to production (Kappel 2010). However, there is limited quantitative information on cultivar susceptibility over a range of temperatures. Matzneller et al. (2016) performed controlled-environment experiments on 'Summit' that involved three frost temperatures (−2.5, −5.0, −10.0°C), and developed four empirical functions for calculating frost damage on sweet cherry buds or flowers at four phenological development stages. None of these functions ranged from 0 to 100%, and we considered that all behaved unsatisfactorily outside the range –10 to –2.5°C, and thus are not useful for our modelling.

Ballard et al. (1997) provided general kill rate vs temperature for different development stages from Swollen Bud to Post Bloom, showing that the stages most vulnerable to frost kill are first bloom to post bloom (with a 10% loss at –2.2°C and 90% loss at –3.8°C), with the open cluster and first white stages being a little less vulnerable (a 10% loss at –2.8°C and 90% loss at, respectively, –8.3 and −6.1°C). Assuming a temperature variability of ±2°C around the VCSN temperature within each 25-km^2 grid-square in conjunction with this range of values, we chose a frost suitability curve corresponding to a fruit survival rate of approximately 10% at –5.4°C, and 90% at –1.4°C, with a 50% midpoint at –3.4°C (Figure 25).

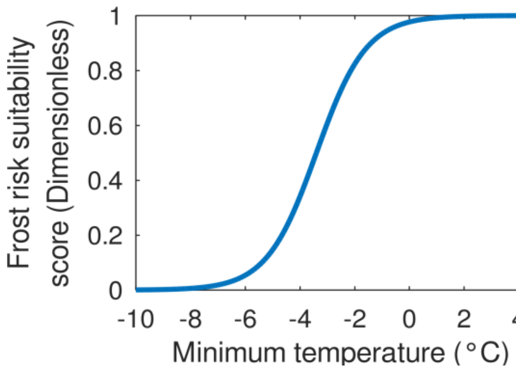

Figure 25. Cherry: frost suitability score as a function of minimum daily temperature

The frost survival score was calculated using the minimum daily temperatures for each day in the frost risk period. The calculated daily loss was weighted by the probability of being in the frost risk period described above, and the cumulative damage calculated for the total period.

Frost damage is calculated for only the period from bud break and consequently cold areas with bud break delayed until well after frost events will not be identified as frost risk areas.

While these areas should be ruled out under GDD considerations, maps of frost suitability could be misleading. Thus we used a combined frost and cold suitability score by multiplying the frost suitability score by a ‘bud-break-day suitability score’, to rule out areas that are too cold for timely bud break to occur. We assumed that if bud break does not occur by 15 October, then the growing season will be too short. We defined the bud-break-day suitability score as a function of the number of days from bud break until an arbitrary date of 31 December, 77 days later. The bud-break-day score was assigned values of 0.15, 0.5 and 0.85 for, respectively, 70, 77 and 84 days from bud break to 31 December (Figure 26), with the latter being calculated by the weighted sum of days from July to December, with weights being the probability that bud break has occurred.

A map showing the number of days from bud break until 31 December for different locations across New Zealand is presented in the left hand panel of Figure 27. Without application of the bud-break-day suitability score (Figure 26), the dark magenta areas in this map would not be identified as frost risk areas despite being among the coldest in the country, because of bud-burst being delayed until outside the frost risk period.

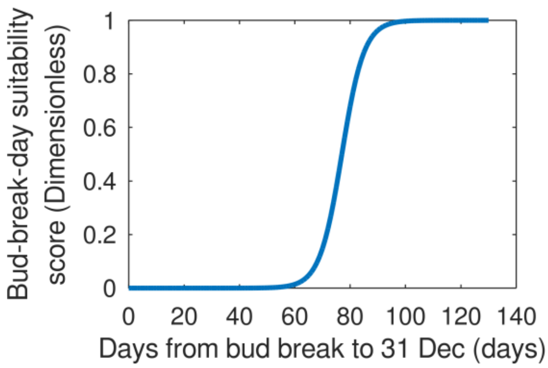

Figure 26. Cherry: suitability score for bud break as a function of effective days from bud break to 31 December.

The combined frost and cold suitability that takes both frost and severely delayed bud-burst into account is mapped in the right hand panel of Figure 27. Most of the North Island, including Hawke’s Bay, have very low to low frost risk for cherry, with only inland areas showing moderate to high risk. Coastal areas of the South Island have very low to moderate frost risk, including Marlborough, whilst inland areas have moderate to high risk. The valleys of Central Otago regions have moderate risk, suggesting that frost mitigation is important. This is line with known growing regions and use of frost protection in Central Otago.

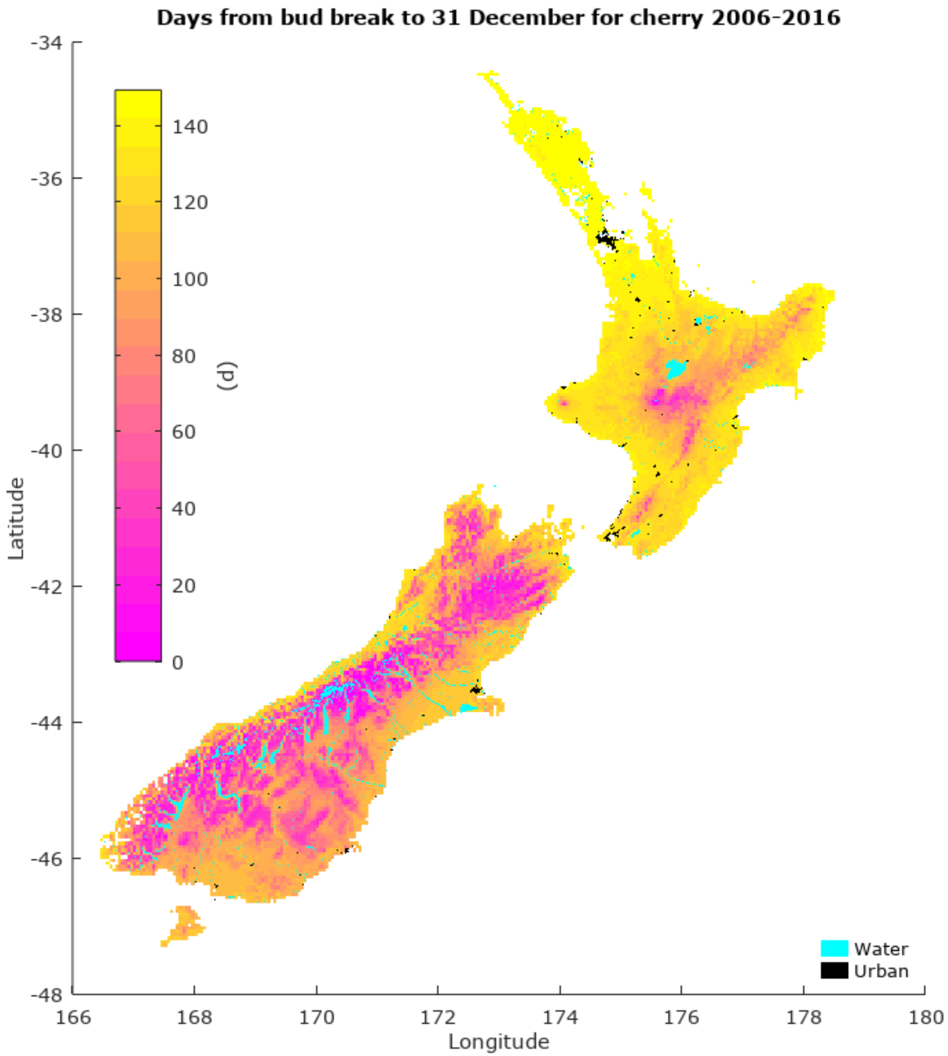

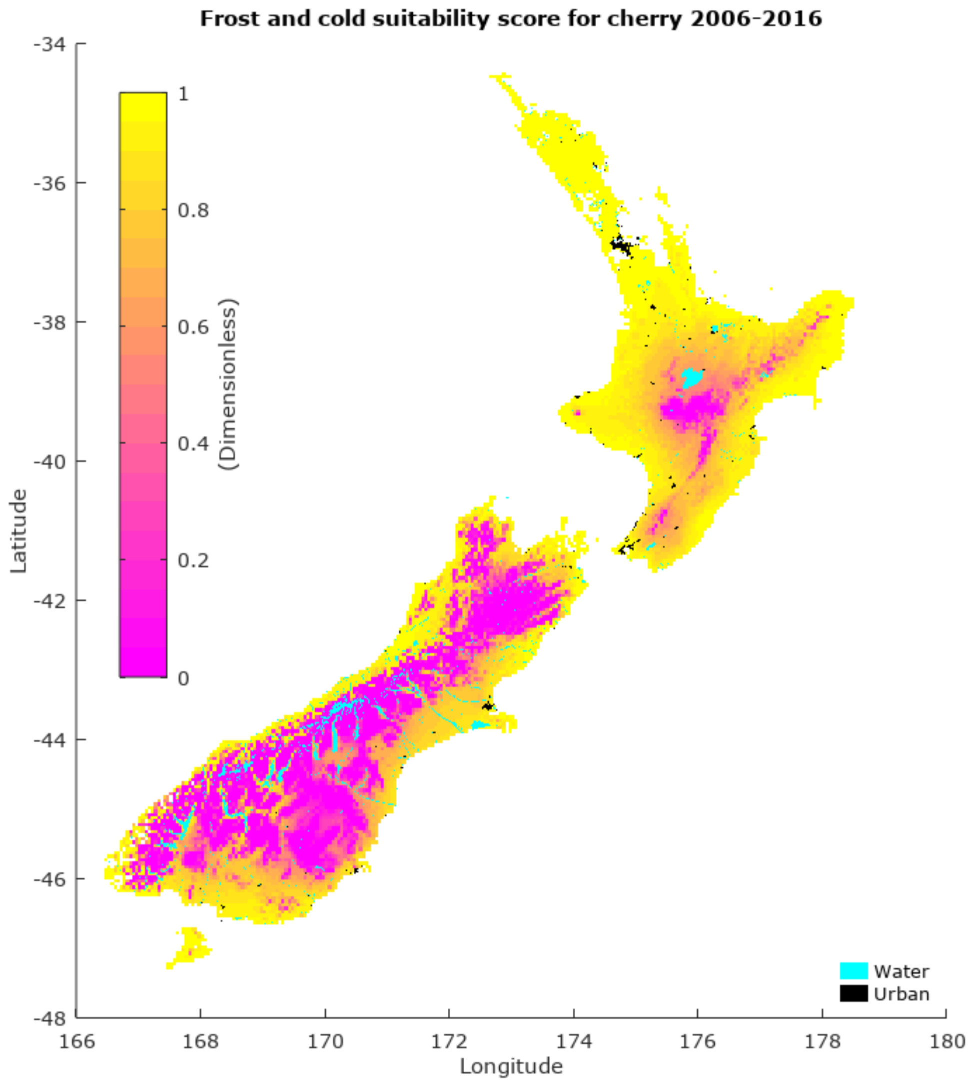

Figure 27. Cherry: map of NZ showing number of days from bud break to 31 December (left), which were used along with minimum temperature to calculate the combined frost/cold suitability score (right). Calculations used Virtual Climate Station Network (VCSN) data.

3.3.6 Wine grape

The impact of freezing temperatures varies between species, cultivars, locations on the cane and vine, and is lower in dormant plants compared with actively growing plants, and buds are more susceptible to freeze damage than canes, trunks and roots (Fennell 2004). In *Vitis vinifera* cultivars, bud freezing tolerance from dormancy induction to bud break ranges from –5 to –15°C in mid-autumn to –20 to –30°C in mid-winter (Fennell 2004). In contrast, green, actively growing tissues can be damaged by temperatures slightly below 0°C or even higher if radiative cooling leads to sub-zero tissue temperatures (Ferguson et al. 2014).

Plant tissues become more susceptible to cold injury as grapes develop from bud burst through shoot development (Poling 2008). For example, LT_{50} values for Pinot noir were –2.2°C at bud break, and −2.0°C, −1.7°C, and −1.2°C for the first, second and fourth leaf stages, respectively (Gardea (1987) cited by Ferguson et al. (2014)). Cold damage before bud burst may not reduce yield, depending on timing with relation to pruning and on the abundance of secondary buds that are less prone to freezing than primary buds and potentially productive (Fennell 2004). Given New Zealand’s relatively warm climate, we ignored autumn and winter frost damage.

We assumed that Sauvignon blanc has similar frost tolerance to Pinot noir. Based on the trend in the LT_{50} described above, we chose –1.7°C as a nominal LT_{50} across all stages for spring frost. The difference between LT_{10} and LT_{90} for ‘Concord’ grape averaged 3°C for the same growth stages (Proebsting et al. (1978) cited by Ferguson et al. (2014)). Given that ‘Concord’ is more frost tolerant we would expect the difference in LT_{10} to LT_{90} to be less than 3°C in Pinot noir and Sauvignon blanc. However, temperature variations within a grid will flatten LT responses and thus we assumed that LT_{10} and LT_{90} would vary by 4°C, and took them to be 0.3 and –3.7°C (Figure 28, left panel).

Frost damage is calculated only for the period from bud break (when growing tissue becomes vulnerable) to 31 December. As was the case for cherry, very cold areas with bud break delayed until after frost events will not be identified as frost risk areas and might be depicted as warmer than they really are in frost suitability maps. Thus, we used the same approach for cherry, and multiplied the frost suitability score by a bud-break-day suitability score to obtain a combined frost/cold suitability score.

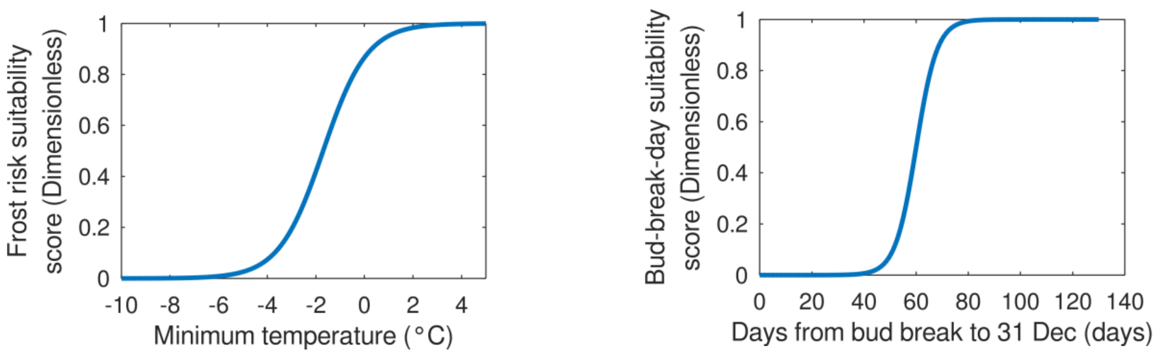

Figure 28. Grape: Frost suitability score as a function of minimum daily temperature (left) and bud-break-day suitability score as a function of days from bud break to 31 December (right).

If bud break does not occur by 1 November, the growing season will be too short for grape production (Damian Martin, pers. comm.). Thus the bud-break-day score (Figure 28, right panel) was assigned values of 0.15, 0.5 and 0.85 for 53, 60 and 67 effective days from bud break to 31 December, the latter being the daily probabilities that bud break has occurred from 1 July. Separate maps for Pinot noir and Sauvignon blanc show effective days from bud break until 31 December (Figure 29), and the combined frost/cold suitability scores (Figure 30) across New Zealand.

For the most part, frost and cold susceptibility scores for Pinot noir and Sauvignon blanc are calculated as being similar. As expected, the northern part of the North Island has no frost risk, whilst areas such as Gisborne and Hawke's Bay have low to moderate frost risk, as does Marlborough and Nelson. Canterbury has moderate frost risk, moving slightly higher closer to the Alps and slightly higher risk for Sauvignon blanc in some pockets. Central Otago shows high frost risk for Sauvignon blanc, whereas Pinot noir is moderate to high, which would suggest frost mitigation will be essential in those areas. These calculations of frost risk appears to be mostly in line with what is experienced in known growing regions, although in practice Pinot noir in Central Otago may be faced with slightly less frost risk than predicted, and fare much better than Sauvignon blanc.

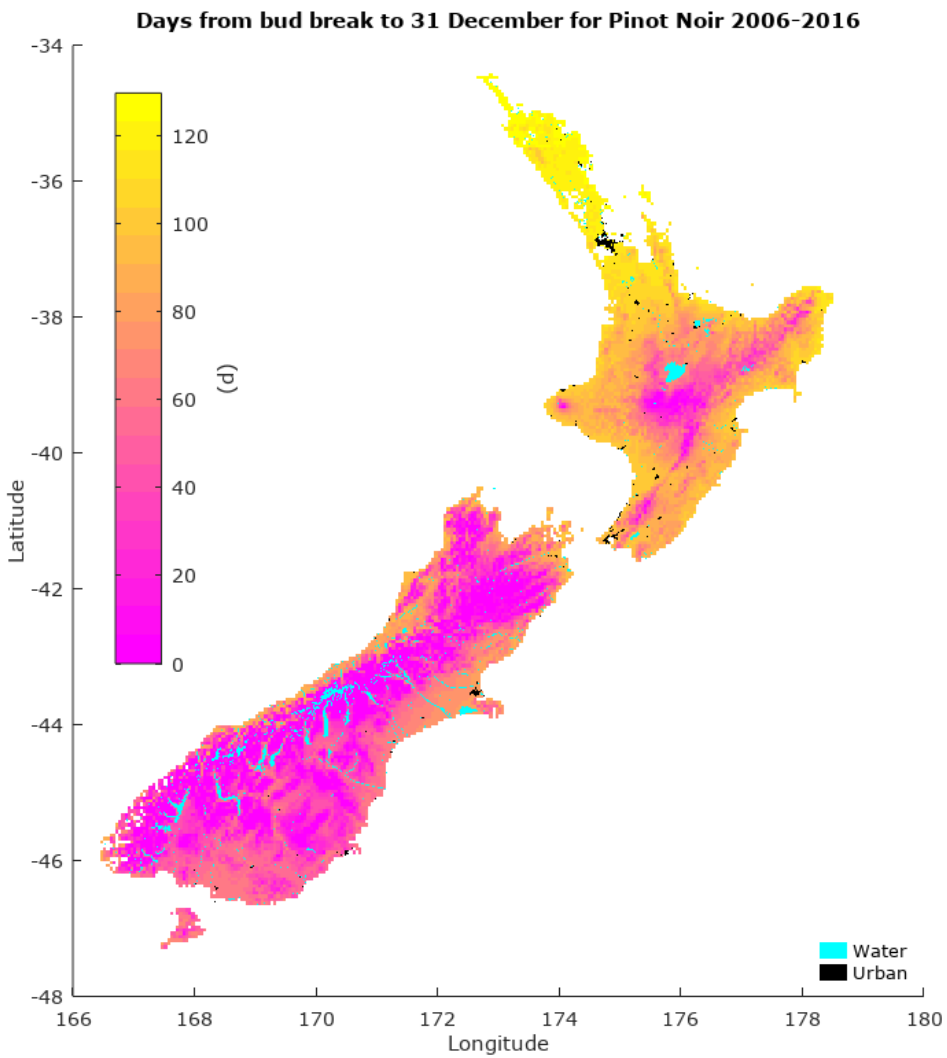

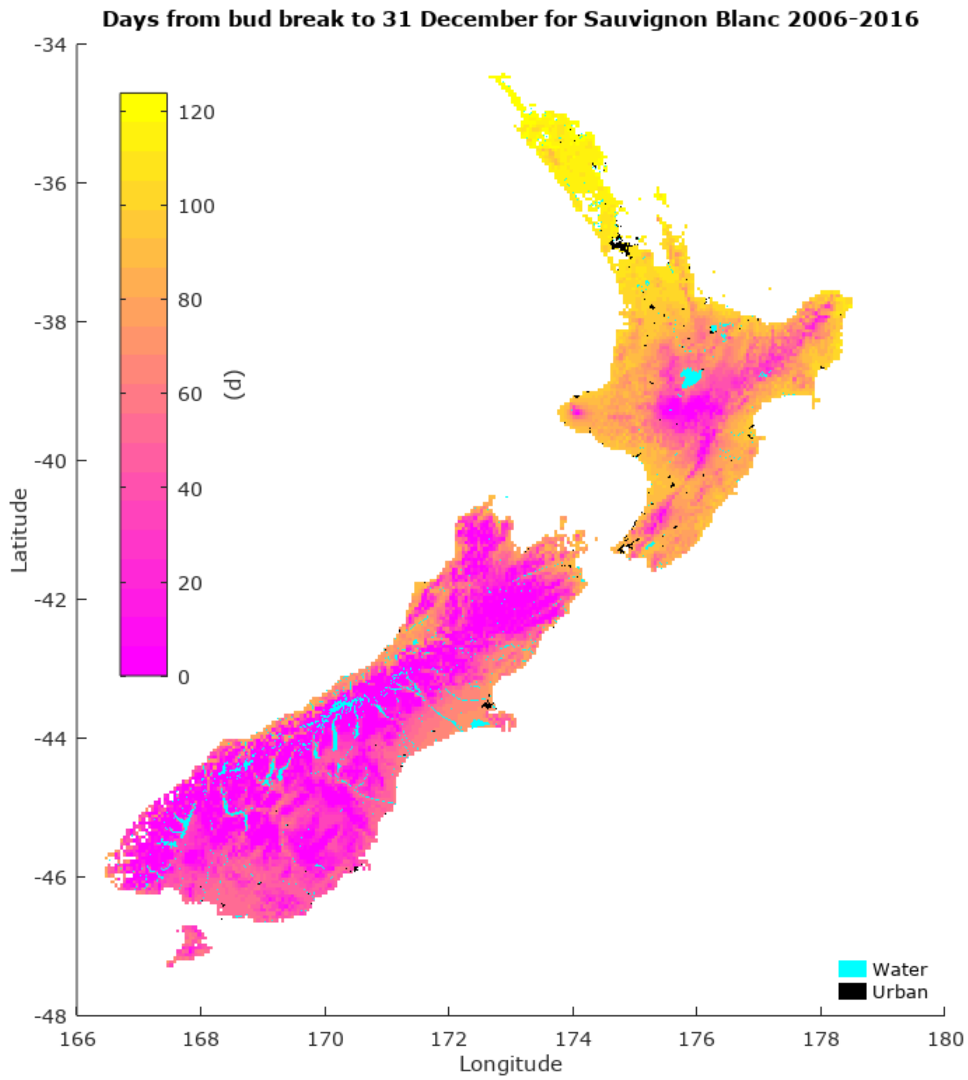

Figure 29. Grape: days from bud break to 31 December for locations across the country for Pinot noir (left) and Sauvignon blanc (right). Calculations used Virtual Climate Station Network (VCSN) data.

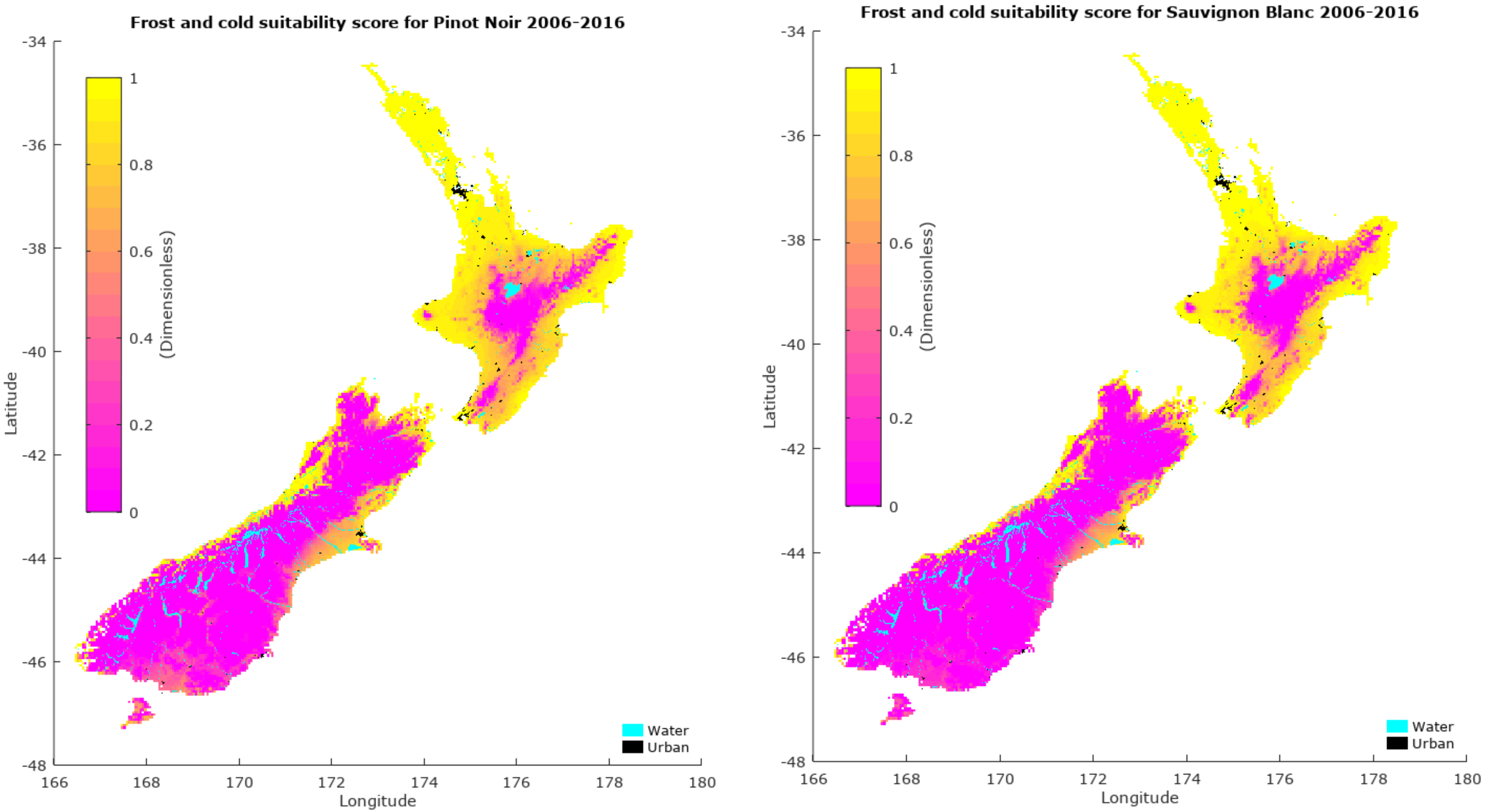

Figure 30. Grape: frost suitability scores for Pinot noir (left) and Sauvignon blanc (right). Calculations used Virtual Climate Station Network (VCSN) data.

3.4 Temperature and warmth for crop maturation

Horticultural production requires warm conditions for fruit maturation, and depending on the crop, is expressed in terms of growing degree days (GDD), growing degree hours (GDH), or mean temperatures over a period.

3.4.1 Apple

For apple production, van den Dijssel et al. (2014) and Clothier et al. (2018) suggested a minimum GDD requirement of 800 d°C for October to April using a 10°C base. Singh and Bhatia (2012) found that 10 different cultivars had a 28% variation in GGD (4°C base) requirement. Jangra (2012) found a 39% variation between two cultivars in their GDD requirement to maturity.

We used the 10°C base suggested by van den Dijssel et al. (2014), but accommodated the variation between cultivars found by other authors. Thus we chose a suitability score with a response curve that was approximately 0.05, 0.5, and 0.95 for GDD values of 500, 800 and 1100 d°C, respectively, calculated using a 10°C base (Figure 31). The annual calculation uses the October to December temperatures for that year, and January to April temperatures for the following year (e.g. GGD for 2008 used temperatures from 2008 and 2009).

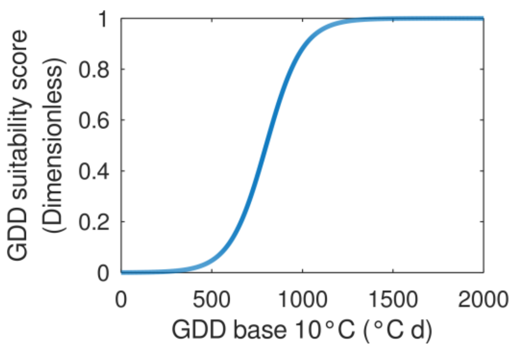

Figure 31. Growing degree days (GDD) score assigned to different GDD values base 10°C for apple. A higher score indicates a more satisfactory maturation of fruit.

The accumulation of GDD base 10°C is shown for different locations across the country in Figure 32, and the corresponding suitability scores for apple are mapped in the left panel of Figure 34 alongside a map of GDD suitability scores for kiwifruit, which were calculated using the same GDD accumulations as for apple.

The GDD accumulations look very suitable for maturing apple in the Waikato and further north, and for the rest of the North Island in all the regions that are not overly elevated, which is reflected in the correspondingly high GDD scores. For the South Island, good maturity of the fruit can be reached in pockets around Marlborough, Nelson, Tasman, the West Coast, Canterbury and Central Otago. These predictions are in line with known growing regions.

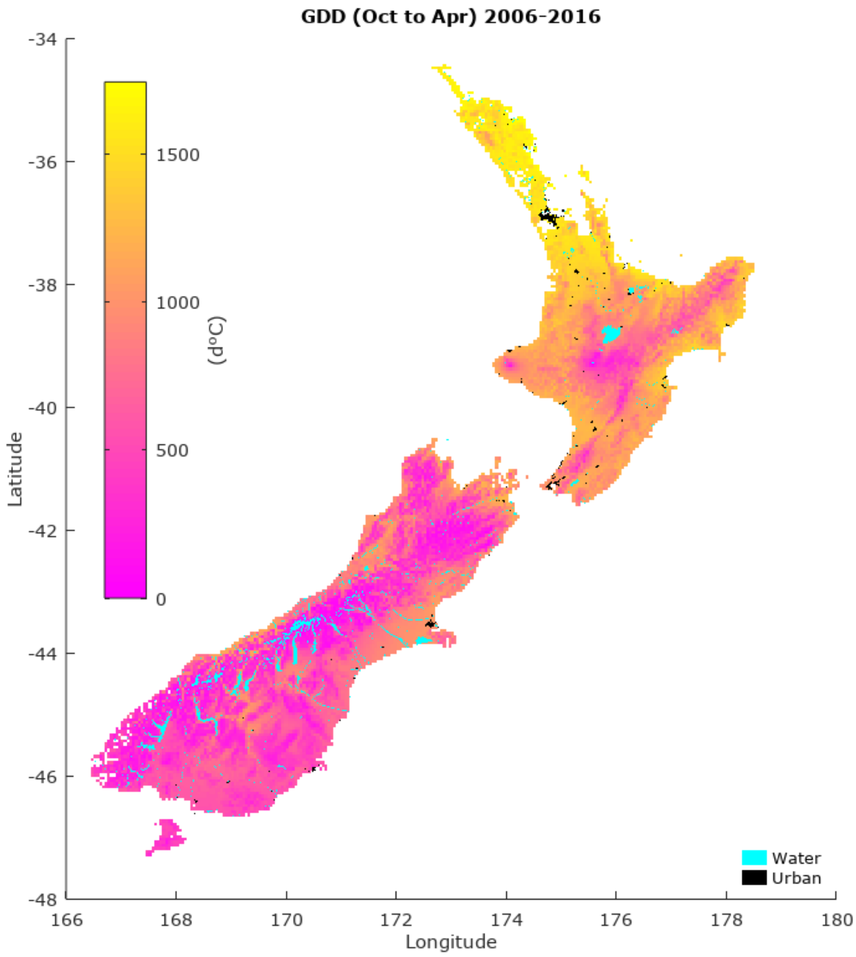

Figure 32. Accumulation of growing degree days (GDD) from October to April using a 10°C base, mapped for New Zealand, and used for calculating GDD suitability scores for both apple and kiwifruit. Calculations used Virtual Climate Station Network (VCSN) data.

3.4.2 Kiwifruit

Salinger & Kenny (1995) specified GDD requirements for adequate 'Hayward' kiwifruit growth to be 1100 d°C accumulated during October to April using a GDD base of 10°C. Interestingly, this base is higher than the base temperature of 7°C that Salinger et al. (1993) reported for calculating forcing during flower development. For kiwifruit, the GDD accumulation period, base and thus calculation was the same as that for apple, and thus the map of GDD accumulation is the same (Figure 32).

In the absence of data of GDD requirements for other cultivars, we used the information for 'Hayward' to construct a GDD suitability curve to represent current and future cultivars, assigning the values 0.05, 0.5, and 0.95 respectively for GDD values of 690, 900 and 1110 d°C, base 10°C (Figure 33).

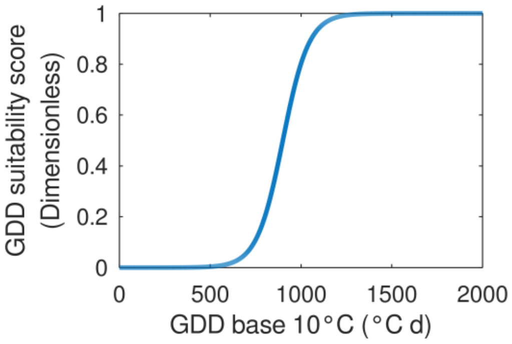

Figure 33. Growing degree days (GDD) score assigned to different GDD values base 10°C for kiwifruit. A higher score indicates a more satisfactory maturation of fruit.

The GDD base 10°C accumulations across New Zealand are mapped in Figure 32. The corresponding suitability scores for kiwifruit are mapped in the right panel of Figure 34, alongside those for apple. Kiwifruit require a little more warmth to reach maturity than apple, but the predicted spatial suitability pattern is overall is very similar to apple. These predictions are in line with known growing regions, but Nelson might be represented as having a little lower GDD suitability than the present production might suggest.

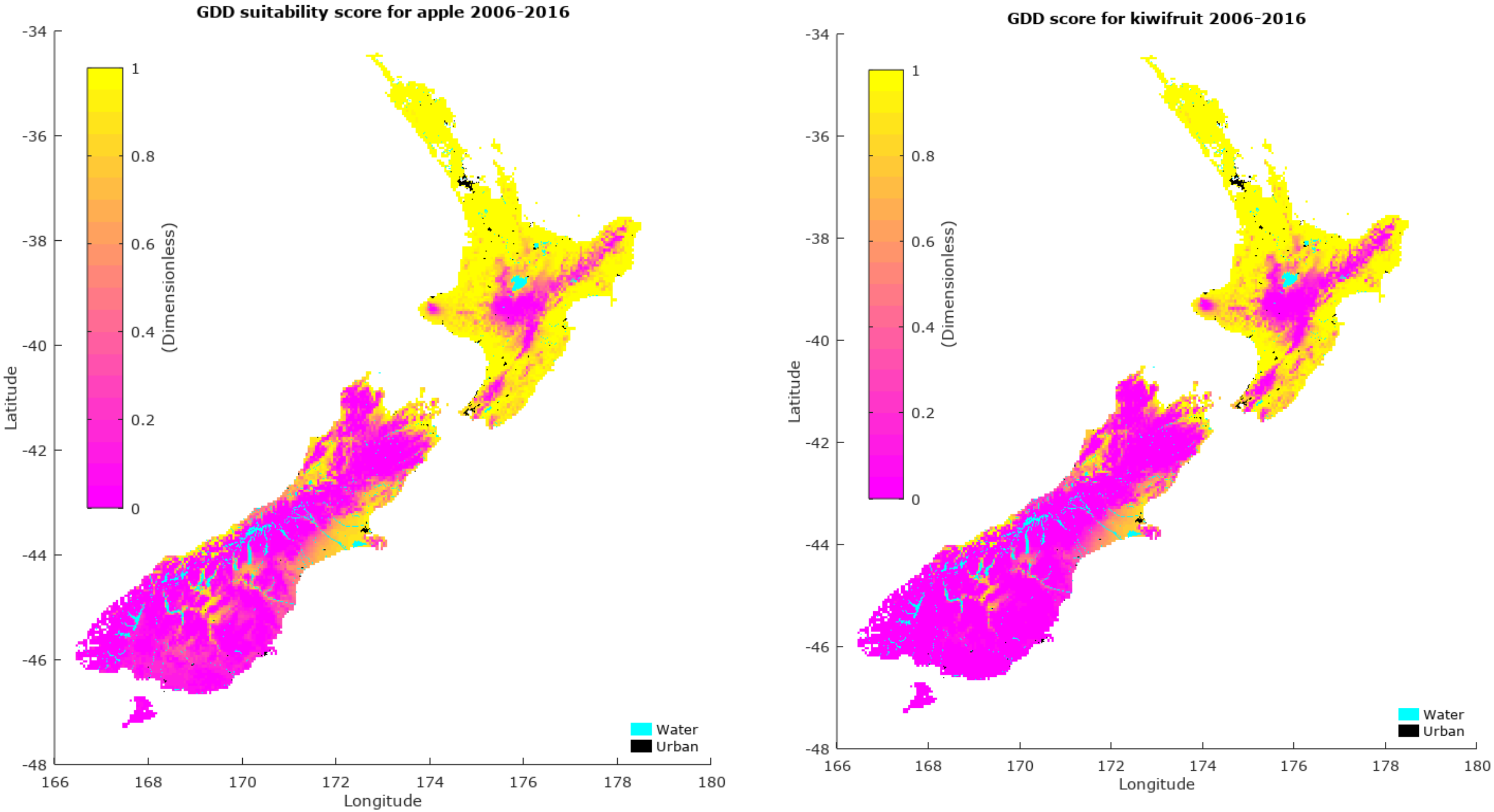

Figure 34. Growing degree day (GDD) suitability scores for apple (left) and kiwifruit (right) corresponding to GDD accumulations shown in Figure 32. Calculations used Virtual Climate Station Network (VCSN) data.

3.4.3 Avocado

Dubrovina & Bautista (2014) noted that the literature has conflicting views on optimal temperature ranges for avocado, and stated that the limiting temperature factors for avocado are frosts, low average minimum temperatures during flowering and fertilisation, and heat waves during fruit development. The lack of consensus may be because of the variation between cultivars depending on whether they are Type A or Type B. In the Type A cultivars, the flowers open in the morning in the female stage, close at mid-day and reopen the afternoon of the following day at the male stage, while in the Type B cultivars, the flowers open in the afternoon at the female stage, close in the evening and reopen the following morning at the male stage (Davenport 1986). Type B cultivars may be more sensitive to low temperatures than Type A cultivars (such as 'Hass') during pollination (Ish-Am & Eisikowitch 1991).

Floral bud initiation in New Zealand generally occurs in April or May, but could occur in March in the western Bay of Plenty (Dixon et al. 2006). Temperatures above 20°C inhibit flower initiation (Buttrose & Alexander 1978; Nevin & Lovatt 1989). In New Zealand, the main flowering period is mid-October to mid-November (Dixon & Barber 2008). Optimal pollination and yield occurs for a daily temperature range of 20°C at night to 25°C during the day (Dixon & Barber 2008). At higher temperatures, the flowering period and number of open flowers decreased in 'Hass' avocado (Sedgley & Annells 1981). Lower temperatures can disrupt pollen tube growth (Sedgley 1977). These studies used specific temperature bands that represent a small fraction of possible temperature variations, and are not suitable for developing rules.

Selim et al. (2018) used the suitability criterion that mean temperature during flowing should be between 10 and 35°C. Optimal growth occurs with a 25/20°C day/night (Sedgley & Annells 1981). We took the approach of Dubrovina & Bautista (2014) and characterised climates with mean annual temperatures of 15–20°C as optimal for avocado, with yield decreasing outside this zone, and climates with mean annual temperatures less than 12°C as unsuitable. Allowing for a 2°C variation within a grid cell around its nominal temperature, we chose a suitability score curve with approximate values of 0.15 for mean annual temperatures of 12 and 23°C and 0.9 for mean annual temperatures of 15 and 20°C (Figure 35). Temperature additionally affects fatty acid composition and other nutritional qualities of 'Hass' avocado (Ferreyra et al. 2016). However, we have not considered nutritional attributes of the fruit in our suitability modelling.

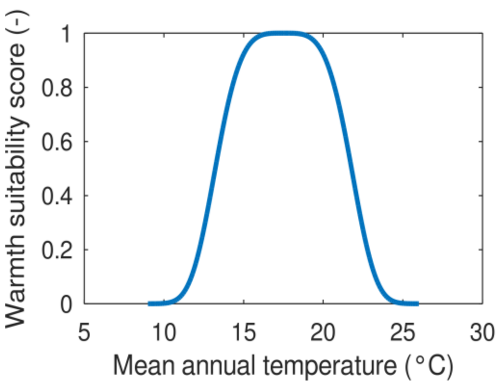

Figure 35. Avocado: warmth suitability score.

For consistency with other crops, we performed calculations for the 1 July to 30 June year. Scores were calculated for the years 2006 to 2016 for each location, and averaged across years to indicate location suitability (Figure 36). This suitability maps highlights Northland and Auckland as very suitable for growing avocado from a warmth perspective along with parts of Waikato, the Bay of Plenty and Gisborne. Nearby areas are indicated as suboptimal along with parts of the Hawke's Bay and Manawatu, but in practice are likely to have pockets of land with microclimates suitable for avocado production. The South Island is largely unsuitable. These suitability calculations appear in line with the experience in known growing regions.

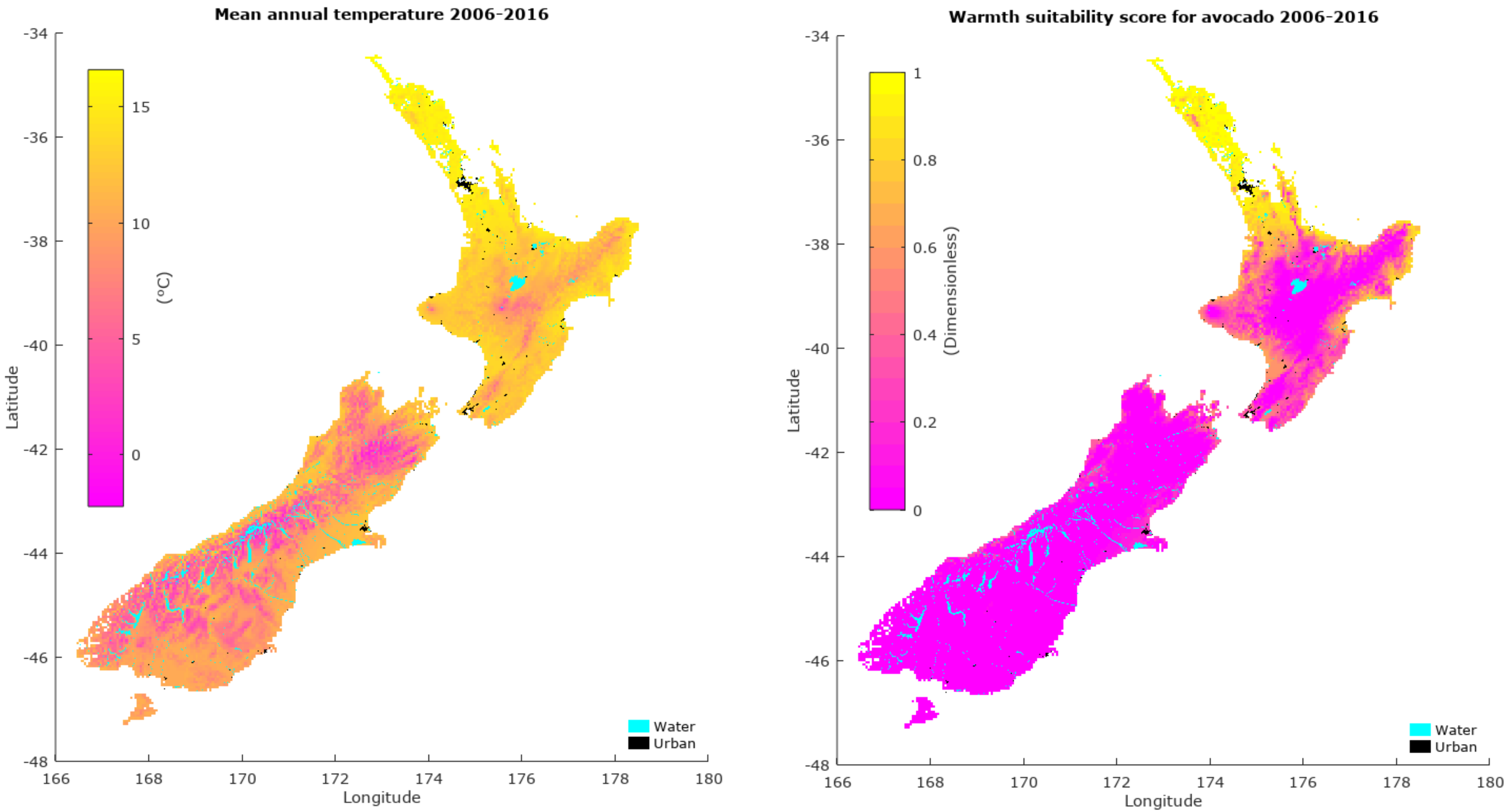

Figure 36. Avocado: map of location suitability score for warmth criteria (right), based on calculated mean annual temperature (right) using VCSN data from 2006 to 2016. Calculations used Virtual Climate Station Network (VCSN) data.

3.4.4 Blueberry

The mean time from 50% flowering to 50% maturity ranged from 75 to 94 days in a trial involving seven Rabbiteye cultivars, and accumulated GDD base 7°C ranged from 1789 to 2554 d°C (NeSmith 2006). In a trial involving seven Southern Highbush varieties, mean time and accumulated GDD from 50% flowering to 50% maturity ranged from 56 to 83 days and from 587 to 824 d°C (NeSmith 2012). Mainland (2002) developed a heat unit model analogous to Richardson chill units, in which heat unit accumulation was increasingly graduated with increasing temperature bands, with negative accumulation for temperatures below 7.2°C. Çelik (2009) gave a thermal time requirement of 120 to 160 GDD for Northern Highbush, but did not indicate a base temperature. Hall et al. (2018) used a requirement of at least a 600 d°C of accumulation of GDD base 10°C from October to April.

Allowing for a long growing season across cultivars, we assumed a ripening window from October to April and calculated GDD base 10°C accumulation for this period. We assigned a GDD suitability score of 0.5 to 700 d°C, which is approximately the average of Southern Highbush range, and values of 0.25 and 0.75 for values of 600 and 800 d°C, which are approximately the extrema for the Southern Highbush range above. The corresponding suitability function is shown in Figure 37. The Rabbiteye GDD requirement seemed excessive and was treated as unreliable.

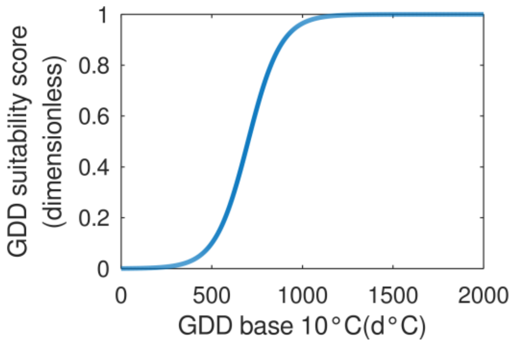

Figure 37. Blueberry: growing degree day (GDD) suitability score as a function of GDD.

Average GDD for locations across the country are the same as for apple and kiwifruit (Figure 32); however, blueberry are more tolerant in terms of GDD accumulation than apple. Thus while the suitability scores map for blueberry (shown in Figure 38) has clear similarities with the apple suitability maps (Figure 34, left panel), it also has extended areas of suitability, which is in line with known growing regions for blueberry and apple.

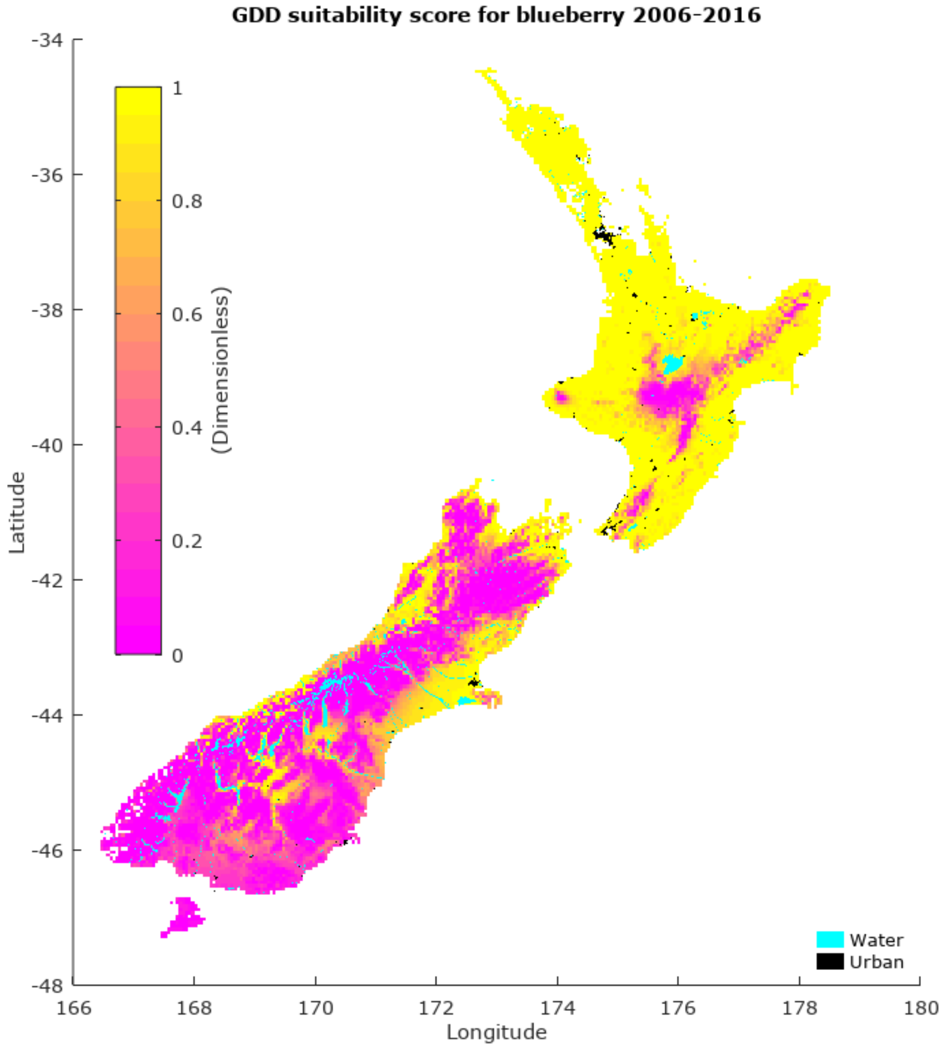

Figure 38. Blueberry: GDD suitability scores for locations across the country. Calculations used Virtual Climate Station Network (VCSN) data.

3.4.5 Cherry

The literature is sparse on information on the thermal requirements of cherry during the growing season. Hall et al. (2018) considered that fruit ripening in cherry requires a GDD base 10°C accumulation of at least 800 d°C from October to April.

Hochmaier (2014) developed simple phenological models for 'Bing', 'Van', 'Lapins' and Sweetheart®, for the phenological stages: swollen bud, visible flower bud, white tip, first bloom, full bloom, petal fall, fruit set and harvest, and found that the average thermal requirements from swollen bud stage to harvest ranged from 765 (for ‘Van’) to 916 GDD base 4.5°C (for Sweetheart).

We used a sigmoidal GDD suitability curve that had values of 0.25, 0.5 and 0.75 for, respectively, 765, 840 and 915 GDD base 4.5°C from bud break to the end of April, which we assumed would be the latest acceptable harvest date. This GDD suitability curve is shown in Figure 39.

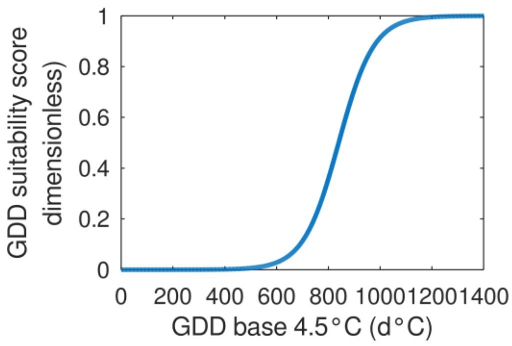

Figure 39. Cherry: Growing degree day (GDD) suitability score as a function of GDD.

Figure 40 shows mean annual October to April GDD base 4.5°C for locations across the country and the corresponding GDD suitability scores. The moderate requirements of cherry for warmth to mature is reflected in all of the North Island, bar the highest peaks, being very suitable in this respect. In the South Island, the pattern for unsuitability again appears to be dominated by high elevation. This leaves large areas of land very suitable for cherry production from a GDD perspective.

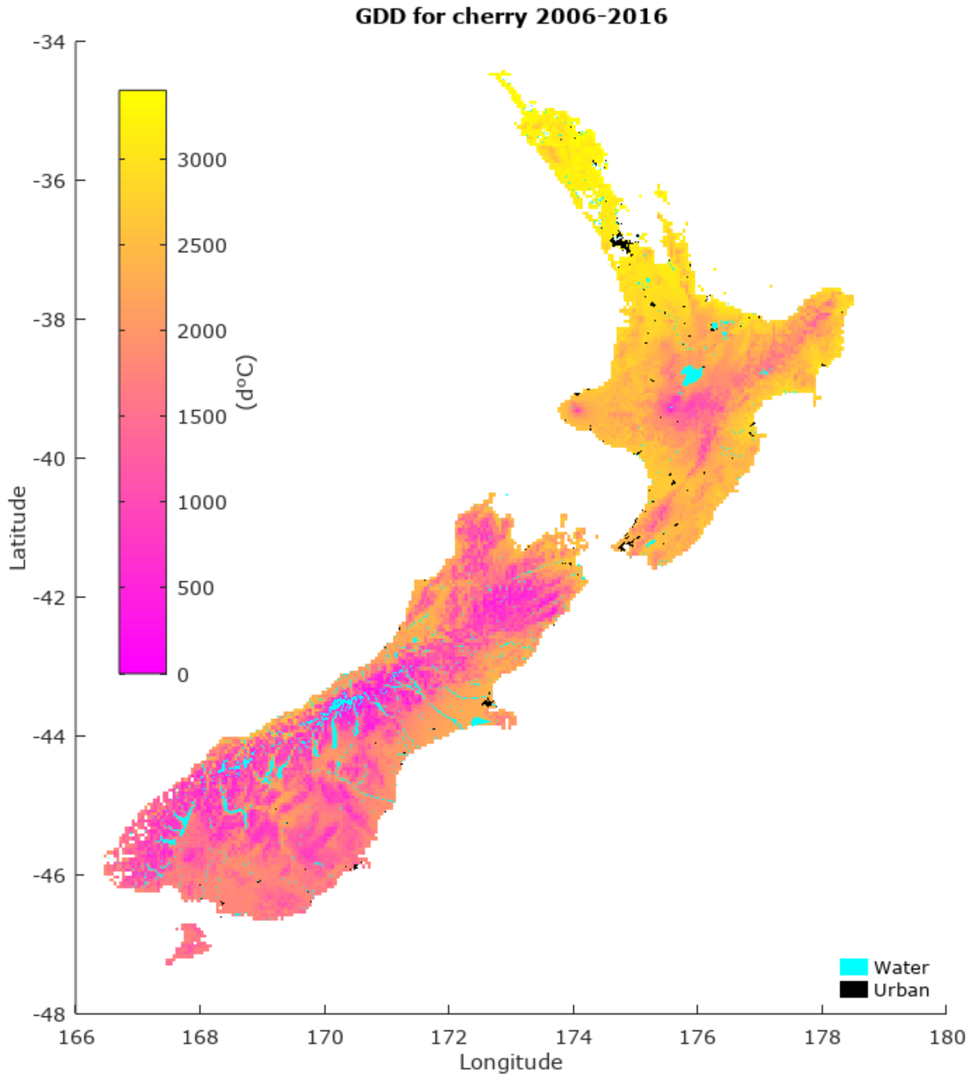

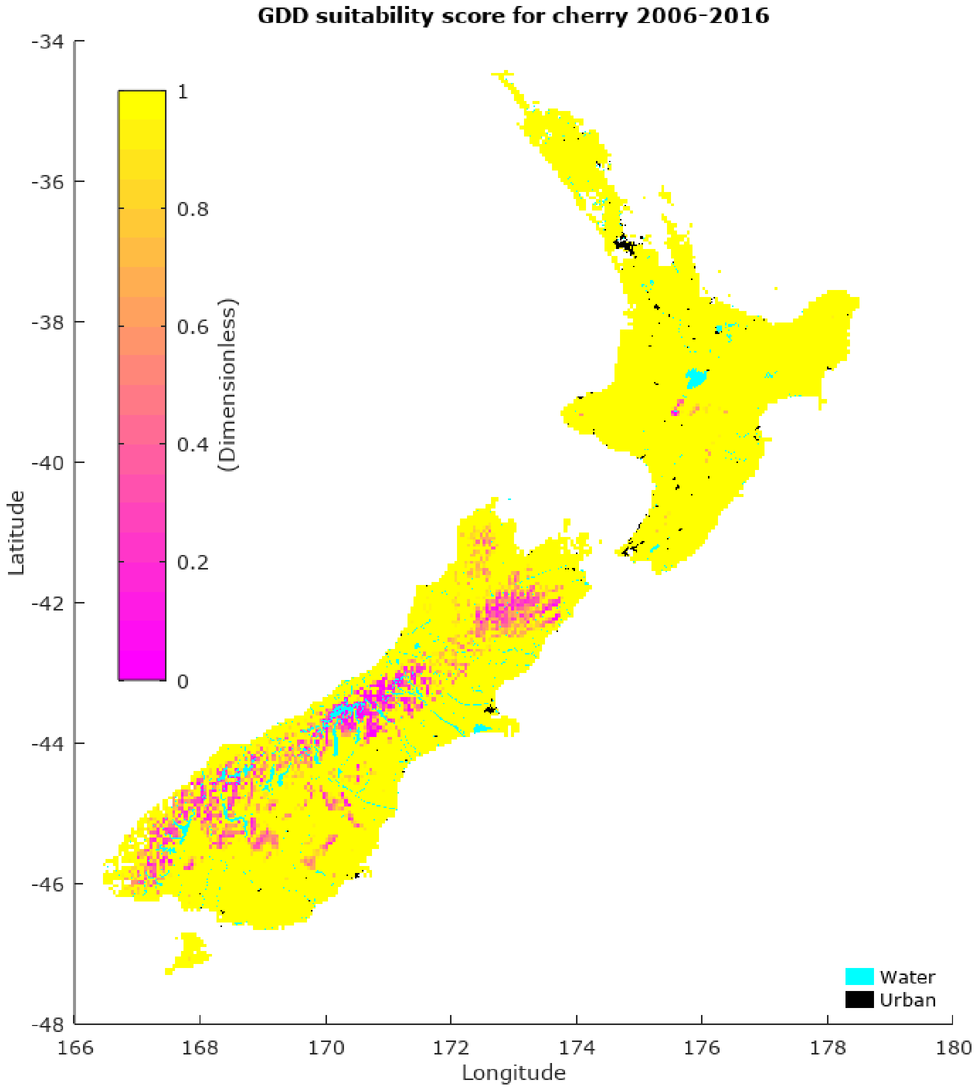

Figure 40. Cherry: growing degree days (GDD) base 4.5°C (left) and corresponding GDD suitability score (right) for locations across the country. Calculations used Virtual Climate Station Network (VCSN) data.

3.4.6 Wine grape

Not all grape cultivars reach maturity at similar sugar levels (Van Leeuwen et al. 2008), and grapes are harvested at different compositions depending on logistics and requirements. There is not one set of parameters that equates to maturity (Parker 2012). Since maturity cannot be defined with precision (Van Leeuwen et al. 2008), we have investigated requirements for veraison and/or maturity. 10°C was generally considered as the thermal baseline for grapevine development either using growing degree hours (GDH) (Mohamed & El-Sese 2009) or days (GDD) (Van Leeuwen et al. 2008; Neethling et al. 2012), although other thermal bases have been investigated (Zapata et al. 2015; 2017). While GDH may give more precision, given that we have only daily minimums and maximums available, GDD was a more suitable option. GDD base 10 accumulation from bud break to veraison ranged from 900 to 1025 d°C across 17 cultivars, with 967 and 947 d°C for Pinot noir and Sauvignon blanc, respectively (Zapata et al. 2017). Van Leeuwen et al. (2008), using European data, found that Pinot noir and Sauvignon blanc needed heat accumulations of 957 and 1011 d°C from bud break to veraison, with accumulations for other cultivars ranging up to 1209 d°C, and harvest for Pinot noir when GDD accumulation reached 1251 d°C.

For New Zealand conditions, a GDD base of 4.5°C is preferable (Damian Martin, pers. comm.) following the work of Hall & Blackman (2019) who modelled wine grape phenology for regions in Australia. Although the heat requirements for Sauvignon blanc and Pinot noir that are reported in the literature are similar, in New Zealand the management of the two cultivars is different, with Sauvignon blanc typically grown to be more high-producing than Pinot noir and therefore having a higher GDD requirement by about 150 d°C. Further GDD accumulations that exceed an optimal band reflect areas that are less suitable for viticulture (Damian Martin, pers. comm.). Thus we used GDD base 4.5°C and used suitability curves with optimal bands having value 1.0: 1075 to 1325 d°C centred around 1200 d°C for Pinot noir and 1225 to 1475 d°C centred around 1350 d°C for Sauvignon blanc. Suitability scores declined as GDD accumulations deviated from the band, with the value of 0.6 at 800 and 1600 d°C for Pinot noir and 950 and 1750 d°C for Sauvignon blanc (Figure 41).

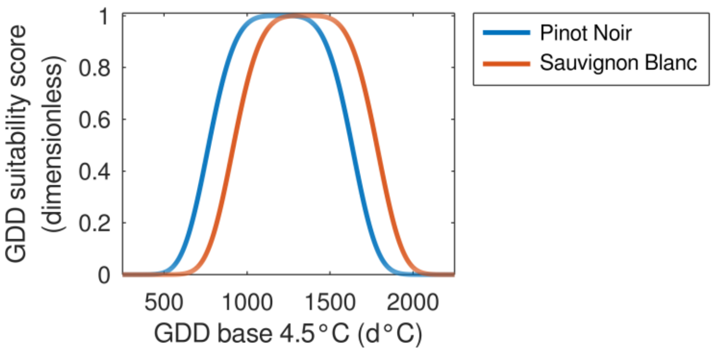

Figure 41. Grape: growing degree day (GDD) suitability score vs GDD for Pinot noir and Sauvignon blanc.

To calculate GDD suitability scores, GDD calculated for each day of the growing season (1 Jul to 30 Jun), and weighted by the corresponding daily probability that the growing season was continuing. The weighted sum of GDD contributions gave the total GDD. This was done separately for Pinot noir and Sauvignon blanc (Figure 42), with suitability scores shown in Figure 43. The predictions indicate that large areas of Northland, Auckland, Waikato and the Bay of Plenty are unsuitable, and this will be because of too much warmth rather than too litle. The patterns of suitability accord with locations where Pinot noir and Sauvignon blanc are known to be grown.

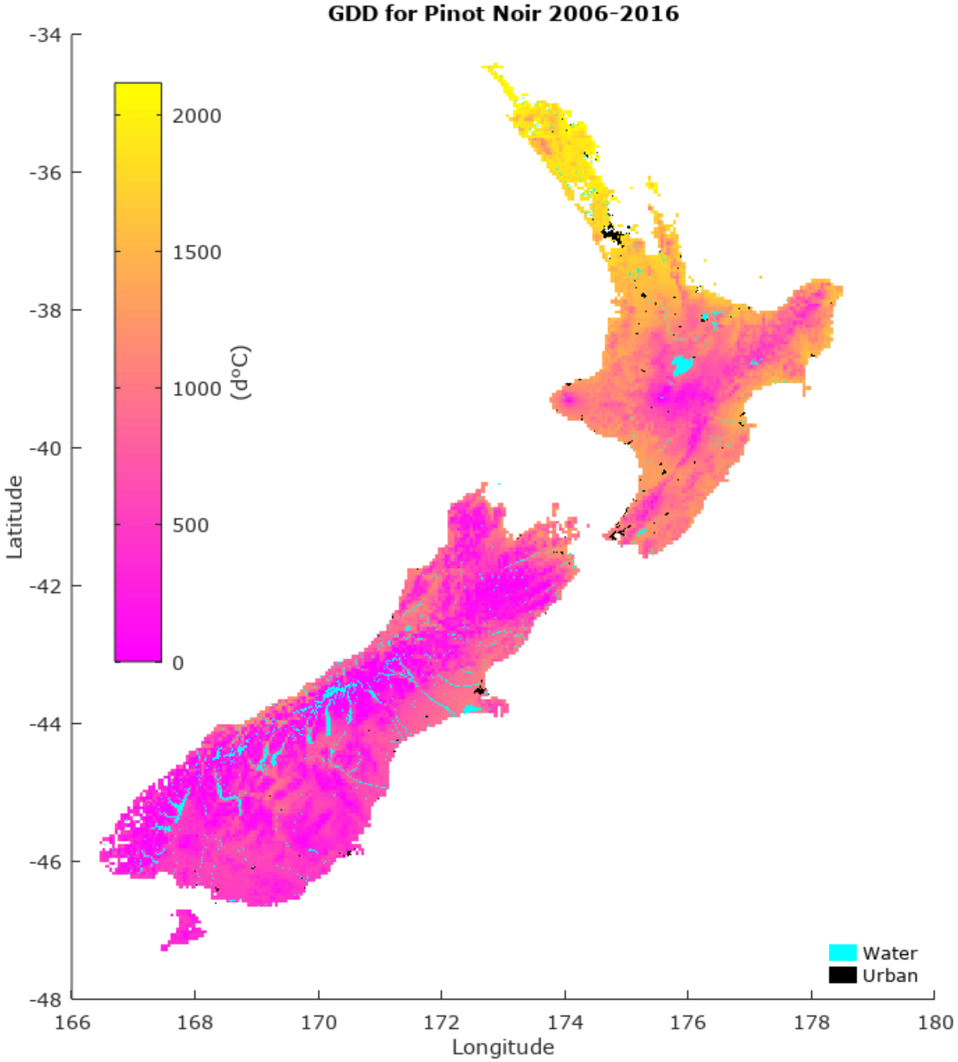

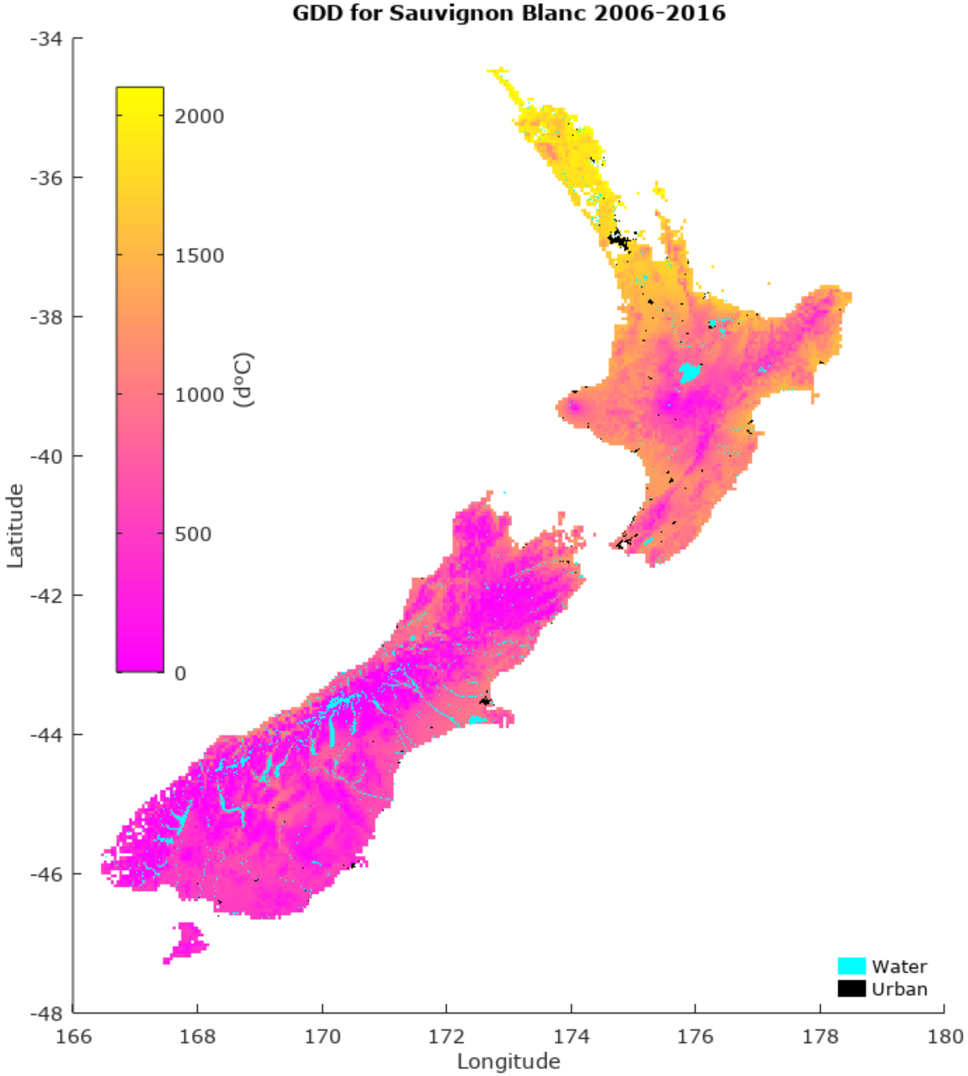

Figure 42. Grape: growing degree day (GDD) accumulation for Pinot noir (left) and Sauvignon blanc (right). Calculations used Virtual Climate Station Network (VCSN) data.

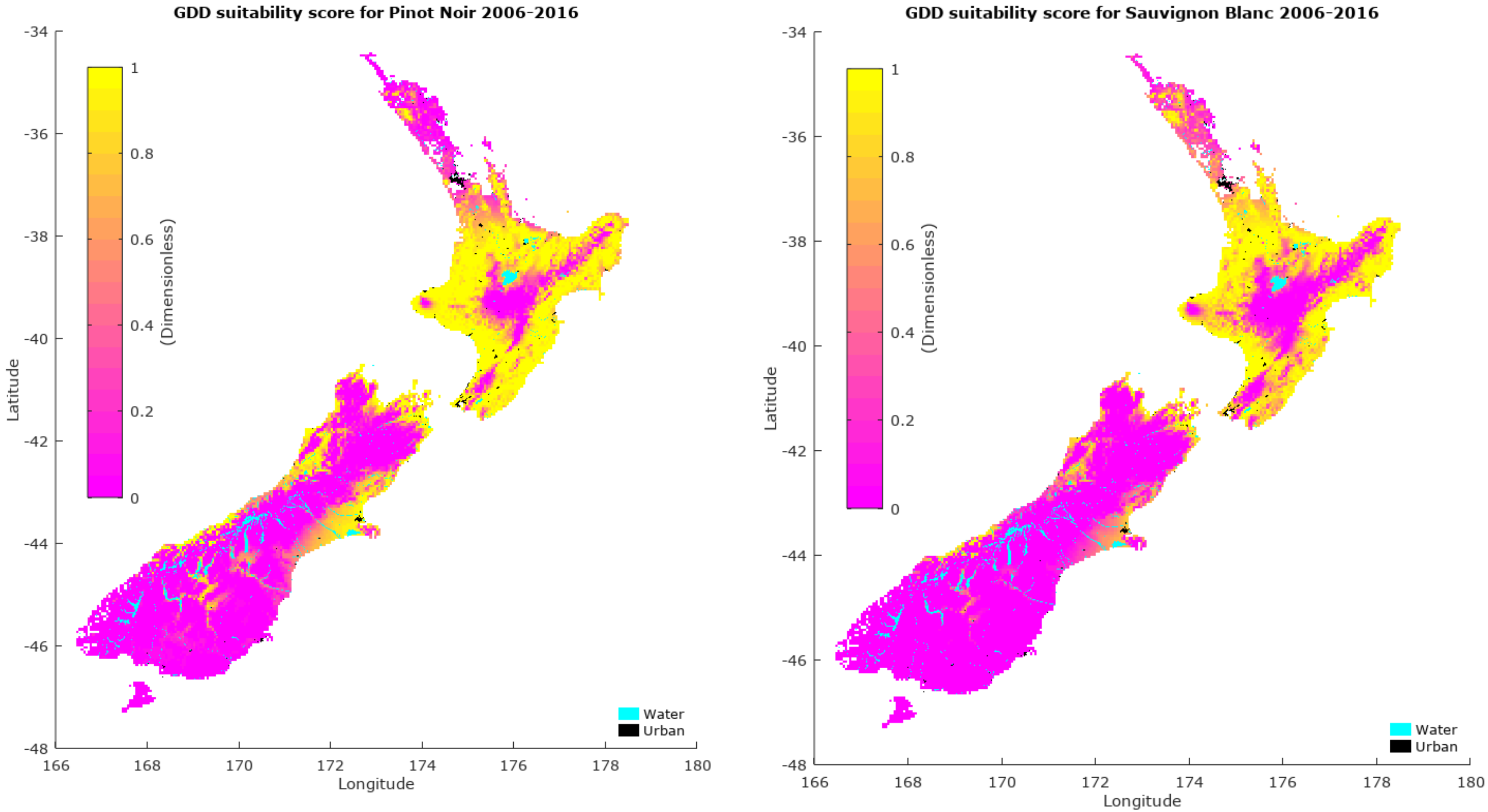

Figure 43. Grape: growing degree day (GDD) suitability scores for Pinot noir (left) and Sauvignon blanc (right). Calculations used Virtual Climate Station Network (VCSN) data.

3.5 Fruit size

3.5.1 Apple: early growing season sufficient for good fruit size

Stanley et al. (2000) found that if GDD accumulation in the first 50 days after DFB (DAFB) was doubled from 120 to 240 d°C, then this resulted in an increase in fruit weight of approximately 90% and increase in fruit diameter of 20%. Thus to assess suitability of a location for producing sizeable fruit, we calculated GDD base 10°C (GDD_{10}) for the first 50 days from the same DFB that we calculated for assessing frost risk.

Chaves et al. (2017) found that different cultivars had different effective GDD reference bases, due to differences in harvest dates. This suggests that cultivars would vary in their GDD_{10} requirements for good sized fruit, which is well suited to a continuous suitability score approach. We chose a suitability score curve that gave values of approximately 0.05, 0.5, and 0.95 for GDD_{10} values of 60, 120, 180 d°C, respectively, in the first 50 DAFB (Figure 44).

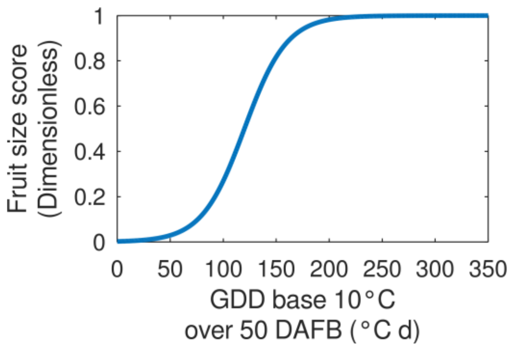

Figure 44. Fruit-size score assigned to growing degree days (GDD) base 10°C in the first 50 days after full bloom (DAFB) for apple. Lower scores correspond to smaller-sized fruit.

Figure 45 shows the corresponding fruit size suitability scores for locations across the country. While total GDD accumulation for maturation could be expected to be correlated with GDD accumulation in the first 50 DAFB, the correlation is not as strong as might be expected.

While there are many areas where fruit-size suitability and GDD (for maturation) suitability are both high or both low, some areas had moderate or low fruit-size suitability despite scoring high GDD for the growing season, which would indicate relatively cooler spring temperatures in these areas despite good summer warmth. Conversely, some elevated areas throughout New Zealand are indicated as having moderate to high suitability scores for fruit size despite having low suitability scores for October-to-April GDD accumulation, which identifies them as cold locations. This apparent inconsistency can arise because of the calculated DFB in cold locations being considerably delayed into warmer weather.

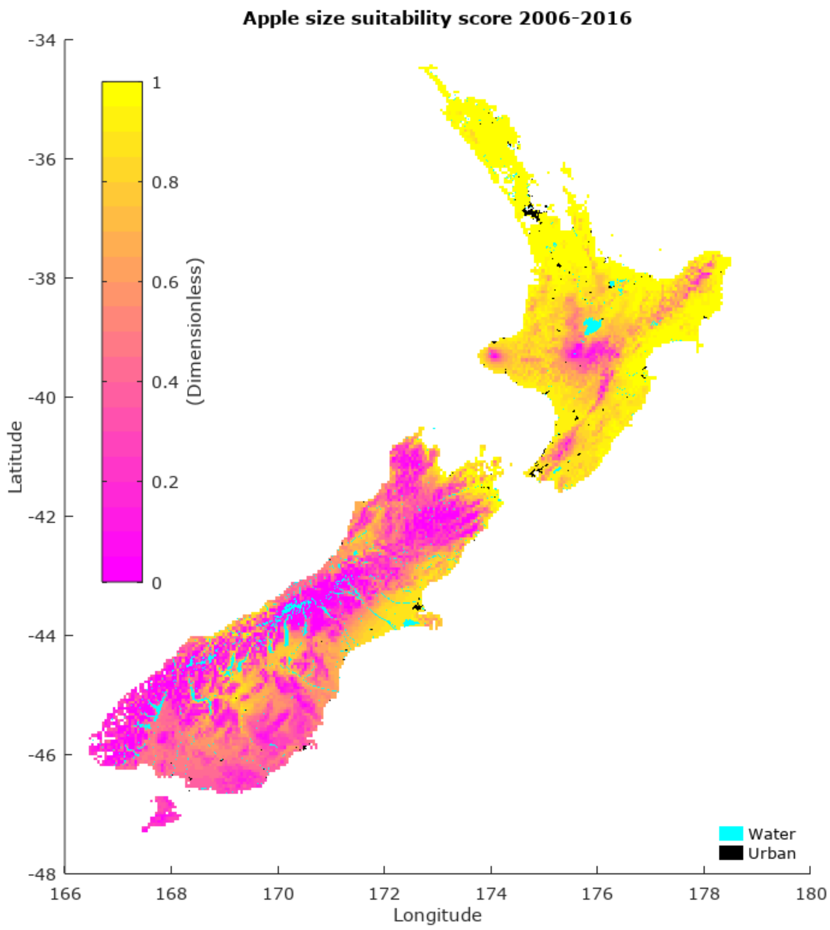

Figure 45. Apple fruit size suitability score mapped for locations across the country for 2006–2016. Calculations used Virtual Climate Station Network (VCSN) data.

3.6 Damage from weather extremes

3.6.1 Apple: Sunburn risk

Air temperature in the shade as an indicator of sunburn risk in apple can be categorised as follows (http://mvcitrus.org.au/mvcb/wp-content/uploads/2012/09/Sun-Protection-for-Apples-Agnote.pdf):

- Greater than 40°C = High risk of a necrotic patch
- Greater than 35°C = High risk of browning damage
- 30–35°C = Damage is variable, depending on wind, sunlight intensity (cloud cover), humidity and degree of fruit acclimatisation to sunlight.

For example, in the Goulburn Valley, estimated fruit losses vary from 6 to 30%, depending on the season and the type of fruit. Losses in susceptible cultivars such as 'Granny Smith' and 'Gala' fruit have been reported to be as high as 40–50%.

We assume that only fruit directly exposed to sunlight are prone to sunburn damage and that the risk period starts in October and ends in April. Further, we assumed that days of high temperature did not have to be consecutive to cause cumulative damage. We also introduced a decreased weighting for sunburn effects occurring later in April. This accounts for early harvested cultivars that are not exposed to potentially high temperatures occurring after harvest.

We represented the percent of fruit surviving sunburn by a sigmoidal curve with values of 99, 75 and 51% at maximum VCSN temperatures of 29, 37.5 and 46°C, respectively. The sunburn survival score was then chosen to be one minus twice the survival rate, ensuring a range from zero to one (Figure 46). This assumes, for example, that for a maximum VCSN temperature of 29°C the maximum temperature for the corresponding 25-km^2 grid-square ranges from 27 to 31°C.

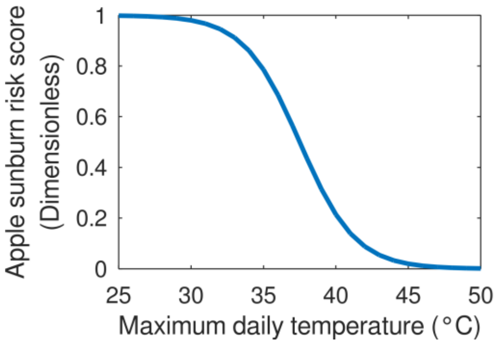

Figure 46. Sunburn survival score for apple as a function of maximum temperature. The higher the score, the lower is the sunburn risk.

Calculations for sunburn suitability scores are mapped in Figure 47, indicating excess heat resulting in sunburn in apple is most likely to occur in Canterbury and Otago and to a lesser extent in areas around the North Island. However, no areas of New Zealand were identified as having a high risk of sunburn, which is in line with known growing regions.

Sunburn will affect the bottom line but not cause sustained damage and therefore would be expected to have less impact on overall suitability than the other climate-related criteria that we considered for apple.

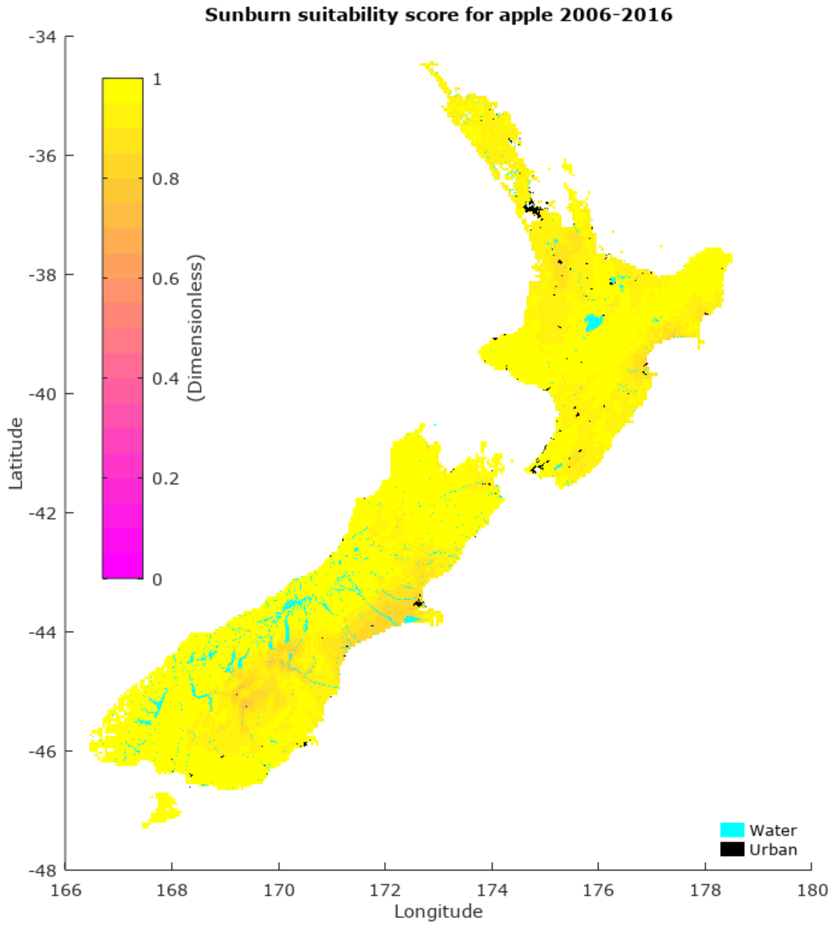

Figure 47. Apple: sunburn suitability score for locations across the country. Calculations used Virtual Climate Station Network (VCSN) data.

3.6.2 Kiwifruit: cane damage from extreme cold

Pyke et al. (1986) found that temperatures below –7°C can kill some dormant kiwifruit vines in May, with frosts of –9°C and –11°C both killing 100% of 1-year-old plants in the same month. However, in June, no plants were killed by a frost treatment of –7°C, and 17, 33 and 67% of 1-year-old plants were killed by frost treatments of respectively –9°C, –11°C and –13°C. Weet (1979) found that North American kiwifruit plants when fully dormant can survive –17.5°C. Additionally, Testolin and Messina (1987) found that the cultivar 'Hayward' survived temperatures of –18°C, although with shoot damage. Based on these findings, we assigned a suitability score of 0.5 to a temperature of –13°C, with a slow sliding scale as shown in Figure 48.

Calculations for a cold-damage suitability score are mapped in Figure 49, which shows that only the coldest places in New Zealand could cause cane damage in this context and the bulk of the country is ideally suited to avoid such damage. None of the known growing regions would be affected at all.

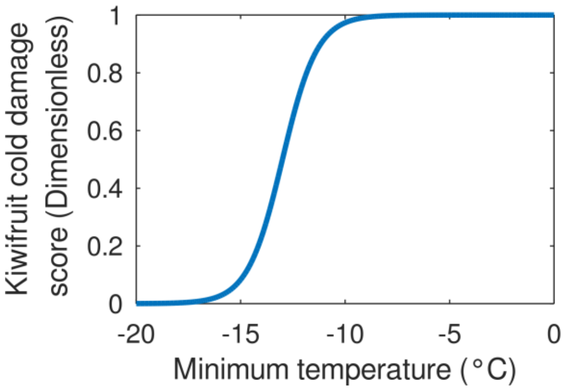

Figure 48. Cane damage score for kiwifruit as a function of minimum temperature. A higher score reflects less cane damage.

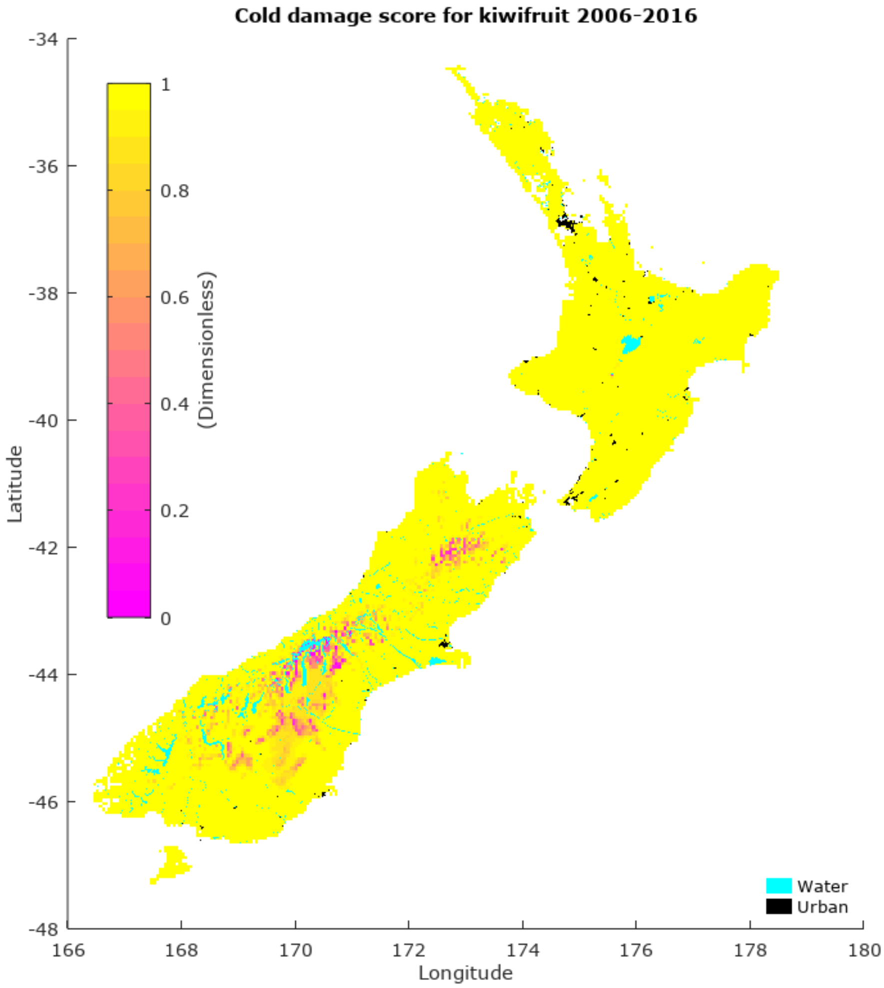

Figure 49. Kiwifruit: cold-kill suitability score for locations across the country. Calculations used Virtual Climate Station Network (VCSN) data.

3.6.3 Cherry: moisture-induced fruit cracking

Rain-induced fruit cracking and splitting of fruit is a serious economic concern that occurs during the later stages of fruit development and is associated with multiple factors including cultivar, rootstock, growing conditions, soil moisture and irrigation, stage of fruit development and several fruit characteristics, and high temperatures (Balbontín et al. 2013; Correia et al. 2018). Although rain cracking is commonly thought to be caused by excessive water uptake, Measham (2011) found that while initial cracking of fruit coincided with rainfall there was no relationship between the amount of rain and the incidence of cracking, and that application of excess water to the root zone induced fruit cracking. Alternative theories include the view that rapid cooling of the fruit surface increases the tensile stress on its skin (Koumanov 2015), or that rain cracking is caused by localised skin phenomena involving localised water uptake through microcracks (Winkler et al. 2016; Winkler 2017). In earlier work, Knoche and Peschel (2006) had identified that surface water aggravated microscopic cracking in the skin of sweet cherry cuticle, and found that although temperature had no significant effect, increases in RH increased the number of microcracks, with about a 50% increase when RH went from 84 to 92%, and over a two-fold increase in cracking as RH went from 92 to 100%. We have therefore used RH rather than rainfall as a predictor for fruit cracking, in light of Measham's (2011) observations that there was no relationship between amount of rain and the incidence of cracking. We developed a function of fruit surviving cracking with survival rates of 95%, 87.5% and 75% from one day of exposure to RH of 84, 92 and 100%, respectively (Figure 50). The climate database provide only one daily RH value (taken in the morning), and this was taken as representative of the day, which will of course result in a degree of inaccuracy.

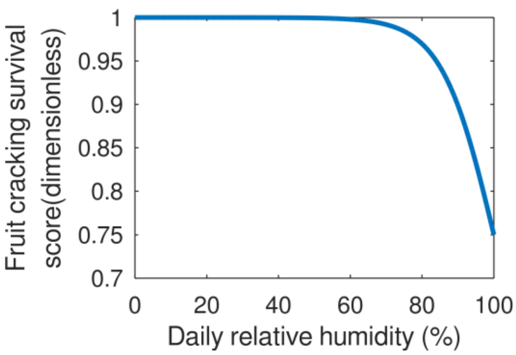

Figure 50. Cherry: fraction of fruit prone to cracking as a function of relative humidity.

Microcracks can occur on immature and mature sweet cherry fruit, and can subsequently develop into fruit cracking (Knoche & Peschel 2006). Thus we allowed for the possibility of fruit cracking stemming from microcracks formed early in the season. Nominal cracking survival was calculated for each day from 1 November onwards, and losses weighted by the corresponding daily probability that the crop has not been harvested (based on phenology modelling as illustrated in Figure 2).

The cumulative loss from cracking was then calculated from the daily weighted losses, and the fraction of surviving fruit used as the suitability score. Resulting fruit cracking suitability scores for different locations are shown in Figure 51. These calculations indicate very high suitability for a reduced likelihood of moisture-induced cracking in Northland, Auckland, Gisborne and the Hawke's Bay, with plenty of moderately high suitability around the rest of the country including the New Zealand cherry growing hotspot of Central Otago. This prediction of some moisture-induced cracking occurring in Central Otago and very little occurring in the Hawke's Bay is in line with what is observed in the industry.

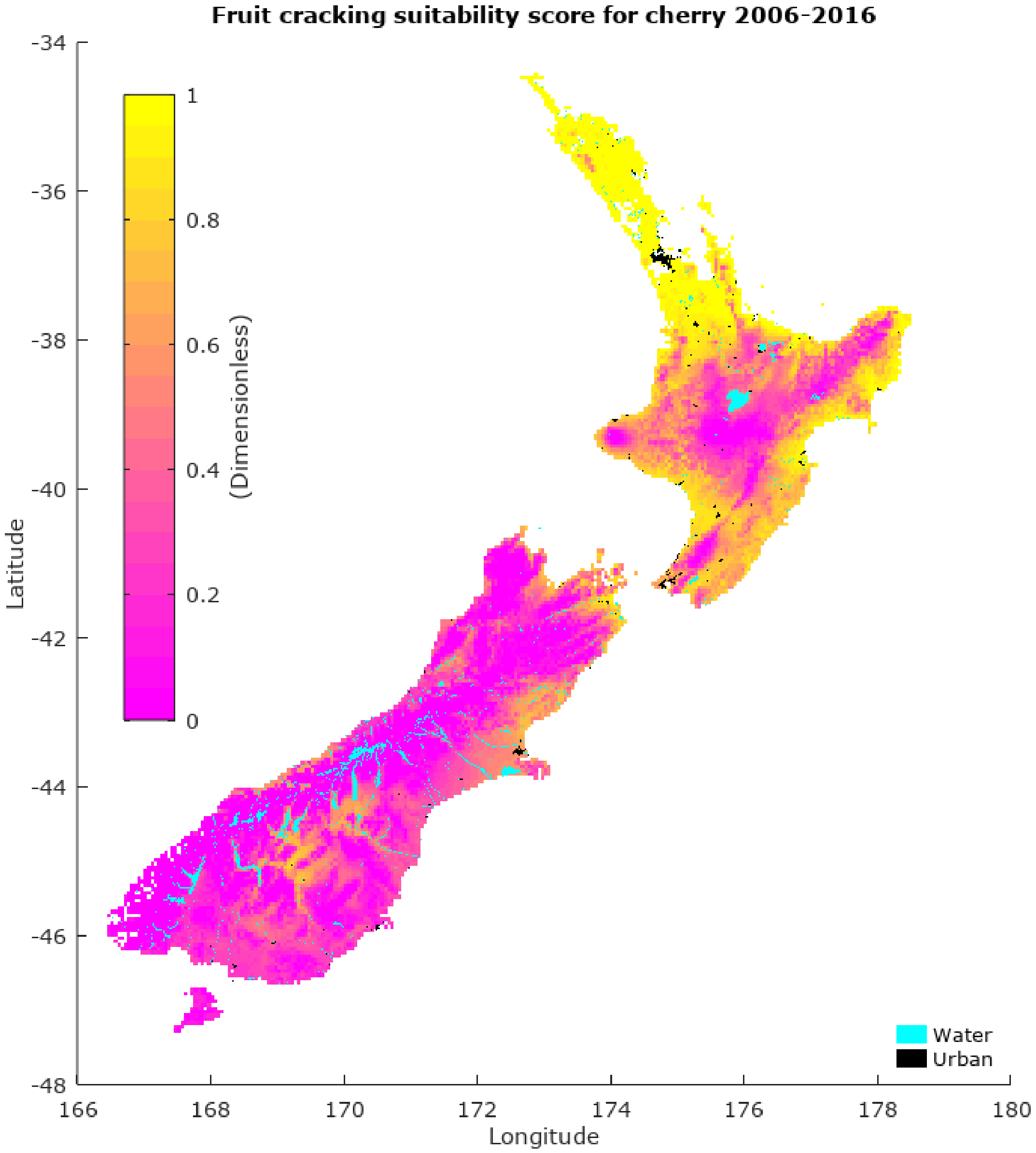

Figure 51. Cherry: fruit crack suitability score for locations across the country. Calculations used Virtual Climate Station Network (VCSN) data.

3.6.4 Wine grape: heat stress

Temperatures greater than 35°C in either the growing season or the maturation period negatively affect wine-grape production by inhibiting photosynthesis and reducing colour development and anthocyanin production (Jones 2015). Grapevine susceptibility to yield and quality losses from extreme heat vary according to development stage, with heat stress at the flowering stage potentially reducing fruit set, while berries may shrivel or get sunburnt (Hayman et al. 2012). Temperature treatments of 25, 35 and 40°C during bloom set resulted in, respectively, 83, 85 and 54% fruit set and berry weights of 1.10, 1.03 and 0.99 g in Pinot noir (Kliewer 1977).

Maturation may benefit from a few days of temperatures over 30°C, but prolonged periods can induce heat stress, premature veraison, reduce flavour and lead to loss of berries (Jones 2015). Excessive temperatures inhibit berry growth, delay sugar accumulation, impede fruit colouration, cause fruit to shrivel and may cause abnormal pigmentation of white fruit (Hashim-Buckey 2006). However, during Australian heat waves with air and canopy temperatures exceeding 40°C for 2 weeks, yield was not significantly affected by high temperatures, although berry damage reduced bunch quality and reduced wine quality (Greer & Weedon 2013).

The effect of heat waves (five consecutive maximum daily temperatures >35°C or three consecutive maximum daily temperatures >40°C) varies with location, vineyard management and vine acclimatisation (Hayman et al. 2012). Losses resulting from heatwaves that were reported by growers in different regions of Australia ranged from 0 to 48% (Webb et al. 2009). The nature of the information provided in that reference does not specify an obvious relationship between daily temperature profiles and loss.

Thus we have developed a sigmoid function to express a decrease in yield with maximum temperature for each day of the growing season (Figure 52); this gives a yield reduction of 1% for five non-consecutive days of temperature highs of 30°C and a yield reduction of 7% for three non-consecutive days of temperature highs of 40°C.

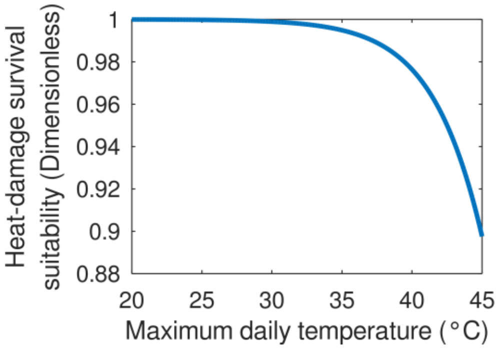

Figure 52. Fraction of berries surviving heat damage as a function of maximum daily temperature.

Maps of heat stress averaged over the 2006–16 growing seasons are shown for Pinot noir and Sauvignon blanc in Figure 53, indicating that heat stress is unlikely to be an issue anywhere in New Zealand, which is in line with experience in known growing areas.

The loss function in Figure 52 may seem mild in relation to the upper range of the reported losses discussed above. We have, however, sought to represent average losses. Additionally, since losses from day-to-day are accumulated, losses over a growing season could potentially be significant in warmer climates.

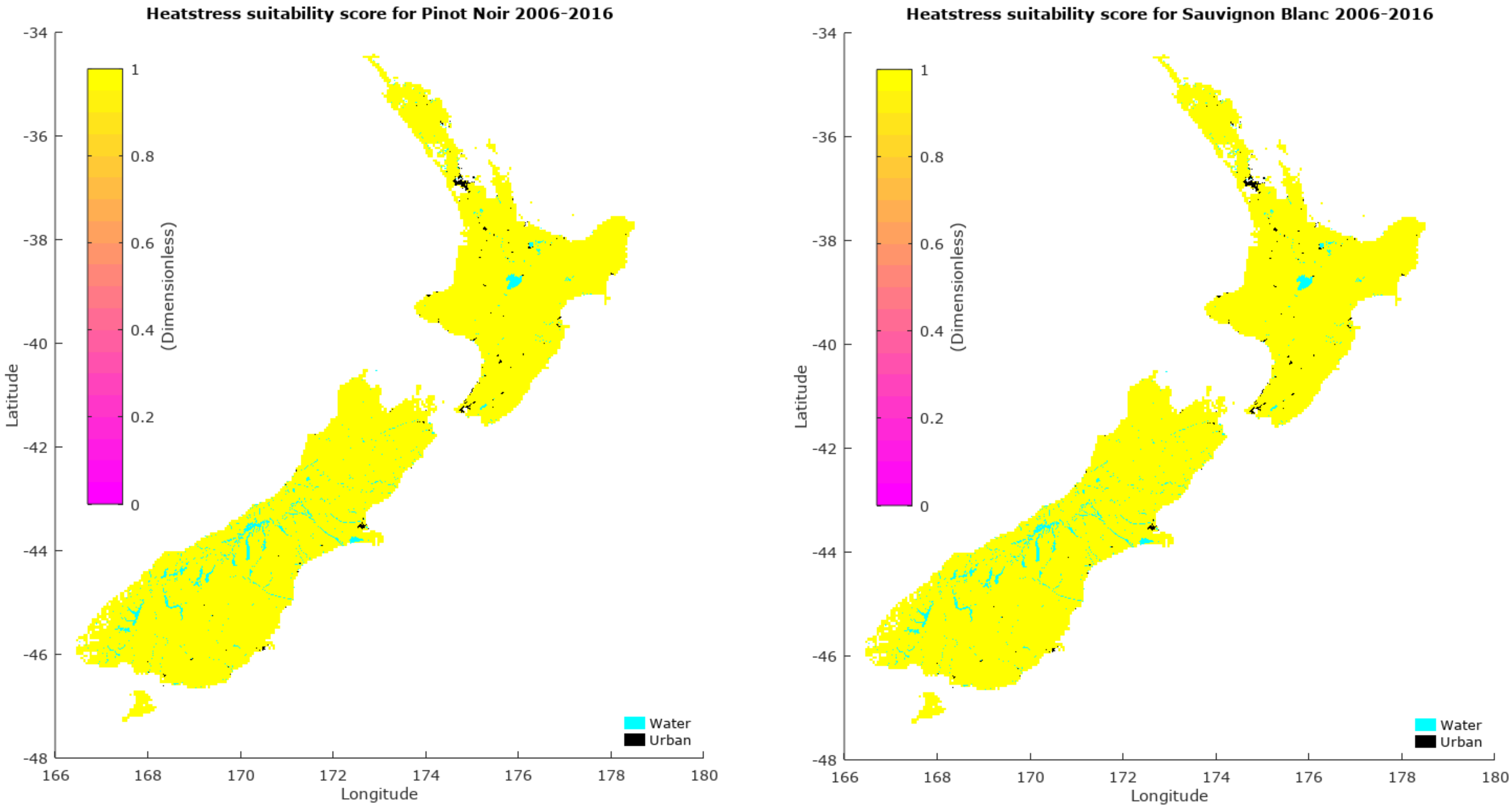

Figure 53. Heat stress suitability scores for Pinot noir (left) and Sauvignon blanc (right). Calculations used Virtual Climate Station Network (VCSN) data.

3.7 Disease risk

At the time of developing the project proposal, it was planned to deal with the risk of pest and diseases in a qualitative manner because of the complexity of the interactions between pathogens, crops and environment. However, during our industry and expert consultations the absence of an assessment of this risk was a recurring topic. Thus we developed a simple mathematical model to evaluate a general, broad-brush risk of pest and diseases of perennial crops under projected climate change scenarios in different geographical locations of New Zealand.

Velásquez et al. (2018) summarised major causes of concern for plant diseases in the context of climate change: incidence of plant pathogen overwintering, emergence of new pathogenic strains and rise of aggressive plant disease vectors. Different plant pests and diseases have different optimal environmental conditions and respond differently to variations in atmospheric CO_2 concentrations, temperature and water availability, which are the environmental factors most likely affected by climate change. The general understanding how crops, pests and diseases interact with climate change is still relatively poor (DeLucia et al. 2012; Juroszek & von Tiedemann 2015). Climate simultaneously affects plant immune response, pathogen virulence and disease development and influences all life stages of crops and pathogens. Tissue damage from hail or storms offers increased opportunity for microbial attack, thus the projected increase in intensity and frequency of storm events would be expected to increase the risk of crop infection. Additionally, climate change occurs on a scale much slower than the evolutionary speed of microbial life, allowing existing pathogens to adapt to environmental changes. A warming climate could speed up pathogen life cycles and also allow tropical pathogens to become a threat in New Zealand. Thus, our current understanding of phytopathology might no longer be valid under changing climates (Nick Waipara, pers. comm., 13 July 2019).

A number of diseases are common to several crops. For example, grapevines and fruit trees including avocado and cherry can be affected by white root rot, which is caused by *Rosellinia necatrix*, a fungus that has optimal growth at 22–24°C, does not grow below 5°C or above 32°C, and is favoured by moderate soil moisture levels and aerobic conditions (Santomauro & Faretra 2002; Pérez-Jiménez 2006). Phytophthora root rot, which can also cause canker in the lower trunk is a threat to avocado (Everett 2002; Pérez-Jiménez 2008), blueberry (Silva et al. 1999), cherry (Blodgett et al. 1990) and grapevines (Latorre et al. 2015). Botryosphaeria dieback causes branch canker and dieback in avocado (Pérez-Jiménez 2008), blueberry (Sammonds et al. 2009) and grapevines (Mundy & Manning 2010).

Additionally, avocado is affected by pythium root rot that causes necrosis of feeder roots, while stem-end rot and anthracnose are post-harvest diseases that damage fruit, with the latter also affecting leaves (Pérez-Jiménez 2008), with the latter two diseases, such as botryosphaeria dieback, being significant in New Zealand (Everett 2002). Cercospora (black spot) and scab both affect leaves, stems and fruit in avocado (Pérez-Jiménez 2008), but have not been recorded in New Zealand (Everett & Siebert 2018). Two other avocado diseases currently not in New Zealand are laurel wilt, which causes wilting of terminal leaves, defoliation and eventual death of the tree over a period of weeks to several months, and *Avocado sunblotch viroid* (ASBVd), which renders fruit unsaleable by causing skin distortions and chlorotic patches, as well as similarly affecting leaves and shoots (Everett & Siebert 2018). The ASBVd could readily become established in New Zealand, and laurel wilt could become a threat if New Zealand becomes sufficiently warm under climate change (Everett & Siebert 2018).

Blueberry plants are also susceptible to phomopsis twig blight or stem canker. They can suffer from a range of fungal leaf spots, which are generally minor diseases but some fungi can cause severe dieback of young stems. Further, blueberry is susceptible to a range of viruses, which are insect vectored rather than associated with climate (Fulcher et al. 2015).

In addition *to Rosellinia necatrix*, *Armillaria mellea* can cause root rot in cherry and cause significant damage in orchards (Santomauro & Faretra 2002). In cherry, the fungus *Blumeriella jaapii* causes cherry leaf spot, which under humid conditions, can lead to severe defoliation later in the growing season (Holb et al. 2010). Brown rot blossom blight caused by *Monilinia* spp., which attacks cherry, is favoured by the presence of moisture and temperatures in the 4 to 30°C range with an optimal temperature of 25°C (Holb 2008). Post-harvest loss in cherry can be caused by a number of different fungi, including *Botrytis* (Aminifard & Mohammadi 2013).

Wine grape is at risk from a number of diseases in addition to those discussed above. There is economic risk from fungal pathogens such as *Botrytis,* which causes significant damage to grapes in New Zealand and international vineyards (Elmer & Reglinski 2006). Grapevine trunk diseases include esca, which is associated with a range of fungi, eutypa dieback and petri disease (Mundy & Manning 2010). Surveys at a global level, indicated that downy mildew and powdery mildew were regarded as the most damaging diseases, ahead of botrytis (Bois et al. 2017).

3.7.1 Modelling approach

Different plant pests and diseases vary in their optimal environmental requirements, and there is limited understanding on how they will respond to variations in environmental factors such as atmospheric CO_2 concentrations, temperature and water availability caused by climate change (DeLucia et al. 2012; Juroszek & von Tiedemann 2015). The range of current and potential diseases, and the complexity of their interaction with environmental factors precludes modelling of individual pathogens and diseases in a project of this nature, and this topic is better handled via qualitative discussion (Hall et al. 2018). Thus here the disease modelling has been pitched at a broad-brush approach.

Nevertheless, since industry feedback was that disease is a major consideration, we developed a general mathematical model and suitability score for disease risk. This does not include the risk of root diseases, which is reflected in consideration of soil properties.

In addition to this general model, since the wine industry expressed a strong desire for botrytis risk to be modelled (Hall et al. 2018), we developed an additional botrytis risk suitability score specifically for grape.

3.7.2 General disease risk model

Moisture availability is a common factor for many trunk diseases and botryosphaeria dieback infections can occur in the temperature range 15 to 26°C with an optimal infection range of 23 to 26°C (Mundy & Manning 2010). Humidity has a significant role in grapevine infection by powdery mildew, with an optimum RH of 85% and an infection range of 39 to 98% in the optimal temperature band 23 to 27°C (Carroll & Wilcox 2003). Kadam et al. (2014) stated that downy mildew is favoured by temperatures of 10 to 23°C or 23 to 27°C if RH is greater than 80%. However, Williams et al. (2007) found that although downy mildew zoospores germinated at temperatures from 5 to 30°C, infection occurred mainly in the range of 10 to 25°C, but not at 30°C or higher and rarely at 5°C, and that optimal infection occurred at 20°C in a dark environment. In avocado, since stem-end rot can be caused by diverse organisms (Pérez-Jiménez 2008), the conditions that favour it vary with the causative pathogen (Everett 2002). However, other avocado diseases such as anthracnose, cercospora (black spot) and scab are favoured by high humidity or rainfall (Pérez-Jiménez 2008).

These issues preclude a detailed projection of how climate change might affect disease risk at the national level, thus we took a broad-brush approach using moisture and temperature as input variables. RH was used as a proxy for moisture availability, since some studies have found it a more reliable indicator than rainfall (Creasy 1980). Wilks & Shen (1991) used a risk threshold for RH of ≥90%, while Beresford et al. (2016) used a value of 81%. Following our sliding-scale approach, we developed a sigmoidal curve to represent relative microbial threat as a function of RH (assuming temperature is optimal for microbial attack), with values of 0.5 and 0.99 at RHs of 80 and 95%, respectively.

We note that some plant-pathogen interactions are enhanced by low moisture conditions, but these are exceptions (Velásquez et al. 2018). Instead, most promulgate at high moisture conditions. Different pathogens also have different optimal growing temperatures, thus there will be a microbial threat over a band of temperatures (Nick Waipara, pers. comm., 13 July 2019). Therefore, we used a temperature risk curve (assuming RH is optimal for microbial attack) with the value 1.0 for the range 15 to 25°C, and then falling off to zero as temperatures deviated from that range.

Multiplying the RH risk curve and the temperature risk curve gives disease risk as a function of RH and temperature. The overall disease suitability score is the inverse of the disease risk, and was obtained by subtracting disease risk from 1.0. Thus a disease risk close to zero corresponds to a disease suitability score close to 1, and a disease risk close to 1.0 corresponds to disease suitability score close to 0 (Figure 54).

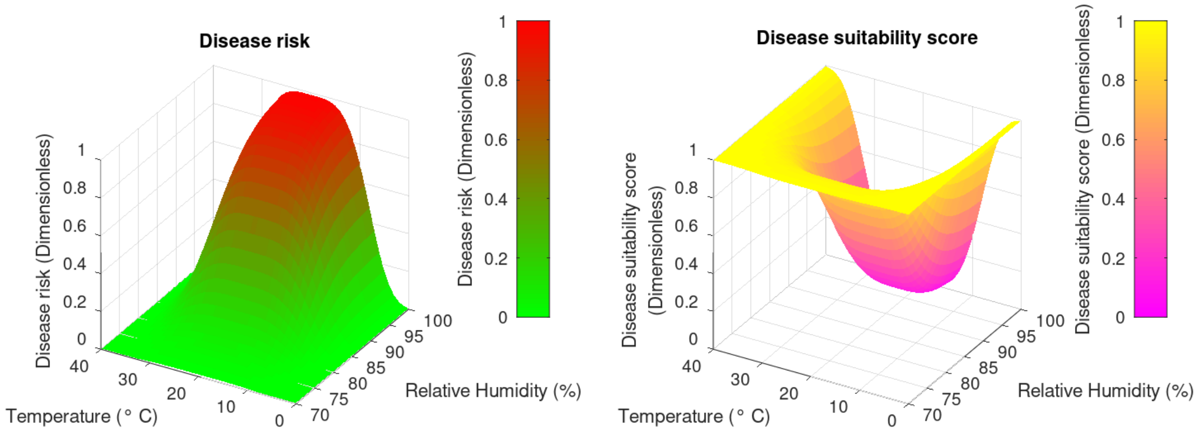

Figure 54. Disease risk (left) and disease suitability score (right) as functions of relative humidity and temperature. A higher disease suitability score (yellow) corresponds to less risk of disease (green) and is more desirable, whereas a lower score (magenta) indicates greater disease risk (red) and is less desirable. The highest disease risk is identified as high relative humidity (95–100%) at moderate temperatures (15–25°C), and this receives a low disease suitability score close to 0. Calculations used Virtual Climate Station Network (VCSN) data.

Disease suitability scores are shown for locations across the country in Figure 55, indicating that generally there seems to be some disease risk in any growing region for any crop, and that the risk increases with warmer temperatures in the north and more humid conditions in the west. This follows the general pattern experienced in the different growing regions.

In our earlier progress report on apple and kiwifruit we had made this decision to exclude the general disease suitability score from our overall climate suitability model, because the RCP vapour pressure data were not bias adjusted and were required to calculate RH. Subsequently, in anticipation that this issue would be rectified, we included the general disease suitability score in climate suitability scores for avocado, blueberry, cherry and wine grape.

Our view now, despite bias adjused future RH data becoming available (see Section 6), is that a generic disease risk model is useful for indicative purposes, but has no real predictive power for the risk of individual pathogens, given the disparate nature of potential pathogens with contrasting environmental requirements. Feedback from industry workshops did not support the inclusion of the generic disease suitability score for projecting the impact of climate change on future land suitability for cultivation of crops. Thus we exclude the generic disease risk from climate suitability calculations, although we include botrytis risk as a factor in climate suitability for grape.

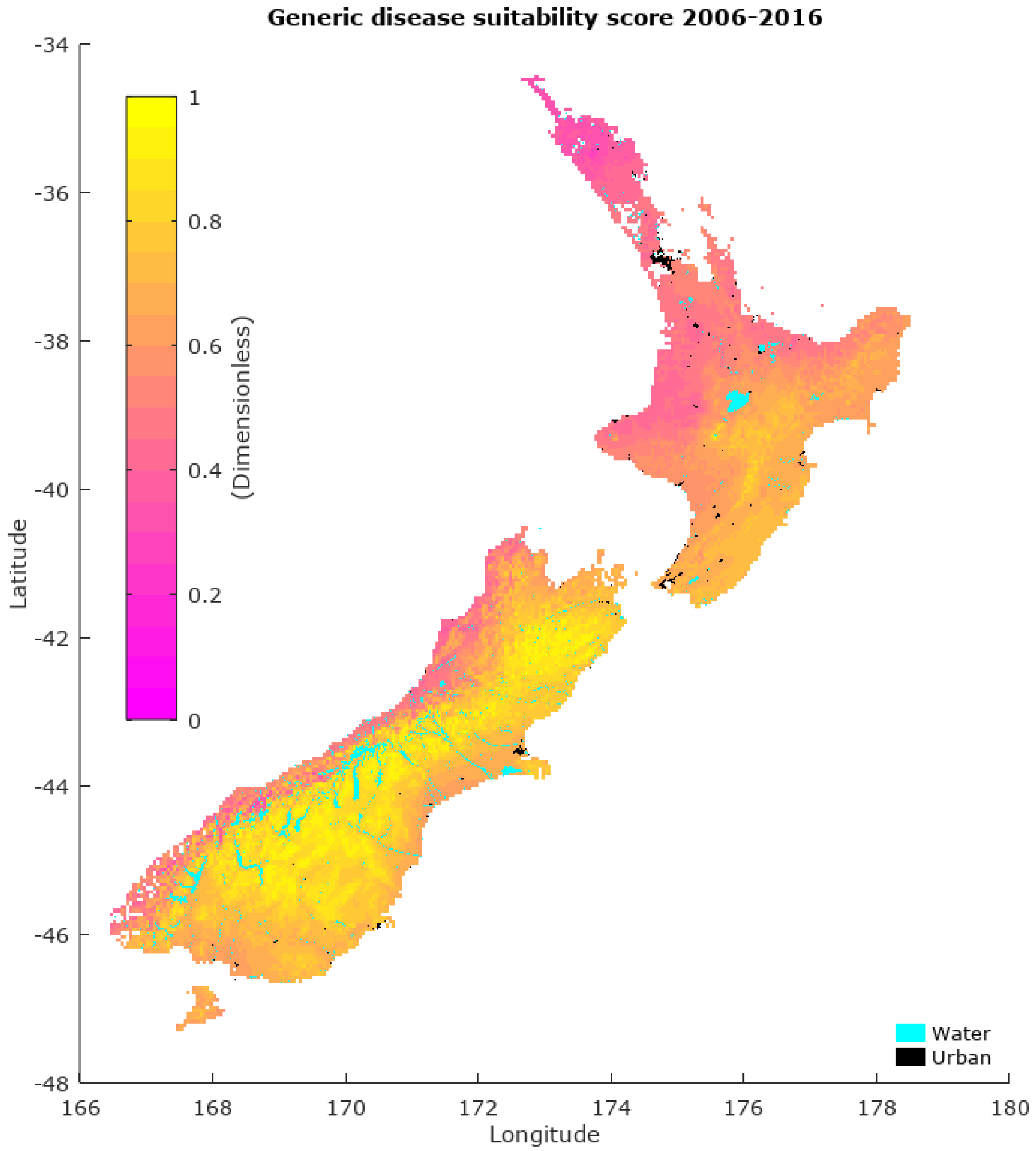

Figure 55. Generic disease suitability score for locations across the country. Calculations used Virtual Climate Station Network (VCSN) data.

3.7.3 Botrytis risk in wine grape

Trials showed that while late season rainfall and mean daily rainfall were strongly correlated with botrytis severity at harvest, they were poor predictors of botrytis when used in models, and more reliable prediction is obtained by considering duration of surface wetness and temperature during wetness (Edwards et al. 2009). In a factorial trial, Thomas et al. (1988) investigated botrytis under air speeds from 0 to 2 km/h, RH of 69 to 94% and temperatures from 16 to 30°C, and found that botrytis development occurred if the evaporative potential of the air was below a temperature-dependent threshold, with air speed and RH having a greater effect on evaporative potential than temperature.

Broome et al. (1995) performed trials to develop an infection model for botrytis development based on surface-wetness duration and temperature, finding that risk peaked at temperatures around 20°C and increased with duration of wetness. Hill et al. (2018) investigated a number of climatic factors as predictors of botrytis and found that combining RH and wetness duration provided the most consistent predictions of botrytis outbreaks, while combining temperature and wetness duration provided good but less consistent prediction. Estimation of the duration of surface wetness of grape berries is not feasible, thus we used temperature together with RH as a proxy for moisture availability.

For botrytis, we investigated using the inverse of the Bacchus model (see Kim et al. (2007) and Hill et al. (2018)) for calculating the botrytis threat with hourly temperature. This equation had been formulated to give an infection risk for each hour with surface wetness. We adapted this to our purpose by scaling it to have a maximum value of 1.0, and interpreting it in the context of relative daily threat calculated from average daily temperatures. Ciliberti et al. (2015) found that botrytis incidence was 30 and 15 times higher at 100 and 90% RH, respectively, than at 80%, with no incidence of botrytis at 65% RH. Thus we used a sigmoidal curve to represent relative botrytis threat as a function of RH, with values of 1.0, 0.5 and 0.03 at RHs of 100%, 90% and 80%, respectively.

However, this approach using temperature and humidity did not yield satisfactory results for predicting the relative risk of botrytis for different locations across the country, based on expert knowledge of wine-growing regions in New Zealand. This is likely because of the limitations of using a daily (9 a.m.) RH value and daily mean temperature in the absence of hourly RH and temperature data. Thus we used total rainfall for March and April as a predictor instead, developing a sigmoidal curve with values of 0.95, 0.5 and 0.05 for March–April rainfalls of 90, 160 and 250 mm, respectively, based on expert parameterisation (Figure 56).

This curve was applied to March–April rainfall data and mapped across the country (Figure 57), indicating botrytis risk is very low in the wine-growing region of Central Otago and low to moderate in the wine-growing regions of Marlborough, Hawke's Bay and Martinborough, which is in line with our knowledge and expectations of the different wine-growing regions. In Marlborough, the upper Southern Valleys and the Blenheim area of the Wairau Valley show the lowest risk, although the Awatere Valley may be the drier.

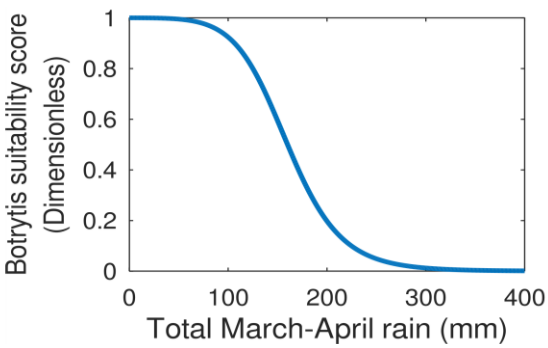

Figure 56. Grape: botrytis suitability score as a function of total rain during March and April.

Of course the production of botrytised dessert wines relies on the prevalence of 'noble rot', and thus this suitability score function would be inverted to represent suitability for such purposes.

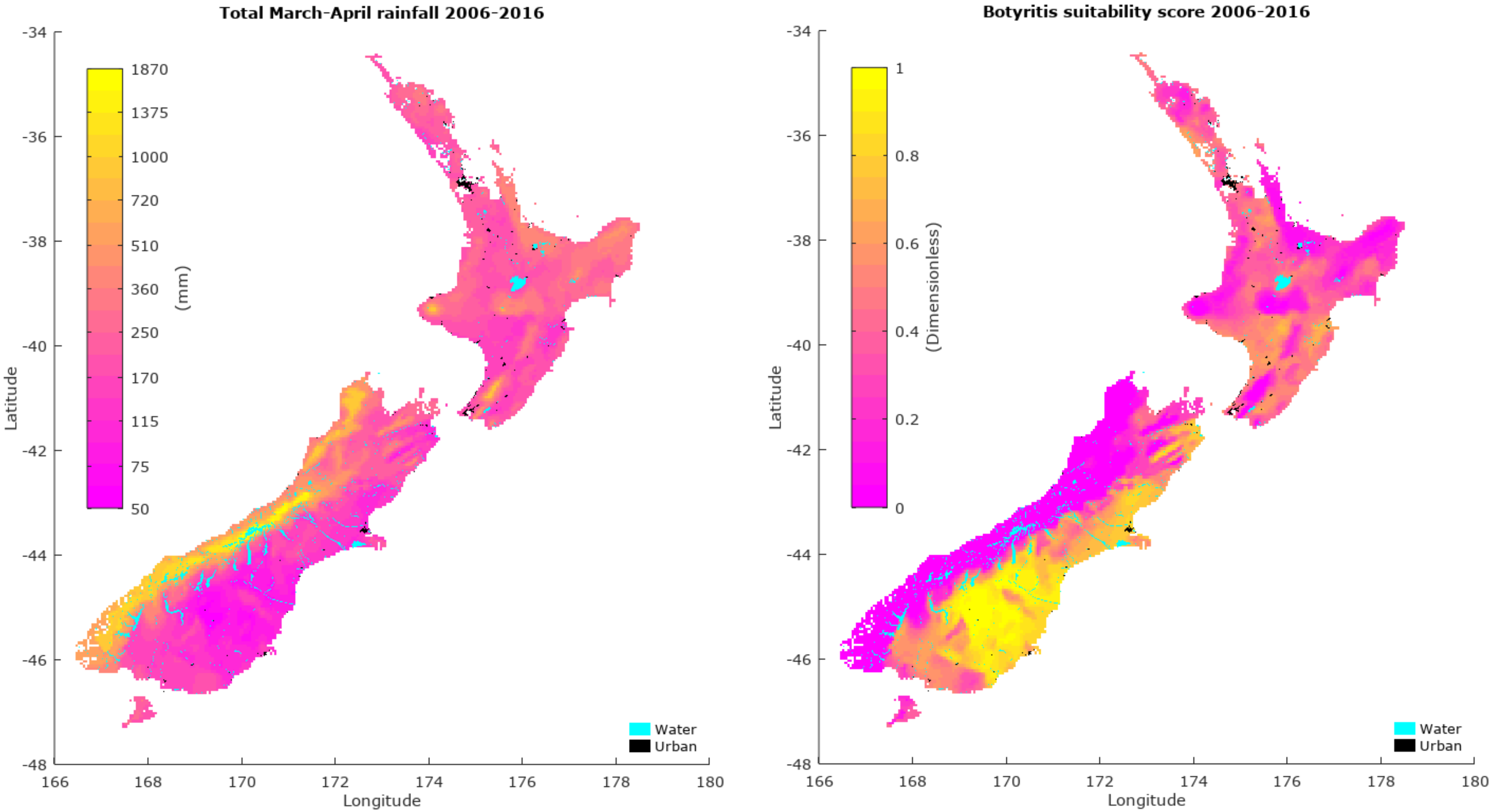

Figure 57. Wine grape: Total rainfall for March and April period, averaged from 2006-2016 (left) and botrytis suitability scores based on rainfall for different locations across the country. A higher score indicates a lower botrytis risk and a more suitable location for growing wine grapes. Calculations used Virtual Climate Station Network (VCSN) data.

3.8 Combined climate-related suitability criteria

The development of continuous suitability scores, in preference to binary rules, offers the opportunity to combine assessments for different criteria in a way that takes into account the relative importance of each criteria. For this purpose we chose to take weighted geometric means of individual scores as an appropriate approach to calculating a combined score. The higher the weight used for a criterion, the greater the influence of its suitability score on the combined score. Conversely, using a lower weight diminishes the influence of a suitability criterion, and a weight of zero removes it from the combined score altogether.

For each climate criterion, suitability scores were calculated for each year of the period 2006 to 2016 and the arithmetic mean taken to obtain an average suitability score for the period. When combining scores, we chose not to use these average suitability scores. Rather, we combined suitability criteria by combining their individual scores for each year by taking the weighted geometric means of those scores to provide an overall climate suitability score for that year. The yearly climate suitability scores were then averaged over a period of years using arithmetic means to provide a climate suitability score for the period.

By combining suitability criteria scores on a yearly basis, we obtain a better reflection of the production loss that could be incurred over a period, than by combining the average criteria scores for the period, since the latter approach will not distinguish between different criteria having poor suitability in the same years or different years. For example, if a location incurred heavy production losses due to severe frost in 2 out of 10 years, and heavy production losses due to poor winter chill in 2 out of 10 years, this could result in the number of poor production years ranging from 2 to 4 out of 10 depending on whether losses from the two criteria occurred in the same years or not.

The weights assigned to the different suitability criteria were assigned based on the opinion of horticultural experts and thus were subjective and reflective of varied experiences. The same criterion could be weighted significantly differently for different industries. For example, frost damage was considered a significant risk by some experts while others considered it minor risk that can be mitigated. Conversely while insufficient GDD accumulation cannot be mitigated, some experts considered it a minor risk while others considered it a significant risk.

3.8.1 Apple

For apple, we chose weights of 1.0 for the chill, GDD and fruit-size suitability scores, 2.0 for the frost suitability score and 0.5 for the sunburn suitability score. The frost suitability score was given a larger weight because of the expert view that it was the major risk to crop loss, while damage from sunburn was considered to be of minor importance. Lower GDD or chill could be mitigated to some extent by selecting cultivars that require less winter chill to produce satisfactory bud break and flower or fewer GDD to reach maturity, respectively. The resulting map is shown in Figure 58 and accords with the main apple growing regions of Hawke's Bay, Nelson and Central Otago, with apple cultivation also taking place in other areas that are indicated as suitable around the North Island and in Canterbury.

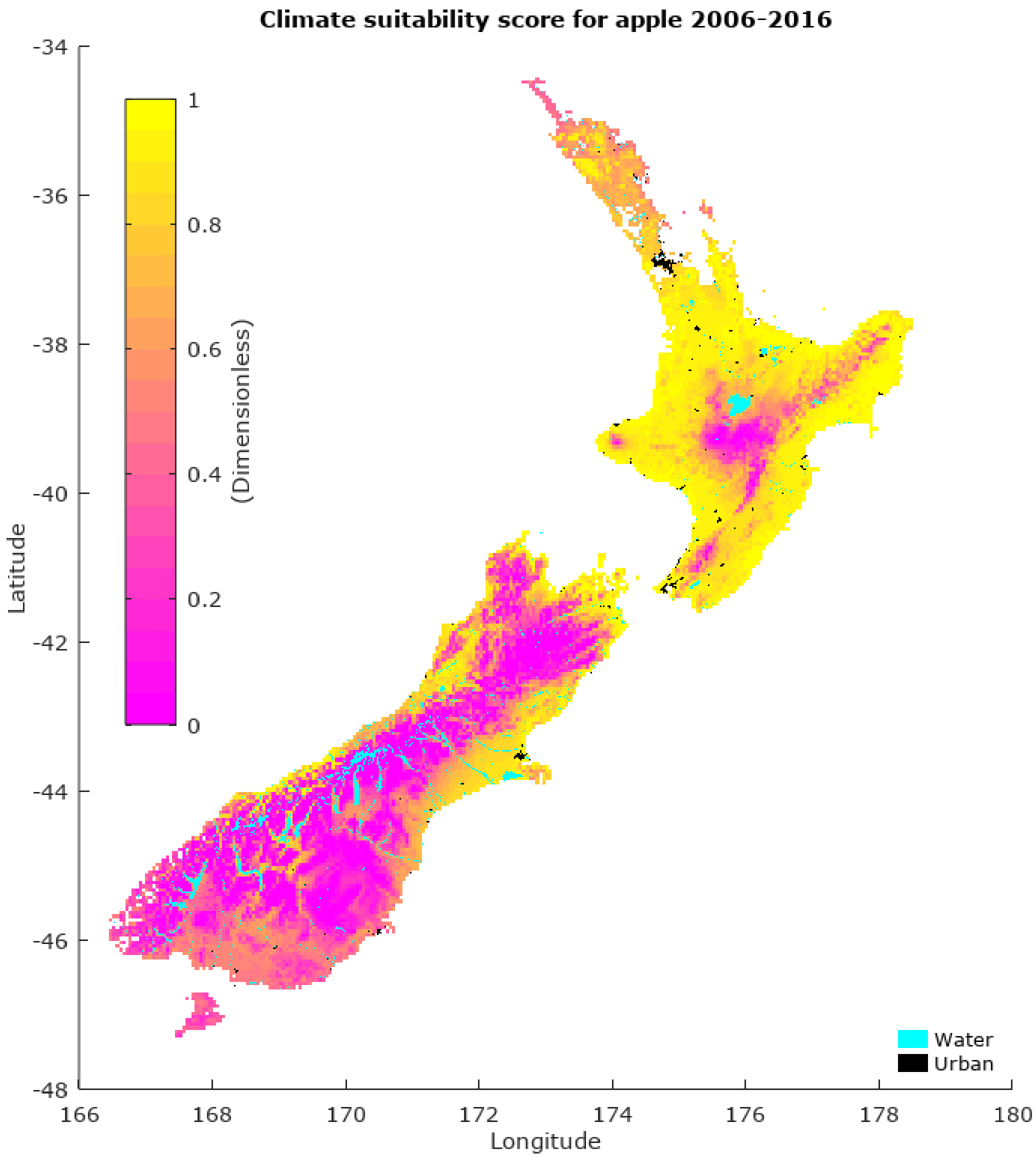

Figure 58. Climate suitability score map for apple. Calculations used Virtual Climate Station Network (VCSN) data.

3.8.2 Kiwifruit

For kiwifruit, we chose weights of 1.0 for the chill, GDD and frost suitability scores, and a weight of 2.0 for the cold-damage suitability score. The latter was given an increased weight because damage to canes could have long-term consequences for vine health. The resulting map is shown in Figure 59 and is in line with the kiwifruit-growing heartland of the Bay of Plenty and strong production in Northland, Gisborne, the Hawke's Bay and Nelson, although climate suitability may be a little less in Nelson than some might expect.

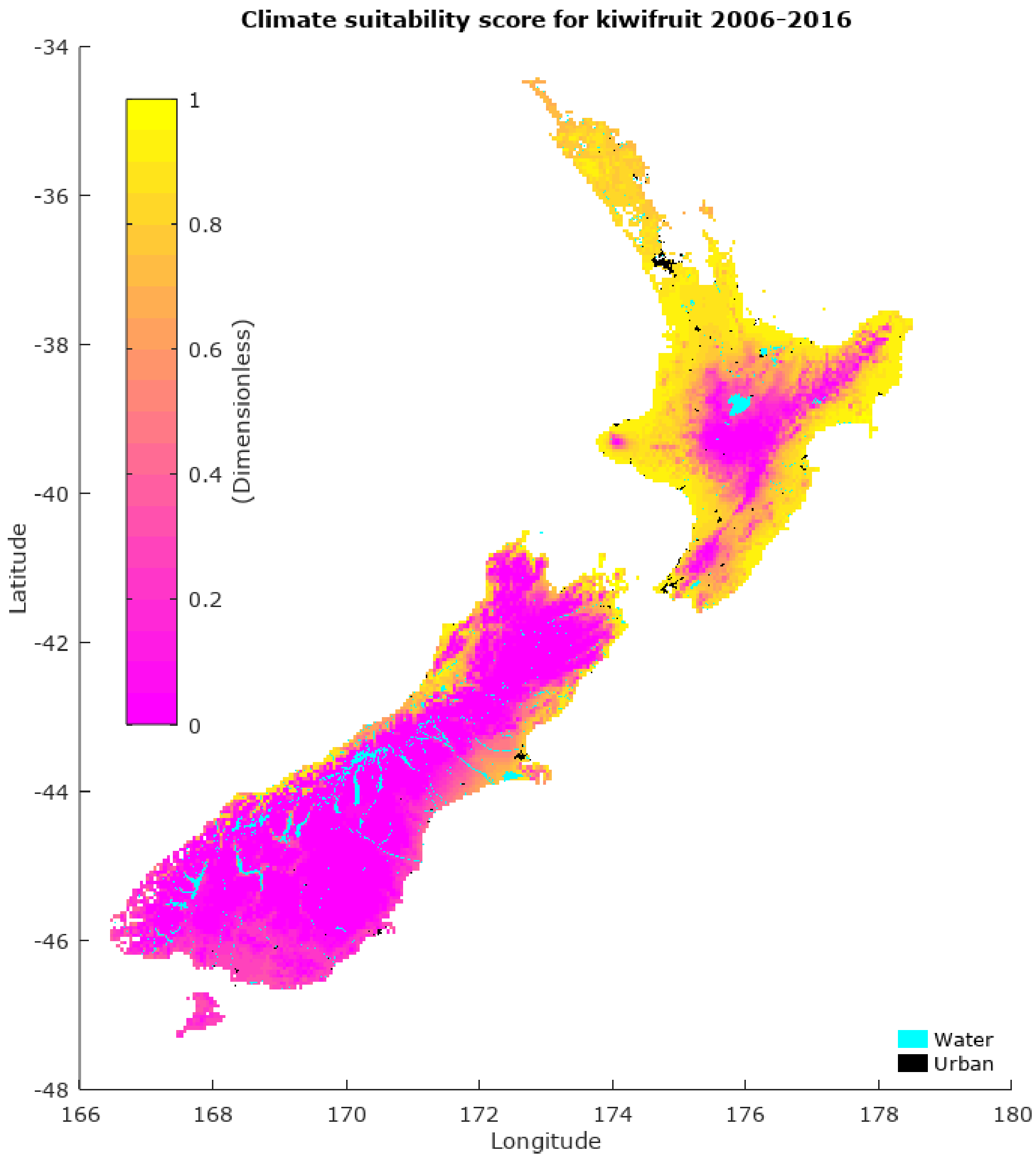

Figure 59. Climate suitability map for kiwifruit. Calculations used Virtual Climate Station Network (VCSN) data.

3.8.3 Avocado

A weighting of 3 was used for each of warmth and frost scores when taking the geometric mean (these were the only two climate-related suitability criteria for avocado). The resulting suitability map is shown in Figure 60. This strongly accords with Northland being the avocado-production heartland of Northland and strong production in some areas of the Bay of Plenty and Gisborne.

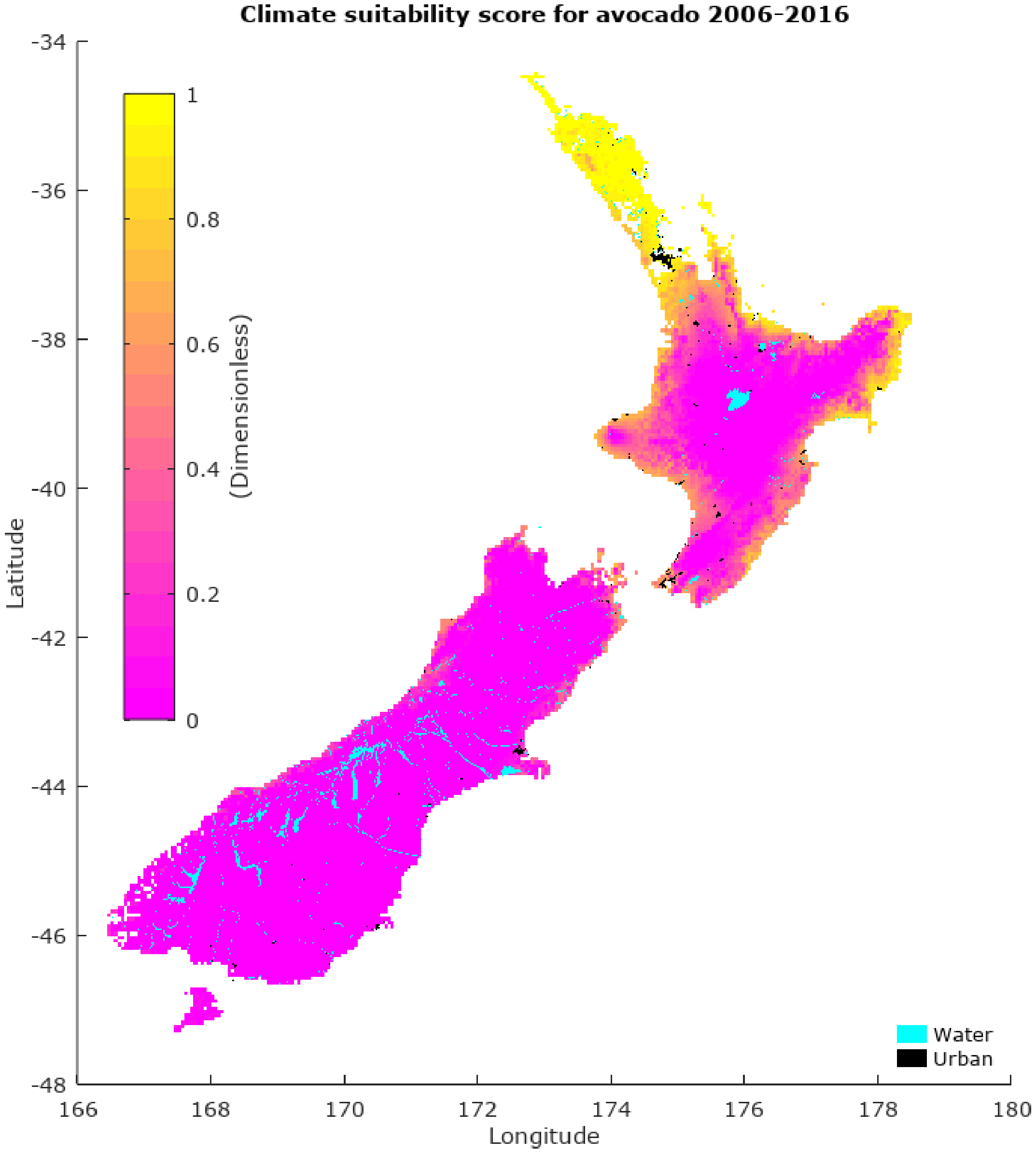

Figure 60. Avocado: map of overall climate suitability. Calculations used Virtual Climate Station Network (VCSN) data.

3.8.4 Blueberry

We chose weight of 2 for each chill, frost and GDD; the resultant map is shown in Figure 61. Although frost or GDD deficiency can be mitigated by a tunnel house, this mitigation would be expensive, hence the increased weight. Much of the North Island and large areas of Canterbury and the West Coast are indicated as having high suitability. The decreased suitability in Northland is associated with lower winter chill suitability, which could be mitigated by using low-chill cultivars. The Waikato and Bay of Plenty, which are significant blueberry growing regions, have areas of good to very high suitability.

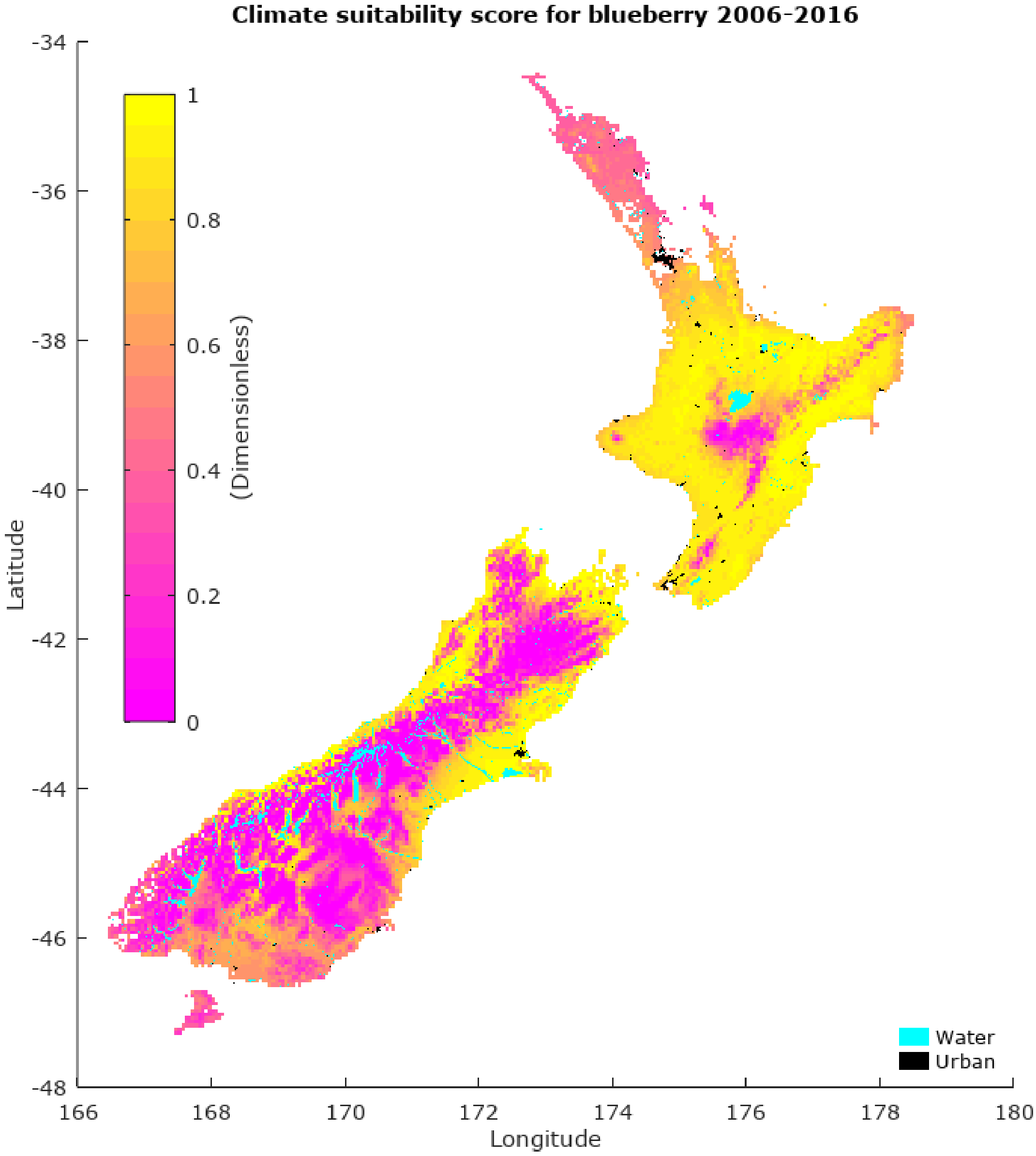

Figure 61. Blueberry: map of overall climate suitability score. Calculations used Virtual Climate Station Network (VCSN) data.

3.8.5 Cherry

We chose weights of 1 for the chill and frost suitability scores, and a weight of 2 for the GDD and fruit cracking suitability scores (Figure 62). Very few areas of good or higher suitability are indicated for cherry. However, areas of Central Otago, which represent the bulk of New Zealand's cherry industry, are indicated as having high suitability scores, with the Hawke's Bay, which has a smaller cherry footprint, having lower but still good suitability.

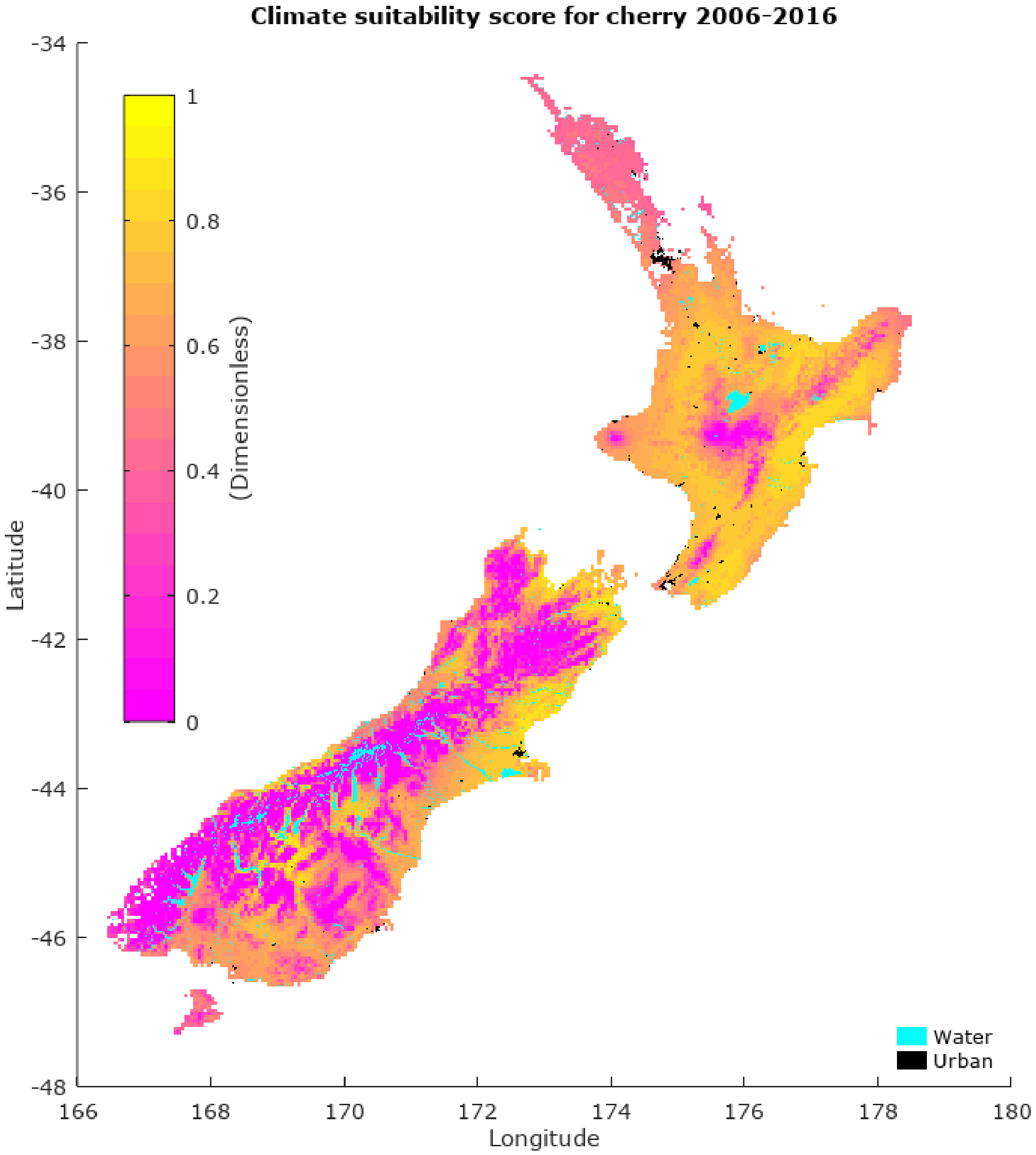

Figure 62. Cherry: overall climate suitability score. Calculations used Virtual Climate Station Network (VCSN) data.

3.8.6 Wine grape

Weights were 1 for frost and heat damage, 0.5 for winter chill, and 3 for GDD and botrytis risk (Figure 63). The footprint of suitable land shown in Figure 63 (left panel) for Pinot noir highlights North Canterbury, Central Otago, parts of Marlborough around the Wairau Valley and the Southern Valleys, parts of the Wairarapa, the Hawke's Bay and, to a lesser extent, Nelson, all of which are established Pinot noir regions. Additionally areas in the Manuwatu and Waikato are indicated has having moderate suitability. The map in Figure 63 (right panel) for Sauvignon blanc shows small suitability footprints in the Marlborough, North Canterbury, Nelson, Hawke's Bay and Wairarapa regions, which encompass the bulk of the Sauvignon blanc growing regions. The suitability footprint for Central Otago is very small compare with Pinot noir. The Manuwatu and Waikato are indicated as having pockets of land with moderate suitability.

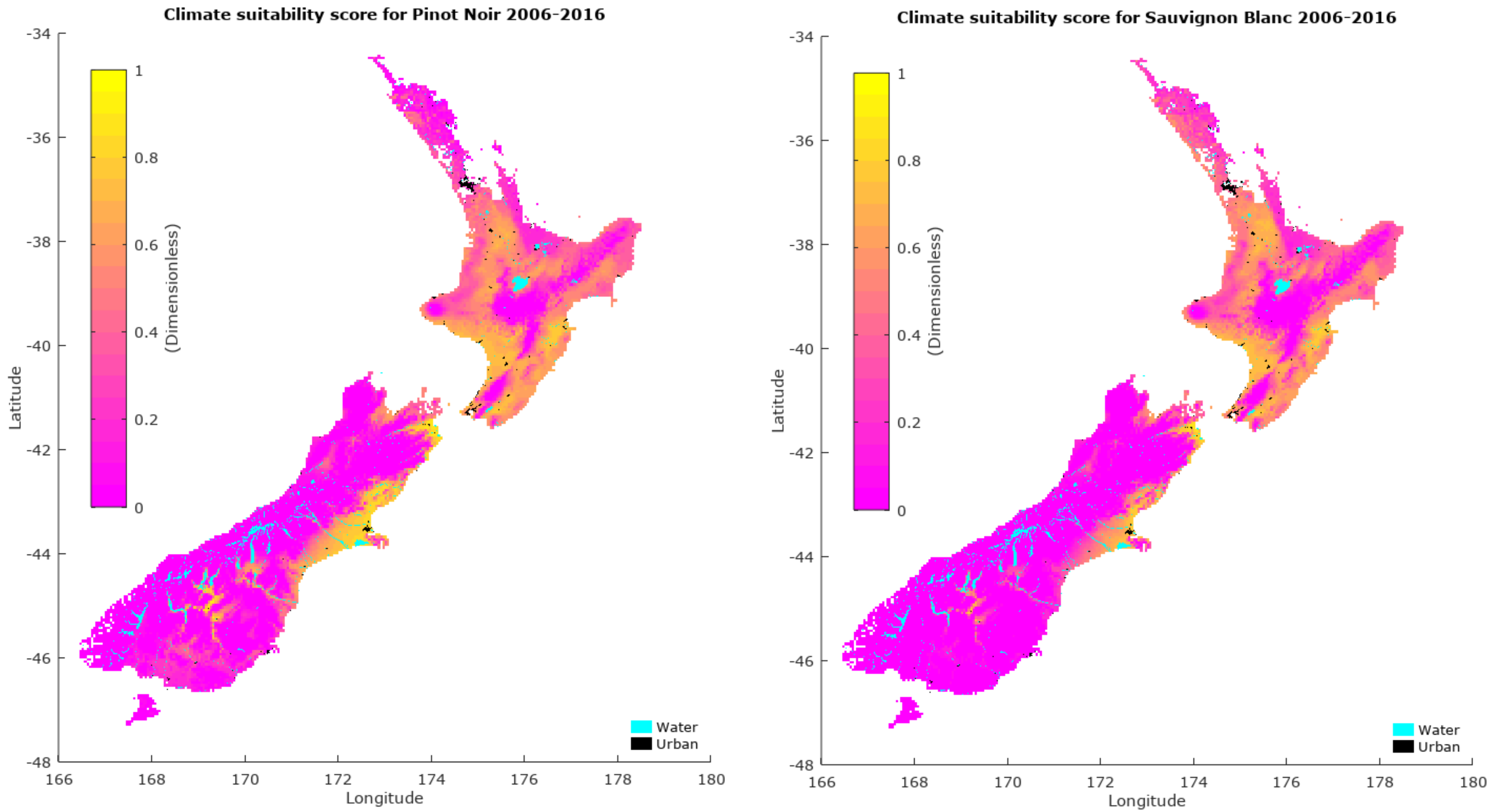

Figure 63. Grape: climate suitability for Pinot noir (left) and Sauvignon blanc (right) for locations across the country. Calculations used Virtual Climate Station Network (VCSN) data.

4 Soil/land-related suitability criteria

In our previous work (Vetharaniam et al. 2019; Vetharaniam et al. 2020b) we used the following four soil- and land-related criteria common all crops, although with different requirements for each crop:

1. Sufficient potential rooting depth (PRD)
2. Adequate drainage
3. Slope of the land not too steep
4. Appropriate land use capability (LUC) class.

   The first three of these had been identified by Hall et al. (2018) as important crop-growing factors, while we had identified the fourth as a useful indicator for the industry, during the ground-truthing process. In addition, we developed suitability scores for avocado and blueberry, corresponding to another soil-related criteria:

5. Soil pH (avocado and blueberry).

A further potential criterion for avocado is soil texture and structure. Ticho & Gefen (1965) considered a medium texture soil to be best suited for avocado. Dubrovina & Bautista (2014) further classified sandy loam, silty loam and loamy sand textures to be more suitable than other soil textures, and a fine to medium structure to be more suitable than other structures. However, McCarthy (2001) also identified a rich sandy loam as ideal, but noted that avocado can be grown successfully in a range of soils from light sands to well-drained clays providing there is suitable management, and good drainage and soil depth were far more important. Thus we have not included soil texture and structure in considerations.

We used extracted LRI data on PRD, drainage quality, slope and LUC to calculate suitability scores for the soil/land-related criteria for different geographical locations in New Zealand with a 1 x 1 km grid resolution. The locations of urban areas, quarries, rivers and lakes were indicated in the LRI data and these locations did not have soil data. Other areas lacked LUC or drainage information, and many of these were in conservation areas (identified in DOC Public Conservation Areas database).

4.1 Potential rooting depth

Information on potential rooting depth (PRD) was presented in terms of depth of topsoil to an impervious barrier (e.g. rock or tight clay). Values are mapped in Figure 64.

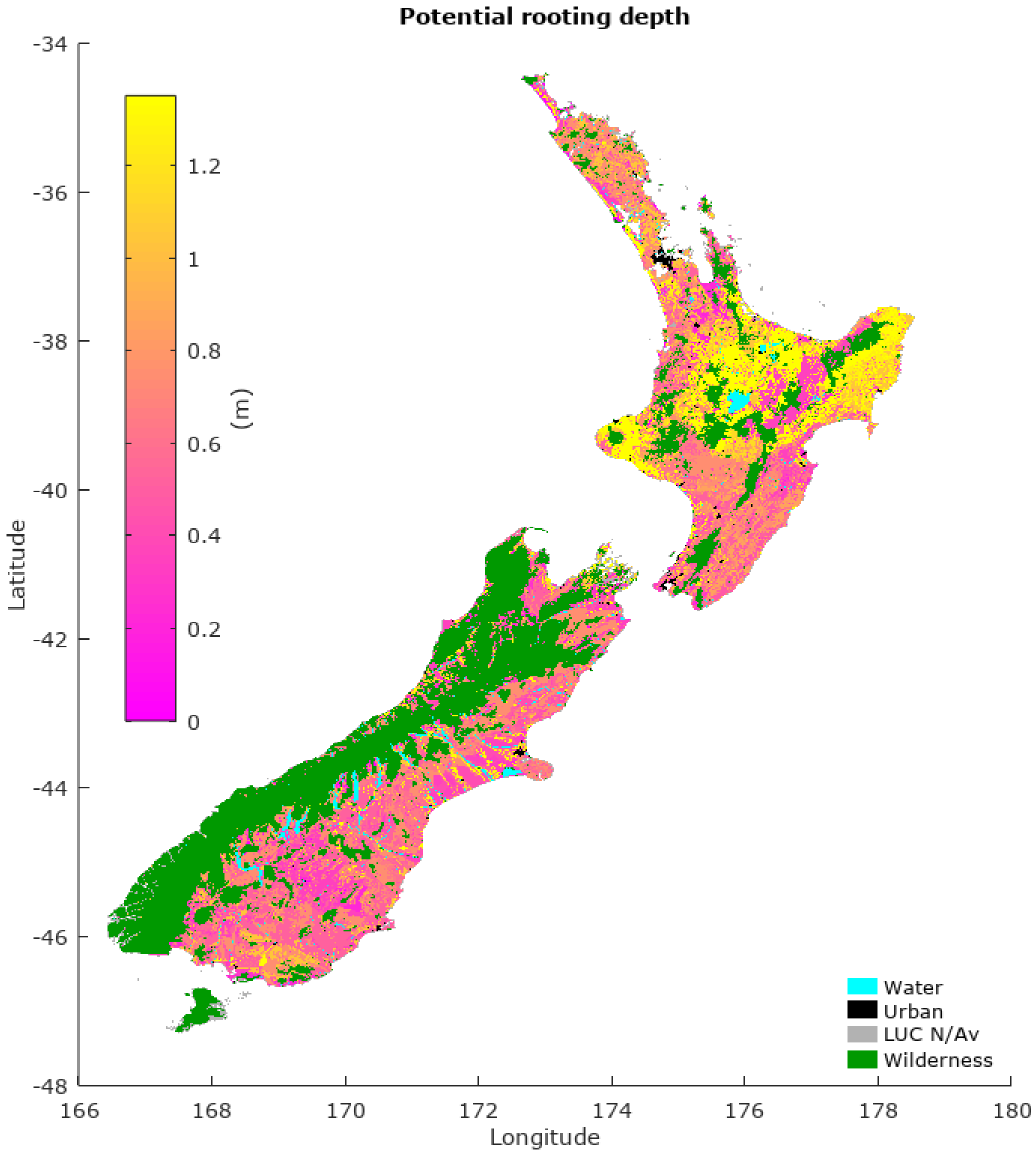

Figure 64. Depth of soil to an impermeable layer (potential rooting depth) in metres.

4.1.1 Apple and kiwifruit

Based on expert opinion, we chose a suitability curve to give values of 0.15, 0.5 and 0.8 for PRDs of 0.25, 0.45 and 0.65 m, respectively (Figure 65). This reflects that while a deeper soil is preferable, both apple trees and kiwifruit vines can perform well over a range of different soil depths, and that a shallow PRD can be mitigated, for example, by mounding or by irrigation. Corresponding potential rooting depth scores for apple and kiwifruit are mapped in Figure 66. This shows that the Hawke's

Bay, Nelson and especially Central Otago, all of which have strong apple industries, have large areas with low scores for rooting depth suitability, although they also contain some very high-suitability locations. The mottled appearance of some areas indicates a high variability in soil properties. Orchards in these locations may have required mitigation of shallow soils by, for example, mounding. For the main kiwifruit production area of Northland and strong production areas of Northland and Gisborne, rooting depth suitability scores are high. For the Hawke's Bay and Nelson, limitations and mitigation requirements will be the same as for apple in those regions.

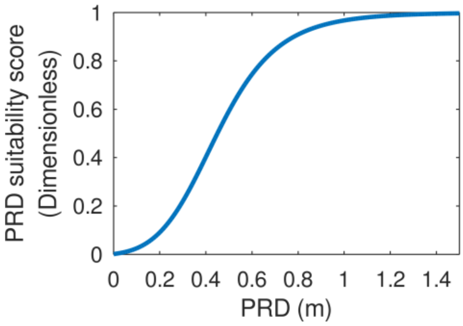

Figure 65. Rooting depth score vs potential rooting depth (PRD) for both apple and kiwifruit.

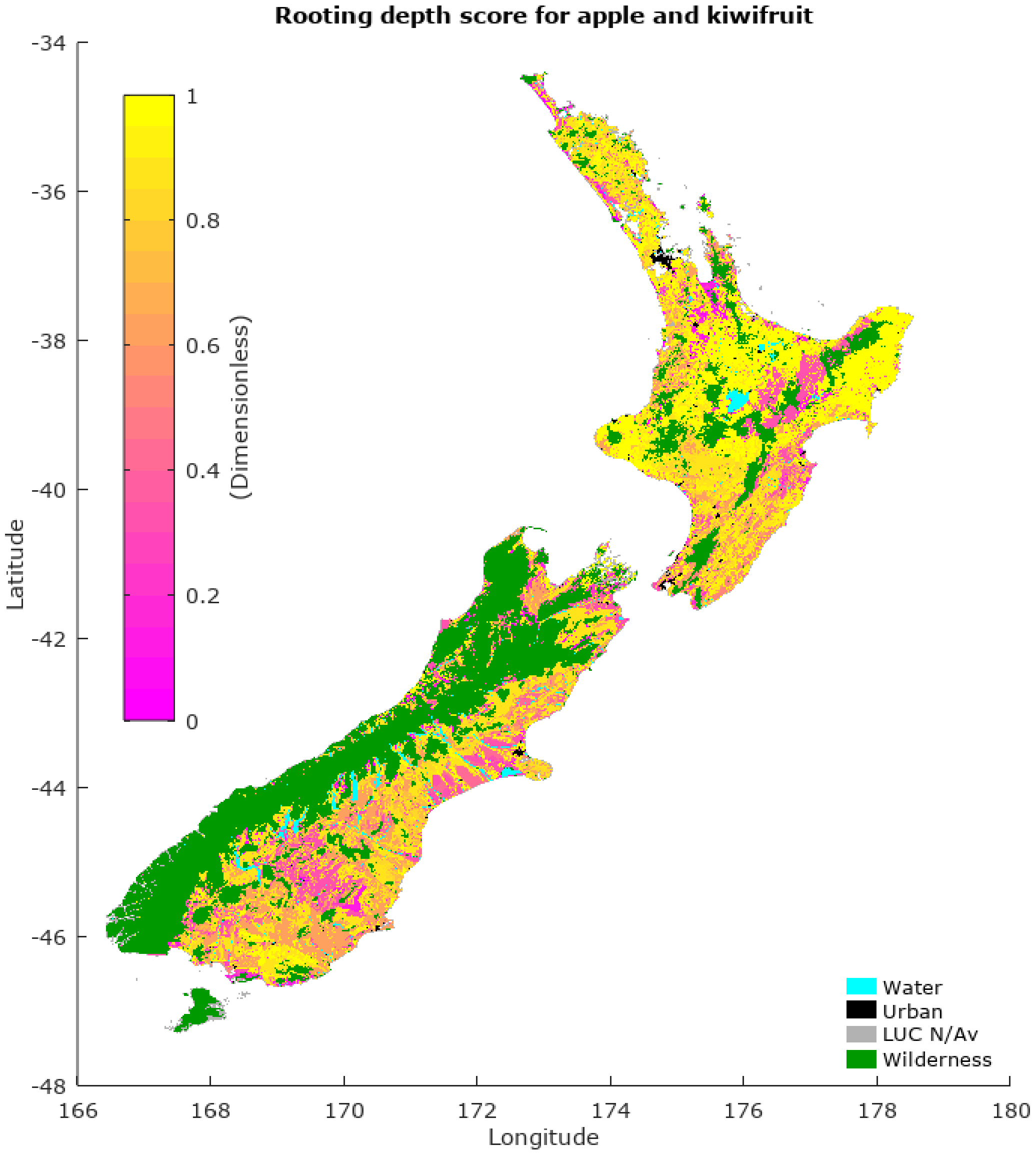

Figure 66. Apple and kiwifruit: Rooting depth suitability scores for locations across the country.

4.1.2 Avocado

Hall et al. (2018) considered PRD ≥0.9 m to be optimal, following Griffiths et al. (2003). McCarthy (2001) considered 1 m a minimum depth for good performance, with 2 m being preferable. Dubrovina & Bautista (2014) classified PRD greater than 1 m as highly suitable, 0.8–1 m as suitable, 0.5–0.8 m as low suitability and below 0.5 m as unsuitable. We chose a suitability score curve that gave values of 0.25, 0.5, 0.85 and 1 for PRDs of 0.5, 0.65, 1.0 and 2.0 m, respectively (Figure 67).

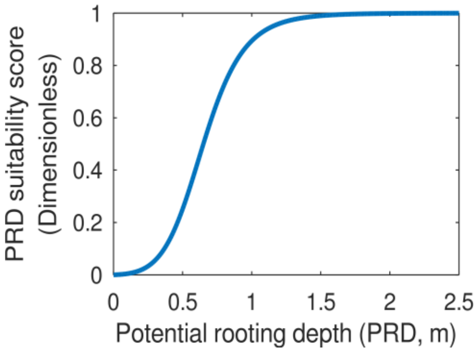

Figure 67. Avocado: rooting depth suitability score vs potential rooting depth.

Scores were calculated for each location (Figure 68), showing good PRD suitability in Gisborne and Bay of Plenty, and varied suitability in Northland, which might require mitigation, for example through irrigation.

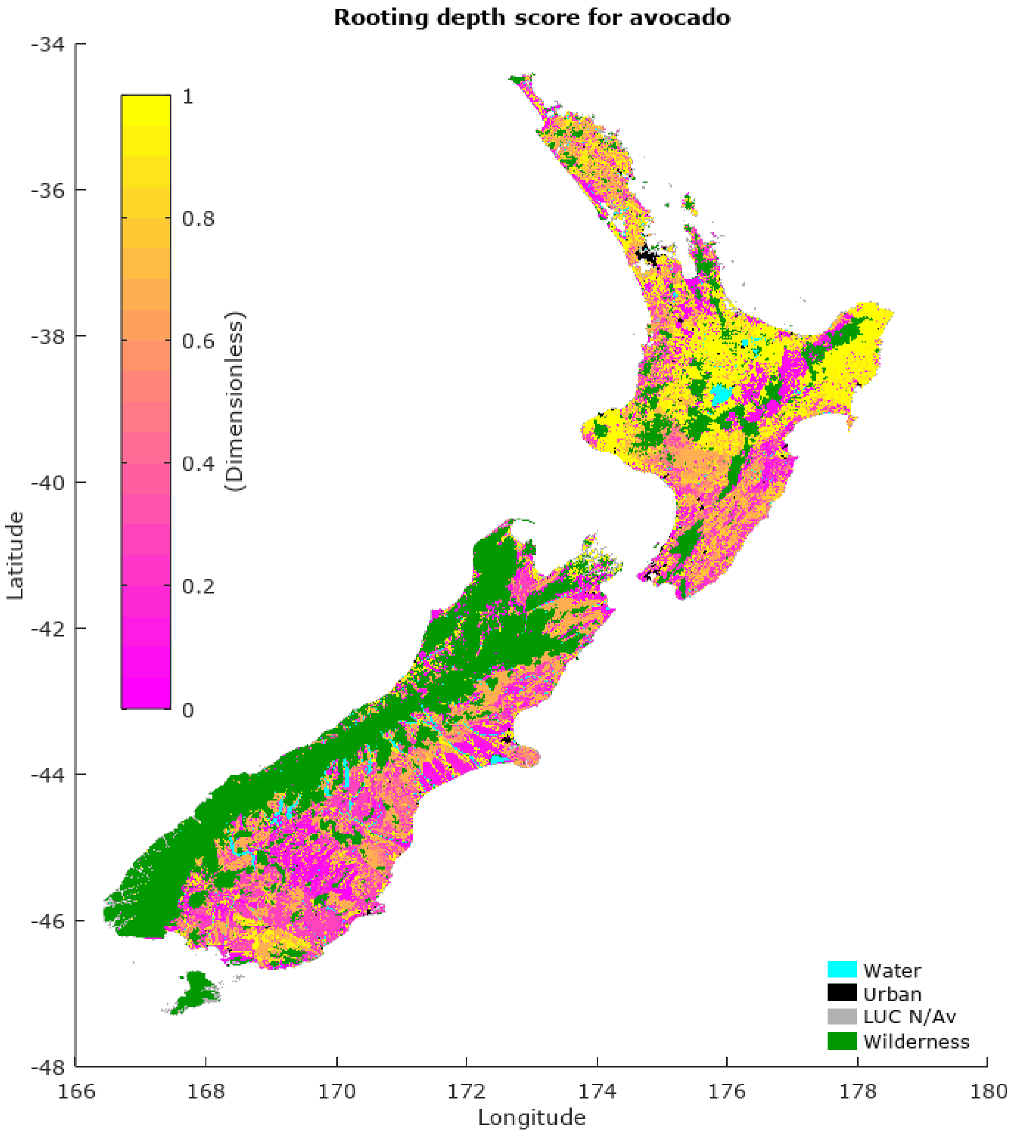

Figure 68. Avocado: rooting depth suitability scores for locations across the country.

4.1.3 Blueberry

Blueberry is shallow rooted, with the depth of the main root mass from 5 to 35 cm (Zydlik et al. 2019), and can be grown in soils of 0.45 m PRD or deeper (Griffiths et al. 2003). Hall et al. (2018) required PRD ≥15 cm; Masabni (2007) gave the minimum soil depth for blueberry cultivation as 24 inches (0.61 m), while Williamson et al. (1997) recommended a minimum depth of 18 inches (46 cm). We used a suitability score with values of 0.15, 0.5 and 0.9 for PRDs of 0.2, 0.35 and 0.6 m, respectively (Figure 69), with resulting suitability scores shown in Figure 70, showing very high rooting depth suitability for most locations across the country.

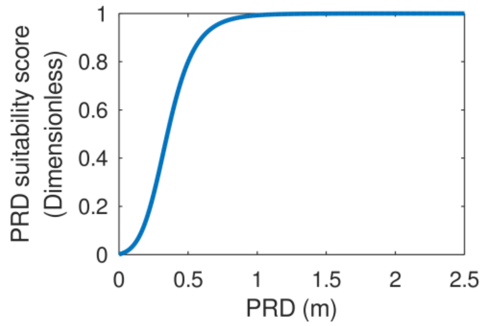

Figure 69. Blueberry: rooting depth score as a function of potential rooting depth (PRD).

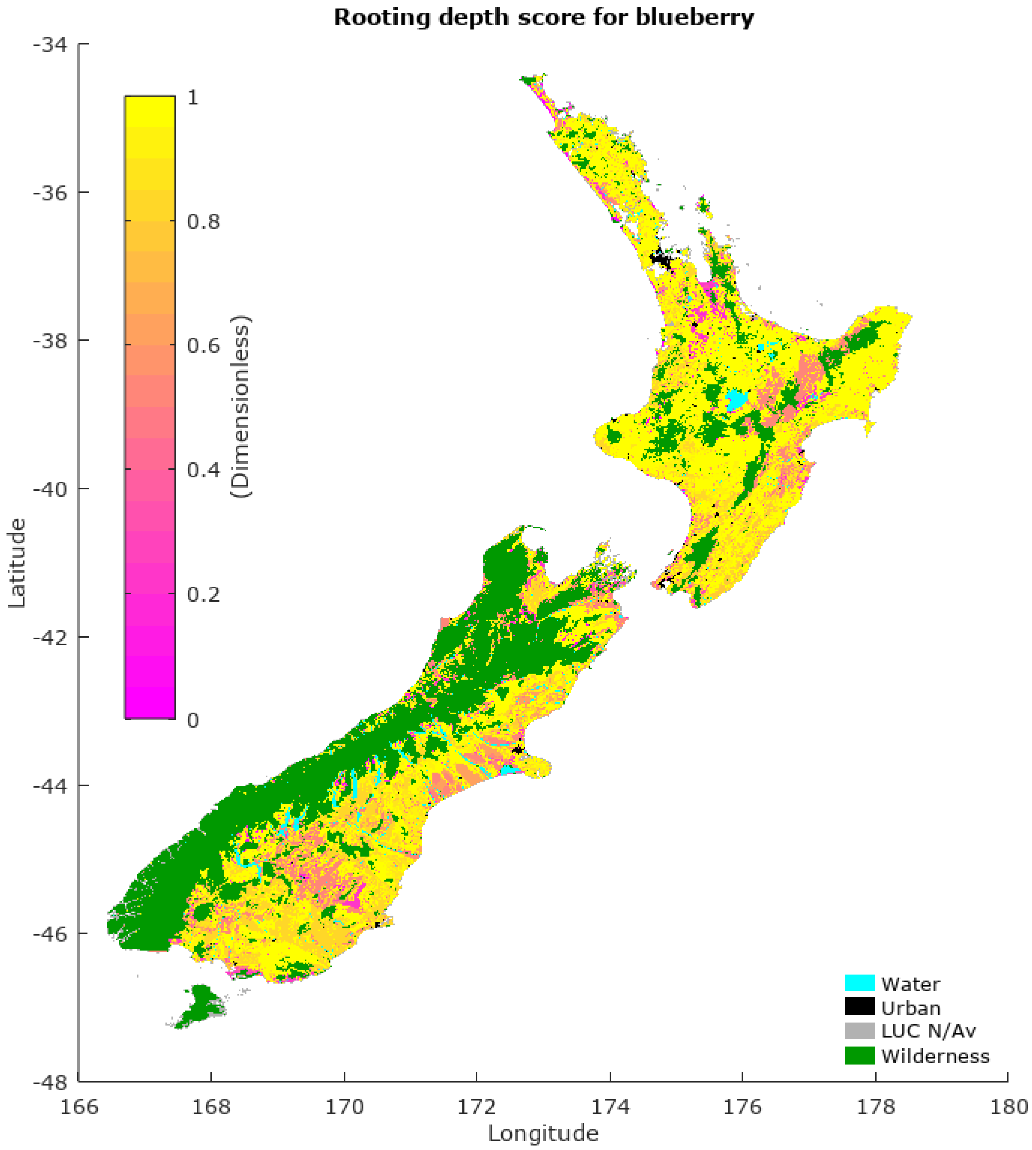

Figure 70. Blueberry: rooting depth score for locations across the country.

4.1.4 Cherry

Dawson et al. (2001) found that in 2-year-old cherry whips, the depth distribution of white roots was affected by competition from grass roots and varied with time, but the majority of roots were in the top 30 cm of soil. Long & Kaiser (2013) considered that soil depths 0.9 to 1.5 m are required for semi-dwarfing root stocks. Bonomelli et al. (2012) found that in the 'Bing' cultivar on 'Gisela 6' rootstock, white roots in the top 90 cm of soil grew up to 1.6 m in length, though these authors did not give a root density distribution. We assigned a suitability curve with values of 0.05, 0.5, 0.9 and 1.0 for potential rooting depths of 0.3, 0.6, 0.9 and 1.5 m, respectively (Figure 71). Suitability scores for locations across the country are shown in Figure 72, indicating poor rooting depth suitability in Central Otago and part of the Hawke's Bay, suggesting mitigation strategies may have been required for orchard establishment in those areas.

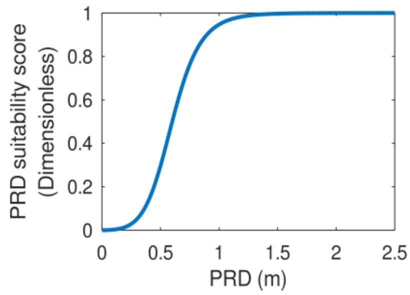

Figure 71. Cherry: rooting depth suitability as a function of potential rooting depth (PRD).

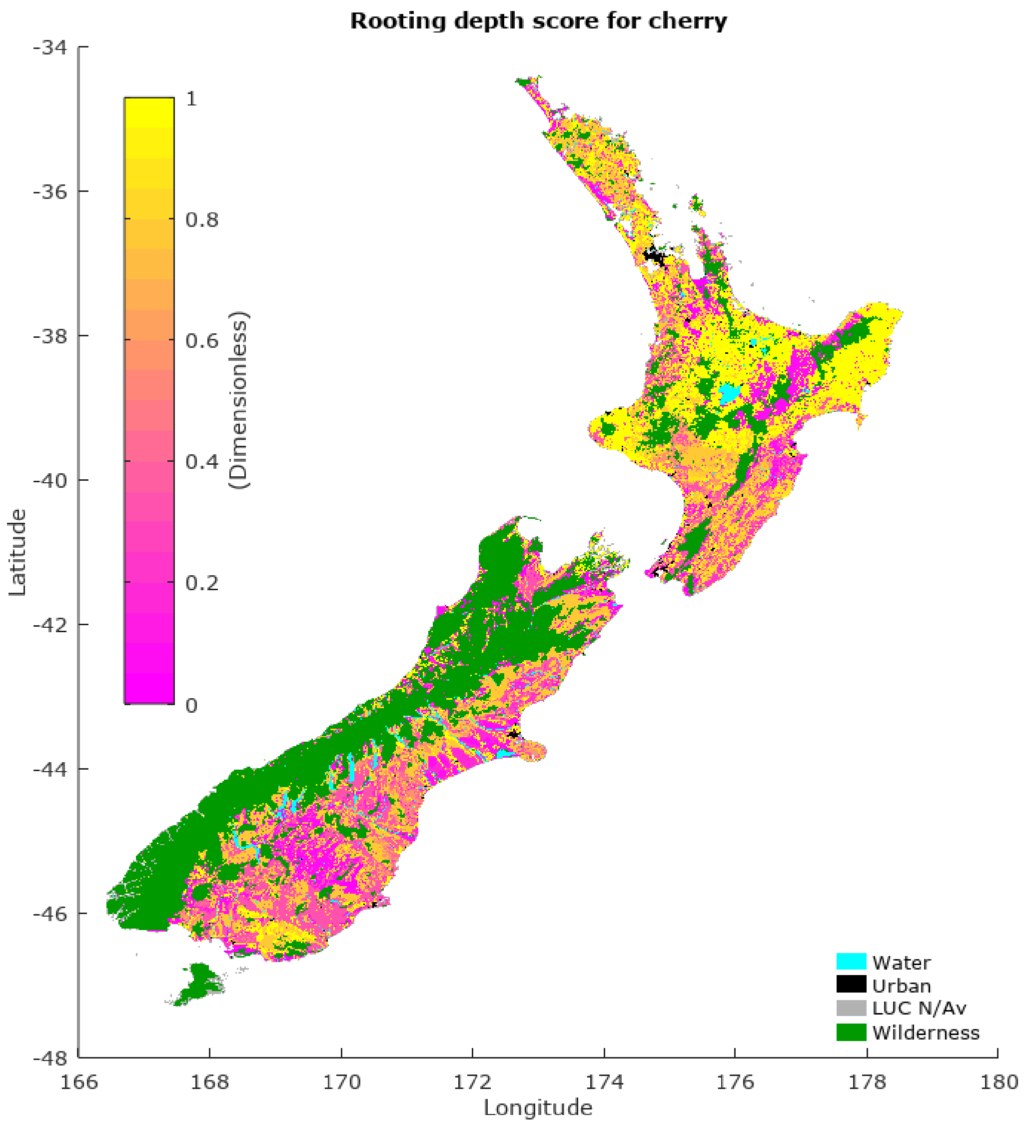

Figure 72. Cherry: rooting depth score for locations across the country.

4.1.5 Wine grape

Root density and distribution in the top layer of soil, down to 1 or 2 m, are influenced by a number of soil properties including depth to an impermeable layer and in turn have a strong influence on grapevine performance and grape quality (Smart et al. 2006; Tomasi 2014). Soil depth, along with water holding capacity and drainage are more important for wine quality than soil composition (Jackson & Lombard 1993).

Although van Leeuwen et al. (2018) noted that some studies found shallower soil gave higher quality grapes, they considered that roots in the top 20 cm of soil are undesirable because of uptake of excessive nitrogen and also excessive water uptake may dilute grape components after rainfall events. However, the validity of this reservation would very much depend on soil type and the distribution of water and nutrients across soil depth. Deeper root systems would confer better protection from water stress during drought or in soils with low absorption and high surface run-off (Jackson & Lombard 1993).

Optimal soil depths may be 0.8 to 1.0 m for non-irrigated vineyards and 0.4 m for irrigated vineyards (Lanyon et al. 2004). Since we are not considering irrigated and non-irrigated vineyards separately, we chose a sigmoidal suitability score as a function of PRD with a value 0.5 for a PRD of 0.4 m and a value of 0.95 for a PRD of 0.9 m (Figure 73). This is a considerably deeper depth requirement than that specified by Hall et al. (2018) who required PRD ≥15 cm with the note that growers could mound soil if needed.

Application of our suitability curve to locations across New Zealand gave the map in Figure 74, which suggests poor rooting depth suitability in many of the major Pinot noir and Sauvignon blanc growing areas. Given the mixed assessments in the literature on rooting depth for wine grape, the poor PRD score for grape may not pose major limitations.

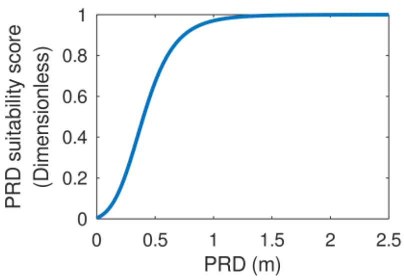

Figure 73. Grape: rooting depth suitability score as a function of potential rooting depth (PRD).

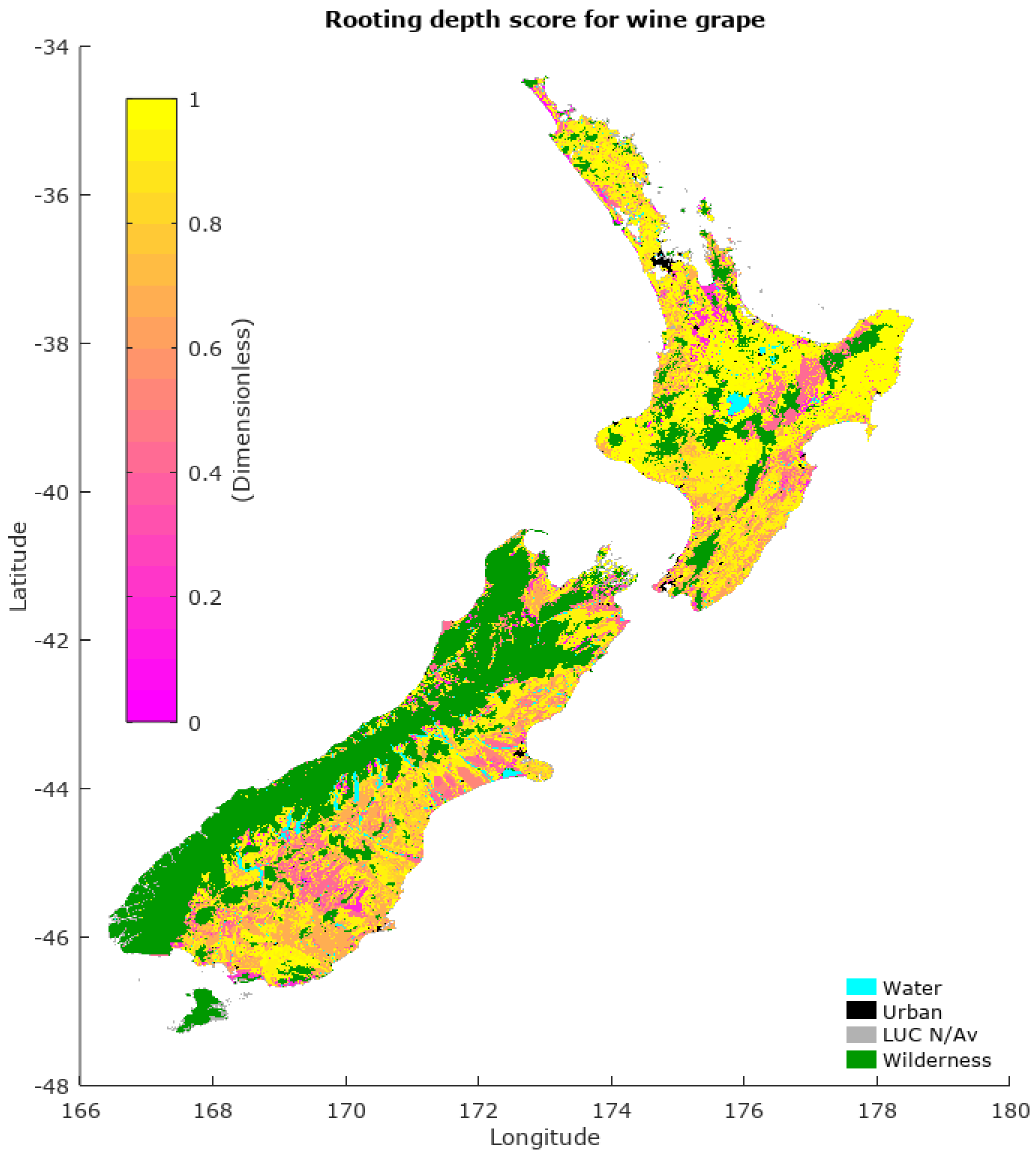

Figure 74. Grape: rooting depth suitability score for wine grape for locations across the country.

4.2 Drainage

Drainage was available for the same locations as PRD, and reported as one of the following drainage classes: well, moderate, imperfect, poor and very poor. These classifications take into account a number of factors, including soil structure, depth, and permeability, and water-table depth. We assigned numerical suitability scores from 0 to 1 to the drainage classes, with the numerical assignment for each class potentially differing between crops (Table 2). While a lower score indicates less suitability, it does not rule out an area for a crop, but rather indicates that extra effort and cost would be needed for successful crop production. This could include, for example, improving soil drainage through subsoil ploughing, installation of surface or subsurface drainage systems, mounding or long-term improvements of soil health through application of soil amendments, and minimising soil compaction through reducing traffic in orchards.

Table 2. Drainage scores assigned to drainage class descriptors for different crops

	Well	Moderate	Imperfect	Poor	Very Poor
Apple	1	1	0.6	0.3	0
Kiwifruit	1	0.9	0.4	0.1	0
Avocado	1	0.9	0.4	0.1	0
Blueberry	1	0.75	0.3	0.1	0
Cherry	1	0.9	0.4	0.2	0
Wine grape	1	0.9	0.4	0.1	0

The values in Table 2 were used to calculate individual drainage suitability maps, which are described in the next subsections. These maps generally indicated favourable drainage, apart from large parts of Northland, significant parts of the Waikato and the Manuwatu, and scattered areas across the Hawke's Bay, Wairarapa and parts of the South Island. These patterns showed more strongly for crops with poor waterlogging tolerance and more patch and less intense for more tolerant crops.

4.2.1 Apple

For apple, we assigned score values of 1, 1, 0.6, 0.3, and 0, respectively, to the drainage classes well, moderately, imperfectly, poorly and very poorly drained (Table 2), with the resulting map shown in Figure 75.

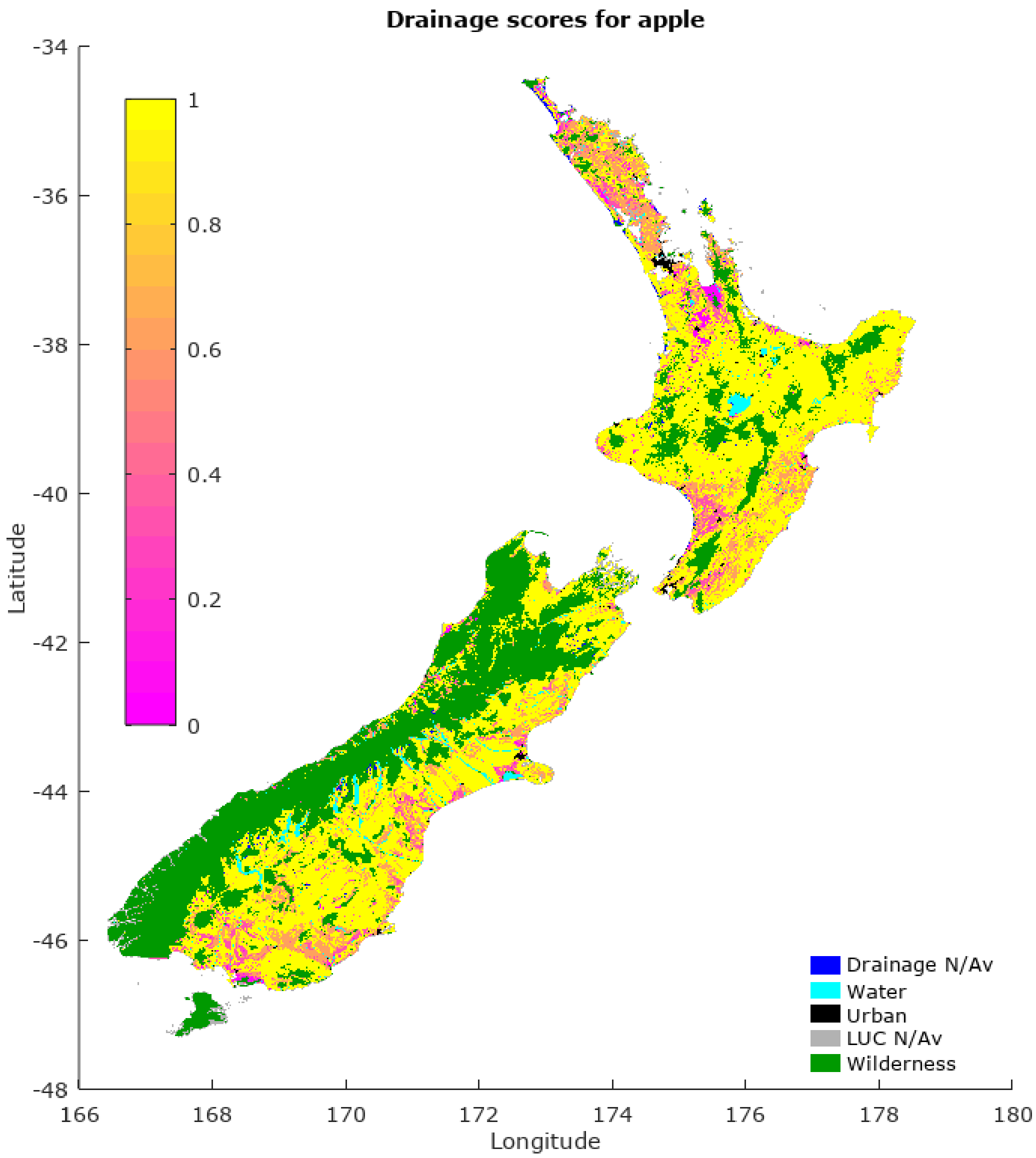

Figure 75. Apple: drainage suitability score for locations across the country.

4.2.2 Kiwifruit, avocado and wine grape

Kiwifruit was considered by horticultural experts to be of higher sensitivity to waterlogged conditions than apple, and thus it was expected that suitability scores would be comparatively lower for drainage class other than “Well drained’. Avocado does not tolerate water logging and requires good drainage (Ticho & Gefen 1965; McCarthy 2001; Dubrovina & Bautista 2014). Wine grape was assessed by horticultural experts as being similarly susceptible to waterlogged conditions as kiwifruit and avocado. Thus for these three crops we assigned score values to the drainage classes of, respectively, 1, 0.9, 0.4, 0.1 and 0 (Table 2). The resulting drainage suitability map for kiwifruit, avocado and wine grape is shown in Figure 76.

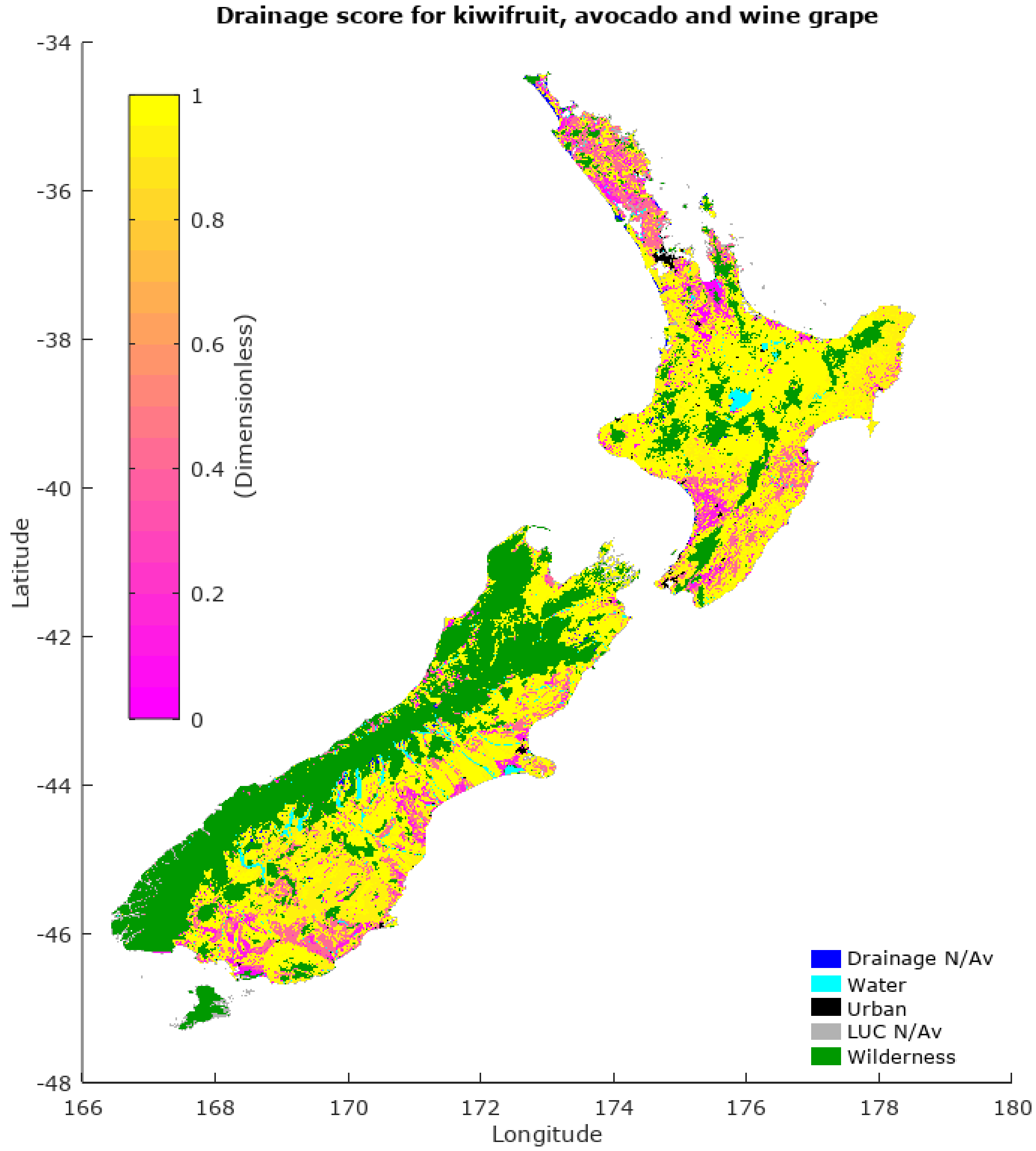

Figure 76. Kiwifruit: drainage suitability score for locations across the country.

4.2.3 Blueberry

Blueberry is highly sensitive to water-logged conditions (Hayes 1988) and duration of flooding events were significantly related to the severity and extent of *Phytophthora* infection causing root rot (Silva et al. 1999), which can be a significant cause of plant mortality when drainage is marginal or worse. In areas where soil is poorly drained, this necessitates planting blueberry in raised beds (Williamson et al. 1997). Griffiths et al. (2003) noted that blueberry should be planted only on either well-drained soils or moderately well-drained soils with artificial drainage. Thus we assigned suitability score values to these drainage classes of, respectively, 1, 0.75, 0.3, 0.1 and 0 (Table 2), with a resulting suitability map shown in Figure 77.

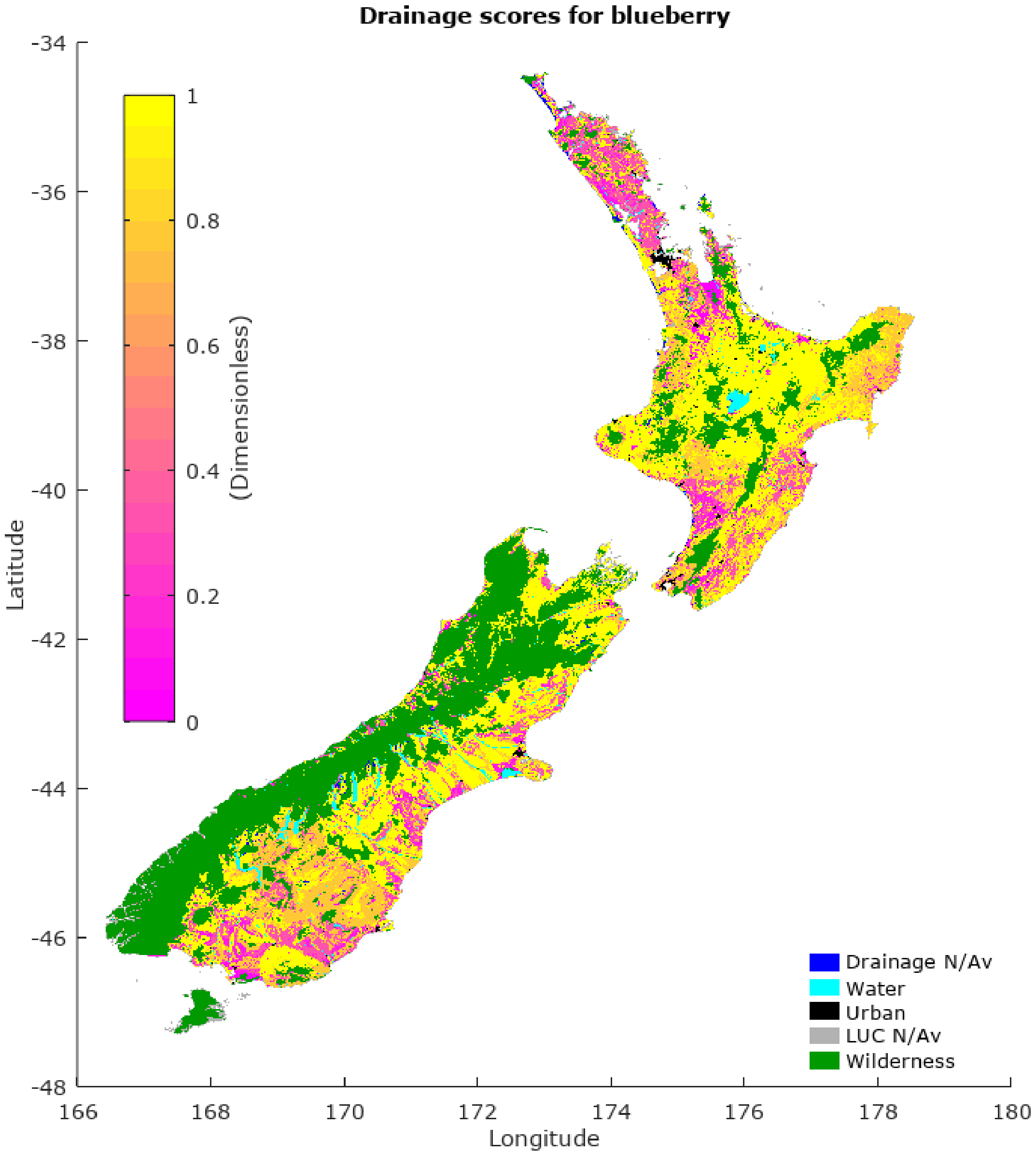

Figure 77. Blueberry: drainage suitability score for locations across the country.

4.2.4 Cherry

Cherry trees (and more so the deeper-rooted cultivars) are very susceptible to waterlogging and often do poorly or die in heavy soils with poor drainage, with the moist soil conditions favouring pathogens such as *Phytophthora* (Blodgett et al. 1990), with the extent of damage increasing with the duration of waterlogging (Wilcox & Mircetich 1985). Additionally, waterlogging can cause hypoxia by lowering oxygen availability to root systems (Pérez-Jiménez et al. 2017). Interestingly, trees with hypoxia-tolerant rootstocks showed less stress from waterlogging when the ambient CO_2 concentration was increased (Pérez-Jiménez et al. 2017). Drainage was available for the same locations as PRD, and reported as: well, moderately, imperfectly, poorly and very poorly drained. These classifications take into account factors such as soil structure, depth and permeability, and water table depth. While there is variation between cherry rootstocks in their tolerance to waterlogging, we have emphasised that good drainage is required by assigning scores that significantly favour the better drainage classes, using respective values of 1, 0.9, 0.4, 0.2 and 0 (Table 2). Figure 78 shows suitability scores for locations across the country.

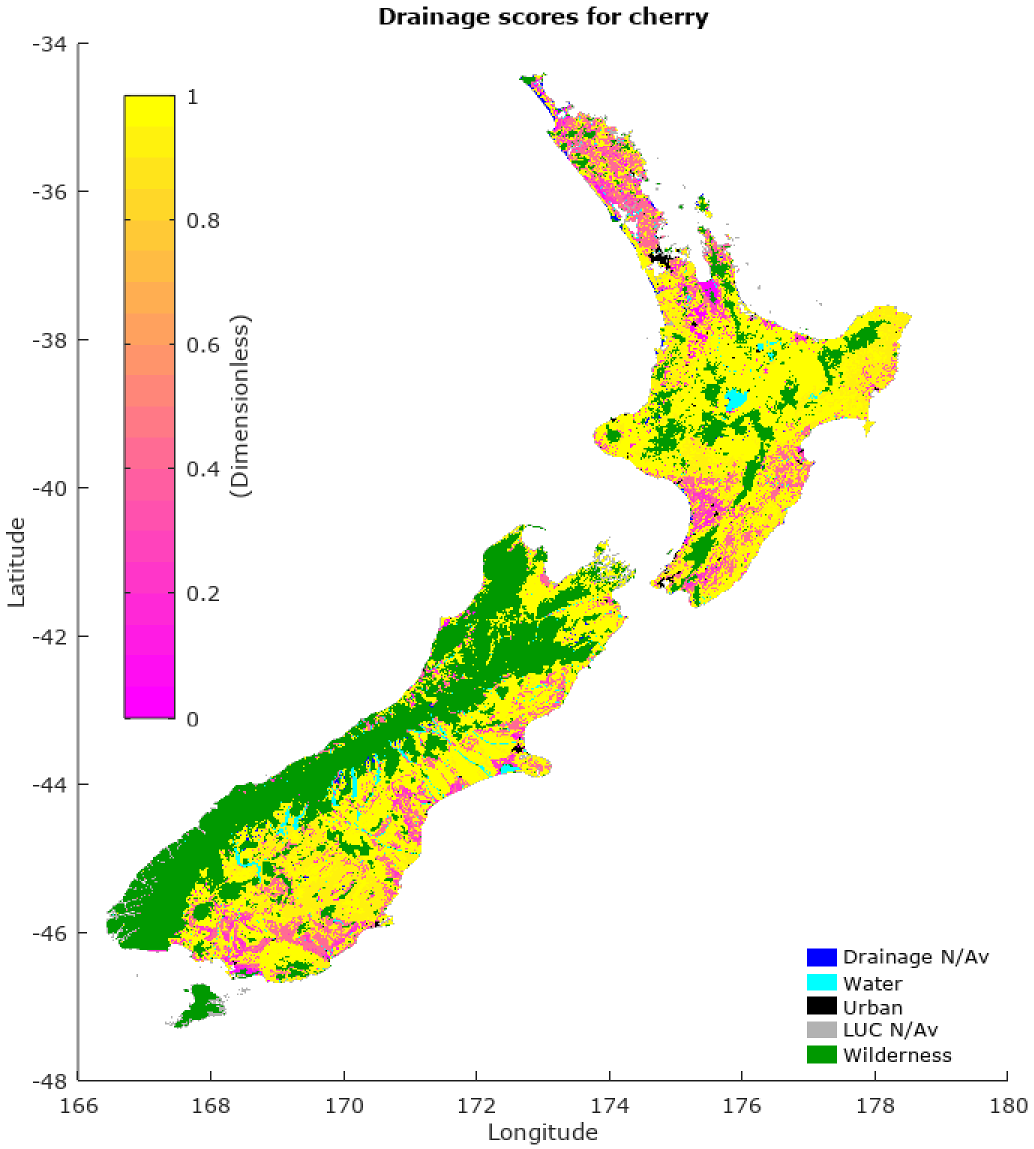

Figure 78. Drainage score for locations across the country.

4.3 Slope

Rowland et al. (2016) state that slopes greater than 30° are not suitable for machinery, and that for well-managed horticultural crops, only slopes greater than 30° pose an erosion risk. In any 1-km^2 grid-square, there will likely be a range of slopes, some suitable for cultivation even if the central latitude value indicates otherwise. Database values for slope are shown in Figure 79. In any 1-km^2 grid-square, there will likely be a range of slopes, some suitable for cultivation even if the central latitude value indicates otherwise.

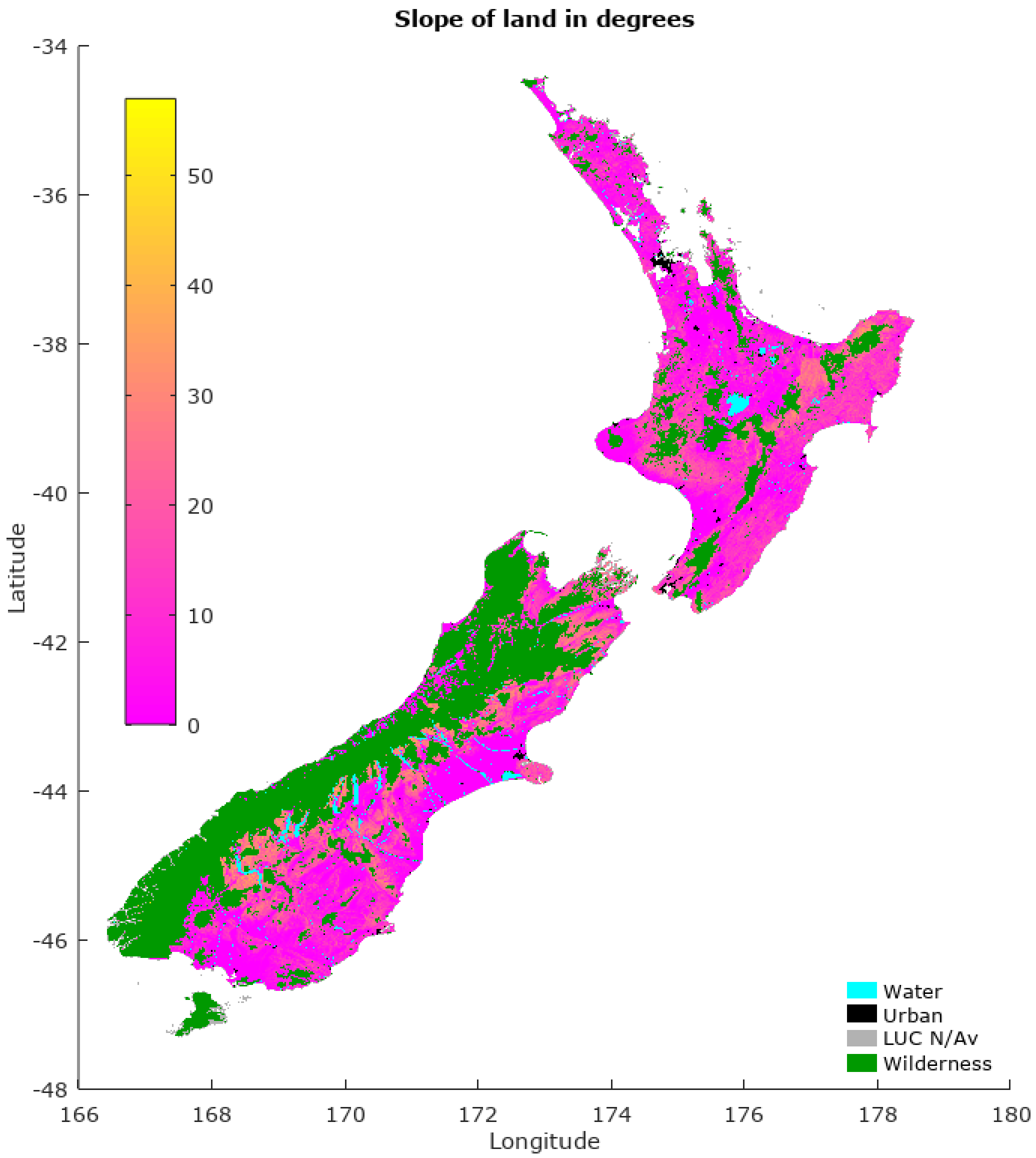

Figure 79. Slope (degrees) for locations across the country.

4.3.1 Apple

We assigned a suitability curve with a mid-point value occurring at a slope of 19° for apple, with high values for slopes ≤8.5°, with a rapid descent to zero as slope increases past the mid-point slope values (Figure 80). The requirements for apple may need to be modified if and when new systems requiring more complex structures become common. The slope suitability score map for apple is shown in Figure 81, showing generally very high suitability across the country.

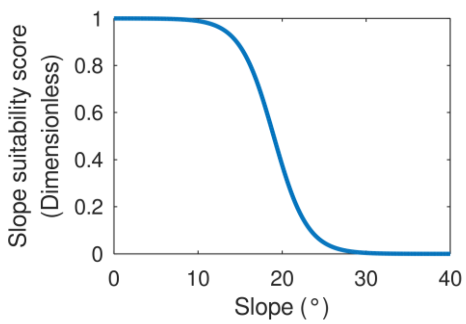

Figure 80. Slope suitability score assigned to slope for apple.

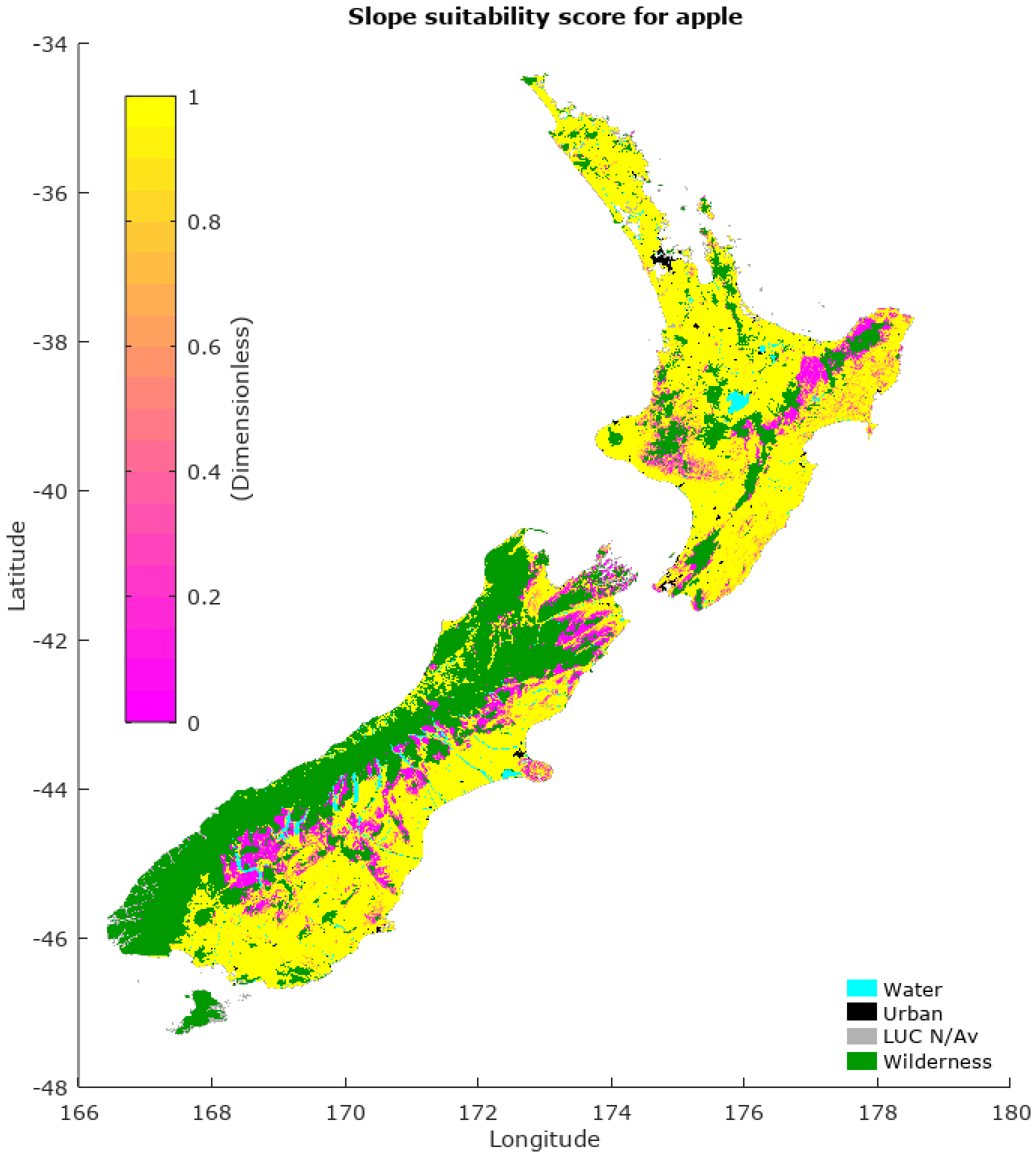

Figure 81. Apple: slope suitability score for locations across the country.

4.3.2 Kiwifruit

Since structures for kiwifruit are currently more difficult to construct on slopes, a more restrictive slope suitability score is appropriate for kiwifruit compared with apple. Thus, we assigned a suitability curve with a mid-point value occurring for a slope of 12°, high values for slopes ≤8.5°, and a rapid descent to zero as slope increases past the mid-point slope values (Figure 82). The corresponding suitability map is shown in Figure 83, showing many locations in Gisborne have slopes that could pose limitations to growing kiwifruit, but otherwise good suitability in other kiwifruit growing areas.

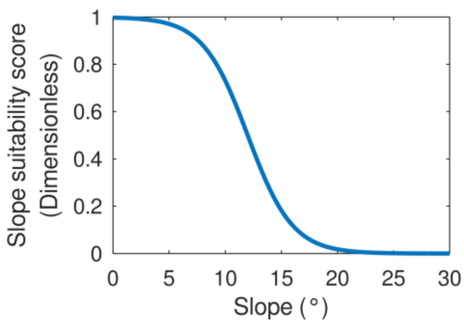

Figure 82. Slope suitability score assigned to slope for kiwifruit.

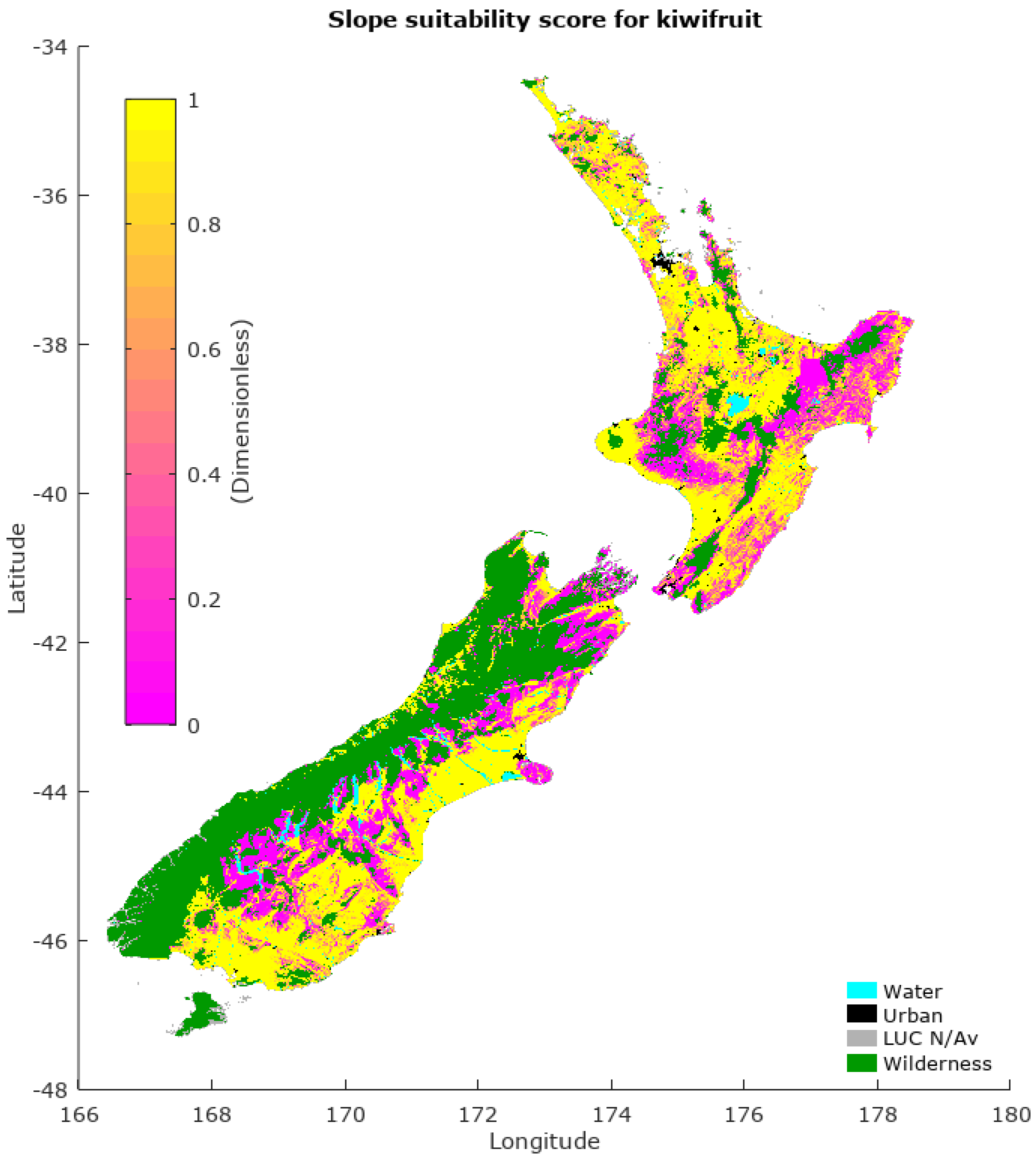

Figure 83. Kiwifruit: slope suitability score for locations across the country.

4.3.3 Avocado

Griffiths et al. (2003) stipulated that the maximum suitable slope for growing avocado is 8.5% or 5°. In contrast, Selim et al. (2018) considered slopes less than 15° to be suitable for growing avocado, and slopes greater than 15° to be more difficult and expensive to farm, and more prone to erosion. Hall et al. (2018) considered slopes ≤7° as optimal, slopes ≤15° as marginal, and slopes >15° as unsuitable. However, we are aware of at least one New Zealand avocado orchard established on a 30° slope. Thus, we assigned a suitability curve with a mid-point value of 19° for avocado, high values for slopes ≤8.5°, and with a rapid descent to zero as

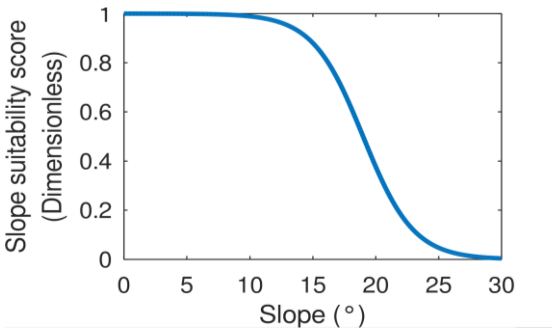

Figure 84. Avocado: slope suitability score vs slope.

slope increases past the mid-point slope value (Figure 84). Calculated suitability scores are mapped across New Zealand in Figure 85, showing generally very high slope suitability across locations.

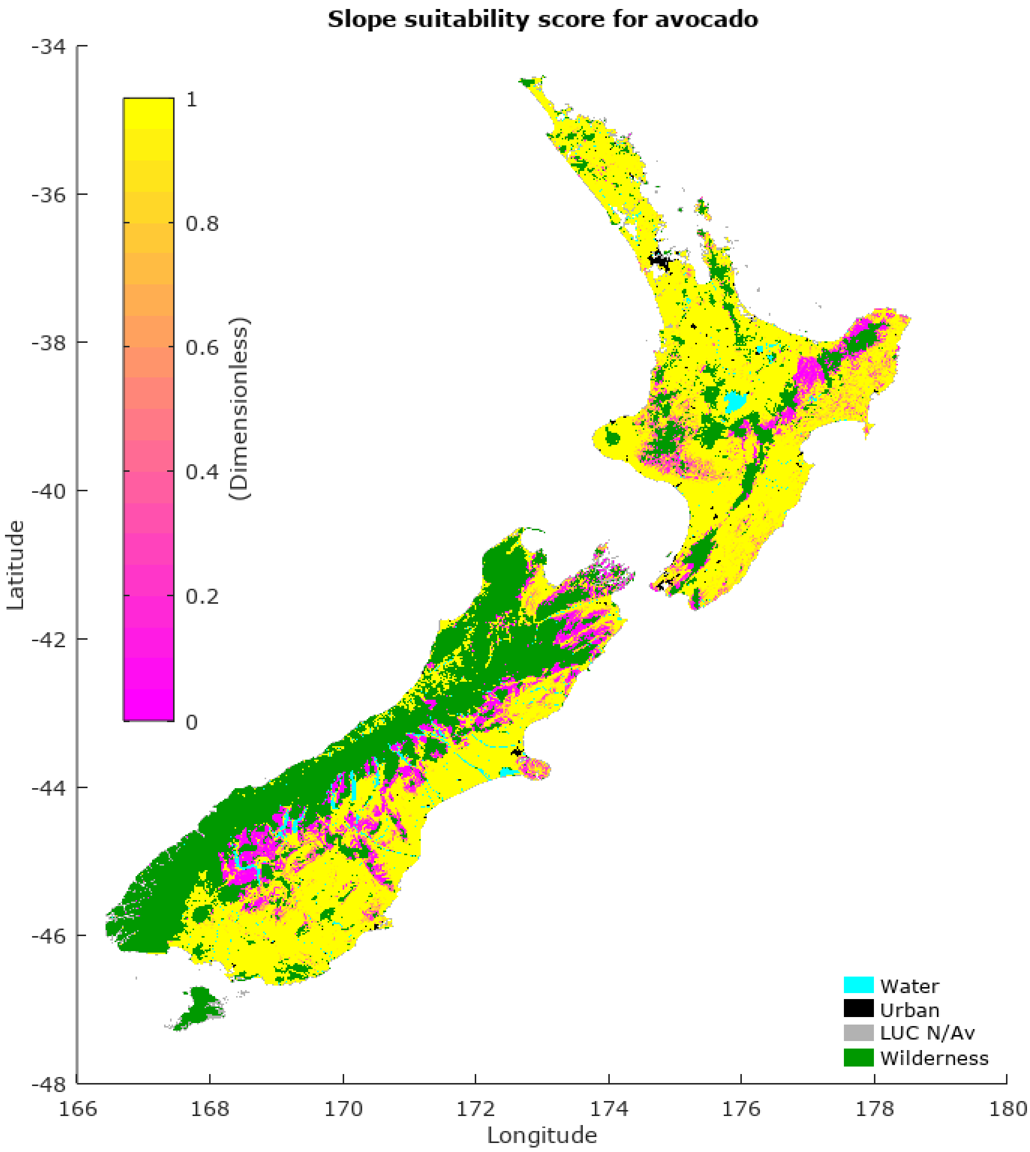

Figure 85. Avocado: slope suitability scores for locations across the country.

4.3.4 Blueberry

Griffiths et al. (2003) state that blueberry should only be grown on flat to gently sloping land to ensure safe and easy access for workers, machinery, installation of infrastructure, and to minimise erosion. Hall et al. (2018) required that slope ≤15°. Balancing these positions with that of Rowland et al. (2016) who considered that slopes of 30° or less are suitable for well managed crops, we assigned a sliding score with a mid-point value of 12° with a rapid descent to zero as slope increases past the mid-point slope value (Figure 86). Suitability scores for locations across the country are shown in Figure 87. Large areas of land across the country show good slope suitability for blueberry, especially in the Waikato and Bay of Plenty where blueberry production is strong.

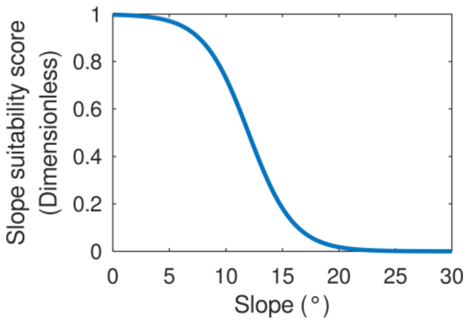

Figure 86. Blueberry: slope suitability score as a function of slope.

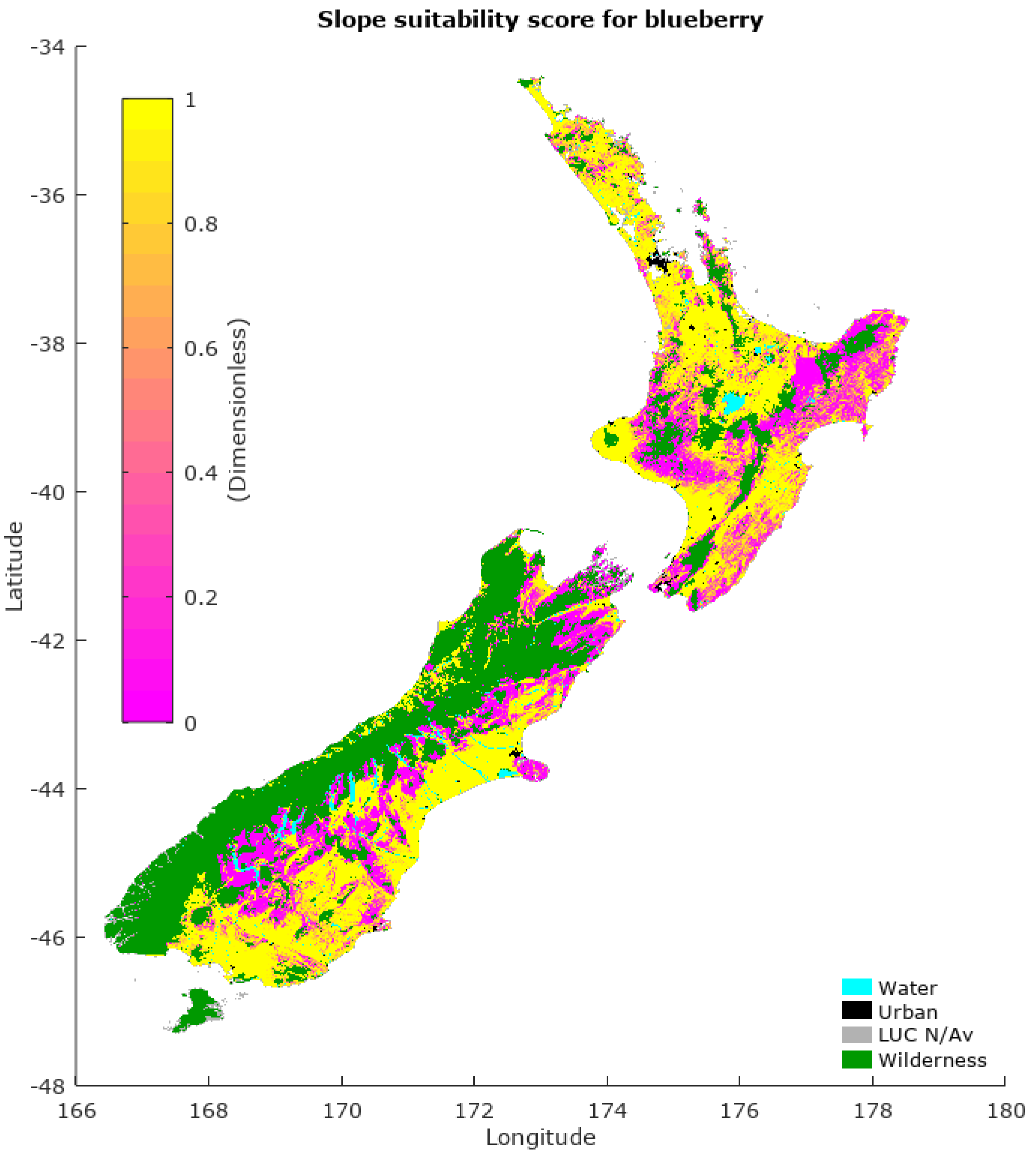

Figure 87. Blueberry: slope suitability score for locations across the country.

4.3.5 Cherry

Cherry tree planting systems can be tailored to suit the steepness of the land (Brown 1932), thus higher slopes should not be a limitation to establishing orchards. For example, cherry and apple orchards have been established on sites with maximum and mean slopes of 30° and 13° in Australia (Oliver et al. 2012), and cherry and apricot orchards on slopes of 15° in Lebanon (Zurayk et al. 2001), and the suitability of slopes of ≤30° is supported by Rowland et al. (2016).

We assigned a sliding score with a mid-point value of 15° with a rapid descent to zero as slope increases past the mid-point slope value (Figure 88). Slope suitability scores for locations across the country are shown in Figure 89. For both Central Otago and the Hawke's Bay, which contain the majority of the cherry industry footprint, slope suitability is high.

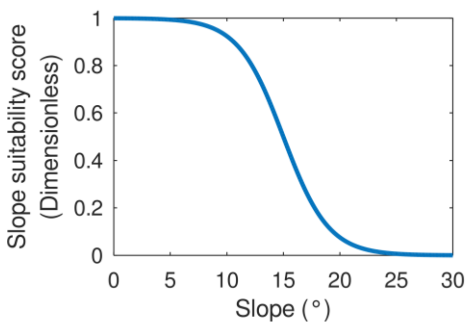

Figure 88. Cherry: slope suitability score as a function of slope.

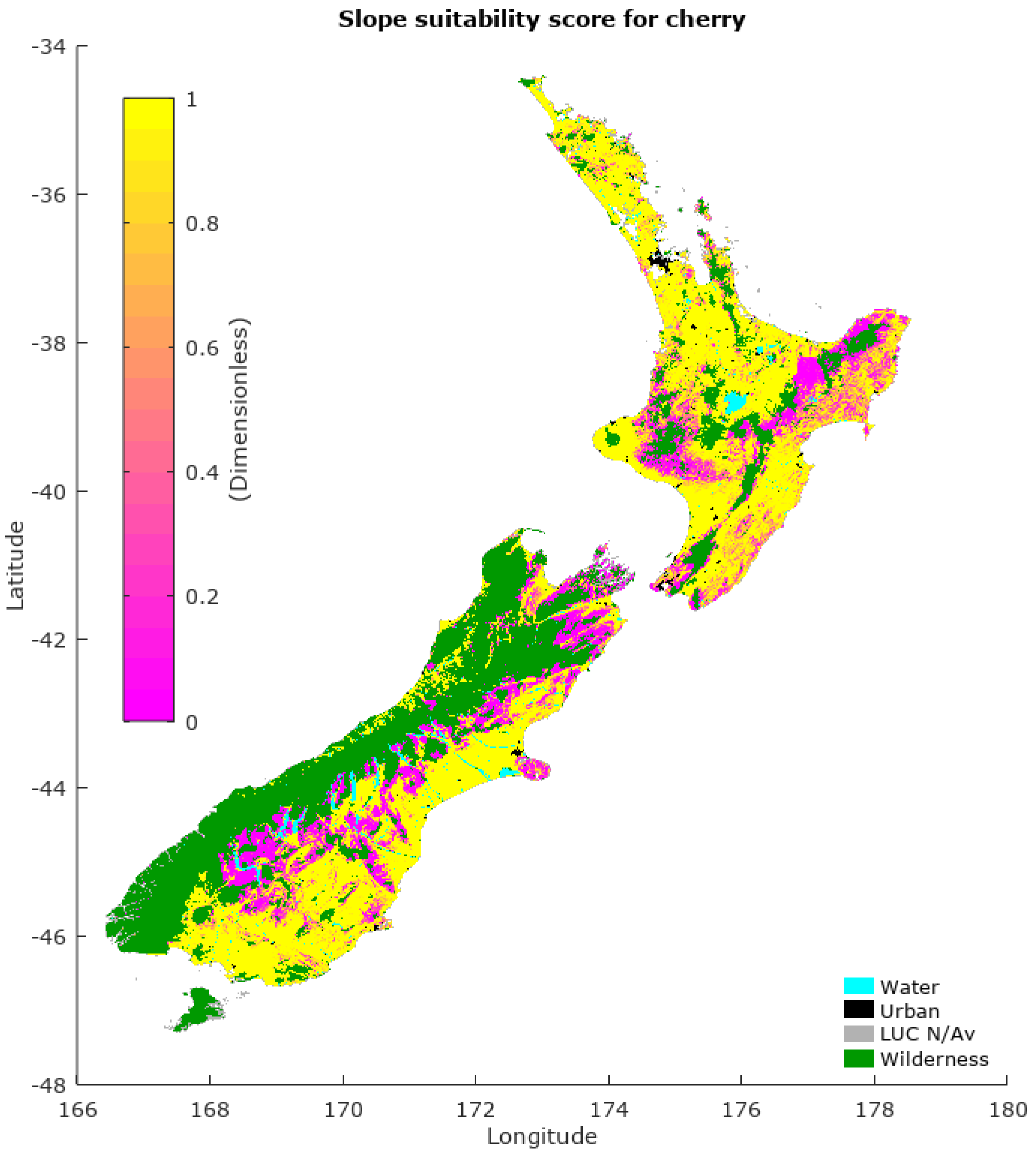

Figure 89. Cherry: suitability score for slope for locations across the country.

4.3.6 Wine grape

Hall et al. (2018) stipulated a maximum slope of 11.3°, reduced to 8.5° if mechanical harvesting was to be used, a value considerably lower than the 30° limit that Rowland et al. (2016) gave for the use of machinery. However, since support structures for grape may be more difficult to construct on slopes, and because of the need for mechanised harvest, we assigned a suitability curve with mid-point values of 12°. The curve has high values for slopes ≤8.5°, with a rapid descent to zero as slope increases past the mid-point slope values (Figure 90). Slope suitability scores across New Zealand are shown in Figure 91, reflecting good suitability of slope in locations where the wine industry is established.

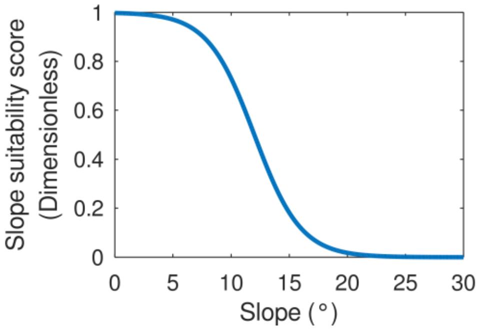

Figure 90. Grape: slope suitability score as a function of slope.

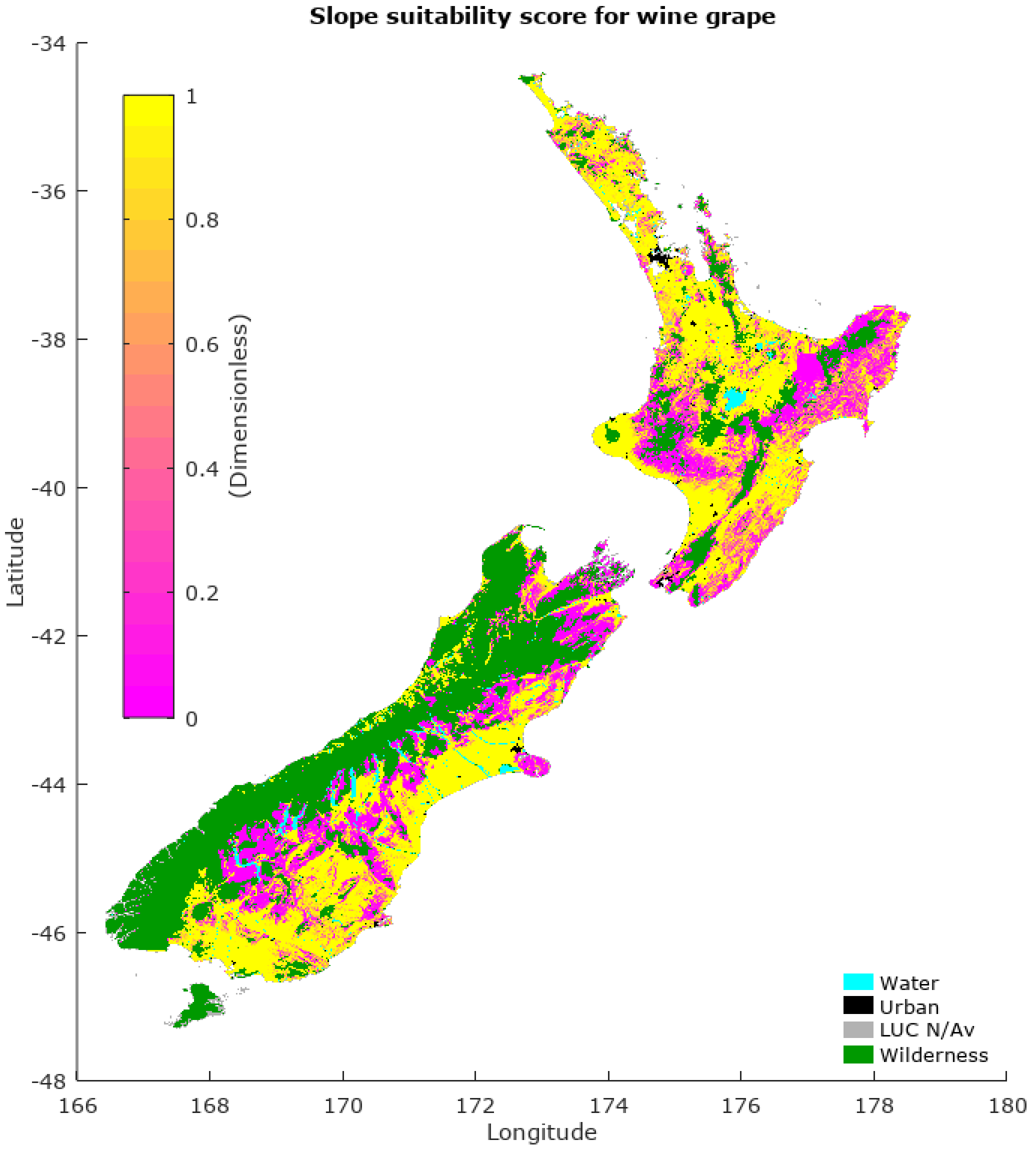

Figure 91. Grape: slope suitability scores for locations across the country.

4.4 Land use capability class

Land use capability (LUC) class descriptors are divided into eight main categories (numbered 1 to 8), with 1 indicating land classes that are considered to have virtually no limitations for arable use and 8 indicating land classes considered to have very severe limitations or hazards that make it unsuitable for cropping, pasture or forestry. However, some crops are better grown on land with a higher LUC category, depending on their requirements.

There is also some overlap between LUC class descriptors and the slope, PRD and drainage information, However, LUC class also contains extra information regarding the soil properties, thus it is important to consider all four of the land-related requirements above.

We assigned suitability scores to LUC classes to facilitate the development of sliding-scale or continuous suitability scoring (Table 3). LUC classes 4 to 6 that are typically not considered suitable for horticulture were generally given moderate to moderately low scores rather than very low scores, in order to be consistent with what could be happening on the ground. For example, data on known apple orchard locations indicated that less than 90% of these orchards were on LUC 1 to 3, with the remainder mostly on LUC 4 and 6.

Table 3. Land use capability (LUC) scores assigned to LUC classes, for different crops.

	LUC 1	LUC 2	LUC 3	LUC 4	LUC 5	LUC 6	LUC 7	LUC 8
Apple	1	0.95	0.9	0.8	0.65	0.5	0.05	0
Kiwifruit	1	0.95	0.9	0.8	0.65	0.5	0.05	0
Avocado	1	0.95	0.9	0.8	0.65	0.5	0.05	0
Blueberry	1	0.95	0.9	0.8	0.6	0.4	0.2	0
Cherry	1	0.95	0.9	0.8	0.65	0.5	0.05	0
Wine grape	1	0.95	0.9	0.8	0.7	0.65	0.6	0

4.4.1 Apple, kiwifruit, avocado and cherry

For apple, kiwifruit, avocado and cherry, LUC classes 1 to 8 were (in discussion with crop experts) assigned the respective score values of 1, 0.95, 0.9, 0.8, 0.65, 0.5, 0.05 and 0 (Table 3), and the resulting suitability map is shown in Figure 92. Large areas of the main growing regions for avocado and kiwifruit have quite low LUC suitability scores, although there are some locations that have high LUC suitability scores, and these are distributed in a somewhat mottled fashion. Orchards may be more predominantly situated in these higher suitability score locations, or there may be considerable variation within individual grid cells that cannot be reflected by a single grid value. The Nelson, Central Otago and Hawke’s Bay regions have large areas of high LUC suitability, which is line with the main apple footprints, and also the main cherry footprint which occurs in the latter two locations.

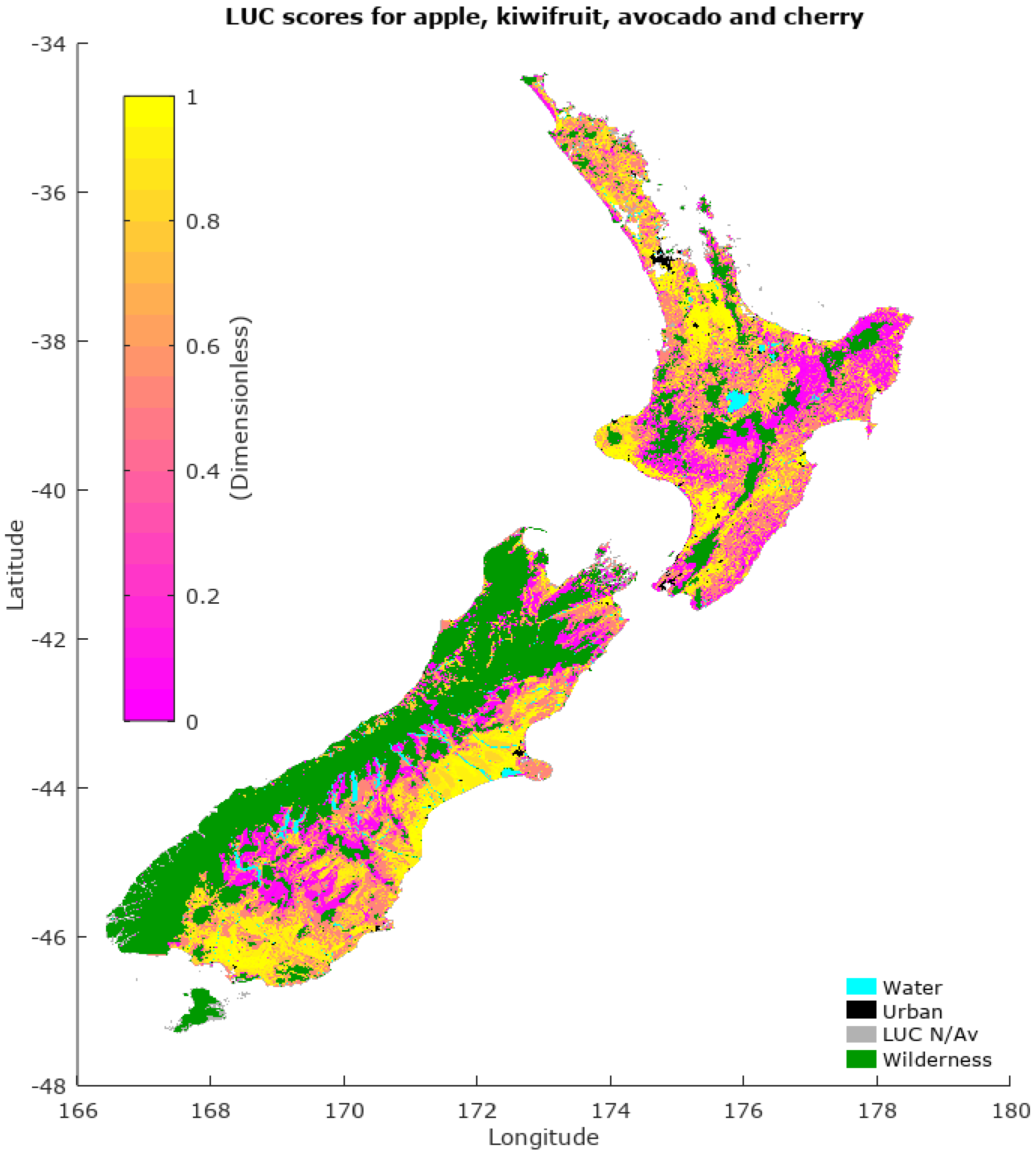

Figure 92. Land use capability (LUC) suitability scores for apple, kiwifruit, avocado and cherry.

4.4.2 Blueberry

For blueberry, we assigned the respective score values of 1, 0.95, 0.9, 0.8, 0.6, 0.4, 0.2 and 0, after discussion with crop experts (Table 3). The resulting map is shown in Figure 93, indicating that large areas of the country are unsuitable for blueberry. However, the Waikato has large areas of high LUC suitability land, as does the Bay of Plenty, which represent the main centres for blueberry production. Many scattered locations around the North Island also have high LUC suitability for blueberry, which is consistent with strong production distributed around the North Island.

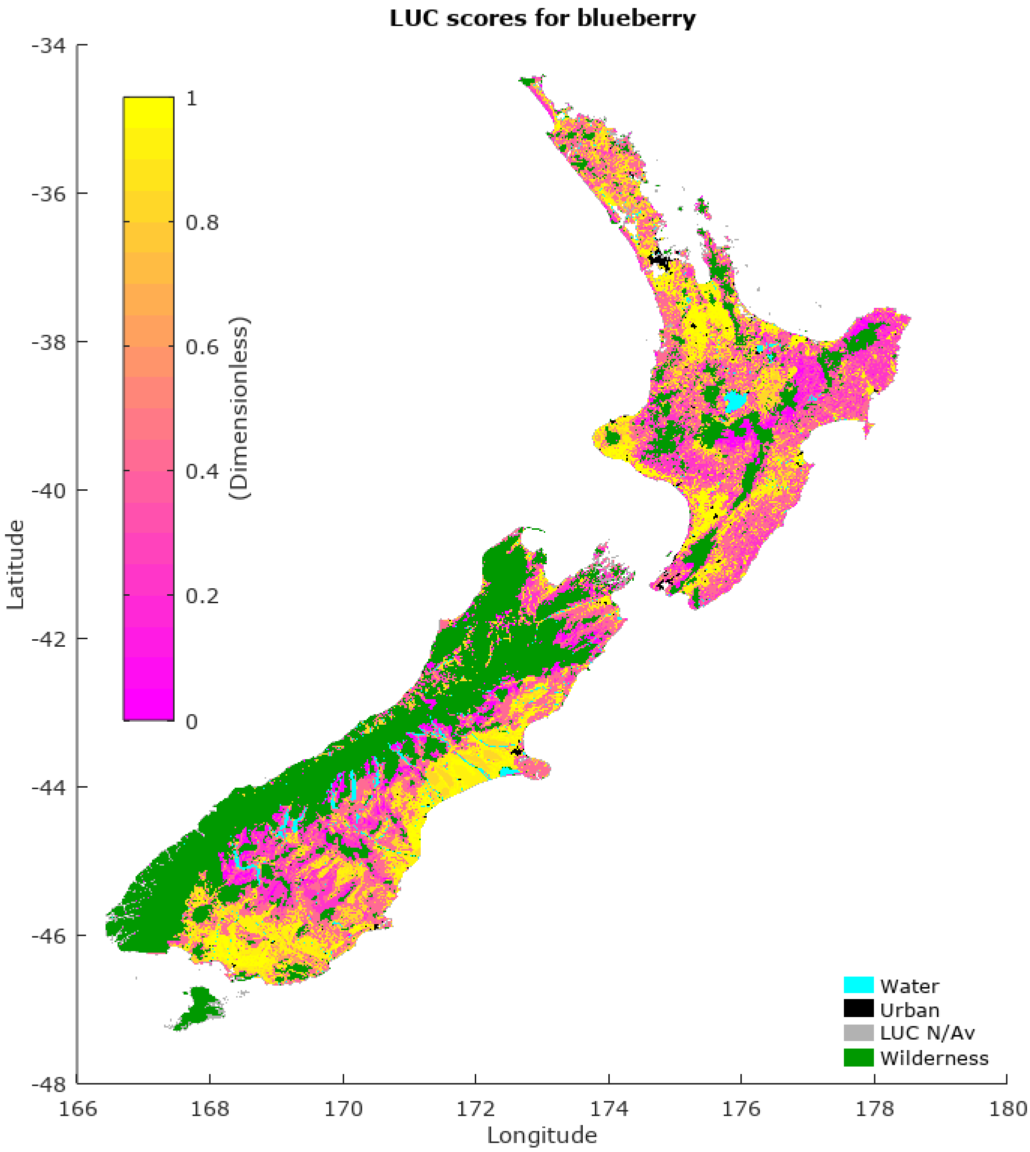

Figure 93. Blueberry: land use capability (LUC) class suitability score for locations across the country.

4.4.3 Wine grape

Hall et al. (2018) reported that LUC classes 1 to 3, or LUC 4s to 7s were suitable for grape. The LUC Survey Handbook (Lynn et al. 2009) represents LUC classes 1 to 7 as having decreasing suitability for viticulture, and class 8 as unsuitable. However, successful wine grape cultivation occurs in some areas considered marginal. Classes 1 to 8 were assigned the respective score values of 1, 0.95, 0.9, 0.8, 0.7, 0.65, 0.6 and 0 (Table 3). LUC suitability scores for locations across the country are shown in Figure 94, with high or moderately high LUC suitability locations being distributed around the wine-growing regions.

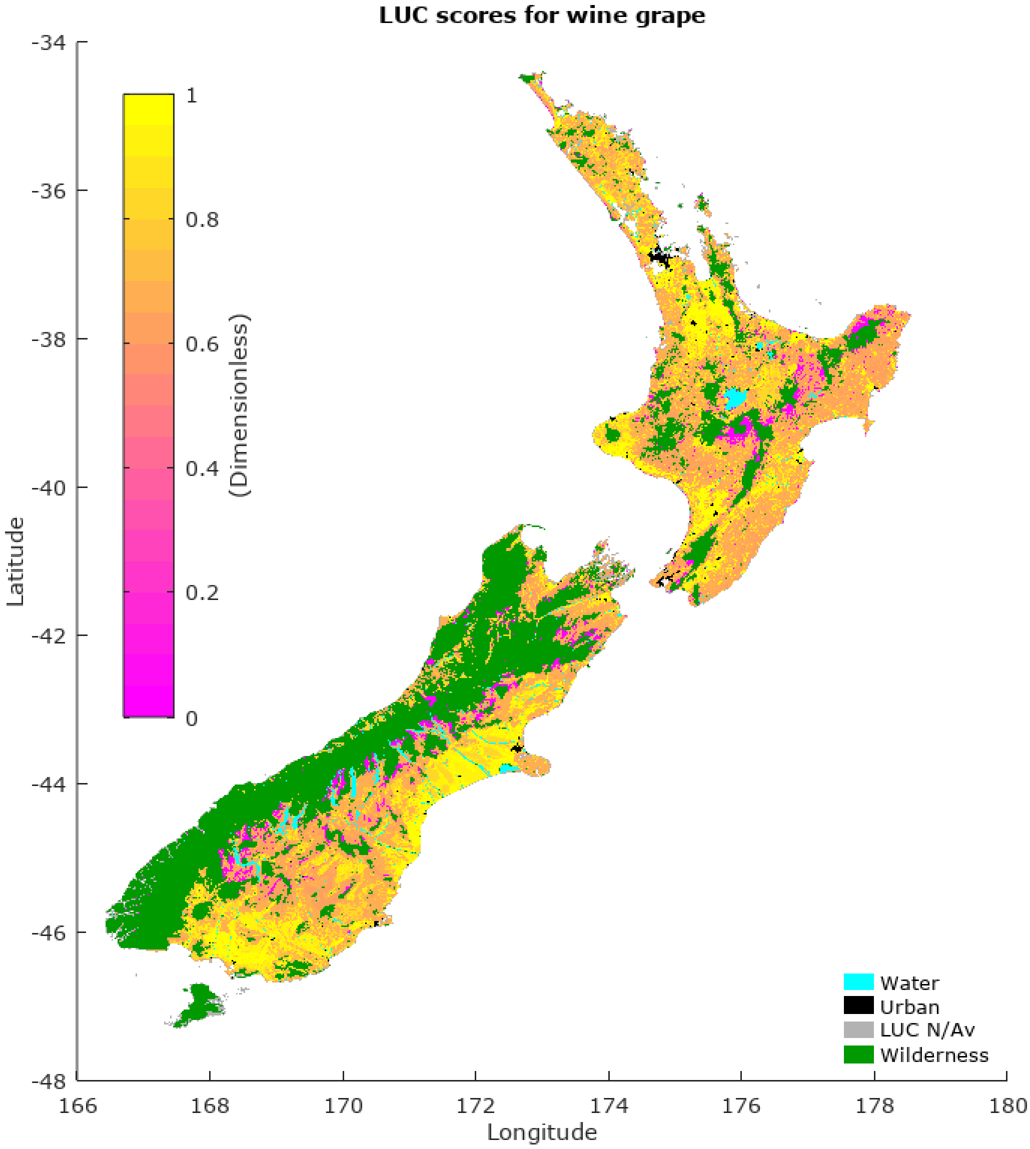

Figure 94. Grape: land use capability (LUC) suitability scores for locations across the country.

4.5 Soil pH

4.5.1 Avocado

Griffiths et al. (2003) state that the ideal soil pH for avocado is 6.0 to 6.5, with the range 5.5 to 6.9 being satisfactory. In contrast, Dubrovina & Bautista (2014) classified a soil pH of 6.7 to 7.3 as highly suitable, with ranges 5.5 to 6.7 and 7.3 to 8.0 considered suitable, 4.5 to 5.5 and 8.0 to 9.0 considered low suitability, and <4.5 or >9.0 being unsuitable. Selladurai & Awachare (2020) noted that in alkaline soil there is a risk of zinc deficiency, and in soils with a pH <6 there is a risk of manganese toxicity if manganese levels are high. These authors recommend that soil should be neutral or slightly acidic in reaction, and alkaline conditions are not suitable for avocado. We chose a pH suitability score with value 1 at pH 6.5, value 0.9 at pH 6 and 7, and value 0.1 at pH 4.5 and 8.5 (Figure 95).

Scores for each location are mapped across New Zealand in Figure 96, showing a huge contrast from high pH suitability to low suitability between neighbouring locations in Northland, large areas of land in the Gisborne region with low suitability but interspersed with locations of high suitability, and generally favourable soil pH conditions in many parts of the Bay of Plenty. These three regions contain the bulk of the New Zealand avocado footprint, and in Gisborne and Northland, orchard location may strongly coincide with the higher suitability locations or require ongoing mitigation to adjust pH.

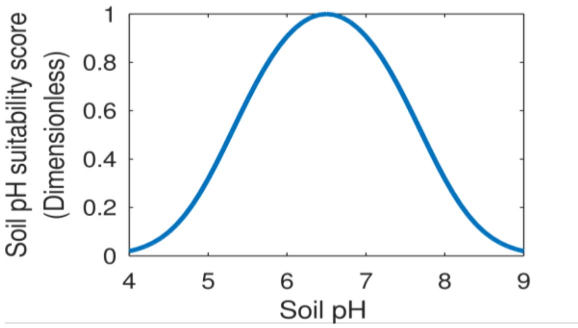

Figure 95. Avocado: soil pH suitability score vs soil pH.

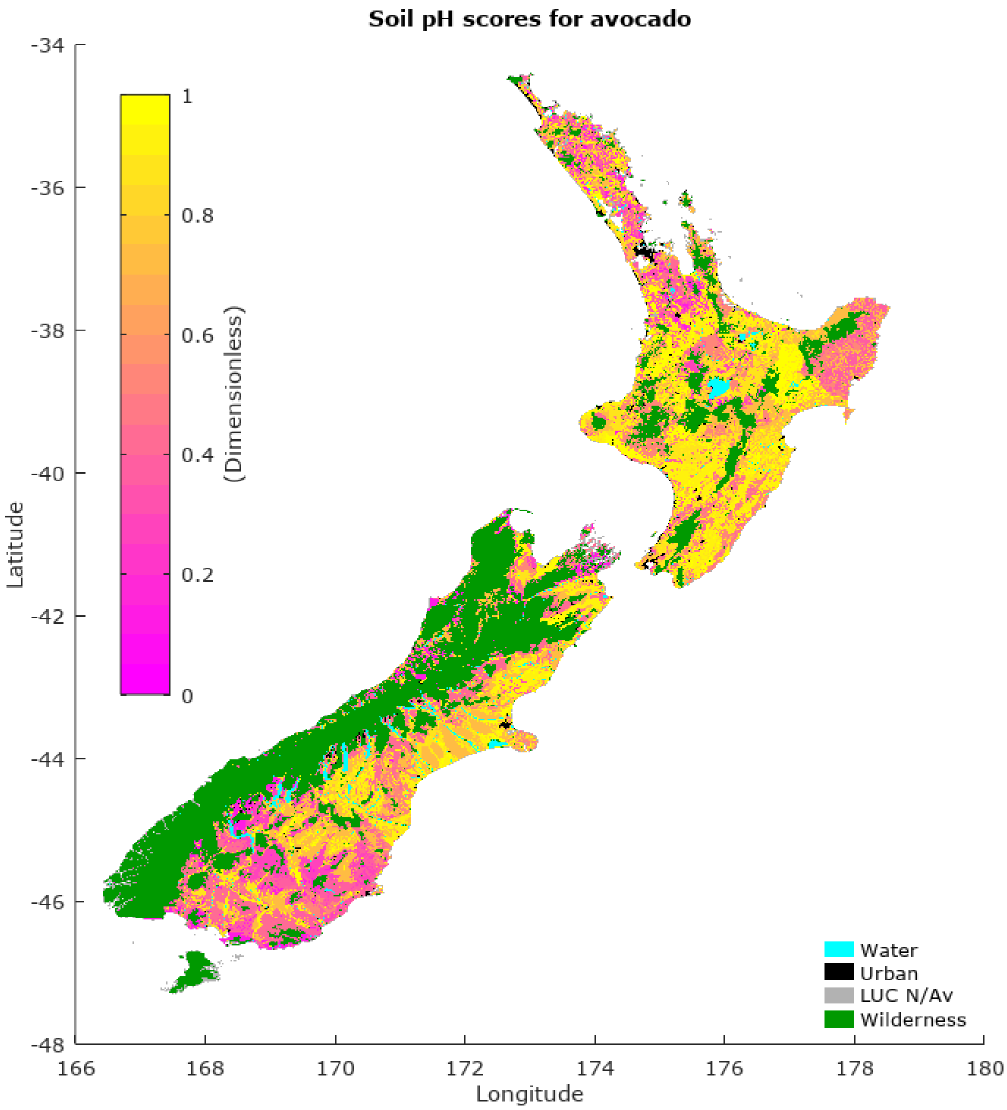

Figure 96. Avocado: soil pH suitability scores for locations across the country.

4.5.2 Blueberry

Both Highbush and Rabbiteye blueberry exhibit optimal growth in organic soils when soil pH is between 4 and 5, but in mineral soils, because of the potential for aluminium and manganese being bioavailable at low pH, best growth occurs in soil pH of 5 to 5.5 (Hayes 1988). For blueberry, Griffiths et al. (2003) give a soil pH requirement of 4.0 to 5.5, Masabni (2007) gives a range of 4.5 to 5.2, while Zydlik et al. (2019) give a pH requirement of 3.5 to 4.0 in peat soils. Jiang et al. (2019) found that at soil values of pH 5.5 and 6.0, the decrease in yield compared with pH 4.5 was 20 and 92% in cultivar ‘Climax’ and 32 and 76% in ‘Chaoyue No. 1’. However, the optimal pH can vary with the medium used for planting, and in trials with five clonal lines, using four different types of potting media with varied pH, optimal growth occurred at pH values at 4.2, 4.9, 5.0 and 5.5 (Hall et al. 1964). Blueberries New Zealand give a pH requirement of 4.0 to 5.5, and state that the optimum pH is 4.8 (https://www.blueberriesnz.co.nz/industries/growing).

We used a suitability score that had values ≥0.99 in the soil pH band 4 to 5 (1.0 at 4.5), and sharply declining outside that range, with a value of 0.65 and 0 at pH 5.5 and 6.0, respectively. The function is symmetrical and would give a suitability score of 0.65 at pH 3.5, although the pH values in the database do not go that low (Figure 97). Figure 98 shows suitability scores for locations across New Zealand, indicating many areas of high suitability for soil pH distributed across the country, with large areas of the Waikato being favourable. The Bay of Plenty is generally less favourable, indicating that orchards located there may require some mitigation of unfavourable soil pH.

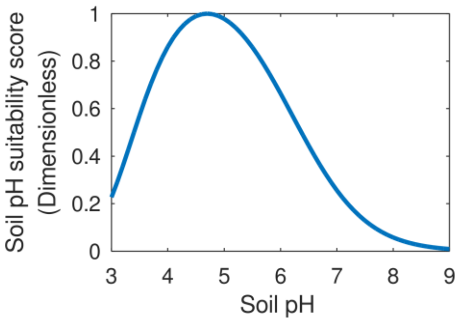

Figure 97. Blueberry: pH suitability score as a function of soil pH.

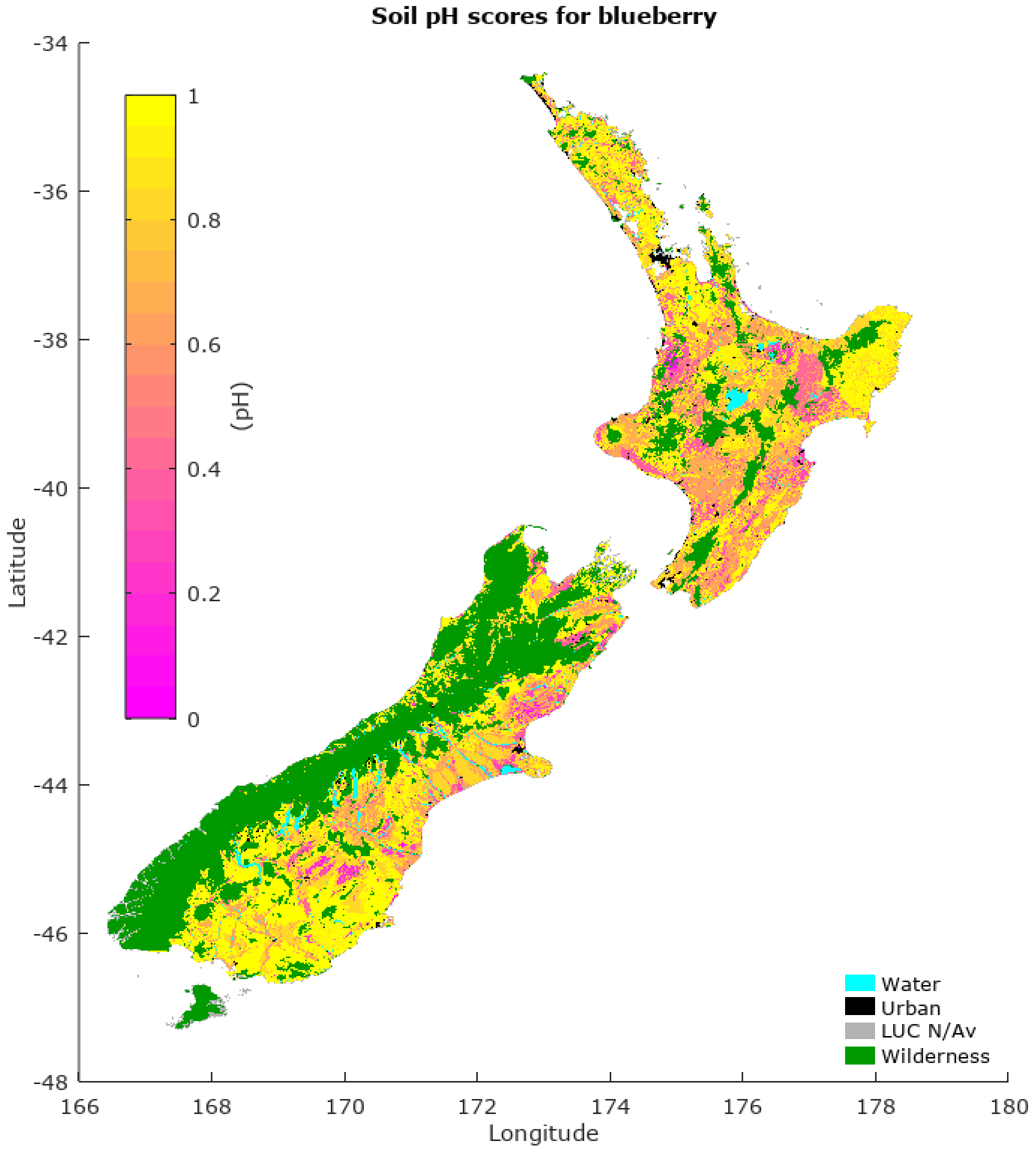

Figure 98. Blueberry: suitability score for soil pH for locations across the country.

4.6 Combined soil/land-related suitability criteria

We used extracted LRI data on PRD, drainage quality, slope and LUC to calculate suitability scores for the soil/land-related criteria for different geographical locations in New Zealand with a 1 x 1 km grid resolution. The location of urban areas, quarries, rivers and lakes were indicated in the LRI data and correspondingly were not associated with data. Other areas lacked LUC or drainage information, and many of these were in conservation areas (identified in DOC Public Conservation Areas database).

Suitability scores for slope, drainage, PRD, LUC and pH (where appropriate) were combined for each grid-square by taking weighted geometric means of the scores to provide an overall land suitability score. As with combing the climate criteria scores, a higher weight reflects a higher significance placed on the corresponding criterion. Weights were finalised after feedback from the consultation process.

4.6.1 Apple

For apple, the suitability scores for PRD and LUC were given weights of 1.0 while a weight of 2.0 was used for drainage, indicating the importance of drainage for good plant health and survival. Slope suitability was weighted 0.5, reflecting that this was considered to have less importance. The resulting map of land suitability is shown in Figure 99.

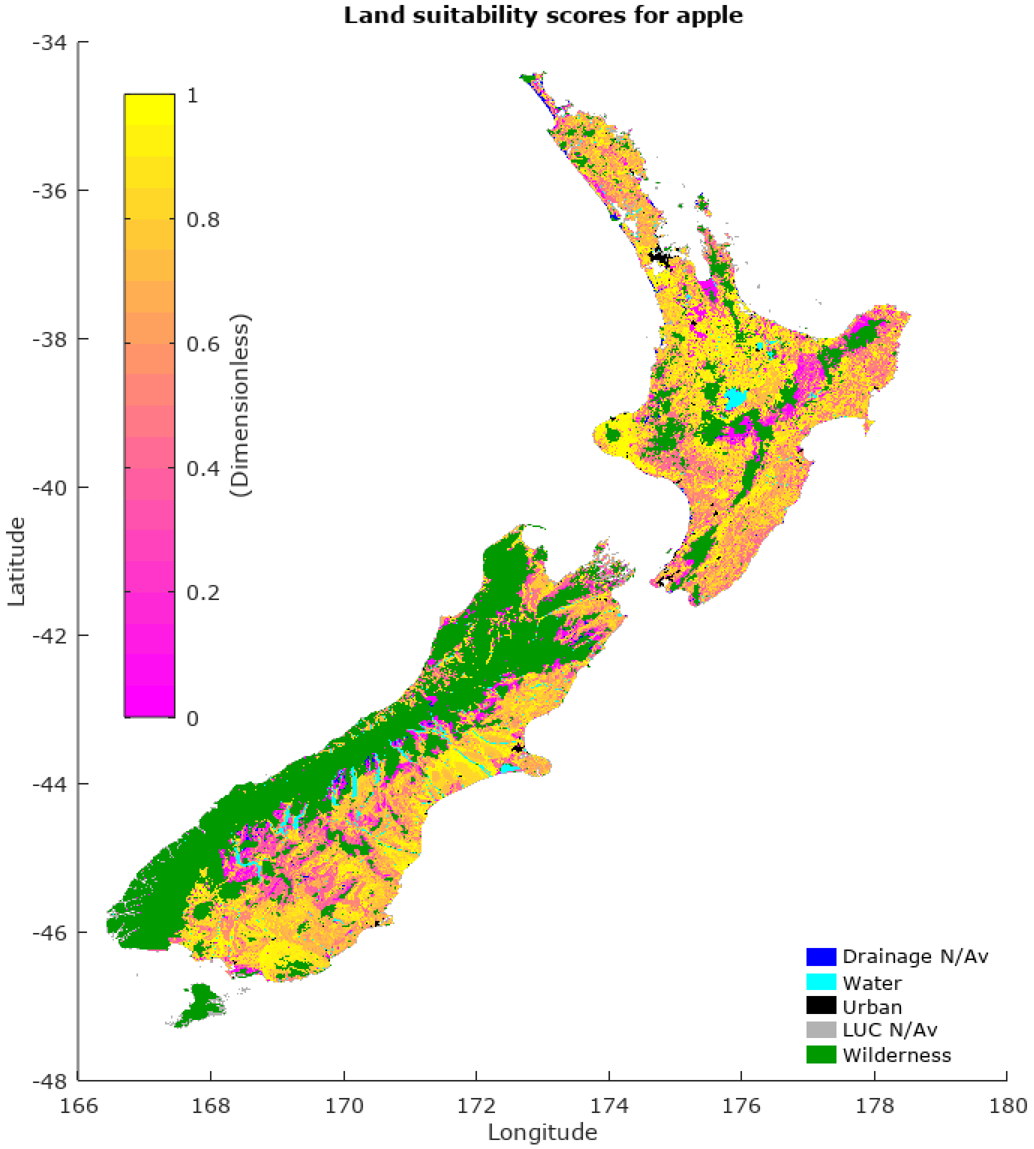

Figure 99. Land/soil suitability score map for apple.

4.6.2 Kiwifruit

For kiwifruit, a weight of 2.0 was used for drainage suitability, while weights of 1.0 were used for PRD and LUC and slope. The higher weight for the latter compared with apple reflects the impediment that slopes pose for constructing supporting structures for kiwifruit. Maps of land suitability for the country are shown for both, kiwifruit and apple in Figure 100.

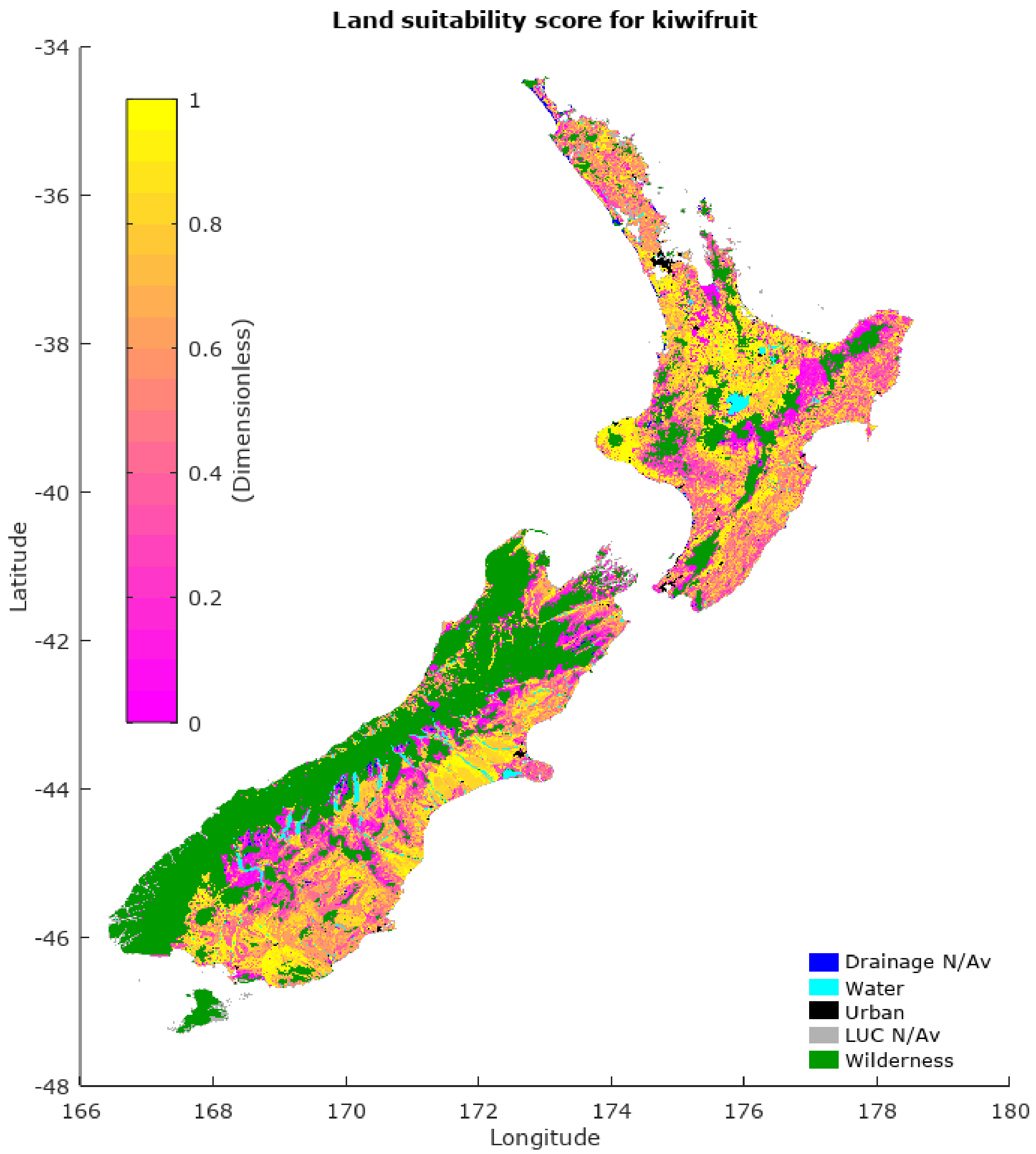

Figure 100. Land/soil suitability score map for kiwifruit.

4.6.3 Avocado

We used a value of 0.25 for the weight for the slope score to reflect reduced importance, while giving drainage a weighting of 3. Rooting depth, LUC and soil pH were given weights of 1 (Figure 101).

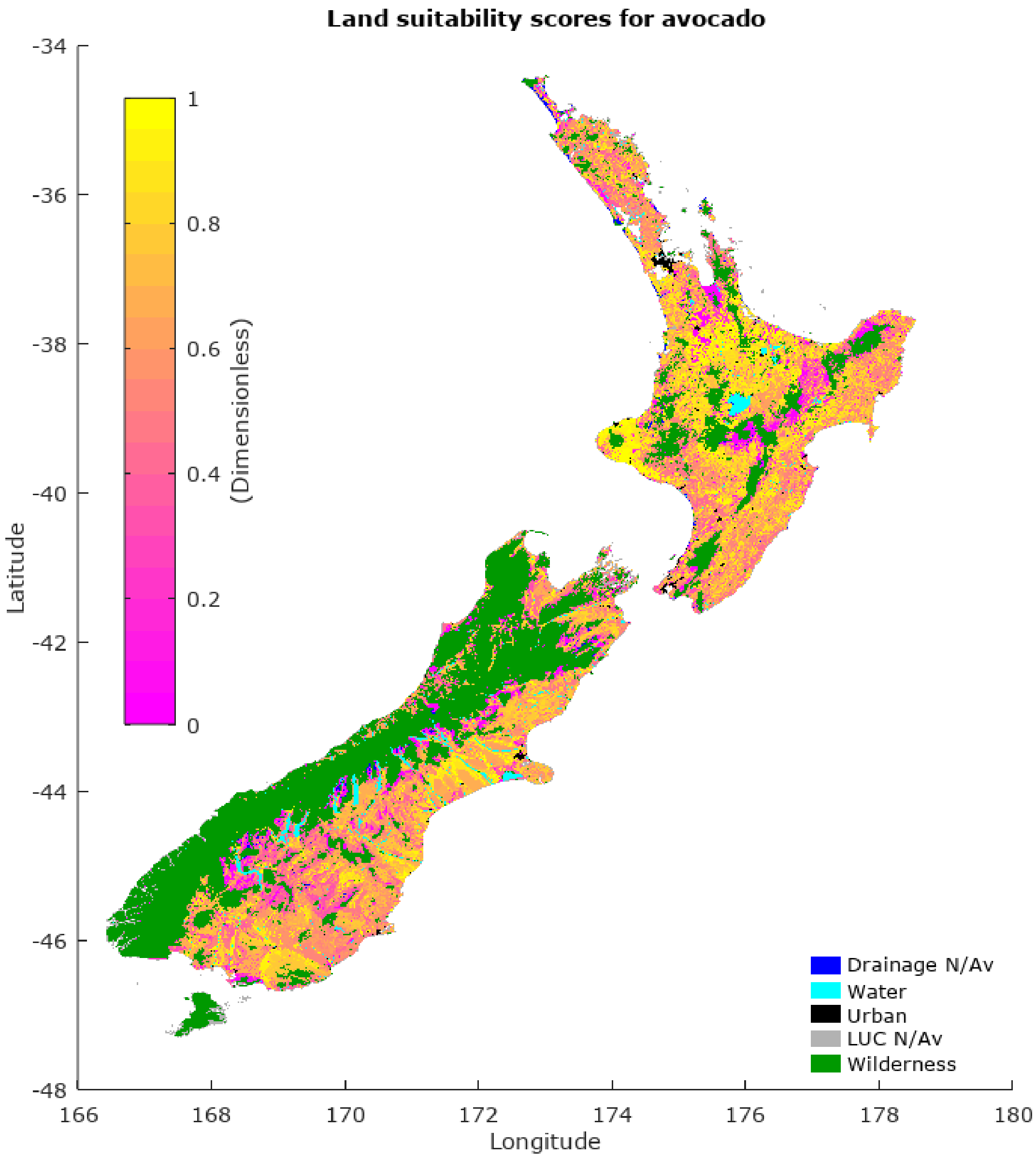

Figure 101. Avocado: overall land/soil suitability scores for locations across the country.

4.6.4 Blueberry

We used weights of 0.5 for slope, and 1 for LUC and rooting depth, 3 for drainage and 2 for soil pH (Figure 102). While drainage and soil pH are critical, these parameters can be mitigated by growing blueberry in containers; however, this would entail extra setup costs and hence the weights are set relatively high. Similarly, rooting depth can be mitigated by container growing or mounding.

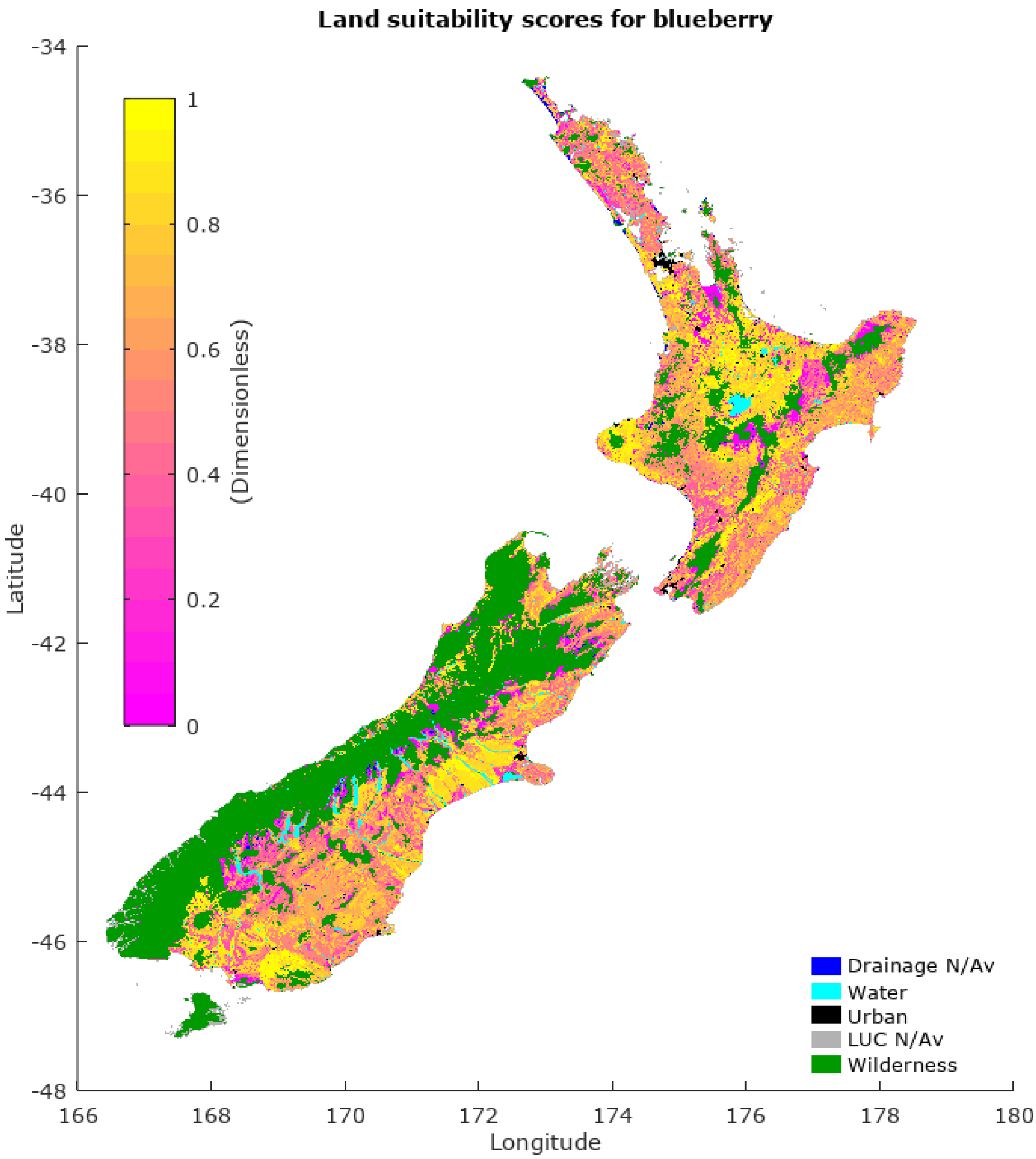

Figure 102. Blueberry: overall soil suitability for locations across the country.

4.6.5 Cherry

We chose weights of 0.5 for slope, 1 for rooting depth and LUC, and a weight of 2 for drainage. This gave the overall land suitability map in Figure 103.

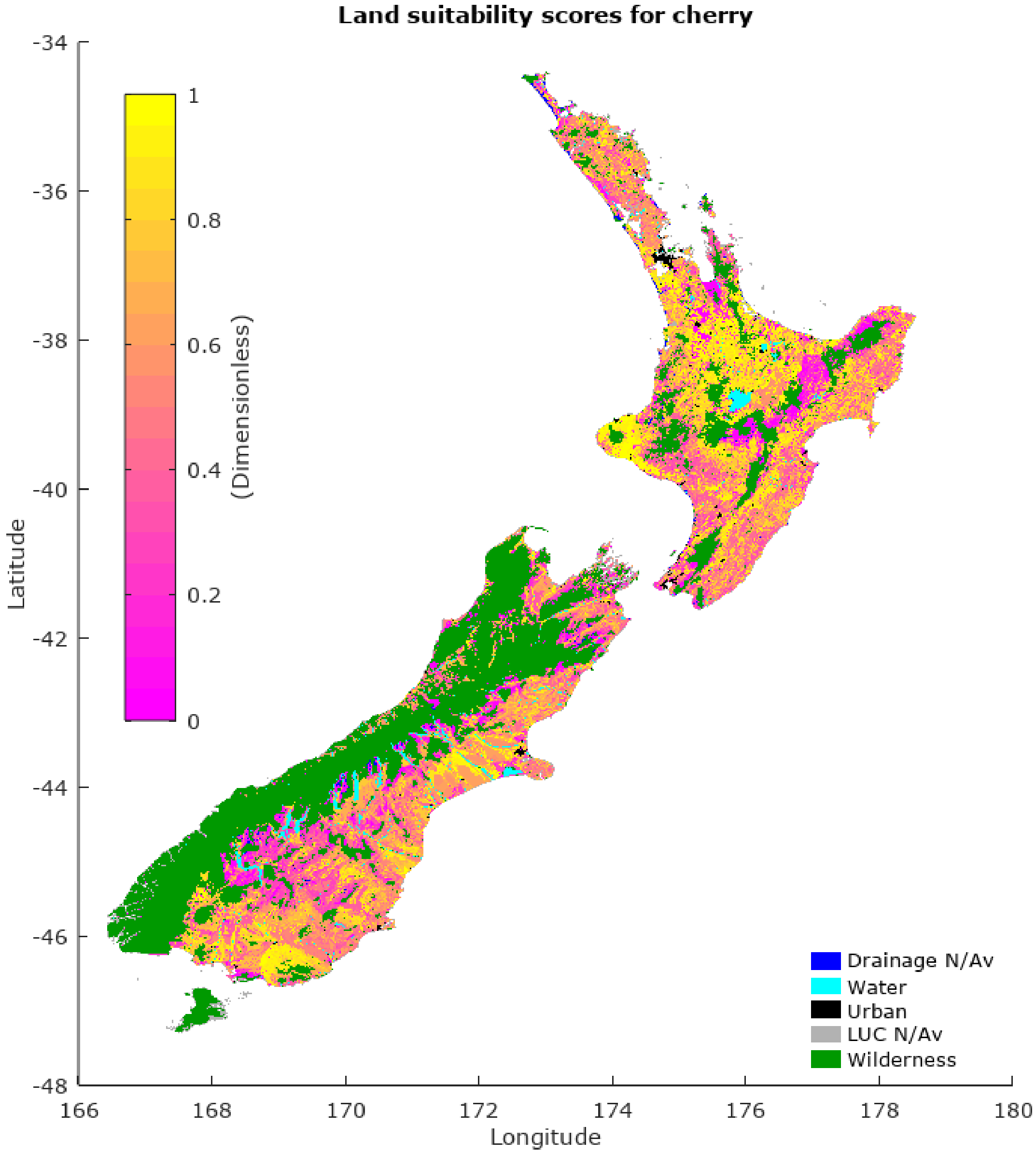

Figure 103. Cherry: overall soil suitability for locations across the country.

4.6.6 Wine grape

We chose weights of 1 for slope and drainage, 0.5 for PRD and 0.25 for LUC (Figure 104).

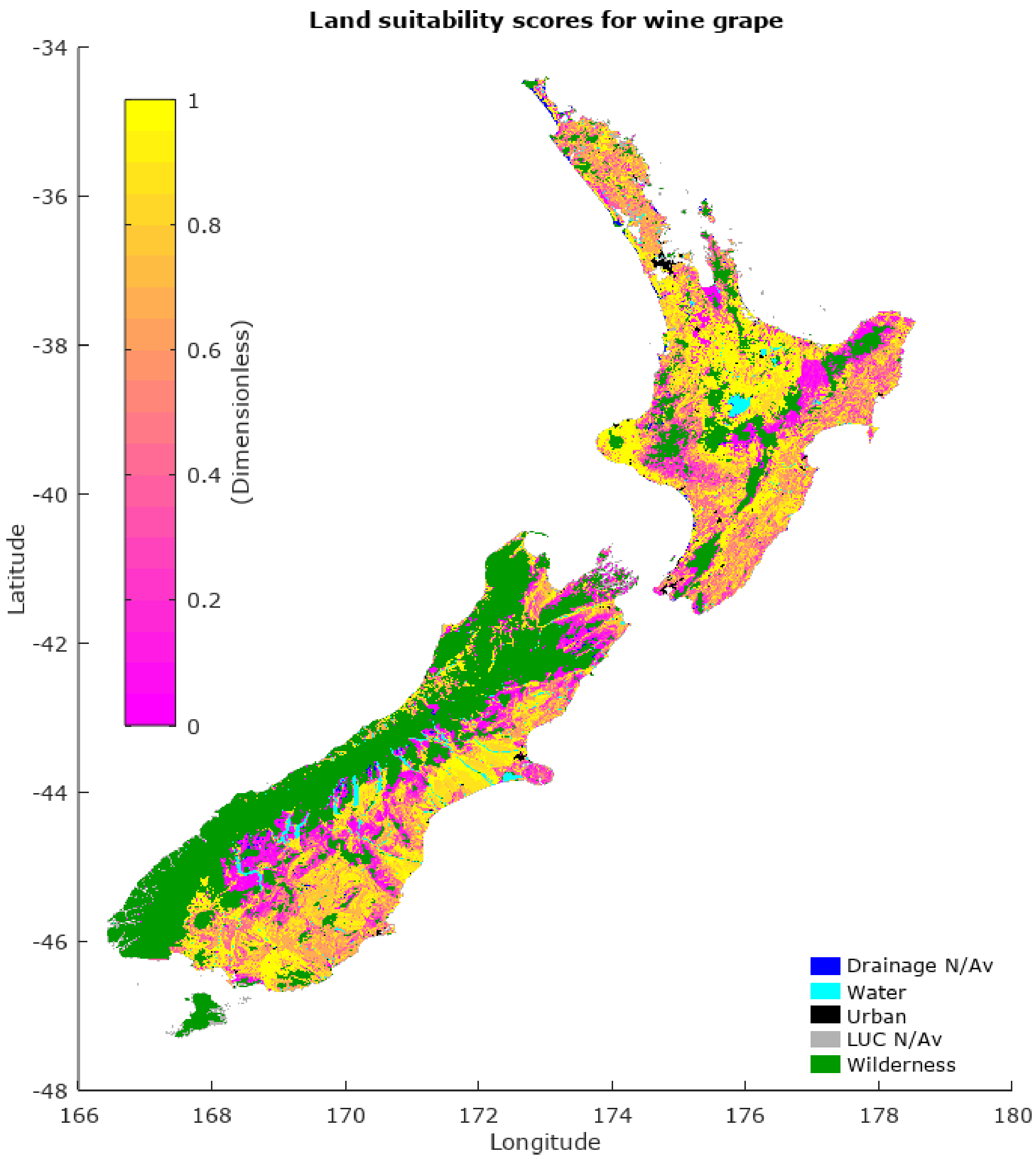

Figure 104. Grape: overall soil suitability scores for locations across the country.

5 Cultivation suitability

A cultivation suitability score was computed as the geometric mean of the land suitability score and average climate suitability score, weighted by a function of the underlying criteria weights. Cultivation suitability maps constructed from the LRI data and VCSN data for the period from 2006 to 2016 are shown for all crops in Figure 105 to Figure 110 below.

5.1 Apple

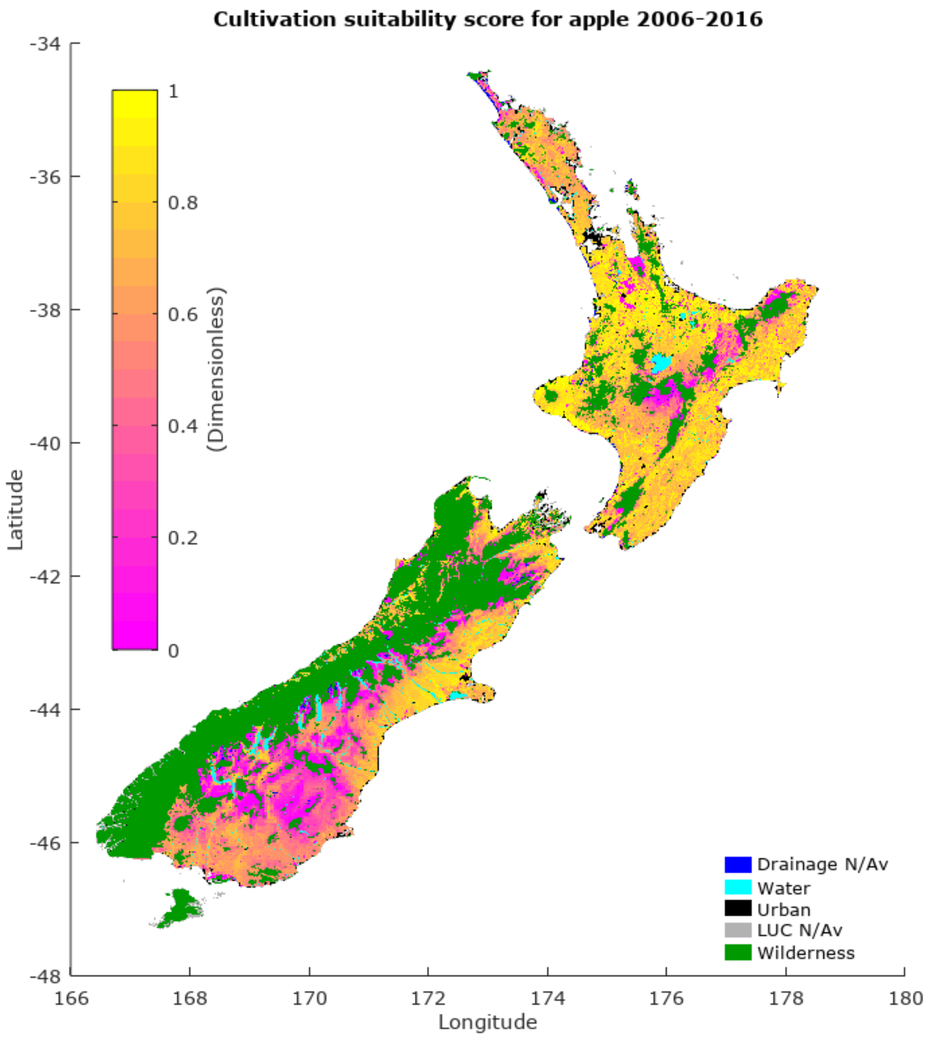

Figure 105. Cultivation suitability scores for apple across New Zealand when all climate- and soil/land-related scores are combined. This map is in line with the main apple growing regions of Hawke's Bay, Nelson and Central Otago with growing also taking place in other areas found suitable around the North Island and in Canterbury. Additionally, Taranaki is indicated has having high suitability. Calculations used Virtual Climate Station Network (VCSN) data.

5.2 Kiwifruit

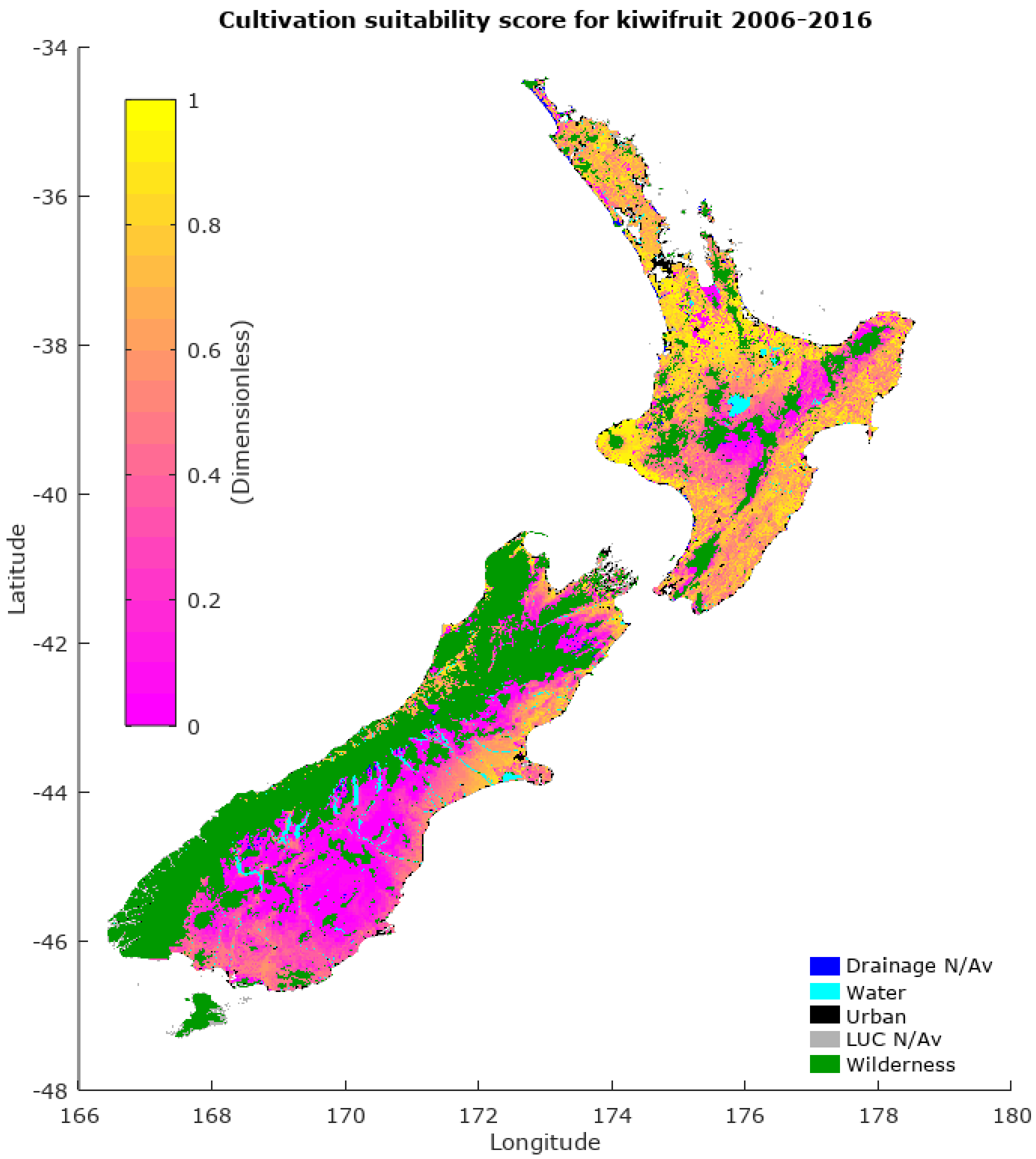

Figure 106. Cultivation suitability scores for kiwifruit across New Zealand when all climate- and soil/land-related scores are combined. The map prediction reflects the current kiwifruit footprint, which has its main production area in the Bay of Plenty and strong production in Northland, Gisborne, the Hawke's Bay and Nelson. Additionally, Taranaki is indicated as having high suitability for kiwifruit, with some areas of North Canterbury predicted to have moderately high suitability. Calculations used Virtual Climate Station Network (VCSN) data.

5.3 Avocado

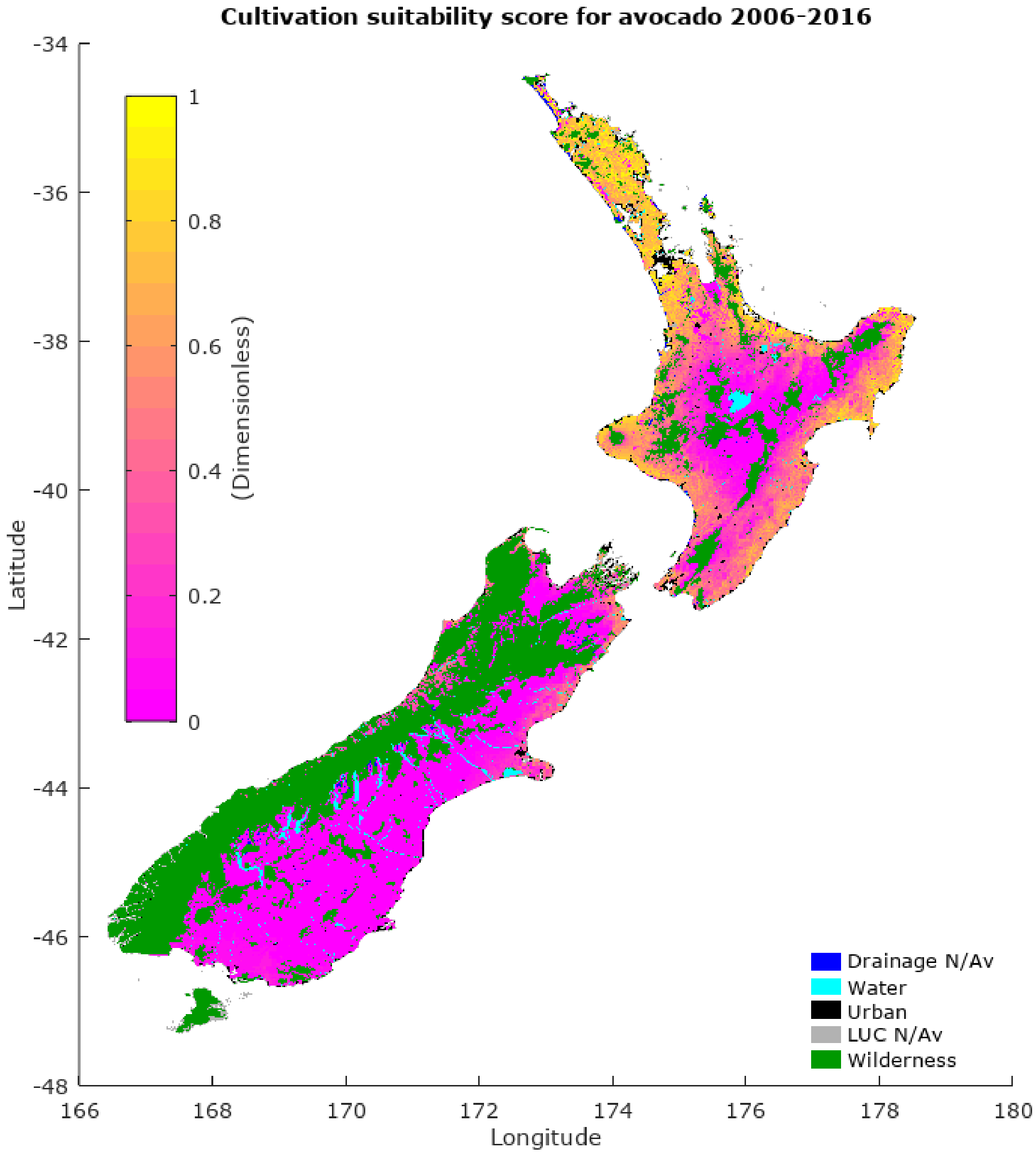

Figure 107. Avocado: overall cultivation suitability scores for locations across the country. The map is consistent with avocado production having its main production area in Northland but with strong production in the Bay of Plenty and Gisborne. Calculations used Virtual Climate Station Network (VCSN) data.

5.4 Blueberry

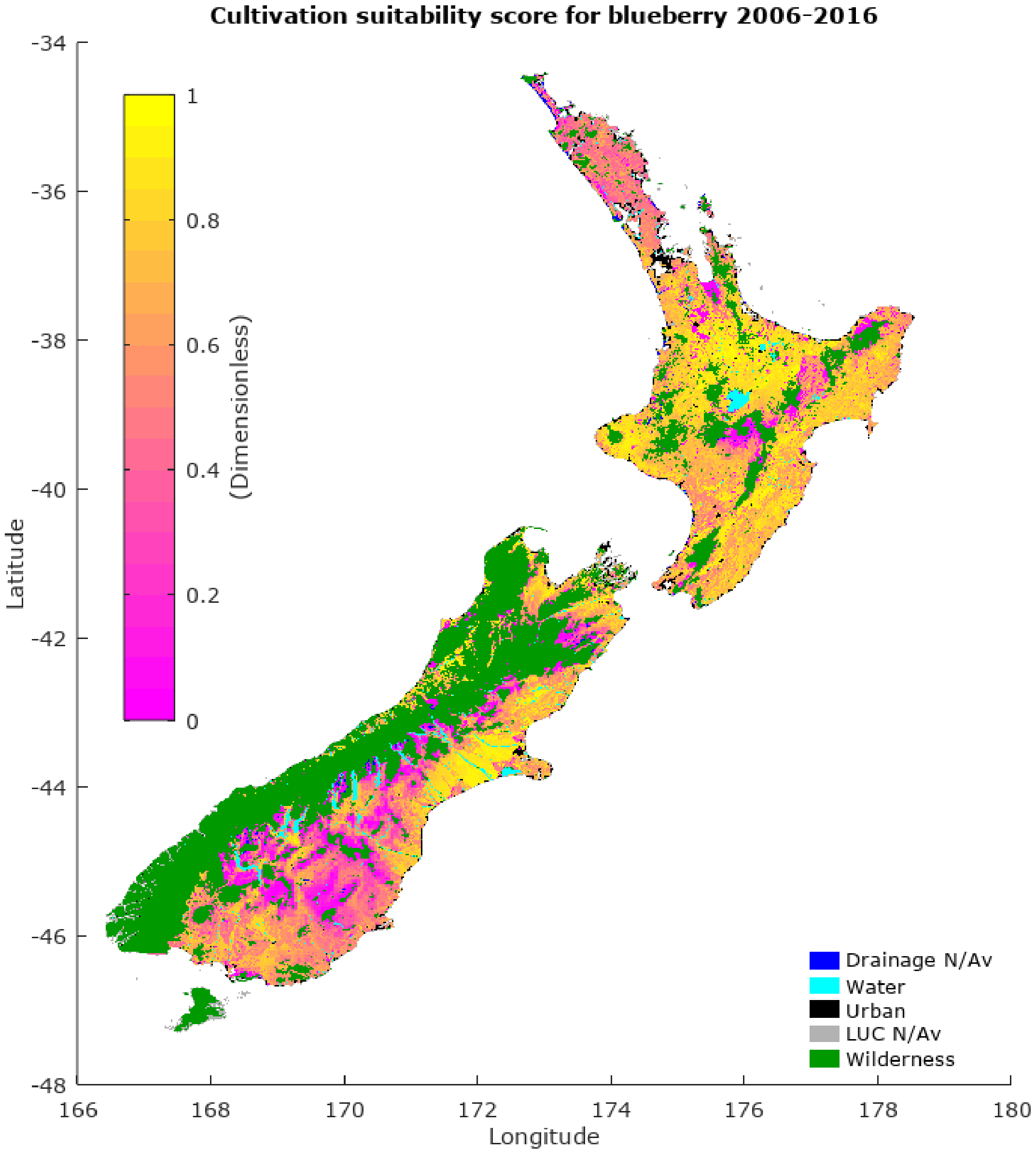

Figure 108. Blueberry: overall cultivation suitability for locations across the country. This map is in line with blueberry production occurring around the North Island and parts of the South Island, with the main production areas being located in the Waikato and to a lesser extent in the Bay of Plenty. Calculations used Virtual Climate Station Network (VCSN) data.

5.5 Cherry

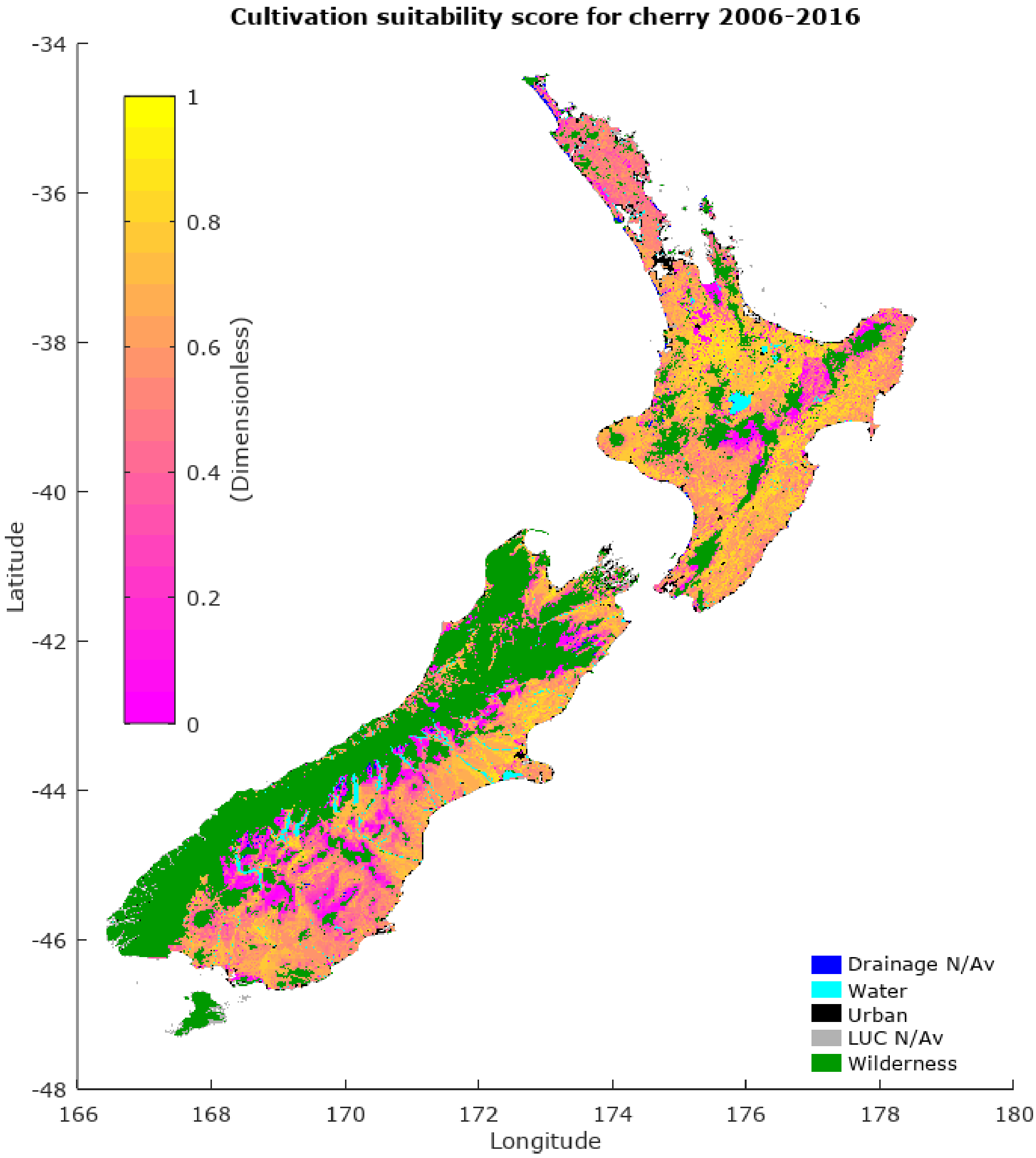

Figure 109. Cherry: overall cultivation suitability for locations across the country. This map is in line with cherry having a small footprint with its main production areas being Central Otago, and with strong production in the Hawke's Bay. Calculations used Virtual Climate Station Network (VCSN) data.

5.6 Wine grape

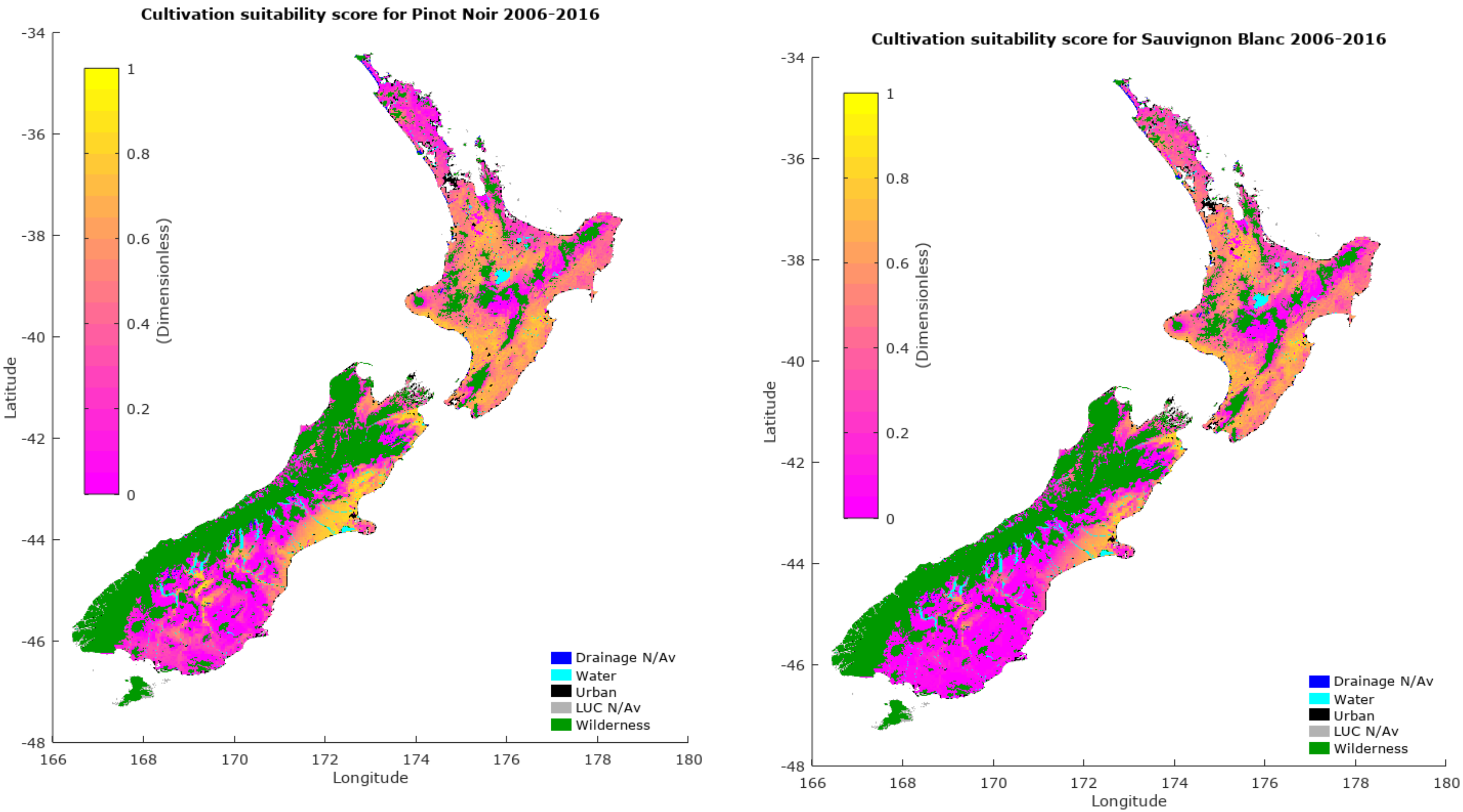

Figure 110. Overall cultivation suitability scores for Pinot noir (left) and Sauvignon blanc (right) for location across the country. These maps are consistent with current Pinot noir production occurring mainly in Marlborough, Central Otago, North Canterbury, Nelson, the Wairarapa and Hawke's Bay, and with current Sauvignon blanc production occurring mainly in Marlborough, the Hawke's Bay, North Canterbury, Nelson, the Wairarapa and Gisborne. Calculations used Virtual Climate Station Network (VCSN) data.

6 Adjustment of future-climate projection data

For purposes of consistency when assessing climate-change impacts on crop suitability, suitability maps that are developed using data from the future period of climate model simulations should be compared with suitability maps developed using data from the historical period of the same climate model simulations. However, for such comparisons to provide meaningful estimates of future change, the latter maps must closely resemble suitability maps developed from observed data for the same historical period. If this is not the case, then it is imperative to make adjustments to the climate model data (Challinor et al. 2018).

6.1 Modelled climate data

The modelled climate data were supplied by NIWA, and were derived from NIWA's high resolution Regional Climate Model (RCM), which was applied on a domain that encompasses all of New Zealand. When the RCM is run, it is constrained by conditions for the boundary of this domain. In alternative simulations, these 'boundary conditions' were provided by outputs from the six CMIP5 GCMs: BCC-CSM1.1, CESM1-CAM5, GFDL-CM3, GISS-EL-R, HadGEM2-ES and NorESM1-M. Each was run under four RCPs. Each RCP represents a different scenario of future atmospheric GHG concentrations, and thus four different levels of global and regional warming were considered.

The daily RCM data start in 1971 and extend until at least 2099, with the end date of simulations varying with climate model and RCP. Simulations for the period 1971 to 2005 are considered to be historical simulations and are referred to as 'RCP Past'; for each CMIP5 model, all four RCPs share the same RCP Past dataset. Simulations from 2006 onwards are considered to be future simulations.

The Raw RCM data were "bias corrected" with the aim that they would reflect the same climatology as the observed data (VCSN), although year-to-year variability would be different (Ministry for the Environment 2018). Such corrections are necessary because inherent errors in the representation of local surface conditions and processes in RCMs can lead to considerable systematic biases in RCM data, and reducing these biases will increase the confidence of regional climate impact studies (Sood 2015). Two corrections were performed. The first addressed errors in the probability distribution of model data by determining correction factors for a training period (1980–1999) at a coarse model resolution (30 km), and then applying them consistently to RCM data for the historical period and the future projections. The second calculated, at each grid point, the mean bias between observations and model data over the period 1986 to 2005, and subtracted it from the entire model dataset for the historical and future periods (Ministry for the Environment 2018).

6.2 Differences between RCM- and VCSN-based maps

Crop suitability rules are generally sensitive to extremes in temperatures, as well as means of maximum and/or minimum temperatures. Thus a minimum requirement for agreement in baseline maps generated from different climate datasets is that the climate datasets have similar statistical properties. However, in an investigation into the cause of the differences between the RCP Past and VCSN Past maps (Vetharaniam et al. 2020a), we found differences in statistics between the climate model datasets and the VCSN datasets, and identified these as the main cause of the observed biases in maps.

6.3 Statistical differences between RCM and VCSN data

Here we present some of our key findings from Vetharaniam et al. (2020a), where we found that the means and variances of annual maximum and minimum temperatures for all six climate model datasets showed notable differences from those calculated for the VCSN data.

6.3.1 Bias and variance ratio for annual daily maximum and minimum temperatures

For each RCM climate dataset, we calculated the mean and variance for annual daily maximum temperature for the 1972–2000 period, individually for each location, and from these calculated the mean bias and variance ratio with respect to the corresponding VCSN statistics ratio (Vetharaniam et al. 2020a). We performed the same calculations for annual daily minimum temperature study, and found that for both maximum and minimum temperature, mean biases were small across the locations, but variance ratios varied widely across locations and could be appreciably different from unity for elevations under 500m, which are more likely than higher elevations to be suited for horticulture (see Table 4). The period 1972–2000 was chosen to coincide with another climate model data series that was under examination in that study; the differences were similar if calculations were performed on the entire 1972–2005 RCP Past period.

Table 4. Mean bias and variance ratio for maximum and minimum temperature, calculated for six Regional Climate Model datasets with respect to the Virtual Climate Station Network (VCSN) data, calculated across all VCSN grid locations with elevations below 500m, for the years 1972–2000. Adapted from Vetharaniam et al. (2020a). Minimum and maximum values represent the extreme cases and correspond to only a few grid locations.

Dataset	Mean Bias			Variance ratio		
	Min.	Max.	Mean	Min.	Max.	Mean
Maximum temperature						
BCC-CSM1.1	–0.02	0.02	–0.01	0.58	2.13	0.96
CESM1-CAM5	–0.02	0.00	–0.01	0.58	2.15	0.94
GFDL-CM3	–0.02	0.02	0.00	0.58	2.17	0.97
GISS-EL-R	–0.03	0.01	–0.01	0.60	2.21	0.98
HadGEM2-ES	–0.04	0.01	–0.01	0.57	2.14	0.95
NorESM1-M	–0.01	0.03	0.00	0.58	2.17	0.98
Minimum temperature						
BCC-CSM1.1	–0.01	0.02	0.00	0.56	1.39	0.88
CESM1-CAM5	–0.02	0.01	0.00	0.56	1.36	0.87
GFDL-CM3	–0.01	0.03	0.01	0.55	1.40	0.88
GISS-EL-R	–0.02	0.02	0.00	0.56	1.38	0.88
HadGEM2-ES	–0.03	0.01	–0.01	0.55	1.37	0.88
NorESM1-M	–0.02	0.02	0.00	0.56	1.41	0.89

These results show that although the previous bias correction of the RCM datasets (Ministry for the Environment 2018) ensured agreement with the VCSN dataset on annual mean temperatures, it did not ensure that the agreement in the range of temperatures about the means at all locations. For example, a variance ratio of 0.5 corresponds to roughly a 30% reduction in temperature spread about the mean, while a variance ratio of 2.0 corresponds to approximately a 40% increase in the temperature spread about the mean. Furthermore, we found differences between the RCP Past datasets and the VCSN Past datasets in the distribution of monthly minimum and maximum temperatures, and since many crop suitability rules are sensitive to seasonal or monthly temperatures, this would also be a major contributor to the differences in the baseline suitability maps.

6.4 Adjustment of RCP datasets

We have identified that a large component of the differences between the RCP-Past-based crop suitability maps and VCSN-based crop suitability maps arise from differences in the statistical properties between the RCP Past and VCSN datasets, despite the RCP Past datasets being bias corrected to the VCSN datasets. In our previous report investigating this, we suggested that the main statistical differences between the RCP Past datasets and the VCSN dataset related to both (i) differences in the distributions of annual means for maximum and minimum temperature within the bias-correction period and (ii) differences in the variances of yearly maximum and minimum temperatures within the bias-correction period, and suggested that adjustments to address these differences would provide closer agreement in past-period suitability maps (Vetharaniam et al. 2020a).

However, we found that although performing adjustments to yearly statistics improved the alignment of climate model suitability scores with the VCSN suitability scores, adjustment on quarterly data statistics gave more improvement overall (Vetharaniam et al. 2020a). Subsequent to that report, we chose to perform adjustment of the RCP Past temperature data at the level of monthly statistics, which would also ensure better alignment for quarterly and annual levels. Since adjustment for bias in annual mean temperatures does not guarantee zero bias for monthly mean temperatures, our adjustment included bias adjustment for each month.

In adjusting the RCP data to the VCSN data, we have assumed that the latter provide a reasonable representation of New Zealand weather patterns. The biases for means and variance ratios in the RCP data with respect to the VSCN data are considered to be due to errors inherent in representing local surface conditions and processes (Ministry for the Environment 2018), and it is assumed that these biases are invariant over time. The adjustments we applied were designed to maintain trends in the RCP data, and be compatible with non-stationary climates.

Challinor et al. (2018, Supplementary material) noted that a variety of bias adjustment methods exist but none can fully correct the errors that are inherent in all GCMs without compromising the climate change physics. Those authors recommended using multiple correction methods if possible. However, we used only one method (adjustments of monthly means and adjustments of variance on two time scales) for temperature, a simple mean bias adjustment for RH, and a simple scaling of rainfall, which we found gave satisfactory improvement in alignment of baseline suitability scores for our purpose. When discussing unresolved issues and limitations of bias correction, Maraun et al. (2017) raised the possibility that adjusting data might alter climate change signals. We present an evaluation of the impact of our adjustments in Section 6.5.

6.4.1 Adjustment of RCP Past temperature datasets to align monthly statistics

We have refrained from presenting equations in earlier sections of this report and used graphs to represent relationships, in order to improve accessibility. However, the use of equations is required in this subsection for precision and clarity.

The approach that we developed for adjusting the daily temperature time series in the RCP datasets incorporates the variance-scaling-of-temperature methods described in the literature (Chen et al. 2011; Teutschbein & Seibert 2012) but applies successive variance adjustments to adjust for differences in intra-month variance (Step 1) and inter-year monthly variance (Step 2), for maximum and minimum temperature. The inter-year monthly adjustment scales monthly means around the trend in monthly means. This was then followed by a standard mean bias adjustment (Maraun 2016) but on a monthly rather than annual level (Step 3). The adjustments are applied separately for each month from January to December. A schema to explain Steps 1 and 2 below is presented in Figure 111.

1. Adjustment for differences between each RCP dataset and the VCSN dataset in the mean variance of daily maximum and minimum temperatures for each month:
   $T_i^j \rightarrow (T_i^j - \overline{T_i}) \cdot \sigma_{d,V} / \sigma_{d,R} + \overline{T_i}$, for each day, j, of the month and year, $i = 1972, \ldots, 2005$
   a) T_i^j is the maximum or minimum temperature on the j^{th} day of the month in year i
   b) $\overline{T_i}$ is the mean daily maximum or minimum temperature for the month in year i
   c) $\sigma_{d,R}$ is the standard deviation of daily RCP maximum or minimum temperature for the month, calculated over the 1972–2005 period using the formula
   $\sigma_{d,R}^2 = \frac{1}{N} \sum_{i=1}^{N} \sum_{j=1}^{n_i} \frac{\left(T_i^j - \overline{T_i}\right)^2}{n_i - 1}$,
   with N being the number of years and n_i being the number of days in the month for year i.
   d) $\sigma_{d,V}$ is the standard deviation of daily VCSN temperatures for the month over the same period, calculated by applying the equation in b) to the VCSN data.
2. Adjustment for the difference between each RCP dataset and the VCSN dataset in the variation of monthly mean maximum or minimum temperature around the corresponding monthly mean for the period :
   $T_i^j \rightarrow T_i^j - \Delta T_i$
   $\Delta T_i = (\overline{T_i} - \overline{T_i^s})(1 - \sigma_{m,V}/\sigma_{m,R})$, where:
   a) T_i^j and $\overline{T_i}$ are the same as in 1a) and 1b) above
   b) $\overline{T_i^s}$ is the value at year i of the spline smooth to the entire 1972-2099 data series
   c) $\sigma_{m,R}$ is the standard deviation of the RCP monthly mean of individual years around $\overline{T}_i$, calculated as:
   $\sigma_{m,R}^2 = \frac{1}{N-1} \sum_{i=1}^{N} \left(\overline{T_i} - \overline{T}\right)^2$ where $\overline{T}$ is the mean of $\overline{T_i}$ for the 1972-2005 period
   d) $\sigma_{m,v}$ is the standard deviation of VCSN mean (maximum or minimum) temperature for the month over individual years, calculated around the VCSN mean monthly (maximum or minimum) temperature over the 1972–2005 period using an analogous equation to that in 1 b).
3. Bias adjustment with respect to monthly means for RCP maximum and minimum temperature
   $T_i^j \rightarrow T_i^j - (\overline{T} - \overline{V})$, where

   $\overline{T}$ and $\overline{V}$ are RCP and VCSN mean (maximum or minimum) temperature for the month over the entire1972-2005 period.

Quantities pertaining to the adjustments for maximum and minimum temperatures are summarised in Figure 112 for elevations under 500m. There is little difference between the six RCP datasets in the pattern of their anomalies because the different RCP datasets were simulated using the same RCM but forced by different GCMS providing inputs at the spatial boundary of the simulation.

Additionally, we adjusted for an anomaly in the RCP data where some locations and some days, the value for the maximum temperature was lower than the value of the minimum temperature. We addressed this by swapping the values in such instances.

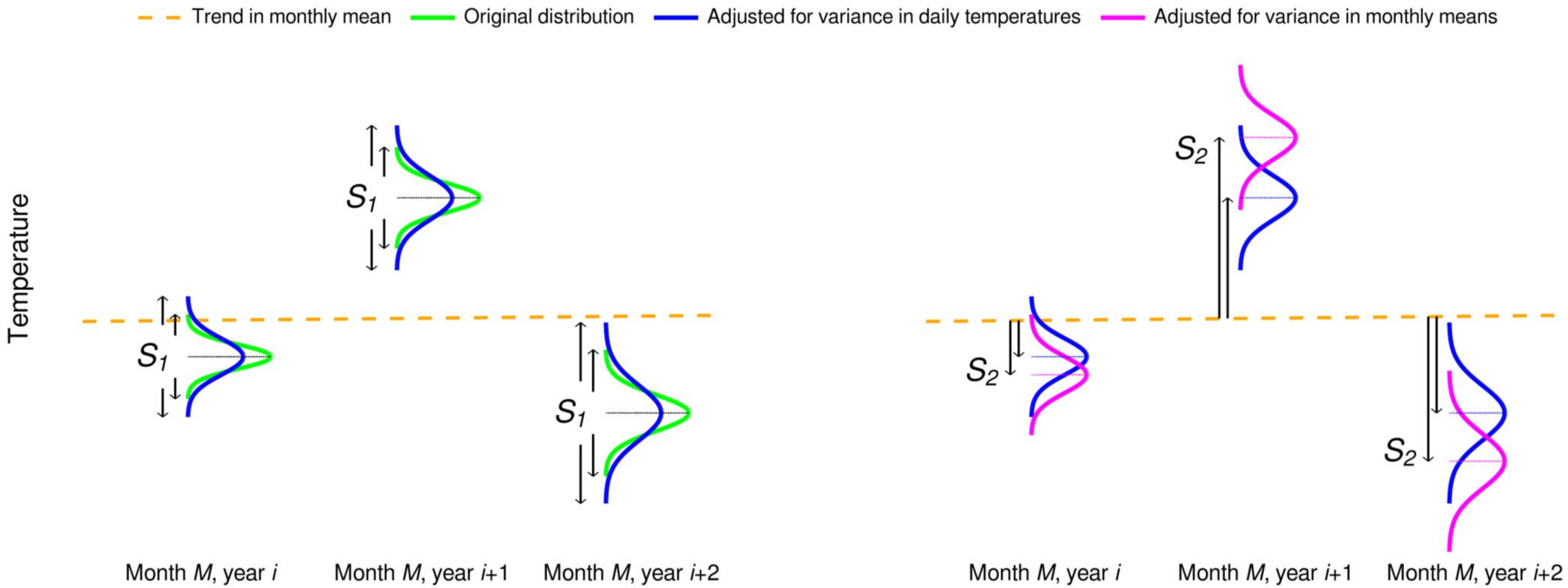

Figure 111. Schema showing the effect of Steps 1 and 2 in the adjustment procedure in Section 6.4.1. For each calendar month, M, Step 1 (left hand side) scales daily temperatures around their mean by the same scale factor, S_1, for each year. Step 2 (right hand side) scales the monthly means around the trend in the monthly mean by the same scale factor, S_2, for each year. This results in a translation of the temperature distributions for each month and year that is proportional to the scale factor and the deviation of the mean from the trend, without affecting the variance of the daily temperatures.

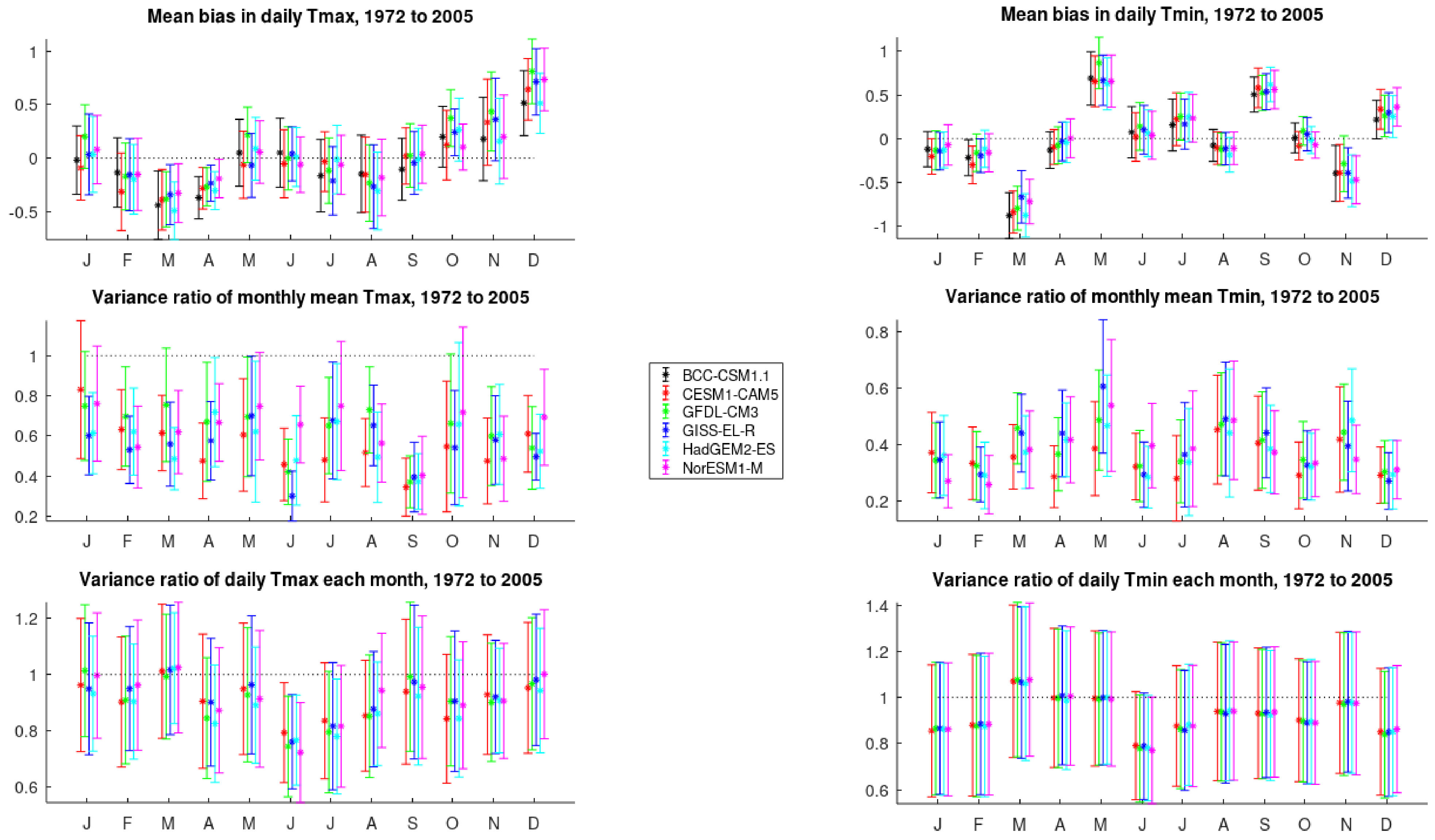

Figure 112. Distribution of mean biases and variance ratios for maximum and minimum temperatures for the RCP data series with respect to the VCSN data series, used in the adjustment of the RCP temperature data. Each error bar shows the mean and ±1 standard deviation over grid locations with elevations below 500 m across the country.

6.4.2 Adjustment of monthly RCP Past relative humidity data and rainfall data

While the VCSN datasets provide RH values, the RCP datasets instead contain daily vapour pressure data from which we calculated RH. The vapour pressure data had not been bias corrected, thus this bias is transferred to the RH data. Data on bias and variance ratio for RH values derived from the six RCPs with respect to the VCSN RH data are shown in Figure 113 for elevations under 500m. However, because RH is bounded above and below by 100 and 0%, performing the adjustments in Steps 1 and 2 for the temperature data was not appropriate. We investigated performing these adjustments on unbounded transformations of the RH data, but this approach was susceptible to numerical rounding issues. Thus for RH, we performed only a mean bias adjustment (analogous to Step 3 for the temperature data adjustments).

The rainfall data in the RCP datasets had been bias corrected on an annual basis. Means and standard deviations of mean biases and variance ratios for RCP rainfall values with respect to the VCSN rainfall data are shown in Figure 113, for grid locations with elevation below 500 m. Small mean biases in daily rainfall scale up when considering rainfall at the monthly level, and can be significant when calculating suitability scores that are rainfall dependent. Rainfall data are bounded below by zero, and also have a binary aspect of no rain versus rain. None of the adjustments applied to the temperature data were appropriate here, thus we obtained agreement in monthly rainfall by applying a scaling factor (Maraun 2016) to ensure agreement in mean rainfall.

6.4.3 Applying adjustments to RCP future datasets

The adjustments to the RCP Past temperature data in Steps 1 and 2 of Section 6.4.1 were applied to the RCP future temperature data using the same standard deviation ratios calculated for the Past period. The use of spline-smooth values in Step 2 ensures the extension of the adjustment to the future is consistent. The adjustments to the RH and rainfall data in Section 6.4.2 were also extended to the future, using the statistics calculated for the RCP Past period. To distinguish the new climate model datasets, we refer to them as “SLM RCP” data.

6.5 Effect of bias adjustments on climate change signals

Ministry for the Environment (2018) calculated climate change signals for the RCP Past data by comparing how key climate statistics changes from a reference period of 1986–2005 to the periods 2031–2050 and 2081–2100. We calculated differences between the SLM RCP datasets and RCP datasets in their change signals for the same time periods to gauge the impact of our bias adjustments on climate change signals. The SLM RCP datasets were calculated to only 2099 because not all of the 24 RCP datasets extended past 2099. Thus we used a late-century period of 2080–2099.

Climate signals for maximum and minimum temperatures and for RH were calculated by subtracting annual means for 1986–2005 from those for 2031–2050 and 2080–2099. Variance signals for maximum and minimum temperatures were calculated by taking annual variance ratios for 2031–2050 and 2080–2099 with respect to 1986–2005.

The change signal for rainfall was calculated as a percentage change from mean 1986–2005 rainfall to mean 2031–2050 and mean 2080–2099 rainfall. Change signals were calculated for each of the six GCM-driven datasets within each RCP, and also for the ensemble of datasets within each RCP.

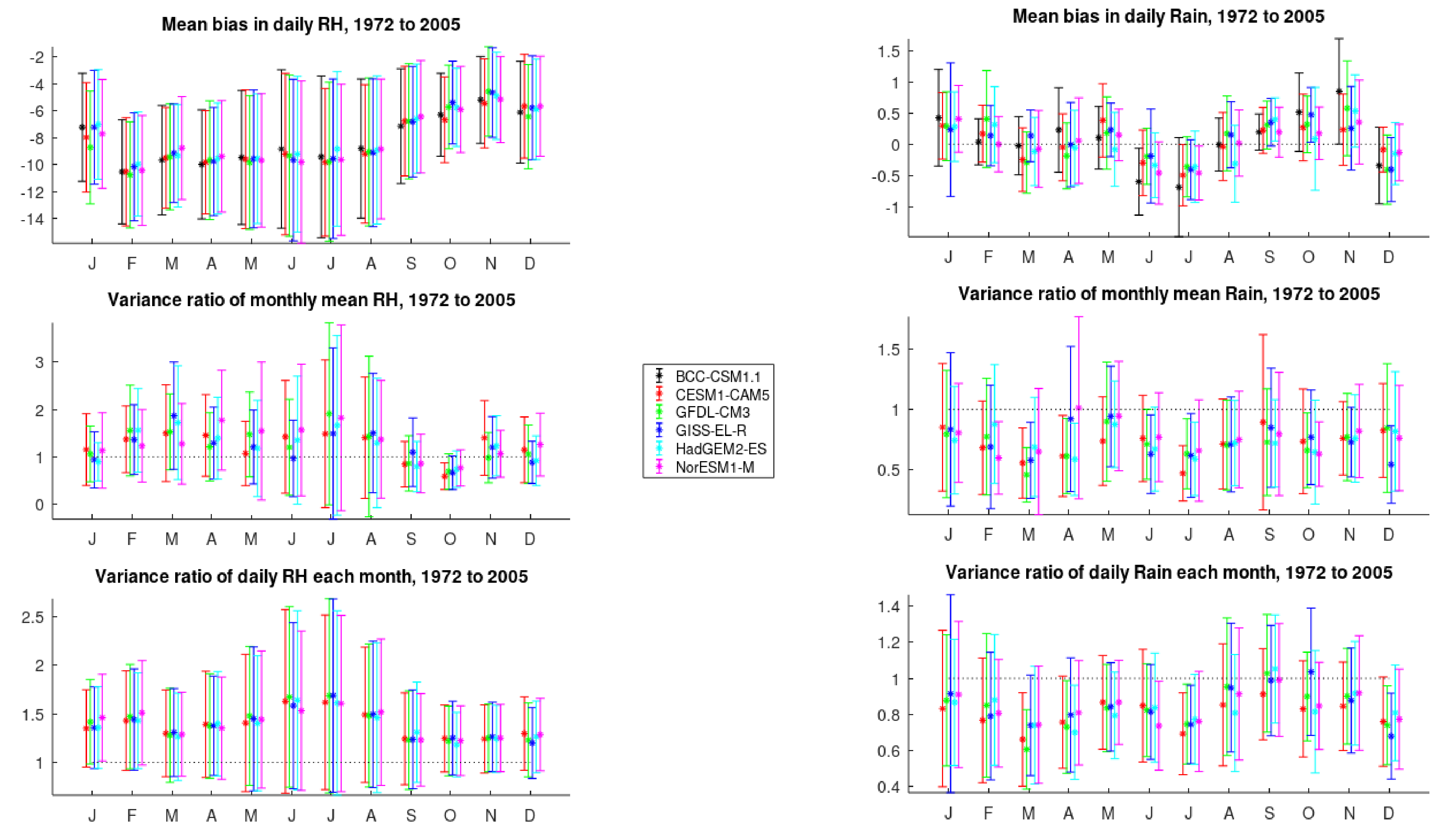

Figure 113. Distribution of mean biases and variance ratios for relative humidity (RH) and daily rainfall (rain) for the RCP data series with respect to the VCSN data series, used in the adjustment of the RH and rain data in the RCP datasets. Each error bar shows the mean and ±1 standard deviation for mean bias or variance ratio over grid locations with elevations below 500m across the country.

Bias-adjustment impacts for ensembles are presented in Table 5, showing generally very little impact on locations with elevations below 500m, which are more likely than locations with higher elevations to be used for horticulture. Ranking the impacts on change signals across locations by magnitude, the first percentile (P_1) of impacts for minimum temperature ranged across RCPs from −0.03°C to −0.02°C for both the 2031–2050 and 2080–2099 periods, and the corresponding 99th percentile (P_{99}) ranged from 0.00°C to 0.02°C (Table 5). That is, the bias adjustments affected the change signal for minimum temperature by at most a magnitude of 0.03°C for 98% of locations with elevations below 500m. Impacts on change signals were of similar magnitude for maximum temperature, and slightly smaller for mean temperature (Table 5). For all elevations, the P_1 for impacts on change signals for minimum and maximum temperature ranged from −0.06°C to −0.01°C across RCPs for both periods, and the P_{99} varied from 0.00°C to 0.06°C; the lowest extremum across RCPs and periods was −0.21°C and the highest was 0.21°C (Table 5), which in the context of our continuous suitability rules would have little significance. Across all elevations and periods, the impact on the change signals for mean annual temperature was very small (Table 5) because of the impacts of opposing sign cancelling when averaging minimum and maximum temperature.

In Section 6.4.1, the monthly mean bias adjustment in Step 3 will not affect annual change signals that are calculated as differences. Neither will the variance adjustment in Step 1 affect mean annual trends, since it scales around monthly means. In principle, the variance adjustment in Step 2 should not affect mean trends; however, a fitted spline may have small deviations from the average over a period, and this is likely the cause for the slight impacts on change signal for temperature. While a moving average could have been used instead of a spline, it would have been subject to end-point problems preventing symmetrical averaging near the beginning and end of the data series.

Impacts on change signals for annual temperature variance ratios tended to be small. For elevations under 500m, across RCPs and periods, for minimum temperature P_1 varied between −0.04 and 0.00 and P_{99} varied from 0.00 to 0.04 for minimum temperature and for maximum temperature varied P_1 between −0.05 and −0.02 and P_{99} varied between 0.00 and 0.02 (Table 5). For all elevations, across RCPs and periods, for minimum temperature P_1 varied between −0.04 and −0.02 and P_{99} varied from 0.00 to 0.04 and for maximum temperature P_1 varied between −0.05 and −0.02 and P_{99} varied between 0.00 and 0.02 (Table 5). The magnitude of impacts increased with RCP number, and tended to be skewed towards negative change (see Section 33 in the supplementary material). A few locations experienced an impact on the change signal for annual temperature variance that was significantly lower than the P_1 value, and some of these were for elevations lower than 500m, and for RCPs 6.0 and 8.5 the lower extrema were, respectively, −0.12 and −0.15 and occurred for the 2080–2099 period (Table 5 and see Section 33 in the supplementary material).

The monthly variance adjustments are expected to have an impact on the change signal for annual temperature variance since the adjustment factors vary with month of the year. When these monthly adjustment factors are applied to the future period of the RCP data, they scale monthly variance change signals differently for each month of the year. Unless variances for each month of the year are changed over time by the same factor, this will result in an impact for the annual variance change signal, although monthly change signals are not affected.

Similarly, the adjustment to rainfall involved adjustment factors that varied by month and thus will impact the change signal for annual rainfall (expressed as a percent change), although the change signal for monthly rainfall will not be, unless all monthly rainfall change signals are the same.

Table 5. Impact on climate change signals of the bias adjustments, expressed for each representative concentration pathway (RCP) as the difference in change signals between the ensemble of six adjusted "SLM RCP" datasets and the ensemble of six original RCP datasets. Change signals were calculated for 2031–2050 and 2080–2099 using a reference period of 1986–2005. Change signals for temperature and relative humidity were calculated as differences between period means, while change signals for temperature variances were calculated as the ratio of variances. The change signals for rain were calculated as a percentage change. Change signals were calculated individual for each location. Statistics are for all grid locations mapping the country. P_1 and P_{99} are the first and 99th percentile values, and LE and UE are the lower and upper extrema, respectively.

	Elevations <500m				All elevations							
Period	2031–2050		2080–2099		2031–2050				2080–2099			
	P_1	P_{99}	P_1	P_{99}	P_1	P_{99}	LE	UE	P_1	P_{99}	LE	UE
Annual minimum temperature signal impact (°C)												
RCP 2.6	−0.02	0.02	−0.02	0.01	−0.04	0.02	−0.17	0.03	−0.04	0.02	−0.20	0.02
RCP 4.5	−0.03	0.00	−0.03	0.01	−0.06	0.00	−0.19	0.01	−0.05	0.01	−0.17	0.01
RCP 6.0	−0.03	0.02	−0.02	0.02	−0.04	0.02	−0.19	0.02	−0.04	0.02	−0.21	0.02
RCP 8.5	−0.02	0.02	−0.02	0.01	−0.04	0.02	−0.20	0.03	−0.05	0.01	−0.21	0.01
Mean annual maximum temperature signal impact (°C)												
RCP 2.6	−0.01	0.02	−0.01	0.02	−0.01	0.06	−0.02	0.22	−0.01	0.06	−0.03	0.19
RCP 4.5	−0.02	0.01	−0.01	0.01	−0.03	0.02	−0.06	0.13	−0.01	0.04	−0.03	0.16
RCP 6.0	−0.01	0.01	−0.01	0.02	−0.01	0.04	−0.02	0.18	−0.01	0.06	−0.03	0.21
RCP 8.5	−0.02	0.02	−0.01	0.02	−0.02	0.05	−0.03	0.20	−0.01	0.05	−0.03	0.18
Mean annual mean temperature signal impact (°C)												
RCP 2.6	−0.01	0.01	−0.01	0.01	−0.01	0.02	−0.02	0.04	−0.01	0.02	−0.03	0.05
RCP 4.5	−0.02	0.00	−0.01	0.00	−0.03	0.00	−0.06	0.01	−0.02	0.01	−0.03	0.02
RCP 6.0	−0.02	0.01	−0.01	0.01	−0.02	0.01	−0.04	0.03	−0.01	0.02	−0.03	0.03
RCP 8.5	−0.01	0.01	−0.01	0.01	−0.01	0.02	−0.03	0.05	−0.01	0.01	−0.03	0.01
Annual minimum temperature variance ratio signal impact (1)												
RCP 2.6	−0.02	0.00	−0.02	0.01	−0.02	0.00	−0.05	0.01	−0.02	0.01	−0.04	0.01
RCP 4.5	−0.02	0.01	−0.02	0.01	−0.02	0.01	−0.03	0.02	−0.02	0.01	−0.04	0.03
RCP 6.0	−0.02	0.01	−0.03	0.02	−0.02	0.01	−0.05	0.01	−0.03	0.02	−0.05	0.03
RCP8.5	−0.03	0.01	−0.04	0.04	−0.02	0.01	−0.05	0.02	−0.04	0.04	−0.07	0.06
Annual maximum temperature variance ratio signal impact (1)												
RCP 2.6	−0.02	0.00	−0.03	0.00	−0.04	0.00	−0.08	0.00	−0.03	0.00	−0.07	0.01
RCP 4.5	−0.02	0.01	−0.03	0.01	−0.03	0.01	−0.08	0.02	−0.05	0.01	−0.09	0.02
RCP 6.0	−0.02	0.00	−0.04	0.01	−0.03	0.00	−0.08	0.01	−0.06	0.02	−0.12	0.03
RCP8.5	−0.02	0.01	−0.05	0.02	−0.04	0.01	−0.10	0.02	−0.07	0.03	−0.15	0.05
Mean annual rainfall signal impact (%)												
RCP 2.6	−1.28	0.02	−1.44	−0.05	−1.28	−0.01	−1.79	0.41	−1.42	0.11	−2.04	0.44
RCP 4.5	−1.65	0.12	−1.70	0.03	−1.59	0.23	−2.70	0.62	−1.64	0.07	−2.58	0.52
RCP 6.0	−1.33	0.04	−2.23	0.01	−1.32	0.03	−1.87	0.39	−2.15	0.16	−3.11	0.49
RCP 8.5	−1.66	0.02	−2.78	0.73	−1.55	0.04	−2.36	0.38	−2.65	0.82	−3.54	1.51
Mean annual relative humidity signal impact (%)												
RCP 2.6	−0.04	0.06	−0.07	0.05	−0.08	0.07	−0.19	0.12	−0.10	0.05	−0.18	0.10
RCP 4.5	−0.06	0.09	−0.04	0.07	−0.11	0.09	−0.24	0.14	−0.16	0.07	−0.35	0.23
RCP 6.0	−0.03	0.06	−0.05	0.09	−0.10	0.07	−0.24	0.14	−0.18	0.09	−0.41	0.25
RCP 8.5	−0.08	0.09	−0.05	0.08	−0.14	0.09	−0.29	0.15	−0.27	0.09	−0.56	0.41

Across both periods and locations with elevations under 500m, P_1 for impacts on the rainfall signal varied from −1.3% to −2.8%, while P_2 varied from −0.05% to 0.73%. These ranges were not significantly altered when all locations were considered. The upper extremum of 1.5% occurred for a very high elevation, while the lower extremum of −3.5% occurred for a very low elevation (Table 5) and see Section 33 in the supplementary material). When change signals have been negatively affected by bias adjustments this will be due to downward adjustments for means having higher values in the RCP data than in the VCSN data for that location, and vice versa for positive impacts.

Change signals for relative humidity were slightly affected by the bias adjustments with P_1 and P_{99} across all RCPs and both time periods having magnitudes under 0.1% for elevations under 500m, and magnitudes under 0.3% for all elevations. Upper and lower extrema across all RCPs and both time periods had magnitudes under 0.6% (Table 5).

The sizes of the impacts on change signals would have little effect in the context of our continuous suitability models.

6.6 Impact of adjustments to RCP Past data

The new SLM RCP datasets that resulted from the adjustments to the RCP data showed closer statistical agreement with the VCSN data and generally resulted in improved agreement between suitability scores derived from the new data and the VCSN-based suitability scores for the Past period.

As an example, we consider a case study on September temperatures for three locations and their relevance to a frost risk assessment that was presented in our earlier investigation (Vetharaniam et al. 2020a) for the original RCP data, and extend it to include the SLM RCP dataset.

6.6.1 Case study: September temperatures and frost risk

Three example locations of Alexandra, Hamilton and Whangarei were chosen for their differing climates. Histograms of mean and variance for September maximum and minimum temperatures for the period 1972–2005 were constructed for the original six RCP Past datasets, the SLM RCP dataset and the VCSN dataset.

For all locations, the mean maximum and mean minimum September temperatures from all six original RCP Past datasets showed a smaller spread than the VCSN data, and generally had smaller variances in September maximum and minimum temperatures, which can be seen in the left hand side (LHS) panels in Figure 114, Figure 115 and Figure 116. This was more pronounced for the minimum temperatures, with the climate models having more representation in the higher range of minimum temperatures than the VCSN data, and less or no representation in the lower range of minimum temperatures. For Alexandra, the climate model data tended to have lower mean September maximum temperatures than the VCSN data (LHS of Figure 114), while for Hamilton and Whangarei the climate model data tended to have higher means (LHS of Figure 115 and Figure 116)

In contrast, the SLM RCP Past temperature data showed a closer agreement with the VCSN temperature data than the original RCP Past data, having an increased range of mean September temperatures over the 1972–2005 period, as well as an increased range of temperatures within the month (right hand side panels of Figure 114, Figure 115 and Figure 116). This is as expected.

The relevance of the discrepancies between the RCP data and the VCSN data for calculation of suitability scores was demonstrated by using the example of frost risk. Although we have developed continuous suitability scores, for the purpose of this demonstration we used a binary risk model with a −2°C threshold since this provides outcomes that are conceptually easier to understand. In this binary model, a frost event occurs when the daily minimum temperature is −2°C or lower, otherwise the day is considered to be frost-free.

Using the binary frost-risk model with September daily minimum temperatures from the original RCP Past datasets for the three locations of Alexandra, Hamilton and Whangarei, showing that the number of September frosts was significantly under-predicted for Alexandra by the RCP Past datasets compared with the VCSN dataset (Table 6). Whereas the VCSN dataset predicted 74 frosts events less than or equal to −2°C for Alexandra over the period 1972–2005, the RCP Past predictions for Alexandra for the same period ranged from 14 frost events (NorESM1-M) to 21 frost events (CESM1-CAM5). Thus all RCP datasets underestimated the frost risk for Alexandra by 70 to 80% compared with the observation-based VCSN datasets. This result is not surprising and is consistent with our assessment in Section 6.3.

Table 6. Number of predicted September frosts ≤ −2°C from 1972 to 2005 for Alexandra, Hamilton and Whangarei, using the VCSN and six original RCP Past datasets (from Vetharaniam et al. (2020a)).

	Alexandra	Hamilton	Whangarei
VCSN	74	2	0
BCC-CSM1.1	15	0	0
CESM1-CAM5	21	0	0
GFDL-CM3	19	0	0
GISS-EL-R	15	0	0
HadGEM2-ES	19	0	0
NorESM1-M	14	0	0

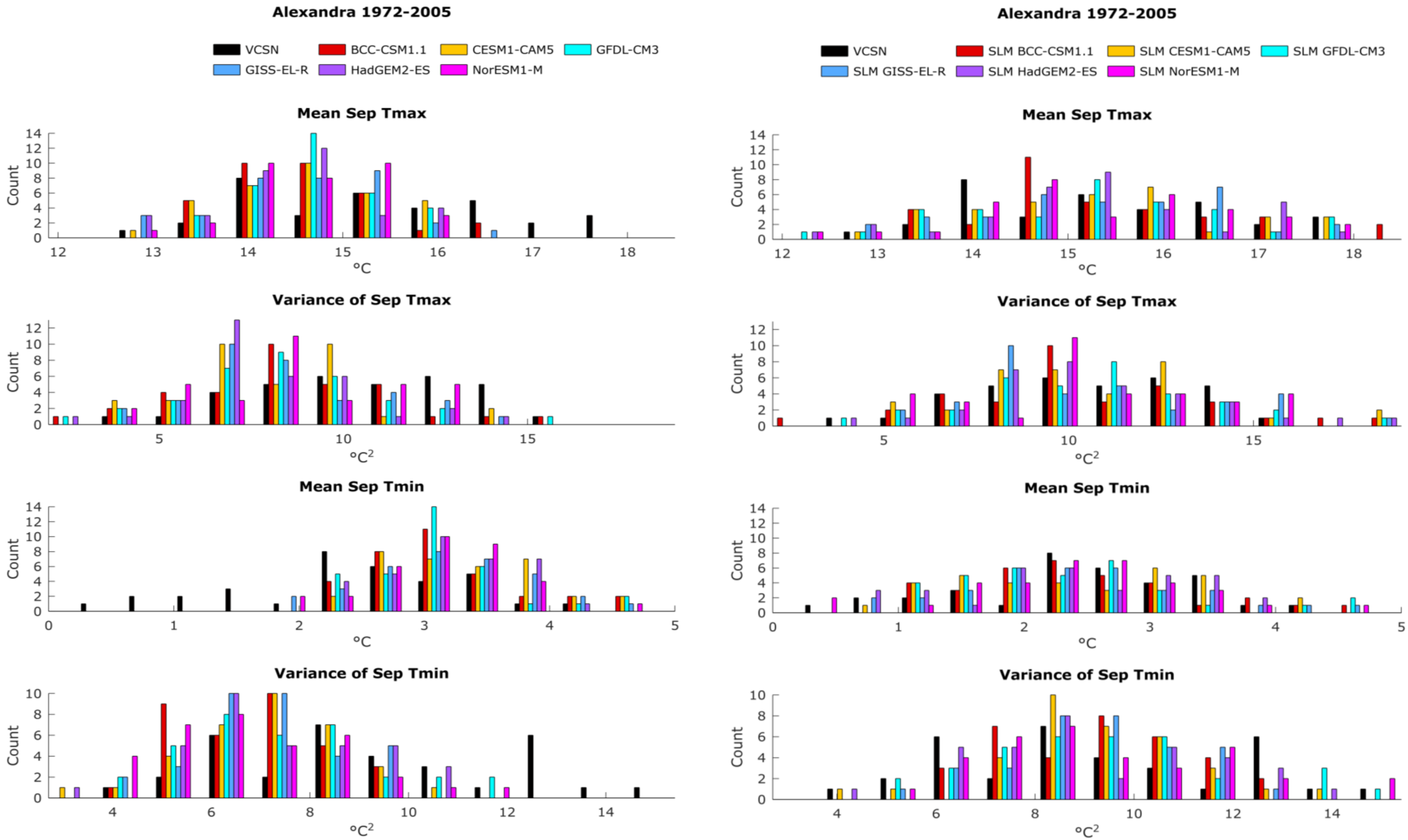

Figure 114. Distribution of annual means and variances of September maximum and minimum temperatures for Alexandra from different climate datasets for the period 1972-2005. Left panel: comparison of original RCP Past and VCSN data. Right panel: comparison of SLM RCP Past and VCSN data.

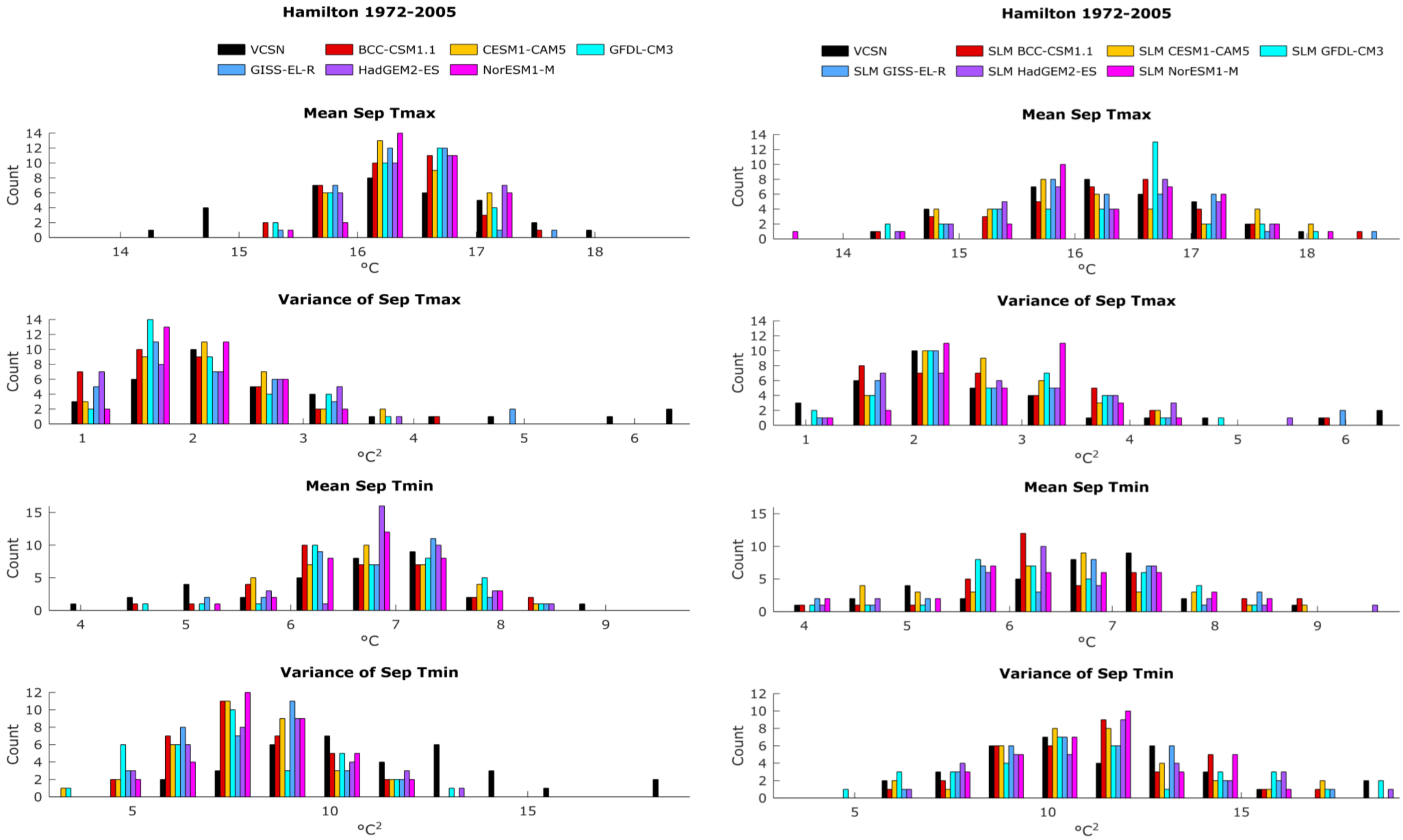

Figure 115. Distribution of annual means and variances of September maximum and minimum temperatures for Hamilton from different climate datasets for the period 1972-2005. Left panel: comparison of original RCP Past and VCSN data. Right panel: comparison of SLM RCP Past and VCSN data.

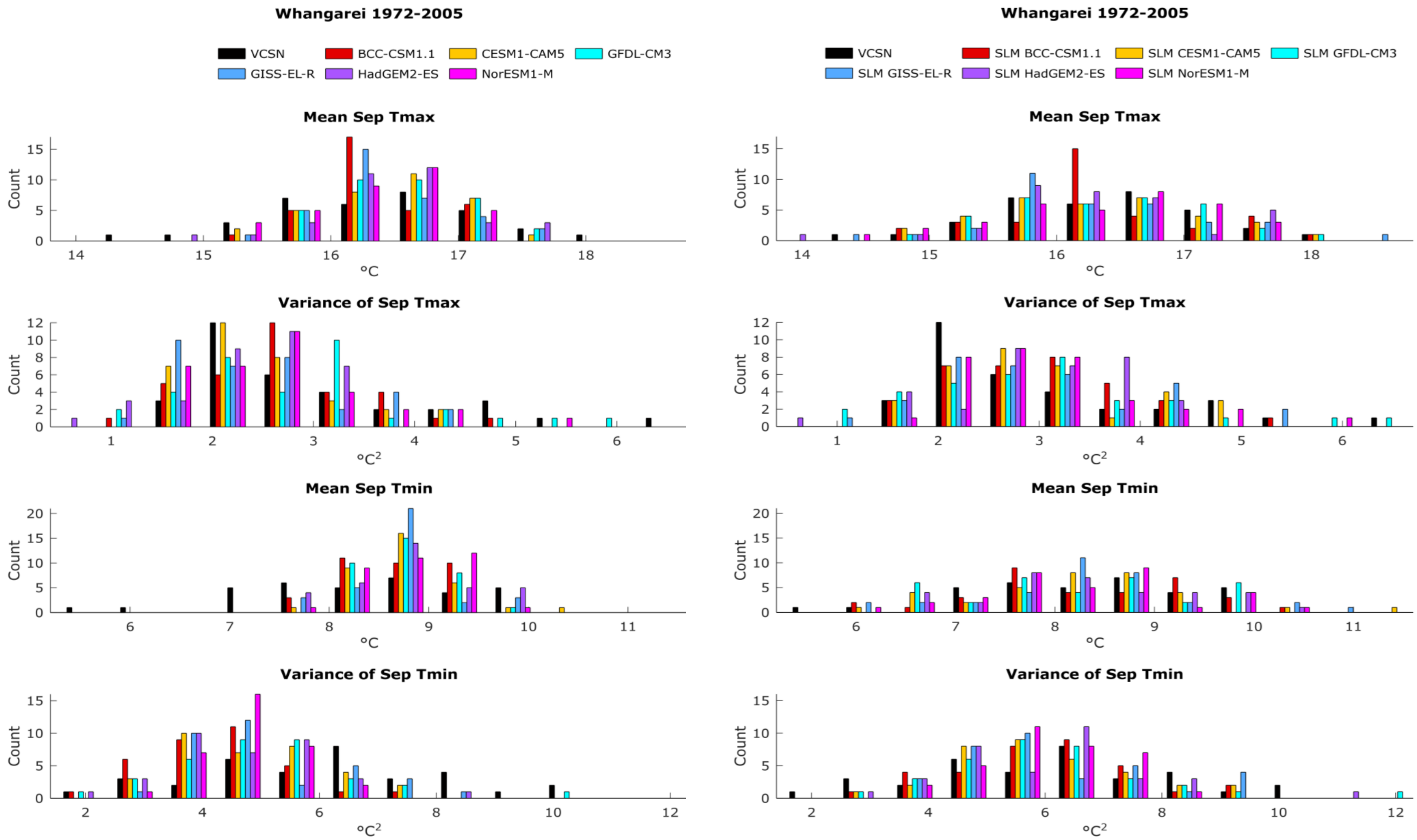

Figure 116. Distribution of annual means and variances of September maximum and minimum temperatures for Whangarei from different climate datasets for the period 1972-2005. Left panel: comparison of original RCP Past and VCSN data. Right panel: comparison of SLM RCP Past and VCSN data.

The VCSN data depicts two frosts ≤ −2°C for Hamilton, while all original RCP Past datasets depict zero frosts. For the warmer location of Whangarei the VCSN and all RCP Past datasets depict zero frosts. The apparent improvement of the RCP datasets in depiction of frosts for warmer locations is purely due to the lack of frost events due to the warmer climate; examination of Figure 115 and Figure 116 show that mean minimum September temperatures from the RCP Past datasets were higher than from the VCSN datasets for Hamilton and even more so for Whangarei, as was the case for Alexandra. VSCN minimum temperatures were also more variable than RCP Past minimum temperatures, increasing the likelihood of dropping below a threshold.

In contrast, the SLM RCP Past datasets showed similar or slightly more variability than the VCSN data and depict more September frosts from 1972 to 2005 than the VCSN data (see Table 7). While the SLM RCP data tended to over-represent the frost risk for Alexandra and Hamilton compared with the VCSN data, the difference is not hugely significant, and in the context of a 34-year period would not affect suitability scores. Thus we considered the new data to be more suitable for representation of these very cold temperatures.

Although our example only used minimum temperatures, it demonstrates that it is important that climate model datasets exhibit similar variability in daily temperatures as the observed historic dataset, in order for better baselining of suitability scores that are sensitive to temperature extremes. This is in addition to the requirement for agreement in mean temperatures. Also, it is important that the agreement in temperature statistics is for individual months of the year, rather than over a long period of years.

Further comparisons of RCP Past and SLM RCP Past are shown in Appendix 1 for annual and May temperatures for the same three locations, demonstrating the effectiveness of the data adjustment that we have developed.

Table 7. Improved prediction of number September frosts < −2°C from 1972 to 2005 for Alexandra, Hamilton and Whangarei, using the Virtual Climate Station Network (VCSN) and six SLM RCP Past datasets.

	Alexandra	Hamilton	Whangarei
VCSN	74	2	0
SLM BCC-CSM1.1	74	2	0
SLM CESM1-CAM5	80	2	0
SLM GFDL-CM3	73	6	0
SLM GISS-EL-R	87	5	0
SLM HadGEM2-ES	77	2	0
SLM NorESM1-M	86	4	0

6.6.2 Improvement in agreement of suitability scores

In our previous investigation into the differences between the RCP-past-based suitability maps and VCSN-based maps, we used one-to-one graphs to indicate the level of agreement for locations across the country (Vetharaniam et al. 2020a). Below we compare one-to-one graphs for scores from the RCP-past vs VCSN datasets with one-to-one graphs for scores from the SLM RCP Past vs VCSN datasets. In these graphs, each point represents the average suitability score over the period 1972-2005 for a single grid location, and every grid location across New Zealand is represented. Thus the graphs include locations with elevations of 500m or higher for which confidence in the VCSN data is lower than for elevations below 500m.For both apple and kiwifruit, baseline agreement for overall climate suitability score was improved by using the SLM RCP Past datasets, with less deviation from the one-to-one line and a reduction in bias being very noticeable for kiwifruit (Figure 117). Although the apple one-to-one scores for the original RCP Past datasets appear to show little bias, this is purely fortuitous since overall suitability is calculated by averaging scores for individual suitability criteria, and some of these underlying scores had significant biases that cancelled out due to differences in their sign and because of the particular (subjective) weightings used when averaging across individual scores.

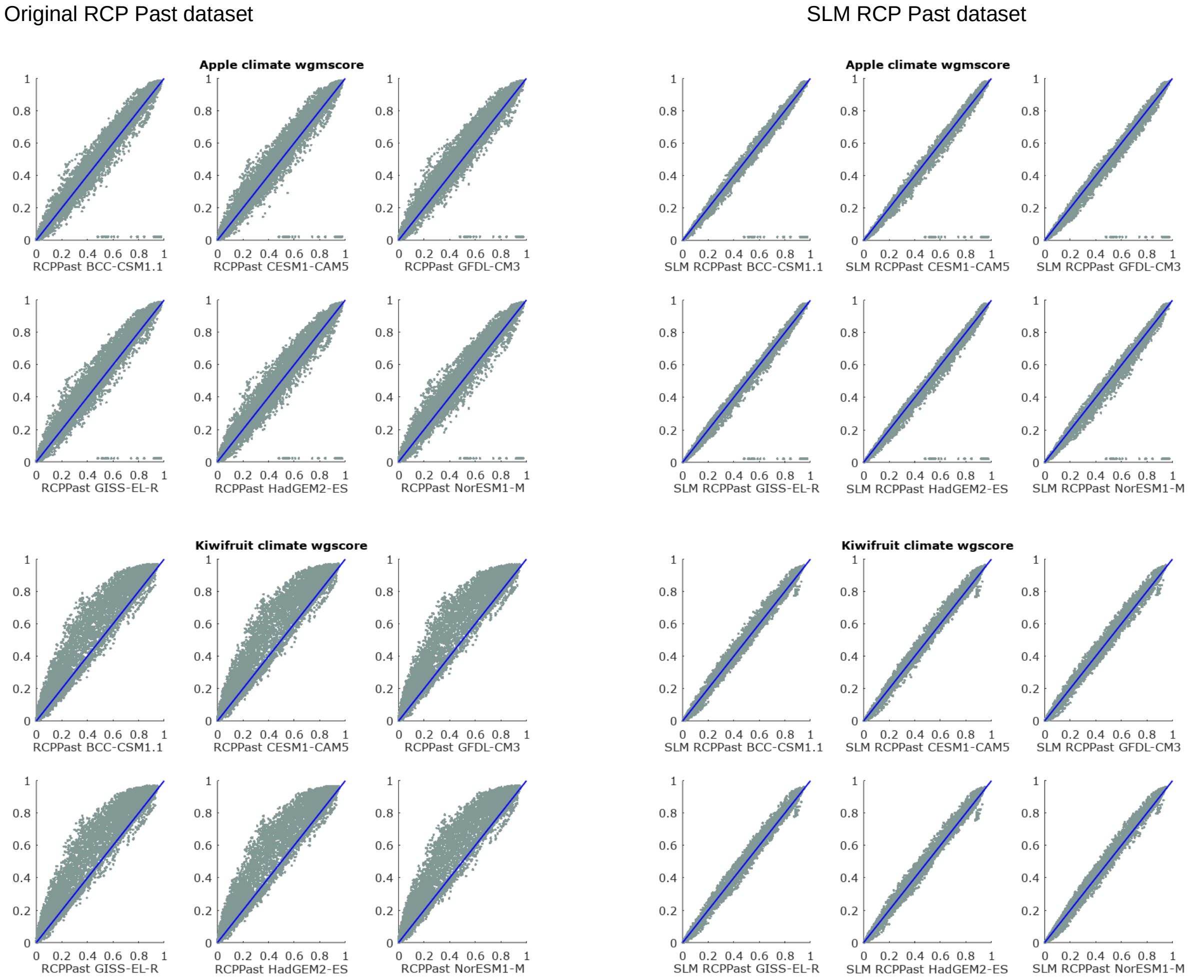

Figure 117. One-to-one graphs comparing performance of the original RCP Past datasets (left panels) and SLM RCP Past datasets (right panels) in terms of baseline agreement with the Overall climate suitability score for apple (upper panels) and kiwifruit (lower panels).

For apple, we considered bias in two common alternatives to calculating winter chill. Using the SLM RCP Past datasets provided a notable improvement over using the original RCP Past dataset in baselining the 7.2°C base chill suitability score (see the top panels of Figure 118); this requires a better estimation of the range of both daily maximum and daily minimum temperatures in order to better estimate hours per day below 7.2°C.

Interestingly, the Richardson-chill suitability scores showed more bias for the SLM RCP Past than for the original RCP Past data (middle panel of Figure 118). The apparently better performance of the original RCP Past data is due to anomalies in that data: for some locations, and a small fraction of days, the value for the maximum temperature was lower than the value of the minimum temperature, leading to significant negative contributions to the calculated chill units and fortuitously lowering an otherwise over-calculated result. These anomalies had been detected and addressed when we developed the SLM RCP data.

Original RCP Past dataset

SLM RCP Past dataset

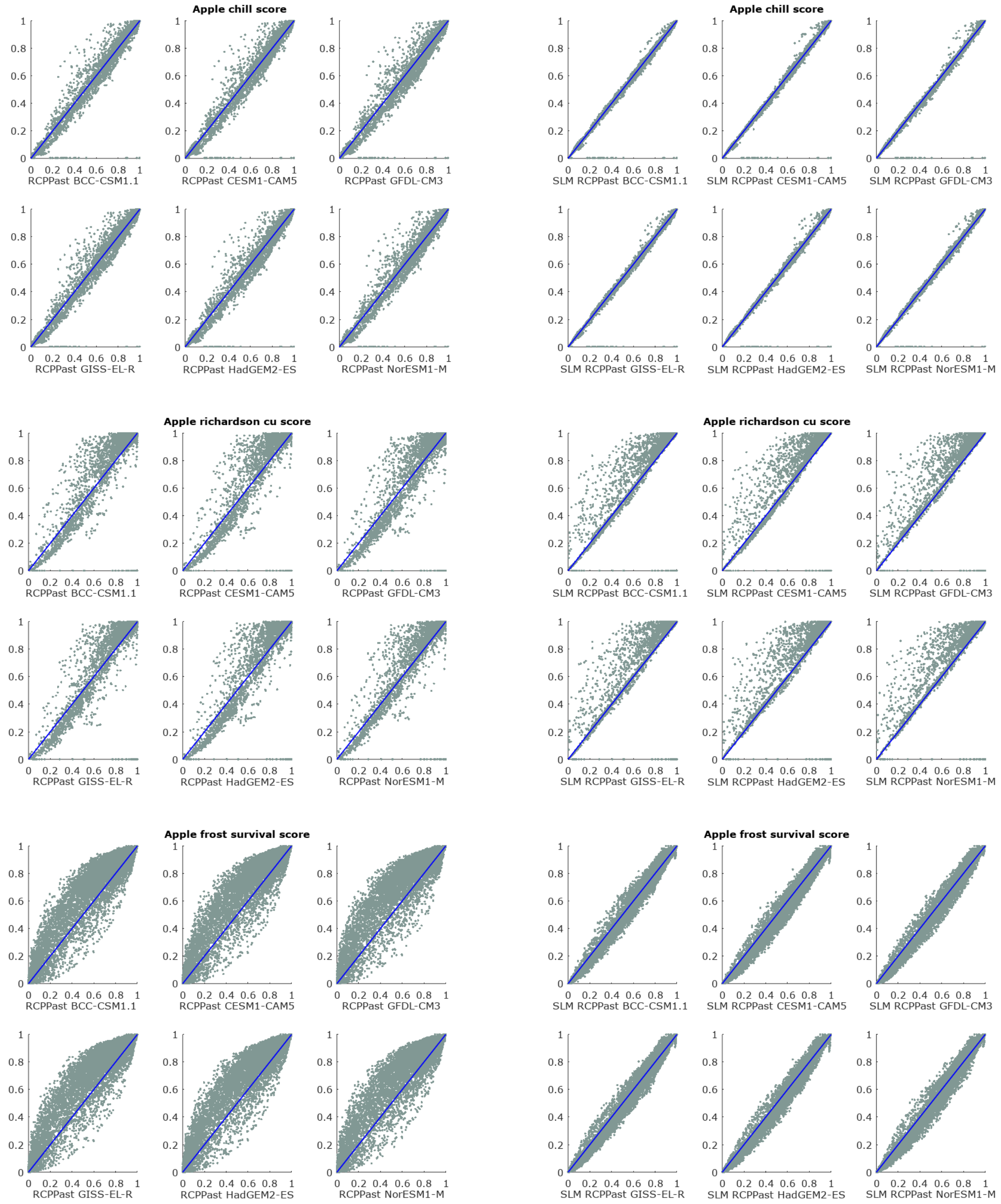

Figure 118. One-to-one graphs comparing performance of the original RCP Past datasets (left panels) and SLM RCP Past datasets (right panels) in terms of baseline agreement in apple for conventional chill-hours suitability score with a 7.2°C base (top panels), Richardson chill units suitability score (middle panels) and frost survival suitability scores (lower panels).

RCU are a non-linear function of the temperature profile over the course of a day, and to improve agreement in RCU calculation between climate model datasets and the VCSN dataset would require investigation of the covariance between daily maximum and daily minimum temperatures in the different datasets, which is outside the scope of this study.

The improvement in frost suitability scores for apple (lower panel of Figure 118) and kiwifruit (upper panel of Figure 119) are to be expected given the case study in Section 6.4.2.

Kiwifruit chill score was calculated in terms of mean winter temperature, and the improvement in baseline agreement of the SLM RCP dataset (lower panel of Figure 119) reflects the benefit of performing adjustments to the means and variance of maximum and minimum temperature for individual months of the year rather than on annual averages over a period.

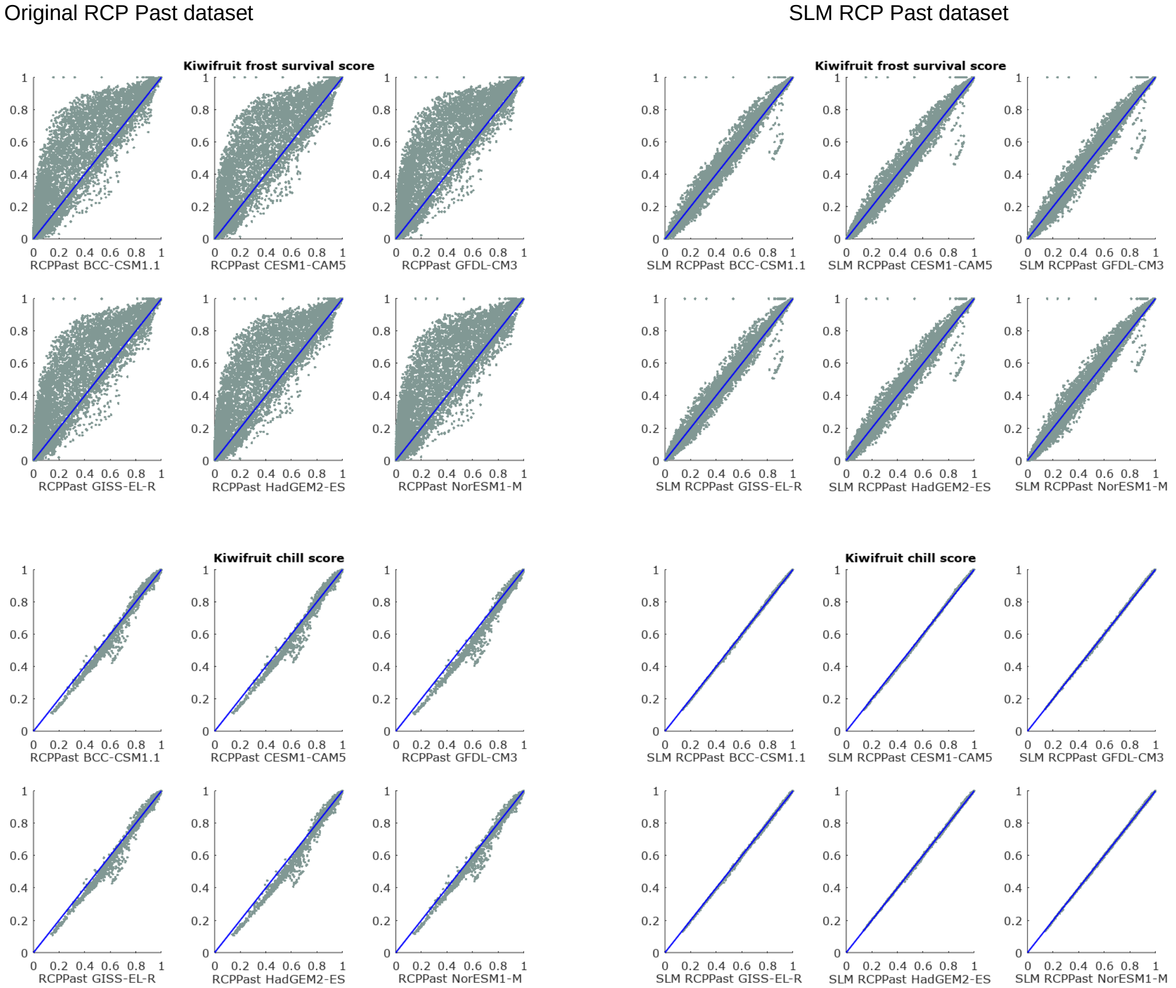

Figure 119. One-to-one graphs comparing performance of the original RCP Past datasets (left panels) and SLM RCP Past datasets (right panels) in terms of baseline agreement in kiwifruit for mean-winter-temperature-based chill suitability score (top panels) and frost-survival suitability (lower panels).

Similarly, Figure 120 shows that there was an improvement in baseline agreement for apple GDD suitability (top panel), which requires both maximum and minimum daily temperatures to be appropriately distributed, and also an improvement in baseline agreement for apple fruit size suitability scores, which depends on the first 50 days of GDD accumulation during the season. The much tighter agreement for GDD suitability scores compared with the fruit size suitability scores suggests that biases in the early stages of calculated GDD accumulation were balanced out by subsequent biases of the opposite sign. GDD suitability scores for kiwifruit showed very similar behaviour to those for apple and are not presented.

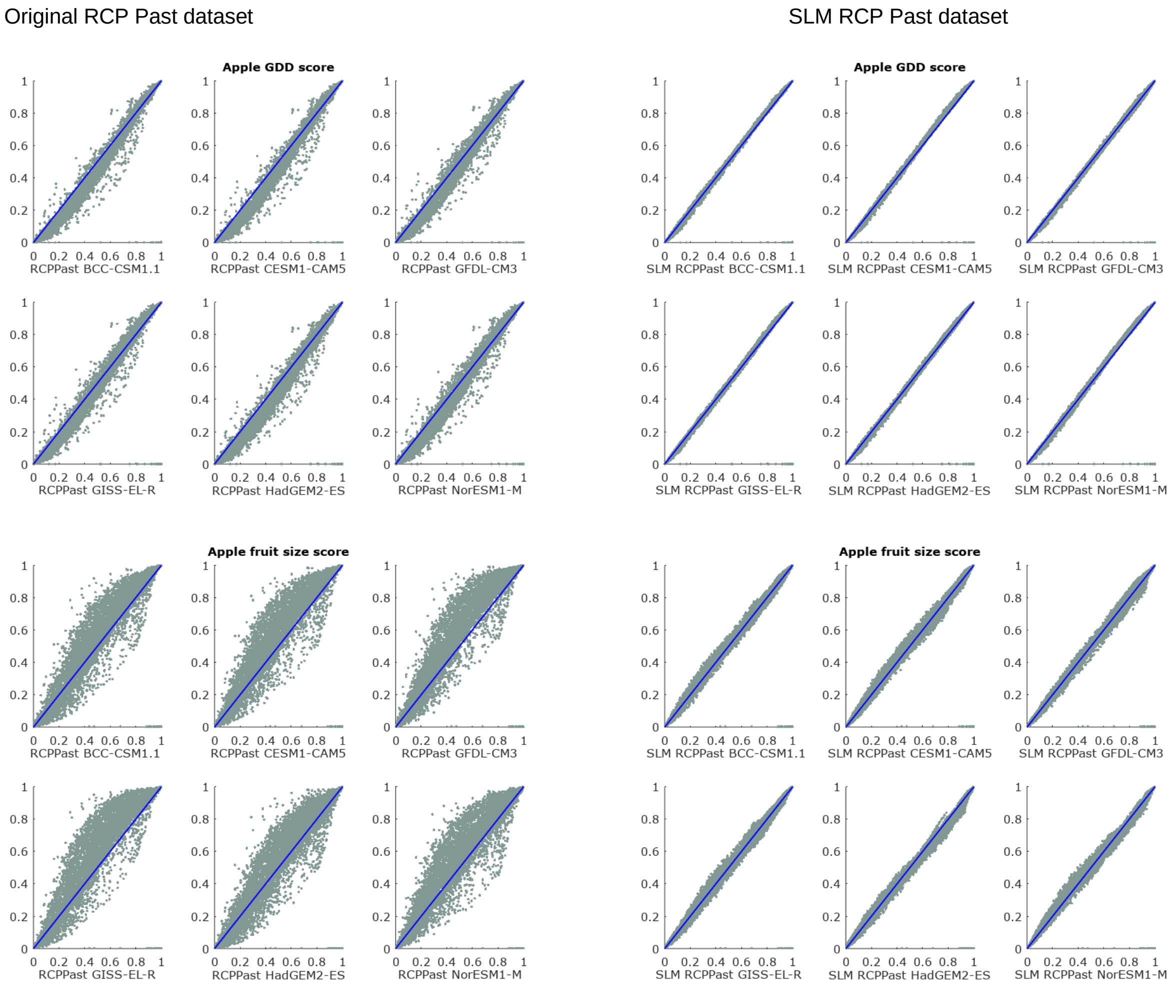

Figure 120. One-to-one graphs comparing performance of the original RCP Past datasets (left panels) and SLM RCP Past datasets (right panels) in terms of baseline agreement in apple growing degree day (GDD) suitability score (upper panels) and GDD-based apple fruit size score (lower panels).

Consistent with their representation of variability of temperatures, the SLM RCP Past datasets provided better agreement with the VCSN-based predictions for apple sunburn suitability score (Figure 121, upper panels), which is sensitive to extreme warmth, and for kiwifruit cold kill suitability score (Figure 121, lower panels).

Much of the focus has been on temperature-dependent suitability scores, since these are the most common factors in climate-related suitability considerations across crops, and much of our focus has been on the representation of maximum and minimum temperatures in the climate model datasets. However, our formulation of a generic disease suitability score to act as a non-specific indicator of disease risk trends across crops is dependent on both RH and temperature, and the wine-grape-specific botrytis suitability score is dependent on rainfall, and the adjustments we made to both RH and rainfall have contributed to improved baselining.

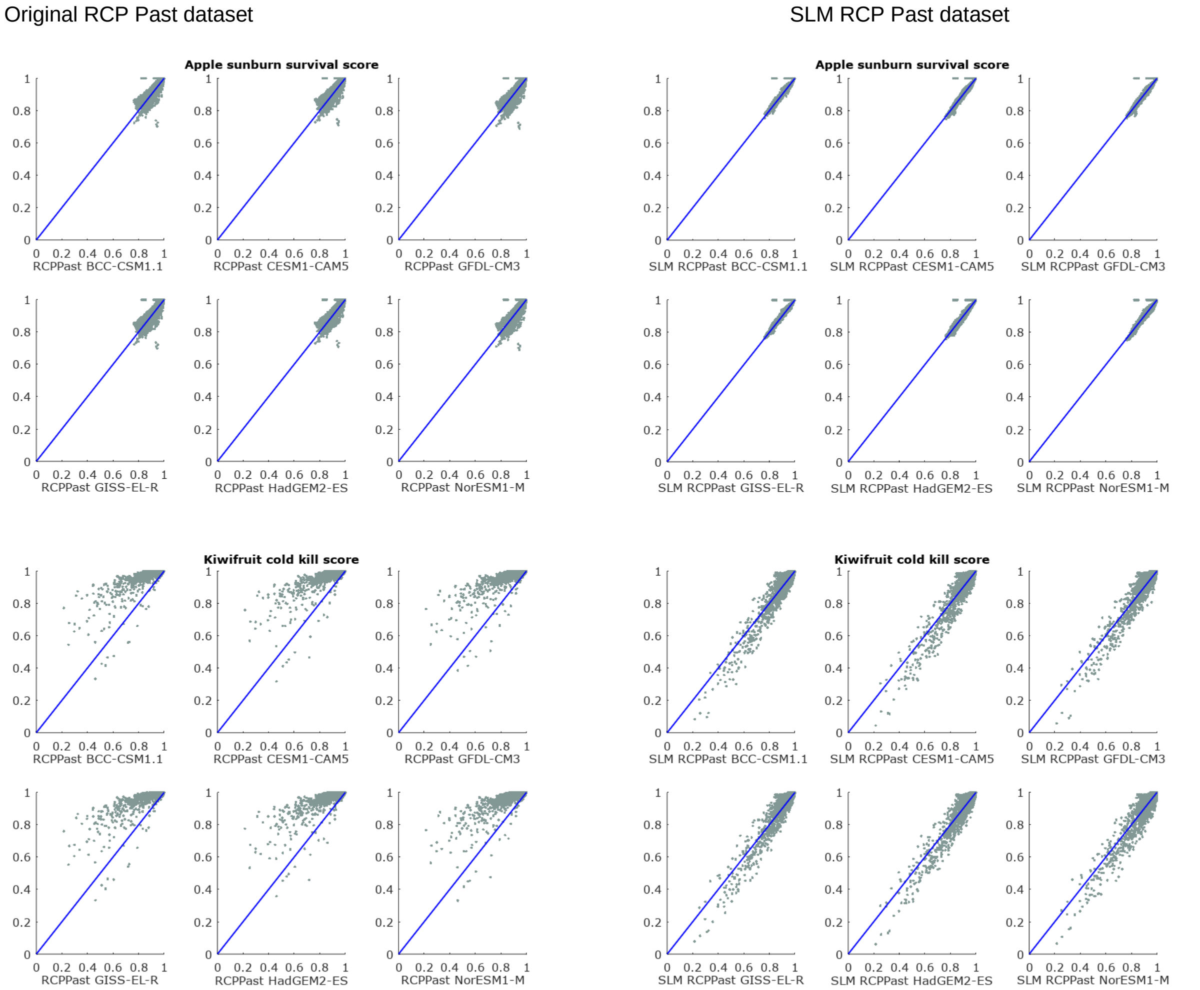

Figure 121. One-to-one graphs comparing performance of the original RCP Past datasets (left panels) and SLM RCP Past datasets (right panels) in terms of baseline agreement in apple sunburn suitability score (upper panels) and kiwifruit cold-kill score (lower panels).

Using the SLM RCP Past dataset provided moderate improvements over using the RCP Past dataset for obtaining agreement in baselines for the botrytis suitability score (Figure 122, upper panels). This reflects that the only adjustment that we made to rainfall data was scaling to ensure agreement with the VCSN data in mean rainfall for each month of the year, and did not address agreement of the variance. Although we adjusted the RH humidity data in the SLM RCP Past dataset only for mean bias, this together with the temperature adjustments provided a good improvement in baseline agreement (Figure 122, lower panels).

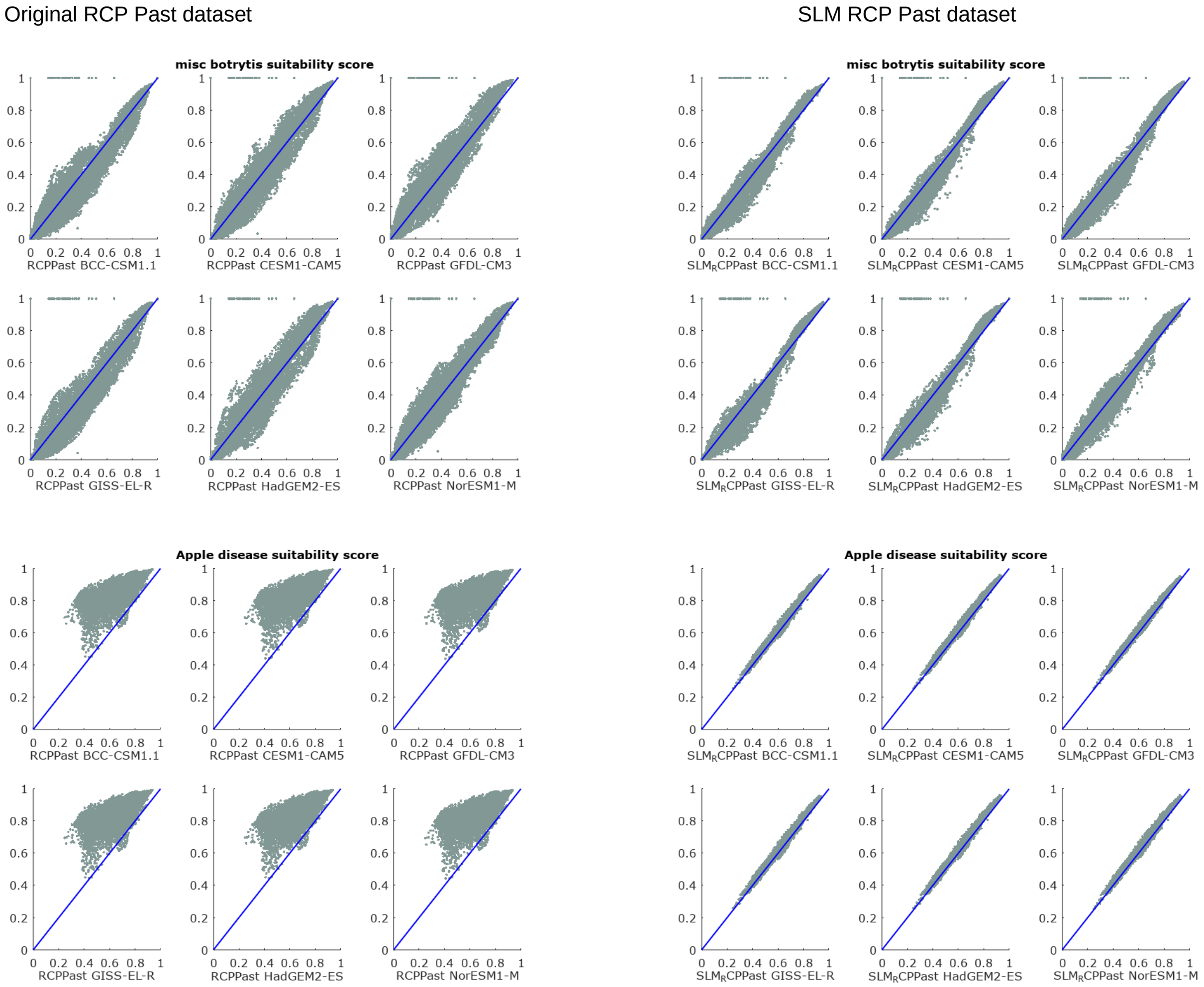

Figure 122. One-to-one graphs comparing performance of the original RCP Past datasets (left panels) and SLM RCP Past datasets (right panels) on baseline agreement of suitability scores for botrytis (upper panels) and disease (lower panels).

6.7 Effect of adjustments on Contemporary period baselining

The adjustments that we made to the RCP dataset were applied consistently to the entire dataset from 1972 to 2099, although the adjustment parameters were calculated from RCP and VCSN data for the Past period (1972–2005). These adjustments provided significant overall improvement in suitability maps between the new SLM RCP datasets and the VCSN dataset, for the Past period.

The RCP future time frames include a period (2006–2017) for which we had observed (VCSN) data. For convenience we refer to this as the “Contemporary” period (corresponding to the growing years 2006–2016). In a previous Progress Report (Vetharaniam et al. 2019) we found that biases in RCP-based suitability maps were significantly worse for the Contemporary period than for the Past period. While a 12-year period of climate data is a short period upon which to calculate statistics, we had anticipated that SLM-RCP-based suitability maps would show significant improvement over RCP-based suitability maps in their agreement with the Contemporary VCSN-based maps. However, while there was some improvement, it was not as great as expected based on the outcomes for the RCP past suitability scores. Figure 123 shows the degree of improvement for climate suitability score for apple.

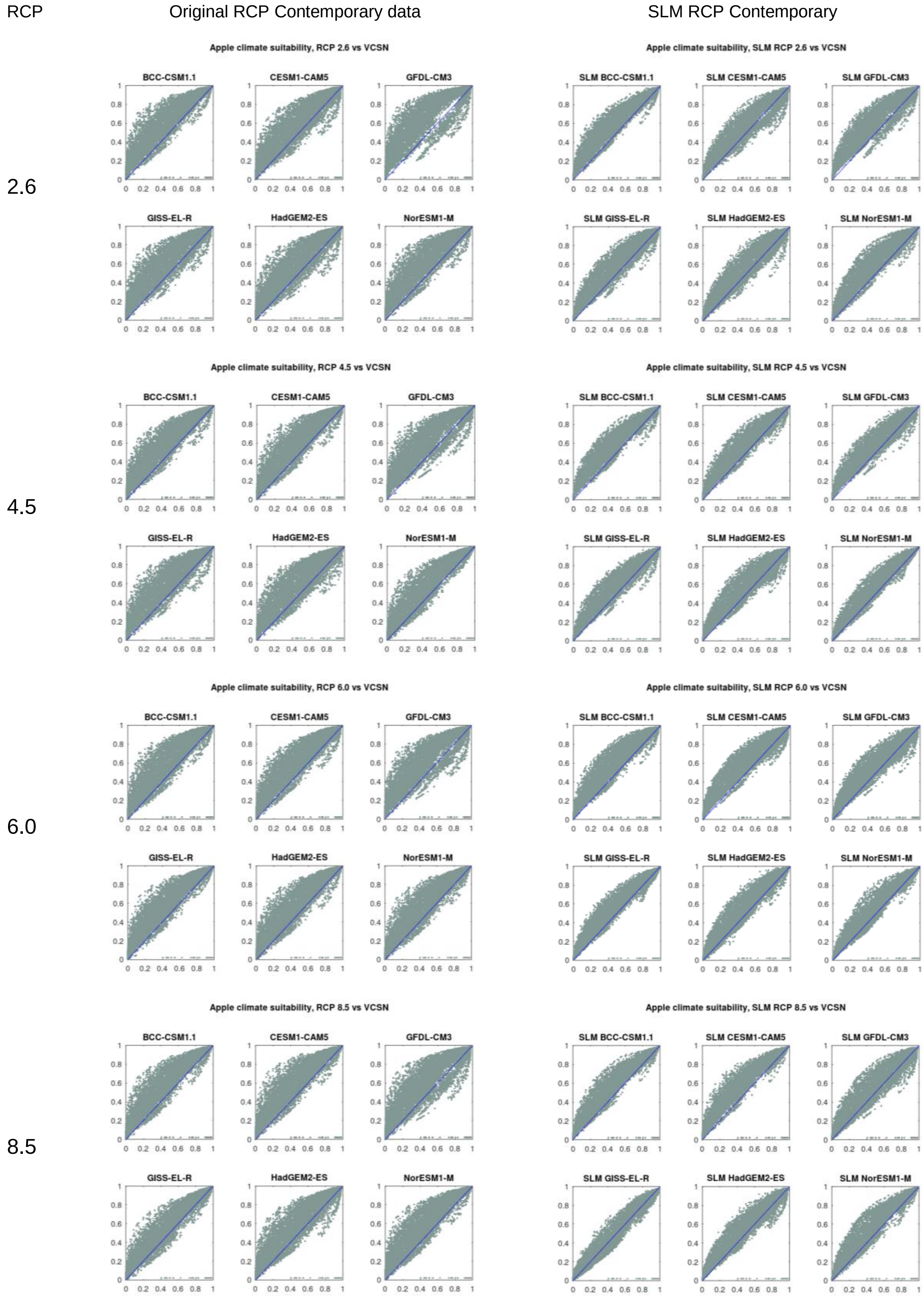

Figure 123. One-to-one plots of Contemporary-period apple climate suitability scores calculated from RCP datasets (left panels) and SLM RCP datasets (right panels) vs VCSN–based scores.

This worsening in agreement for the SLM RCP datasets when going from the Past period to the Contemporary period, is consistent with that experienced with the original RCP datasets. Our adjustments were designed to not affect the climate trends in the RCP data, and so each SLM RCP dataset has essentially the same trends as its counterpart RCP dataset. Thus we attribute this worsening of bias to a short-term divergence in climate trajectory between the climate model data and the VCSN data.

Bias correction is often unavoidable for studies on climate-change impacts because uncorrected RCM simulations are a source of large uncertainties, but the choice of adjustment method is an additional source of uncertainty (Teutschbein & Seibert 2013). Considering alternative adjustment methods as suggested by Challinor et al. (2018) would allow more insight into the impacts of the individual methods.

The RCM simulations to produce the RCP datasets were run for the years 1972–2005 with inputs reflecting known variables and factors that can affect weather patterns. These variables and factors that affect climate include solar variability, volcanoes, other human-produced and natural emissions of GHGs and aerosols, as well as carbon-dioxide levels (Buis 2020). For the years 2006 onwards, the RCM simulations were not informed by such information, and thus were less likely to show the fluctuations in mean temperature found in observation data. Certainly for the period from about 2007 to 2015, observed temperature changes tracked below the ensemble mean from a range of climate models, but from 2016 onwards tended to track above (Buis 2020). Since we have performed a systematic alignment of the RCP data to the VCSN data for the Past period, we consider that large divergence between the SLM RCP datasets and the VCSN datasets for the contemporary period reflects natural variability.

Our approach from here was to use the differences in 2006–2016 suitability scores between the SLM RCP data and VCSN data to estimate an indicative uncertainty in projection of future cultivation suitability maps. While the conventional approach is to use the variability between model runs to infer projection uncertainty, this would not account for systematic effects that are common to the GCMs or intrinsic to the RCM, and observation-based estimation of uncertainties is an alternative approach (Eyring et al. 2019). This uncertainty was calculated individually for each crop, based on the root mean square error (RMSE) of prediction. For each crop, SLM RCP-based scores were assigned to histogram bins of width 0.5, and for each bin the RMSE across locations was calculated for the SLM RCP-based 2006–2016 scores with respect to the corresponding VCSN-based scores. The Contemporary scores are averaged over 11 growing years. For future projections we chose to work with a 30-year average to reduce the effect of volatility in weather patterns. Thus we estimated the uncertainty for each histogram bin by discounting the RMSE calculated for the Contemporary period by $\sqrt{1/3}$.

7 Future climate and cultivation suitability

We used the SLM RCP datasets to project suitability scores for an early-mid-century (2028–2058) period and a late mid-century period (2068–2098), taking the mean of the 30 yearly scores for each period as representative of the period. We chose a 30-year period to reflect the volatile nature of weather patterns over the course of several years: a projection based on a 30-year average is less likely to suffer from misprojection than a projection based on a smaller time frame.

The suitability models were run for each of the four RCP levels (2.6, 4.5, 6.0 and 8.5). For each RCP, scores were calculated for corresponding six SLM RCP datasets (corresponding to forcing by six GCMs) and these scores were averaged to give one projection per RCP for each suitability model, which was then mapped to show the projected climate and cultivation suitability scores at locations across the country. Changes in suitability were calculated with respect to the average of the six SLM RCP Past predictions for that suitability score, and these changes were also mapped to indicate the extent to which suitability scores for each location were projected to change. The regional impacts of climate change projections are more clearly seen in the climate suitability maps than in the cultivation suitability maps. However, the latter maps more clearly show the extent of limitations to crop cultivation by considering both climate and soil/land criteria.

Histograms of past and future suitability scores were constructed to compare future change in the area of land falling into different suitability score ranges. We used the estimated uncertainties in prediction to calculate prediction bands around the histogram values, and these were reported as best and worst cases. The lower the cultivation suitability score, the more the limitations to successful crop production. Thus growers are less likely to be interested in areas with lower suitability scores since these would require more mitigation strategies to reduce risk and improve production. Thus we have focused our discussion on scores above 0.6. For convenience we (arbitrarily) refer to cultivation suitability scores in the 0.9 to 1.0 range as ‘excellent”, 0.8 to 0.9 as “very good”, 0.7 to 0.8 as good, and 0.6 to 0.7 as “acceptable”.

In this section we discuss results of suitability projections for all crops under the RCP 2.6 and 8.5 scenarios, which represent the extremes of the four global warming scenarios. Additionally, climate change impacts on the average risk level across diseases are discussed at the end of this section. Climate and cultivation suitability projections under RCP 4.5 and 6.0 are presented Appendix 2.

The future suitability maps for apple and kiwifruit were integrated into the Land Use in Rural New Zealand (LURNZ) model, which is an economics-based spatial model of rural land use in New Zealand that is used to understand the spatial distributions of rural land use and map likely future land-use patterns. The LURNZ model was used to project the likelihood of land across rural New Zealand being in horticultural use under RCP 2.6 and 8.5, while taking into account the likely extent of major competing land uses of dairy, sheep and beef, and forestry. The cultivation suitability maps provided key input variables for projecting the footprints of the apple and kiwifruit under future climate change projections for LURNZ. Results from the LURNZ model are presented in Section 8.

For each crop and scenario, we indicate the uncertainty in the number of locations in each histogram bin. This uncertainty was calculated from the projection uncertainties described in Section 6.7. Whilst there is considerable variability for individual bands, it is clear there is a general trend for areas of more suitable land to increase or decrease. What is less clear is exactly how much land will be in each category. When histograms are taken of the upper and lower limits around nominal scores, locations will generally be shifted into and out of each bin. However, locations cannot leave the excellent range (the top range) because of an increase in suitability, nor enter the excellent range because of a decrease in suitability, thus this range will have a larger uncertainty variance than other ranges.

7.1 Apple

7.1.1 Apple RCP 2.6

Under RCP 2.6, most change is projected to occur by the mid-century, with trends generally continuing into the late-century. The biggest declines in climate and cultivation suitability occur across most parts of Northland, northern parts of the Auckland Region and around the East Cape (Figure 124 and Figure 125). However, these are not significant apple-growing areas. Smaller declines in suitability are projected to occur across much of the Waikato, in the Coromandel, and in most coastal areas of the Bay of Plenty, Gisborne region and Hawke's Bay. Slight increases in suitability are projected to occur across the central North Island and across the South Island. While areas around Waiouru show the most increase in suitably in the North Island these areas have low to moderate cultivation suitability and thus are unlikely to contribute to an increase in apple footprint (Figure 125). Small increases in cultivation suitability that occur in the Tasman district and in scattered areas of Central Otago (Figure 125) may provide benefit to the apple industry in those regions.

Areas of land with acceptable or higher suitability are projected to have a modest increase through to the late century, although gains in the excellent range that are achieved by the mid-century will subsequently be halved (Table 8).

Table 8 Apple: Land area in the historic period falling into different cultivation suitability ranges, projected changes for the mid- and late-century under RCP 2.6, and best and worst cases. Decreases are shaded red and increases shaded blue. Colour intensity increases with the magnitude of change.

Apple SLM RCP 2.6	Historic (km^2) 1972–2004	Area change from historic (km^2) 2028–2058			Area change from historic (km^2) 2068–2098		
Suitability range		Projected	Best case	Worst case	Projected	Best case	Worst case
0–0.1	14891	−1498	−3175	354	−1603	−3176	83
0.1–0.2	4286	−828	−1980	−673	−909	−2126	−648
0.2–0.3	4972	−1266	−617	−134	−1404	−711	−358
0.3–0.4	8321	−2494	−4201	−367	−2711	−4302	−479
0.4–0.5	12457	−2057	−4464	393	−1947	−4767	582
0.5–0.6	22444	−2387	−6174	855	−2340	−5949	1101
0.6–0.7	31668	3815	916	4969	4474	1137	5157
0.7–0.8	32230	948	3752	−2846	507	3689	−2872
0.8–0.9	31947	4558	5270	2744	5380	6011	3525
0.9–1.0	20509	1209	10673	−5295	553	10194	−6091

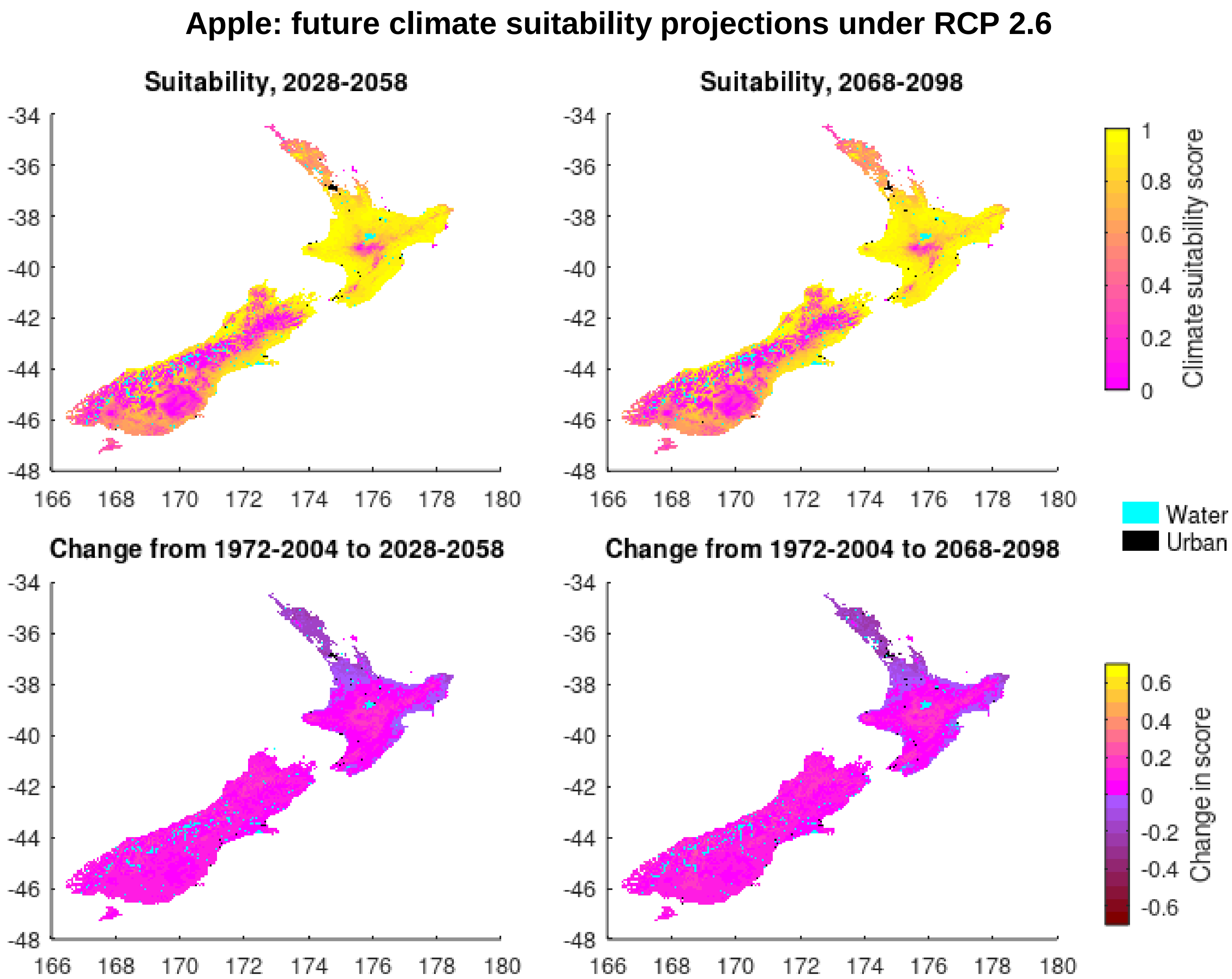

Figure 124. Apple: Projected climate suitability (top panels) and projected changes in climate suitability from the historic period (bottom panels) for the mid-century (left panels) and late century (right panels) under RCP 2.6.

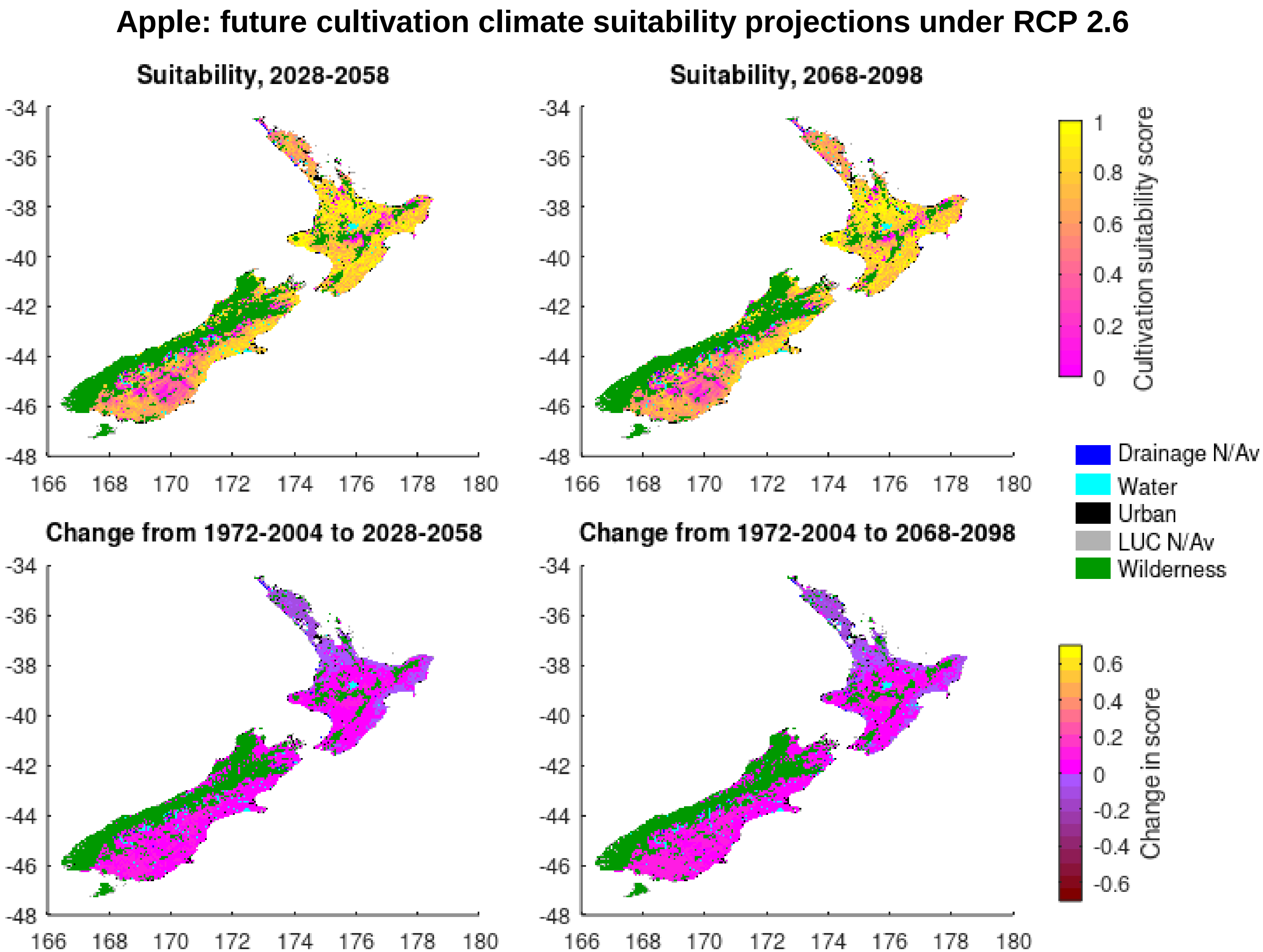

Figure 125. Apple: Projected cultivation suitability (top panels) and projected changes in cultivation suitability from the historic period (bottom panels) for the mid-century (left panels) and late century (right panels) under RCP 2.6.

Within projection uncertainty, under RCP 2.6 the change in area of excellent suitability land ranges from −26% to 53% for the mid-century and from −30% to 50% for the late-century. However, very good suitability land is consistency projected to increase by 9% to 19% for both periods (Table 8).

7.1.2 Apple RCP 8.5

Under RCP 8.5, projected changes in the suitability of land for apple are much larger in many locations than under RCP 2.6, but the spatial patterns of change are similar. The projected climate suitability and cultivation suitability maps for the mid-century under RCP 8.5 (Figure 126 and Figure 127) are similar to the late-century suitability maps projected for RCP 2.6 (Figure 124 and Figure 125). Under RCP 8.5, climate and cultivation suitability for apple have severe declines in Northland, the Auckland Region and around the East Cape, and significant declines in the coastal areas of the Bay of Plenty, the Coromandel, and many Northern and Western locations of the Waikato (Figure 126 and Figure 127). This could pose a threat to the small number of established apple orchards in the Waikato and Coromandel. Smaller declines in suitability are projected to occur across much of the North Island except for central and elevated areas, with notable improvement around Waiouru. Many of these areas are projected to have good cultivation suitability or higher. The South Island is projected to experience low to moderate increases in suitability except for northeast Marlborough and parts of coastal Canterbury, which are projected to decline in suitability by the late century (Figure 126 and Figure 127). This pattern of change is likely to shift the footprint of apple further south.

Under RCP 8.5, the simulations project a very small increase in the area of land with excellent suitability by mid-century, but significant increases of land with suitability scores in the acceptable to very good ranges; however, a loss of 50% of excellent suitability land (10,000 km^2) is projected to occur by the late-century, although accompanied by about a 14,000km^2 increase in the area of land falling into the slightly lower suitability range of ‘very good’ (Table 9). Within projection uncertainty a loss of excellent suitability land would lie between 20% and 71% by the late-century; however, the areas of acceptable, good and very good suitability land are consistently projected to increase within prediction uncertainty (Table 9).

Table 9. Apple: Land area in the historic period falling into different cultivation suitability ranges, projected changes for the mid- and late-century under RCP 8.5, and best and worst cases. Decreases are shaded red and increases shaded blue. Colour intensity increases with the magnitude of change.

Apple SLM RCP 8.5	Historic (km^2) 1972–2004	Area change from historic (km^2) 2028–2058			Area change from historic (km^2) 2068–2098		
Suitability range		Projection	Best case	Worst case	Projection	Best case	Worst case
0–0.1	14891	−2027	−3173	−778	−2803	−3182	−2319
0.1–0.2	4286	−1442	−2263	−1235	−3032	−3575	−2289
0.2–0.3	4972	−1606	−1245	−956	−609	−2420	3118
0.3–0.4	8321	−3184	−4552	−1291	2473	−1186	2765
0.4–0.5	12457	−2104	−4868	312	−1299	−276	−576
0.5–0.6	22444	−2675	−5170	481	−2841	−6048	−320
0.6–0.7	31668	3690	887	4116	1518	420	2898
0.7–0.8	32230	886	3221	−1587	2695	516	3576
0.8–0.9	31947	8143	9460	5662	14150	19873	7711
0.9–1.0	20509	319	7703	−4724	−10252	−4122	−14564

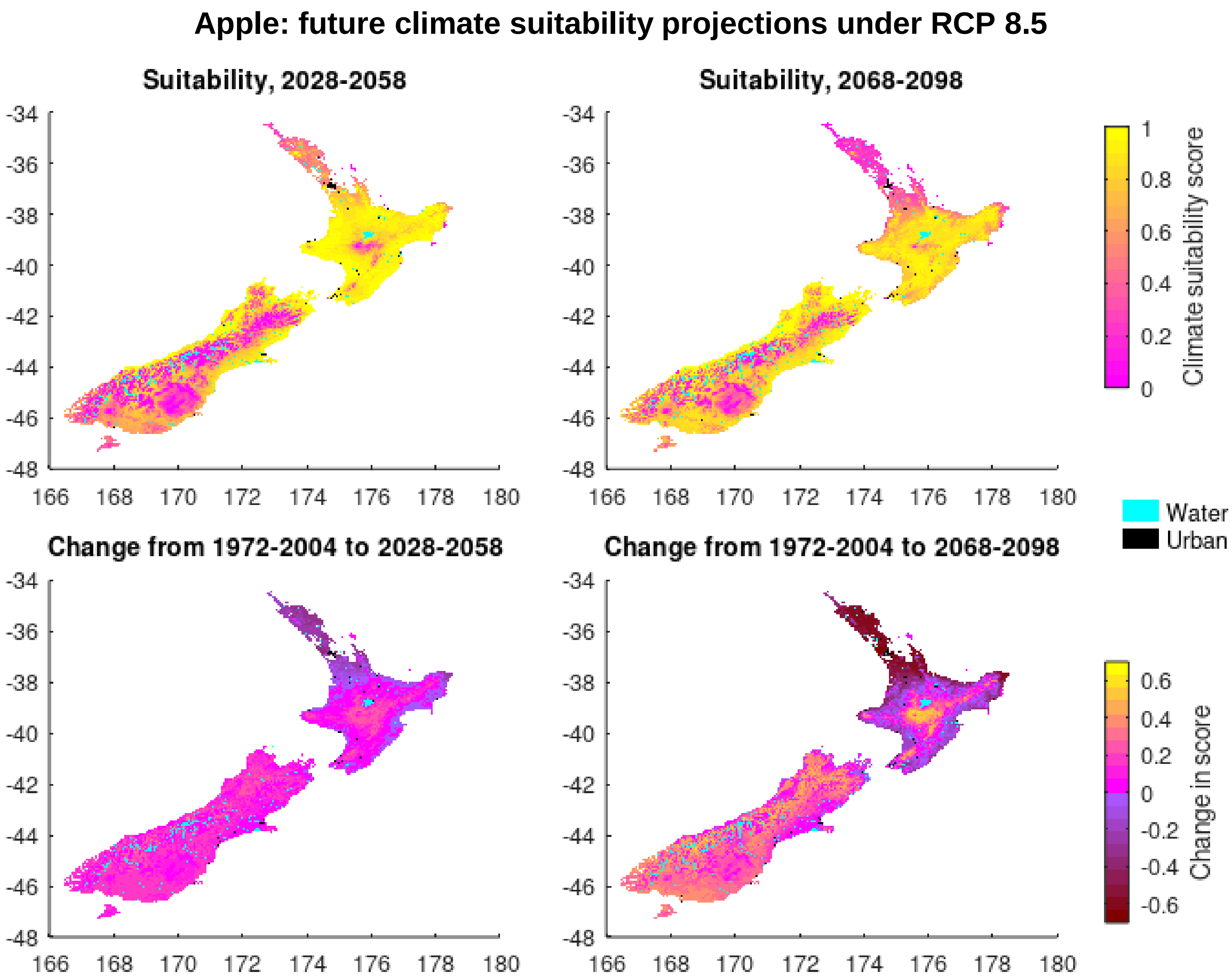

Figure 126. Apple: Projected climate suitability (top panels) and projected changes in climate suitability from the historic period (bottom panels) for the mid-century (left panels) and late century (right panels) under RCP 8.5.

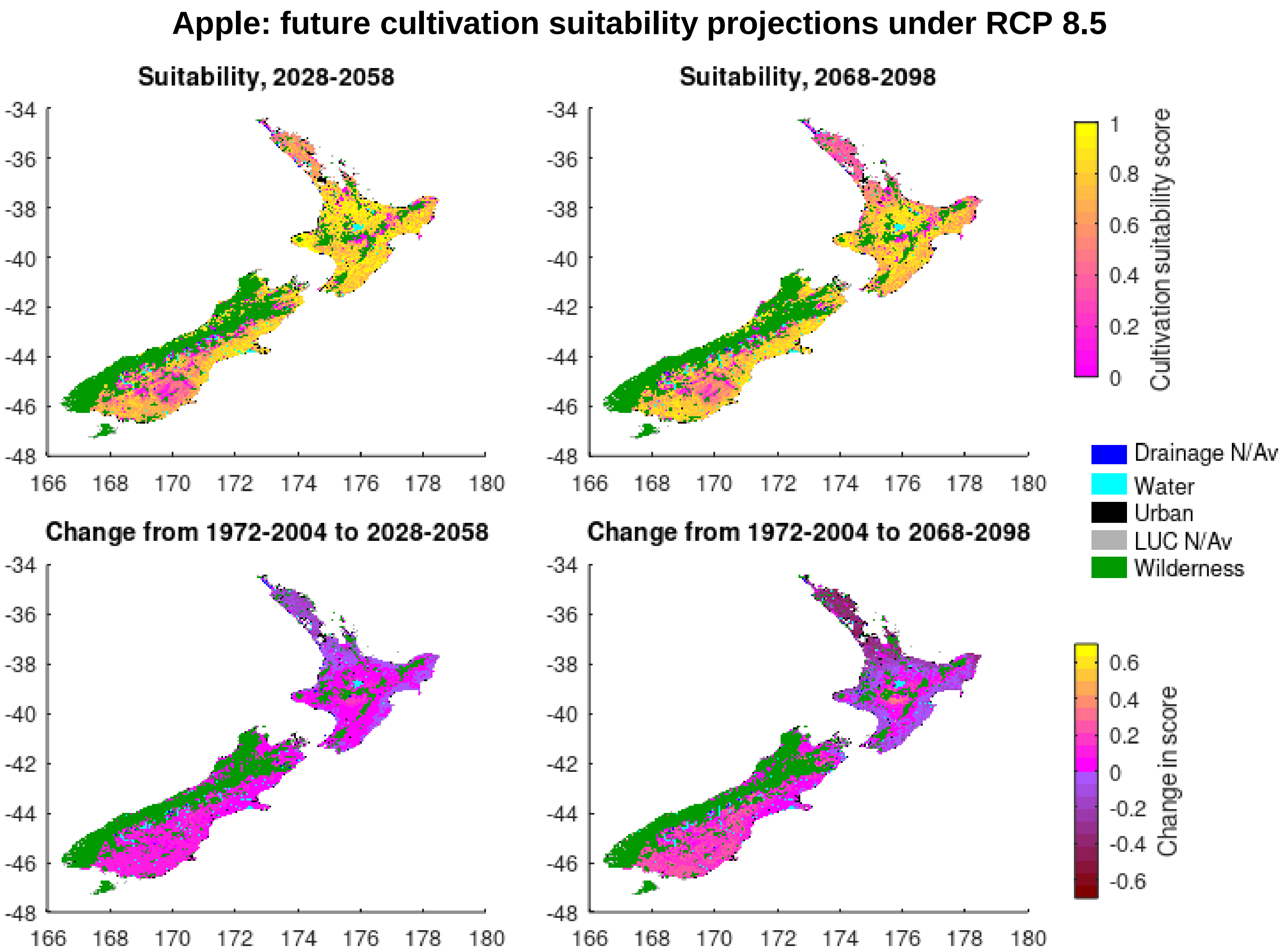

Figure 127. Apple: Projected cultivation suitability (top panels) and projected changes in cultivation suitability from the historic period (bottom panels) for the mid-century (left panels) and late century (right panels) under RCP 8.5.

7.1.3 Apple: key criteria underlying change

Under both RCP 2.6 and 8.5, suitability scores for fruit size, frost risk, and GDD improved consistently across all locations when compared with RCP Past values, for both mid- and late-century. In contrast, under both RCPs and for both time periods, sunburn suitability decreased in all locations except for those scoring very highly in the historic period; and chill suitability notably decreased in many areas, but increased in others but to a lesser extent (see supplementary file ‘Comparison future vs historic scores’). Under RCP 2.6 there was little difference in patterns of change between mid- and late-century, indicative of a stabilising of temperatures, while under RCP 8.5, the difference between the two periods was profound.

A reduction in winter chill is the predominant factor in areas experiencing reduced cultivation suitability under both scenarios, with increased sunburn also contributing.

The bifurcating behaviour for the change in chill suitability likely occurred because there is a narrow temperature band for optimal accrual of RCU. In very cold areas where hourly winter temperatures are predominantly below the optimal band, a warming of climates will push temperatures closer to the optimal band and thus increase suitability scores. However, in areas currently receiving high RCU, a warming climate can push temperatures above the optimal temperature band, and potentially into temperature bands where negative accumulation of RCU occurs, decreasing suitability scores more sharply. This effect was extremely pronounced under RCP 8.5 compared with RCP 2.6.

7.2 Kiwifruit

7.2.1 Kiwifruit RCP 2.6

Under RCP 2.6, climate and cultivation suitability for kiwifruit are projected to have moderate declines in Northland and smaller declines in Auckland, northern and some eastern areas of the Waikato, northeast areas of Gisborne region, and some coastal areas of the Bay of Plenty, the Hawke’s Bay and some coastal locations around other parts of the North Island (Figure 128 and Figure 129). Given the current horticultural footprint for kiwifruit, orchards in Northland would be negatively affected by these changes in suitability, although a few areas in Northland are projected to still have good suitability in the future, while the majority of kiwifruit orchards elsewhere are likely to experience a small positive impact. Most change in suitability is projected to occur by mid-century, with little change from then until the late century.

Under RCP 2.6, the projection indicates moderate increases in the areas of land with suitability scores falling into the acceptable range or higher, although increases in the area of land with excellent suitability is expected to be modest (Table 10). Since suitability is projected to decrease in Northland, these changes may result in the kiwifruit footprint decreasing in Northland and increasing further south. Notably, high suitability areas are projected in areas around Taranaki.

The projection uncertainty encompasses a change in area of excellent suitability land between −16% and 67% for the mid-century and a range of −20% to 62% for the late century. However, within uncertainty limits, the areas of land with acceptable or very good suitability are consistently projected to increase slightly to moderately by the mid-century and slightly to significantly by the late-century (Table 10). Although the worst-case projections for good suitability land are decreases of 5 to 6% for the two periods, the best-case projections are for increases of 15%, and thus the expectation is an increase (Table 10).

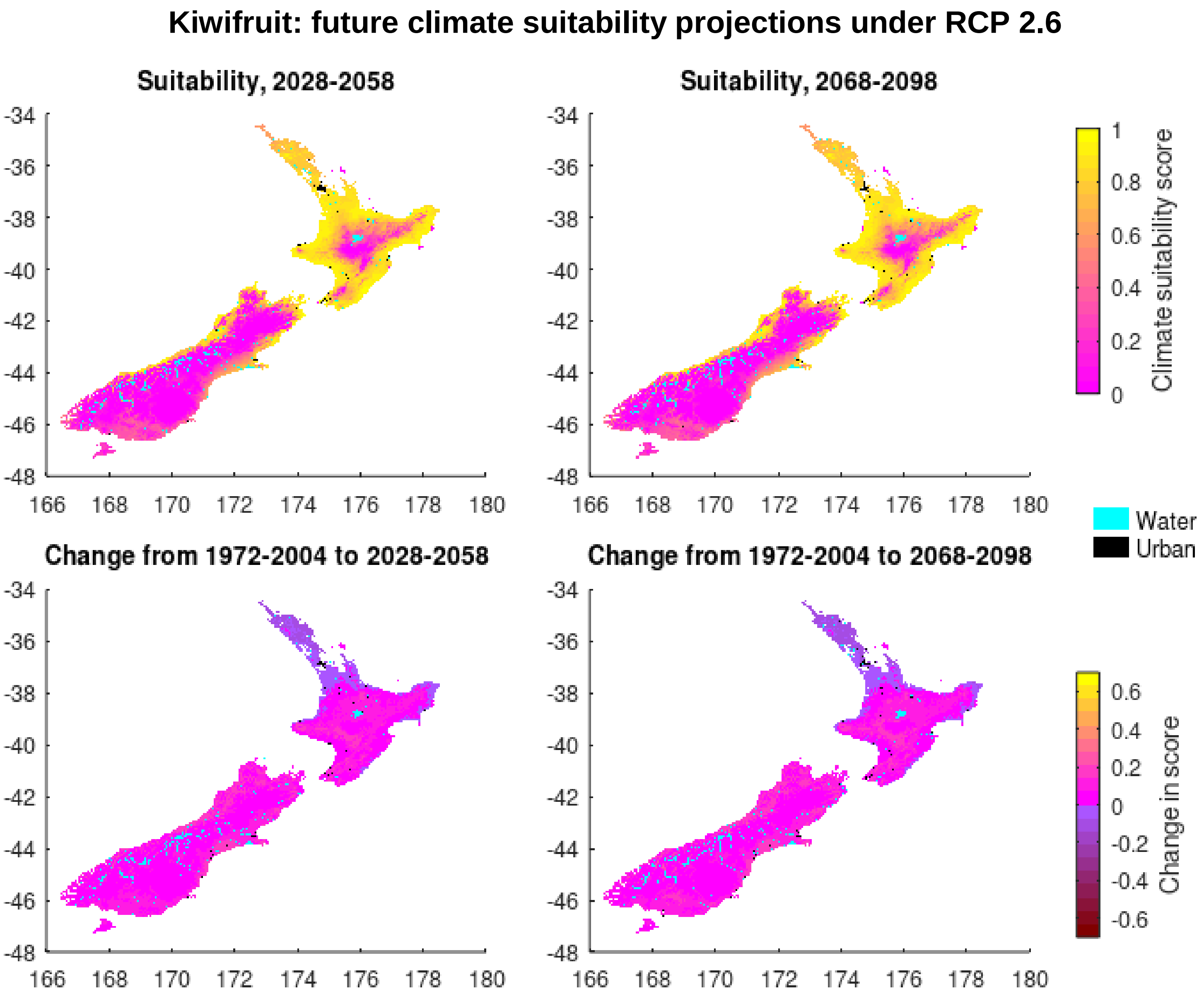

Figure 128. Kiwifruit: Projected climate suitability (top panels) and projected changes in climate suitability from the historic period (bottom panels) for the mid-century (left panels) and late century (right panels) under RCP 2.6.

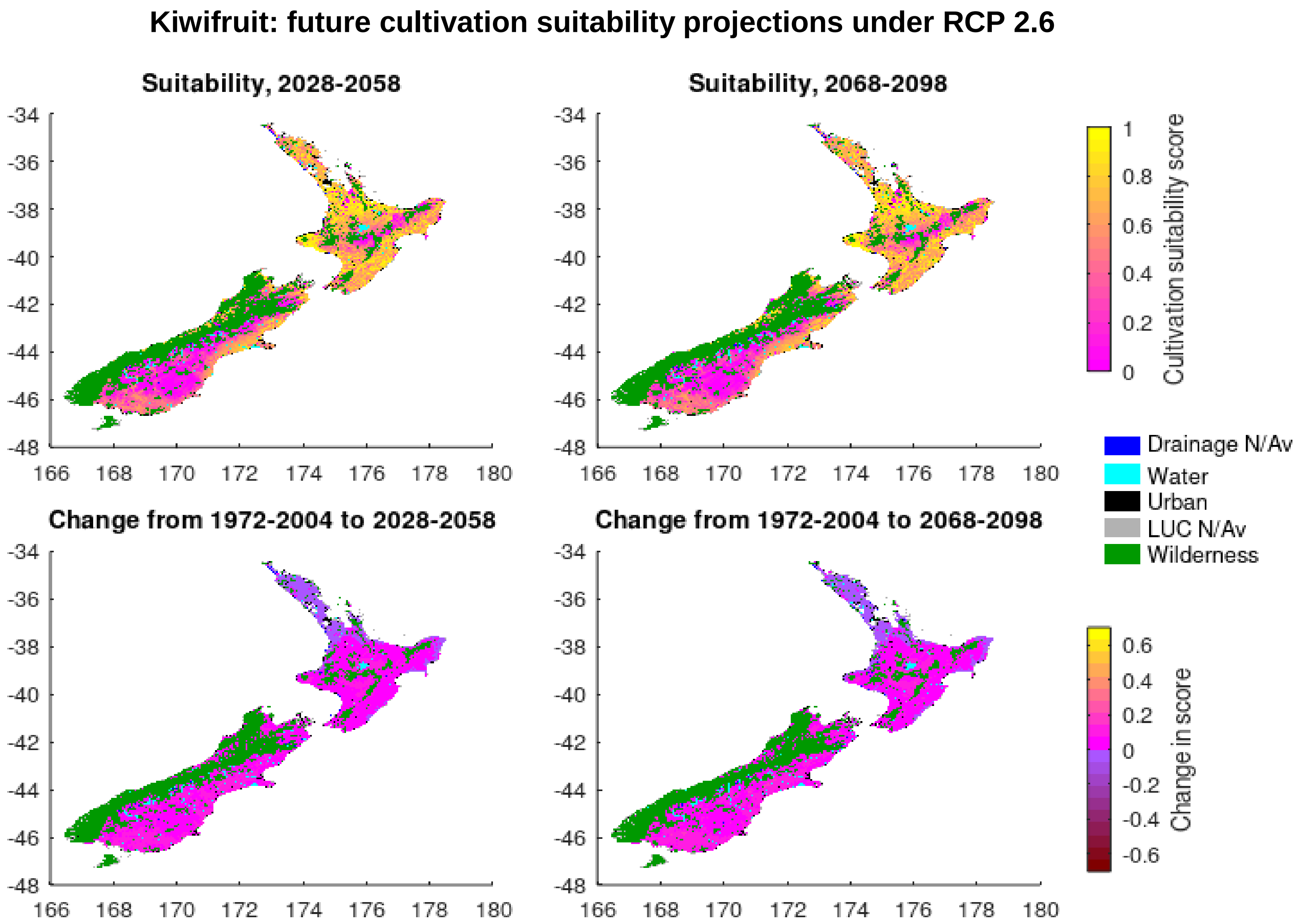

Figure 129. Kiwifruit: Projected cultivation suitability (top panels) and projected changes in cultivation suitability from the historic period (bottom panels) for the mid-century (left panels) and late century (right panels) under RCP 2.6.

Table 10. Kiwifruit: Land area in the historic period falling into different cultivation suitability ranges, projected changes for the mid- and late-century under RCP 2.6, and best and worst cases. Decreases are shaded red and increases shaded blue. Colour intensity increases with the magnitude of change.

Kiwifruit SLM RCP 2.6	Historic (km²) 1972–2004	Area change from historic (km²) 2028–2058			Area change from historic (km²) 2068–2098		
Suitability range		Projection	Best case	Worst case	Projection	Best case	Worst case
0–0.1	37541	−6215	−13048	−1090	−6716	−13358	−1591
0.1–0.2	12757	−1983	475	−3079	−2080	256	−3287
0.2–0.3	14845	−2929	−2971	−1100	−3176	−3311	−1417
0.3–0.4	16808	−1861	−2746	−1457	−1891	−2890	−1636
0.4–0.5	19596	1515	−698	3121	1578	−677	3637
0.5–0.6	21305	2873	3919	1477	3035	3968	1774
0.6–0.7	19058	4377	4089	3680	4988	4894	4079
0.7–0.8	18653	763	2778	−1107	784	2765	−956
0.8–0.9	16787	2604	3936	586	2884	4414	698
0.9–1.0	6375	856	4266	−1031	594	3939	−1301

7.2.2 Kiwifruit RCP 8.5

Under RCP 8.5, the climate and cultivation suitability projections for mid-century are similar to late-century projections under RCP 2.6. However, by late century, climate suitability is projected to decline significantly and cultivation suitability is projected to decline moderately in Northland, the Auckland region, the Waikato, the Coromandel, and coastal areas of the Bay of Plenty and Gisborne region with suitability scores dropping below acceptable in many locations in these areas, especially in Northland (Figure 130 and Figure 131). Many other areas of the North Island and all of the South Island are projected to have modest to moderate increases in suitability. Large areas around Taranaki, and scattered locations further south across the country are projected to have very good or excellent cultivation suitability scores. These changes could see a significant reduction in Northland's kiwifruit footprint accompanied by new kiwifruit orchards in areas that are not currently favoured for kiwifruit.

A closer examination of the climatic reasons for the change in suitability would indicate whether or not mitigation strategies may be possible. For example, adopting more suitable cultivars and/or acceptable bud break enhancers might enable successful kiwifruit production in areas that have become lower in suitability.

Strong increases in the areas of land in the excellent suitability categories are projected for mid-century, although the gains for the excellent suitability category are expected to reverse to a small loss by late century. Within the uncertainty limits of the projection, the areas of land with suitability scores lying in the acceptable, good and very good categories are consistently projected to increase for both the mid- and late-century (Table 11). However, for excellent category land, projected change is in the range −2% to 59% for the mid-century and in the range −35% to 39% for the late century.

Table 11. Kiwifruit: Land area in the historic period falling into different cultivation suitability ranges, projected change for the mid- and late-century under RCP 8.5, and best and worst cases. Decreases are shaded red and increases shaded blue. Colour intensity increases with the magnitude of change.

Kiwifruit SLM RCP 8.5	Historic (km^2) 1972–2004	Area change from historic (km^2) 2028–2058			Area change from historic (km^2) 2068–2098		
Suitability range		Projection	Best case	Worst case	Projection	Best case	Worst case
0–0.1	37541	−9686	−14697	−4759	−17463	−19709	−15442
0.1–0.2	12757	−2002	−889	−4351	−5839	−6114	−5716
0.2–0.3	14845	−4198	−3394	−3249	−5741	−5724	−5195
0.3–0.4	16808	−2418	−3948	−1778	−5228	−5849	−3959
0.4–0.5	19596	383	−613	2948	338	−1100	1939
0.5–0.6	21305	4372	3953	3224	6462	4249	7256
0.6–0.7	19058	6768	6813	5570	7760	8058	7735
0.7–0.8	18653	1655	3830	706	10464	10312	9672
0.8–0.9	16787	3650	5184	1842	9716	13421	5911
0.9–1.0	6375	1476	3761	−153	−469	2456	−2201

7.2.3 Kiwifruit: key criteria underlying change

The climatic reasons for the change in suitability can be seen by examining the individual one-to-one graphs comparing future scores against historic scores for each location, in the supplementary file ‘Comparison future vs historic scores’. Under both RCP 2.6 and 8.5, suitability scores for frost risk, risk of cold damage to canes (‘cold kill’) and GDD increased consistently across locations for both mid- and late-century, compared with the historic period. This increase was much more pronounced for GDD suitability, especially for RCP 8.5 under which GDD suitability increased to 0.8 or higher for most locations by the late century. However, as would be expected, suitability for winter chill showed a pattern of change that was in the opposite direction to that of GDD suitability, but to a lesser extent.

In many areas, the decrease in chill suitability was more than offset by increases in suitability scores for other criteria leading to an improvement overall; however, in other areas, the decrease in chill suitability dominated, leading to a decrease in overall suitability.

The decrease in chill suitability was moderate enough under RCP 2.6 that many locations could provide sufficient winter chill for ‘Hayward’, but under RCP 8.5 the number of locations with sufficient chill for ‘Hayward’ is projected to be significantly reduced, and ‘Zesy002’ would perform better in these areas. Mitigation strategies, such as more suitable cultivars and/or acceptable bud break enhancers, would be needed to enable successful kiwifruit production in areas that have become too low in suitability.

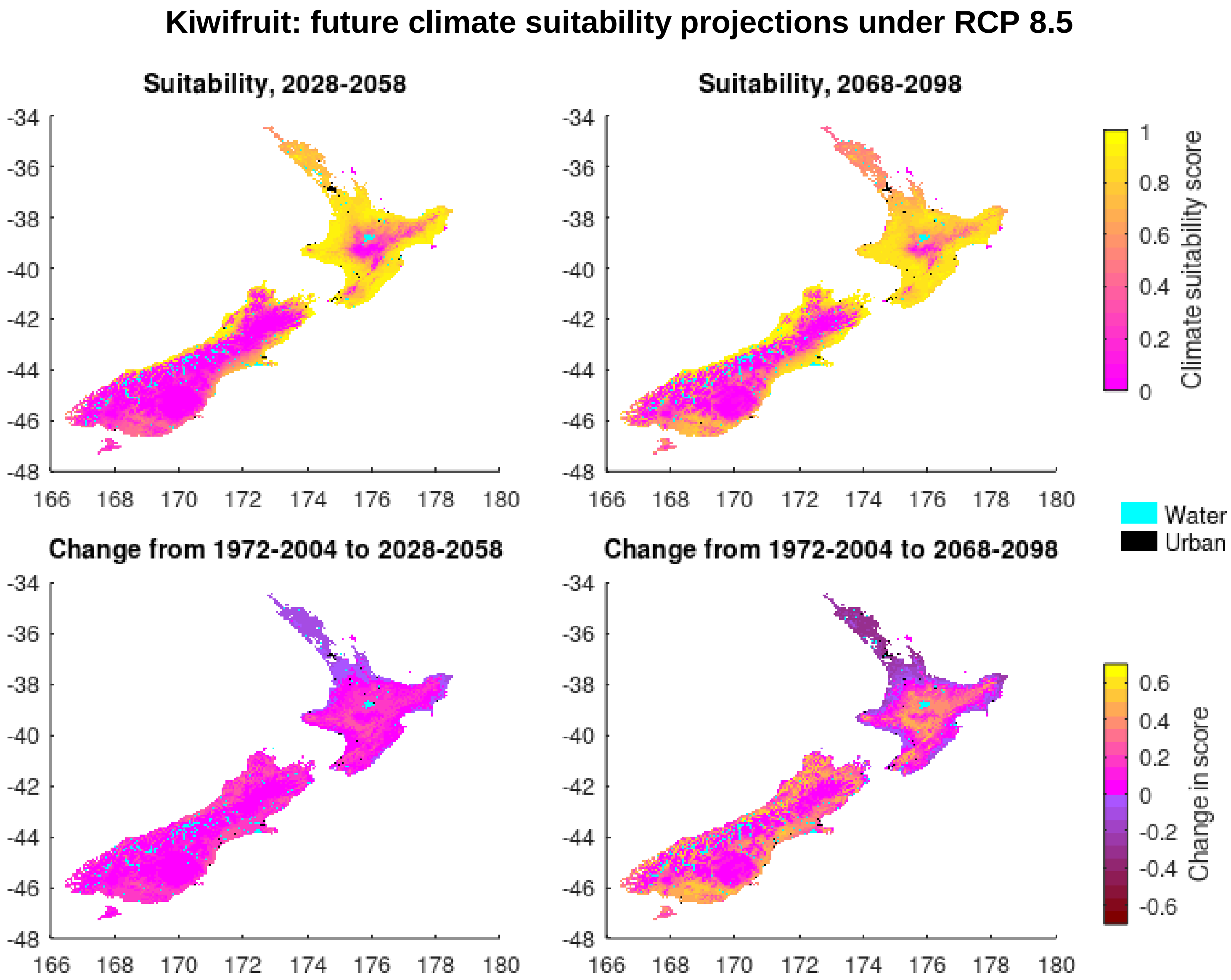

Figure 130. Kiwifruit: Projected climate suitability (top panels) and projected changes in climate suitability from the historic period (bottom panels) for the mid-century (left panels) and late century (right panels) under RCP 8.5.

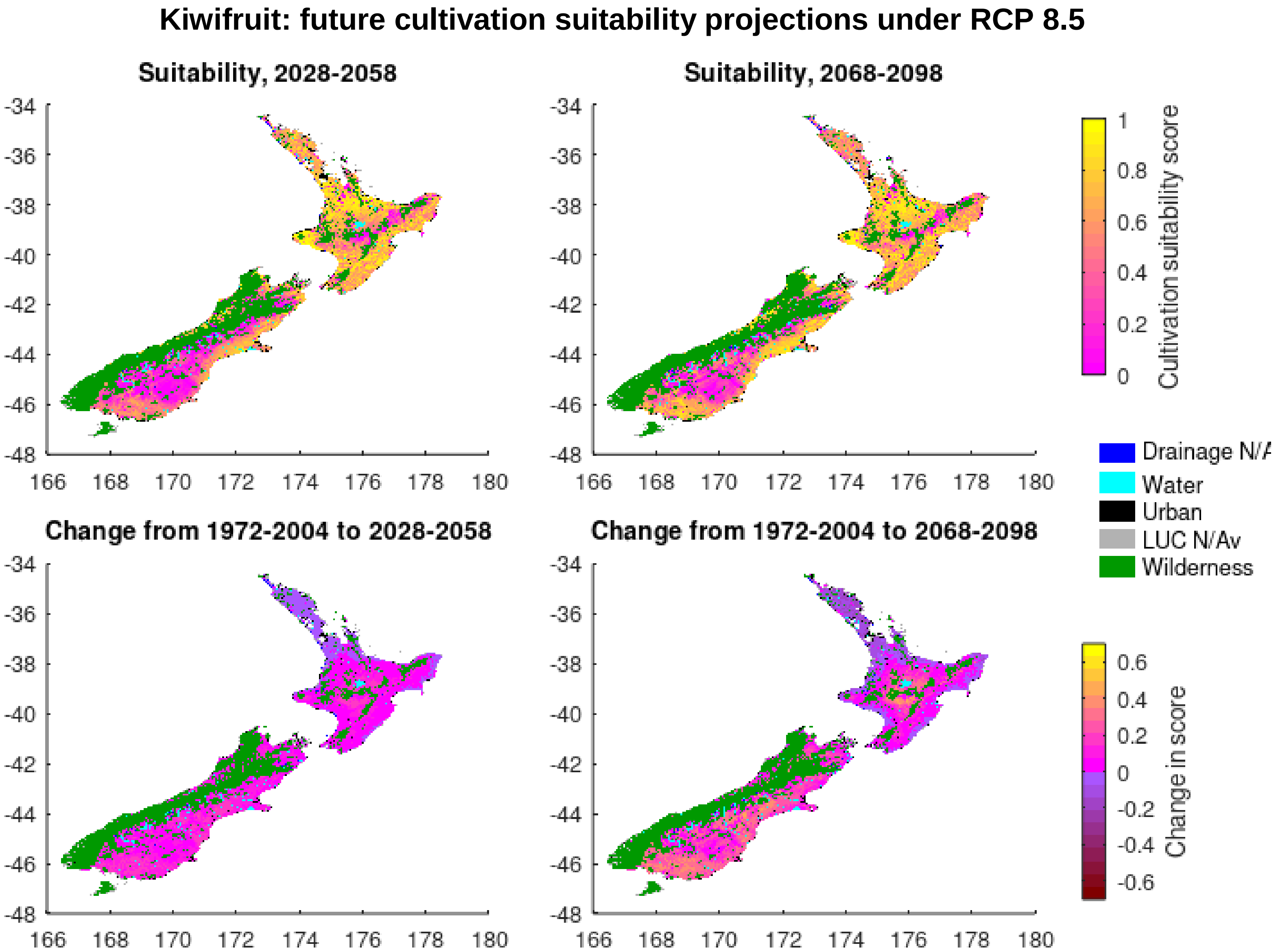

Figure 131. Kiwifruit: Projected cultivation suitability (top panels) and projected changes in cultivation suitability from the historic period (bottom panels) for the mid-century (left panels) and late century (right panels) under RCP 8.5.

7.3 Avocado

7.3.1 Avocado RCP 2.6

Climate suitability and cultivation suitability are both projected to increase modestly across the entire country by mid-century under RCP 2.6, with little further increase in suitability by the end of the century. The suitability maps are little changed from the historic period suitability maps, with Northland and a number of coastal areas round the North Island having good or higher suitability scores (Figure 132 and Figure 133).

The areas of land for each of the score ranges from acceptable to excellent are projected to increase significantly, with the area of excellent suitability land projected to increase by 77% and 80% at the mid- and late-century periods under RCP 2.6. Within projection uncertainty, the areas of land with suitability scores lying in the acceptable, good, very good and excellent categories are consistently projected to increase for both the mid- and the late-century periods with respect to the historic period (Table 12).

Table 12. Avocado: Land area in the historic period falling into different cultivation suitability ranges, projected changes for the mid- and late-century under RCP 2.6, and best and worst cases. Decreases are shaded red and increases shaded blue. Colour intensity increases with the magnitude of change.

Avocado SLM RCP 2.6	Historic (km^2) 1972–2004	Area change from historic (km^2) 2028–2058			Area change from historic (km^2) 2068–2098		
Suitability range		Projection	Best case	Worst case	Projection	Best case	Worst case
0–0.1	100734	−9534	−16716	−4064	−10345	−18544	−4631
0.1–0.2	13592	500	3145	−326	678	4329	−261
0.2–0.3	12048	−1256	−1402	−791	−1075	−1294	−948
0.3–0.4	12659	−696	−1101	−298	−894	−1162	−199
0.4–0.5	11530	1098	767	579	1070	728	665
0.5–0.6	10603	2243	3225	1599	2509	3328	1698
0.6–0.7	9360	2706	4145	989	2915	4417	1133
0.7–0.8	7953	2502	3392	1191	2601	3570	1410
0.8–0.9	4092	1543	2878	582	1617	2901	586
0.9–1.0	1154	894	1667	539	924	1727	547

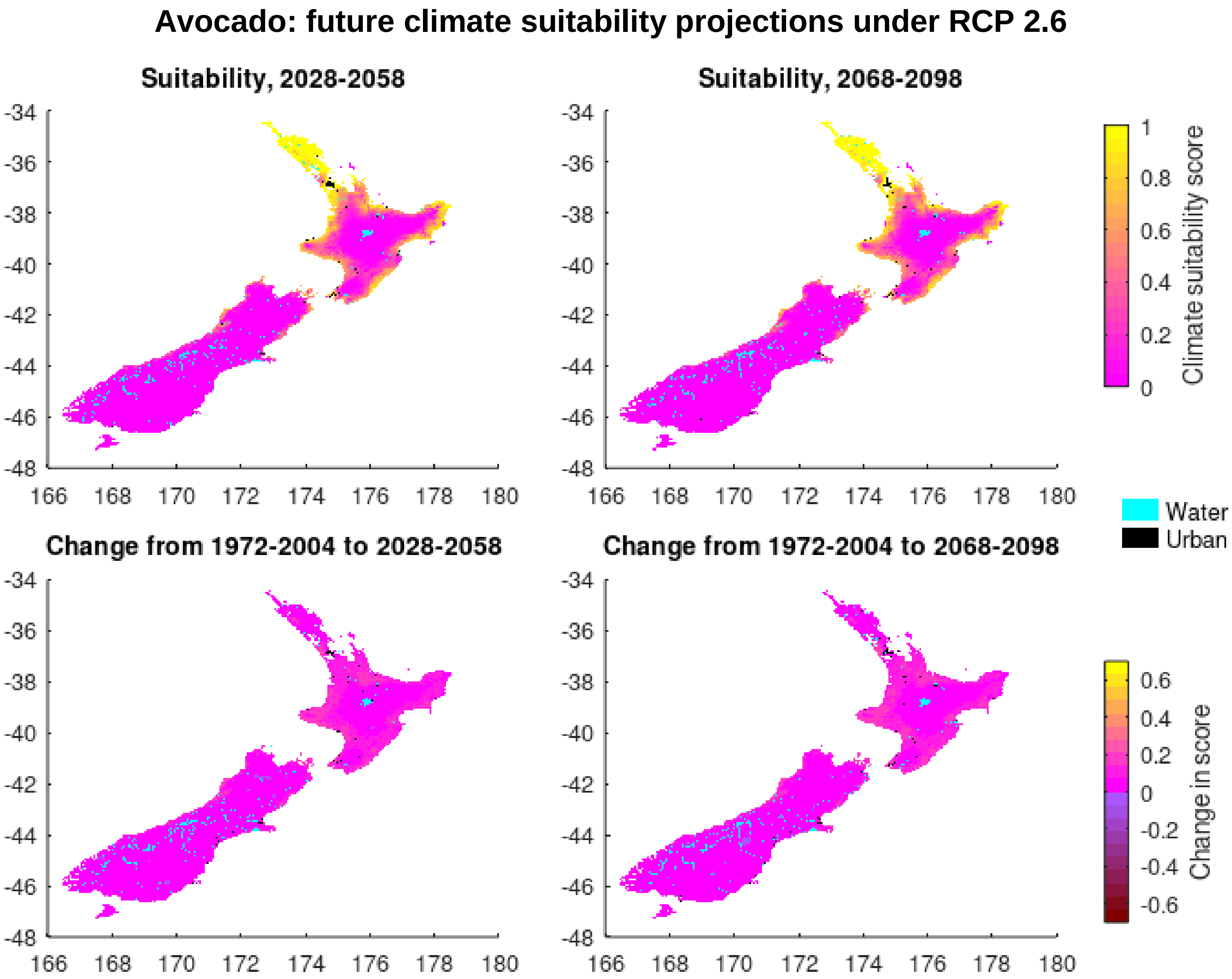

Figure 132. Avocado: Projected climate suitability (top panels) and projected changes in climate suitability from the historic period (bottom panels) for the mid-century (left panels) and late century (right panels) under RCP 2.6

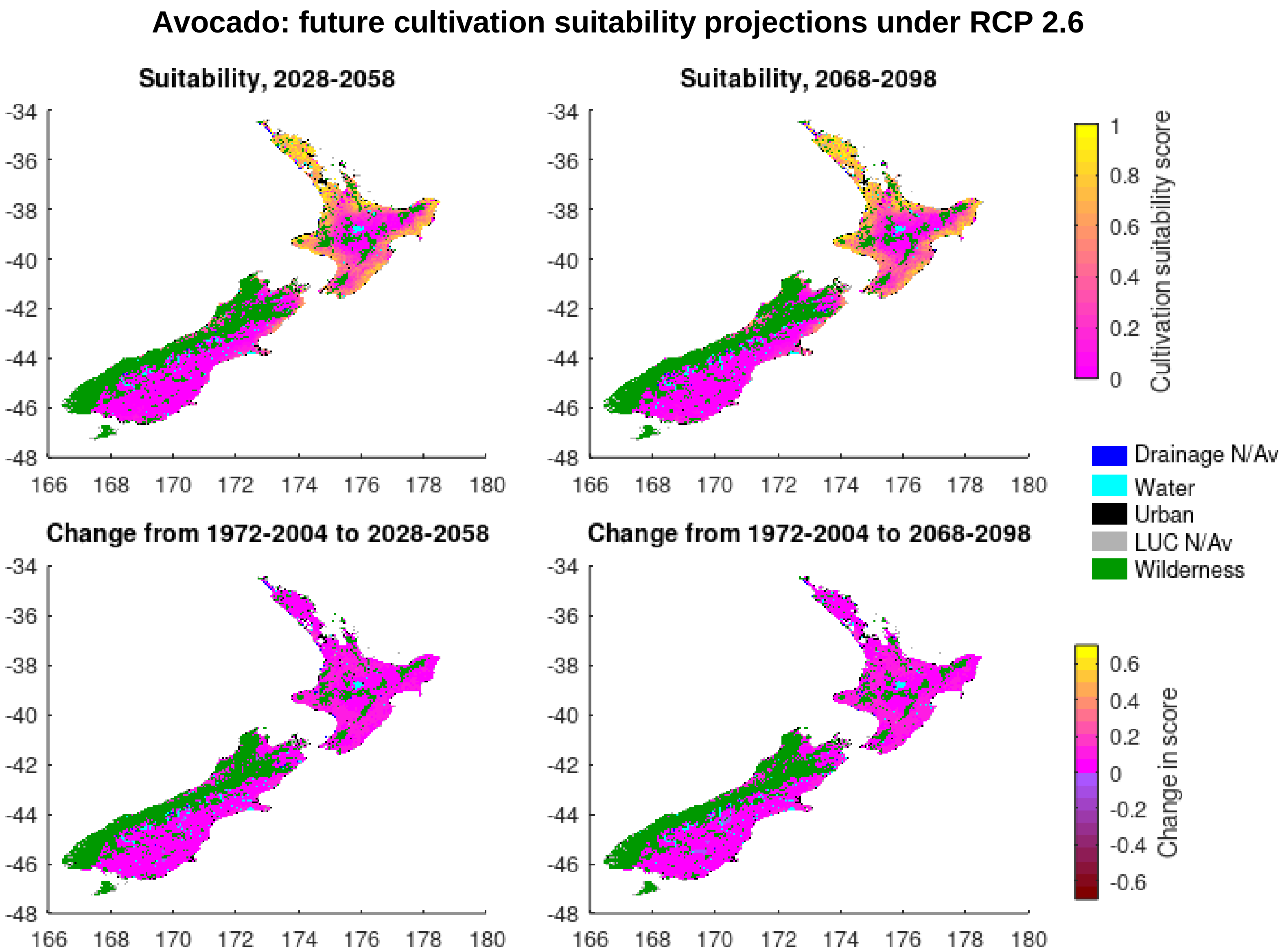

Figure 133. Avocado: Projected cultivation suitability (top panels) and projected changes in cultivation suitability from the historic period (bottom panels) for the mid-century (left panels) and late century (right panels) under RCP 2.6.

7.3.2 Avocado RCP 8.5

The mid-century projection under RCP 8.5 is similar in pattern to the late-century projection under RCP 2.6, although a little more favourable. The late-century projection under RCP 8.5 is for modest through to significant increases in climate and cultivation suitability across the country (Figure 134 and Figure 135). Some areas that had a modest suitability increase, such as Northland, already had excellent suitability scores for the historic period and thus did not have the potential for significant further increase. In addition to changes in Northland, this will result in most coastal areas of the North Island, and pockets on the north and east coast of the South Island, having very good to excellent suitability.

Within projection uncertainty, the areas of land with suitability scores lying in the acceptable, good, very good and excellent categories are consistently projected to increase. In particular, the increased area of excellent category land is projected to lie between 93% and 190% for the mid-century and 360% to 540% for the late-century (Table 13).

Table 13. Avocado: Land area in the historic period falling into different cultivation suitability ranges, projected changes for the mid- and late-century under RCP 8.5, and best and worst cases. Decreases are shaded red and increases shaded blue. Colour intensity increases with the magnitude of change.

Avocado SLM RCP 8.5	Historic (km^2) 1972–2004	Area change from historic (km^2) 2028–2058			Area change from historic (km^2) 2068–2098		
Suitability range		Projection	Best case	Worst case	Projection	Best case	Worst case
0–0.1	100734	−15888	−25633	−9068	−40731	−46497	−35139
0.1–0.2	13592	1998	6916	751	1435	1759	3069
0.2–0.3	12048	−1047	−1252	−1486	2576	1173	1835
0.3–0.4	12659	−1488	−2013	−1384	−140	504	−1884
0.4–0.5	11530	1270	1300	1041	233	1369	405
0.5–0.6	10603	3193	4062	1936	4873	4907	4467
0.6–0.7	9360	4383	5922	2964	9679	10723	8545
0.7–0.8	7953	3436	4774	2636	9397	10987	8180
0.8–0.9	4092	2628	3742	1538	7724	8893	6321
0.9–1.0	1154	1515	2182	1072	4954	6182	4201

7.3.3 Avocado: key criteria underlying change

Under RCP 2.6, frost risk suitability increased modestly in almost all locations and negligibly decreased in the other handful of areas, and the main factor underlying the increased climate suitability across the country was that warmth suitability increased moderately across all locations as mean temperatures increased towards the optimal temperature band (see supplementary file ‘Comparison future vs historic scores’). Under RCP 8.5, frost risk suitability showed more increase compared with for RCP 2.6 and by late-century was significantly increased over the historic values. Increases in warmth suitability scores for avocado were also significantly more than under RCP 2.6, at both the mid-century and late-century stages (see supplementary file ‘Comparison future vs historic scores’).

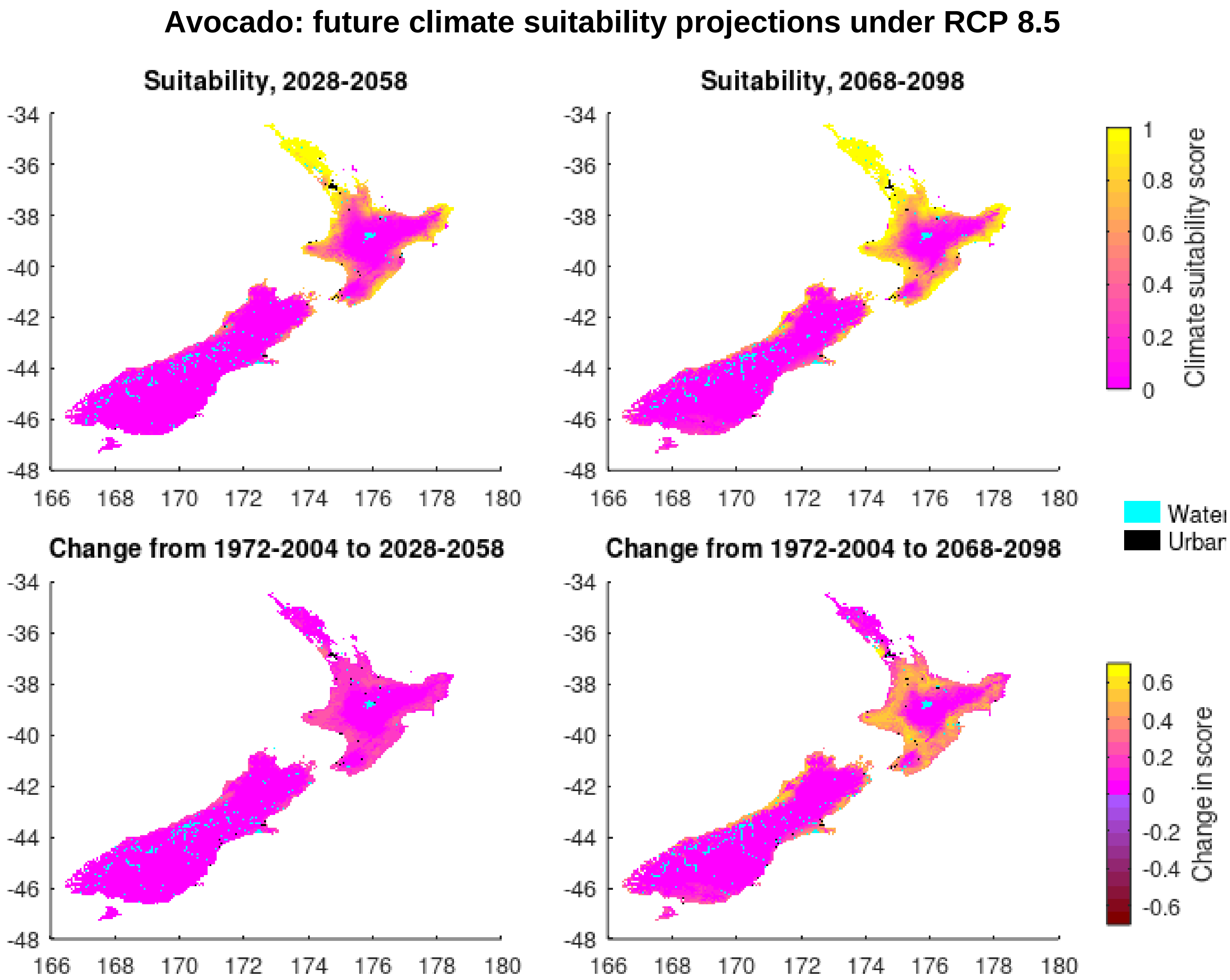

Figure 134. Avocado: Projected climate suitability (top panels) and projected changes in climate suitability from the historic period (bottom panels) for the mid-century (left panels) and late century (right panels) under RCP 8.5.

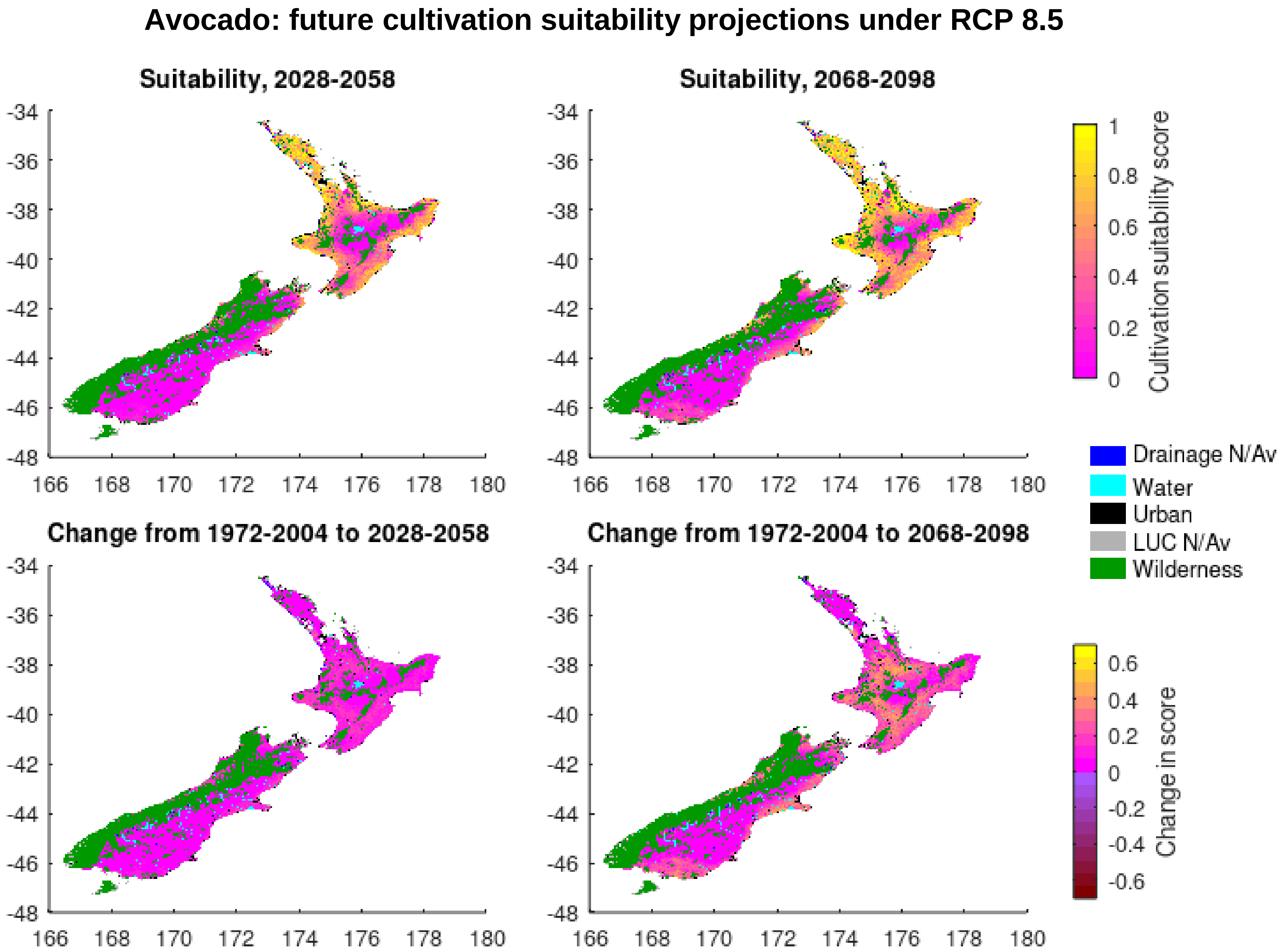

Figure 135. Avocado: Projected cultivation suitability (top panels) and projected changes in cultivation suitability from the historic period (bottom panels) for the mid-century (left panels) and late century (right panels) under RCP 8.5.

7.4 Blueberry

7.4.1 Blueberry RCP 2.6

Under RCP 2.6, climate and cultivation suitability scores are projected to increase slightly or remain constant for the South Island (except for a few coastal areas) and for central and elevated parts of the North Island, with modest decreases in suitability in the northern Waikato and further north, in coastal areas of the Bay of Plenty, and around the East Cape; elsewhere only slight decreases are expected (Figure 136 and Figure 137). The majority of the change occurs by mid-century. The Waikato and Bay of Plenty, which contain a significant number of New Zealand's blueberry orchards, are generally projected to have slight decreases in suitability and are unlikely to experience much impact. Overall, there are likely to be large parts of New Zealand that will be suitable or highly suitable for blueberry production, particularly if appropriate cultivars and mitigation strategies are selected.

Under RCP 2.6, a small relative increase in the area of excellent suitability land is projected to occur by mid-century but largely reverse by late-century, with significant increases in the area of land with suitability scores in the acceptable, good or very good ranges (Table 14). The projected change in excellent suitability land has large uncertainty limits of −22% and 58% for the mid-century and between −25% and 54% for the late century. For very good suitability land these limits are approximately 0% and 20% for both periods. Acceptable and good suitability land is consistently projected to increase, in the range 7% to 13% within uncertainty limits (Table 14). The best case change for the acceptable category (0.6 to 0.7) is lower than the nominal projection value due to the vagaries of considering prediction uncertainties with histogram bins.

Table 14. Blueberry: Land area in the historic period falling into different cultivation suitability ranges, projected changes for the mid- and late-century under RCP 2.6, and best and worst cases. Decreases are shaded red and increases shaded blue. Colour intensity increases with the magnitude of change.

Blueberry SLM RCP 2.6	Historic (km^2) 1972–2004	Area change from historic (km^2) 2028–2058			Area change from historic (km^2) 2068–2098		
Suitability range		Projection	Best case	Worst case	Projection	Best case	Worst case
0–0.1	13684	−1167	−1968	741	−1134	−1968	730
0.1–0.2	3992	−1105	−2776	−890	−1173	−2751	−963
0.2–0.3	4223	−1029	−556	−495	−1072	−654	−593
0.3–0.4	8396	−2619	−3898	−857	−2773	−3848	−996
0.4–0.5	19396	−1394	−6222	1717	−1465	−6384	1529
0.5–0.6	26337	−4039	−3529	−2883	−4132	−3733	−2901
0.6–0.7	30662	4044	3236	2927	4348	3556	3377
0.7–0.8	31696	2140	2608	2108	2554	2515	2543
0.8–0.9	34167	4509	6676	99	4668	7235	100
0.9–1.0	11172	660	6429	−2467	179	6032	−2826

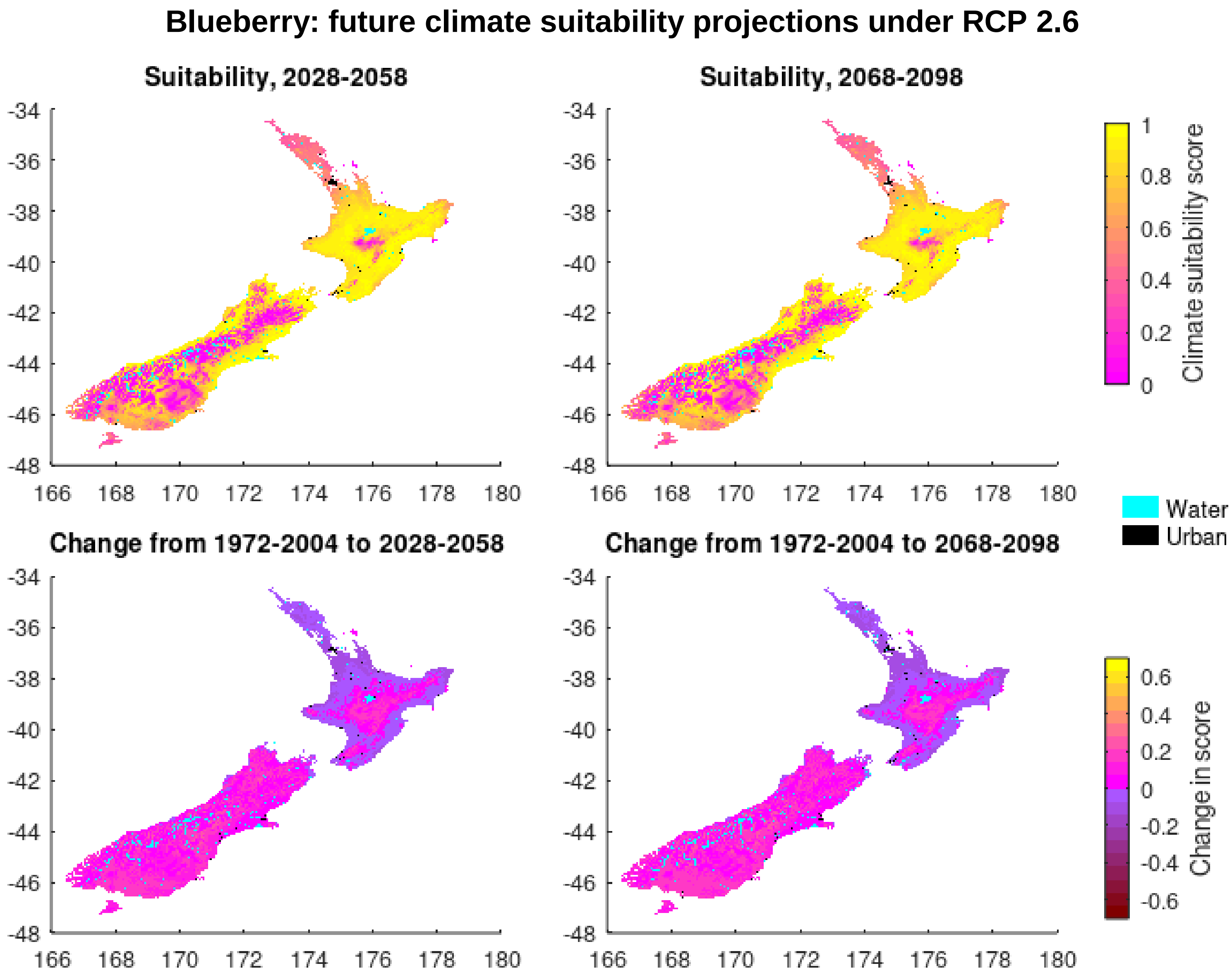

Figure 136. Blueberry: Projected climate suitability (top panels) and projected changes in climate suitability from the historic period (bottom panels) for the mid-century (left panels) and late century (right panels) under RCP 2.6.

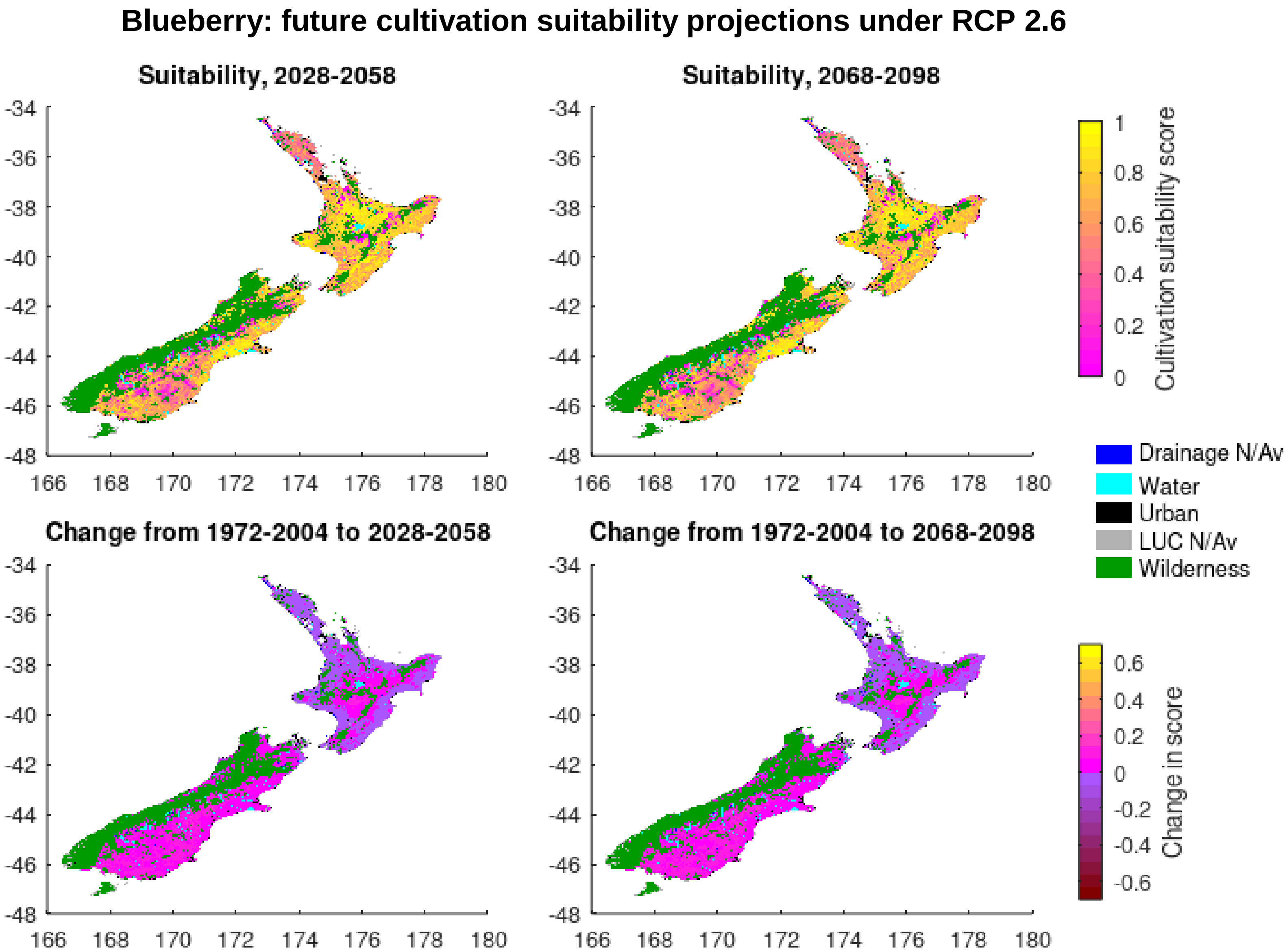

Figure 137. Blueberry: Projected cultivation suitability (top panels) and projected changes in cultivation suitability from the historic period (bottom panels) for the mid-century (left panels) and late century (right panels) under RCP 2.6.

7.4.2 Blueberry RCP 8.5

Under RCP 8.5, projected changes in suitability scores showed similar spatial patterns to those projected for the late-century under RCP 2.6, though the magnitude of changes are much more pronounced. These trends were projected to continue through to the end of the century, with the most of the North Island experiencing moderate declines in cultivation suitability except for elevated areas of the central North Island which were mostly projected to experience no change with a few areas experiencing moderate increases in suitability.

By the end of the century, the majority of the South Island, apart from areas around Blenheim was projected to have little increase in suitability, with isolated areas in Otago and Southland projected to have moderate increases in suitability with resulting suitability scores in the good to excellent range (see Figure 138 and Figure 139). As for the scenario under RCP 2.6, we expect that large numbers of locations in New Zealand will be suitable or highly suitable for blueberry production if appropriate cultivars and mitigation strategies are selected.

Under RCP 8.5, the areas of land with suitability scores in the excellent and very good range is projected to increase by 24% and 6%, respectively, by the late-century. The uncertainty limits around these late-century projections are 4% and 51% for excellent suitability land and −3% and 15% for very good suitability land (Table 15). An increase of between 7% and 17% in the area of very good suitability land is projected for the mid-century, but much of this gain is expected to be lost by late-century with concomitant gains in the excellent and good suitability categories (Table 15).

Table 15. Blueberry: Land area in the historic period falling into different cultivation suitability ranges, projected changes for the mid- and late-century under RCP 8.5, and best and worst cases. Decreases are shaded red and increases shaded blue. Colour intensity increases with the magnitude of change.

Blueberry SLM RCP 8.5	Historic (km^2) 1972–2004	Area change from historic (km^2) 2028–2058			Area change from historic (km^2) 2068–2098		
Suitability range		Projection	Best case	Worst case	Projection	Best case	Worst case
0–0.1	13684	−1431	−1971	33	−1839	−1975	−1317
0.1–0.2	3992	−1607	−2972	−1771	−3282	−3717	−3457
0.2–0.3	4223	−1447	−1076	−1005	−2848	−3274	−1549
0.3–0.4	8396	−3046	−3555	−1964	−1608	−3952	1330
0.4–0.5	19396	−2254	−5333	−324	−4220	−4158	−4730
0.5–0.6	26337	−5130	−5385	−3901	−3035	−5815	−1388
0.6–0.7	30662	4934	4581	4496	4974	3415	7113
0.7–0.8	31696	3176	2640	3375	7215	8573	4562
0.8–0.9	34167	5924	7997	2360	1926	5249	−970
0.9–1.0	11172	881	5074	−1299	2717	5654	406

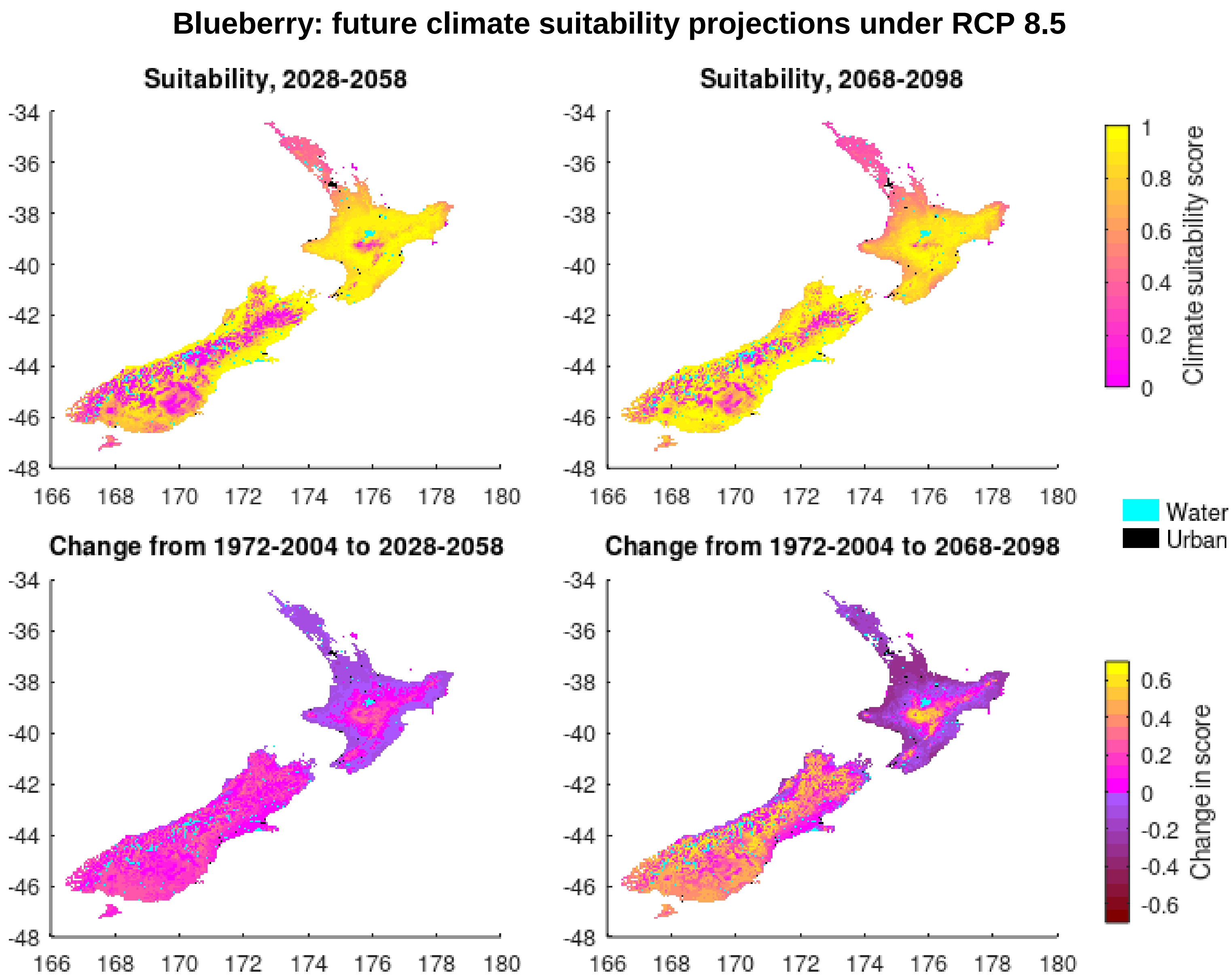

Figure 138. Blueberry: Projected climate suitability (top panels) and projected changes in climate suitability from the historic period (bottom panels) for the mid-century (left panels) and late century (right panels) under RCP 8.5.

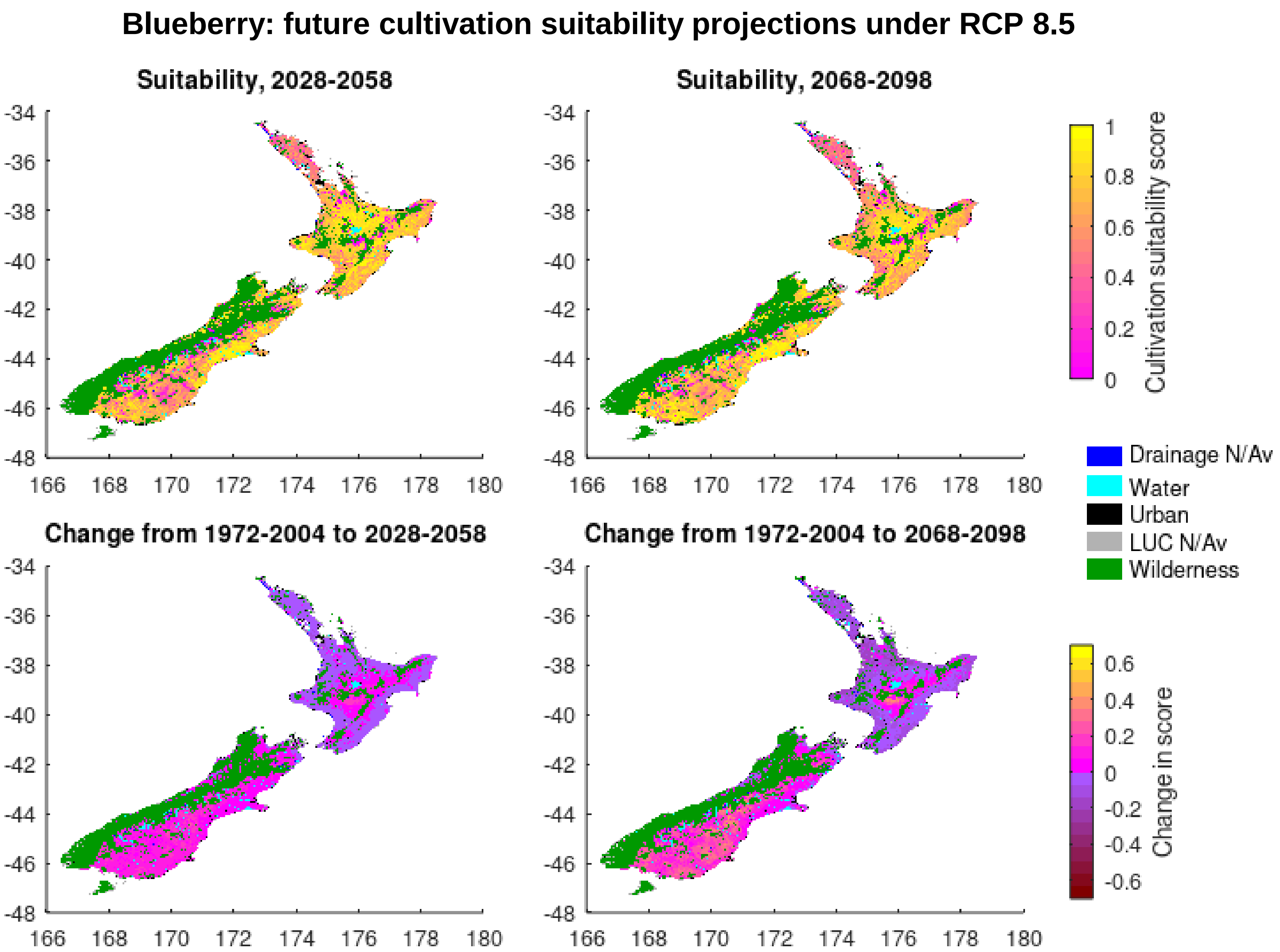

Figure 139. Blueberry: Projected cultivation suitability (top panels) and projected changes in cultivation suitability from the historic period (bottom panels) for the mid-century (left panels) and late century (right panels) under RCP.

7.4.3 Blueberry: key criteria underlying change

In comparison with the historic values, chill suitability scores for blueberry were decreased moderately under RCP 2.6, at mid- and late-century, and moderate and substantial for the same time periods under RCP 8.5. Frost risk moderately increased under RCP 2.6 and moderately and significantly increased under RCP 8.5 for respectively the mid- and late-century periods. GDD suitability was significantly increased under RCP 2.6 and significantly and substantially increased under RCP 8.5 for respectively the mid- and late-century (see supplementary file 'Comparison future vs historic scores').

The changes resulted in either moderate increases or modest decreases in overall climate suitability under RCP 2.6, and under RCP 8.5 either significant increases or moderate decreases in climate suitability by mid-century, and either substantial increases or modest to significant decreases in suitability by late-century.

Despite the increases overall climate suitability projected to occur in the majority of area, an emphasis on low-chill cultivars will be needed to capitalise on the increased GDD accumulation.

7.5 Cherry

7.5.1 Cherry RCP 2.6

Under RCP 2.6, most areas of the South Island and central and elevated areas of the North Island are projected to have either no change or a small increase in climate and cultivation suitability, while other areas are projected to have small declines in suitability by mid-century, with little change from then until late-century (Figure 140 and Figure 141). This would have a positive impact on cherry orchards in Central Otago, which represent the bulk of New Zealand's cherry industry, although in the Hawke's Bay the impact on orchards will depend on their location. For example, inland areas of the Hawke's Bay are projected to experience an increase in suitability, whereas a decrease in suitability is projected for coastal and hinterland areas, which in the historic period already had less than ideal chill suitability.

The projection indicates that, with respect to the historic footprint, there would be a 10% increase in the area of the excellent suitability areas by mid-century, followed by a 14% decrease in footprint by the late century. Areas of land with suitability scores in the acceptable, good and very good categories are projected to have modest to moderate increases by the mid-century that are more or less maintained in the late-century (Table 16). For both the mid-century and late-century, the uncertainty limits of the projection allow for large increases or decreases in land with excellent suitability, and significant increases or small decreases in land with very good suitability. Land with good suitability is consistently projected to increase in area (Table 16).

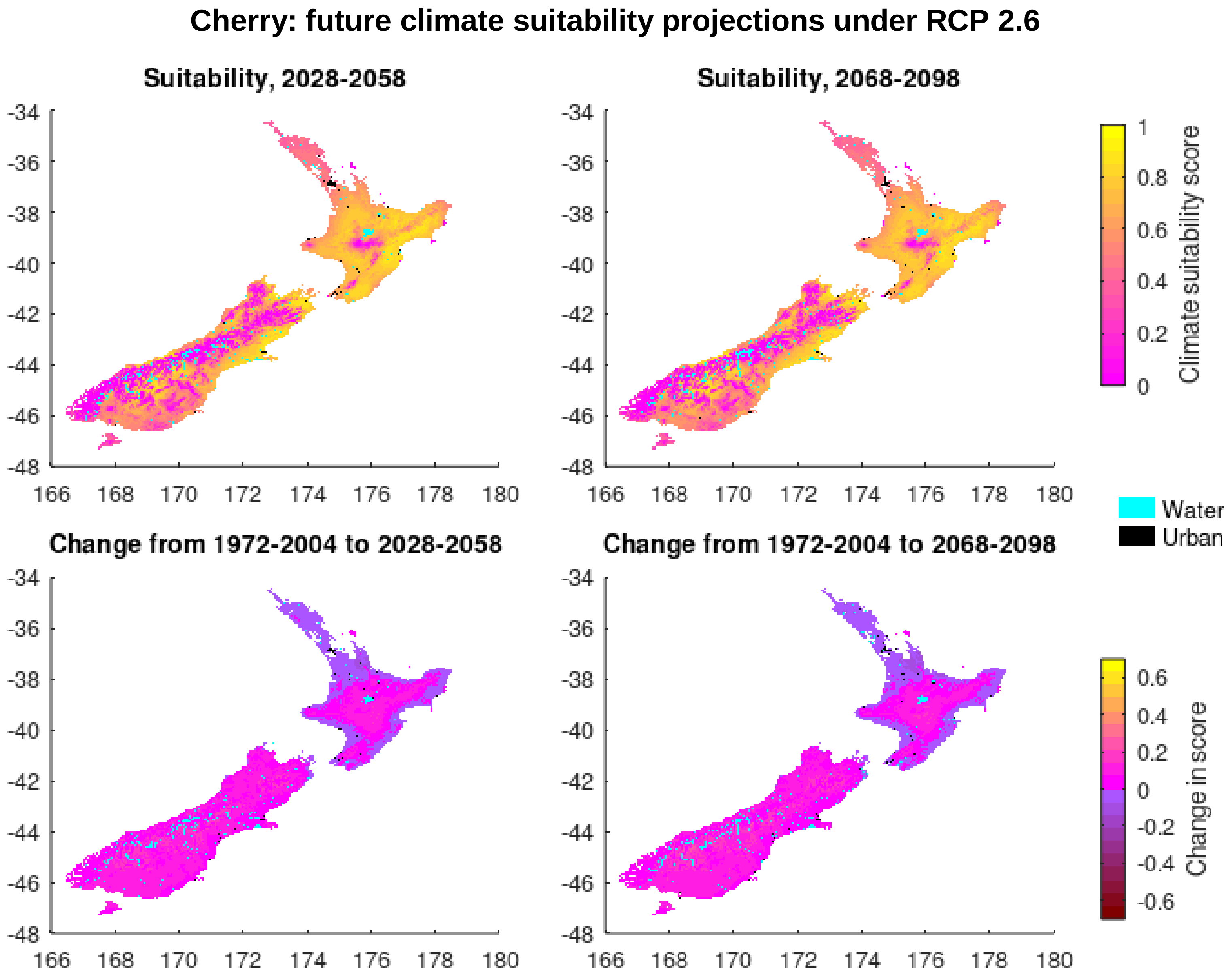

Figure 140. Cherry: Projected climate suitability (top panels) and projected changes in climate suitability from the historic period (bottom panels) for the mid-century (left panels) and late century (right panels) under RCP 2.6.

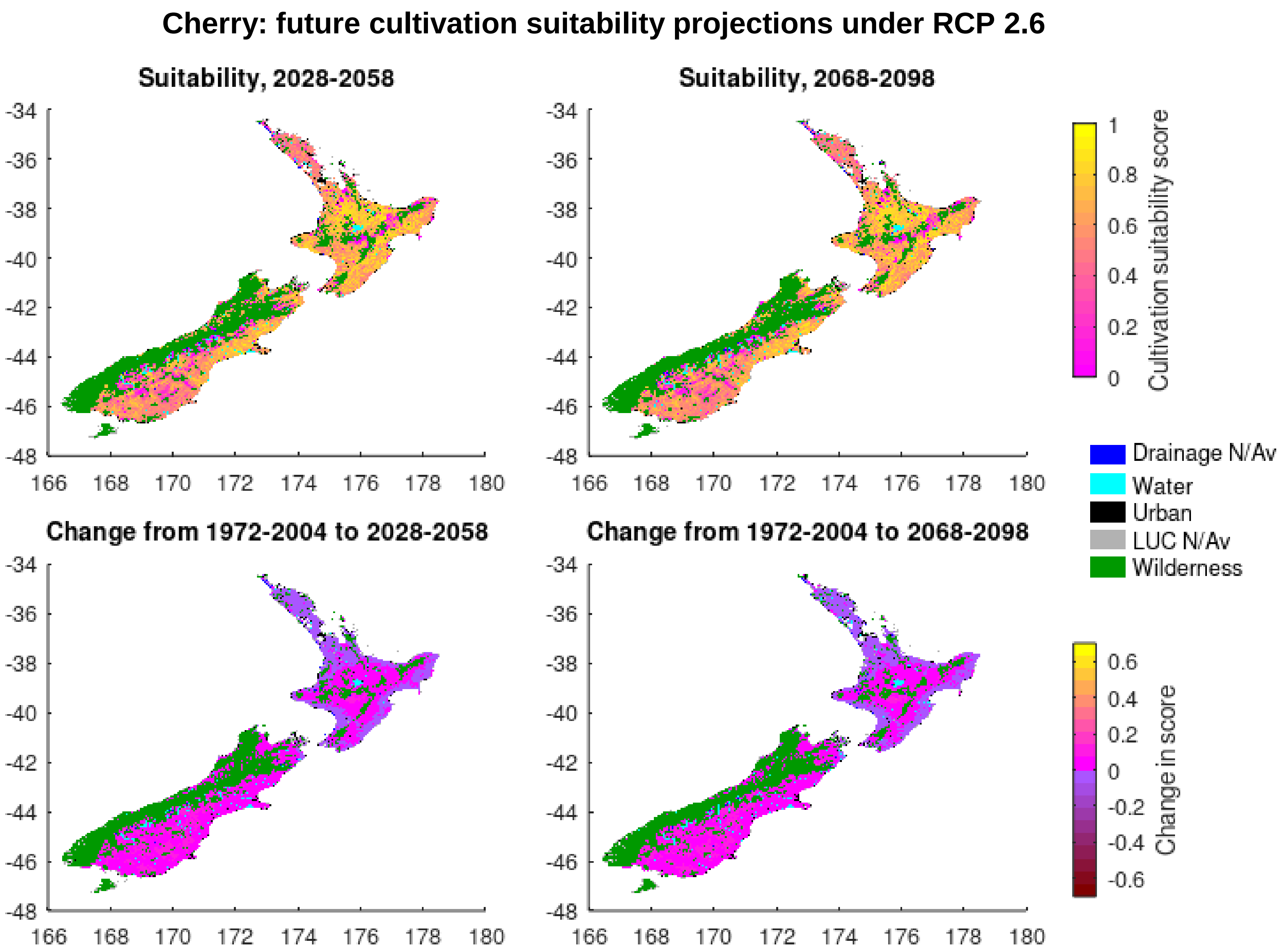

Figure 141. Cherry: Projected cultivation suitability (top panels) and projected changes in cultivation suitability from the historic period (bottom panels) for the mid-century (left panels) and late century (right panels) under RCP 2.6.

Table 16. Cherry: Land area in the historic period falling into different cultivation suitability ranges, projected changes for the mid- and late-century under RCP 2.6, and best and worst cases. Decreases are shaded red and increases shaded blue. Colour intensity increases with the magnitude of change.

Cherry SLM RCP 2.6	Historic (km^2) 1972–2004	Area change from historic (km^2) 2028–2058			Area change from historic (km^2) 2068–2098		
Suitability range		Projection	Best case	Worst case	Projection	Best case	Worst case
0–0.1	14847	−2034	−3016	−1437	−2115	−3009	−1566
0.1–0.2	3325	−1105	−1448	−342	−1301	−1627	−476
0.2–0.3	4934	−1161	−1661	−761	−1187	−1779	−815
0.3–0.4	11732	−2332	−3814	−647	−2356	−3716	−618
0.4–0.5	29866	−4239	−8417	−91	−4002	−8402	238
0.5–0.6	38953	1173	1486	372	1556	1754	862
0.6–0.7	36713	2320	3981	114	2369	4243	43
0.7–0.8	28351	4677	7012	3383	5066	7130	3587
0.8–0.9	14687	2668	5602	−444	2014	5229	−1041
0.9–1.0	317	33	275	−147	−44	177	−214

7.5.2 Cherry RCP 8.5

The mid-century spatial patterns of climate and cultivation suitability change projected for cherry under RCP 8.5 resemble those for the late-century under RCP 2.6, and these changes are projected to intensify for the late-century (Figure 142 and Figure 143). Most areas of the North Island (apart from central, elevated areas) are projected to become increasingly less suitable for cherry cultivation, while most of the South Island (apart from northeast parts of the Marlborough region) are projected to become increasingly suitable, especially in scattered locations in Otago and Southland.

Only a small fraction of land had excellent suitability for cherry in the historic period, and this is projected to have an increase of 32% by mid-century and of 340% by late-century, with significant increases to the areas of land with very good and good suitability (Table 17). Within the uncertainty limits of the projection, change in acceptable, good, and very good suitability land is consistently positive for both mid- and late-century periods. For excellent suitability land, the projected change would lie between −52% and 216% at the mid-century, and between 94% and 1500% by late century which promises the potential for significant growing opportunities (Table 17).

Table 17. Cherry: Land area in the historic period falling into different cultivation suitability ranges, projected changes for the mid- and late-century under RCP 8.5, and best and worst cases. Decreases are shaded red and increases shaded blue. Colour intensity increases with the magnitude of change.

Cherry SLM RCP 8.5	Historic (km^2) 1972–2004	Area change from historic (km^2) 2028–2058			Area change from historic (km^2) 2068–2098		
Suitability range		Projection	Best case	Worst case	Projection	Best case	Worst case
0–0.1	14847	−2444	−3006	−2116	−2643	−3110	732
0.1–0.2	3325	−2131	−2151	−1430	−3232	−2895	−3177
0.2–0.3	4934	−1591	−2231	−1250	−4083	−4367	−3499
0.3–0.4	11732	−2906	−4142	−1441	−2783	−5113	−589
0.4–0.5	29866	−5756	−9174	−2610	−4035	−5868	−2218
0.5–0.6	38953	936	255	1090	−4688	−6034	−4469
0.6–0.7	36713	3120	4732	1351	3983	3203	2584
0.7–0.8	28351	7183	8295	6264	11936	12999	9552
0.8–0.9	14687	3486	6737	306	4462	6531	786
0.9–1.0	317	103	685	−164	1083	4654	298

7.5.3 Cherry: key criteria underlying change

Under RCP 2.6, suitability scores for fruit cracking are projected to consistently increase to a modest extent (and thus fruit-cracking risk to decrease), while GDD suitability scores are projected to consistently increase significantly and chill suitability is projected to decrease consistently across locations. Frost risk suitability, however, is projected to have minor to moderate increases in many areas and minor to small decreases in others locations and remain unchanged in yet others. Change in overall climate suitability is similarly projected under RCP 2.6 to vary from small decreases to moderate increases. Under RCP 8.5, these patterns of change are similar but occur on an exaggerated scale (see supplementary file ‘Comparison future vs historic scores’).

Under RCP 2.6, while growing conditions are projected to generally improve by mid-century, an increased reliance on moderate and low-chill cultivars is expected. The minor decrease in frost suitability projected for some locations is likely to occur due to changes in timing of flowering with respect to the start of the frost risk periods.

Under RCP 8.5, the number of locations suitable for high-chill varieties of cherry is expected to decrease significantly, and it is likely that the industry will be reliant on low-chill varieties in much of its footprint. This of course depends on whether or not locations with high chill suitability have high suitability scores for other criteria. Answering this would require a detailed location-by-location analysis, which is out of scope for this study. Generally, however, the number of locations with high suitability scores for GDD, fruit cracking and frost are expected to increase under RCP 8.5, although advanced development times for budburst and flowering stages due to increased accumulation of GDD are expected to increase frost risk in some areas.

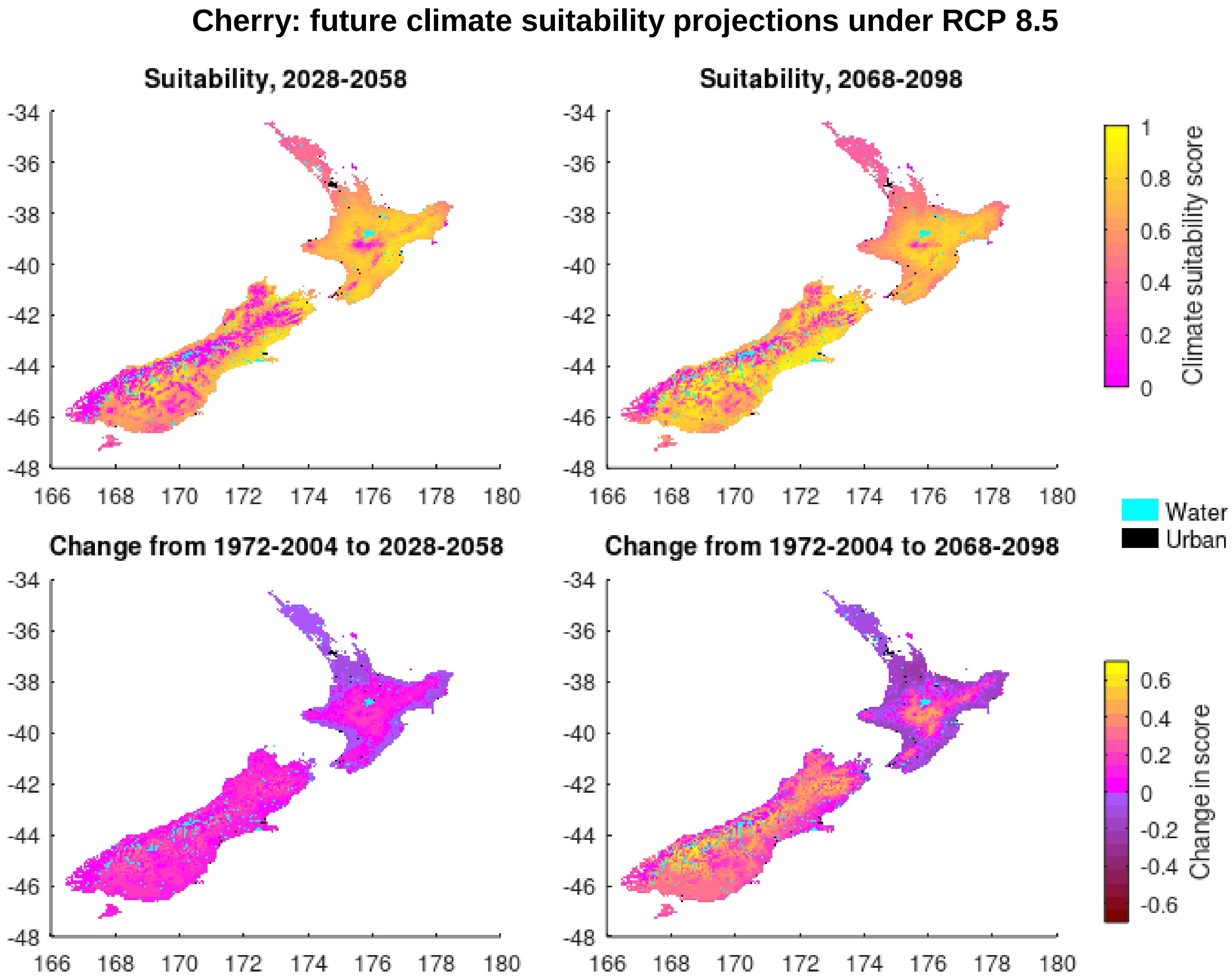

Figure 142. Cherry: Projected climate suitability (top panels) and projected changes in climate suitability from the historic period (bottom panels) for the mid-century (left panels) and late century (right panels) under RCP 8.5.

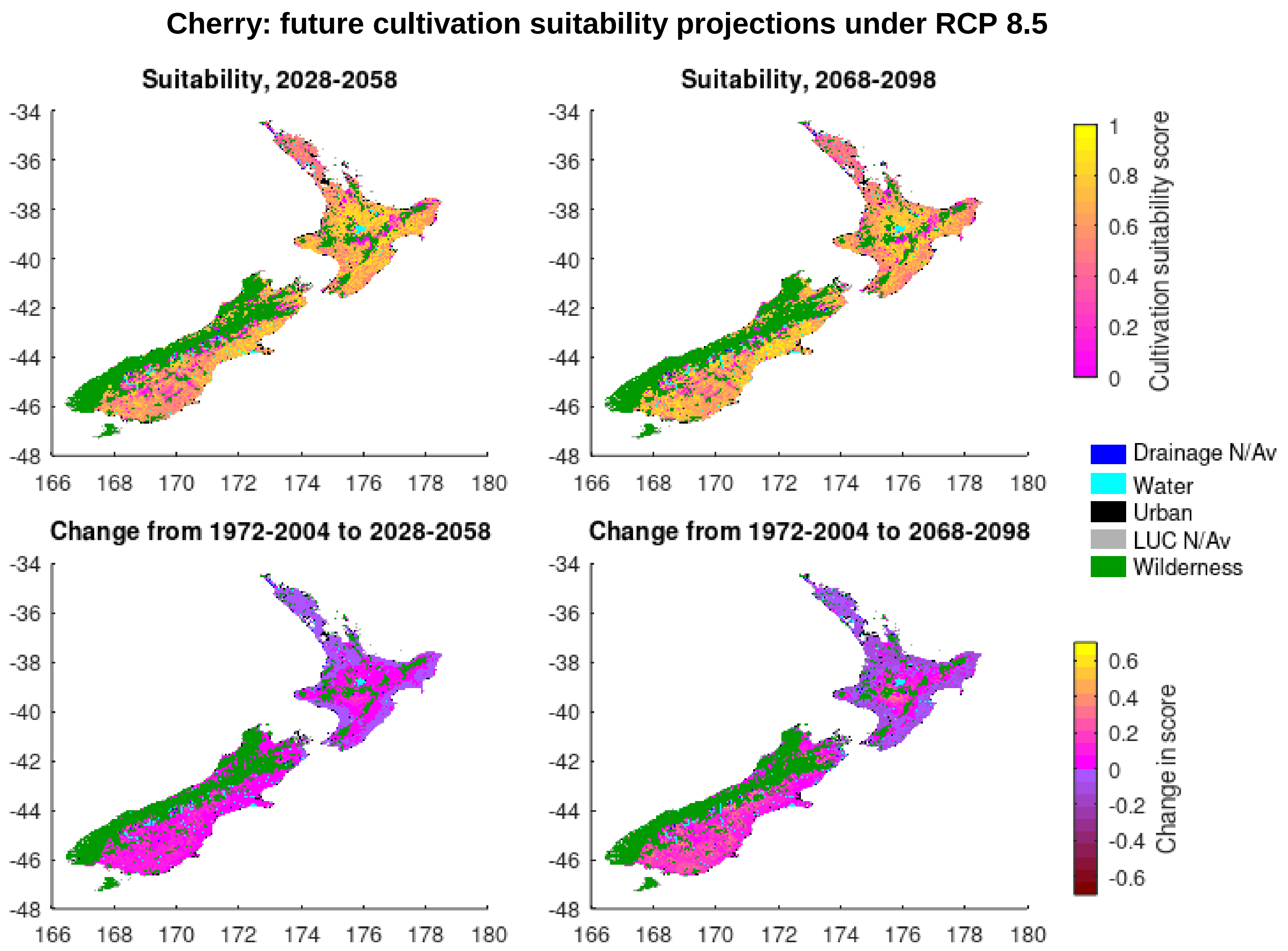

Figure 143. Cherry: Projected cultivation suitability (top panels) and projected changes in cultivation suitability from the historic period (bottom panels) for the mid-century (left panels) and late century (right panels) under RCP 8.5.

7.6 Pinot noir

7.6.1 Pinot noir RCP 2.6

Under RCP 2.6, climate and cultivation suitability scores are projected to remain constant or increase across the South Island apart from the Blenheim area where a slight decrease in suitability is expected. Slight decreases in suitability are projected across the North Island, apart from central and elevated areas, and large parts of the Wairarapa, which are expected to remain unchanged or very slightly increased in suitability (see Figure 144 and Figure 145). These changes are projected to occur by mid-century with an overall slight decrease in suitability from mid- to late-century. In particular, a small decrease in suitability is projected to occur in additional northern areas of Marlborough and some coastal areas of the Nelson region, which might impact on vineyards in these areas. Overall, these climate change impacts under RCP 2.6 would appear to be favourable for the current Pinot noir footprints in Central Otago and North Canterbury. Despite the projected decreases in suitability around Blenheim, cultivation suitability will generally remain excellent for many areas of the region, and some areas of the Wairarapa will have very good cultivation suitability.

Under RCP 2.6, the area of land with excellent suitability is projected to double by the late century with a transient higher increase occurring for the mid-century period (Table 18), with most of this gain appearing in the Central Otago area. Very good and good suitability land is also projected to substantially increase in area over these periods. However, for excellent suitability land the projection uncertainties are very large, and the projected change would lie between −90% and 1300% at the mid-century, and between −90% and 1100% by late century (Table 18). These large percentage values for potential increases are due to the very small area of excellent suitability land in the historic period. Since the uncertainty interval for excellent suitability land predominantly lies in the positive region of change, the overall view picture points to new growing opportunities, although a loss of excellent suitability land cannot be ruled out.

Table 18. Pinot noir: Land area in the historic period falling into different cultivation suitability ranges, projected changes for the mid- and late-century under RCP 2.6, and best and worst cases. Decreases are shaded red and increases shaded blue. Colour intensity increases with the magnitude of change.

Pinot noir SLM RCP 2.6	Historic (km^2) 1972–2004	Area change from historic (km^2) 2028–2058			Area change from historic (km^2) 2068–2098		
Suitability range		Projection	Best case	Worst case	Projection	Best case	Worst case
0–0.1	42923	−10414	−18366	−183	−10078	−18481	278
0.1–0.2	20376	1152	−273	2871	556	−53	2209
0.2–0.3	20274	2154	−1267	5529	2778	−1766	6353
0.3–0.4	24613	682	−1236	−2745	663	−230	−3240
0.4–0.5	21422	1301	4894	−2142	787	4156	−1864
0.5–0.6	20731	−380	1440	282	1004	2017	280
0.6–0.7	19718	322	3276	−3318	−597	3197	−3656
0.7–0.8	9765	2124	5284	−456	2191	5100	−134
0.8–0.9	3727	2604	3984	320	2336	4087	−68
0.9–1.0	176	455	2264	−158	360	1973	−158

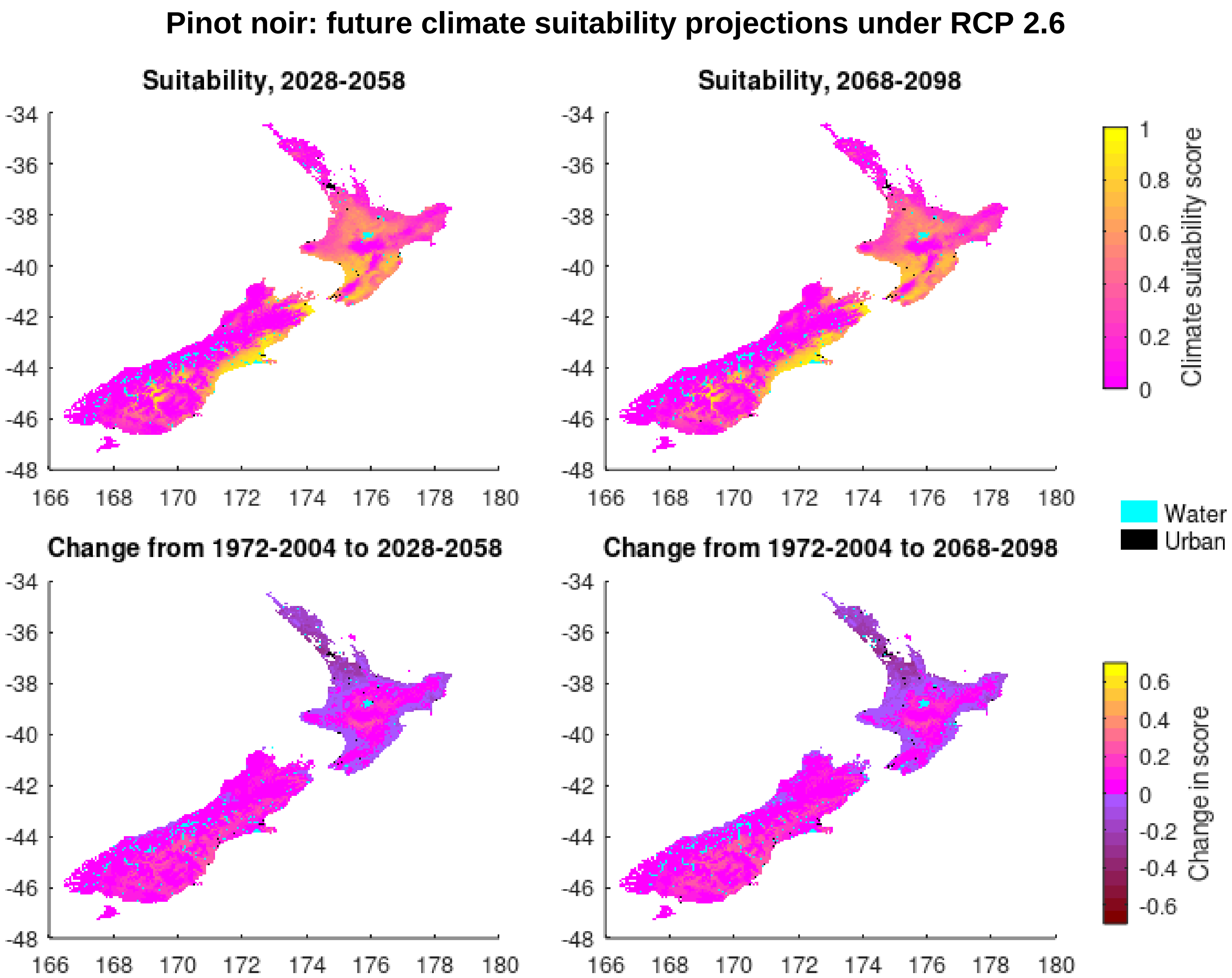

Figure 144. Pinot noir: Projected climate suitability (top panels) and projected changes in climate suitability from the historic period (bottom panels) for the mid-century (left panels) and late century (right panels) under RCP 2.6.

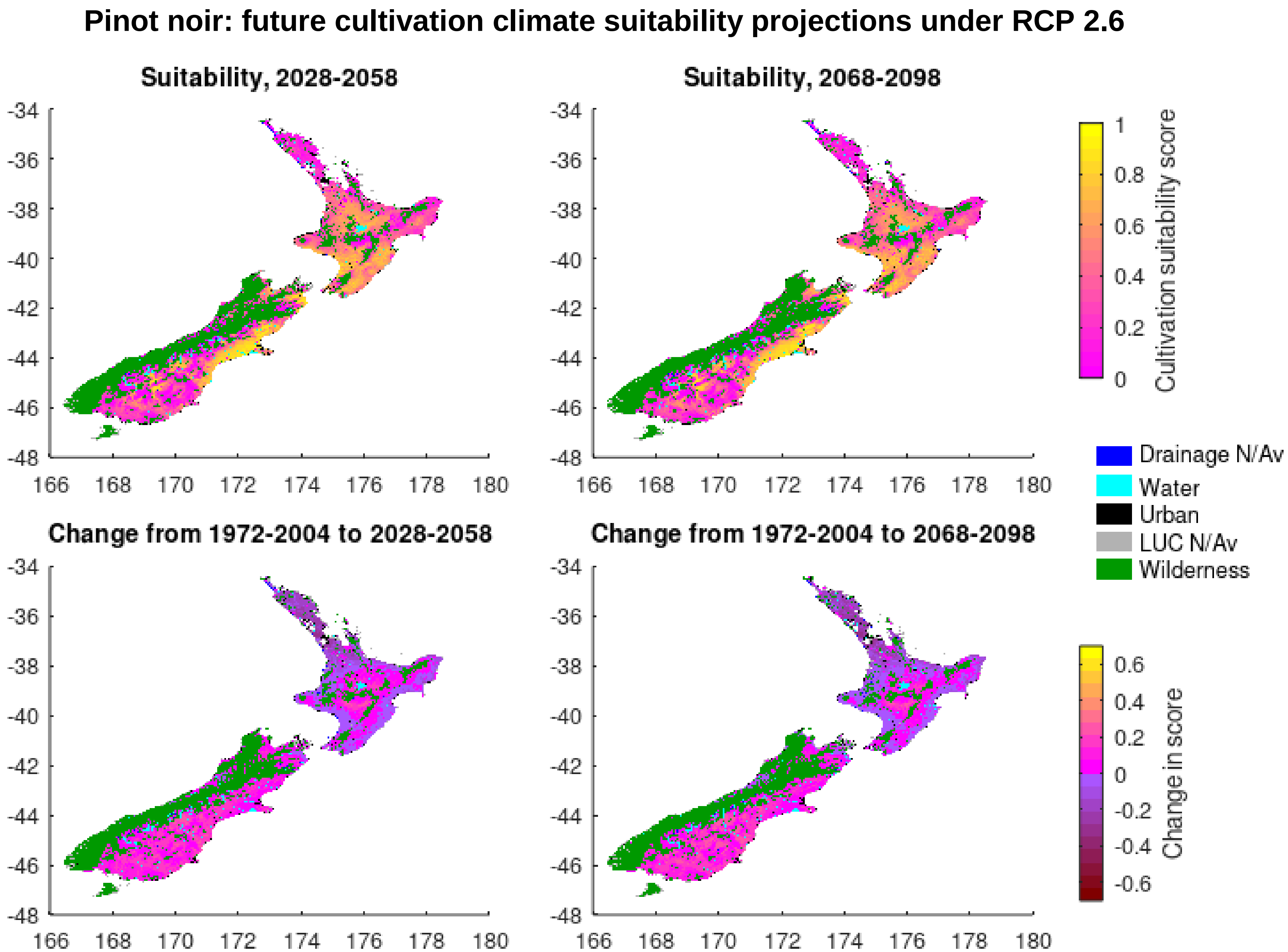

Figure 145. Pinot noir: Projected cultivation suitability (top panels) and projected changes in cultivation suitability from the historic period (bottom panels) for the mid-century (left panels) and late century (right panels) under RCP 2.6.

7.6.2 Pinot noir RCP 8.5

Projected suitability change for the mid-century period under RCP 8.5 showed patterns of change that were qualitatively similar to those projected for the late-century under RCP 2.6, although the magnitudes of change (both increases and decreases in suitability scores) were larger. Projected suitability scores for the end late-century under RCP 8.5 magnified these trends, with large changes from the historic period (see Figure 146 and Figure 147). In particular, climate and cultivation suitability decreased in much of the North Island, and of note, the Wairarapa was projected to decline in suitability for Pinot noir to the extent that all areas there fell below good suitability. However, cultivation suitability in some lower-central regions of the North Island were projected to improve to the very good and excellent categories. In the South Island, cultivation suitability for Nelson and most areas of Marlborough (and especially around Blenheim) were projected to drop below good suitability. Some inland areas of North Canterbury were projected to improve slightly, and within these areas are locations that are expected to have very good suitability. Large increases in suitability are projected across much of Otago, with many of these locations improving to very good or excellent suitability, especially around Oamaru.

The footprint area of excellent suitability land is projected to almost double by late-century with a transient greater increase at mid-century, and very good suitability land is projected to consistently increase and more than double in footprint area by late-century (Table 19). The uncertainty limits of the projection for the late-century allow from a possible disappearance of excellent suitability land to a substantial increase, but indicate that the areas of good suitability and very good suitability land would increase even for the worst case, and substantially so in the best case.

Table 19. Pinot noir: Land area in the historic period falling into different cultivation suitability ranges, projected changes for the mid- and late-century under RCP 8.5, and best and worst cases. Decreases are shaded red and increases shaded blue. Colour intensity increases with the magnitude of change.

Pinot noir SLM RCP 8.5	Historic (km^2) 1972–2004	Area change from historic (km^2) 2028–2058			Area change from historic (km^2) 2068–2098		
Suitability range		Projection	Best case	Worst case	Projection	Best case	Worst case
0–0.1	42923	−10967	−19379	−5785	3778	−2550	8576
0.1–0.2	20376	−2076	318	−165	−3591	−3020	−1925
0.2–0.3	20274	1742	−1458	6134	−726	−2667	2070
0.3–0.4	24613	1813	−89	−299	−3434	−4155	−4973
0.4–0.5	21422	917	3647	−585	−1841	−780	−2642
0.5–0.6	20731	2613	2644	1424	−2084	−518	−4657
0.6–0.7	19718	20	3620	−2235	−3481	−2487	−2900
0.7–0.8	9765	1961	3456	925	7187	6379	6396
0.8–0.9	3727	3655	5240	738	4043	8082	231
0.9–1.0	176	322	2001	−152	149	1716	−176

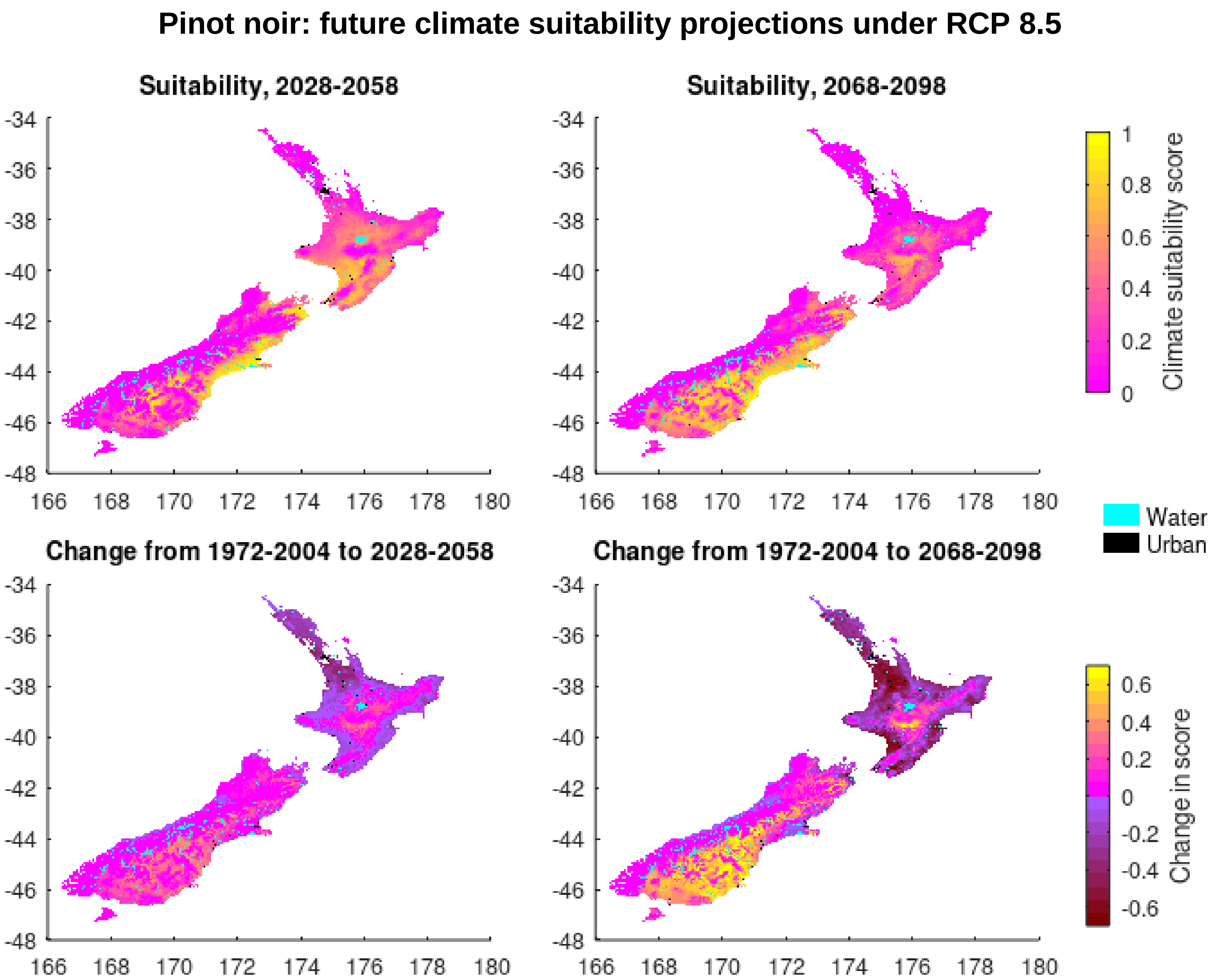

Figure 146. Pinot noir: Projected climate suitability (top panels) and projected changes in climate suitability from the historic period (bottom panels) for the mid-century (left panels) and late century (right panels) under RCP 8.5.

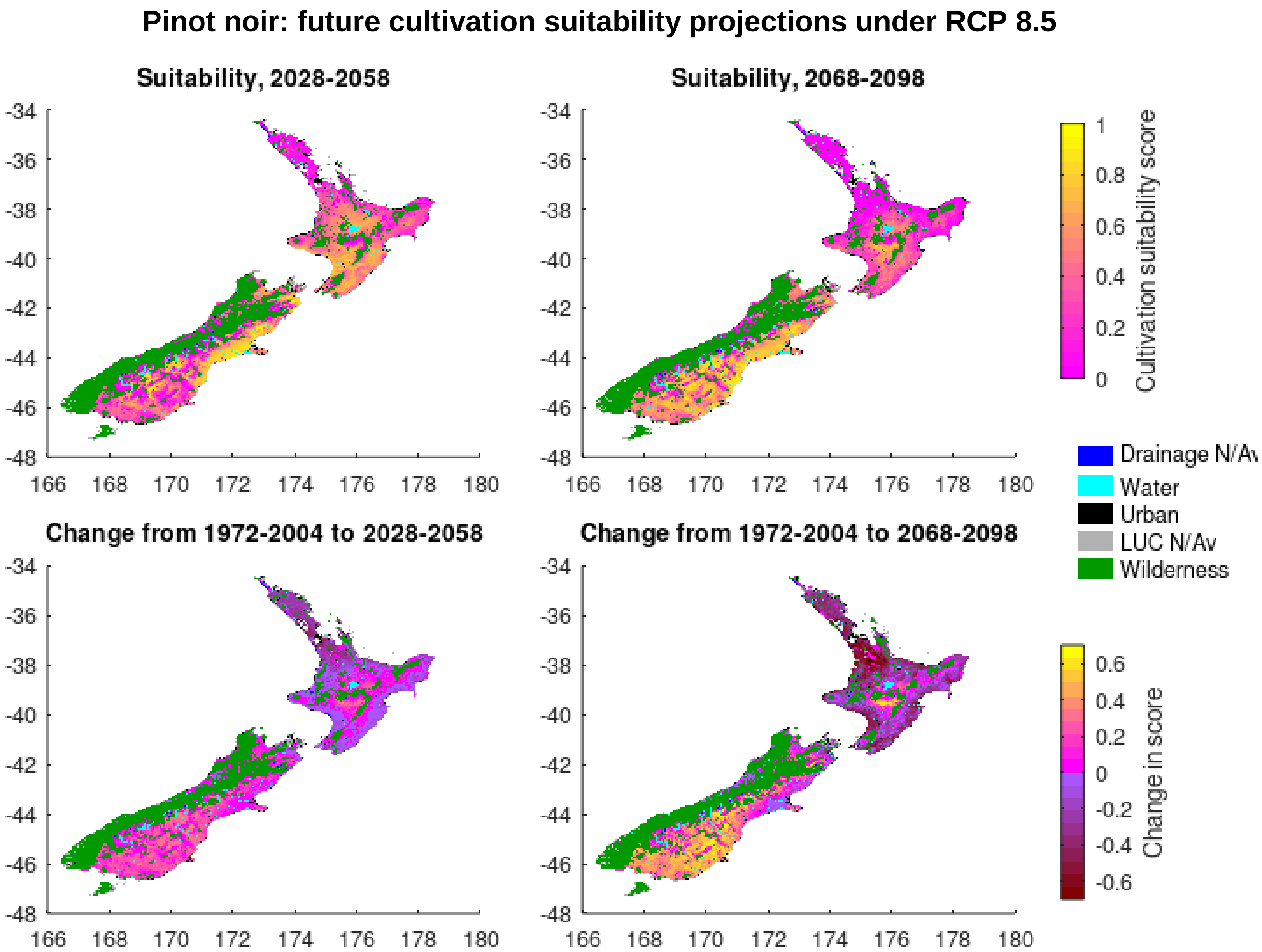

Figure 147. Pinot noir: Projected cultivation suitability (top panels) and projected changes in cultivation suitability from the historic period (bottom panels) for the mid-century (left panels) and late century (right panels) under RCP 8.5.

7.6.3 Pinot noir: key criteria underlying change

Under RCP 2.6, the change in suitability for botrytis risk ranged from minor increases in some locations to modest decreases in others. Winter chill showed little or no change for locations with chill suitability scores close to 1.0 in the historic period, for lower historic values showed a decreases, with the magnitude of the decrease increasing (by up to 0.2) the lower the historic value. Frost suitability was significantly improved for most locations, with some small decreases for locations with suitability scores of 0.7 or over. Heat stress suitability, which historically fell in the 0.95 or higher range, remained tightly clustered and showed only a very minor decrease for the future period. However, for GDD suitability, locations tended to show either a very sharp decrease or a very sharp increase, although some locations with scores that for the historic period were in the 0.95 to 1.0 range or were close to zero showed little change (see supplementary file ‘Comparison future vs historic scores’). The pattern of change for GDD suitability arises because the Pinot noir requirement for GDD accumulation has an optimal band. An increase in temperature could increase GDD suitability by pushing GDD accumulation closer to or into the optimal zone (increased suitability score), within the optimal zone (no change in suitability), or out of or away from the optimal zone (decreased suitability score) depending on the starting point for GDD accumulation and the magnitude of the change. Accordingly, the patterns of changes in overall climate suitability varied considerably from significant decreases through to no change, through to significant increases. Locations with the highest climate suitability, however, did not experience significant change.

Under RCP 8.5, suitability for botrytis risk had similar patterns to those projected for RPC 2.6, though by the late-century the decreases in suitability were larger, although the highest suitability location showed little change. Patterns of decline in chill suitability were also similar to those for RCP 2.6, but larger, especially for the late-century, which numerous locations with very high historic scores decline substantially in suitability. Frost suitability by mid-century were modestly higher than for RCP 2.6, and substantially greater by the late-century, although some locations had a moderate decrease. By late-century, heat stress suitability had decreased in some locations to the extent that heat damage might be an issue in some years. As for RCP 2.6, change in GDD suitability showed a bifurcating behaviour, and by late-century changes were so great locations with historic GDD scores above 0.9 would have their scores fall below 0.8 (mostly under 0.5). However, many locations with historic GDD suitability scores below 0.6, were projected to improve above 0.9 by late-century. Projected patterns of change for climate suitability were similar in pattern to those for RCP 2.6, but of moderately greater magnitude by mid-century and substantially greater by late-century. Many locations that had historic climate suitability scores of good to excellent would incur only moderate decreases in suitability by late-century, although many others would become unviable. However, previously unviable areas would become viable (see supplementary file ‘Comparison future vs historic scores’).

7.7 Sauvignon blanc

7.7.1 Sauvignon blanc RCP 2.6

Under RCP 2.6, the mid-century projection is that climate and cultivation suitability will remain constant or increase across the South Island and most non-coastal areas of the North Island south of the Waikato by mid-century, with increases generally being modest, but more significant in some areas of Otago, Canterbury and the lower central North Island; these trends are expected to strengthen a little by the late-century (Figure 148 and Figure 149). However, some areas of the Gisborne region and the Hawke's Bay are projected to have modest to moderate decreases in suitability. These trends would favour the majority of Sauvignon blanc vineyards in Marlborough, other South Island regions such as Nelson, North Canterbury and Otago, and the Wairarapa in the North Island. However, growers in the Hawke's Bay and Gisborne regions may find growing conditions decrease or increase depending on their location.

The area of land in the excellent suitability category, which historically was only 38 km^2, is projected to increase by a factor of 2.5 by the late century, and land with very good suitability expected to triple (Table 20). While the limits of the projection uncertainty allow an almost complete loss of excellent suitability land by the mid-century, these limits also allow very large increases, and since the uncertainty interval is predominantly positive the expectation is an increase.

The area of land in the good and very good categories are projected to higher with respect to the historic period at both the mid-century and late-century, with small increases in land for the worst case and approximately 400% increases for the best case. Thus the overall outlook is positive.

Table 20. Sauvignon blanc: Land area in the historic period falling into different cultivation suitability ranges, projected changes for the mid- and late-century under RCP 2.6, and best and worst cases. Decreases are shaded red and increases shaded blue. Colour intensity increases with the magnitude of change.

Sauvignon blanc SLM RCP 2.6	Historic (km^2) 1972 – 2004	Area change from historic (km^2) 2028 –2058			Area change from historic (km^2) 2068–2098		
Suitability range		Projection	Best case	Worst case	Projection	Best case	Worst case
0–0.1	67747	−18779	−27209	−9666	−20042	−28436	−10408
0.1–0.2	14643	4976	5494	6438	5544	5938	7523
0.2–0.3	15576	5577	1977	8202	7038	3031	9186
0.3–0.4	21047	1390	−110	−753	1705	376	−1259
0.4–0.5	21684	−1487	722	−3822	−1803	811	−3726
0.5–0.6	19098	804	2490	863	1008	2462	511
0.6–0.7	17136	1853	4212	−2204	956	3711	−2547
0.7–0.8	5654	3126	6758	842	3231	6745	686
0.8–0.9	1102	2416	4529	137	2259	4314	71
0.9–1.0	38	124	1137	−37	104	1048	−37

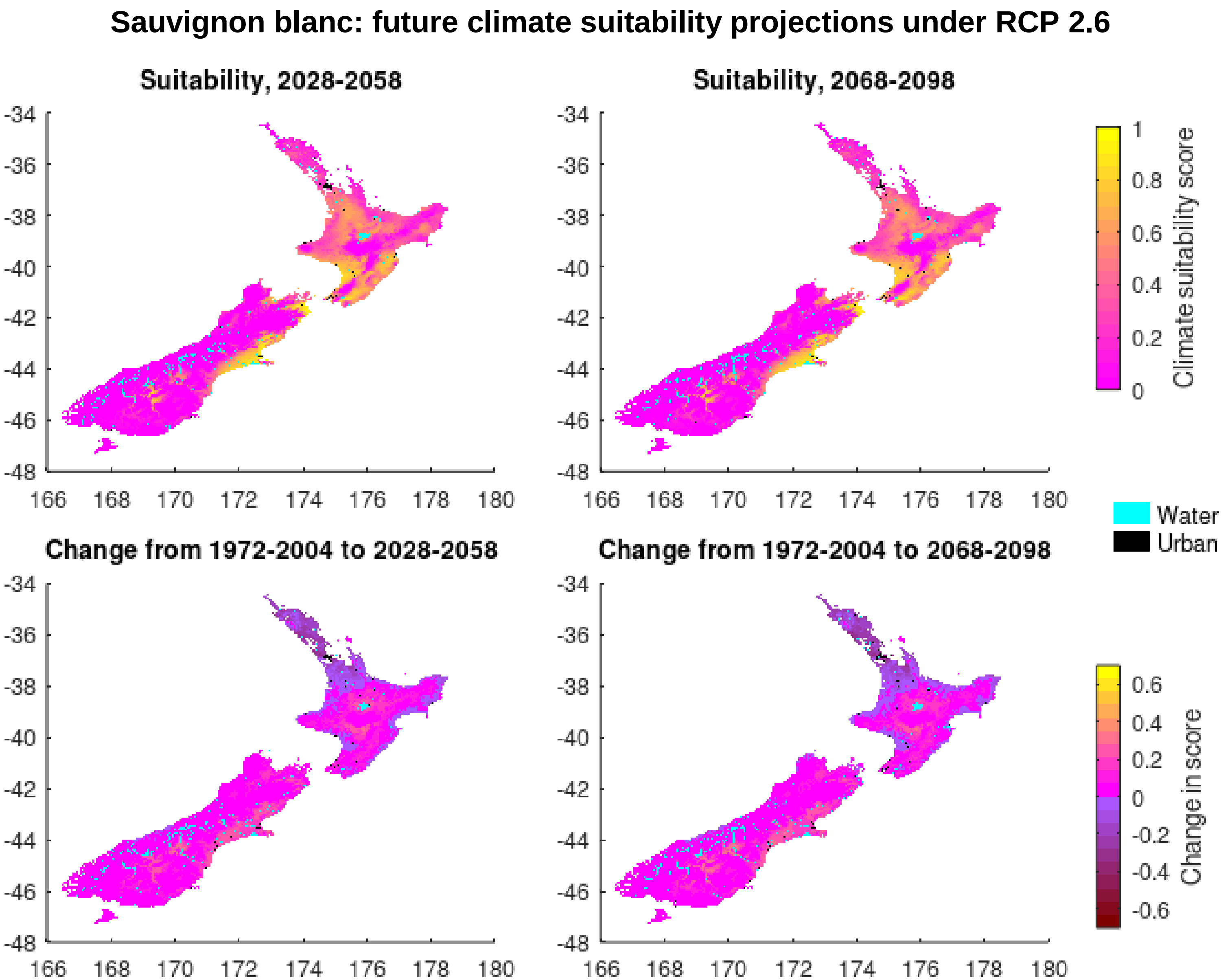

Figure 148. Sauvignon blanc: Projected climate suitability (top panels) and projected changes in climate suitability from the historic period (bottom panels) for the mid-century (left panels) and late century (right panels) under RCP 2.6.

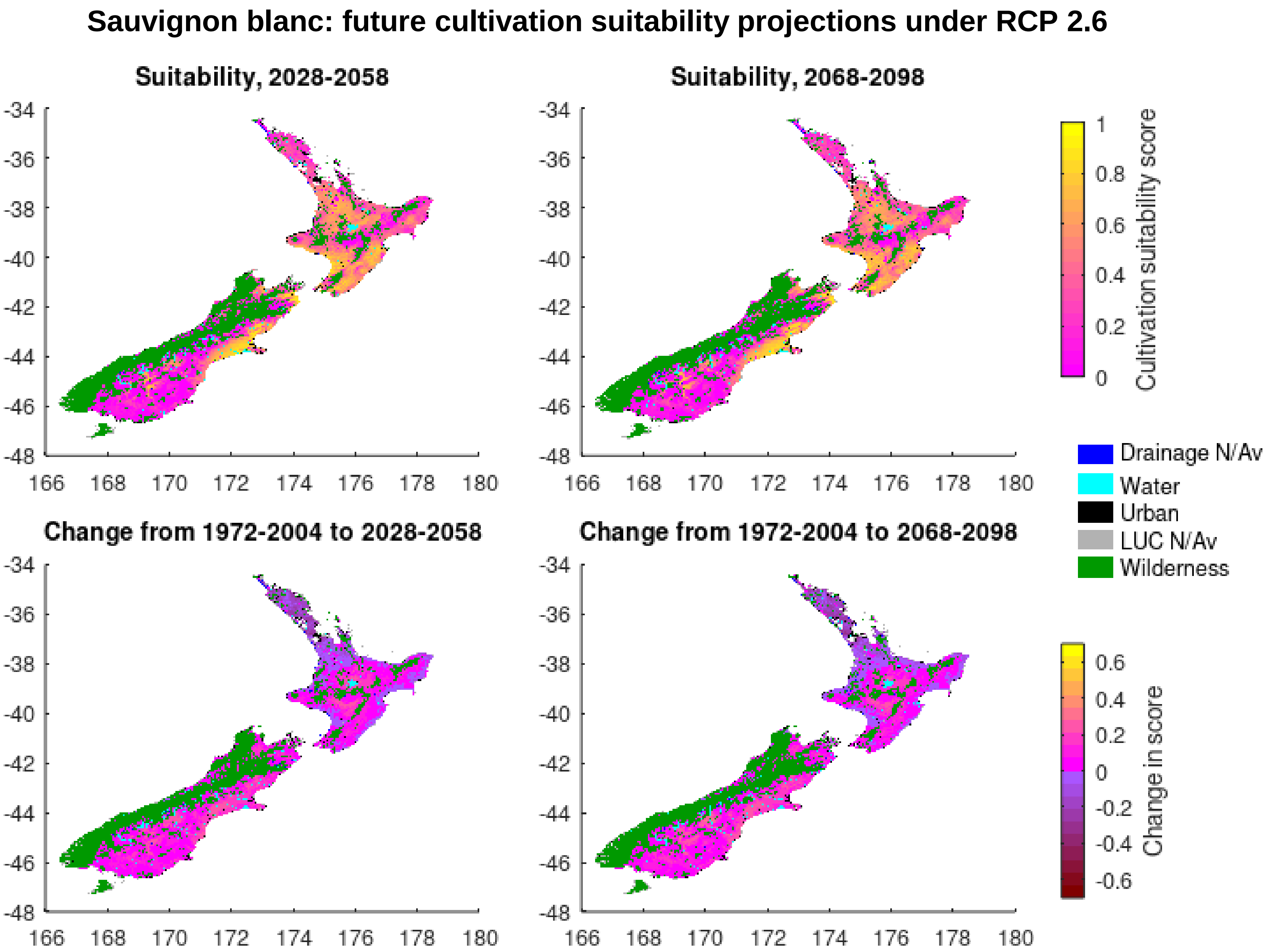

Figure 149. Sauvignon blanc: Projected cultivation suitability (top panels) and projected changes in cultivation suitability from the historic period (bottom panels) for the mid-century (left panels) and late century (right panels) under RCP 2.6.

7.7.2 Sauvignon blanc RCP 8.5

The RCP 8.5 projection for the mid-century suggests modest to significant improvements in climate and cultivation suitability across much of the South Island and central parts of the North Island and non-coastal areas of the Wairarapa; however, decreases in suitability are expected for much of the coastal and hinterland areas of the Hawke's Bay and Gisborne regions, but increases further inland. Thus the mid-century outlook for Sauvignon blanc is for improved growing conditions in the South Island, parts of the Wairarapa, and southern areas of the Hawke's Bay, with poorer growing conditions for the northern areas of the Hawke's Bay and for Gisborne region (see Figure 150 and Figure 151).

By the late-century, the RCP 8.5 projection indicates that large areas of Otago and some areas of Canterbury will have experienced very significant increases in climate and cultivation suitability, while Marlborough will have experienced a small decrease in suitability in its northern areas, and generally only a slight increase in suitability in other areas (apart from pockets of moderate suitability increase). The outlook for the South Island under this scenario is that Central Otago will contain much of the highest (excellent) suitability land for Sauvignon blanc, with large areas of very good suitability land in Canterbury. The outlook for the North Island is generally poor with large areas of land that have regressed in suitability compared with the historic period, including some areas that had shown improvement at mid-century. The exception to this is an elongated area south of Waiouru with very significant suitability increase: this area and surrounding areas are projected to have the best suitability for Sauvignon blanc in the North Island in the late-century, with suitability scores in the good to very good range (see Figure 150 and Figure 151).

The area of excellent suitability land is projected to increase 8-fold and 9-fold by mid-century and late-century, respectively, under RCP 8.5, and the area of very good suitability land is projected to increase almost 4-fold and 9-fold for the same periods (Table 21). Within projection uncertainty areas of good, very good and excellent category land would be higher by mid-century compared with the historic period, Within projection uncertainty for the late century, areas of good and very good suitability land would be substantially higher than in the historic period, while excellent suitability land would be 61% lower in the worst case, but 55-fold higher in the best case. (The large fold increase is due to the very small historic value (Table 21). Overall, this paints an optimistic picture for Sauvignon blanc at a national level, though the industry could face threats in some regions.

Table 21. Sauvignon blanc: Land area in the historic period falling into different cultivation suitability ranges, projected changes for the mid- and late-century under RCP 8.5, and best and worst cases. Decreases are shaded red and increases shaded blue. Colour intensity increases with the magnitude of change.

Sauvignon blanc SLM RCP 8.5	Historic (km^2) 1972–2004	Area change from historic (km^2) 2028–2058			Area change from historic (km^2) 2068–2098		
Suitability range		Projection	Best case	Worst case	Projection	Best case	Worst case
0–0.1	67747	−29203	−35324	−23087	−26681	−31707	−21702
0.1–0.2	14643	10159	7522	12941	3234	2357	5389
0.2–0.3	15576	6569	7047	7143	4186	2057	4464
0.3–0.4	21047	2569	2144	1958	726	−125	3621
0.4–0.5	21684	−400	−238	−2247	3117	2259	1448
0.5–0.6	19098	994	1269	1485	3965	5398	1339
0.6–0.7	17136	1572	4062	−1253	−1946	1574	−2946
0.7–0.8	5654	4310	6794	1813	5695	6329	4803
0.8–0.9	1102	3145	5716	1230	7389	9769	3607
0.9–1.0	38	285	1008	17	315	2089	−23

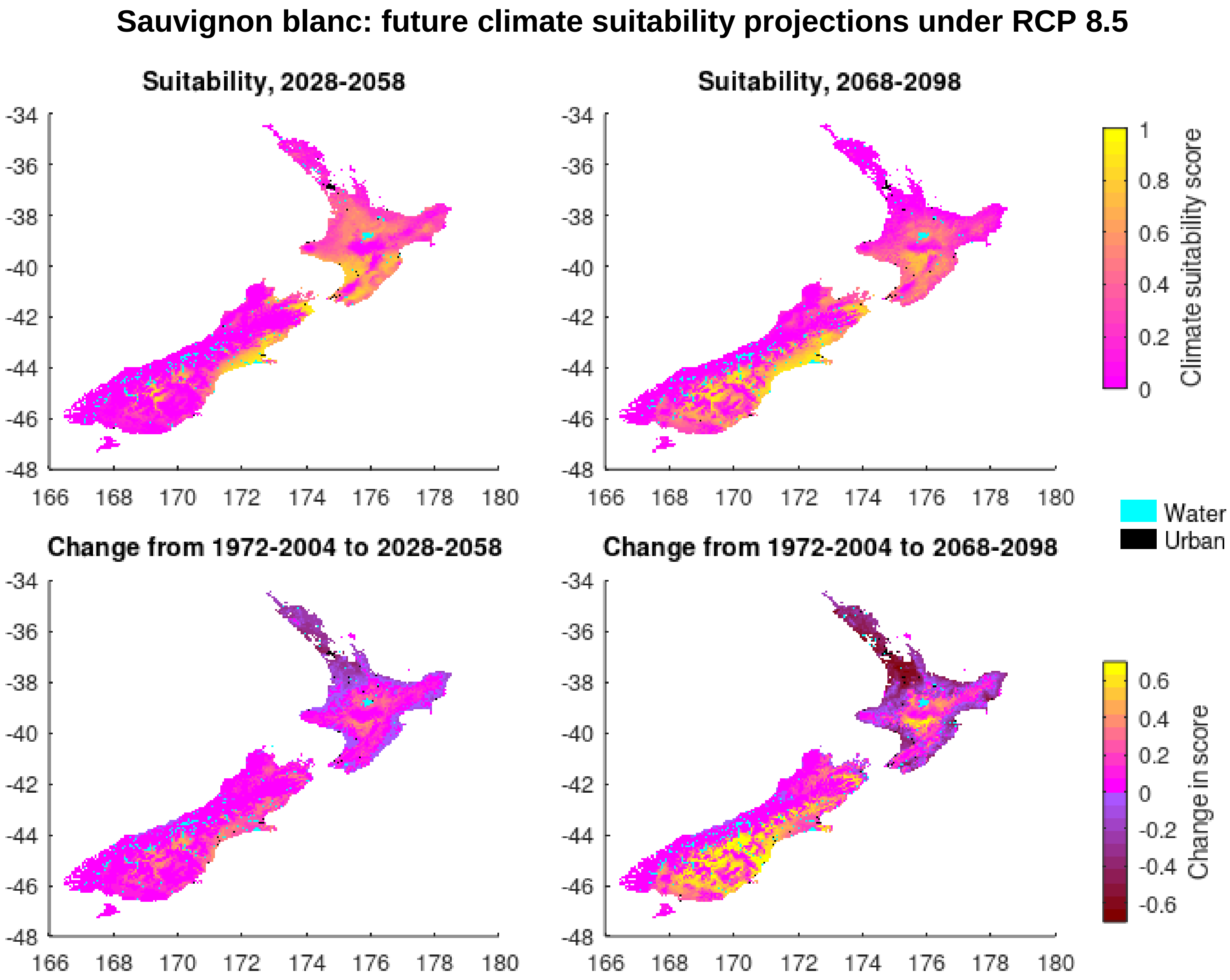

Figure 150. Sauvignon blanc: Projected climate suitability (top panels) and projected changes in climate suitability from the historic period (bottom panels) for the mid-century (left panels) and late century (right panels) under RCP 8.5.

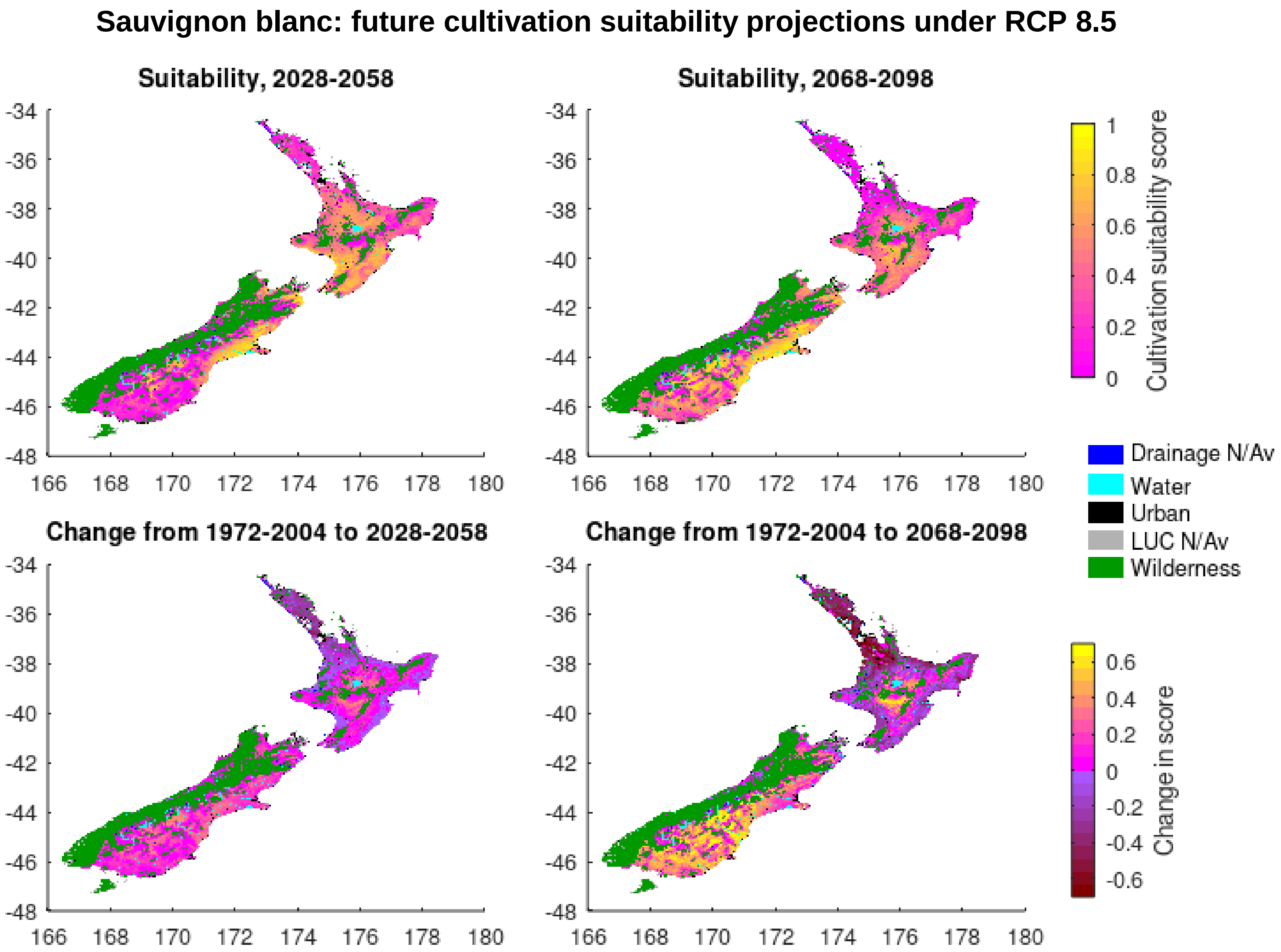

Figure 151. Sauvignon blanc: Projected cultivation suitability (top panels) and projected changes in cultivation suitability from the historic period (bottom panels) for the mid-century (left panels) and late century (right panels) under RCP 8.5.

7.7.3 Sauvignon blanc: key criteria underlying change

Although Sauvignon blanc has slightly different GDD requirements from Pinot noir and thus slightly different development times and thus slightly different frost risk and heat stress profiles, the underlying responses of suitability criteria are very similar. Suitability scores for winter chill and botrytis risk are exactly the same as for Pinot noir, and their responses under climate change are discussed above.

Frost risk suitability scores showed very similar patterns of change for Sauvignon blanc as for Pinot noir, under both RCP 2.6 and 8.5. However, increases in suitability for Sauvignon blanc were slightly greater and slightly more consistent in magnitude than for Pinot noir, and decreases in frost risk suitability slightly smaller. GDD suitability scores were marginally smaller in the historic period for Sauvignon blanc compared with Pinot noir, which is expected given the difference in GDD requirement. Change in GDD suitability score for Sauvignon blanc under RPC 2.6 and 8.5 showed a similar bifurcating pattern to that for Pinot noir, indicating that many areas that are favourable for optimal GDD accumulation would become unsuitable and vice versa. Damage from heat stress is likely to be an issue for Sauvignon blanc in some locations in some years under RCP 8.5, as for Pinot noir. Expectedly, the patterns of change in overall climate suitability for Sauvignon blanc is similar to that for Pinot noir (see supplementary file ‘Comparison future vs historic scores’).

7.8 General disease risk suitability

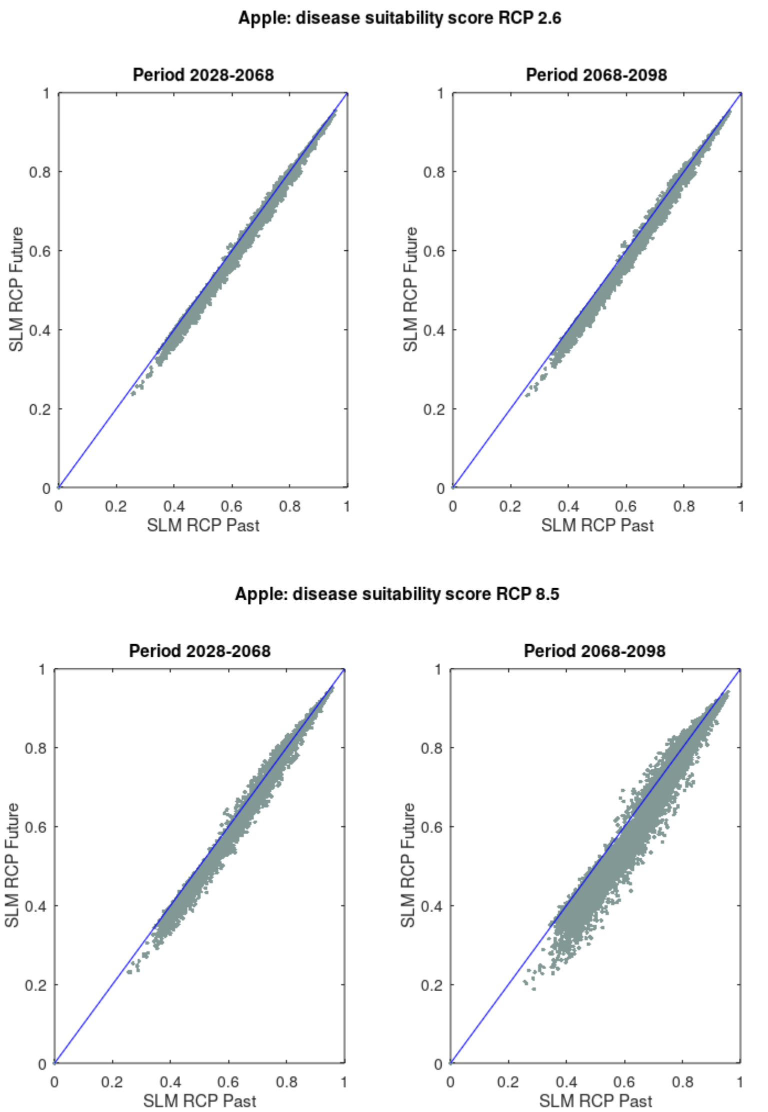

Figure 152. Individual one-to-one graphs comparing future vs historic disease suitability scores under RCP 2.6 (top panels) and RCP 8.5 (lower panels) for mid-century (left panels) and late-century (right panels).

Under RPC 2.6, general disease suitability (for non-root diseases) was projected to have a slight decrease (disease risk slightly elevated) across most of the country by mid-century with little subsequent change by late-century, as can be seen in the top panels of the individual one-to-one graphs in Figure 152 comparing future versus past disease suitability scores for each grid location. Figure 153 indicates that the relatively few areas with improved disease suitability are located in national parks and thus inconsequential.

Under RCP 8.5 there is a progressive worsening of disease suitability across most areas of the country, with the worsening being more significant in the late-century than the mid-century (Figure 152). The relatively few areas with increased suitability are located in mountainous regions or conservation areas (Figure 154), as was the case under RCP 2.6. The spatial patterns for risk profiles shown in the historic disease suitability map are generally preserved, with the west coast of the South Island, western areas north of Taranaki in the North Island, the Waikato and Northland, and parts of the Auckland region projected to have a higher risk of disease than other areas. Central, elevated areas of the South Island and to a lesser extent in the North Island are projected to have high disease suitability scores and thus less overall disease risk. Other areas are projected to have moderate disease suitability risk.

The individual one-to-one graphs (Figure 152) indicate that the biggest declines in disease suitability tend to occur in locations with already poor disease suitability.

.

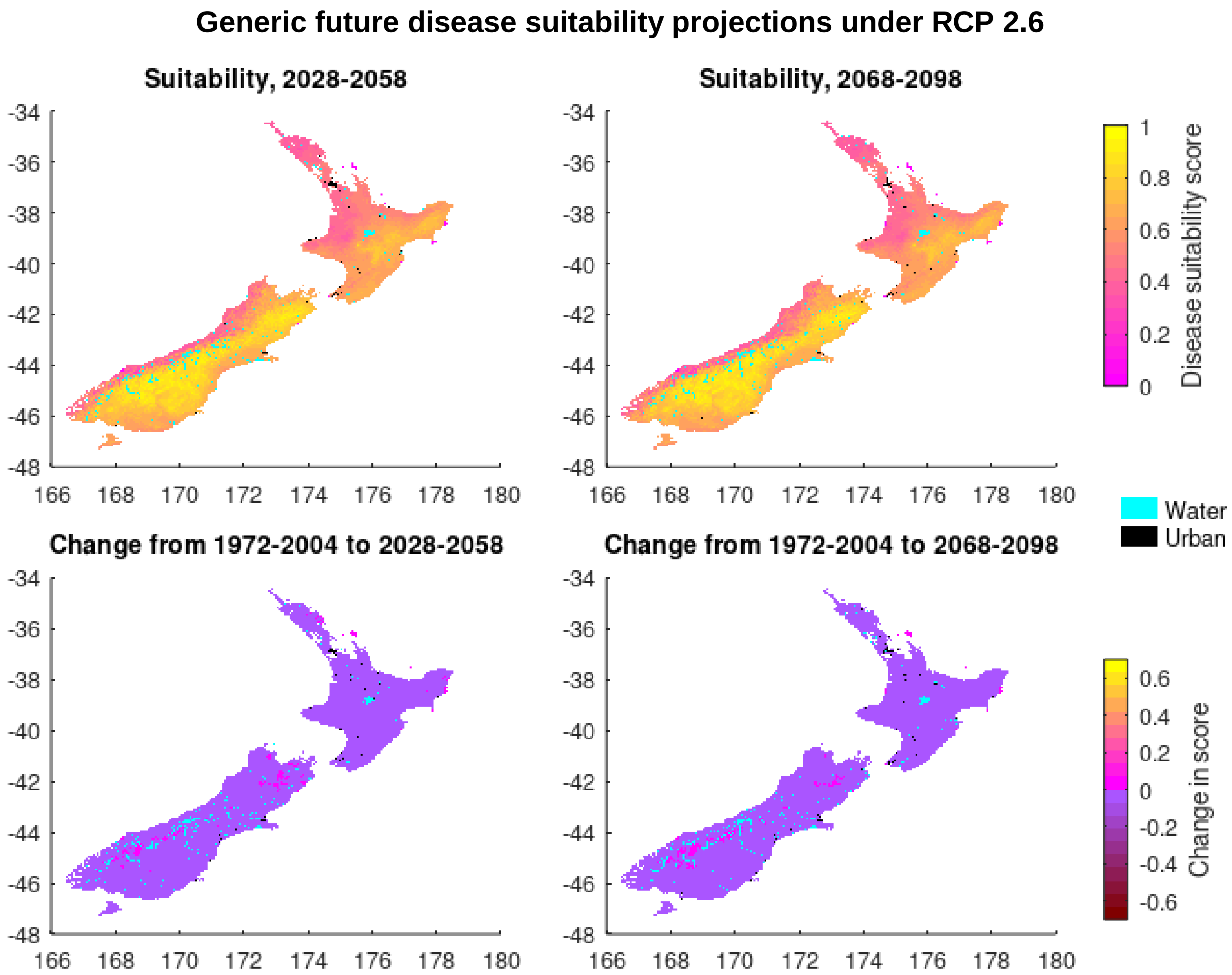

Figure 153. Mid-century and late-century projection maps for disease suitability and change from historic period under RCP 2.6.

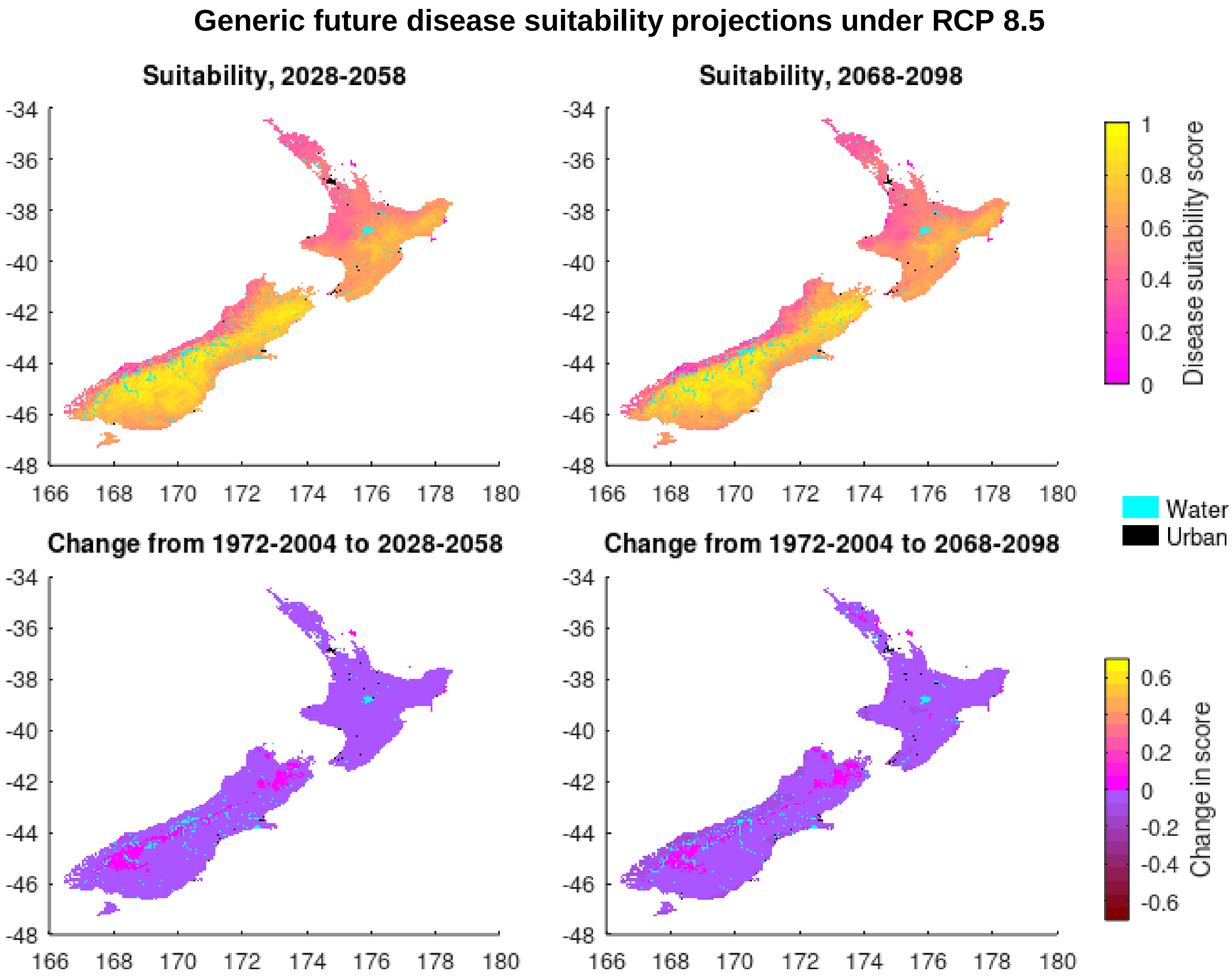

Figure 154. Mid-century and late-century projection maps for disease suitability and change from historic period under RCP 8.5.

8 LURNZ modelling

Land-use simulations were carried out in the Land Use in Rural New Zealand (LURNZ) model. The LURNZ analysis considered land-use change that could result from changing suitability under future climate for kiwifruit and apple, and focused on climate scenarios representing mild climate change (RCP 2.6) and severe climate change (RCP 8.5).

8.1 The LURNZ Model

LURNZ is national-scale, spatial model designed to consider the implications of environmental policies on future land use, production and GHG emissions. It is a partial equilibrium model (Kerr et al. 2012), it includes all private rural land in New Zealand and can produce annual maps of land use at a 25-ha resolution.

The foundation of LURNZ is provided by econometrically estimated models that establish the relationship between observed drivers of land use and land-use outcomes (Timar 2011; Kerr & Olssen 2012; Timar 2016). The revealed preference nature of these models enables us to make relatively few assumptions about farmers' objectives and decision processes: LURNZ results are largely driven by how land use has responded to its main drivers in the past. The model's underlying datasets and processes have been validated (Anastasiadis et al. 2014), and its results are consistent with data and trends at the national scale, including New Zealand's Greenhouse Gas Inventory (Timar & Kerr 2014).

The land-use basemap of LURNZ combines remote-sensing land-cover data from the 2012 Land Cover Database 4 (LCDB4) with land-use data from the Land Use New Zealand (LUNZ) map. Data on land ownership and land tenure are also used to identify and classify privately owned land. In addition, a forest age map is included in LURNZ to constrain simulated harvest and deforestation decisions (Kerr et al. 2012; Anastasiadis et al. 2014).

LURNZ can be used to simulate changes in dairy farming, sheep-beef farming, plantation forestry and unproductive scrub in response to changes in economic incentives. In addition, it can spatially allocate land-use change for horticulture. Kiwifruit and apple were added to its spatial modelling capabilities in this project.

Recent examples of empirical research relying on LURNZ for land-sector modelling include the reports of the Productivity Commission (2018) and the Parliamentary Commissioner for the Environment (2019). Unless otherwise noted below, LURNZ assumptions and processes used in this project are based on those documented in Appendix 2 of the latter report.

8.2 Data for kiwifruit and apple

The following GIS data layers were used in the LURNZ modelling:

- Two maps identifying apple and kiwifruit blocks, respectively
- Apple and kiwifruit cultivation suitability scores under RCP past and VCSN past climate
- Mid-century (2028–2058) apple and kiwifruit cultivation suitability scores under RCP 2.6 and RCP 8.5
- End-of-century (2068–2098) apple and kiwifruit cultivation suitability scores under RCP 2.6 and RCP 8.5.

All layers had been adjusted to the geographic grid used in the LURNZ model.

8.3 Assigning baseline land use

The total land area represented by the kiwifruit and apple block maps is larger than total land area under kiwifruit and apple cultivation according to Stats NZ data for 2019. As shown by the first two data columns of Table 22, kiwifruit area in the map overestimates Stats NZ kiwifruit area by more than a factor of two, and apple area in the map overestimates Stats NZ apple area by about a third.

Table 22. Land-use area (hectares) for kiwifruit and apple.

	Block maps	Stats NZ (2019)	Block maps & horticulture	Modelled
Kiwifruit	32,650	14,922	15,600	15,500
Apple	12,500	9,761	10,075	9,400

These differences in land area are likely due to property boundaries (rather than true block boundaries) being reported in the block maps. That is, the maps capture all areas of farms that have any kiwifruit or apple blocks in them, even areas not containing orchards. This also explains why some blocks are simultaneously classified as apple and kiwifruit: these are properties that cultivate both. Thus taking the intersection of each block map with a layer identifying horticulture land use (from the LURNZ basemap) is a reasonable strategy to identify areas under apple and kiwifruit land use.

Therefore, we assigned kiwifruit land use to those cells in horticulture use that are identified as kiwifruit blocks. Likewise, we assigned apple land use to those cells in horticulture use that are identified as apple blocks (unless the cell is also a kiwifruit block). Doing so greatly decreased the discrepancy between mapped area and Stats NZ area for both apple and kiwifruit, as shown in the third column of Table 22.

Modelled area for both land uses, in column 4 of Table 22, is slightly smaller for two reasons. First, as noted above, we assign kiwifruit use to cells that are simultaneously classified as apple and kiwifruit blocks: this reduces apple area by 650 ha. Second, a handful of apple and kiwifruit cells have missing data for some variables and cannot therefore be included in the estimation. This affects 25 ha of apple and 100 ha of kiwifruit area.

The regional distribution of land use in the updated LURNZ basemap is displayed in Table 23 below. Land-use figures in Table 23 also include grid cells with missing data on explanatory variables. In simulations of future scenarios, the baseline land use is assumed to persist on these cells.

Table 23. Land use (hectares) by region and outside regional council (RC) boundaries.

Region	Kiwifruit	Apple	Horticulture	Dairy	Sheep-beef	Forestry	Scrub
Auckland	375	75	11,050	45,175	148,450	52,300	51,000
Bay of Plenty	11,625	0	18,075	100,575	113,475	275,400	54,525
Canterbury	0	50	252,200	275,375	1,718,475	130,075	297,675
Gisborne	600	150	15,825	650	329,150	171,950	130,900
Hawke's Bay	350	5,900	28,550	29,275	624,850	156,850	127,625
Manawatu-Wanganui	100	0	17,500	165,425	1,012,900	148,925	182,025
Marlborough	0	0	32,950	9,900	236,175	77,075	113,200
Nelson	0	0	25	450	2,725	11,475	7,300
Northland	1,000	0	8,150	167,925	357,500	182,825	119,450
Otago	0	725	20,625	120,125	1,720,600	143,375	176,700
Southland	0	0	7,125	207,925	729,300	92,275	55,125
Taranaki	0	0	1,650	215,275	147,550	28,775	58,250
Tasman	700	2,250	6,150	30,600	65,875	101,925	47,475
Waikato	825	150	18,300	602,850	592,975	308,200	133,925
Wellington	0	100	8,225	35,950	302,050	76,450	127,450
West Coast	0	0	0	87,475	35,750	40,650	47,575
Outside RC boundaries	25	25	1,050	3,250	15,025	3,550	12,800
Total	15,600	9,425	447,450	2,098,200	8,152,825	2,002,075	1,743,000

8.3.1 Cultivation suitability

Climate change is represented by changes in kiwifruit and apple suitability scores. Consistent with NIWA's approach for projecting climate impacts, the RCP future data have continuity back to the RCP past data (but not the VCSN past maps). Consequently, we regard the RCP past maps as representing suitability with current climate; we use these maps to estimate a land-use choice model and to calibrate LURNZ, and we used the RCP future maps for simulation.

The (smoothed) frequency distribution of kiwifruit and apple suitability scores by baseline land use is shown in Figure 155 and Figure 156, respectively. The mean score is also shown (by a dotted vertical line) and labelled within each panel. On average, kiwifruit suitability is highest on land currently used to grow kiwifruit and apple suitability is highest on land currently used to grow apple. Dairy and other horticulture land also have relatively high average suitability for apple.

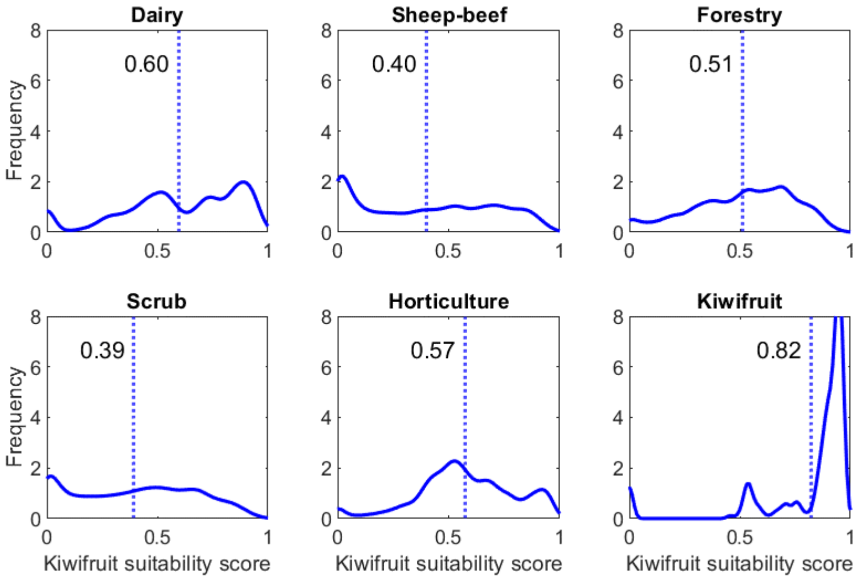

Figure 155. The frequency distribution of kiwifruit suitability scores (RCP past) by land use.

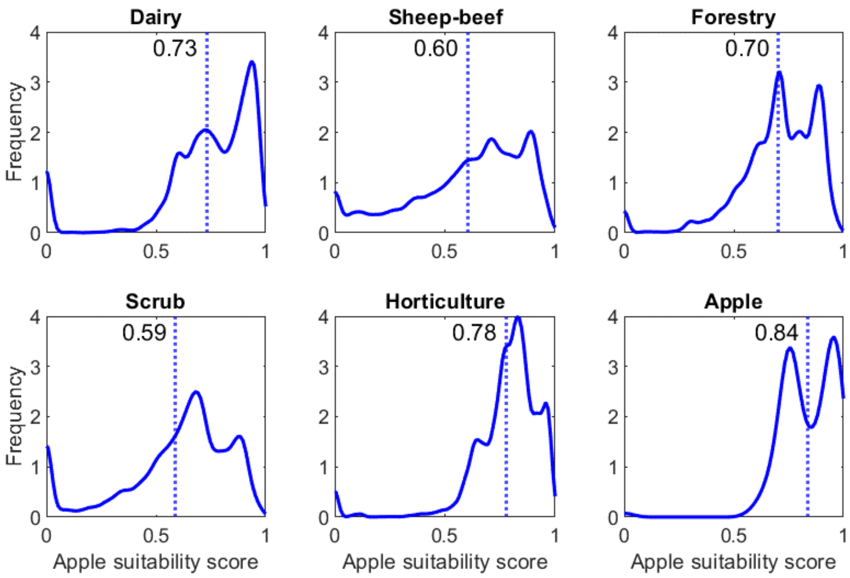

Figure 156. The frequency distribution of apple suitability scores (RCP past) by land use.

With climate change, average kiwifruit suitability across New Zealand is projected to rise (by 9% under RCP 2.6 and by 24% under RCP 8.5) by the end of the century. Changes in average apple suitability are proportionally smaller (4% under RCP 2.6 and only 2.5% under RCP 8.5) over the same period.

Figure 157 and Figure 158 illustrate suitability changes graphically by current land-use type, focusing on land uses with relatively high baseline suitability for kiwifruit and apple. A solid line in each panel reproduces the distribution of current suitability (from Figure 155 or Figure 156, as applicable), and a dashed line depicts the distribution of future suitability with severe climate change at the end of the century. Kiwifruit suitability decreases significantly on current kiwifruit land, but it increases in current dairy and horticulture production areas. Apple suitability also decreases significantly on current apple land. Apple suitability decreases on current dairy land as well, but it increases slightly on current horticulture land.

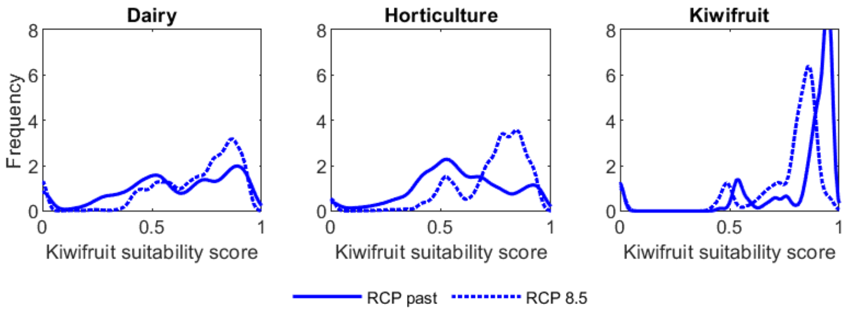

Figure 157. Changes in kiwifruit suitability (RCP past vs. RCP 8.5) by current land use.

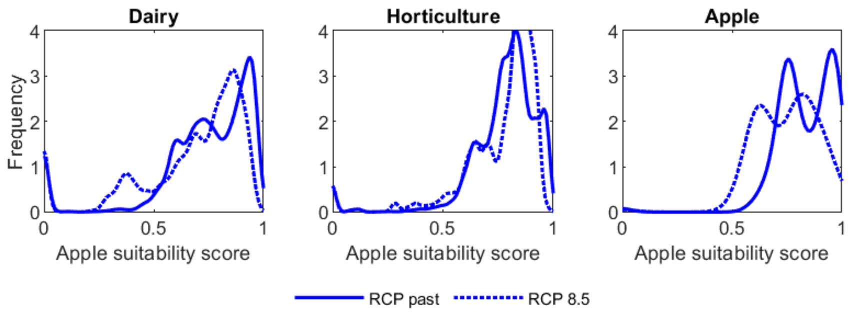

Figure 158. Changes in apple suitability (RCP past vs RCP 8.5) by current land use.

In the following section, we estimate a model to formally analyse the effect of suitability on land-use outcomes.

8.4 Econometric land-use model

Underlying LURNZ's spatial module is an econometric model describing the relationship between current land use, current kiwifruit and apple suitability scores and other drivers of land use. Applying the estimated relationship to future suitability under climate change allows us to simulate the consequent land-use change.

8.4.1 Estimation

The econometric model is a multinomial logit choice model, similar to that described in Timar (2016). The choice set includes the seven land uses from Table 22: kiwifruit, apple, other horticulture, dairy farming, sheep and beef farming, plantation forestry and scrub (or unproductive). Land use is modelled as a function of variables characterising land quality (slope and LUC class), accessibility to markets (distances to nearest port and to nearest town) and land tenure (general land or Māori freehold). In addition, for kiwifruit we include kiwifruit suitability and for apple we include apple suitability. The estimation is performed on 555,224 observations, each corresponding to a 25-ha grid cell. The model predicts choice probabilities for each land-use type at each grid cell, given the characteristics associated with the cell.

Table 24 contains parameter estimates and standard errors from the multinomial logit. A negative parameter estimate in the table indicates that an increase in the value of the variable decreases the log odds (ratio of probabilities) of the given land use versus scrub. For example, holding all other variables in the model constant, a one degree increase in slope would be expected to decrease the multinomial log-odds for apple relative to scrub by 0.471. The discussion below focuses on the estimates for apple and kiwifruit. Other results are similar to those presented by Timar (2011). LUC class and slope also contribute to cultivation suitability for kiwifruit and apple. The estimates for kiwifruit score and apple score could therefore capture some of the effect of these variables on land-use decisions.

Table 24. Multinomial logit estimation results. Standard errors are shown in parentheses. Asterisks indicate statistical significance at the 1% (**) and at the 5% (*) level.

Variable	Kiwifruit	Apple	Other horticulture	Dairy	Sheep-beef	Forestry
Land use capability class	–0.736**	–1.179**	–0.923**	–0.563**	–0.409**	–0.029**
	(0.035)	(0.060)	(0.010)	(0.006)	(0.005)	(0.006)
Slope	–0.134**	–0.471**	–0.407**	–0.202**	–0.055**	–0.065**
	(0.016)	(0.057)	(0.006)	(0.001)	(0.001)	(0.001)
Distance to nearest port	–0.216**	–0.378**	–0.100**	–0.024**	0.012**	–0.049**
	(0.011)	(0.019)	(0.002)	(0.001)	(0.001)	(0.001)
Distance to nearest town	–0.851**	–1.412**	–0.279**	–0.231**	0.017**	0.013**
	(0.058)	(0.110)	(0.008)	(0.003)	(0.001)	(0.002)
Māori freehold	–1.323**	–1.798**	–1.435**	–1.623**	–1.621**	–0.713**
	(0.195)	(0.388)	(0.056)	(0.028)	(0.016)	(0.018)
Kiwifruit score	5.285**	-	-	-	-	-
	(0.271)					
Apple score	-	2.226**	-	-	-	-
		(0.380)				
Constant	0.006	4.346**	6.335**	5.759**	4.541**	1.893**
	(0.275)	(0.382)	(0.040)	(0.030)	(0.028)	(0.032)

Results in Table 24 indicate that the included variables are important parameters for kiwifruit and apple land uses. Lower land quality (as reflected in higher LUC class and higher slope), higher cost of market access (increased distance to ports and towns) and Māori freehold tenure all decrease the log odds of both kiwifruit and apple relative to scrub.[1] As expected, higher kiwifruit suitability increases the probability of kiwifruit land use, and higher apple suitability increases the probability of apple land use. We note that LUC class and slope also contribute to cultivation suitability for kiwifruit and apple, so the estimates for kiwifruit score and apple score could capture some of the effect of these variables on land-use decisions.

8.4.2 Projected land-use change

The predicted choice probabilities from the multinomial logit model can be aggregated into predicted land-use areas. At observed values of all explanatory variables, the model's aggregate predictions exactly match observed land-use areas in the estimation sample. By substituting future values of

[1] In multinomial logit models, the sign of the parameter estimate does not always necessarily match the direction of the marginal effect on choice probability. However, negative estimates are generally associated with decreasing probability of apple and kiwifruit in our model.

suitability into the equation, one can use the estimation results to project future land-use change for kiwifruit and apple under a given climate scenario (assuming no change in other variables).

Table 25 includes mid-century and end-of-century projections under two climate scenarios. In all cases, the area changes shown are relative to baseline land-use areas. In general, kiwifruit area is projected to expand with climate change, growing by 3800 ha (about 25% of current land area) by the end of the century under severe climate change. Apple area changes only marginally under mild climate change but contracts by 1050 ha (about 10% of current land area) by the end of the century under severe climate change. Mid-century and end-of century outcomes are nearly identical under RCP 2.6.

Table 25. Projected land-use change (hectares) for kiwifruit and apple from the multinomial logit by climate scenario.

Land use	RCP 2.6 mid	RCP 2.6 end	RCP 8.5 mid	RCP 8.5 end
Kiwifruit	1875	1825	2675	3800
Apple	150	125	100	–1050

Climate change impacts for other land uses are not directly modelled (but there will be offsetting changes to these uses to accommodate changes in kiwifruit and apple so that total modelled land area does not change).

8.5 Integration with LURNZ

The projected land-use changes from the multinomial logit model are effectively used as inputs into LURNZ model runs. LURNZ combines these inputs with other land-use changes representing the impact of economic drivers, and it also applies various constraints on future land-use change. Therefore, the simulation outcomes from LURNZ will not exactly match the projections of the econometric model.

LURNZ also allocates land-use changes spatially across the country. During this process, it considers any changes in location-specific, land-use probabilities resulting from climate change.

8.5.1 Climate-driven land-use change

LURNZ integrates information from current and future suitability layers during execution of the desired climate scenario. Current (RCP past) climate is assumed to apply until 2027. The model does not therefore project any climate-driven, land-use change in this period. Mid-century climate is assumed to apply in the period 2028–2062. LURNZ determines the overall land-use change projected for this period and attempts to allocate it (subject to some constraints), in a linear manner in annual steps over the period. End-of-century climate is assumed to apply in the period 2063–2098. LURNZ determines the additional (compared with mid-century) land-use change for the period and attempts to allocate it linearly over the period. However, as LURNZ simulations end in 2075, land use will not have fully adjusted to end-of-century climate by the final simulation year.

8.5.2 Economic and policy context

Economic and policy parameters affect simulation outcomes for dairy farming, sheep-beef farming, plantation forestry and scrub. The parameters applied for LURNZ scenarios in this project reflect integrated Model Run 7 in the study by the Parliamentary Commissioner for the Environment (2019). Model Run 7 explores a two-basket approach to climate policy, where emissions from the land sector are treated separately to emissions from other sectors of the economy (collectively referred to as the fossil sector). The objective in Run 7 is for the fossil sector to meet net zero emissions by 2050, and for the land sector to reach a 20% emissions reduction from 2016 levels. Forestry offsets are allowed in the land sector only. The two-basket approach combined with the low policy stringency for the land sector leads to relatively low emissions prices in the land sector. The carbon price applied to the land sector increases along a sigmoid function to NZD 48 by 2075, the end of the simulation period. As a larger share of mitigation is performed by the fossil sector, there is relatively small disruption to the land sector (compared with other policy scenarios considered). Therefore, this run is thought to be the most consistent with the assumption of no exogenously driven growth in horticulture, kiwifruit and apple land area.

Consistent with assumptions in the reports of both the Productivity Commission (2018) and the Parliamentary Commissioner for the Environment (2019), we constrain the expansion of dairy farming in the simulations: no new land may be converted to dairying beyond 2025. This constraint reflects an anticipation of regional councils setting water quality limits in their regions in compliance with the Freshwater National Policy Statement.

8.5.3 Implementation

The geographic allocation of simulated land-use change in LURNZ is documented in detail in Anastasiadis et al. (2014). Here, we amend the original allocation algorithm to deal with changes in kiwifruit and apple land use.

In each simulation year, changes to kiwifruit are allocated first, and changes to apple are allocated next (then the algorithm moves on to other horticulture, dairy farming, sheep and beef farming, forestry and finally scrub). If kiwifruit land area increases, cells in other land uses with the highest kiwifruit land-use probability are converted to kiwifruit use. If kiwifruit land decreases, kiwifruit cells with the lowest kiwifruit land-use probability are assumed to convert to other horticulture land. The allocation of apple changes proceeds similarly (with the exception that kiwifruit land is not available for conversion to apple).

Simulated land-use conversions must satisfy some constraints. For example, deforestation of a plantation forestry cell is not allowed unless the forest is of harvestable age, and pre-1990 forests are not allowed to change land use (if a positive carbon price applies).

The algorithm deals only with changes in land use each year thereby minimising the number of cells that change use: reshuffling across land uses does not happen. This feature, a reflection of both unobservable factors and costs associated with land conversions, leads to patterns of land-use change that match observed short- and medium-term changes reasonably well (Anastasiadis et al. 2014). However, it is not well suited to long-term simulations in the context of climate change. By considering only changes in land use, the algorithm will not allow any cells to convert out of a use as long as the area of that land use increases nationally. Of particular concern in this respect is the projected shift of kiwifruit cultivation suitability across New Zealand. Although suitability with climate change increases on average, it decreases significantly in some current production areas. It is expected that over time, land use would respond to declining suitability, but this cannot be captured in the standard LURNZ output.

Therefore, we perform an additional modelling step to simulate conversions out of kiwifruit and apple. For each of these two land uses, we assume that the loss of land area within a region is proportional to the change in mean land-use probability on land in the given use. That is, a 50% fall in mean kiwifruit land-use probability on current kiwifruit land would lead to a projected loss of half of the region's kiwifruit land. The land area lost is then reallocated elsewhere by the standard algorithm in LURNZ. Essentially, this leads to a reallocation of kiwifruit an apple land areas away from regions with falling suitability to areas with the highest suitability (or, more precisely, highest probability).

8.6 LURNZ simulation results

Combining the effects of climate, economic and policy parameters, Table 26 and Table 27 report simulated land-use outcomes over time at the national level for RCPs 2.6 and 8.5, respectively. As economic and policy parameters are fixed across the runs, differences across the tables reflect the effect of changing kiwifruit and apple cultivation suitability.

Table 26. Simulated land-use (hectares) with mild climate change (RCP 2.6).

Land use	Basemap	2030	2045	2060	2075
Kiwifruit	15,600	15,750	16,550	17,350	17,475
Apple	9,425	9,425	9,500	9,550	9,575
Other horticulture	447,450	447,425	447,075	446,800	446,775
Dairy	2,098,200	2,291,375	2,290,925	2,290,500	2,290,450
Sheep-beef	8,152,825	7,488,125	7,243,025	6,916,975	6,685,075
Forestry	2,002,075	2,426,775	2,894,325	3,387,875	3,687,350
Scrub	1,743,000	1,789,700	1,567,175	1,399,525	1,331,875

Table 27. Simulated land-use (hectares) with severe climate change (RCP 8.5).

Land use	Basemap	2030	2045	2060	2075
Kiwifruit	15,600	15,825	16,975	18,375	18,675
Apple	9,425	9,425	9,475	9,425	9,125
Other horticulture	447,450	447,400	446,950	446,550	446,850
Dairy	2,098,200	2,291,325	2,290,750	2,290,050	2,290,025
Sheep-beef	8,152,825	7,488,025	7,242,575	6,823,850	6,683,325
Forestry	2,002,075	2,426,775	2,894,300	3,508,800	3,687,300
Scrub	1,743,000	1,789,800	1,567,550	1,371,525	1,333,275

In Table 28 and Table 29, a more detailed regional analysis of simulated land-use changes for kiwifruit and apple is presented. Under each climate scenario, regional losses and gains in land area are shown separately. For example, under the severe climate change scenario represented by RCP 8.5, kiwifruit area across New Zealand is projected to grow to 18,675 ha by 2075 – an increase of 3075 ha. This increase is the net effect of a loss of 5425 ha of current kiwifruit land and a growth of 8500 ha elsewhere.

For kiwifruit, area losses tend to be relatively large in the Bay of Plenty and Northland regions. At the same time, conversions to kiwifruit are projected to happen in some regions that are not traditionally associated with kiwifruit production. Hawke's Bay and Taranaki experience relatively large increases under both scenarios, while conversions to kiwifruit happen only with severe climate change in Canterbury.

Several previous studies (including Kenny 2001; Warrick et al. 2001; Pearce 2017) suggest that a lack of winter chilling due to climate change may make 'Hayward' kiwifruit production uneconomic in Northland (these studies also indicate a large potential decline in production in the Bay of Plenty.) However, our cultivation suitability scores assess suitability across all cultivars, not just 'Hayward'; while rising temperatures may result in 'Hayward' vines not receiving sufficient winter chill, lower-chill cultivars such as 'Zesy002' could still be viable. Thus, while kiwifruit cultivation suitability falls significantly in Northland under RCP 8.5, it does not fall to zero, precisely because kiwifruit cultivars other than 'Hayward' are available. Consequently, we have not projected a complete loss of kiwifruit land in Northland. More detail on the difference between our and previous studies are given in Section 9.2.

For apple, impacts under mild climate change are negligible. Under severe climate change, a large decrease of land use area is projected for the Hawke's Bay with partly offsetting increases in the South Island regions of Canterbury and Otago. The net effect is a projected decline of 300 ha in apple land area by 2075.

Table 28. Simulated land-use (hectares) by region and outside regional council (RC) boundaries for kiwifruit in 2075.

		RCP 2.6			RCP 8.5		
Region	**Basemap**	**loss**	**gain**	**Year 2075**	**loss**	**gain**	**Year 2075**
Auckland	375	50	0	325	200	0	175
Bay of Plenty	11,625	650	75	11,050	4,275	75	7,425
Canterbury	0	0	0	0	0	1,625	1,625
Gisborne	600	25	25	600	125	150	625
Hawke's Bay	350	0	325	675	0	2,325	2,675
Manawatu-Wanganui	100	0	0	100	0	0	100
Marlborough	0	0	0	0	0	950	950
Nelson	0	0	0	0	0	50	50
Northland	1,000	225	0	775	600	0	400
Otago	0	0	0	0	0	400	400
Southland	0	0	0	0	0	0	0
Taranaki	0	0	2,425	2,425	0	2,275	2,275
Tasman	700	0	0	700	0	625	1,325
Waikato	825	25	0	800	225	0	600
Wellington	0	0	0	0	0	25	25
West Coast	0	0	0	0	0	0	0
Outside RC boundaries	25	0	0	25	0	0	25
Total	15,600	975	2,850	17,475	5,425	8,500	18,675

Table 29. Simulated land-use (hectares) by region and outside regional council (RC) boundaries for apple in 2075.

		RCP 2.6			RCP 8.5		
Region	Basemap	loss	gain	Year 2075	loss	gain	Year 2075
Auckland	75	0	0	75	50	0	25
Bay of Plenty	0	0	0	0	0	0	0
Canterbury	50	0	50	100	0	875	925
Gisborne	150	0	25	175	50	25	125
Hawke's Bay	5,900	175	125	5,850	1,600	25	4,325
Manawatu-Wanganui	0	0	0	0	0	0	0
Marlborough	0	0	0	0	0	0	0
Nelson	0	0	0	0	0	0	0
Northland	0	0	0	0	0	0	0
Otago	725	0	0	725	0	525	1,250
Southland	0	0	0	0	0	0	0
Taranaki	0	0	125	125	0	75	75
Tasman	2,250	0	0	2,250	50	0	2,200
Waikato	150	0	0	150	50	0	100
Wellington	100	0	0	100	25	0	75
West Coast	0	0	0	0	0	0	0
Outside RC boundaries	25	0	0	25	0	0	25
Total	9,425	175	325	9,575	1,825	1,525	9,125

9 Workshops for industry and feedback

A separate workshop was held for each of apple, kiwifruit, avocado, cherry and wine grape, to present the work done in the project to the industries associated with these crops. Attendees included industry representatives, PFR crop experts and business managers, and members of the project team. The structure was the same for each workshop and reflected the structure of this report. However, since we modified some aspects of the modelling (such as not including the generic disease suitability score in overall suitability calculations), some of the presented results were in effect preliminary, with the final results presented in this report.

Additionally, we obtained feedback on how the different industries felt regarding how a crop fact sheet summarising this work should be presented. We also briefly described the purpose and intention of the SLMACC Adaptation project that will extend this work, by quantifying production and financial risk to the kiwifruit and avocado under climate change, and assessing and valuing different mitigation strategies.

Below we present salient information from the workshops along with our subsequent considerations.

9.1 Apple industry

While there was strong interest in the suitability modelling and the potential for future extensions, the industry view was that the modelling missed the opportunity to provide guidance to growers on the daily operations in the orchard. From a grower’s viewpoint, the risks of frost, hail and sunburn damage can be mitigated, as can drainage to a lesser extent. However, the number of rainfall days could be an operational issue, especially in spring, but at other times too: rain and weather events affected whether a location is suitable, and thus growers are interested in long-term forecasts of daily rain and additionally wind for the current season. However, the work done in the project was seen as having value for long-term strategic planning, and would be of more interest to large companies than individual growers.

The industry expressed the view that rather than modelling and projecting cultivation suitability at the national level, an approach that paid individual attention to the main current apple-growing regions (Hawke’s Bay, Nelson, Central Otago, Gisborne plus perhaps Timaru and Waikato) would provide more insight on how these areas will be affected over the next 50 years. It would be also desirable to have the biggest climate risk factor for each region identified. The industry highlighted that it has GPS coordinates for orchard boundaries that could be incorporated to enhance regional-scale suitability modelling and projections.

Certainly our focus in this project has been at the national level, and although projected climate change impacts on apple cultivation at the regional level are shown on our future suitability maps this does not provide the resolution that the apple industry would like. Refining our suitability modelling to separately focus on current apple-growing regions, especially incorporating industry GPS data for boundaries would be an invaluable extension, and additionally strategic value could be gained by applying a focus on the new areas of future suitability that we have projected in this project. However, given the stochastic nature of weather patterns, the ability of models to provide guidance on daily operations in the long-term future is limited.

The industry had the view that rain was a better predictor of disease than relative humidity and suggested a reformulation of our generic disease model to incorporate rainfall per month or the number of rain days a month, based on work done for the industry by PFR disease expert, Robert

Beresford. An alternative view (Ken Breen) was that the predictor should be pathogen specific, with the example that russet disease was more accurately predicted by leaf surface wetness or RH >80%. Modelling disease risk in apple by addressing the different risk factors for individual pathogens would require more resources than available in this project and thus was out of scope. The feedback from the industry has highlighted the need to address this gap in the future.

9.2 Kiwifruit industry workshop

A key concern raised by the kiwifruit industry was that our projections on the suitability for Northland for kiwifruit differed from earlier projections by NIWA (Tait et al. 2018) for which timeline projections are available at https://well-shny-vp.shinyapps.io/CCII/. While Tait et al. (2018) focused on Te Puke, the timeline projections encompasses all of New Zealand. This timeline and other reports (which are referenced in the LURNZ section) suggest that suitability for kiwifruit in Northland would reduce to the point that it would become uneconomic. In contrast, our projection was far more favourable. Our response at the meeting was followed by subsequent email communication and investigation. Given the importance of this apparent conflict in projections, we summarise the main details below.

Reassuringly, both the NIWA study and our study project a decline in suitability for Northland, with a minor impact projected under the RCP 2.6 and a more significant decrease in suitability under RCP 8.5. However, comparison of the studies is complicated a little because the two studies used different suitability scales, different suitability rules and different future climate model datasets.

Additionally, while the NIWA study focused on the viability of the green 'Hayward' cultivar, we considered suitability for a range of cultivars, including 'Hayward', 'Zesy002' (which has a lower chill requirement than 'Hayward'), and future cultivars bred to have even lower chill requirements.

While the NIWA study expressed suitability in terms of used the three categories of "Poor", "Marginal" and "Good", we used a continuous scale from 0 to 1. Additionally, while the NIWA study used a temperature index approach to identify threshold 'production risk' temperatures for four phenologically important seasons (Tait et al. 2018), we considered the range of climate and soil suitability criteria that we have described in this report. Also, we used the new SLM RCP climate datasets (discussed in Section 6) rather than NIWA's RCP climate datasets.

Thus the studies do differ in the starting and end points for suitability assessment.

Our study assessed that in the contemporary period (2006–2016) most areas in Northland had average to good cultivation suitability (0.5 to 0.8) across kiwifruit cultivars but with some very poor and some very excellent suitability (>0.9) areas. Our end of century projection for RCP 8.5 indicates that while there will be no areas with excellent suitability across all cultivars, there will be still be a number of areas in the average to good range.

The NIWA study assessed Northland as having marginal to poor suitability for 'Hayward' over the contemporary period (2006–2016) and earlier years, and projected all of Northland would have poor suitability for 'Hayward' by the end of the century under RCP 8.5.

A key point here is that although Northland may become too warm for 'Hayward', it may still prove sufficient for other cultivars. Thus how scores are interpreted is very important. For example, within our suitability score system, a lower chill suitability score could suggest that 'Hayward' would not receive adequate chill, but 'Zesy002' or other new cultivars might, or that Hi-Cane® (or suitable replacement) will be needed for successful growing of 'Hayward'.

Another area of concern was that the preliminary projections from the LURNZ model suggested that the kiwifruit footprint would increase in Northland in the future despite our projections that kiwifruit suitability would decline. The LURNZ model had been extended in this project to include apple and kiwifruit, and investigations showed that a parameter spuriously linked an increase in kiwifruit area to a decrease in the apple suitability. Thus as a result of the workshop feedback, the model has been updated to remove the spurious effect, in order to improve the robustness of the LURNZ model projections.

The kiwifruit industry saw value in the modelling to help individual growers undertake risk assessments and develop farm plans for mitigation, and for the industry to perform risk assessment at the regional level. The modelling is also invaluable for identifying where the industry can grow, and for understanding risks and opportunities from a strategic/governance perspective.

9.3 Avocado industry workshop

There was broad support for our approach of continuous suitability score formulated from a plant physiology perspective, and industry members made the observation that our ground-truthed suitability maps for avocado were in line with industry experience and improved on other approaches they were aware off, especially for projection of suitability in the South Island.

However, it was felt that our modelling of frost and warmth suitability scores could be further refined, with the observation that avocado is relatively plastic with respect to soil properties but very sensitive to climate. Thus it was felt that we could further reduce our weightings for soil criteria which, with the exception of drainage, are already low relative to climate criteria weightings. Our soil pH model was considered to provide a good representation of avocado sensitivity to soil pH.

The industry has found that non-frost spring temperatures less than 7°C can damage leaves, which we have not represented in our modelling. Thus there is interest is having a separate model for spring temperatures. Alternatively our frost suitability model could be extended to include cold damage from non-frost temperatures with season-dependent sensitivity.

Additionally, since low temperatures can affect avocado pollination, the avocado industry would be keen on the development of a separate suitability model for pollination that included low spring temperatures, which can affect pollination. The literature provides some data on the temperature conditions needed for successful pollination, and in this project we had incorporated this information into our warmth suitability score. However, unpublished data on individual flowers, temperature and fruit set have been collected on behalf of the industry, and this would be available to us for further model development.

The view from the industry was that the generic disease model should be excluded from calculations since the industry has tools to control disease, so disease considerations are not as important as other criteria when decisions are made on whether to establish a new orchard, and our disease module is too generic to aid in disease. However, the industry does have future pest incursions due to climate change on its radar, and had observed an increased expression of fungal disease in avocado trees. Productivity loss from phytophthora root rot is hard for the industry to quantify. There is also interest in a separate project dedicated to pest and disease as future work, since the industry has a lot of data collection on pest and disease in the pipeline. It was felt that our generic disease model had the appropriate structure to incorporate data on specific organisms (with suitable parameterisation) and that at least two disease models were needed, to distinguish between tree diseases and fruit diseases. We had used drainage suitability in our modelling to indicate the risk of root diseases; however, a better understanding of root diseases would be desirable.

The avocado industry would like to use the results from our climate suitability studies to inform investment decisions in new avocado orchards by identifying where best to buy land, and to increase grower awareness of increasing or decreasing challenges. Knowledge of potential future climate impacts on productivity would also usefully feed into choice of cultivars as a mitigation strategy that would be underpinned by a breeding programme for future cultivars. A question the industry has, is how much variation in production can be explained by climate versus management, since this feeds into the inherent value proposition of mitigation strategies.

Philip West (Research Manager, New Zealand Avocado) shared research results that indicated summer temperatures were the biggest factor for avocado production under climate change, which was contrary to the expectation that spring temperatures would have the most influence.

9.4 Blueberry industry workshop

No workshop for the blueberry industry was held.

9.5 Cherry industry workshop

A key interest expressed by the cherry industry is using the suitability modelling as a tool to inform on whether or not to replace the current cultivar in a location with a different one in the future, based on how suitability in that location is projected to change. Therefore, as for the apple industry, value was seen in refining our suitability modelling to separately focus on the different locations within growing regions, and to project with much more precision than the uncertainty limits in our study would allow. Growers would be interested in data and future projections at a localised level that would guide investment decisions with a 40-year time-frame (a tree having a 30-year lifespan).

Conversely, the industry would like tools to examine areas that are not growing cherry but appear suitable and investigate why not, and to identify opportunities for new orchard locations.

It was noted by the industry that areas of the Hawke’s Bay showed only moderate suitability for winter chill, yet cherries are successfully grown there because of appropriate (low-chill) cultivar choice. This was actually in accord with our chill suitability score, which reflects the range of cultivars receiving adequate chill: the lower the score, the greater the restriction to low-chill cultivars.

The relevance of the LUC classes was questioned, with the suggestion that LUC scores be ground-truthed for perennial tree crops to check the validity of including LUC classes in suitability rules.

The industry representatives also expressed a desire for the model to be made available as a tool that allowed researchers and growers an ability to test different assumptions and to assign different weights to suitability criteria based on their personal views and experience. For example, frost risk could be mitigated to some extent, thus it was suggested there should be the ability to run scenarios with and without frost as a suitability criterion.

This is an avenue of work that would be of benefit across all industries, and not just cherry, and would especially enhance further work on developing suitability models for individual pathogens by allowing focus on the main known disease risks in a locale.

9.6 Wine grape industry workshop

While there was interest in the model and approach, the industry view was that the 5km×5km climate data grid cells and the 1km×1km soil data grid cells were too course for the industry, given that the footprints on Pinot noir and Sauvignon blanc were very small in some regions. Additionally, despite the use of expert validation in the development of suitability maps, industry representatives would feel more confident if maps were checked for validity using location data. An observation by Damian Martin was that the maps might over-predict suitability for the Waikato.

There was interest in applying the suitability modelling to look at climate risks over a 12- to 18-month basis rather than using it to project for periods of time far into the future. However, such an application would require reliable predictions of weather patterns up to 18 months into the future, and given the stochastic nature of weather patterns, a climate model cannot be relied upon to provide such accuracy.

Industry representatives were also keen on having the ability to interrogate the model to identify how the individual suitability criteria contribute to projected suitability changes for individual locations, and also to compare suitability scores for other crops at individual locations in order to aid decisions on planting.

This functionality would be complementary to the functionality requested by the cherry industry, and could be provided by the same modelling tool. This of course would provide benefit across industries and thus would be a compelling line of research.

10 Discussion

10.1 Outlook for future projections

Under RCP2.6, the low GHG concentration pathway, for all crops there is very little difference between the mid-century suitability maps and late-century maps, most changes having occurred by the mid-century. This is not surprising since under RCP2.6 GHG emissions are assumed to have peaked in 2020. For each crop the area of land with excellent suitability (0.9 to 0.1) is projected to increase modestly by mid-century compared with the historic period. For crops such as cherry and wine grape, starting with very small areas of land in this category, the relative increase ranged from 30 to 400%. However, between the mid- and late-century, a small loss of excellent suitability land is projected to occur for all crops except avocado, with cherry dropping below its historic-period level.

Under this RCP, the pattern of change in suitability for apple disadvantages the Hawke's Bay (the main apple-growing region), Gisborne and the Waikato, but favours other apple regions such as Central Otago and Nelson. The suitability maps indicate that areas in the Taranaki could have the highest suitability land for apple. In contrast, the kiwifruit heartland in the Bay of Plenty is projected to have an increase in suitability apart from coastal areas. However, from Northland down to the Waikato, the Coromandel and areas around the East Cape are projected to decrease, and given that Northland does not have a high suitability for winter chill, these changes would increasingly favour low-chill cultivars such as 'Zesy002' in this region. Since areas with highest suitability for avocado are predominantly in the Northland region and suitability is projected to increase, some change in land use from kiwifruit to avocado could be expected in Northland.

Although suitability for blueberry is expected to experience a small decrease in its main growing regions under RCP.2.6, the Waikato and Bay of Plenty, suitability will remain high, as it is in many locations throughout New Zealand. Thus footprints are unlikely to be significantly affected, although this is not clear for Northland where lower-chill varieties of blueberry would currently be required. Since low-chill varieties of cherry are required in the Hawke's Bay, the decrease in suitability in most areas of that region could place further limitations on cherry cultivation; however, significant areas of very good to excellent suitability land are expected to remain. Cultivation suitability for cherry in Central Otago shows little change.

Both the Pinot noir and Sauvignon blanc industries would have the opportunity to substantially increase their growing footprint under RCP2.6. Although suitability for Pinot noir decreases a fraction in parts of Marlborough and Nelson, but suitability for Sauvignon blanc increases in the same regions, the overall suitability for both wine grape cultivars will remain excellent in many areas of the region, thus there is little likelihood of a climate-driven change in land use between the cultivars in these areas or other wine-growing areas.

Mid-century suitability maps projected under RCP 8.5 show similarities to the late-century maps projected under RCP 2.6. In comparison with the historic period, the total area of land with excellent cultivation suitability is projected to halve for apple by the late-century, remain more or less constant for kiwifruit, have a modest 24% increase for blueberry, double for Pinot noir and have several-fold increases for Sauvignon blanc, avocado and cherry.

Under the RCP 8.5 projections, a reduction in the footprint of apple in its main growing area of Hawke's Bay is expected (as well as Waikato and Gisborne), but some new opportunities for orchard establishment could occur in Southland. Decreasing suitability in kiwifruit strongholds such as the Bay of Plenty and Northland could see the kiwifruit footprint shift to new locations such as the Taranaki and

North Canterbury where suitability is expected to increase. Suitability for avocado is projected to be very good or excellent in many scattered locations around the North Island away from the centre of the central plateau, offering the opportunity for a significantly increased footprint. Many of these locations coincide with areas that current support kiwifruit but that are projected to become unsuitable. Thus significant land-use change from kiwifruit to avocado would be expected.

Under RCP8.5, the projected reduction in suitability for blueberry in Northland and coastal areas around the North Island and the increased appearance of highly suitable land across Canterbury, parts of Otago and Southland could result in a wider distribution of the blueberry footprint, especially in the South Island. A similar trend for cherry is expected, with the Hawke's Bay projected to reduce in suitability and increasing locations in Otago and Southland becoming of very good or excellent suitability.

The warmer late-century temperatures under RCP8.5 are projected to make most of the North Island unsuitable for Pinot noir, and greatly reduce the suitability of the Nelson and Marlborough regions, while opening up a few new areas of land in Canterbury and Otago with very good or excellent suitability. A similar situation is projected for Sauvignon blanc by the late-century under RCP 8.5, with the North Island and Nelson becoming more or less unsuitable, while areas in Central Otago and South Canterbury developing excellent cultivation suitability. Although around the Blenheim area in Marlborough is projected to reduce in suitability, a few locations are expected to have very good suitability.

10.2 Continuous suitability scoring

Our development of a new nonlinear suitability model composed of modular suitability score functions provides for increased power and flexibility for assessing land-use suitability.

Crop growth is a biological process and relationships between crop development and temperature, or in fact any other environmental parameter, are subject to natural variation. In this context, we consider the commonly used binary assessment of 'suitable' or 'unsuitable' to be inflexible, and not ideal for dealing with diversity of horticultural production systems. Thus, we have adopted sliding scale suitability scoring functions to evaluate each assessment criterion. This approach has several advantages over a binary assessment method: the model outputs not only highlight regions with optimal growing conditions for a certain crop but also delineate and rank other regions with lesser suitability for this crop. The scores for the individual suitability criteria can then help to identify which measures or management practices would be required for viable crop production in regions with lesser suitability.

Further, the interpretation of the assessment scores could be extended from pure "suitability" assessments to projections of potential yields and productivity, or to ongoing mitigation costs. Alternatively, the suitability scores could be adapted to expressing exposure to risk and potential loss.

Through consultation with industry and expert researchers, we found that opinions about the relative importance of individual suitability criteria are quite diverse. In our modelling, we represented a "consensus" view of importance by taking a weighted combination of the individual climate-related and land-related suitability criteria to form a final suitability score, with criteria believed to be more important having a larger weight. The criteria weights can readily be changed to accommodate different views.

Another advantage of our model is its modular framework, which provides flexibility for potential future extension of the model. Other environmental factors projected to change, such as frequency and intensity of rain or atmospheric CO_2 concentrations, could be easily considered, provided that necessary input data were available. Also, additional suitability criteria such as the risk of pest and diseases or the occurrence of flooding could similarly be developed and integrated into the model as new modules. Likewise, currently integrated suitability assessment criteria could be removed or given lower weightings if new system understanding was obtained or new cultivars that have greater tolerance to certain climate criteria were developed e.g. lower chill requirements.

While developing the suitability models for avocado, blueberry, cherry and wine grape, we extended our ‘sliding scale’ continuous suitability score methodology that we developed for apple and kiwifruit to incorporate more phenological-based modelling. Compared with a binary approach, a continuous approach is more suitable for incorporating natural variations that occur between environmental parameters and the biological processes that underpin crop performance. Further advantages over a binary assessment method include that the model outputs not only highlight regions with optimal growing conditions for a certain crop but also delineate and rank other regions with lesser suitability for this crop. The scores for the individual suitability criteria can then help to identify which measures or management practices would be required for viable crop production in regions with lesser suitability, e.g. frost protection or rooting depth.

10.3 Adjustments to climate model datasets

At the start of the project it was envisaged that we would perform future projections using 24 future weather datasets generated by NIWA’s regional climate model (separately forced by six GCMs under four RCPs). However, we found deficiencies in the RCP datasets in that they did not accurately reflect NZ weather patterns for their hindcast period (1972–2005), for which we had observation-based data. Thus we performed adjustments in order to obtain future climate datasets that more closely matched observed weather patterns, and this created new datasets, which we refer to as the SLM RCP datasets. These new SLM RCP datasets were used instead for future projections.

The importance of these adjustments is to an extent dependent on the nature of the suitability models. For example, the temperature data in the original RCP datasets had been biased corrected for agreement with the VCSN data for annual mean temperatures, and would be adequate for suitability models that were formulated in terms of mean annual temperatures. However, the temperature data in the original RCP dataset showed biases at the month-of-the-year level, and differences in the variance of both monthly temperatures across years and daily temperatures within months. Thus these datasets could result in misleading assessments when used with suitability rules that required monthly data or that are sensitive to temperature extremes, as we have shown.

10.4 LURNZ modelling

We have incorporated data on the location of kiwifruit and apple blocks as well as on present and future cultivation suitability for kiwifruit and apple in the Land Use in Rural New Zealand (LURNZ) model to analyse the future spatial footprint of these sectors.

Nationally, mean kiwifruit suitability rises with climate change. Mean apple suitability also rises, but it rises less under severe climate change than it does under mild climate change. Despite the increasing average suitability in both sectors, suitability for kiwifruit decreases in current kiwifruit areas, and suitability for apple decreases in current apple areas.

Our simulations suggest that mild climate change is unlikely to disrupt either sector significantly. However, reflecting changing suitability, we see potentially large shifts in the spatial footprints of kiwifruit and apple under severe climate change. Both sectors experience relatively large losses of land area in currently important production regions. For kiwifruit, the losses are more than offset by increases in land area elsewhere. For apple, this is not the case as total apple area is projected to decline.

The results discussed reflect direct climate impacts only. They do not consider other important drivers of land-use change such as global market prices for these crops. Changes in the future suitability of other land uses are also not modelled. Environmental policies, climate variability and extreme weather events, the potential development of new fruit varieties and the adoption of new technologies will also all affect future land-use decisions, sometimes in unforeseeable ways. Nonetheless, we believe the simulations presented in this paper for kiwifruit and apple are of interest because they help identify and characterise pressures and opportunities from climate change in these sectors.

10.5 Final industry workshops

Feedback from the industry workshops provided valuable guidance in a final refining of our suitability modelling, in particular the exclusion of the generic disease score in overall suitability analyses. Approaches. Additionally feedback was valuable for refining the LURNZ model and improving its projection for kiwifruit.

Industries generally viewed the suitability modelling as a long-term strategic tool that could help identify areas of new opportunity to grow their footprints in new areas while at the same time mitigating the impact of climate change. However, there was also a desire for suitability modelling with a 1- or 2-year horizon to aid tactical decisions around orchard management. Unfortunately, because of the stochastic nature of weather patterns and events, a short-term predictive tool may lack predictive power due to larger uncertainties than for projecting the average over a number of years.

A reservation voiced by the wine grape industry in particular is that the 5x5-km climate grid and 1x1-km land information grid are too coarse a resolution to capture microclimate effects and to accurately portray the experiences of individual orchards. Thus there was a call to validate the model predictions against individual orchard experience. This would be a valuable future project that extended our suitability modelling, but would require the availability of GIS-based data collected at different orchard sites.

A strong wish expressed across several industries is the establishment of a project to extend our generic suitability model to predict the risks of individual diseases, especially since some industries are seeing increased incidence of disease. Additionally, industry members saw value in having the suitability model available as a tool that would allow them to set the weights of individual criteria and to explore the relative impacts of different criteria on suitability assessments. Such a tool would allow industry members to explore the climate-change risks to small geographical regions in detail, and this could be both a guidance and educational tool. Establishment of projects to address both these issues would have strong industry support and be seen as a high priority.

11 Acknowledgements

We thank NIWA for making climate data available and Abha Sood and Andrew Tait for discussions during the project. We thank Annette Richardson, Ben van Hooijdonk, Damian Martin, Grant Thorpe, Janice Turner, Ken Breen and Nick Gould for their expertise in ground-truthing the suitability maps, and to industry representatives from the apple, kiwifruit, avocado, blueberry, cherry and wine grape industries for their feedback on progress at different stages of the project. We thank Brent Clothier, Duncan Hedderley, Maryam Alavi, and Rodelyn Jacksons for technical discussions. Finally we thank Brent Clothier for reviewing the report.

12 References

Alburquerque N, García-Montiel F, Carrillo A, Burgos L 2008. Chilling and heat requirements of sweet cherry cultivars and the relationship between altitude and the probability of satisfying the chill requirements. Environ Exp Bot 64(2): 162-170.

Aminifard MH, Mohammadi S 2013. Efficacy of plant essential oils to control post-harvest decay of sweet cherry (Prunus avium L.) fruit. J Hortic Sci Biotec 88(1): 79-84 doi:10.1080/14620316.2013.11512939.

Anastasiadis S, Kerr S, Zhang W, Allan C, Power W 2014. Land use in rural New Zealand: Spatial land use, land-use change, and model validation Wellington, New Zealand: Motu Economic and Public Policy Research.

Ausseil AGE, Bodmin K, Daigneault A, Teixeira E, Keller ED, Kirschbaum MUF, Timar L, Dunningham A, Zammit C, Stephens S et al. 2016. Climate change impacts and implications: an integrated assessment in a lowland environment of New Zealand. 8th International Congress on Environmental Modelling and Software, Toulouse, France. p. 76.

Austin ME, Bondari K 1987. The effect of chilling temperature on flower bud expansion of rabbiteye blueberry. Sci Hortic 31(1-2): 71-79.

Austin PT, Hall AJ, Snelgar WP, Currie MJ 2002. Modelling kiwifruit budbreak as a function of temperature and bud interactions. Ann Bot 89(6): 695–706.

Bagherzadeh A, Ghadiri E, Souhani Darban AR, Gholizadeh A 2016. Land suitability modeling by parametric-based neural networks and fuzzy methods for soybean production in a semi-arid region. Modeling Earth Systems and Environment 2(2): 104 doi:10.1007/s40808-016-0152-4.

Balbontín C, Ayala H, M Bastías R, Tapia G, Ellena M, Torres C, Yuri JA, Quero-García J, Ríos JC, Silva H 2013. Cracking in sweet cherries: A comprehensive review from a physiological, molecular, and genomic perspective. Chilean J Agric Res 73(1): 66-72.

Ballard J, Proebsting EL, Tukey R 1997. Cherries: critical temperatures for blossom buds.

Beresford R, Tyson J, Henshall W 2016. Development and validation of an infection risk model for bacterial canker of kiwifruit, using a multiplication and dispersal concept for forecasting bacterial diseases. Phytopathology 107(2): 184-191.

Blodgett EC, Johnson DA, Grove GG, Beers EH 1990. Why cherry trees die Washington State University Cooperative Extension.

Bois B, Zito S, Calonnec A 2017. Climate vs grapevine pests and diseases worldwide: the first results of a global survey. OENO One 51(2): 133-139.

Bonomelli C, Bonilla C, Acuña E, Artacho P 2012. Seasonal pattern of root growth in relation to shoot phenology and soil temperature in sweet cherry trees (Prunus avium): A preliminary study in central Chile. International Journal of Agriculture and Natural Resources 39(1): 10.

Broome J, English J, Marois J, Latorre B, Aviles J 1995. Development of an infection model for Botrytis bunch rot of grapes based on wetness duration and temperature. Phytopathology 85(1): 97-102.

Brown WS 1932. Cherries. Corvallis, Oregon: Oregon State Agricultural College Extension Service.

Brunt C, Darbyshire R, Nissen R, Chapman S 2017. Australian Cherry Production Guide 2017. Chill and heat requirements: From dormancy to flowering. Cherry Growers Australia.

Buis A 2020. Study Confirms Climate Models are Getting Future Warming Projections Right. NASA. https://climate.nasa.gov/news/2943/study-confirms-climate-models-are-getting-future-warming-projections-right/ [accessed January 2021]. https://climate.nasa.gov/news/2943/study-confirms-climate-models-are-getting-future-warming-projections-right/

Buttrose M, Alexander DM 1978. Promotion of floral initiation in 'Fuerte'avocado by low temperature and short daylength. Sci Hortic 8(3): 213-217.

Carroll J, Wilcox W 2003. Effects of humidity on the development of grapevine powdery mildew. Phytopathology 93(9): 1137-1144.

Çelik H 2009. The performance of some Northern Highbush blueberry (Vaccinium corymbosum L.) varieties in North Eastern part of Anatolia. Anadolu Tarım Bilimleri Dergisi 24(3): 141-146.

Cesaraccio C, Spano D, Snyder RL, Duce P 2004. Chilling and forcing model to predict bud-burst of crop and forest species. Agric For Met 126(1-2): 1-13.

Challinor AJ, Müller C, Asseng S, Deva C, Nicklin KJ, Wallach D, Vanuytrecht E, Whitfield S, Ramirez-Villegas J, Koehler A-K 2018. Improving the use of crop models for risk assessment and climate change adaptation. Agricultural Systems 159: 296-306.

Chaves B, Salazar MR, Schmidt T, Dasgupta N, Hoogenboom G 2017. Modeling apple bloom phenology 10.17660/ActaHortic.2017.1160.29. International Society for Horticultural Science (ISHS), Leuven, Belgium. p. 201-206.

Chen J, Brissette FP, Leconte R 2011. Uncertainty of downscaling method in quantifying the impact of climate change on hydrology. J Hydrol 401(3): 190-202 doi:https://doi.org/10.1016/j.jhydrol.2011.02.020.

Chmielewski F-M, Götz K-P 2016. Performance of models for the beginning of sweet cherry blossom under current and changed climate conditions. Agric For Met 218: 85-91.

Ciliberti N, Fermaud M, Roudet J, Rossi V 2015. Environmental conditions affect Botrytis cinerea infection of mature grape berries more than the strain or transposon genotype. Phytopathology 105(8): 1090-1096.

Cittadini ED, de Ridder N, Peri PL, van Keulen H 2006. A method for assessing frost damage risk in sweet cherry orchards of South Patagonia. Agric For Met 141(2-4): 235-243.

Clothier B, Hall A, Green S 2012. Adapting the horticultural and vegetable industries to climate change. In: Clark A, Nottage R, eds Impacts of Climate Change on Land-based Sectors and Adaptation Options. MPI Technical Paper No: 2012/33. p. 237-292.

Clothier BE, Hall A, van den Dijssel C 2018. Potential land uses: A report to Central North Island Iwi Land Management Ltd Plant & Food Research.

Correia S, Schouten R, Silva AP, Gonçalves B 2018. Sweet cherry fruit cracking mechanisms and prevention strategies: A review. Sci Hortic 240: 369-377.

Cradock-Henry NA, Flood S, Buelow F, Blackett P, Wreford AB 2019. Adaptation knowledge for New Zealand's primary industries: Known, not known and needed. Climate Risk Management 25: 100190.

Creasy IL 1980. The correlation of weather parameters with russet of 'Golden Delicious' apples under orchard conditions. J Amer Soc Hort Sci 105: 735-738.

Davenport T 1986. Avocado flowering. Hort Rev 8(257): 89.

Dawson LA, Duff EI, Campbell CD, Hirst DJ 2001. Depth distribution of cherry (Prunus avium L.) tree roots as influenced by grass root competition. Plant Soil 231(1): 11-19 doi:10.1023/A:1010383506446.

DeLucia EH, Nabity PD, Zavala JA, Berenbaum MR 2012. Climate change: Resetting plant-insect interactions. Plant Physiol 160(4): 1677-1685 doi:10.1104/pp.112.204750.

Díez-Palet I, Funes I, Savé R, Biel C, de Herralde F, Miarnau X, Vargas F, Àvila G, Carbó J, Aranda X 2019. Blooming under Mediterranean climate: Estimating cultivar-specific chill and heat requirements of almond and apple trees using a statistical approach. Agron 9(11): 760.

Dixon J, Smith D, Greenwood A, Elmsly T 2006. Putative timing of irreversible commitment to flowering of 'Hass' avocado trees in the Western Bay of Plenty. New Zealand Avocado Growers' Association Annual Research Report 6.

Dixon J, Barber R 2008. Relationship between temperature in October and November and yield. New Zealand Avocado Growers' Association Annual Research Report 88: 59-70.

Dubrovina I, Bautista F 2014. Analysis of the suitability of various soil groups and types of climate for avocado growing in the state of Michoacán, Mexico. Eurasian Soil Sci 47(5): 491-503.

Edwards J, Riches D, Evans K, Beresford R, Hill G, Wood P, Mundy D 2009. The need for a risk-based approach to botrytis management. The Australian & New Zealand Grape Grower & Winemaker(Annual Technical Issue): 6-9.

Ellenwood CW 1941. Bloom period and yield of apples Ohio Agricultural Experiment Station, Wooster, Ohio, Bulletin 618 [accessed 23 June 2019]. https://kb.osu.edu/bitstream/handle/1811/61075/1/OARDC_bulletin_n618.pdf

Elmer P, Reglinski T 2006. Biosuppression of Botrytis cinerea in grapes. Plant Pathol 55(2): 155-177.

Erez A, Fishman S, Linsley-Noakes GC 1990. The Dynamic Model for rest completion in peach buds. Wageningen: Int Soc Horticultural Science.

Everett K 2002. Avocado fruit rots: a review of industry funded research. New Zealand Avocado Growers' Association Annual Research Report 2: 8-16.

Everett KR, Siebert B 2018. Exotic plant disease threats to the New Zealand avocado industry and climatic suitability: a review. N Z Plant Prot 71: 25-38.

Eyring V, Cox PM, Flato GM, Gleckler PJ, Abramowitz G, Caldwell P, Collins WD, Gier BK, Hall AD, Hoffman FM et al. 2019. Taking climate model evaluation to the next level. Nature Climate Change 9(2): 102-110 doi:10.1038/s41558-018-0355-y.

Fennell A 2004. Freezing tolerance and injury in grapevines. Journal of Crop Improvement 10(1-2): 201-235.

Ferguson JC, Moyer MM, Mills LJ, Hoogenboom G, Keller M 2014. Modeling dormant bud cold hardiness and budbreak in twenty-three Vitis genotypes reveals variation by region of origin. Am J Enol Vitic 65(1): 59-71.

Ferreyra R, Sellés G, Saavedra J, Ortiz J, Zúñiga C, Troncoso C, Rivera S, González-Agüero M, Defilippi B 2016. Identification of pre-harvest factors that affect fatty acid profiles of avocado fruit (Persea americana Mill) cv.'Hass' at harvest. S Afr J Bot 104: 15-20.

Fulcher A, Gauthier NW, Klingeman WE, Hale F, White SA 2015. Blueberry culture and pest, disease, and abiotic disorder management during nursery production in the southeastern US: a review. Journal of Environmental Horticulture 33(1): 33-47.

Greer DH, Weedon MM 2013. The impact of high temperatures on Vitis vinifera cv. Semillon grapevine performance and berry ripening. Front Plant Sci 4: 491.

Griffiths G, Tait A, Wratt D, Jessen M, McLeod M, Reid J, Anderson J, Porter N, Halloy S, Richardson A 2003. Use of climate, soil, and crop information for identifying potential land-use change in the Hokianga and Western Kaipara Region. NIWA [accessed 28 January 2020]. http://www.fndc.govt.nz/about-the-district/soil-and-climate study/soilclimate.pdf

Guak S, Neilsen D 2013. Chill unit models for predicting dormancy completion of floral buds in apple and sweet cherry. Horticulture, Environment, and Biotechnology 54(1): 29-36 doi:10.1007/s13580-013-0140-9.

Hall A, Snelgar W 2014. Predicting the start of budbreak for 'Hayward' and Gold3 kiwifruit. A Plant & Food Research Ltd. report prepared for Zespri Group Limited. Milestone No. 59671. Contract No. 31144. SPTS No. 10948.

Hall A, Stanley J, Müller K, van den Dijssel C 2018. Criteria for defining climatic suitability of horticultural crops. A Plant & Food Research report prepared for Ministry for Primary Industries. Milestone No. Milestone No. 73682. Contract No. 34671. SPTS No. 17301.

Hall A, Blackman J 2019. Modelling within-region spatiotemporal variability in grapevine phenology with high resolution temperature data. OENO One 53(2) doi:10.20870/oeno-one.2019.53.2.2450.

Hall IV, Aalders LE, Townsend LR 1964. The effects of soil pH on the mineral composition and growth of the Lowbush blueberry. Can J Plant Sci 44(5): 433-438.

Hancock J 2006. Northern Highbush blueberry breeding. VIII International Symposium on Vaccinium Culture 715. p. 37-40.

Hashim-Buckey J 2006. Grapes suffering from heat wave. Western Farm Press.

Hatfield JL, Prueger JH 2015. Temperature extremes: Effect on plant growth and development. Weather and Climate Extremes 10: 4-10.

Hauagge R, Cummins JN 1991a. Relationships among indices for the end of bud dormancy in apple cultivars and related Malus species under cold winter conditions. J Amer Soc Hort Sci 116(1): 95-99.

Hauagge R, Cummins JN 1991b. Phenotypic variation of length of bud dormancy in apple cultivars and related malus species. J Amer Soc Hort Sci 116(1): 100-106 doi:10.21273/jashs.116.1.100.

Hayes R 1988. Soil requirements of blueberry in relation to their nutrition. Proceedings of Agronomy Society of New Zealand, vol 18. p. 143-147.

Hayman P, Longbottom M, McCarthy M, Thomas D 2012. Managing grapevines during heatwaves. GWRDC, Australia.

Hewett E, Young K 1981. Critical freeze damage temperatures of flower buds of kiwifruit (Actinidia chinensis Planch.). N Z J Agric Res 24(1): 73-75.

Hicklenton PR, Reekie JYC, MacKenzie K, Eaton LJ, Havard P 2002. Freeze damage and frost tolerance thresholds for flowers of the Lowbush blueberry (*Vaccinium angustifolium* Ait.) 10.17660/ActaHortic.2002.574.29. International Society for Horticultural Science (ISHS), Leuven, Belgium. p. 193-201.

Hill GN, Beresford RM, Evans KJ 2018. Automated analysis of aggregated datasets to identify climatic predictors of botrytis bunch rot in wine grapes. Phytopathology 109(1): 84-95.

Hochmaier V 2014. Chilling unit accumulation and degree-day requirements of four sweet cherry (Prunus avium L.) cultivars. In: Ayala M, Zoffoli JP, Lang GA, eds Vi International Cherry Symposium. Leuven 1: Int Soc Horticultural Science. p. 203-207.

Holb I 2008. Brown rot blossom blight of pome and stone fruits: symptom, disease cycle, host resistance, and biological control. International Journal of Horticultural Science 14(3): 15-21.

Holb I, Lakatos P, Abonyi F 2010. Some aspects of disease management of cherry leaf spot (Blumeriella jaapii) with special reference to pesticide use. International Journal of Horticultural Science 16(1): 45-49.

Hopkins D, Campbell-Hunt C, Carter L, Higham JE, Rosin C 2015. Climate change and Aotearoa New Zealand. Wiley Interdisciplinary Reviews: Climate Change 6(6): 559-583.

Hortinfo 2010. Use and interpretation of weather information. Chilling measurement.(A MAF Sustainable Farming Fund extension initiative for Pipfruit and Winegrapes Weather Monitoring:March 2006 Updated May 2010) [accessed 7 January 2020]. http://www.hortinfo.co.nz/downloads_process_fs.asp?fid=weather%5C%5CFS3-7ChillingMeasurement.pdf

Ish-Am G, Eisikowitch D 1991. New insight into avocado flowering in relation to its pollination. California Avocado Society Yearbook 75: 125-137.

Jackson D, Lombard P 1993. Environmental and management practices affecting grape composition and wine quality-a review. Am J Enol Vitic 44(4): 409-430.

Jangra M 2012 Heat unit utilization of new apple cultivar under high density plantation in Kullu valley of Himachal Pradesh. Crop Improv 39: 157-161.

Jiang Y, Zeng Q, Wei J, Jiang J, Li Y, Chen J, Yu H 2019. Growth, fruit yield, photosynthetic characteristics, and leaf microelement concentration of two blueberry cultivars under different long-term soil pH treatments. Agron 9(7): 357.

Jones G 2015. Climate, grapes, and wine: Terroir and the importance of climate to winegrape production. GuildSomm Organization [accessed 18 December 2019]. https://www.guildsomm.com/public_content/features/articles/b/gregory_jones/posts/climate-grapes-and-wine

Jones R 2016. Future scenarios for plant virus pathogens as climate change progresses. Adv Virus Res 95: 87-147.

Juroszek P, von Tiedemann A 2015. Linking plant disease models to climate change scenarios to project future risks of crop diseases: A review. Journal of Plant Diseases and Protection 122(1): 3-15 doi:10.1007/bf03356525.

Kadam V, Shukla M, Ubale A 2014. Prevention of downey mildew disease in grape field. International Journal of Advances in Engineering & Technology 7(1): 200.

Kappel F 2010. Sweet cherry cultivars vary in their susceptibility to spring frosts. HortSci 45(1): 176-177 doi:10.21273/hortsci.45.1.176.

Kaufmann H, Blanke M 2019. Substitution of winter chilling by spring forcing for flowering using sweet cherry as model crop. Sci Hortic 244: 75-81 doi:10.1016/j.scienta.2018.09.021.

Kenny G 2001. Climate change: Likely impacts on New Zealand agriculture. Wellington, New Zealand.

Kerr S, Anastasiadis S, Olssen A, Power W, Timar L, Zhang W 2012. Spatial and temporal responses to an emissions trading scheme covering agriculture and forestry: Simulation results from New Zealand. Forests 3(4): 1133-1156.

Kerr S, Olssen A 2012. Gradual land-use change in New Zealand: Results from a dynamic econometric model. Wellington: Motu Economic and Public Policy Research.

Kidd D, Webb M, Malone B, Minasny B, McBratney A 2015. Digital soil assessment of agricultural suitability, versatility and capital in Tasmania, Australia. Geoderma Regional 6: 7-21.

Kim K, Beresford R, Henshall W 2007. Prediction of disease risk using sitespecific estimates of weather variables. N Z Plant Prot 60: 128-132.

Kliewer W 1977. Effect of high temperatures during the bloom-set period on fruit-set, ovule fertility, and berry growth of several grape cultivars. Am J Enol Vitic 28(4): 215-222.

Knoche M, Peschel S 2006. Water on the surface aggravates microscopic cracking of the sweet cherry fruit cuticle. J Am Soc Hort Sci 131(2): 192-200.

Koumanov KS 2015. On the mechanisms of the sweet cherry (Prunus avium L.) fruit cracking: Swelling or shrinking? Sci Hortic 184: 169-170.

Lang GA 1993. Southern Highbush blueberries: Physiological and cultural factors important for optimal cropping of these complex hybrids. V International Symposium on Vaccinium Culture 346. p. 72-80.

Lanyon DM, Hansen D, Cass A 2004. The effect of soil properties on vine performance: CSIRO Land and Water Black Mountain.

Latorre B, Wilcox W, Bañados M 2015. Crown and root rots of table grapes caused by Phytophthora spp. in Chile. Vitis - Journal of Grapevine Research 36(4): 195.

Lin W, Pliszka K 2003. Comparison of spring frost tolerance among different Highbush blueberry (*Vaccinium corymbosum* L.) cultivars 10.17660/ActaHortic.2003.626.45. International Society for Horticultural Science (ISHS), Leuven, Belgium. p. 329-333.

Londo JP, Johnson LM 2014. Variation in the chilling requirement and budburst rate of wild Vitis species. Environ Exp Bot 106: 138-147.

Long LE, Kaiser C 2013. Sweet cherry orchard establishment in the Pacific Northwest Oregon State University, University of Idaho, Washington State University.

Luedeling E 2012. Climate change impacts on winter chill for temperate fruit and nut production: a review. Sci Hortic 144: 218-229.

Lynn I, Manderson A, Page M, Harmsworth G, Eyles G, Douglas G, MacKay A, Newsome P 2009. Land use capability survey handbook – a New Zealand handbook for the classification of land: AgResearch Ltd; Landcare Research Ltd; Institute of Geological and Nuclear Sciences Ltd.

Lyrene PM, Sherman WB 2000. 'Star' southern Highbush blueberry. HortSci 35(5): 956-957.

Mainland CM 2002. Blueberry fruit set and intervals from blossoming to ripening 10.17660/ActaHortic.2002.574.28. International Society for Horticultural Science (ISHS), Leuven, Belgium. p. 189-192.

Malo SE, Orth PG, Brooks N 1977. Effects of the 1977 freeze on avocados and limes in South Florida. Proc Fla State Hort Soc, vol 90. p. 247-251.

Manning M, Lawrence J, King DN, Chapman R 2015. Dealing with changing risks: a New Zealand perspective on climate change adaptation. Regional Environmental Change 15(4): 581-594.

Maraun D 2016. Bias correcting climate change simulations-a critical review. Current Climate Change Reports 2(4): 211-220.

Maraun D, Shepherd TG, Widmann M, Zappa G, Walton D, Gutiérrez JM, Hagemann S, Richter I, Soares PMM, Hall A et al. 2017. Towards process-informed bias correction of climate change simulations. Nature Climate Change 7(11): 764-773 doi:10.1038/nclimate3418.

Masabni J 2007. Blueberry production. Princeton, Kentucky: University of Kentucky Research and Education Center.

Mason EG, Salekin S, Morgenroth JA 2017. Comparison between meteorological data from the New Zealand National Institute of Water and Atmospheric Research (NIWA) and data from independent meteorological stations. N Z J Fr Sci 47(1): 7.

Matzneller P, Götz KP, Chmielewski FM 2016. Spring frost vulnerability of sweet cherries under controlled conditions. Int J Biometeorol 60(1): 123-130 doi:10.1007/s00484-015-1010-1.

McCarthy A 2001. Avocado culture in Western Australia. Bunbury, Western Australia: Department of Primary Industries and Regional Development.

McIntyre G, Lider L, Ferrari N 1982. The chronological classification of grapevine phenology. Am J Enol Vitic 33(2): 80-85.

Measham PF 2011. Rain-induced fruit cracking in sweet cherry (Prunus avium L.), University of Tasmania.

Measham PF, Darbyshire R, Turpin SR, Murphy-White S 2017. Complexity in chill calculations: A case study in cherries. Sci Hortic 216: 134-140 doi:10.1016/j.scienta.2017.01.006.

Ministry for the Environment 2018. Climate change projections for New Zealand: Atmosphere projections based on simulations from the IPCC Fifth Assessment, 2nd edition. Wellington: Ministry for the Environment.

Miranda C, Urretavizcaya I, Zaragüeta M, Santesteban LG, Royo JB 2012. Phenological modeling of peach and sweet cherry: start dates and threshold temperatures for each phenophase 10.17660/ActaHortic.2012.940.19. International Society for Horticultural Science (ISHS), Leuven, Belgium. p. 155-161.

Mohamed AK, El-Sese AM 2009. Chilling and heat requirements of some grape cultivars (Vitis vinifera L). International Journal of Applied Agricultural Research 4(3): 193-202.

Mundy D, Manning M 2010. Ecology and management of grapevine trunk diseases in New Zealand a review. N Z Plant Prot 63: 160-166.

Murray M 2009. Critical temperatures for frost damage on fruit trees.

Neethling E, Barbeau G, Bonnefoy C, Quénol H 2012. Change in climate and berry composition for grapevine varieties cultivated in the Loire Valley. Clim Res 53(2): 89-101.

NeSmith DS, Krewer G, Lindstrom OM 1999. Fruit set of rabbiteye blueberry (Vaccinium ashei) after subfreezing temperatures. J Am Soc Hort Sci 124(4): 337-340.

NeSmith DS 2006. Fruit development period of several Rabbiteye blueberry cultivars 10.17660/ActaHortic.2006.715.19. International Society for Horticultural Science (ISHS), Leuven, Belgium. p. 137-142.

NeSmith DS 2012. Fruit development period of several Southern Highbush blueberry cultivars. International Journal of Fruit Science 12(1-3): 249-255.

Nevin JM, Lovatt CJ 1989. Changes in starch and ammonia metabolism during low temperature stress-induced flowering in ‘Hass’ avocado-a preliminary report. S African Avocado Grower’s Assn Yrbk 12: 21-25.

Oliver DP, Kookana RS, Anderson JS, Cox JW, Waller N, Smith LH 2012. Off-site transport of pesticides in dissolved and particulate forms from two land uses in the Mt. Lofty Ranges, South Australia. Agric Wat Manag 106: 78-85.

Orwin KH, Stevenson BA, Smaill SJ, Kirschbaum MU, Dickie IA, Clothier BE, Garrett LG, Van der Weerden TJ, Beare MH, Curtin D 2015. Effects of climate change on the delivery of soil-mediated ecosystems services within the primary sector in temperate ecosystems: a review and New Zealand case study. Global Change Biol 21(8): 2844-2860.

Palasciano M, Gaeta L 2017. Comparison of different models for chilling requirements evaluation of sweet cherry cultivars in a Mediterranean area. Acta Hort 1161: 405-410 doi:10.17660/ActaHortic.2017.1161.65.

Parker AK 2012. Modelling phenology and maturation of the grapevine Vitis vinifera L.: varietal differences and the role of leaf area to fruit weight ratio manipulations, Lincoln University.

Parliamentary Commissioner for the Environment 2019. Farms, forests and fossil fuels: The next great landscape transformation?

Patten K, Neuendorff E, Nimr G, Clark JR, Fernandez G 1991. Cold injury of southern blueberries as a function of germplasm and season of flower bud development. 26(1): 18 doi:10.21273/hortsci.26.1.18.

Pearce P 2017. Northland climate change projections and impacts NIWA Client Report for Northland Regional Council, 2017027AK.

Pérez-Jiménez M, Hernández-Munuera M, Piñero MC, López-Ortega G, del Amor FM 2017. CO_2 effects on the waterlogging response of ‘Gisela 5’and ‘Gisela 6’(Prunus cerasus x Prunus canescens) sweet cherry (Prunus avium) rootstocks. J Plant Physiol 213: 178-187.

Pérez-Jiménez RM 2008. Significant avocado diseases caused by fungi and oomycetes. Eur J Plant Sci Biotechnol 2(1): 1-24.

Pérez-Jiménez M, Hernández-Munuera M, Piñero Zapata MC, López-Ortega G, del Amor FM 2017. Two minuses can make a plus: waterlogging and elevated CO_2 interactions in sweet cherry (Prunus avium) cultivars. Physiol Plant 161(2): 257-272.

Pérez-Jiménez R 2006. A review of the biology and pathogenicity of Rosellinia necatrix–the cause of white root rot disease of fruit trees and other plants. J Phytopathol 154(5): 257-266.

Poling EB 2008. Spring cold injury to winegrapes and protection strategies and methods. HortSci 43(6): 1652-1662.

Productivity Commission 2018. Low-emissions economy: Final report. New Zealand.

Pyke NB, Stanley CJ, Warrington IJ 1986. Kiwifruit: Frost tolerance of plants in controlled frost conditions. N Z J Exp Agric 14(4): 443-447 doi:10.1080/03015521.1986.10423063.

Rai R, Joshi S, Roy S, Singh O, Samir M, Chandra A 2015. Implications of changing climate on productivity of temperate fruit crops with special reference to apple. J Horticulture 2: 135. doi:10.4172/2376-0354.1000135.

Rejman A 1977. Frost damage on Highbush blueberries in central poland during the years 1971–1975 10.17660/ActaHortic.1977.61.20. International Society for Horticultural Science (ISHS), Leuven, Belgium. p. 163-174.

Rowland J, Maschmedt D, Liddicoat C 2016. Land use potential for agricultural crops in southern South Australia: Summary of assessment and mapping methodology.(Department of Environment, Water and Natural Resources Technical Note 2016/29) [accessed 29 May 2019]. https://data.environment.sa.gov.au/Content/Publications/LandUsePotential_Descriptions_MappingAndSpatialData.pdf

Rowland LJ, Ogden EL, Takeda F, Glenn DM, Ehlenfeldt MK, Vinyard BT 2013. Variation among Highbush blueberry cultivars for frost tolerance of open flowers. 48(6): 692 doi:10.21273/hortsci.48.6.692.

Salinger MJ, Kenny GJ, Morley-Bunker MJ 1993. Climate and kiwifruit cv. Hayward 1. Influences ondevelopment and growth. N Z J Crop Hortic Sci 21(3): 235-245 doi:10.1080/01140671.1993.9513775.

Salinger MJ, Kenny GJ 1995. Climate and kiwifruit cv. ‘Hayward’ 2. Regions in New Zealand suited for production. N Z J Crop Hortic Sci 23: 173-184.

Sammonds J, Billones R, Ridgway H, Walter M, Jaspers M 2009. Survey of blueberry farms for Botryosphaeria dieback and crown rot pathogens. N Z Plant Prot 62: 238-242.

Santé-Riveira I, Crecente-Maseda R, Miranda-Barrós D 2008. GIS-based planning support system for rural land-use allocation. Comput Electron Agric 63(2): 257-273 doi:https://doi.org/10.1016/j.compag.2008.03.007.

Santomauro A, Faretra F 2002. Fungal diseases of almond and sweet cherry in Southern Italy [Prunus amygdalus Stokes-Prunus avium Moench.-Apulia]. Informatore Fitopatologico (Italy).

Sedgley M 1977. The effect of temperature on floral behaviour, pollen tube growth and fruit set in the avocado. J Hortic Sci 52(1): 135-141.

Sedgley M, Annells C 1981. Flowering and fruit-set response to temperature in the avocado cultivar 'Hass'. Sci Hortic 14(1): 27-33.

Seif S, Gruppe W 1984. Chilling requirements of sweet cherries (Prunus avium) and interspecific cherry hybrids (Prunus x ssp.). International Workshop on Improvement of Sweet and Sour Cherry Varieties and Rootstocks 169. p. 289-294.

Selim S, Koc-San D, Selim C, San BT 2018. Site selection for avocado cultivation using GIS and multi-criteria decision analyses: Case study of Antalya, Turkey. Comput Electron Agric 154: 450-459.

Selladurai R, Awachare CM 2020. Nutrient management for avocado (Persea americana miller). J Plant Nutr 43(1): 138-147.

Silva Ad, Patterson K, Rothrock C, McNew R 1999. Phytophthora root rot of blueberry increases with frequency of flooding. HortSci 34(4): 693 doi:10.21273/hortsci.34.4.693.

Singh M, Bathia H 2012. Thermal indices in relation to crop phenology and fruit yield of apple. Mausam 63: 449-454.

Smart DR, Schwass E, Lakso A, Morano L 2006. Grapevine rooting patterns: a comprehensive analysis and a review. Am J Enol Vitic 57(1): 89-104.

Snelgar W, Hall A, McPherson H 2008. Modelling flower production of kiwifruit (*Actinidia deliciosa*) from winter chilling. N Z J Crop Hortic Sci 36(4): 273-284.

Snyder R 2017. Climate change impacts on water use in horticulture. Horticulturae 3(2): 27.

Sood A 2015. Improved bias corrected and downscaled regional climate model data for climate impact studies: validation and assessment for New Zealand. National Institute of Water and Atmospheric Research (NIWA), Wellington.

Spiers JM, Draper AD 1974. Effect of chilling on bud break in Rabbiteye blueberry. J Am Soc Hort Sci 99(5): 398-399.

Stanley CJ, Tustin DS, Lupton GB, McArtney S, Cashmore WM, Silva HND 2000. Towards understanding the role of temperature in apple fruit growth responses in three geographical regions within New Zealand. J Hortic Sci Biotec 75(4): 413-422 doi:10.1080/14620316.2000.11511261.

Tait A, Henderson R, Turner R, Zheng X 2006. Thin plate smoothing spline interpolation of daily rainfall for New Zealand using a climatological rainfall surface. International Journal of Climatology 26(14): 2097–2115.

Tait A 2008. Future projections of growing degree days and frost in New Zealand and some implications for grape growing. Weather and Climate 28: 17-36.

Tait A, Paul V, Sood A, Mowat A 2018. Potential impact of climate change on Hayward kiwifruit production viability in New Zealand. N Z J Crop Hortic Sci 46(3): 175-197.

Testolin R, Messina R 1987. Winter cold tolerance of kiwifruit. A survey after winter frost injury in Northern Italy. N Z J Exp Agric 15(4): 501-504 doi:10.1080/03015521.1987.10425604.

Teutschbein C, Seibert J 2012. Bias correction of regional climate model simulations for hydrological climate-change impact studies: Review and evaluation of different methods. J Hydrol 456-457: 12-29 doi:https://doi.org/10.1016/j.jhydrol.2012.05.052.

Teutschbein C, Seibert J 2013. Is bias correction of regional climate model (RCM) simulations possible for non-stationary conditions? Hydrol Earth Syst Sci 17(12): 5061-5077 doi:10.5194/hess-17-5061-2013.

Thomas C, Marois J, English J 1988. The effects of wind speed, temperature, and relative humidity on development of aerial mycelium and conidia of Botrytis cinerea on grape. Phytopathology 78(3): 260-265.

Thomas S, Renwick A, Teixeira E, Guo J, Ausseil A, van der Weerden A, Palmer D, Dowling L, Wakelin S, Hol tL et al. 2019. Evaluation of profitability and future potential for low emission productive uses of land that is currently used for livestock – SLMACC Project 405422 Progress report. A Plant & Food Research Ltd. report prepared for Ministry for Primary Industries. Milestone No. 74663. Contract No. 34828. SPTS No. 18281.

Ticho R, Gefen B 1965. The avocado in Israel. California Avocado Society Yearbook 49: 55-60.

Timar L 2011. Rural Land Use and Land Tenure in New Zealand. Wellington: Motu Economic and Public Policy Research.

Timar L, Kerr S 2014. Land-use intensity and greenhouse gas emissions in the LURNZ model. Wellington: Motu Economic and Public Policy Research.

Timar L 2016. Yield to change: Modelling the land-use response to climate-driven changes in pasture production. Wellington: Motu Economic and Public Policy Research.

Tomasi D 2014. Grape quality starts at the roots. I International Symposium on Grapevine Roots 1136. p. 1-10.

Trębicki P, Dáder B, Vassiliadis S, Fereres A 2017. Insect–plant–pathogen interactions as shaped by future climate: effects on biology, distribution, and implications for agriculture. Insect Sci 24(6): 975-989.

Triantafilis J, Ward WT, McBratney AB 2001. Land suitability assessment in the Namoi Valley of Australia, using a continuous model. Soil Research 39(2): 273-289 doi:https://doi.org/10.1071/SR99087.

van den Dijssel C, Hall A, Green S, Clothier B 2014. Kaitiakitanga for economic prosperity through a multi-functional landscape framework for the lands of the Makirikiri Trust Board. A Plant & Food Research report prepared for Landcare Research. Milestone No. Milestone No. 59828. SPTS No. 10576.

Van Leeuwen C, Garnier C, Agut C, Baculat B, Barbeau G, Besnard E, Bois B, Boursiquot J-M, Chuine I, Dessup T 2008. Heat requirements for grapevine varieties is essential information to adapt plant material in a changing climate. Embrapa Uva e Vinho-Resumo em anais de congresso (ALICE). In: Congrès international des terroirs viticoles, 7., 2008, Nyon, Suisse.

van Leeuwen C, Roby J-P, de Rességuier L 2018. Soil-related terroir factors: a review. OENO One 52(2): 173-188.

Velásquez AC, Castroverde CDM, He SY 2018. Plant–pathogen warfare under changing climate conditions. Curr Biol 28(10): R619-R634 doi:https://doi.org/10.1016/j.cub.2018.03.054.

Vetharaniam I, Müller K, van den Dijssel C, Stanley J 2019. Modelling the effect of climate change on land suitability for growing apple and kiwifruit. A Plant & Food Research Ltd. report prepared for Ministry for Primary Industries. Milestone No. 73683. Contract No. 34671. SPTS No. 18297.

Vetharaniam I, Müller K, Stanley J 2020a. Comparison and diagnostics of reanalysis and RCP past climate data for crop suitability mapping. A Plant & Food Research Ltd. report prepared for Ministry for Primary Industries. Milestone No. 87021-A,1. Contract No. 34671 var. Job code: P/423084/01. SPTS No. 19820.

Vetharaniam I, Müller K, Stanley J, Cummins M, van den Dijssel C 2020b. Modelling location suitability for avocado, blueberry, cherry and wine grape. A Plant & Food Research Ltd. report prepared for Ministry for Primary Industries. Milestone No. 86474. Contract No. 34671. SPTS No. 19672.

Wakelin SA, Gomez-Gallego M, Jones E, Smaill S, Lear G, Lambie S 2018. Climate change induced drought impacts on plant diseases in New Zealand. Australas Plant Pathol 47(1): 101-114.

Warrick RA, Kenny GJ, Harman JJ 2001. The effects of climate change and variation in New Zealand: An assessment using the CLIMPACTS system: The International Global Change Institute (IGCI), University of Waikato.

Webb L, Watt A, Hill T, Whiting J, Wigg F, Dunn G, Needs S, Barlow E 2009. Extreme heat: managing grapevine response. GWRDC and University of Melbourne: Melbourne.

Weet CS 1979. Frost damage to kiwi fruit vines. Avocado Grower 59: 26-29.

Wilcox W, Mircetich S 1985. Effects of flooding duration on the development of Phytophthora root and crown rots of cherry. Phytopathology 75(12): 1451-1455.

Wilks DS, Shen KW 1991. Threshold relative humidity duration forecasts for plant disease prediction. Journal of Applied Meteorology 30(4): 463-477.

Williams M, Magarey P, Sivasithamparam K 2007. Effect of temperature and light intensity on early infection behaviour of a Western Australian isolate of Plasmopara viticola, the downy mildew pathogen of grapevine. Australas Plant Pathol 36(4): 325-331.

Williamson J, Lyrene P, Olmstead JW 1997. Blueberry gardener's guide. University of Florida Cooperative Extension Service.

Winkler A, Peschel S, Kohrs K, Knoche M 2016. Rain cracking in sweet cherries is not due to excess water uptake but to localized skin phenomena. J Am Soc Hort Sci 141(6): 653-660.

Winkler A 2017. Rain cracking mechanisms in sweet cherry fruit: drivers and pathways of water uptake, Hannover: Gottfried Wilhelm Leibniz Universität Hannover.

Zapata D, Salazar M, Chaves B, Keller M, Hoogenboom G 2015. Estimation of the base temperature and growth phase duration in terms of thermal time for four grapevine cultivars. Int J Biometeorol 59(12): 1771-1781 doi:10.1007/s00484-015-0985-y.

Zapata D, Salazar-Gutierrez M, Chaves B, Keller M, Hoogenboom G 2017. Predicting key phenological stages for 17 grapevine cultivars (Vitis vinifera L.). Am J Enol Vitic 68(1): 60-72.

Zurayk R, el-Awar F, Hamadeh S, Talhouk S, Sayegh C, Chehab A-G, al Shab K 2001. Using indigenous knowledge in land use investigations: a participatory study in a semi-arid mountainous region of Lebanon. Agric Ecosyst Environ 86(3): 247-262.

Zydlik Z, Cieśliński S, Kafkas NE, Morkunas I 2019. Soil preparation, running Highbush blueberry (Vaccinium corymbosum L.) plantation and biological properties of fruits. Modern Fruit Industry: IntechOpen.

Appendix 1. Impact of adjustment of RCP data

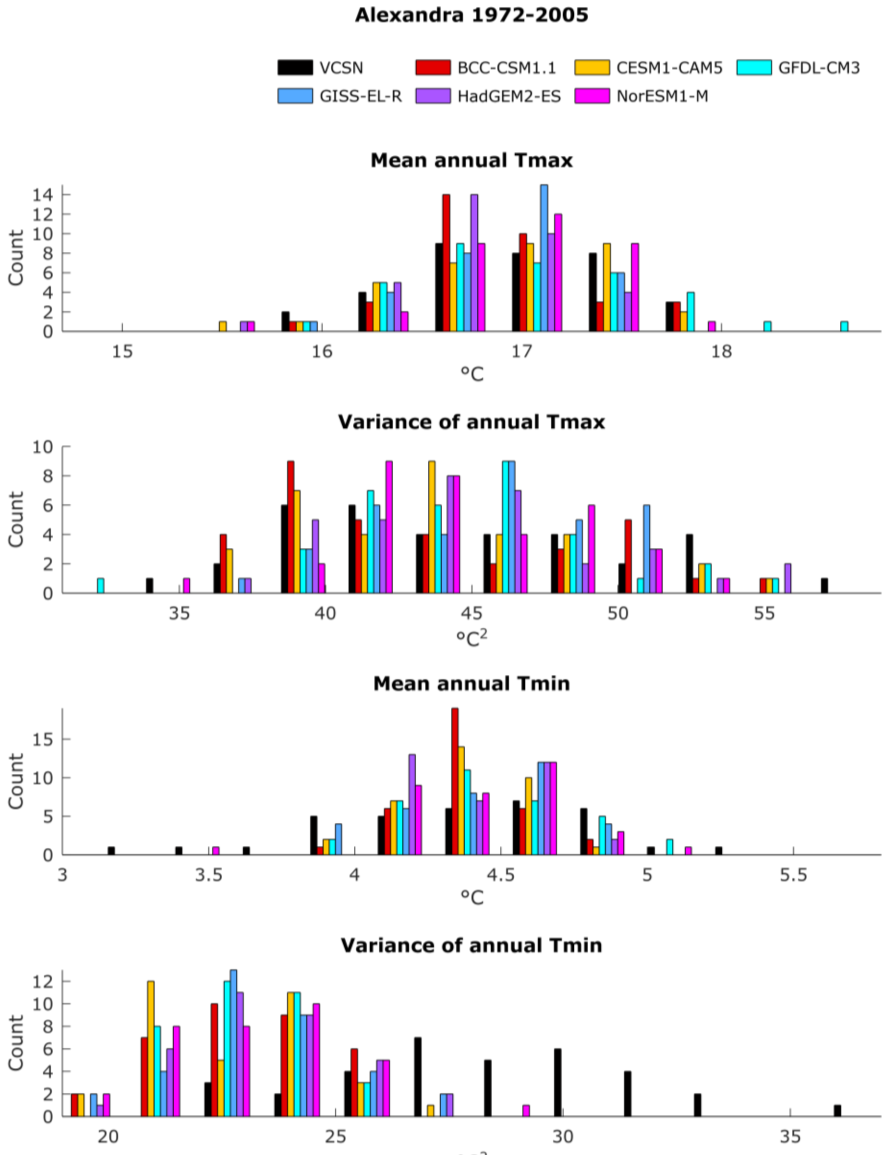

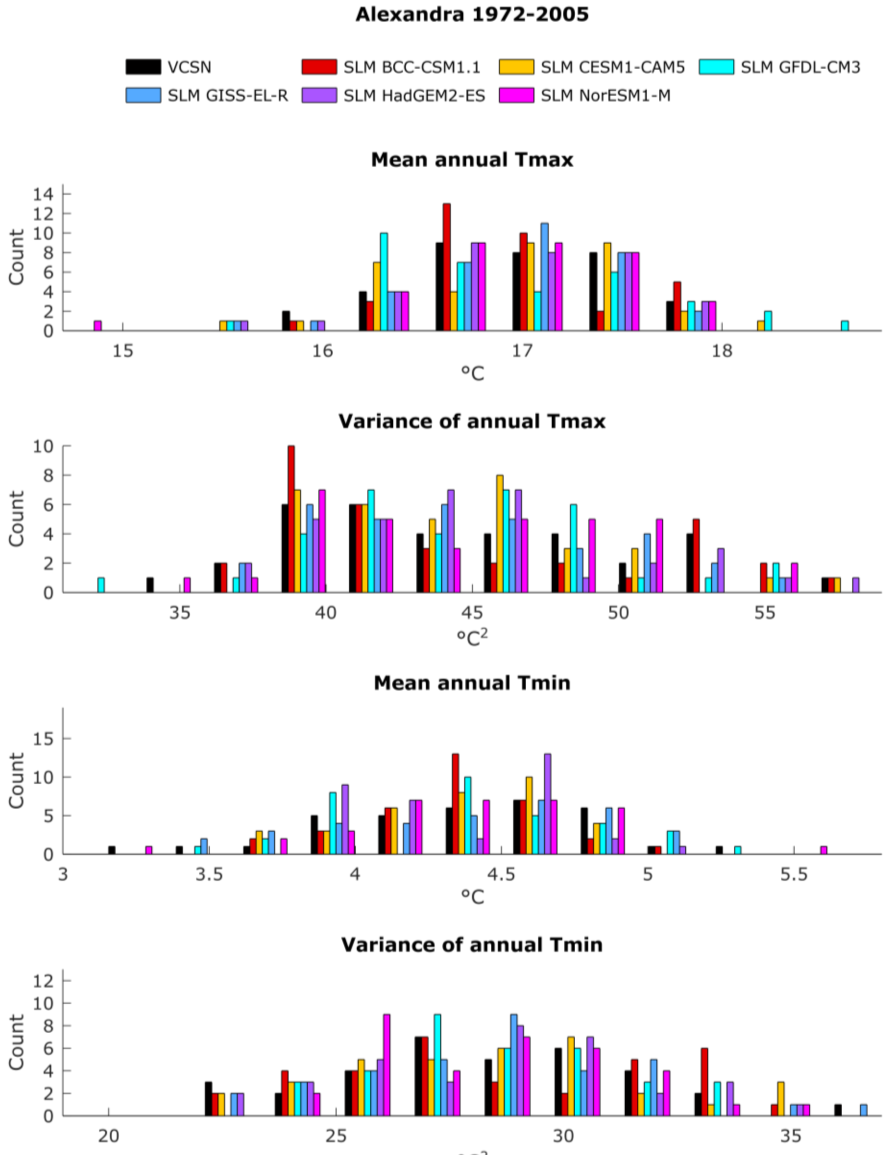

Distribution of annual means and variances annual means of maximum and minimum temperatures for Alexandra from different climate datasets. Left panel: comparison of original RCP Past and VCSN data. Right panel: comparison of SLM RCP Past and VCSN data.

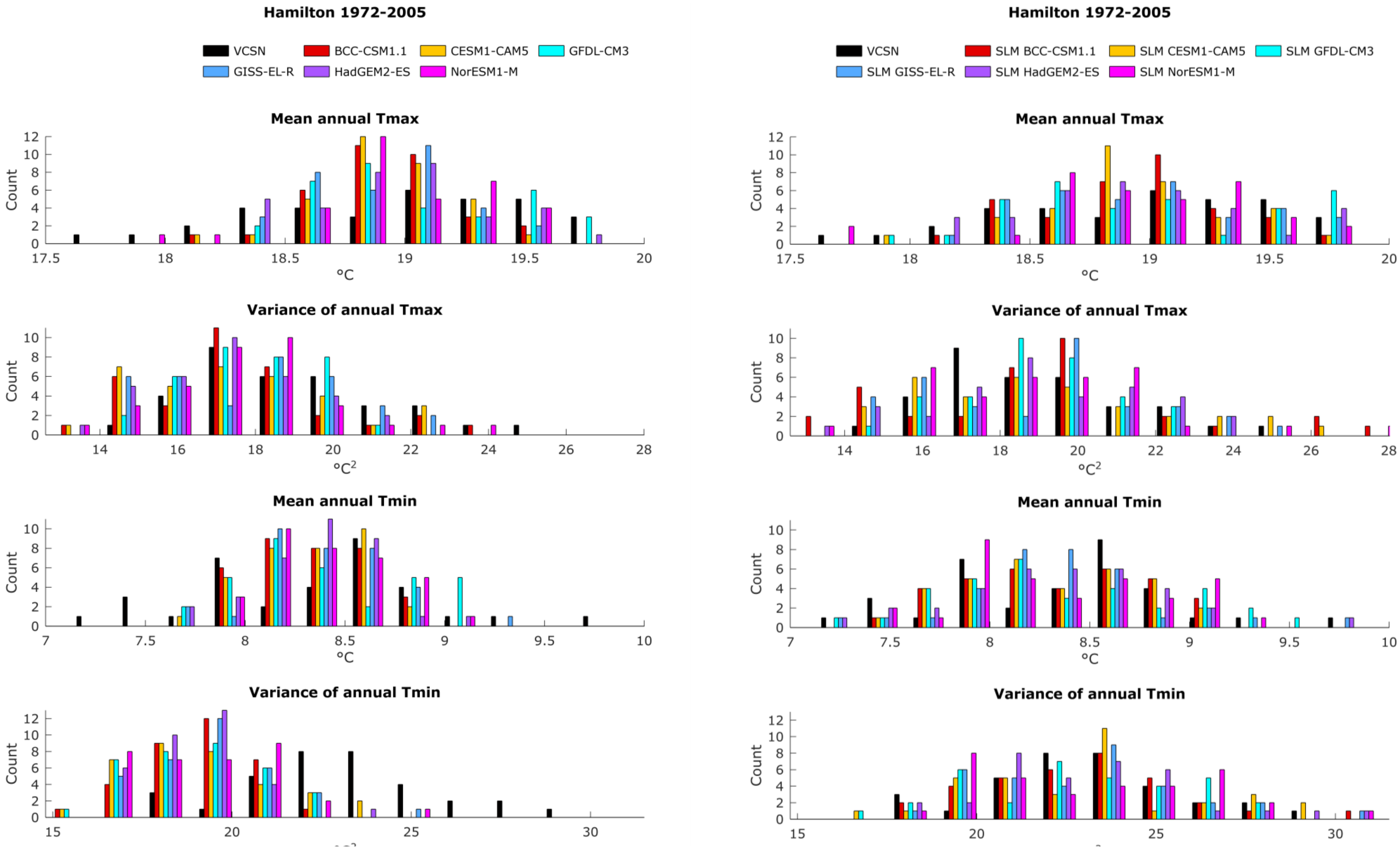

Distribution of annual means and variances annual means of maximum and minimum temperatures for Hamilton from different climate datasets. Left panel: comparison of original RCP Past and VCSN data. Right panel: comparison of SLM RCP Past and VCSN data.

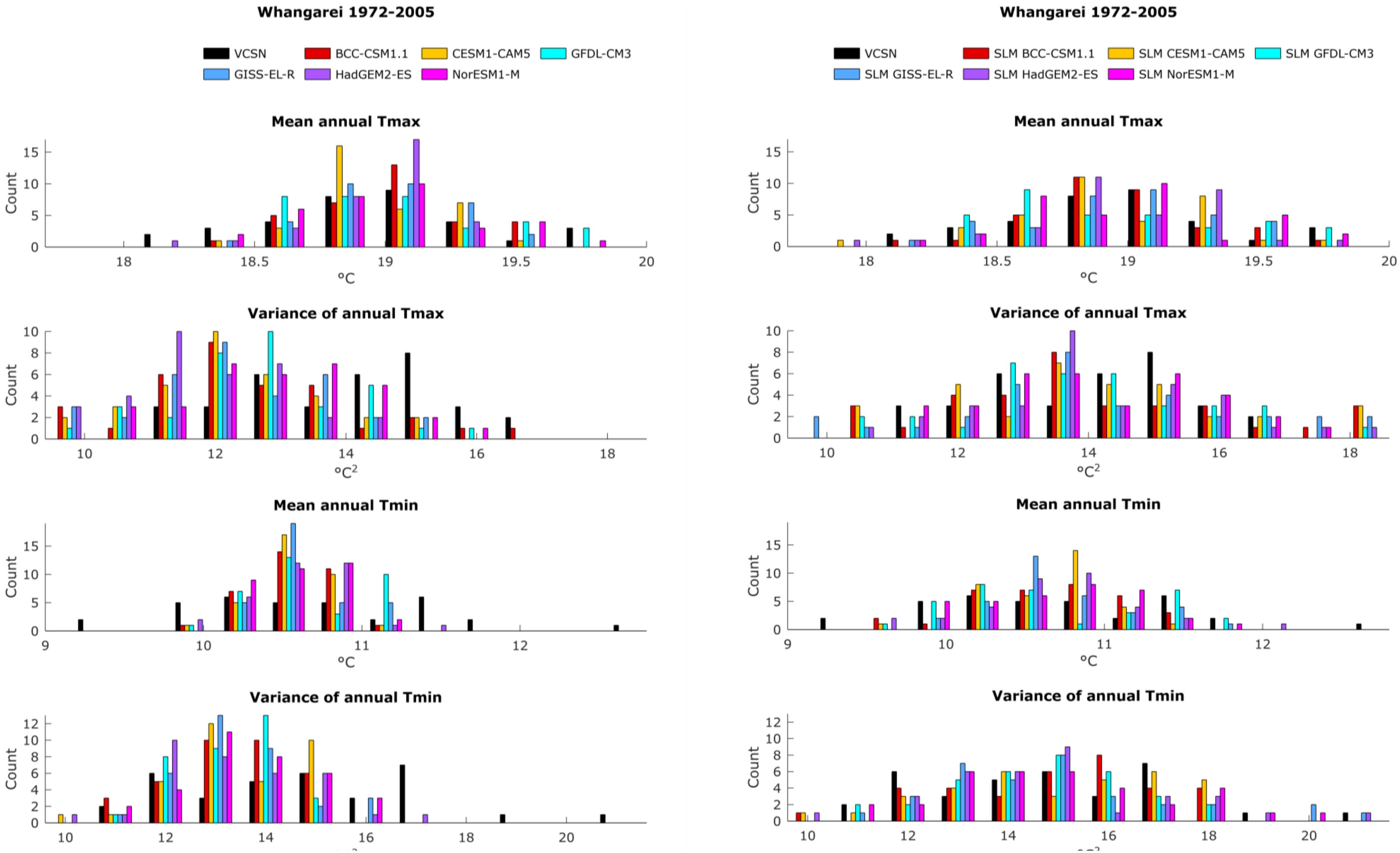

Distribution of annual means and variances annual means of maximum and minimum temperatures for Whangarei from different climate datasets. Left panel: comparison of original RCP Past and VCSN data. Right panel: comparison of SLM RCP Past and VCSN data.

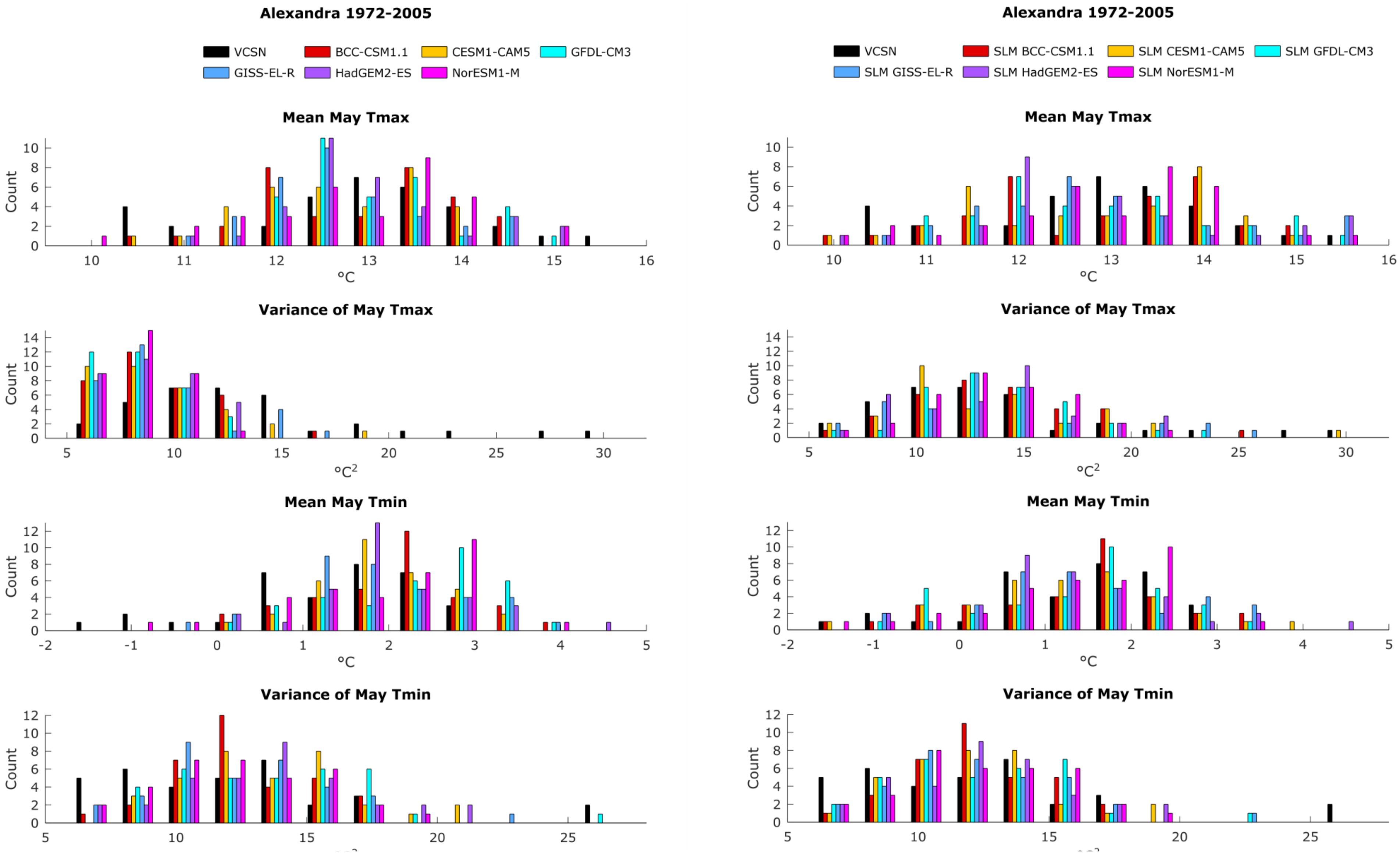

Distribution of annual means and variances of May maximum and minimum temperatures for Alexandra from different climate datasets. Left panel: comparison of original RCP Past and VCSN data. Right panel: comparison of SLM RCP Past and VCSN data.

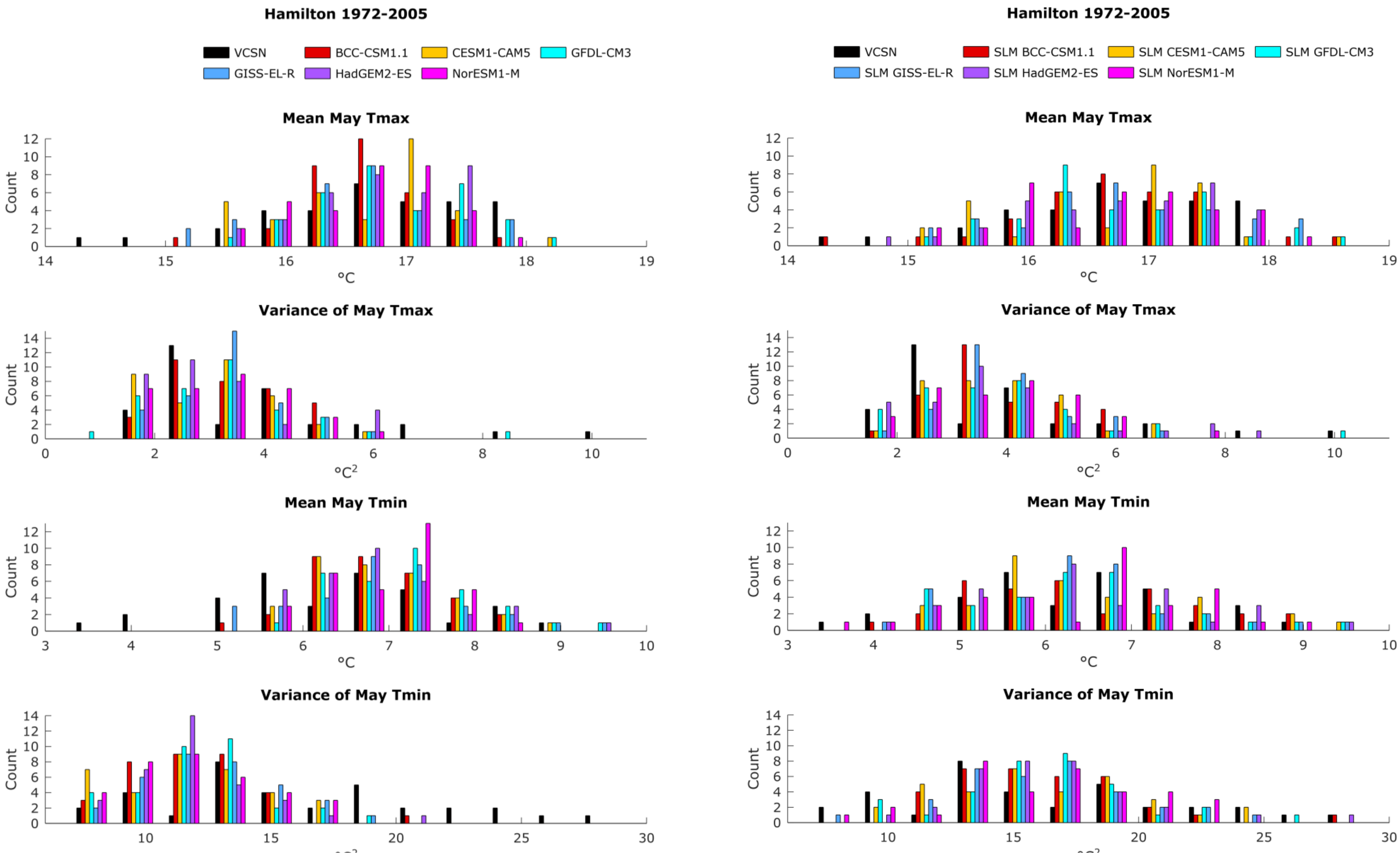

Distribution of annual means and variances of May maximum and minimum temperatures for Hamilton from different climate datasets. Left panel: comparison of original RCP Past and VCSN data. Right panel: comparison of SLM RCP Past and VCSN data.

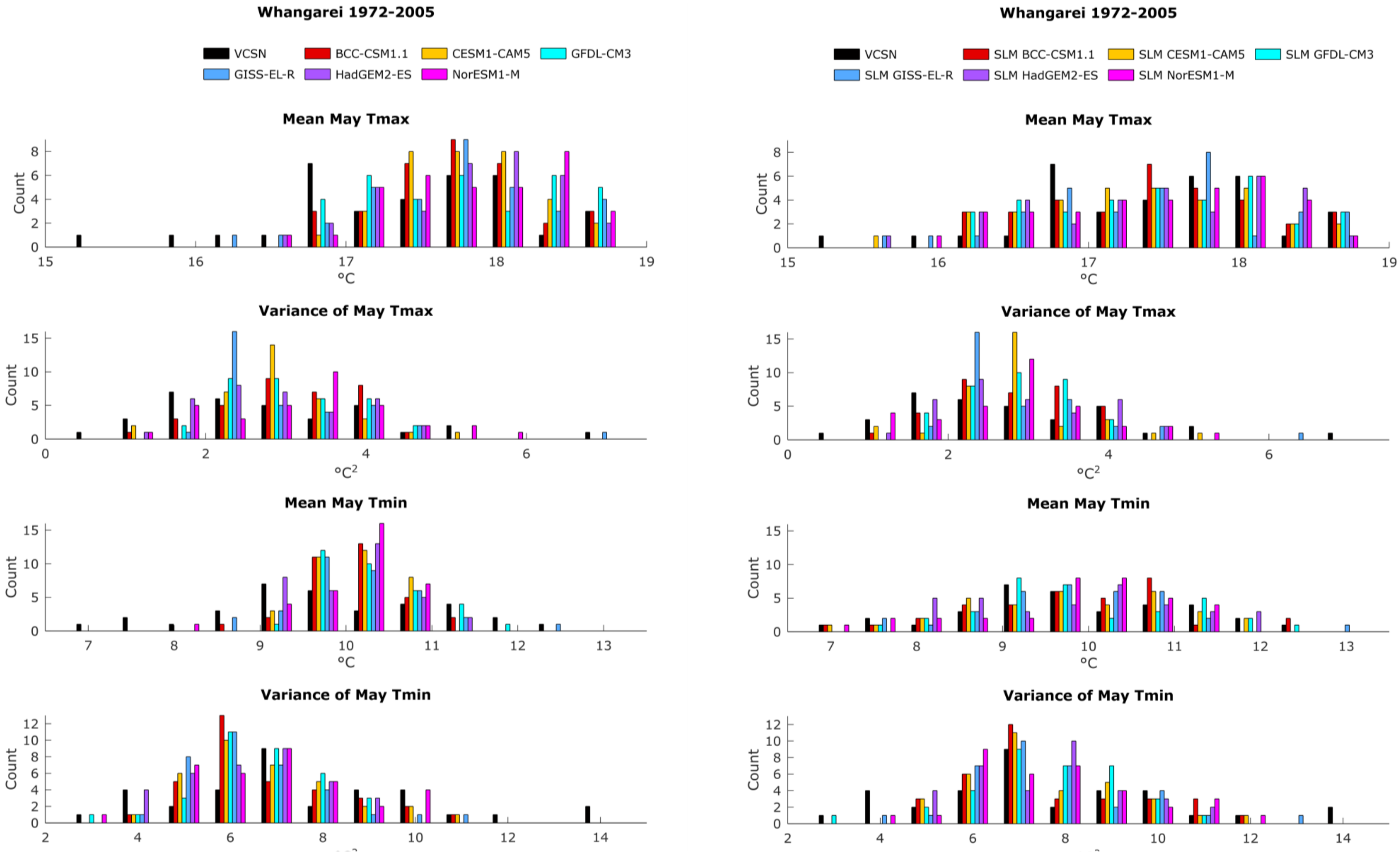

Distribution of annual means and variances of May maximum and minimum temperatures for Whangarei from different climate datasets. Left panel: comparison of original RCP Past and VCSN data. Right panel: comparison of SLM RCP Past and VCSN data.

Appendix 2. Future projections under RCP 4.5 and 6.0

Apple RCP 4.5

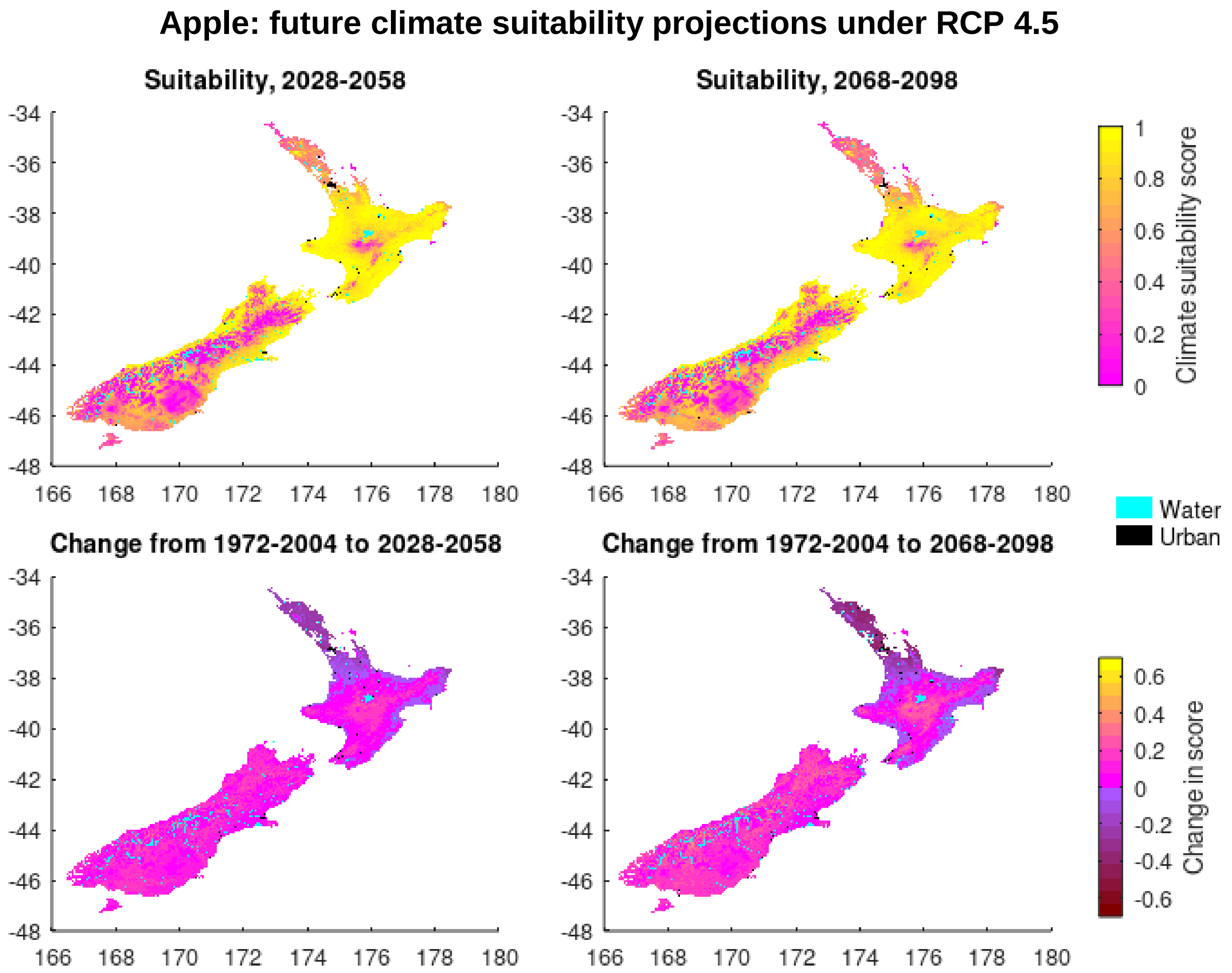

Apple: future cultivation suitability projections under RCP 4.5

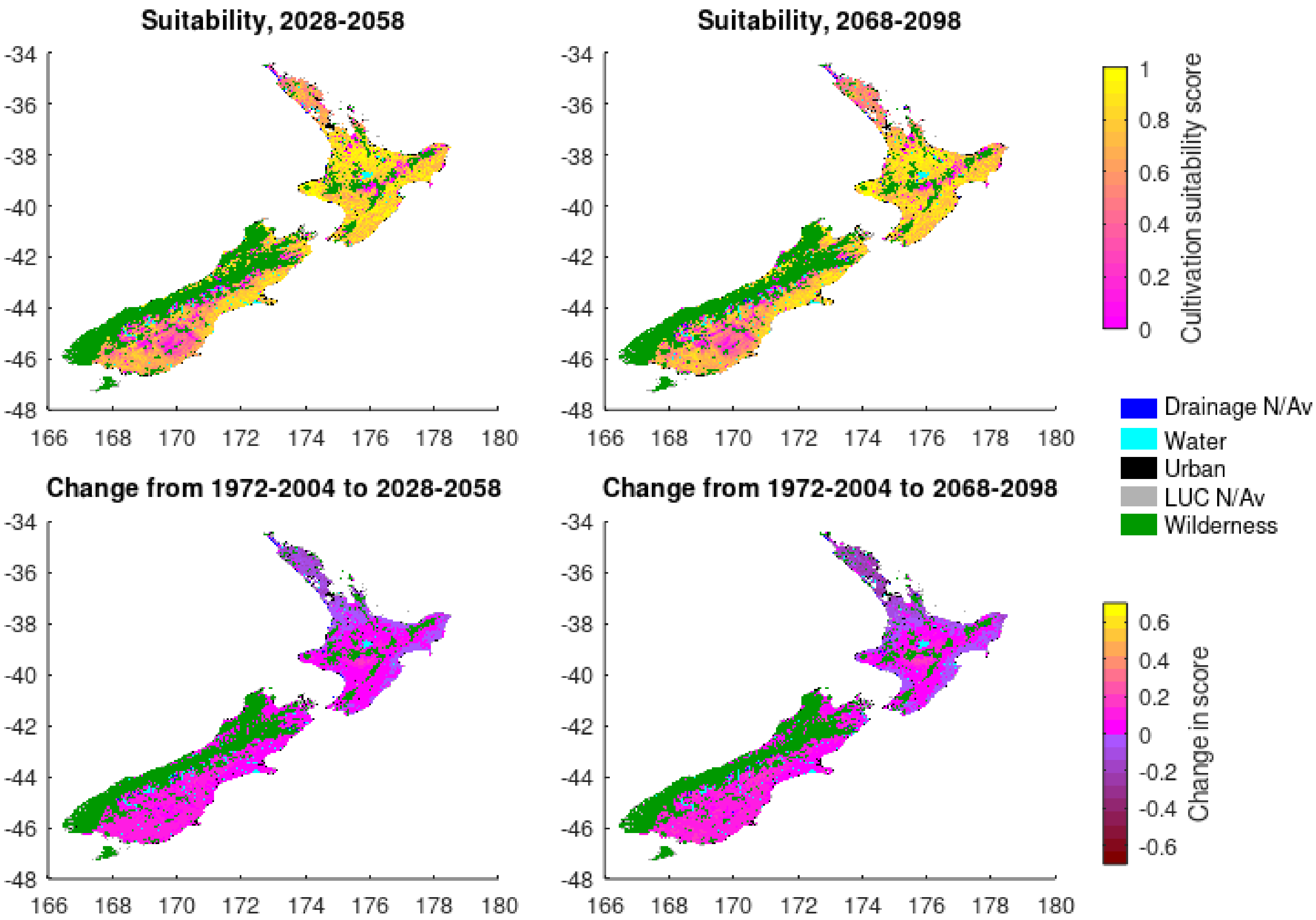

Land area in the historic period falling into different cultivation suitability ranges, projected changes for the mid- and late-century under RCP 4.5, and best and worst cases. Decreases are shaded red and increases shaded blue. Colour intensity increases with the magnitude of change.

Apple SLM RCP 4.5	Historic (km^2) 1972–2004	Area change from historic (km^2) 2028–2058			Area change from historic (km^2) 2068–2098		
Suitability range		Projected	Best case	Worst case	Projected	Best case	Worst case
0–0.1	14891	−1781	−3176	−287	−2206	−3180	−911
0.1–0.2	4286	−1265	−2269	−928	−1715	−2716	−1204
0.2–0.3	4972	−1470	−1058	−755	−1589	−1403	−954
0.3–0.4	8321	−2930	−4493	−832	−3146	−4508	−560
0.4–0.5	12457	−2314	−4849	75	−980	−4418	1581
0.5–0.6	22444	−2589	−5555	716	−1982	−4183	−465
0.6–0.7	31668	4228	886	4738	2558	179	4811
0.7–0.8	32230	970	4569	−1995	1554	2226	−985
0.8–0.9	31947	6306	7050	4246	10198	11481	6537
0.9–1.0	20509	845	8895	−4978	−2692	6522	−7850

Apple RCP 6.0

Land area in the historic period falling into different cultivation suitability ranges, projected changes for the mid- and late-century under RCP 6.0, and best and worst cases. Decreases are shaded red and increases shaded blue. Colour intensity increases with the magnitude of change.

Apple SLM RCP 6.0	Historic (km^2) 1972–2004	Area change from historic (km^2) 2028–2058			Area change from historic (km^2) 2068–2098		
Suitability range		Projected	Best case	Worst case	Projected	Best case	Worst case
0–0.1	14891	−1705	−3167	−215	−2538	−3181	−1629
0.1–0.2	4286	−1122	−2049	−987	−2144	−3070	−1937
0.2–0.3	4972	−1435	−968	−575	−2036	−2135	−712
0.3–0.4	8321	−2949	−4405	−774	−2282	−4359	689
0.4–0.5	12457	−2054	−4673	−107	56	−3460	2153
0.5–0.6	22444	−2521	−5572	1113	−3480	−3576	−3905
0.6–0.7	31668	4240	942	5250	1477	−1927	5457
0.7–0.8	32230	1244	4442	−2300	1586	1738	764
0.8–0.9	31947	5419	5855	3913	13988	14685	8715
0.9–1.0	20509	883	9595	−5318	−4627	5285	−9595

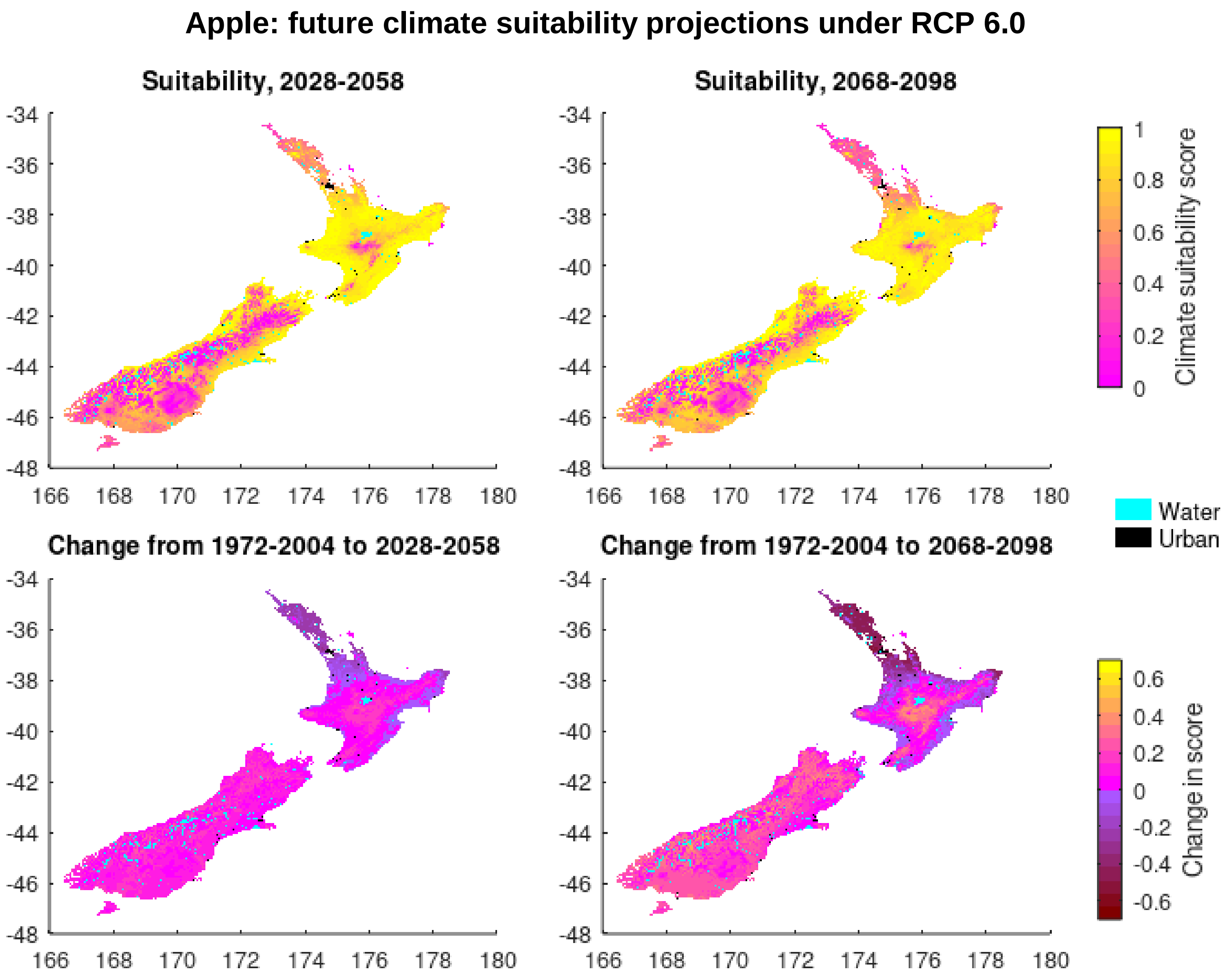
Apple: future climate suitability projections under RCP 6.0
Suitability, 2028-2058
Suitability, 2068-2098
Change from 1972-2004 to 2028-2058
Change from 1972-2004 to 2068-2098
-34
-36
-38
-40
-42
-44
-46
-48
166
168
170
172
174
176
178
180
1
0.8
0.6
0.4
0.2
0
Climate suitability score
Water
Urban
0.6
0.4
0.2
0
-0.2
-0.4
-0.6
Change in score

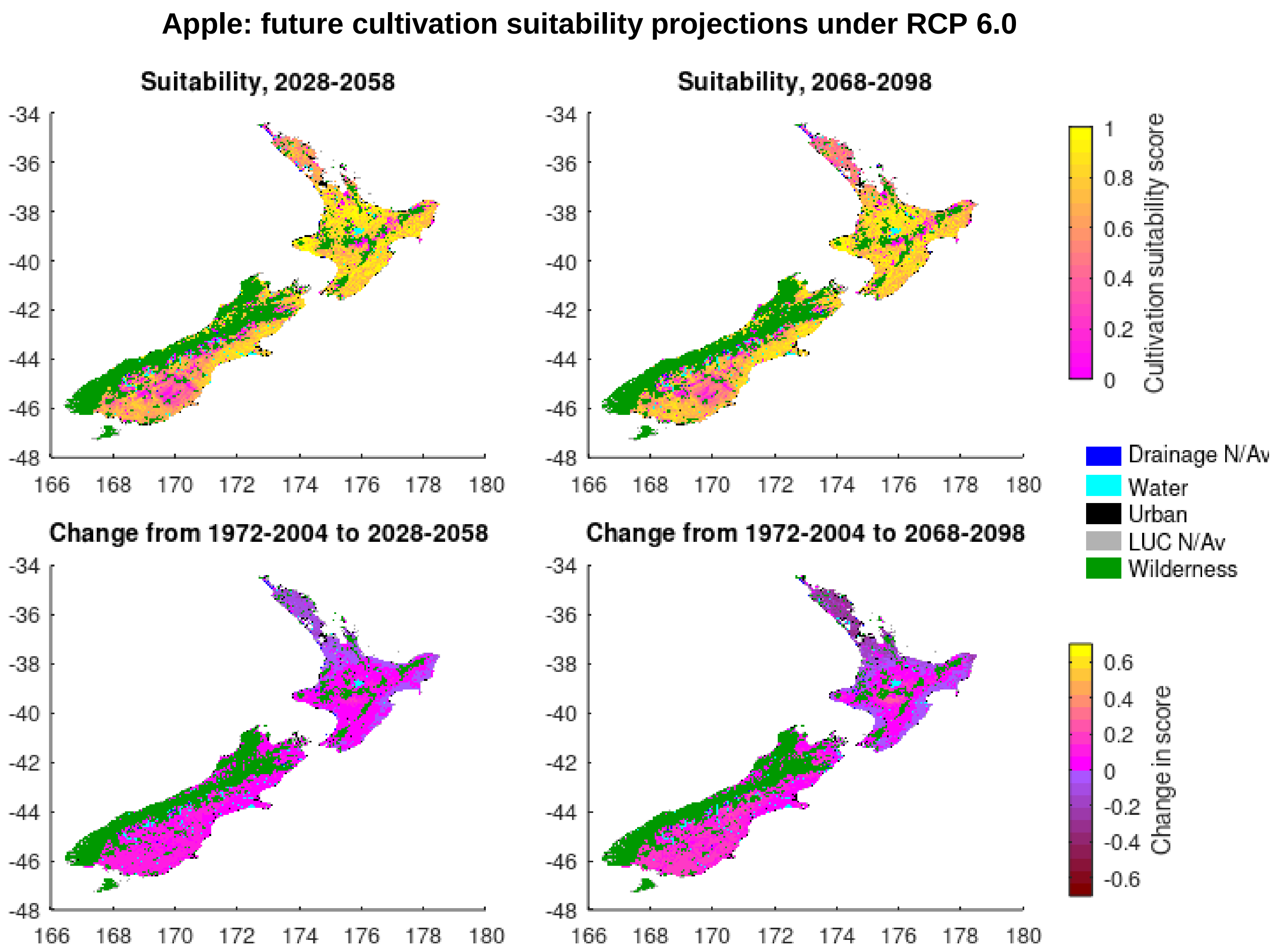
Apple: future cultivation suitability projections under RCP 6.0
Suitability, 2028-2058
Suitability, 2068-2098
Change from 1972-2004 to 2028-2058
Change from 1972-2004 to 2068-2098
-34
-36
-38
-40
-42
-44
-46
-48
166
168
170
172
174
176
178
180
1
0.8
0.6
0.4
0.2
0
Cultivation suitability score
Drainage N/Av
Water
Urban
LUC N/Av
Wilderness
0.6
0.4
0.2
0
-0.2
-0.4
-0.6
Change in score

Kiwifruit RCP 4.5

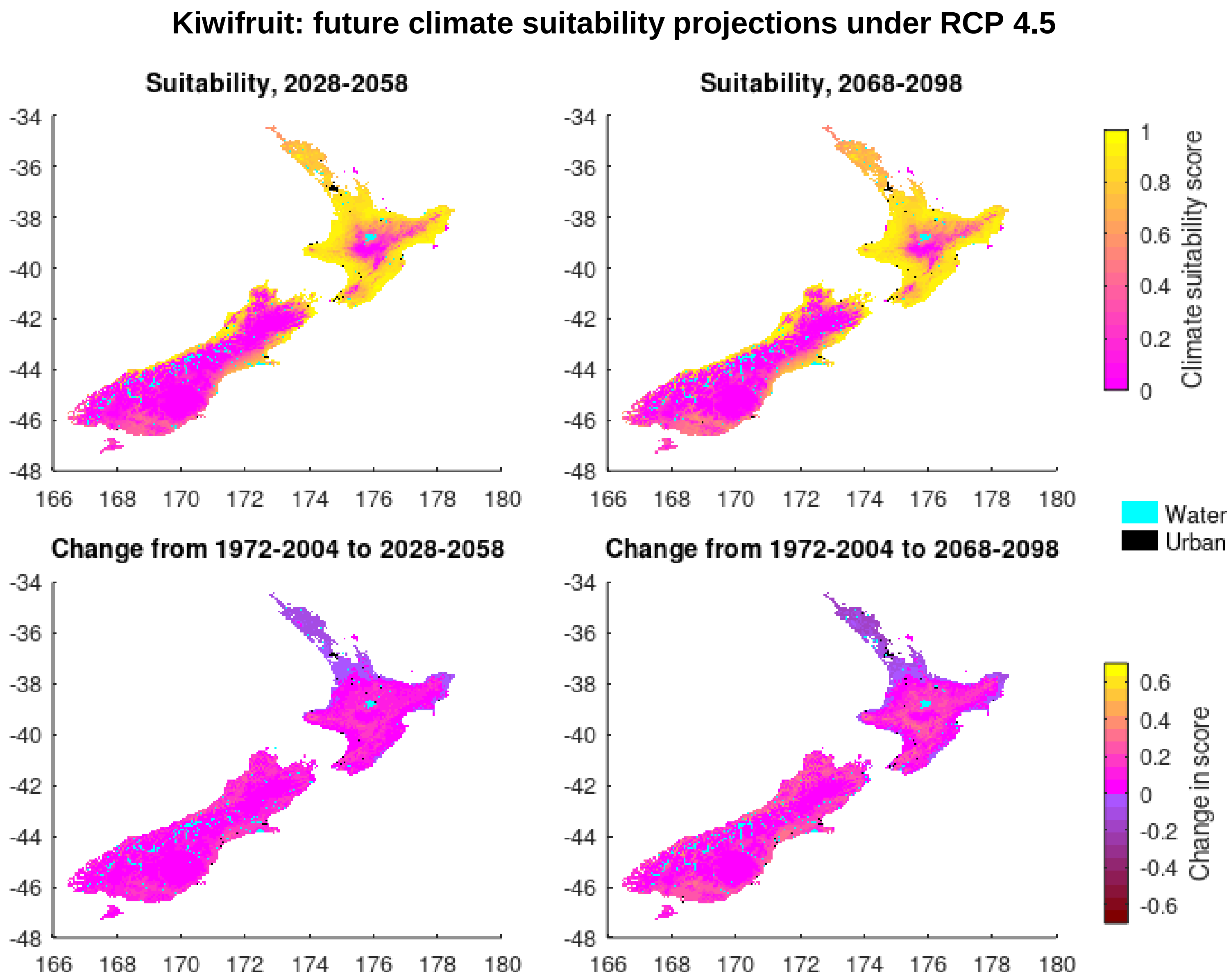

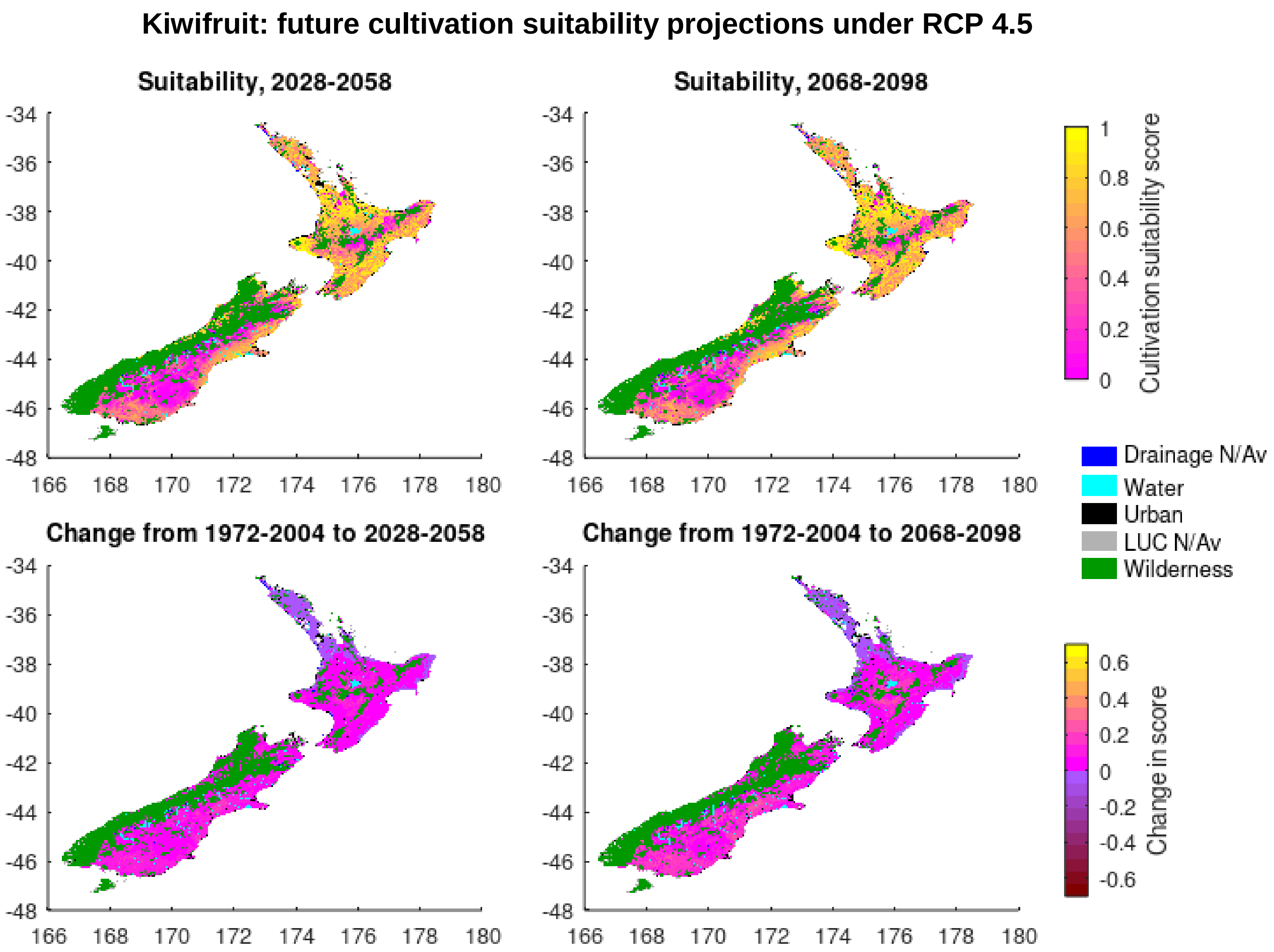
Kiwifruit: future cultivation suitability projections under RCP 4.5
Suitability, 2028-2058
Suitability, 2068-2098
Change from 1972-2004 to 2028-2058
Change from 1972-2004 to 2068-2098
-34
-36
-38
-40
-42
-44
-46
-48
166
168
170
172
174
176
178
180
Cultivation suitability score
1
0.8
0.6
0.4
0.2
0
Drainage N/Av
Water
Urban
LUC N/Av
Wilderness
Change in score
0.6
0.4
0.2
0
-0.2
-0.4
-0.6

Land area in the historic period falling into different cultivation suitability ranges, projected changes for the mid- and late-century under RCP 4.5, and best and worst cases. Decreases are shaded red and increases shaded blue. Colour intensity increases with the magnitude of change.

Kiwifruit SLM RCP 4.5	Historic (km²) 1972–2004	Area change from historic (km²) 2028–2058			Area change from historic (km²) 2068–2098		
Suitability range		Projected	Best case	Worst case	Projected	Best case	Worst case
0–0.1	37541	−7977	−13839	−2801	−11501	−15835	−6600
0.1–0.2	12757	−1941	−167	−3990	−2217	−2068	−4289
0.2–0.3	14845	−3436	−3234	−2197	−4805	−3927	−3740
0.3–0.4	16808	−2134	−3343	−1576	−3426	−4690	−2002
0.4–0.5	19596	1202	−533	3227	1032	−314	2546
0.5–0.6	21305	3428	3963	2544	4520	3729	5072
0.6–0.7	19058	5250	5669	4410	8242	7843	6001
0.7–0.8	18653	1373	3112	−320	2665	5196	1776
0.8–0.9	16787	3001	4339	1226	4220	6049	2144
0.9–1.0	6375	1234	4033	−523	1270	4017	−908

Kiwifruit RCP 6.0

Land area in the historic period falling into different cultivation suitability ranges, projected changes for the mid- and late-century under RCP 6.0, and best and worst cases. Decreases are shaded red and increases shaded blue. Colour intensity increases with the magnitude of change.

Kiwifruit SLM RCP 6.0	Historic (km²) 1972–2004	Area change from historic (km²) 2028–2058			Area change from historic (km²) 2068–2098		
Suitability range		Projected	Best case	Worst case	Projected	Best case	Worst case
0–0.1	37541	−7687	−13505	−2622	−13732	−16941	−9699
0.1–0.2	12757	−1918	3	−3996	−2985	−3664	−4342
0.2–0.3	14845	−3415	−3075	−2370	−5387	−4163	−4966
0.3–0.4	16808	−2186	−3030	−1608	−4618	−5611	−3261
0.4–0.5	19596	1284	−620	3110	847	−117	2036
0.5–0.6	21305	3434	3816	2616	4878	2659	6987
0.6–0.7	19058	5289	5692	4689	8929	8776	7086
0.7–0.8	18653	1156	2752	−467	5278	7282	3579
0.8–0.9	16787	3047	4314	1268	5617	7748	3681
0.9–1.0	6375	996	3653	−620	1173	4031	−1101

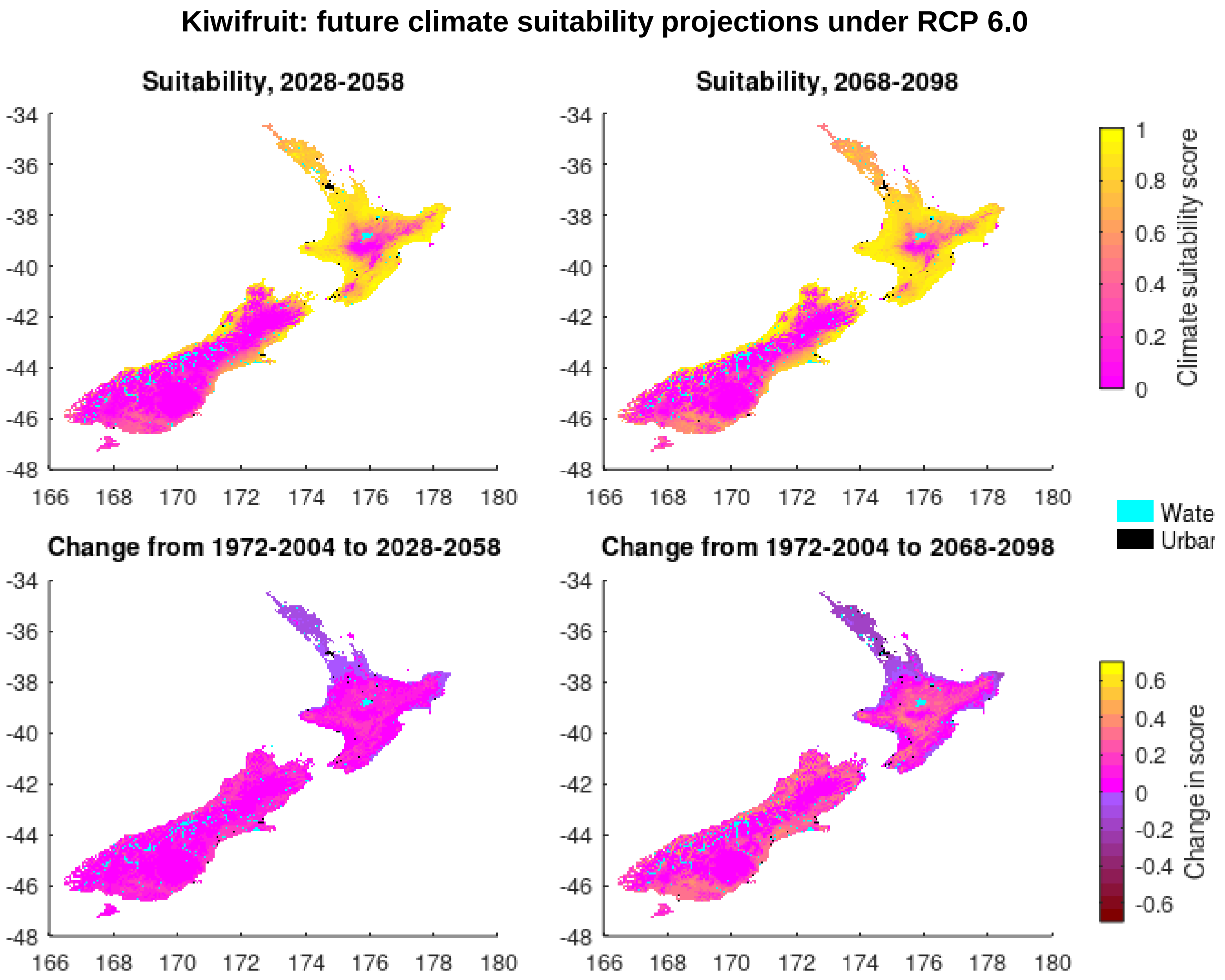
Kiwifruit: future climate suitability projections under RCP 6.0
Suitability, 2028-2058
Suitability, 2068-2098
Change from 1972-2004 to 2028-2058
Change from 1972-2004 to 2068-2098
-34
-36
-38
-40
-42
-44
-46
-48
166
168
170
172
174
176
178
180
1
0.8
0.6
0.4
0.2
0
Climate suitability score
Wate
Urbar
0.6
0.4
0.2
0
-0.2
-0.4
-0.6
Change in score

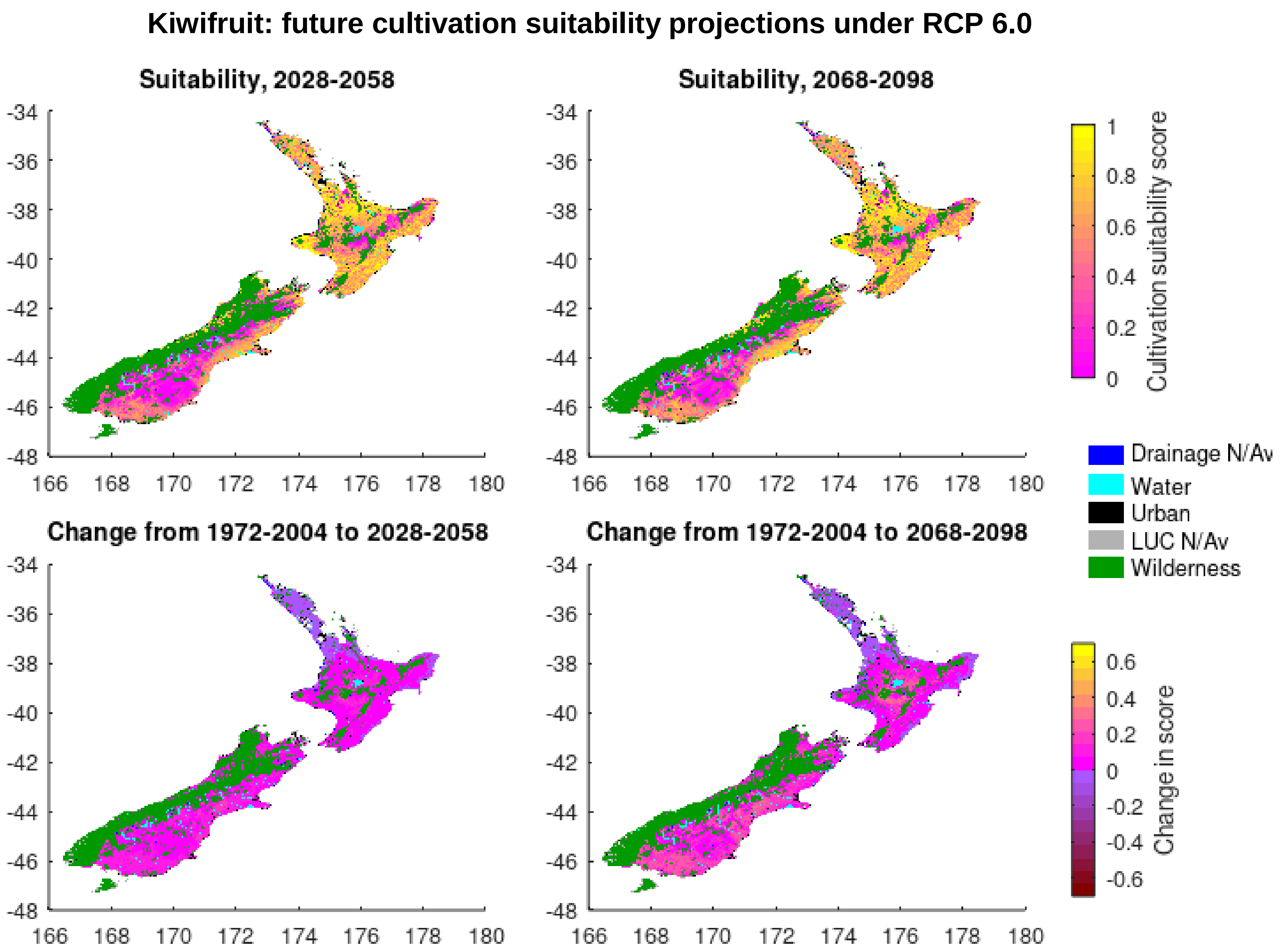
Kiwifruit: future cultivation suitability projections under RCP 6.0
Suitability, 2028-2058
Suitability, 2068-2098
Change from 1972-2004 to 2028-2058
Change from 1972-2004 to 2068-2098
-34
-36
-38
-40
-42
-44
-46
-48
166
168
170
172
174
176
178
180
Cultivation suitability score
1
0.8
0.6
0.4
0.2
0
Drainage N/Av
Water
Urban
LUC N/Av
Wilderness
Change in score
0.6
0.4
0.2
0
-0.2
-0.4
-0.6

Avocado RCP 4.5

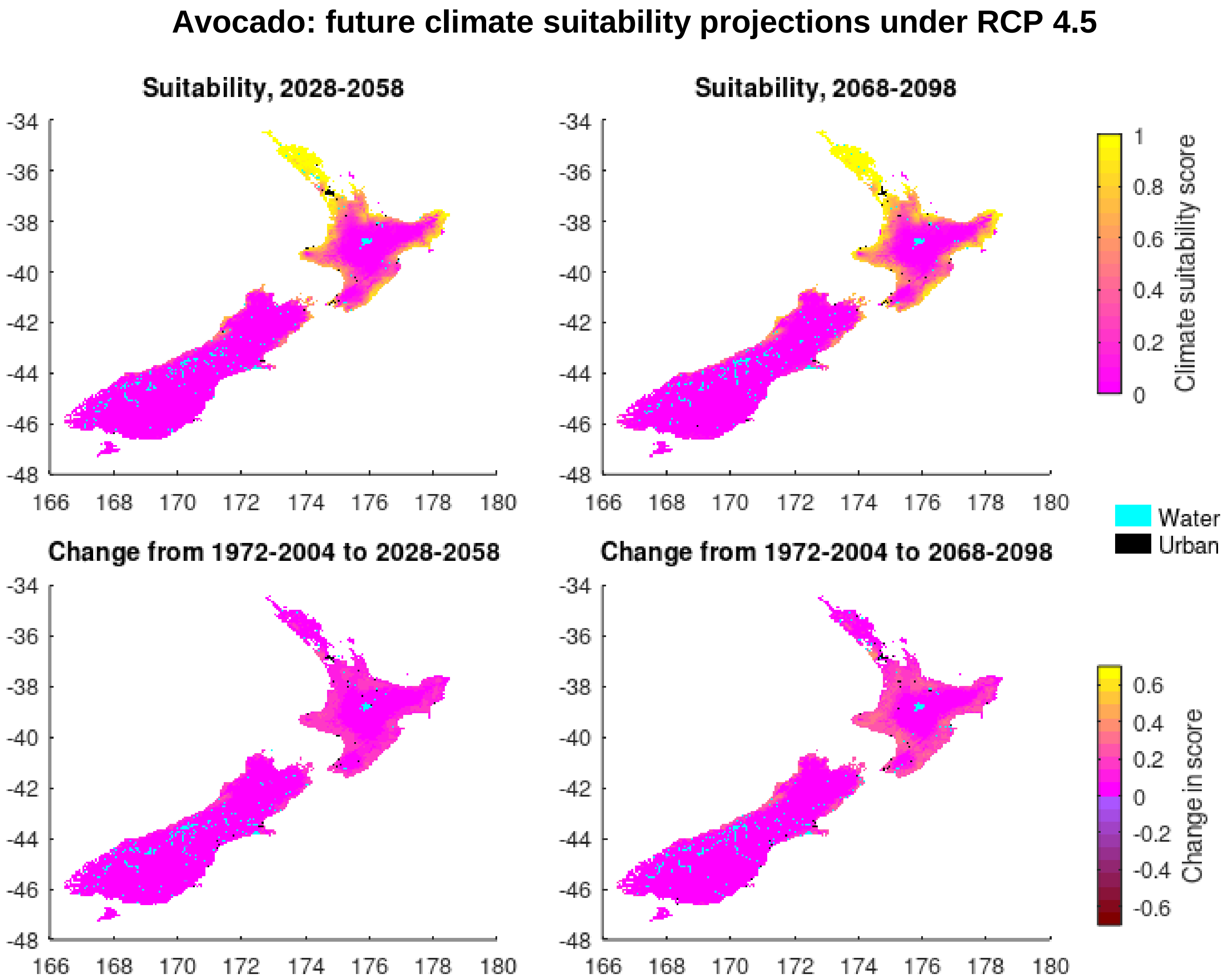

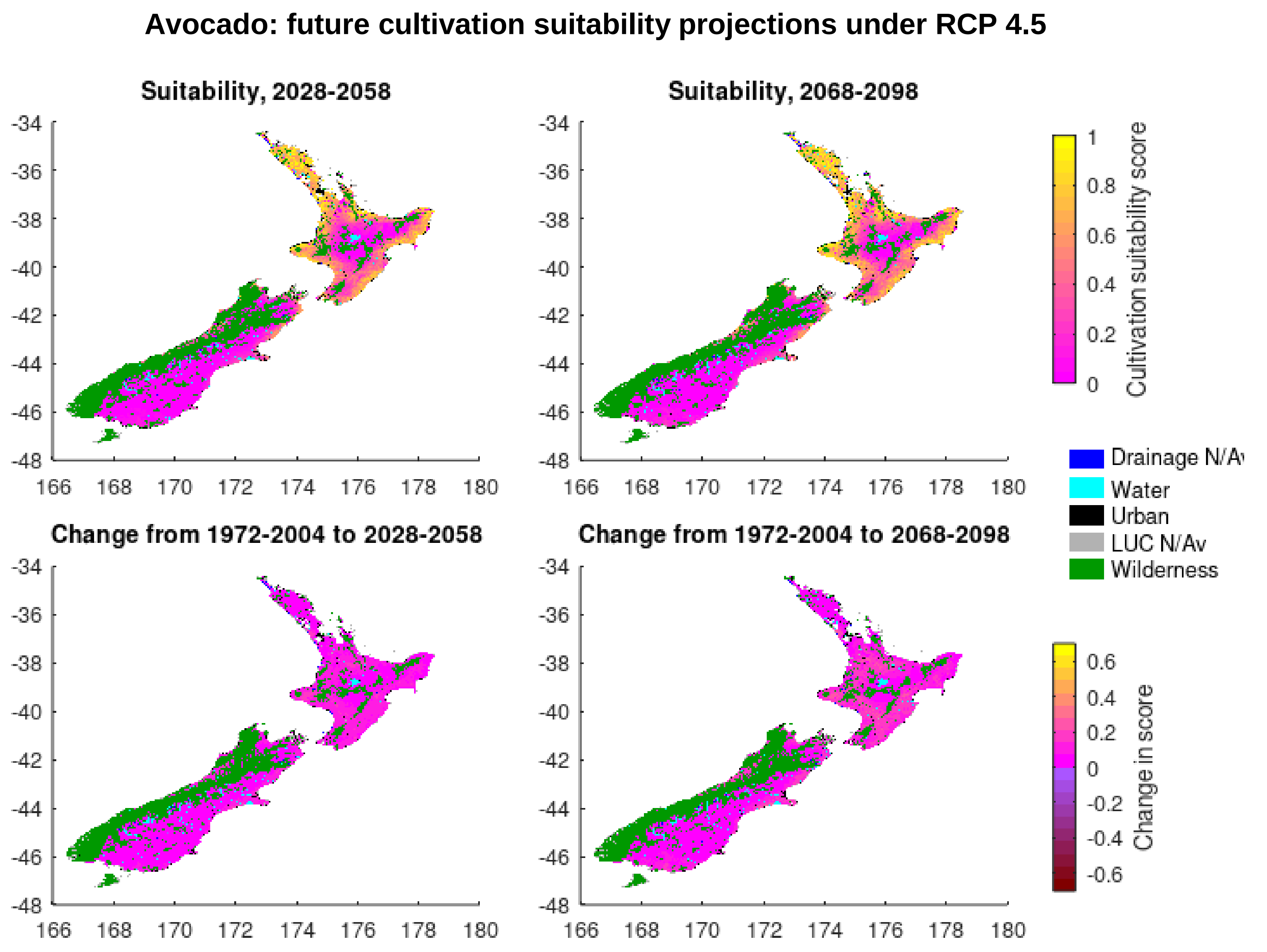

Avocado: future cultivation suitability projections under RCP 4.5
Suitability, 2028-2058
Suitability, 2068-2098
Change from 1972-2004 to 2028-2058
Change from 1972-2004 to 2068-2098
-34
-36
-38
-40
-42
-44
-46
-48
166
168
170
172
174
176
178
180
Cultivation suitability score
1
0.8
0.6
0.4
0.2
0
Drainage N/Av
Water
Urban
LUC N/Av
Wilderness
Change in score
0.6
0.4
0.2
0
-0.2
-0.4
-0.6

Land area in the historic period falling into different cultivation suitability ranges, projected changes for the mid- and late-century under RCP 4.5, and best and worst cases. Decreases are shaded red and increases shaded blue. Colour intensity increases with the magnitude of change.

Avocado SLM RCP 4.5	Historic (km^2) 1972–2004	Area change from historic (km^2) 2028–2058			Area change from historic (km^2) 2068–2098		
Suitability range		Projected	Best case	Worst case	Projected	Best case	Worst case
0–0.1	100734	−12767	−21919	−6641	−20228	−29943	−13073
0.1–0.2	13592	1313	5887	556	3071	7592	1617
0.2–0.3	12048	−812	−1590	−811	−724	−697	−1343
0.3–0.4	12659	−1055	−1202	−547	−1716	−1867	−1342
0.4–0.5	11530	1361	1202	659	1380	1078	1333
0.5–0.6	10603	2714	3567	1379	3824	4290	2490
0.6–0.7	9360	3349	5206	2016	5193	7056	3992
0.7–0.8	7953	2888	3903	1623	4297	5462	3090
0.8–0.9	4092	1835	3155	984	3153	4521	1925
0.9–1.0	1154	1174	1791	782	1750	2508	1311

Avocado RCP 6.0

Land area in the historic period falling into different cultivation suitability ranges, projected changes for the mid- and late-century under RCP 6.0, and best and worst cases. Decreases are shaded red and increases shaded blue. Colour intensity increases with the magnitude of change.

Avocado SLM RCP 6.0	Historic (km^2) 1972–2004	Area change from historic (km^2) 2028–2058			Area change from historic (km^2) 2068–2098		
Suitability range		Projection	Best case	Worst case	Projection	Best case	Worst case
0–0.1	100734	−11715	−20088	−5691	−27849	−35716	−20518
0.1–0.2	13592	1284	4989	399	4479	6959	3135
0.2–0.3	12048	−1117	−1266	−1012	68	200	−770
0.3–0.4	12659	−1120	−1704	−911	−2030	−2082	−2521
0.4–0.5	11530	1210	1406	620	824	1019	940
0.5–0.6	10603	2532	3374	1563	4255	4261	3866
0.6–0.7	9360	3164	4697	1499	6806	8261	5555
0.7–0.8	7953	2805	3861	1819	5890	7290	4601
0.8–0.9	4092	1802	2999	886	4739	6104	3429
0.9–1.0	1154	1155	1732	828	2818	3704	2283

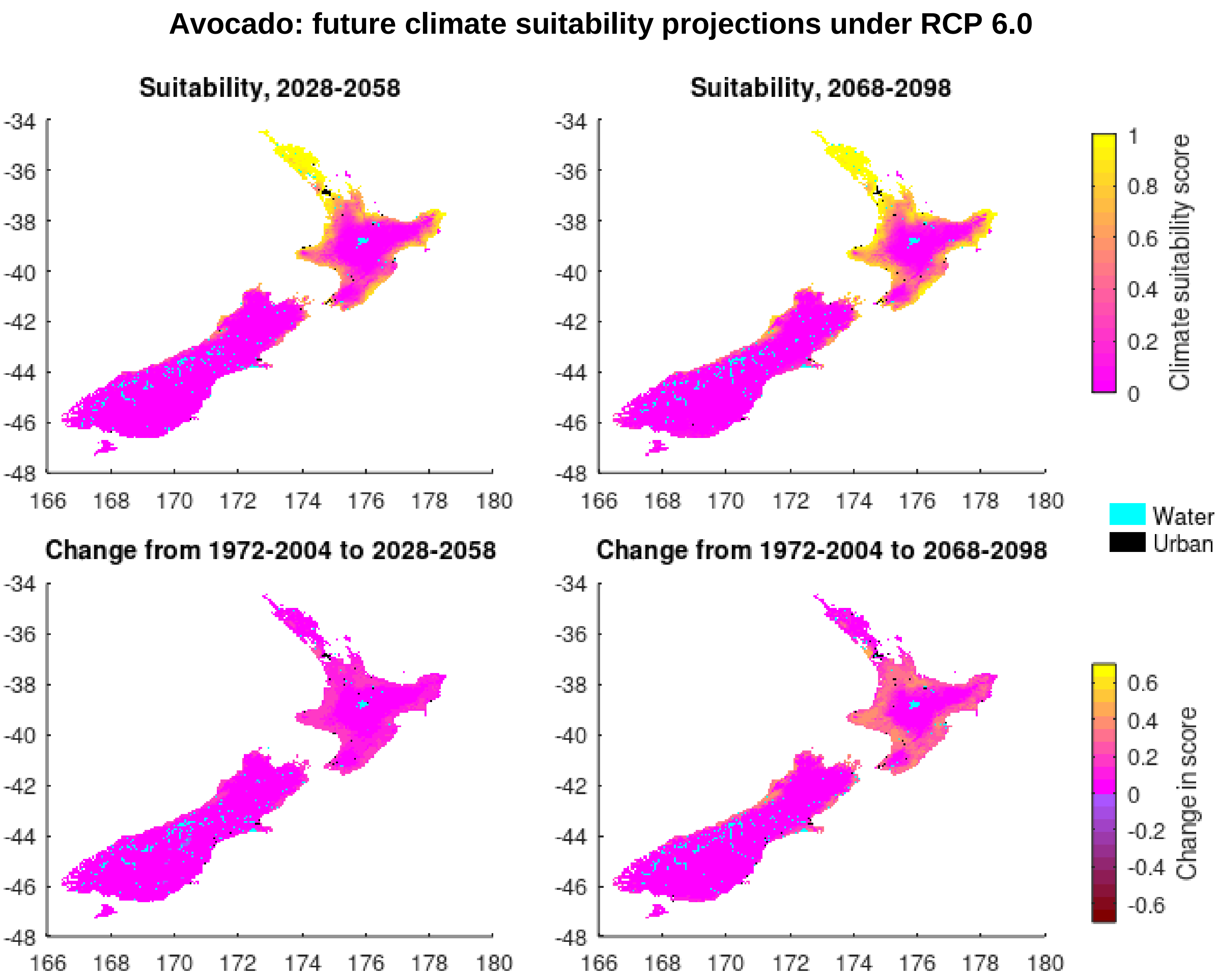
Avocado: future climate suitability projections under RCP 6.0
Suitability, 2028-2058
Suitability, 2068-2098
Change from 1972-2004 to 2028-2058
Change from 1972-2004 to 2068-2098
-34
-36
-38
-40
-42
-44
-46
-48
166
168
170
172
174
176
178
180
Climate suitability score
1
0.8
0.6
0.4
0.2
0
Water
Urban
Change in score
0.6
0.4
0.2
0
-0.2
-0.4
-0.6

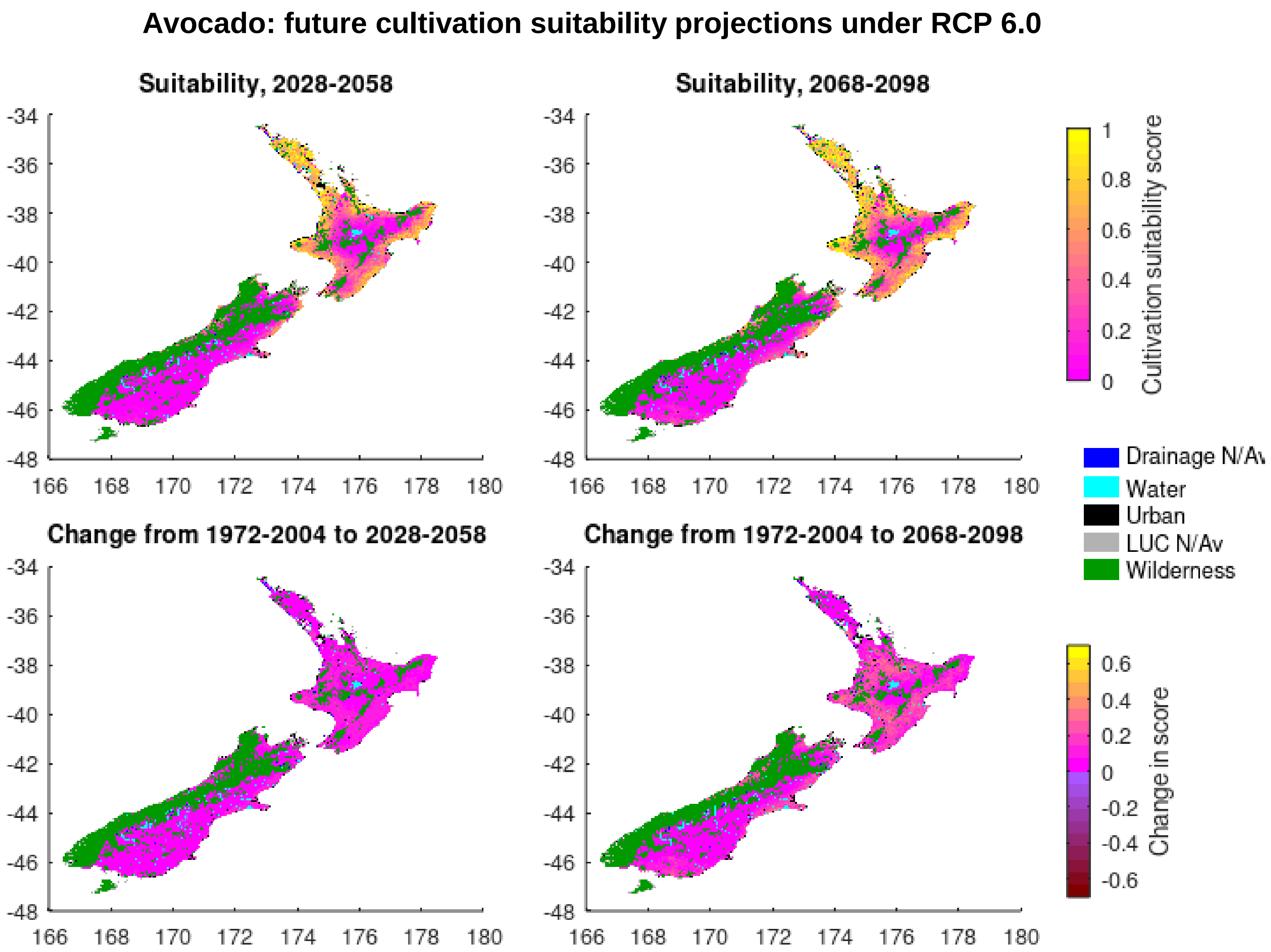
Avocado: future cultivation suitability projections under RCP 6.0
Suitability, 2028-2058
Suitability, 2068-2098
Change from 1972-2004 to 2028-2058
Change from 1972-2004 to 2068-2098
-34
-36
-38
-40
-42
-44
-46
-48
166
168
170
172
174
176
178
180
Cultivation suitability score
1
0.8
0.6
0.4
0.2
0
Drainage N/Av
Water
Urban
LUC N/Av
Wilderness
Change in score
0.6
0.4
0.2
0
-0.2
-0.4
-0.6

Blueberry RCP 4.5

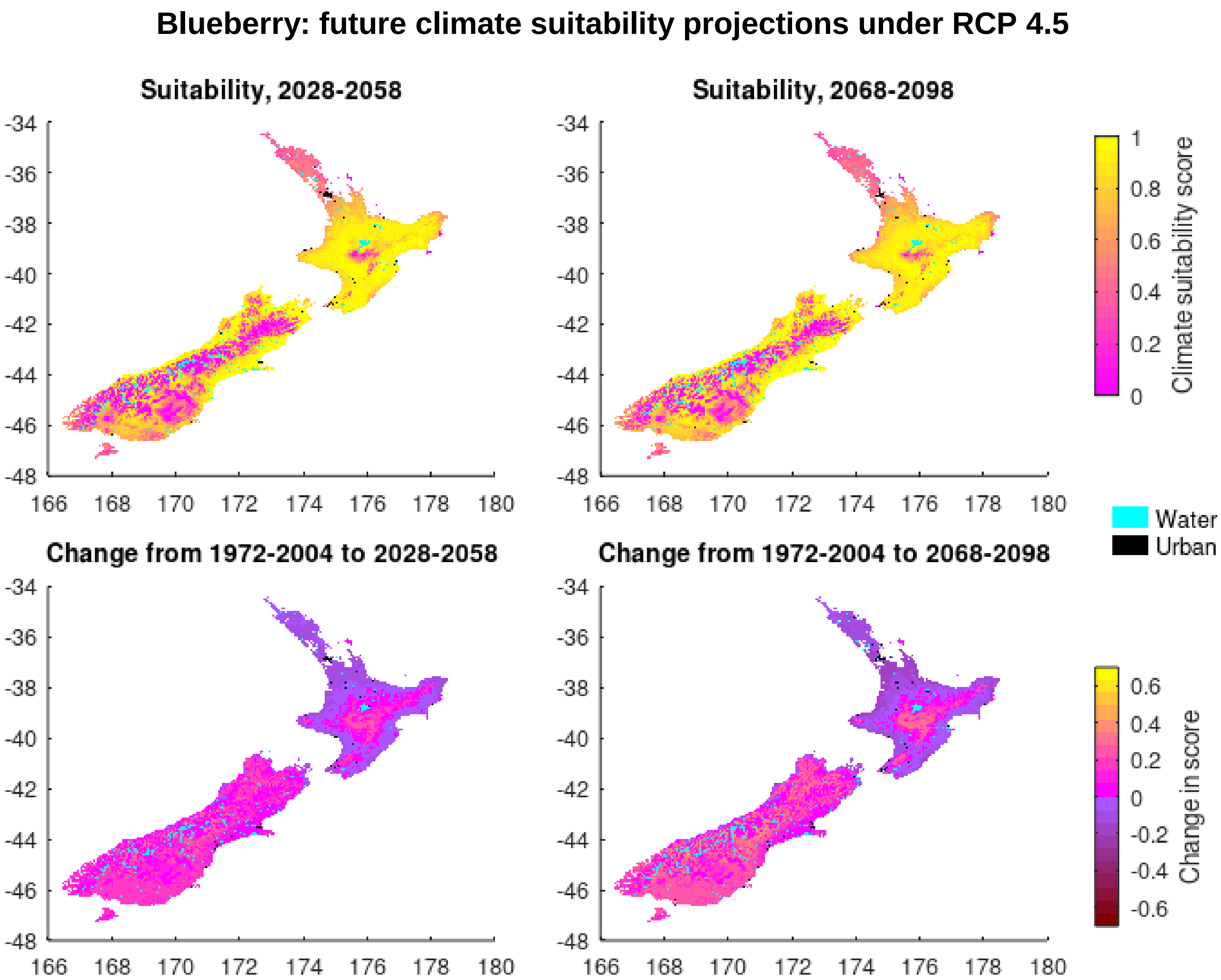

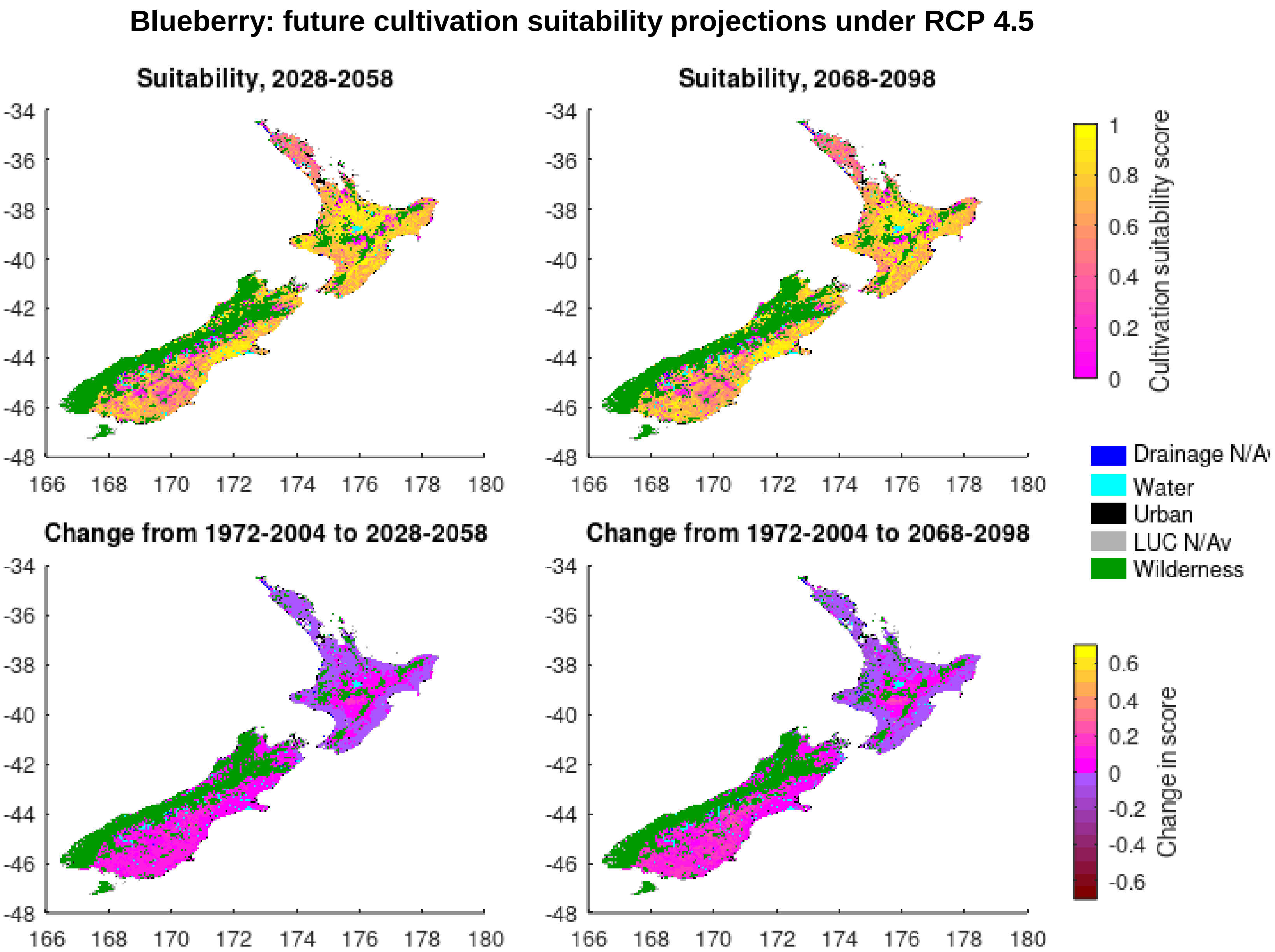

Blueberry: future cultivation suitability projections under RCP 4.5
Suitability, 2028-2058
Suitability, 2068-2098
Change from 1972-2004 to 2028-2058
Change from 1972-2004 to 2068-2098
-34
-36
-38
-40
-42
-44
-46
-48
166
168
170
172
174
176
178
180
Cultivation suitability score
1
0.8
0.6
0.4
0.2
0
Drainage N/Av
Water
Urban
LUC N/Av
Wilderness
Change in score
0.6
0.4
0.2
0
-0.2
-0.4
-0.6

Land area in the historic period falling into different cultivation suitability ranges, projected changes for the mid- and late-century under RCP 4.5, and best and worst cases. Decreases are shaded red and increases shaded blue. Colour intensity increases with the magnitude of change.

Blueberry SLM RCP 4.5	Historic (km²) 1972–2004	Area change from historic (km²) 2028–2058			Area change from historic (km²) 2068–2098		
Suitability range		Projection	Best case	Worst case	Projection	Best case	Worst case
0–0.1	13684	−1238	−1968	393	−1590	−1974	−453
0.1–0.2	3992	−1390	−2833	−1337	−2079	−3262	−1888
0.2–0.3	4223	−1235	−781	−723	−1666	−1617	−892
0.3–0.4	8396	−2920	−3783	−1482	−3122	−3979	−1488
0.4–0.5	19396	−1832	−5880	675	−2463	−5602	−1164
0.5–0.6	26337	−4440	−4468	−3428	−5318	−6443	−3314
0.6–0.7	30662	4439	3980	3657	5305	5243	5153
0.7–0.8	31696	2784	2539	2816	3695	3353	4095
0.8–0.9	34167	5093	7620	1161	6066	8495	1611
0.9–1.0	11172	739	5574	−1732	1172	5786	−1660

Blueberry RCP 6.0

Land area in the historic period falling into different cultivation suitability ranges, projected changes for the mid- and late-century under RCP 6.0, and best and worst cases. Decreases are shaded red and increases shaded blue. Colour intensity increases with the magnitude of change.

Blueberry SLM RCP 6.0	Historic (km²) 1972–2004	Area change from historic (km²) 2028–2058			Area change from historic (km²) 2068–2098		
Suitability range		Projection	Best case	Worst case	Projection	Best case	Worst case
0–0.1	13684	−1240	−1959	460	−1698	−1974	−774
0.1–0.2	3992	−1337	−2719	−1489	−2544	−3397	−2415
0.2–0.3	4223	−1287	−676	−772	−1931	−2070	−1205
0.3–0.4	8396	−2785	−3688	−1782	−2852	−4003	−542
0.4–0.5	19396	−1887	−5597	775	−2573	−4681	−2905
0.5–0.6	26337	−4327	−4194	−3770	−5553	−7017	−2986
0.6–0.7	30662	4381	3819	3748	5980	5271	6066
0.7–0.8	31696	2427	2448	2679	4678	4580	4210
0.8–0.9	34167	5109	7329	1512	4878	8049	1699
0.9–1.0	11172	946	5237	−1361	1615	5242	−1148

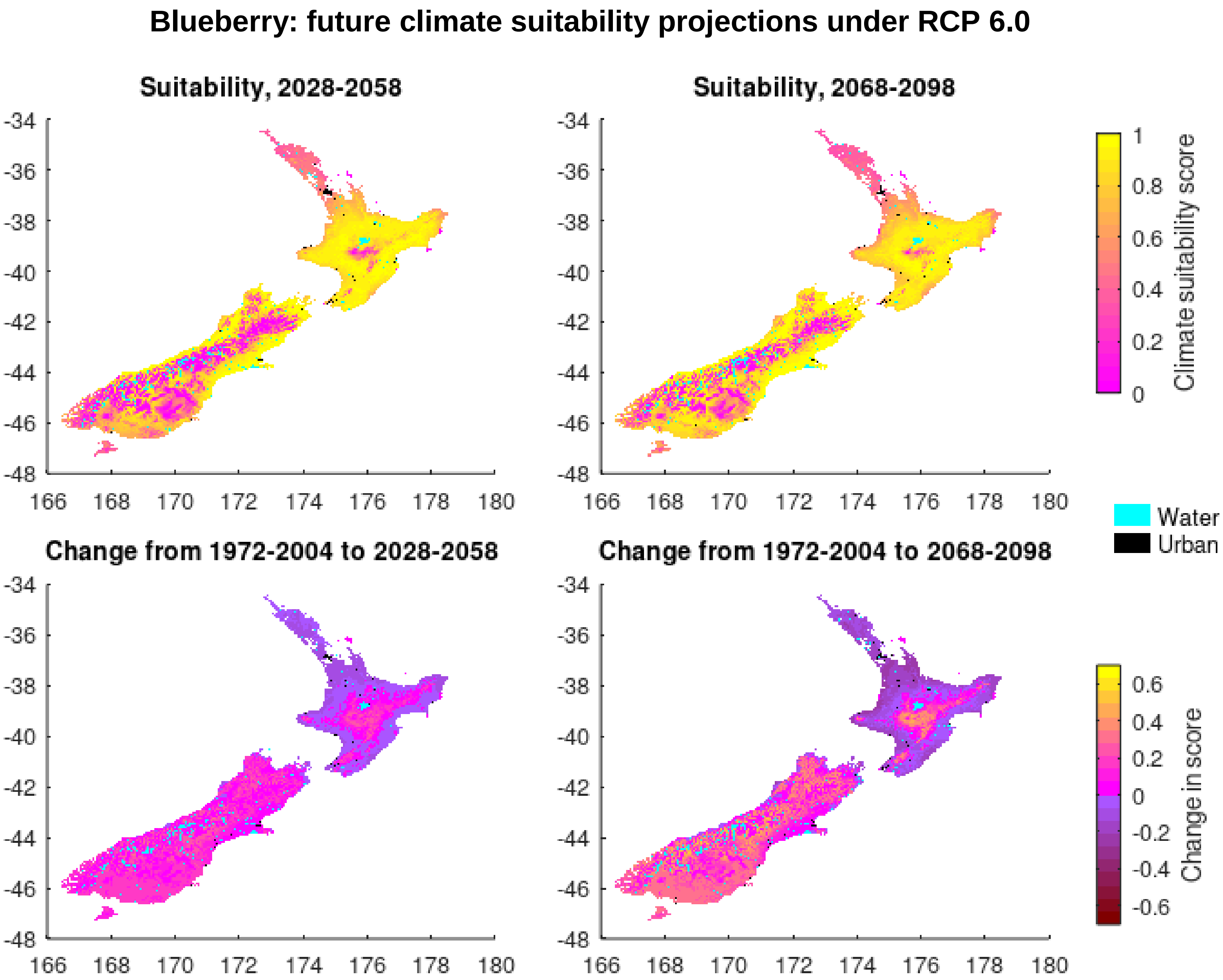
Blueberry: future climate suitability projections under RCP 6.0
Suitability, 2028-2058
Suitability, 2068-2098
Change from 1972-2004 to 2028-2058
Change from 1972-2004 to 2068-2098
-34
-36
-38
-40
-42
-44
-46
-48
166
168
170
172
174
176
178
180
Climate suitability score
1
0.8
0.6
0.4
0.2
0
Water
Urban
Change in score
0.6
0.4
0.2
0
-0.2
-0.4
-0.6

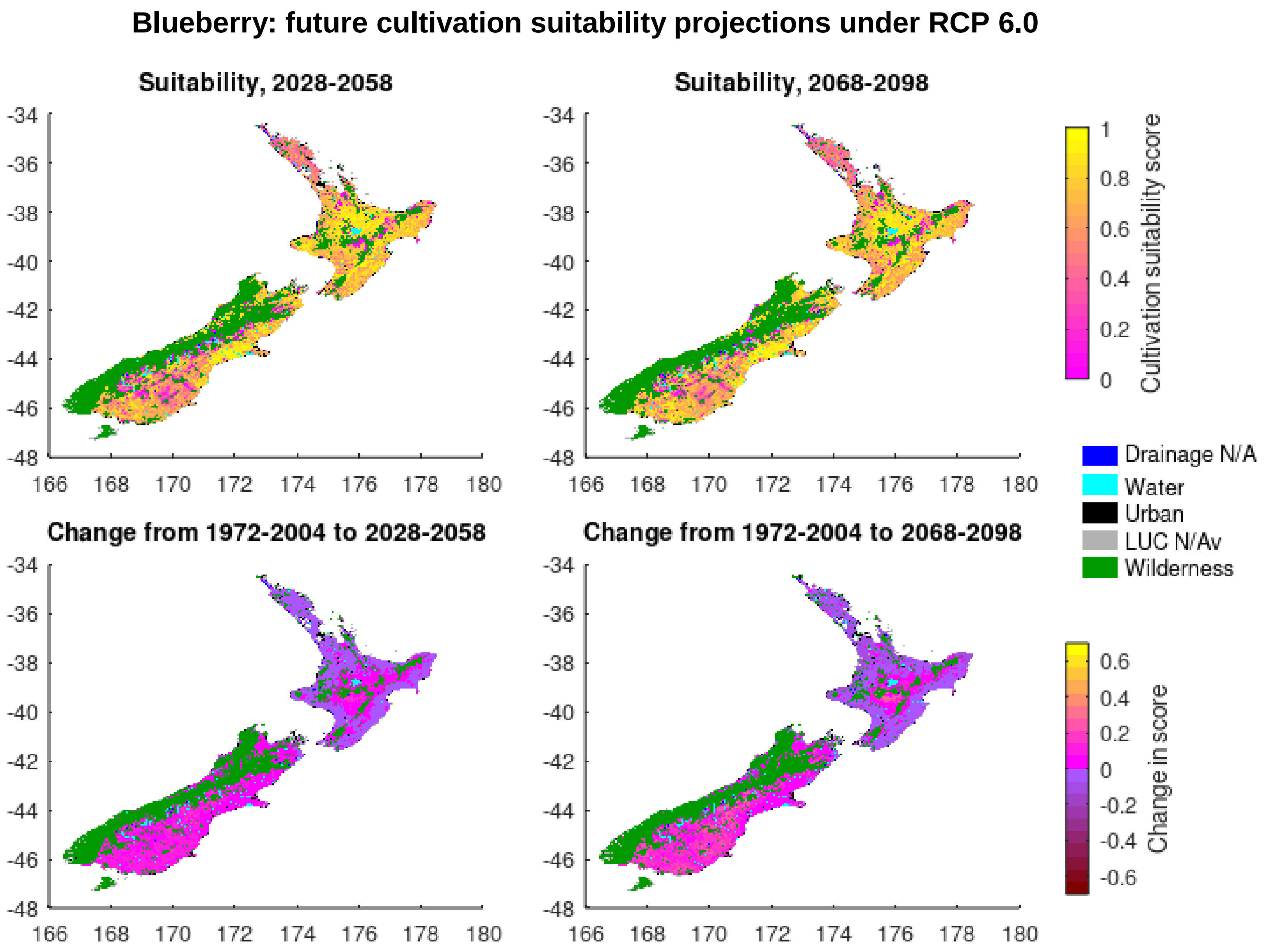
Blueberry: future cultivation suitability projections under RCP 6.0
Suitability, 2028-2058
Suitability, 2068-2098
Change from 1972-2004 to 2028-2058
Change from 1972-2004 to 2068-2098
-34
-36
-38
-40
-42
-44
-46
-48
166
168
170
172
174
176
178
180
1
0.8
0.6
0.4
0.2
0
Cultivation suitability score
Drainage N/A
Water
Urban
LUC N/Av
Wilderness
0.6
0.4
0.2
0
-0.2
-0.4
-0.6
Change in score

Cherry RCP 4.5

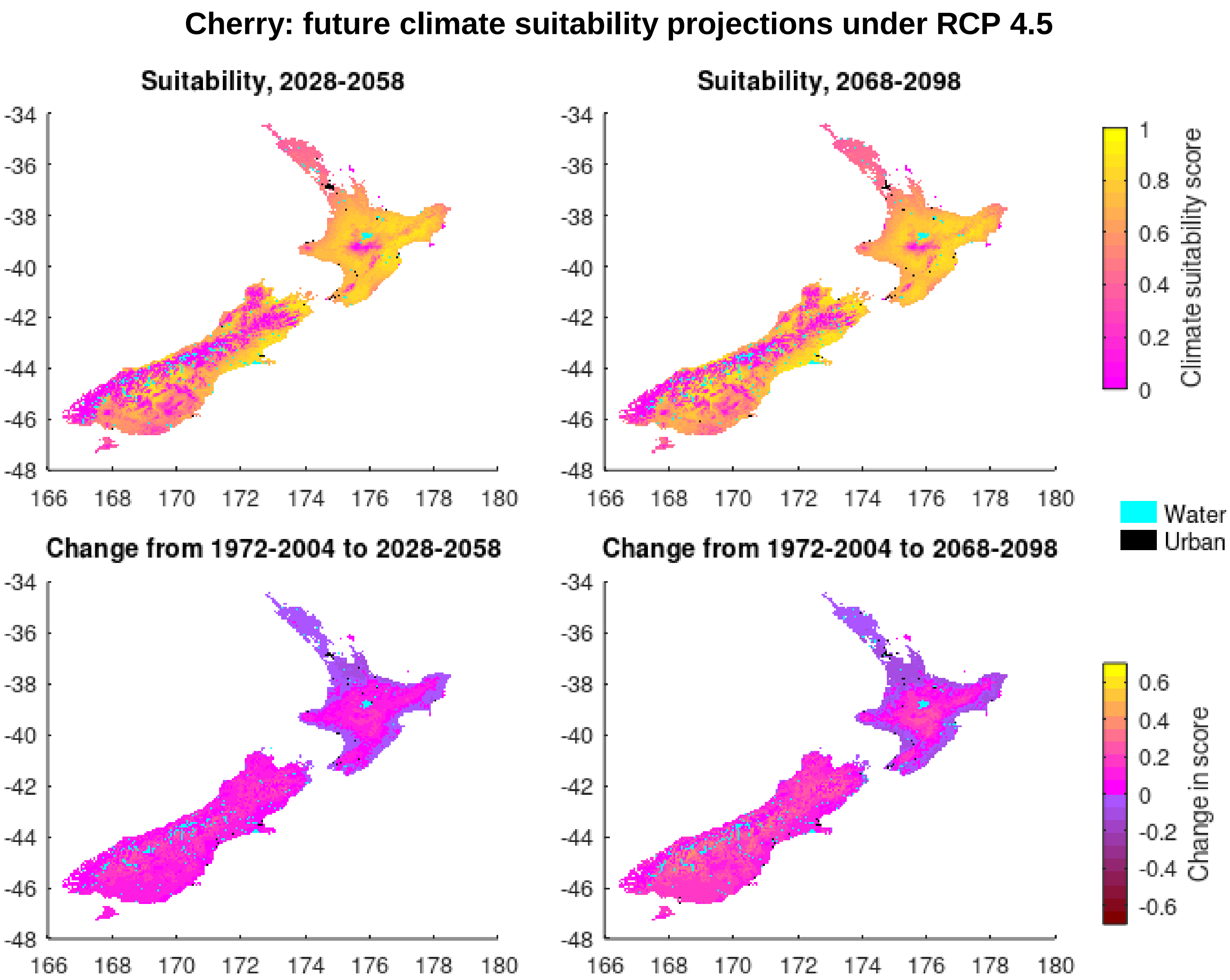

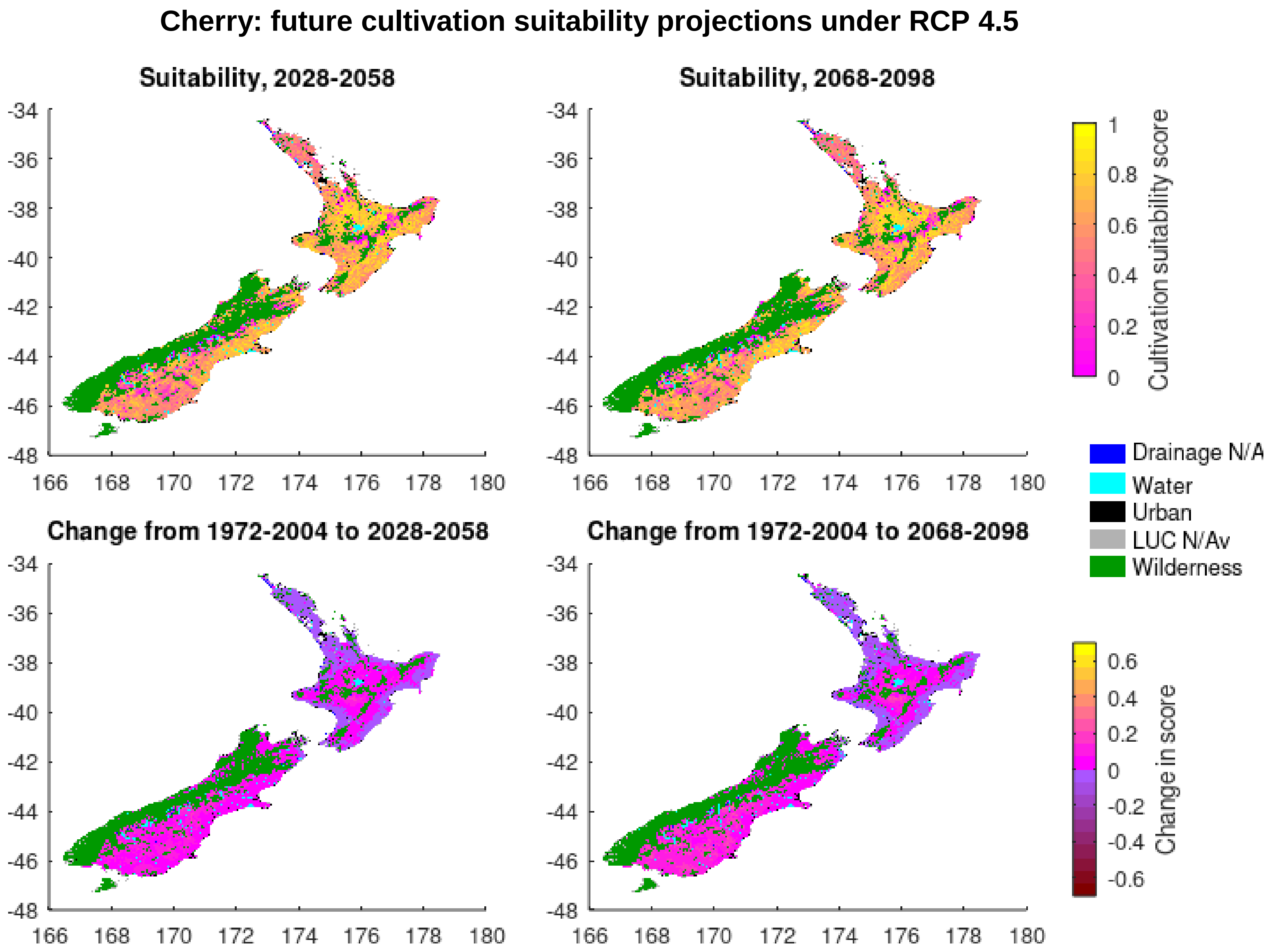
Cherry: future cultivation suitability projections under RCP 4.5
Suitability, 2028-2058
Suitability, 2068-2098
Change from 1972-2004 to 2028-2058
Change from 1972-2004 to 2068-2098
-34
-36
-38
-40
-42
-44
-46
-48
166
168
170
172
174
176
178
180
Cultivation suitability score
1
0.8
0.6
0.4
0.2
0
Drainage N/A
Water
Urban
LUC N/Av
Wilderness
Change in score
0.6
0.4
0.2
0
-0.2
-0.4
-0.6

Land area in the historic period falling into different cultivation suitability ranges, projected changes for the mid- and late-century under RCP 4.5, and best and worst cases. Decreases are shaded red and increases shaded blue. Colour intensity increases with the magnitude of change.

Cherry SLM RCP 4.5	Historic (km^2) 1972–2004	Area change from historic (km^2) 2028–2058			Area change from historic (km^2) 2068–2098		
Suitability range		Projection	Best case	Worst case	Projection	Best case	Worst case
0–0.1	14847	−2311	−3026	−1926	−2509	−3048	−2034
0.1–0.2	3325	−1672	−1942	−868	−2559	−2470	−1911
0.2–0.3	4934	−1483	−2046	−1084	−2243	−2944	−1831
0.3–0.4	11732	−2656	−4073	−1030	−3374	−4543	−1482
0.4–0.5	29866	−4687	−8769	−805	−5825	−9208	−4002
0.5–0.6	38953	1017	982	433	−173	−1137	536
0.6–0.7	36713	2193	4334	631	3488	4878	2245
0.7–0.8	28351	5436	6902	3902	8789	9846	7765
0.8–0.9	14687	4104	7227	910	4093	7704	624
0.9–1.0	317	59	411	−163	313	922	90

Cherry RCP 6.0

Land area in the historic period falling into different cultivation suitability ranges, projected changes for the mid- and late-century under RCP 6.0, and best and worst cases. Decreases are shaded red and increases shaded blue. Colour intensity increases with the magnitude of change.

Cherry SLM RCP 6.0	Historic (km^2) 1972–2004	Area change from historic (km^2) 2028–2058			Area change from historic (km^2) 2068–2098		
Suitability range		Projection	Best case	Worst case	Projection	Best case	Worst case
0–0.1	14847	−2233	−2984	−1874	−2564	−3049	−1620
0.1–0.2	3325	−1512	−1699	−834	−2861	−2695	−2519
0.2–0.3	4934	−1404	−1861	−995	−2742	−3295	−2143
0.3–0.4	11732	−2594	−4027	−885	−3274	−4827	−1263
0.4–0.5	29866	−5029	−9089	−731	−5473	−8318	−4244
0.5–0.6	38953	1605	1102	837	−1648	−2943	−567
0.6–0.7	36713	2684	4762	1018	3094	3864	2017
0.7–0.8	28351	6005	7408	4588	9944	11246	8988
0.8–0.9	14687	2507	6053	−900	4952	8189	1090
0.9–1.0	317	−29	335	−224	572	1828	261

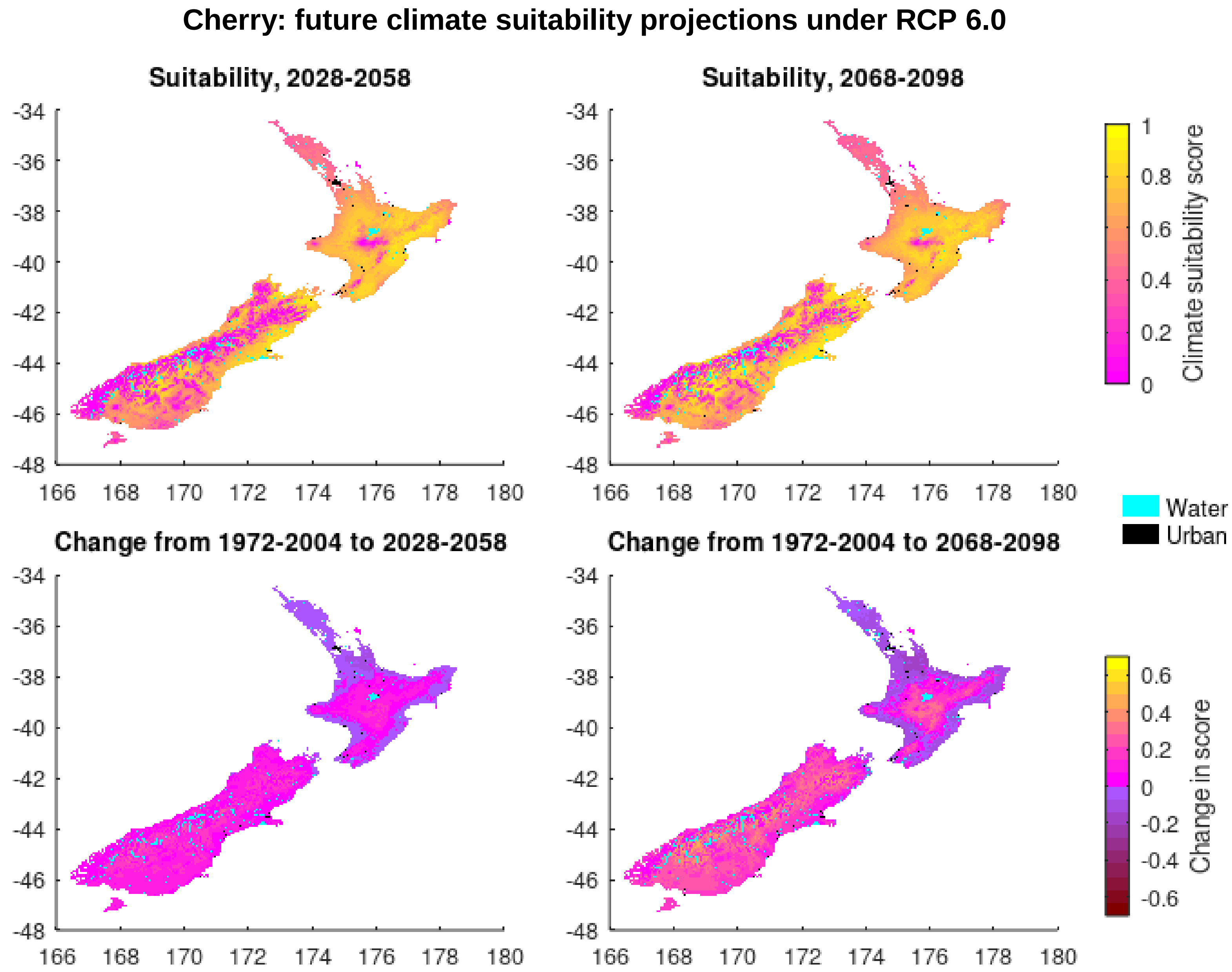
Cherry: future climate suitability projections under RCP 6.0
Suitability, 2028-2058
Suitability, 2068-2098
Change from 1972-2004 to 2028-2058
Change from 1972-2004 to 2068-2098
-34
-36
-38
-40
-42
-44
-46
-48
166
168
170
172
174
176
178
180
1
0.8
0.6
0.4
0.2
0
Climate suitability score
Water
Urban
0.6
0.4
0.2
0
-0.2
-0.4
-0.6
Change in score

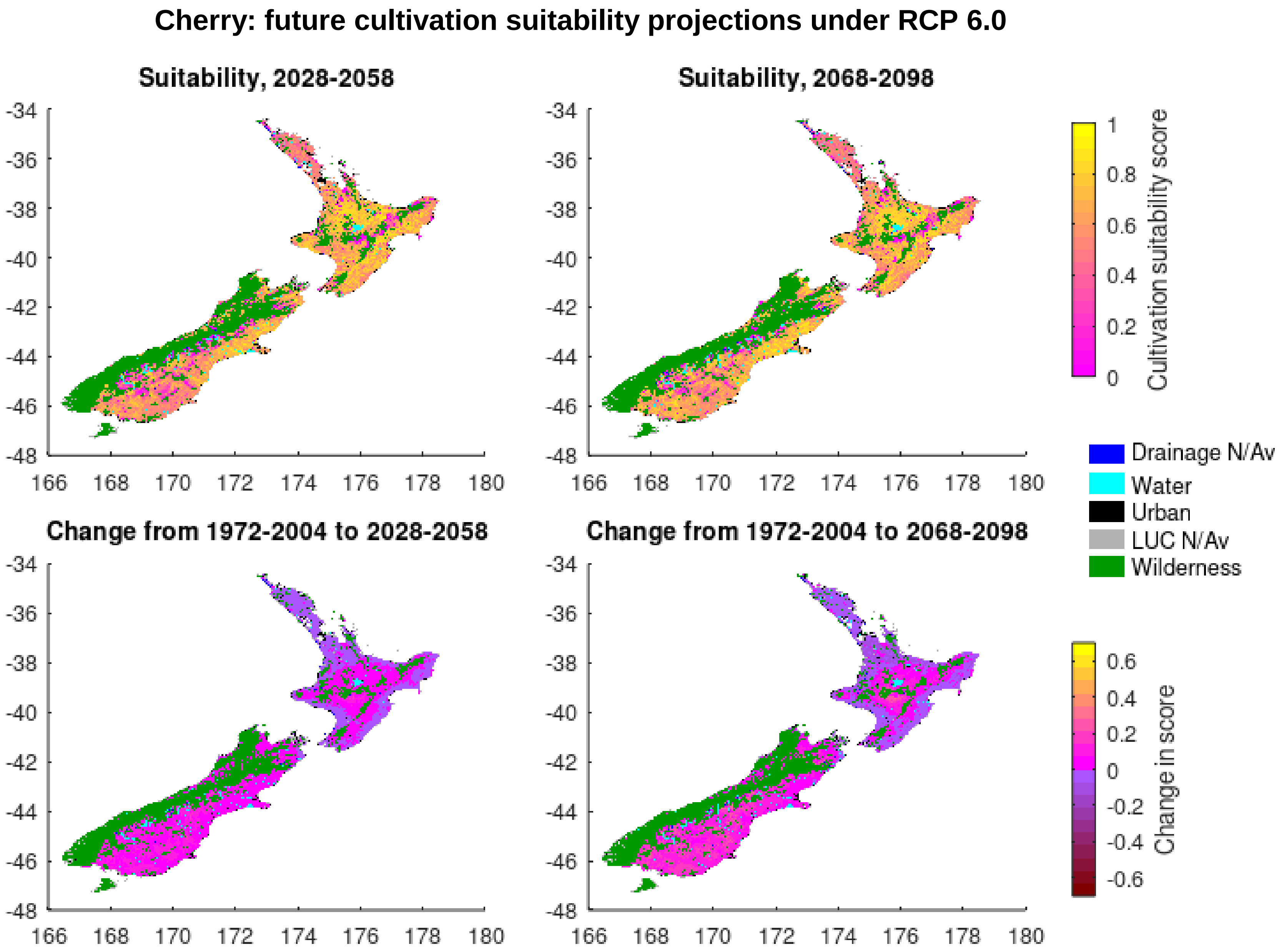
Cherry: future cultivation suitability projections under RCP 6.0
Suitability, 2028-2058
Suitability, 2068-2098
Change from 1972-2004 to 2028-2058
Change from 1972-2004 to 2068-2098
-34
-36
-38
-40
-42
-44
-46
-48
166
168
170
172
174
176
178
180
1
0.8
0.6
0.4
0.2
0
Cultivation suitability score
Drainage N/Av
Water
Urban
LUC N/Av
Wilderness
0.6
0.4
0.2
0
-0.2
-0.4
-0.6
Change in score

Pinot noir RCP 4.5

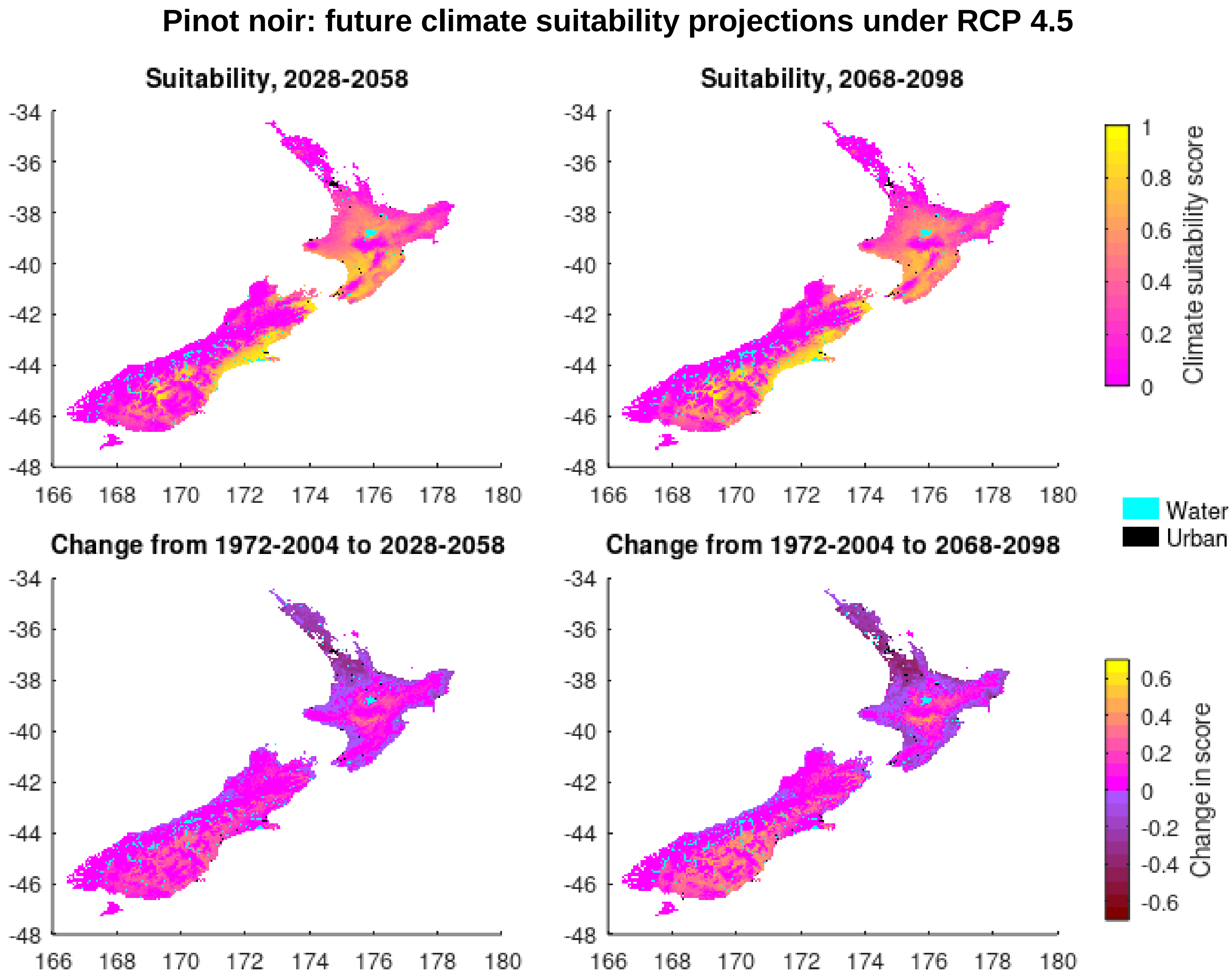

Pinot noir: future cultivation suitability projections under RCP 4.5

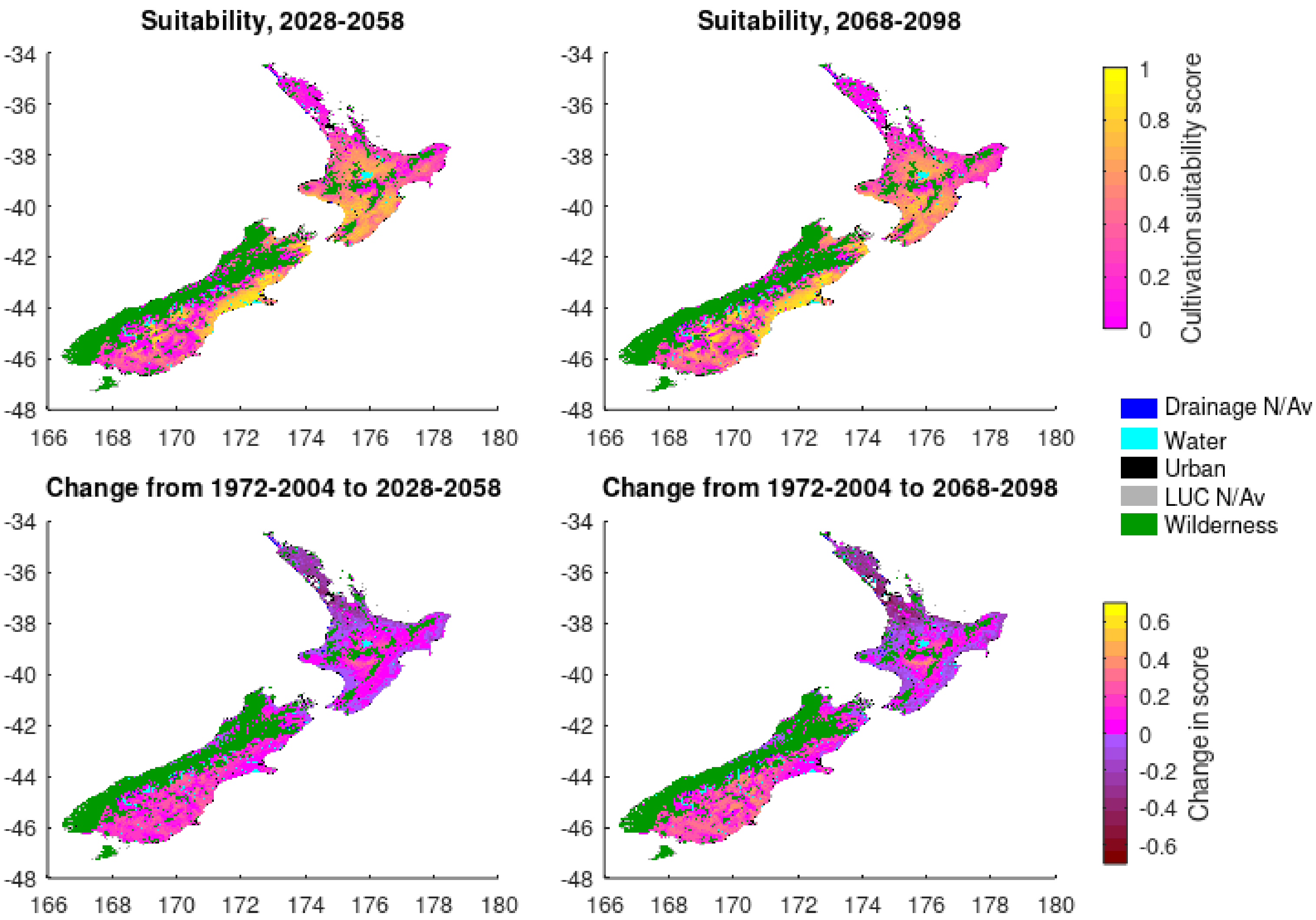

Land area in the historic period falling into different cultivation suitability ranges, projected changes for the mid- and late-century under RCP 4.5, and best and worst cases. Decreases are shaded red and increases shaded blue. Colour intensity increases with the magnitude of change.

Pinot noir SLM RCP 4.5	Historic (km²) 1972–2004	Area change from historic (km²) 2028–2058			Area change from historic (km²) 2068–2098		
Suitability range		Projection	Best case	Worst case	Projection	Best case	Worst case
0–0.1	42923	−10174	−18820	−3910	−9261	−16680	−4251
0.1–0.2	20376	−1637	719	113	−4061	−3099	−770
0.2–0.3	20274	592	−2736	5195	697	−2138	3643
0.3–0.4	24613	1595	−853	−1835	−187	−1861	−1941
0.4–0.5	21422	791	4161	−1347	1651	3809	61
0.5–0.6	20731	502	1305	577	4294	3496	3560
0.6–0.7	19718	1518	4083	−1074	1193	5598	−1935
0.7–0.8	9765	2990	5467	1994	1789	4171	1117
0.8–0.9	3727	3446	4797	427	3577	5133	673
0.9–1.0	176	377	1877	−140	308	1571	−157

Pinot noir RCP 6.0

Land area in the historic period falling into different cultivation suitability ranges, projected changes for the mid- and late-century under RCP 6.0, and best and worst cases. Decreases are shaded red and increases shaded blue. Colour intensity increases with the magnitude of change.

Pinot noir SLM RCP 6.0	Historic (km²) 1972–2004	Area change from historic (km²) 2028–2058			Area change from historic (km²) 2068–2098		
Suitability range		Projection	Best case	Worst case	Projection	Best case	Worst case
0–0.1	42923	−10124	−18296	−3455	−6559	−12146	−1984
0.1–0.2	20376	−487	1179	846	−3788	−4202	−992
0.2–0.3	20274	1848	−1488	5798	−717	−2821	1220
0.3–0.4	24613	1782	389	−2128	−2930	−3518	−4541
0.4–0.5	21422	667	4636	−870	2061	2355	2597
0.5–0.6	20731	2419	1542	1482	5538	6136	3739
0.6–0.7	19718	−986	2451	−2507	−398	2939	−2849
0.7–0.8	9765	1861	3574	1369	1507	2685	1674
0.8–0.9	3727	2724	4250	−381	4983	6100	1312
0.9–1.0	176	296	1763	−154	303	2472	−176

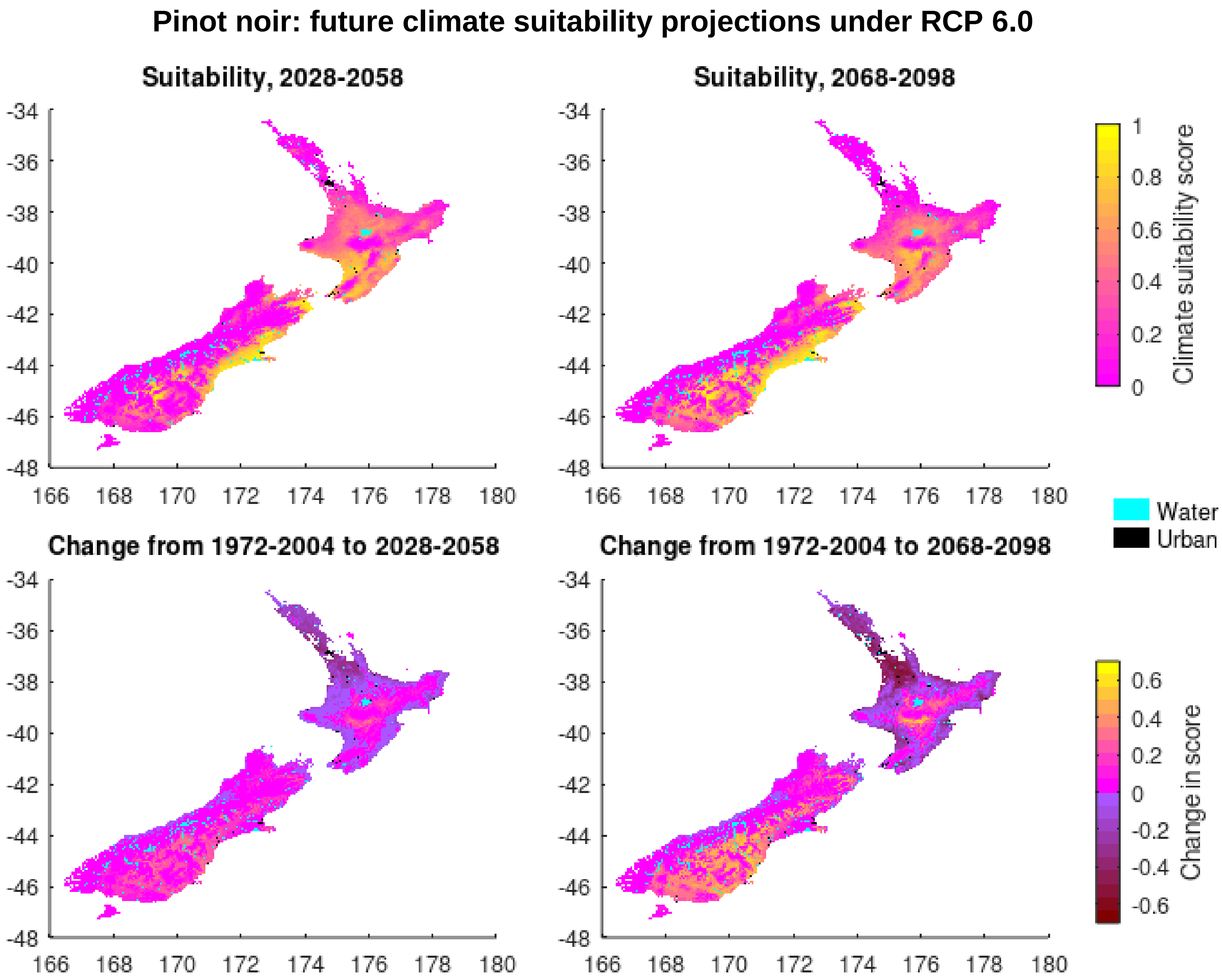
Pinot noir: future climate suitability projections under RCP 6.0
Suitability, 2028-2058
Suitability, 2068-2098
Change from 1972-2004 to 2028-2058
Change from 1972-2004 to 2068-2098
Climate suitability score
1
0.8
0.6
0.4
0.2
0
Water
Urban
Change in score
0.6
0.4
0.2
0
-0.2
-0.4
-0.6
-34
-36
-38
-40
-42
-44
-46
-48
166
168
170
172
174
176
178
180

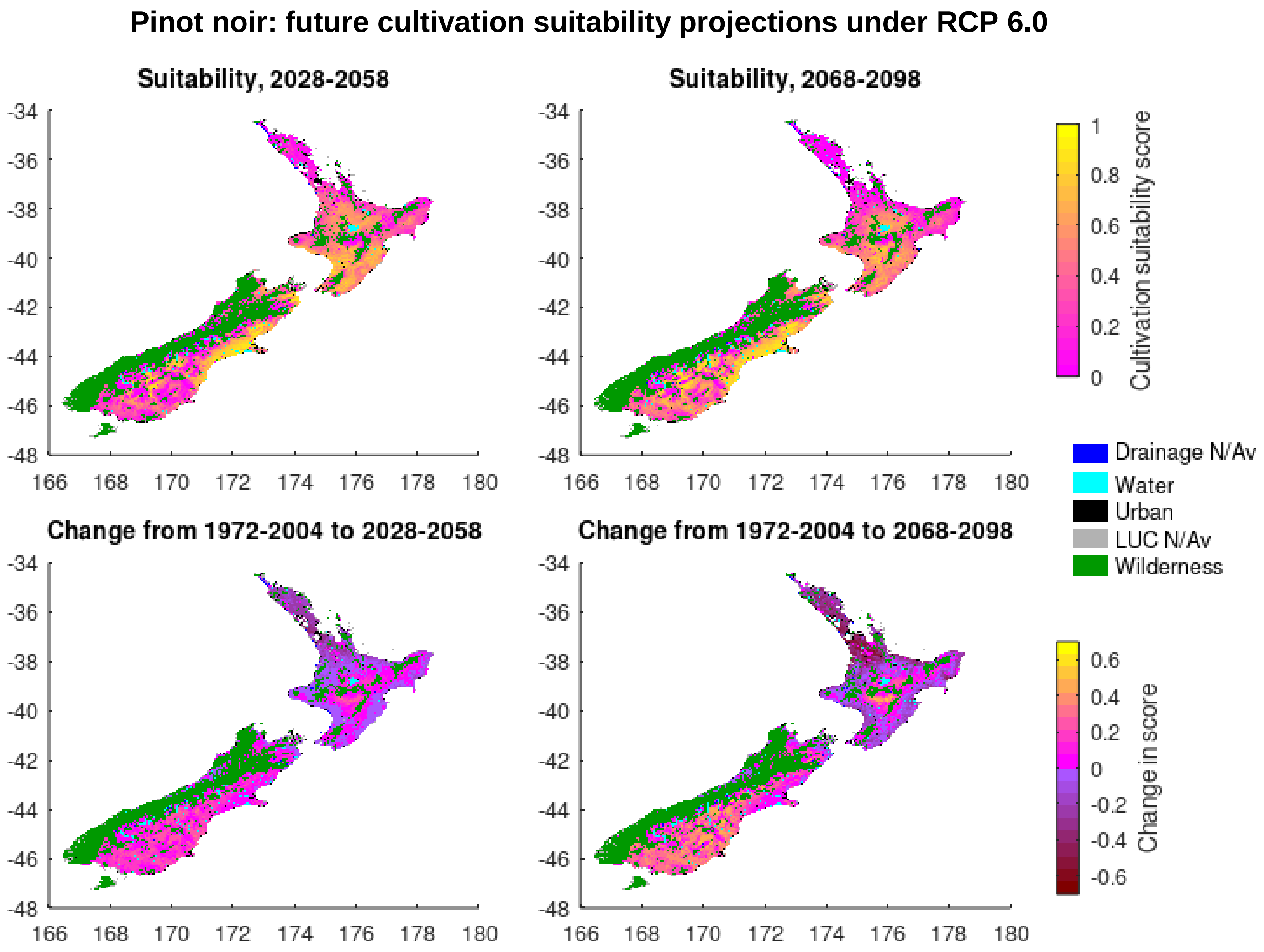
Pinot noir: future cultivation suitability projections under RCP 6.0
Suitability, 2028-2058
Suitability, 2068-2098
Change from 1972-2004 to 2028-2058
Change from 1972-2004 to 2068-2098
Cultivation suitability score
Change in score
Drainage N/Av
Water
Urban
LUC N/Av
Wilderness

Sauvignon blanc RCP 4.5

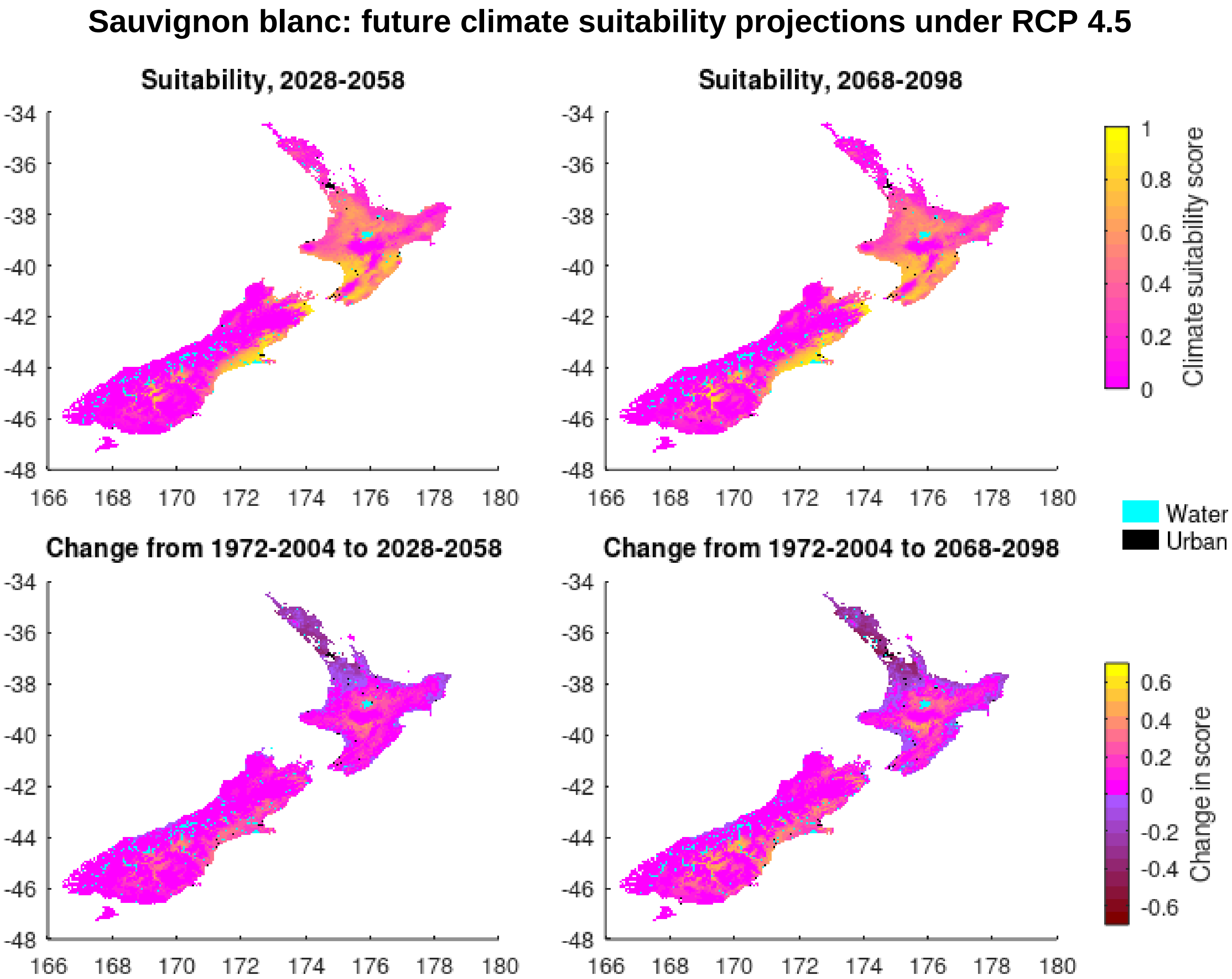

Sauvignon blanc: future cultivation suitability projections under RCP 4.5

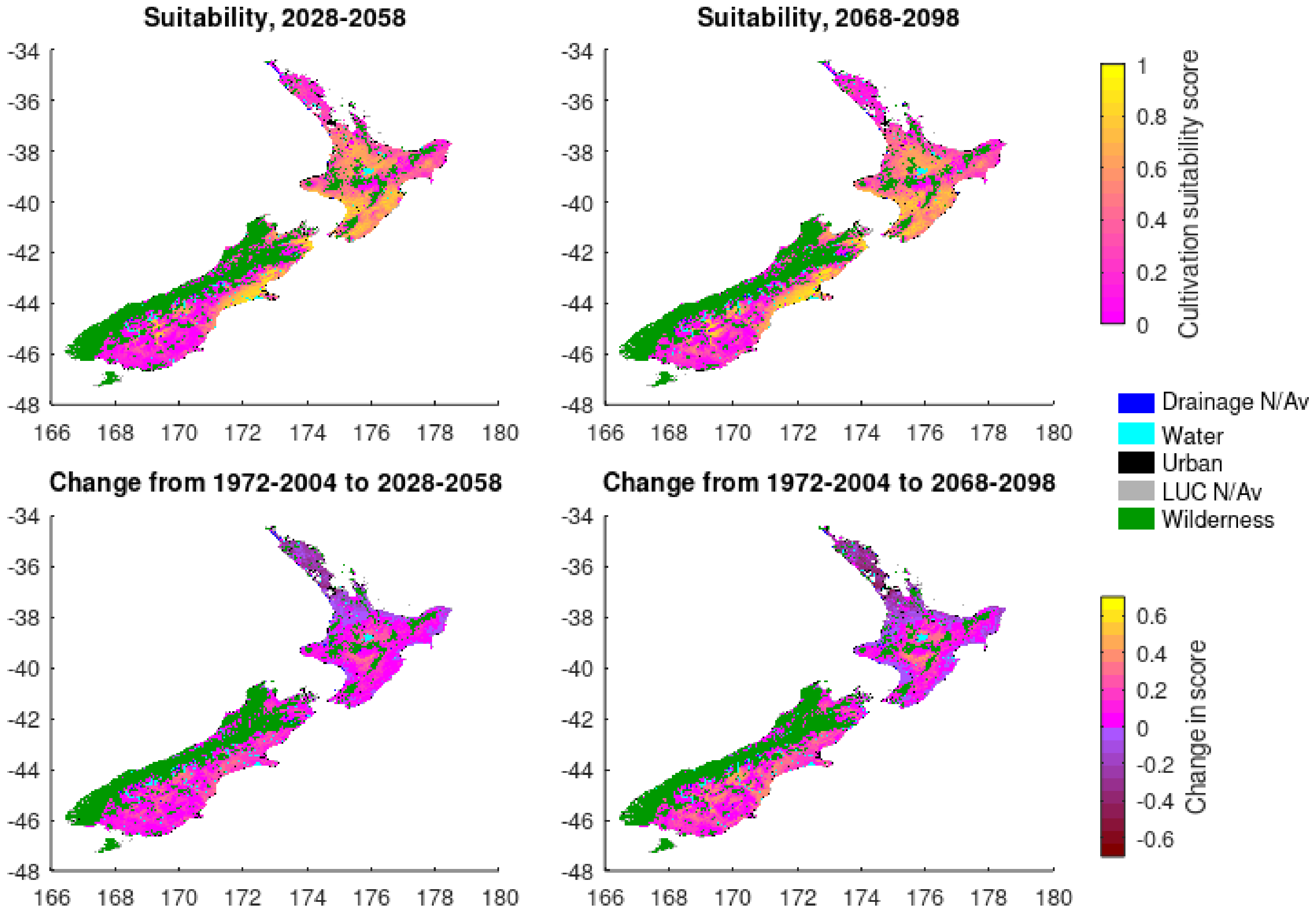

Land area in the historic period falling into different cultivation suitability ranges, projected changes for the mid- and late-century under RCP 4.5, and best and worst cases. Decreases are shaded red and increases shaded blue. Colour intensity increases with the magnitude of change.

Sauvignon blanc SLM RCP 4.5	Historic (km²) 1972–2004	Area change from historic (km²) 2028–2058			Area change from historic (km²) 2068–2098		
Suitability range		Projection	Best case	Worst case	Projection	Best case	Worst case
0–0.1	67747	−24733	−32195	−17037	−30498	−36953	−22366
0.1–0.2	14643	8291	6930	10198	8870	6609	10321
0.2–0.3	15576	5441	5009	5752	6750	5228	7606
0.3–0.4	21047	913	490	−810	2891	2426	1468
0.4–0.5	21684	−1735	−152	−3319	−897	1839	−3642
0.5–0.6	19098	875	1642	1523	706	1191	2338
0.6–0.7	17136	2756	4154	432	3239	5195	293
0.7–0.8	5654	4797	7907	2684	5541	7653	2945
0.8–0.9	1102	3230	5146	614	3098	5502	1029
0.9–1.0	38	165	1069	−37	300	1310	8

Sauvignon blanc RCP 6.0

Land area in the historic period falling into different cultivation suitability ranges, projected changes for the mid- and late-century under RCP 6.0, and best and worst cases. Decreases are shaded red and increases shaded blue. Colour intensity increases with the magnitude of change.

Sauvignon blanc SLM RCP 6.0	Historic (km²) 1972–2004	Area change from historic (km²) 2028–2058			Area change from historic (km²) 2068–2098		
Suitability range		Projection	Best case	Worst case	Projection	Best case	Worst case
0–0.1	67747	−22414	−29605	−15975	−28821	−35346	−23626
0.1–0.2	14643	6212	6749	10227	3698	3614	7925
0.2–0.3	15576	6977	3825	6520	8330	3177	10303
0.3–0.4	21047	1636	2173	−180	3741	5778	−185
0.4–0.5	21684	−1182	764	−2536	−1822	693	−2897
0.5–0.6	19098	2007	1956	935	2380	2125	2857
0.6–0.7	17136	656	2852	−1119	2066	4361	−139
0.7–0.8	5654	3433	5891	1910	5297	7049	4018
0.8–0.9	1102	2576	4418	256	4701	6340	1722
0.9–1.0	38	99	977	−38	430	2209	22

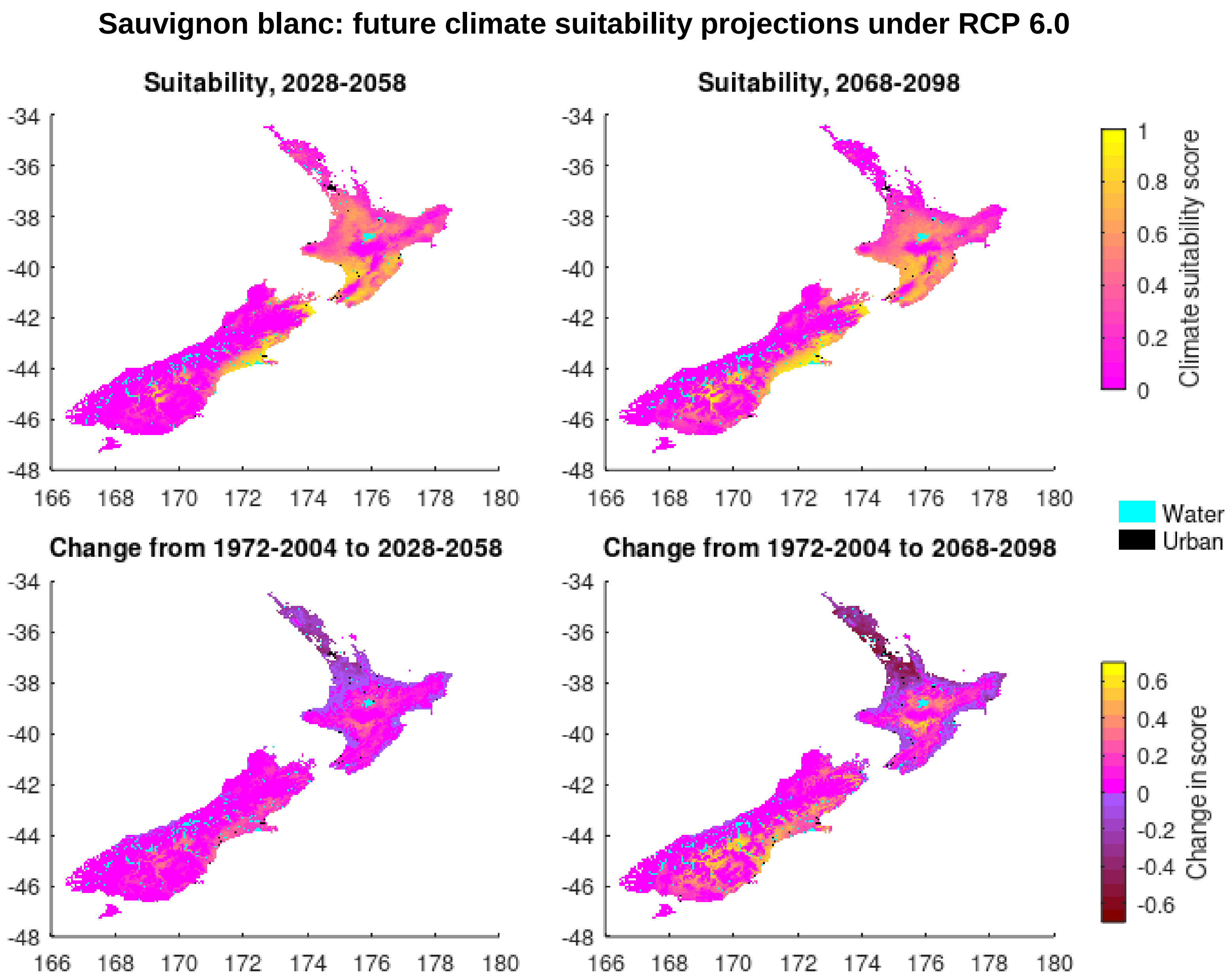
Sauvignon blanc: future climate suitability projections under RCP 6.0
Suitability, 2028-2058
Suitability, 2068-2098
Change from 1972-2004 to 2028-2058
Change from 1972-2004 to 2068-2098
-34
-36
-38
-40
-42
-44
-46
-48
166
168
170
172
174
176
178
180
Climate suitability score
1
0.8
0.6
0.4
0.2
0
Water
Urban
Change in score
0.6
0.4
0.2
0
-0.2
-0.4
-0.6

Sauvignon blanc: future cultivation suitability projections under RCP 6.0

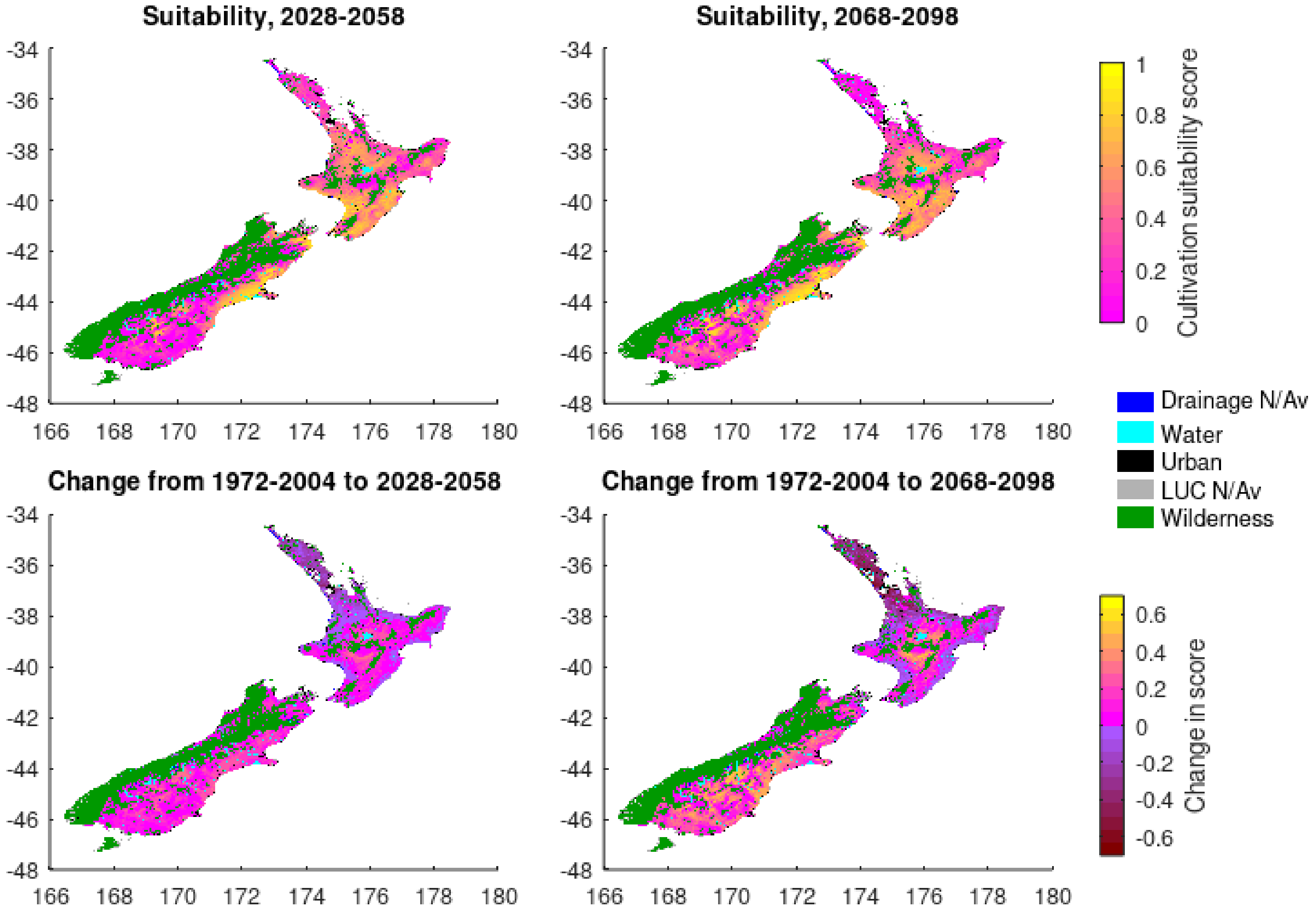

A smart
green
future.
Together.

Supplementary

The following includes supplementary data to support the report

Contents

1 Apple RCP 2.6

Apple: richardson cu suitability score RCP 2.6

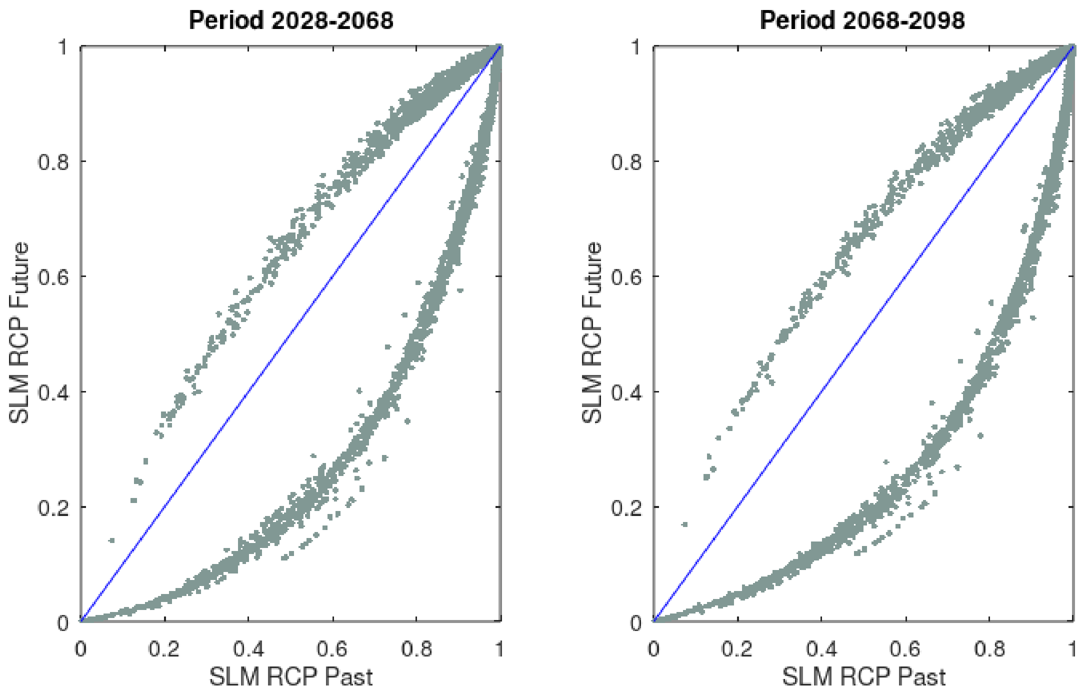

Apple: fruit size suitability score RCP 2.6

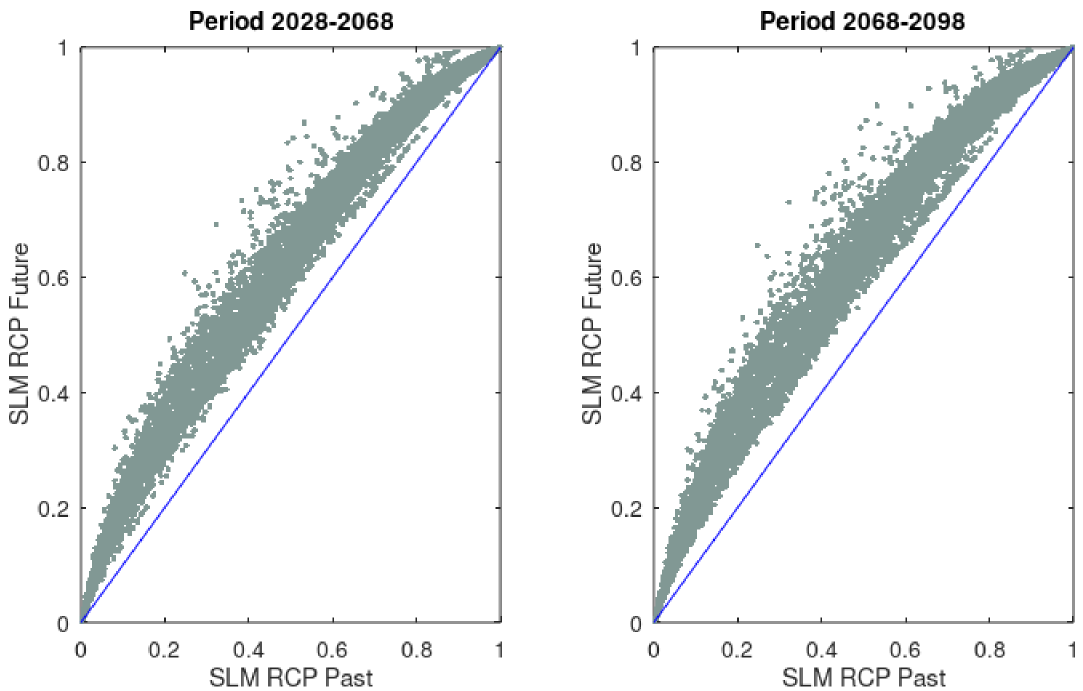

Apple: frost survival suitability score RCP 2.6

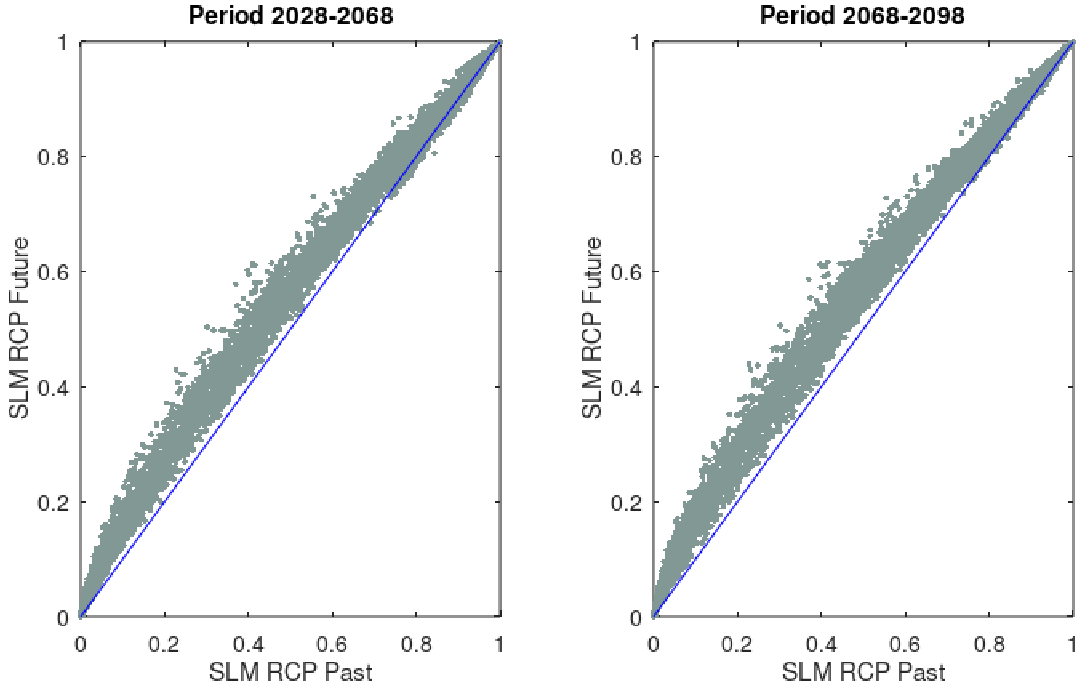

Apple: climate suitability score RCP 2.6

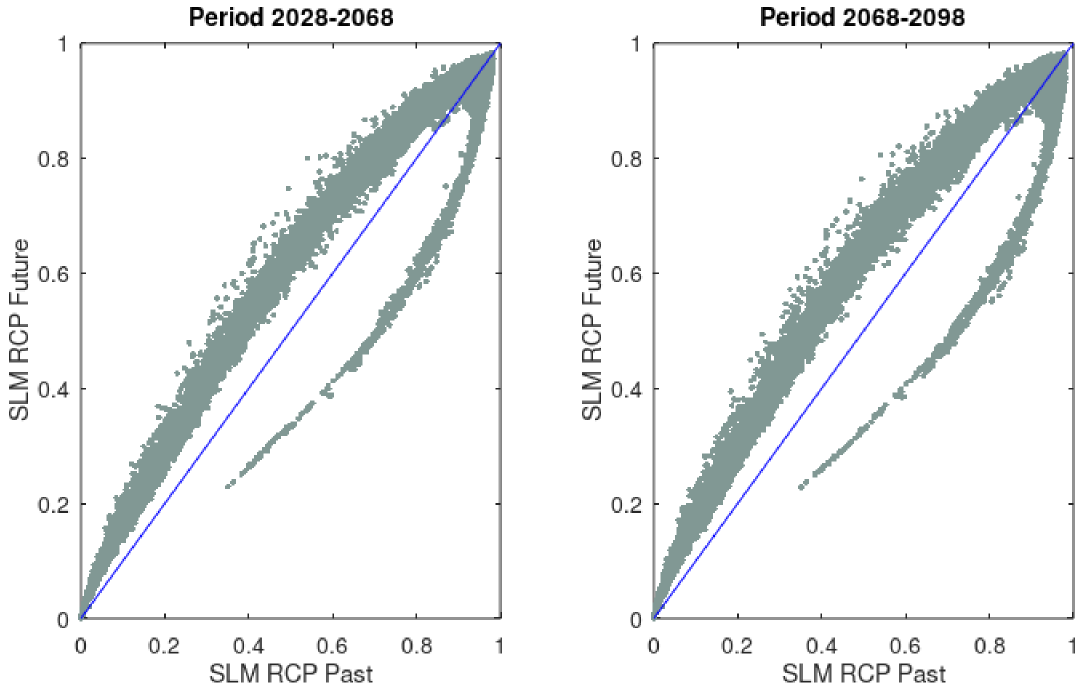

Apple: GDD suitability score RCP 2.6

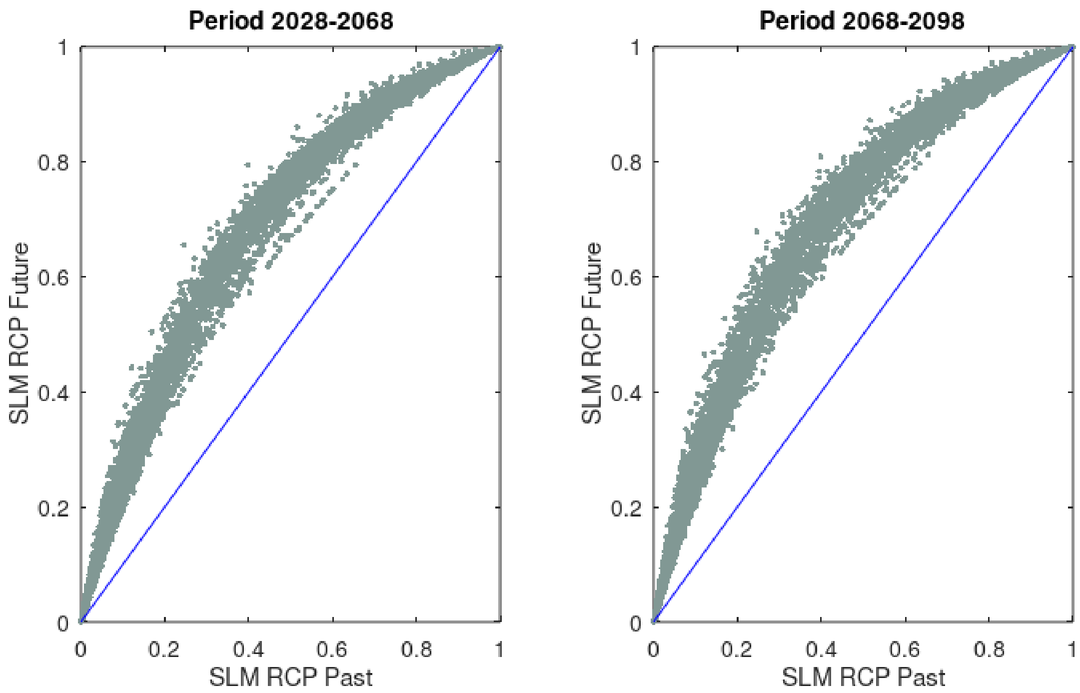

Apple: sunburn survival suitability score RCP 2.6

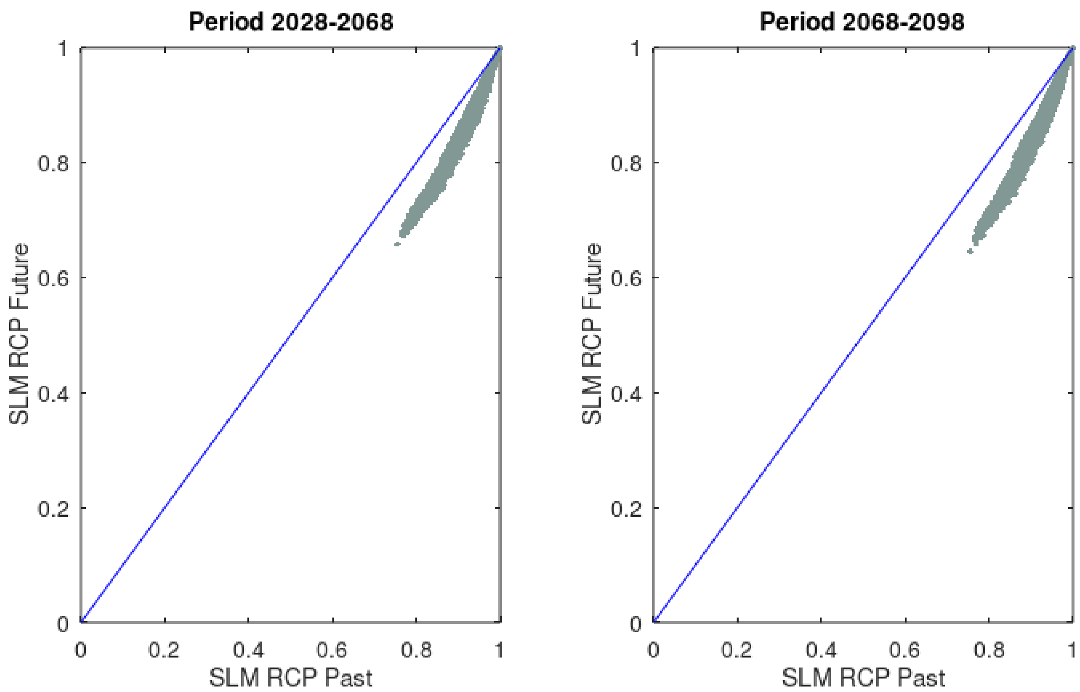

2 Apple RCP 4.5

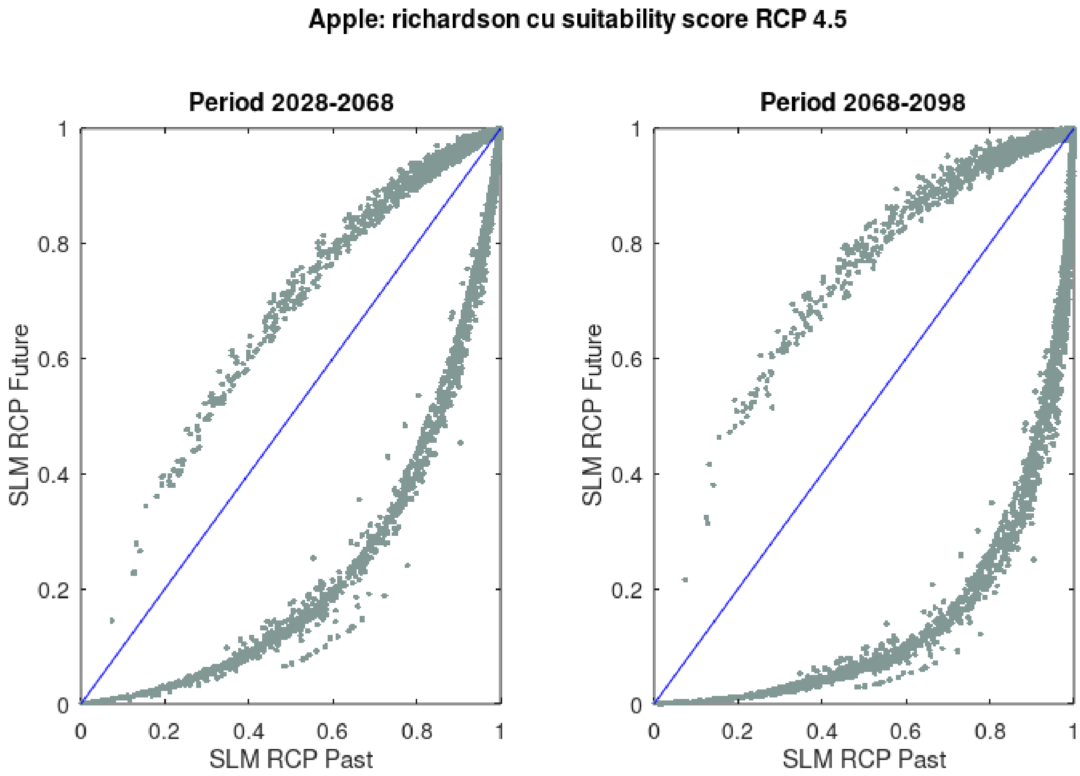

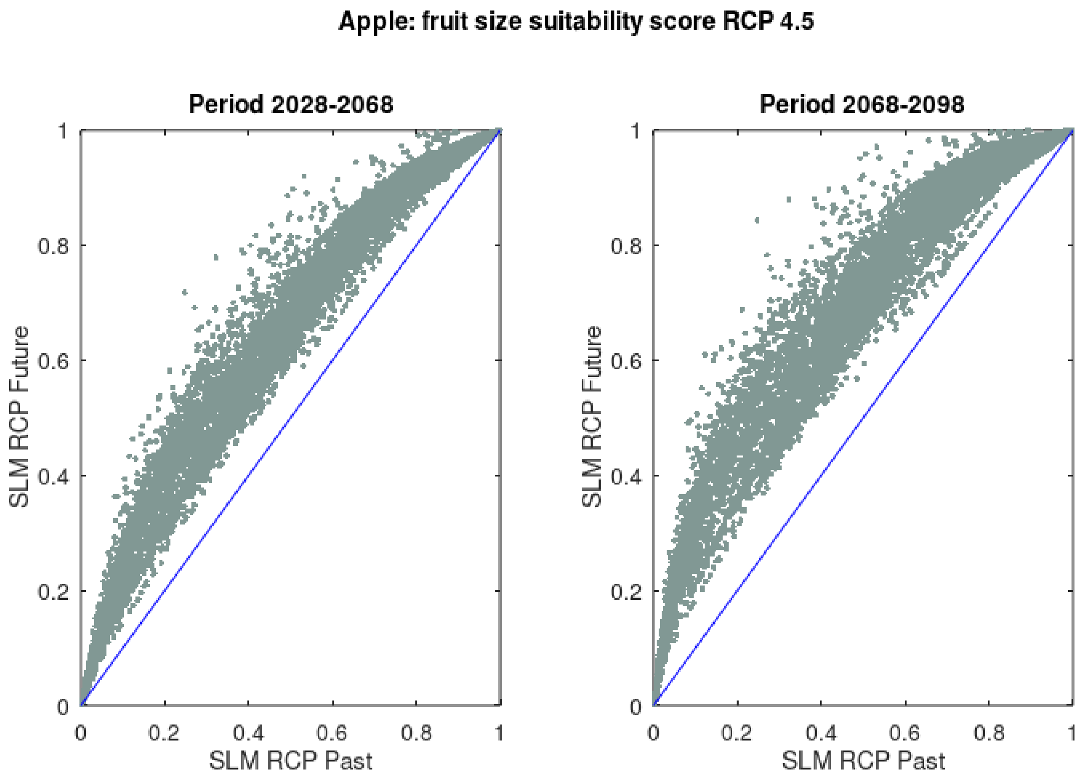

Apple: frost survival suitability score RCP 4.5

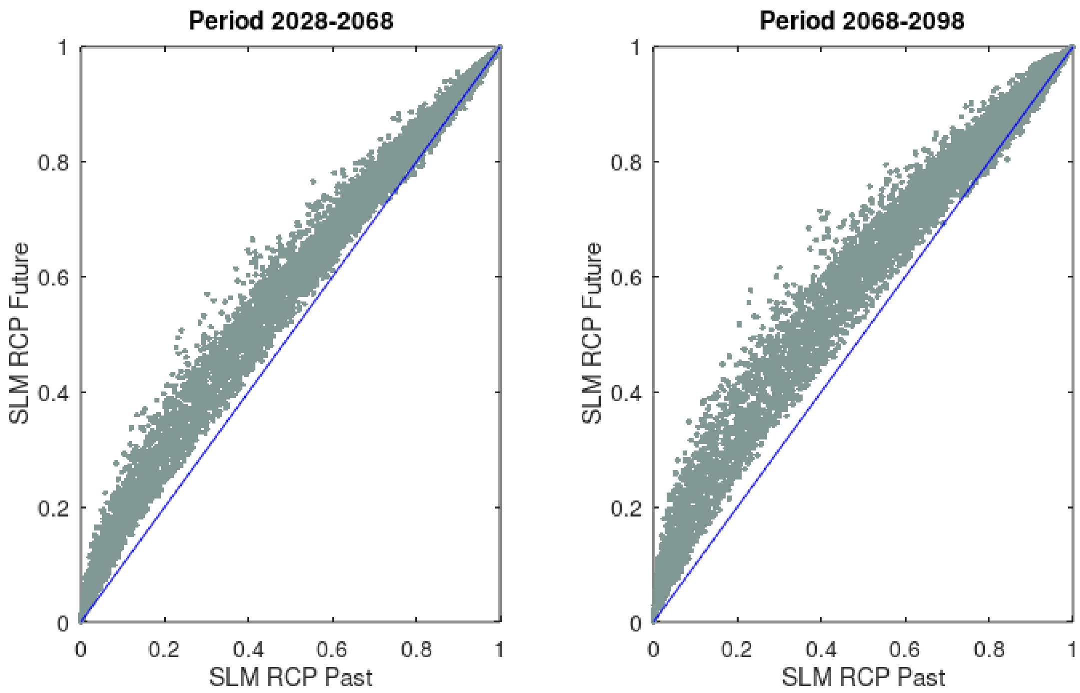

Apple: climate suitability score RCP 4.5

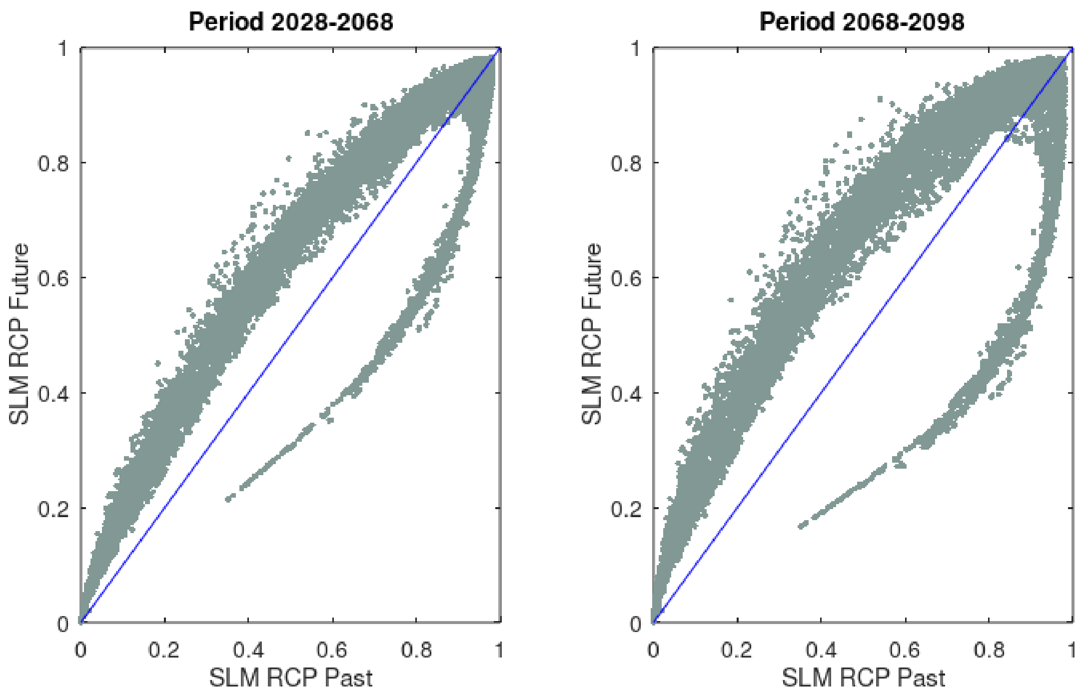

Apple: GDD suitability score RCP 4.5

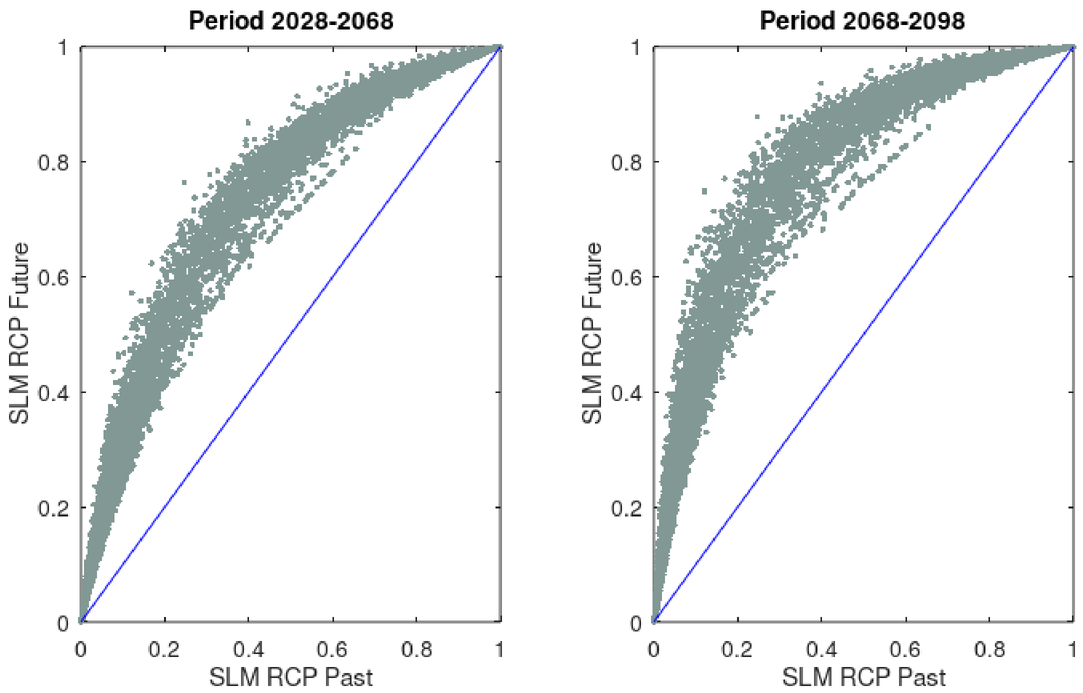

Apple: sunburn survival suitability score RCP 4.5

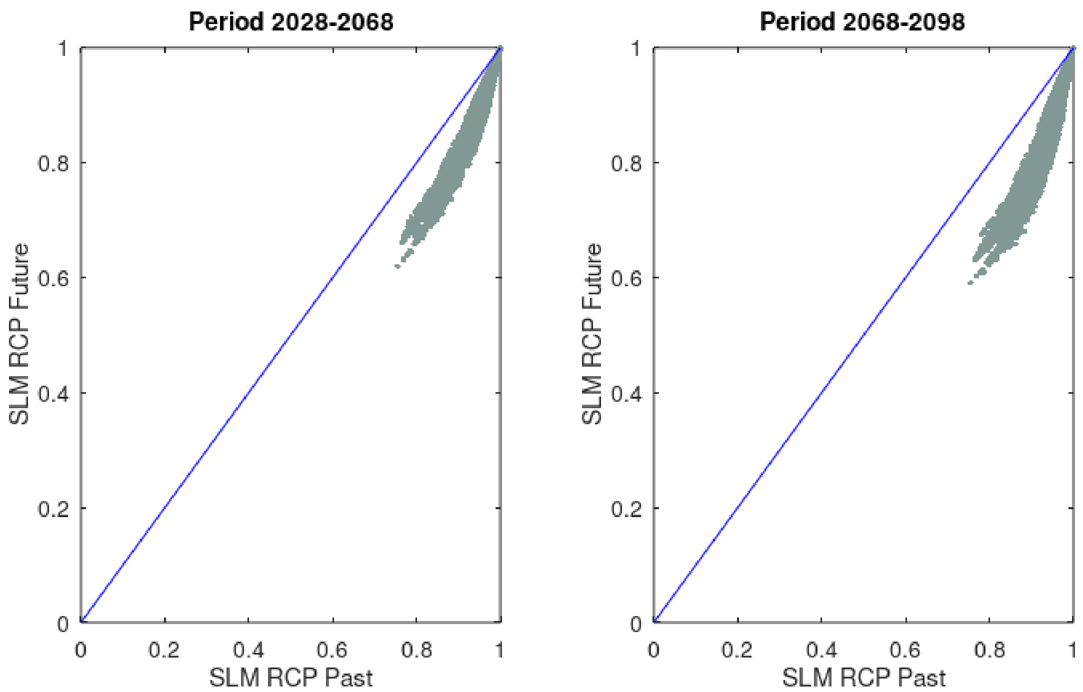

3 Apple RCP 6.0

Apple: richardson cu suitability score RCP 6.0

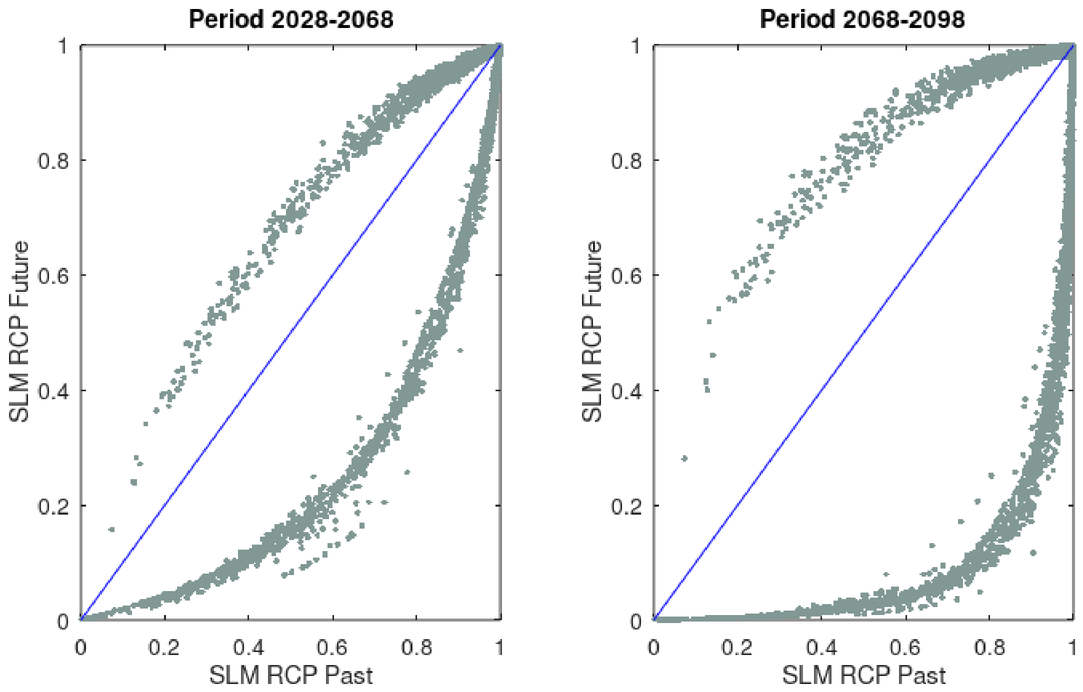

Apple: fruit size suitability score RCP 6.0

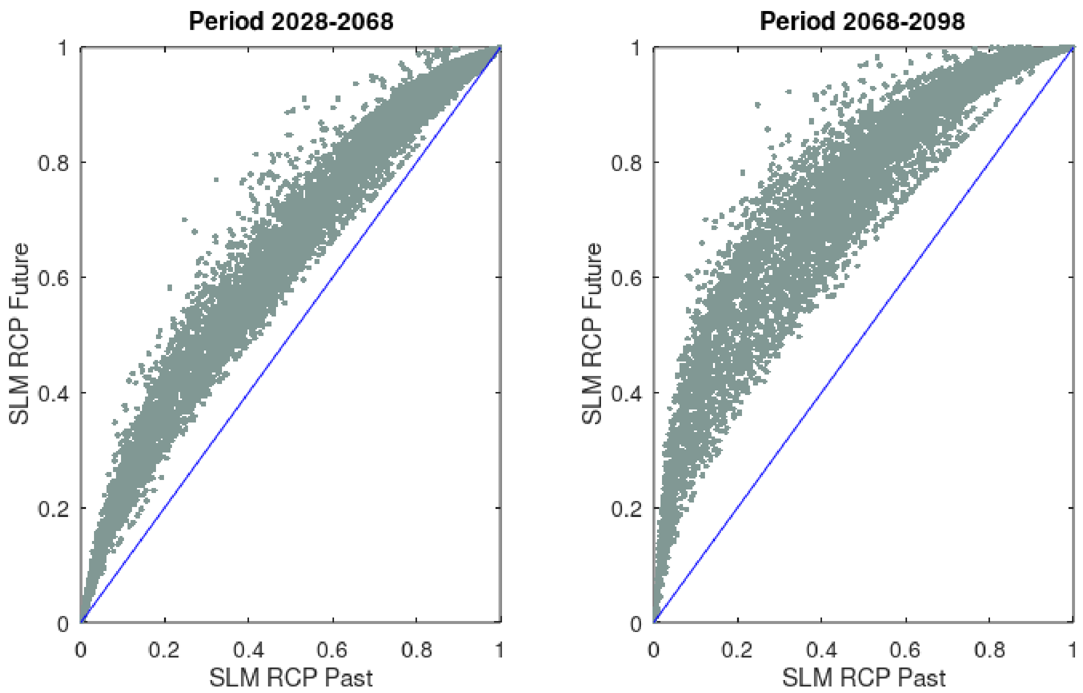

Apple: frost survival suitability score RCP 6.0

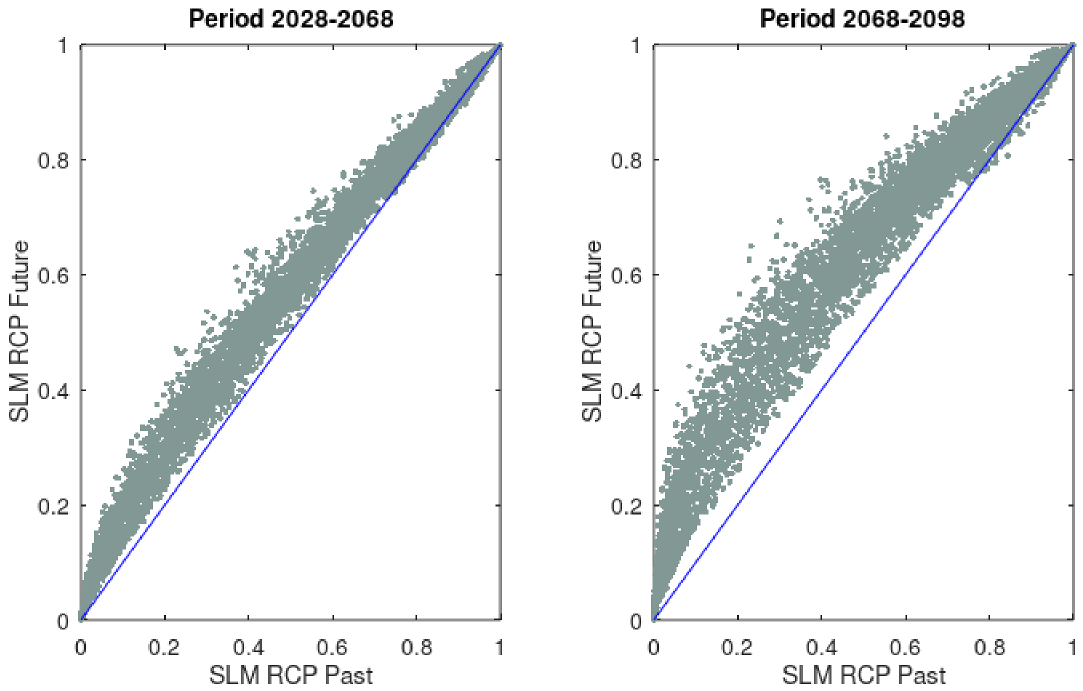

Apple: climate suitability score RCP 6.0

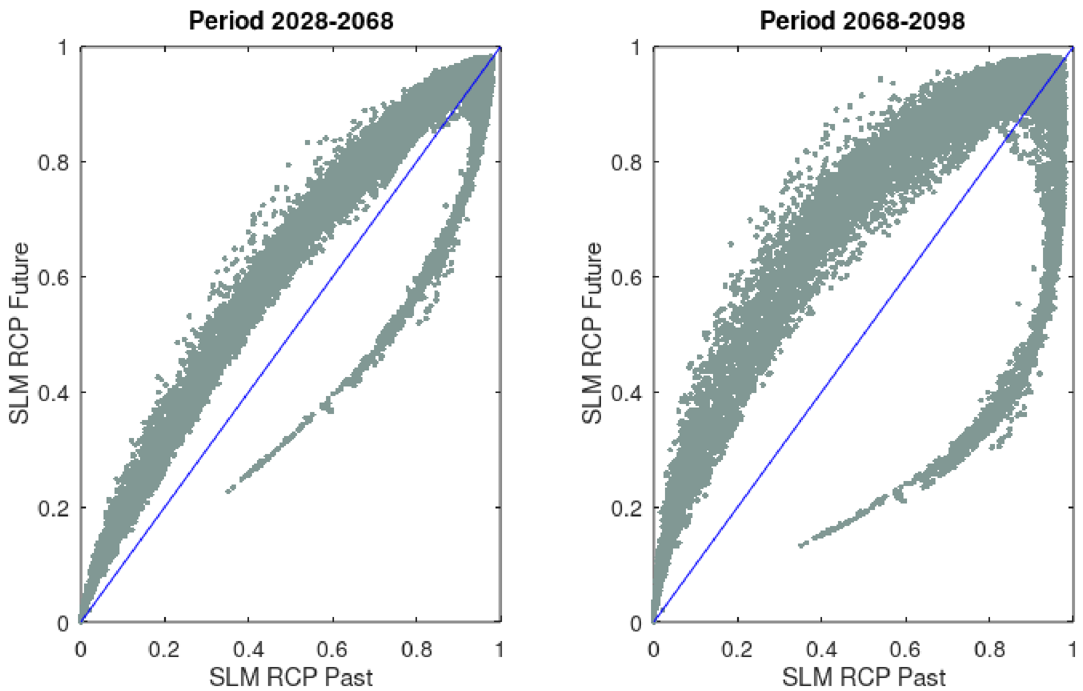

Apple: GDD suitability score RCP 6.0

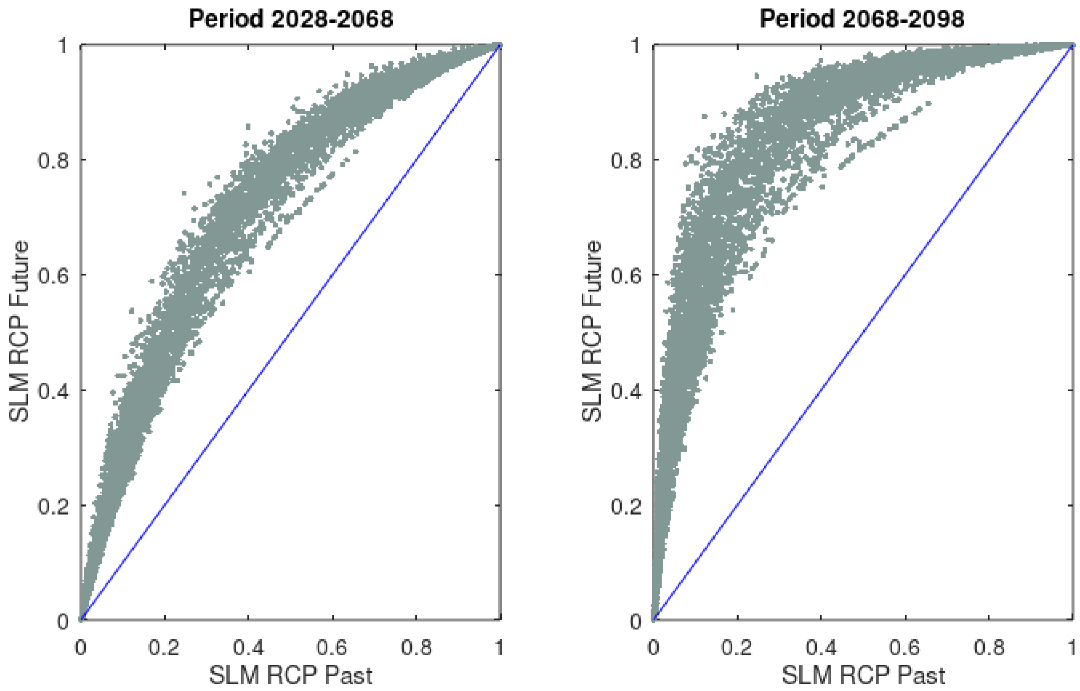

Apple: sunburn survival suitability score RCP 6.0

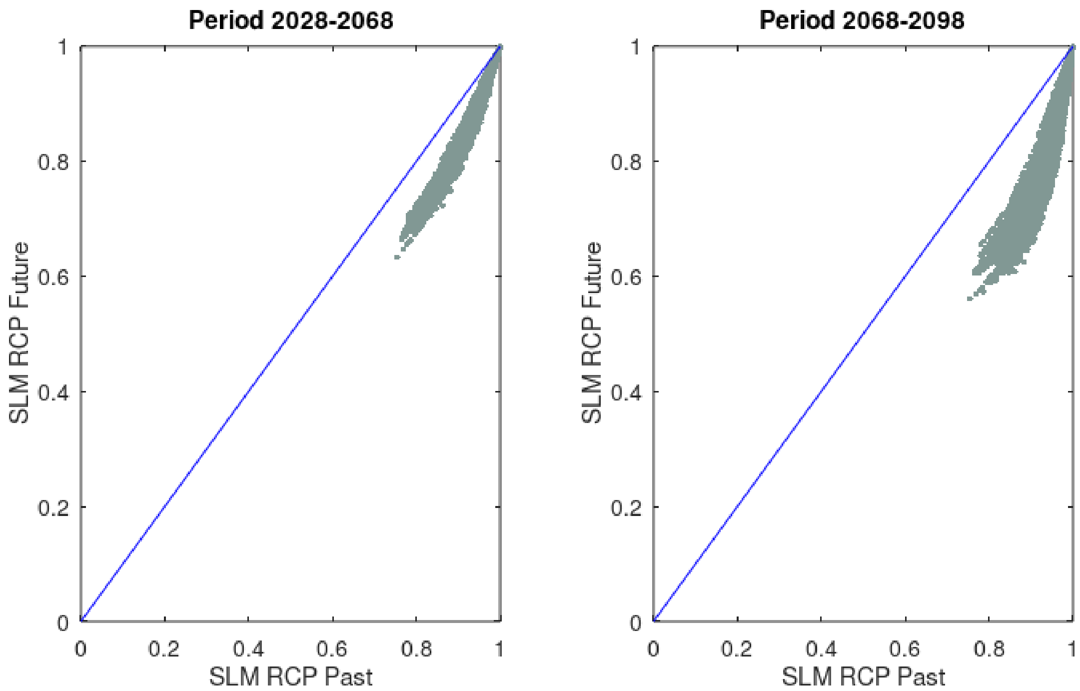

4 Apple RCP 8.5

Apple: richardson cu suitability score RCP 8.5

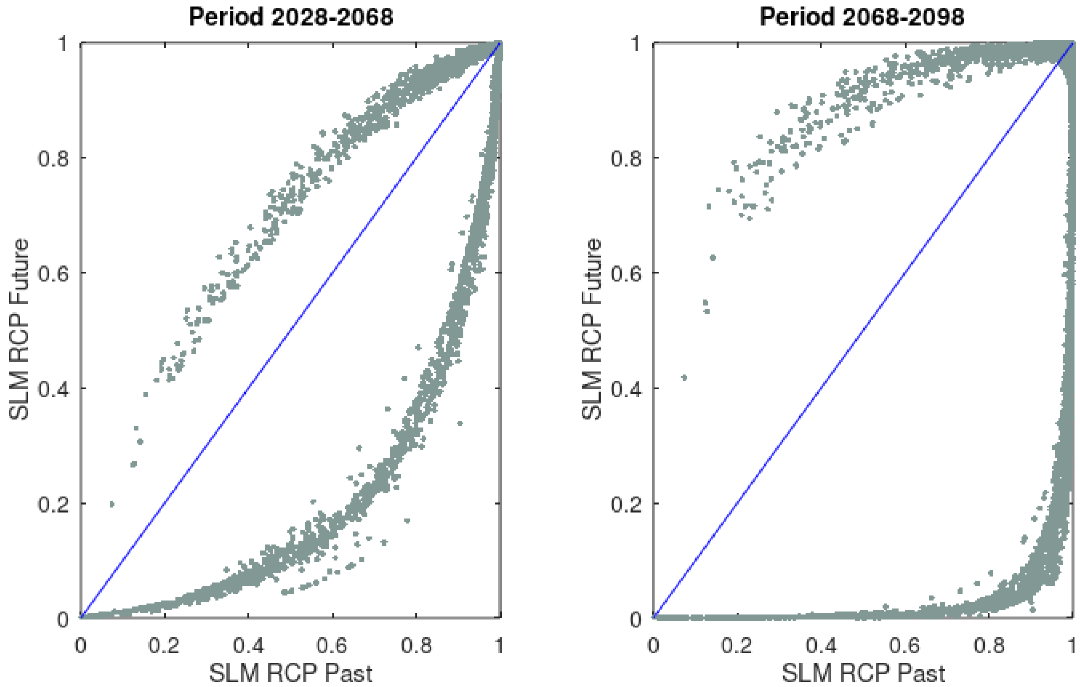

Apple: fruit size suitability score RCP 8.5

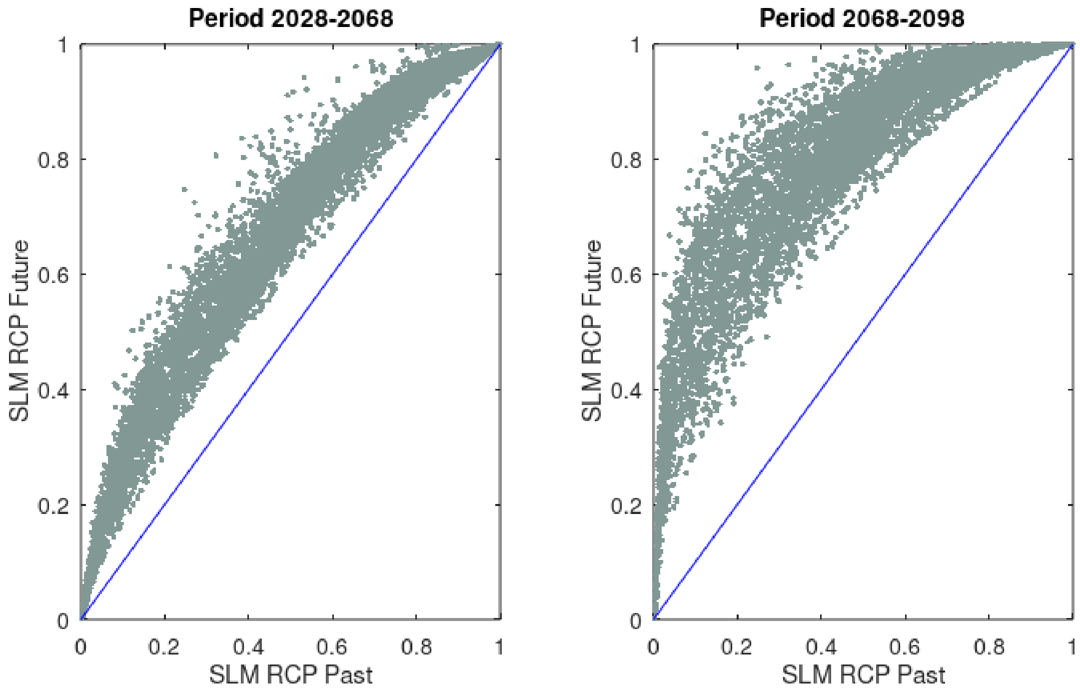

Apple: frost survival suitability score RCP 8.5

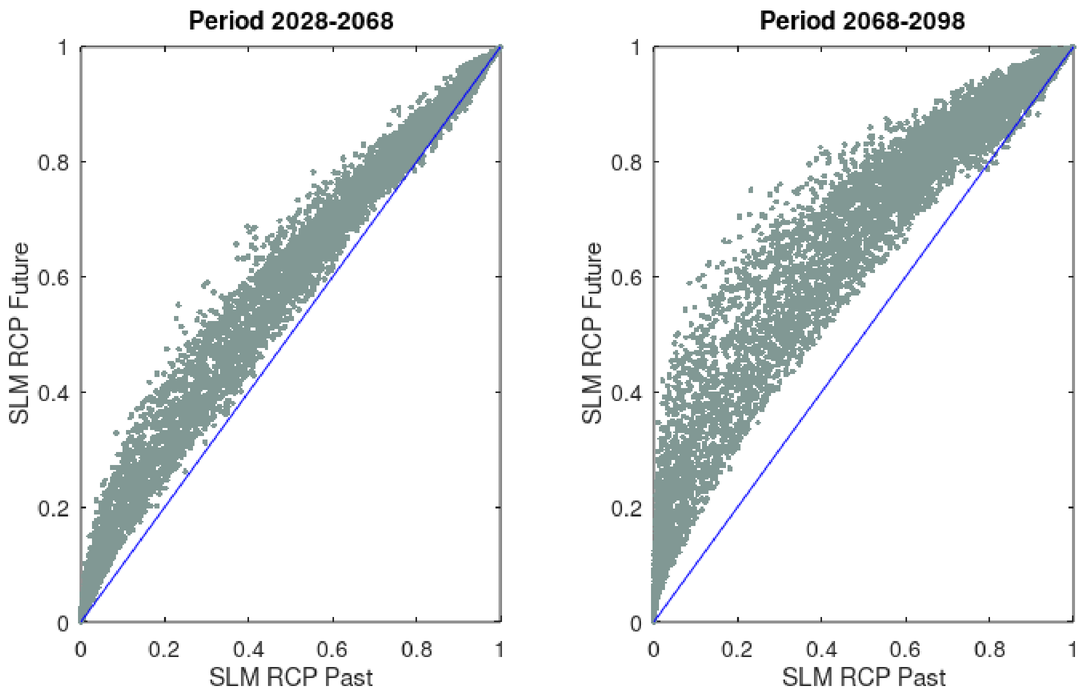

Apple: climate suitability score RCP 8.5

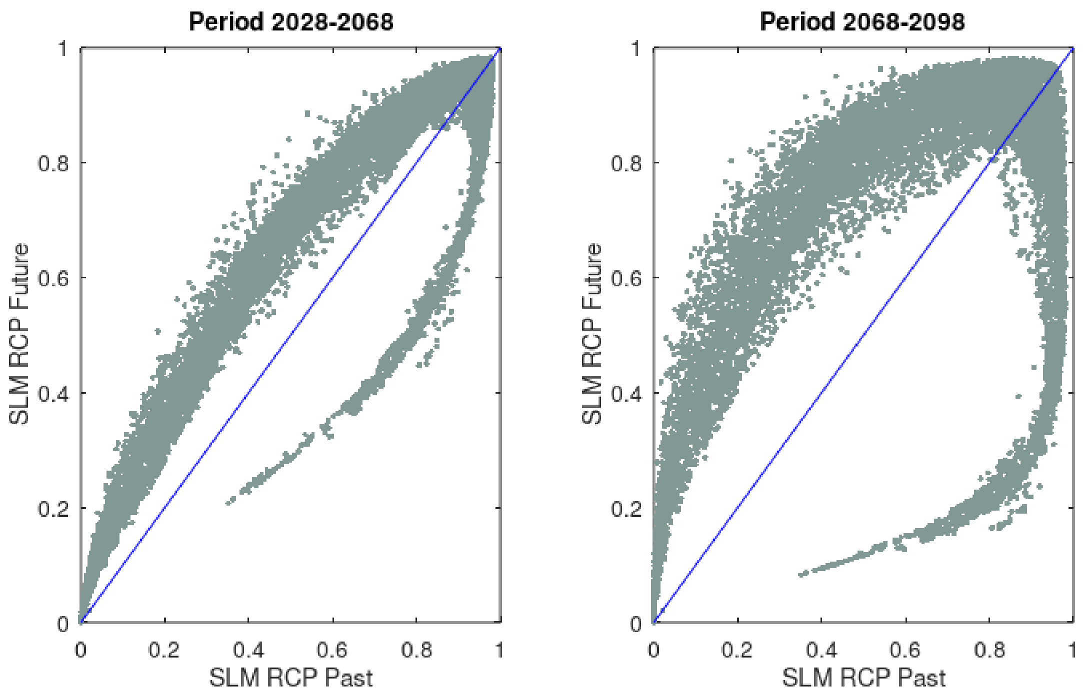

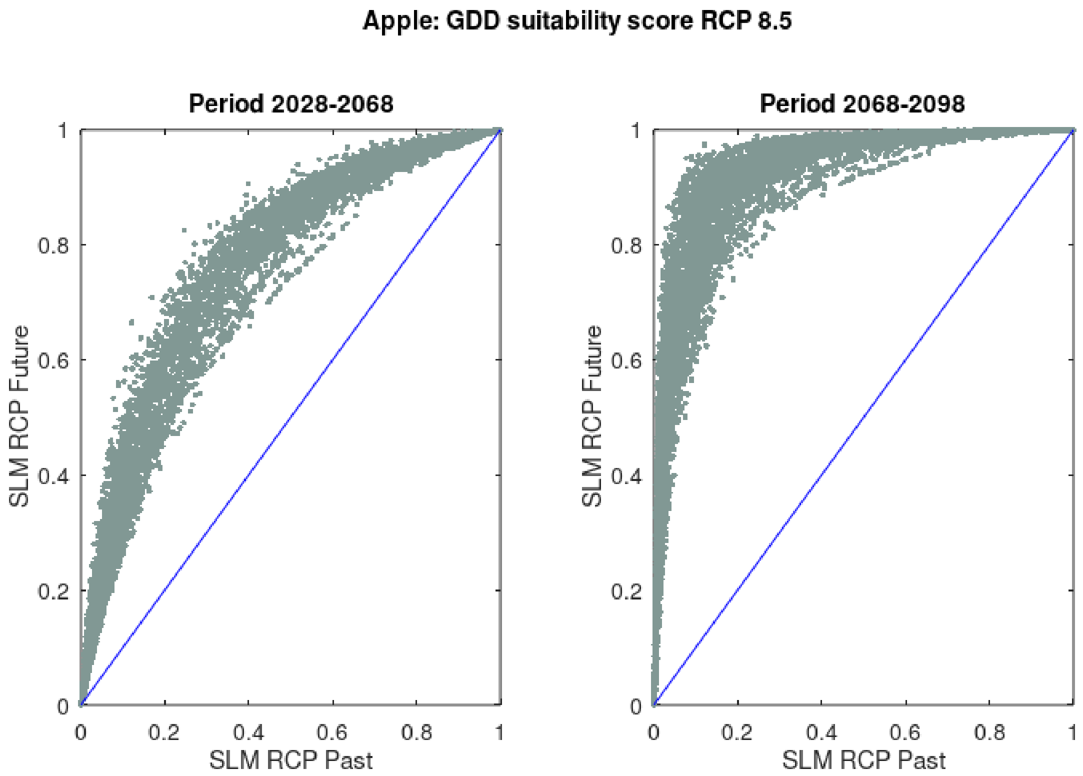
Apple: GDD suitability score RCP 8.5
Period 2028-2068
Period 2068-2098
SLM RCP Future
SLM RCP Past
0
0.2
0.4
0.6
0.8
1

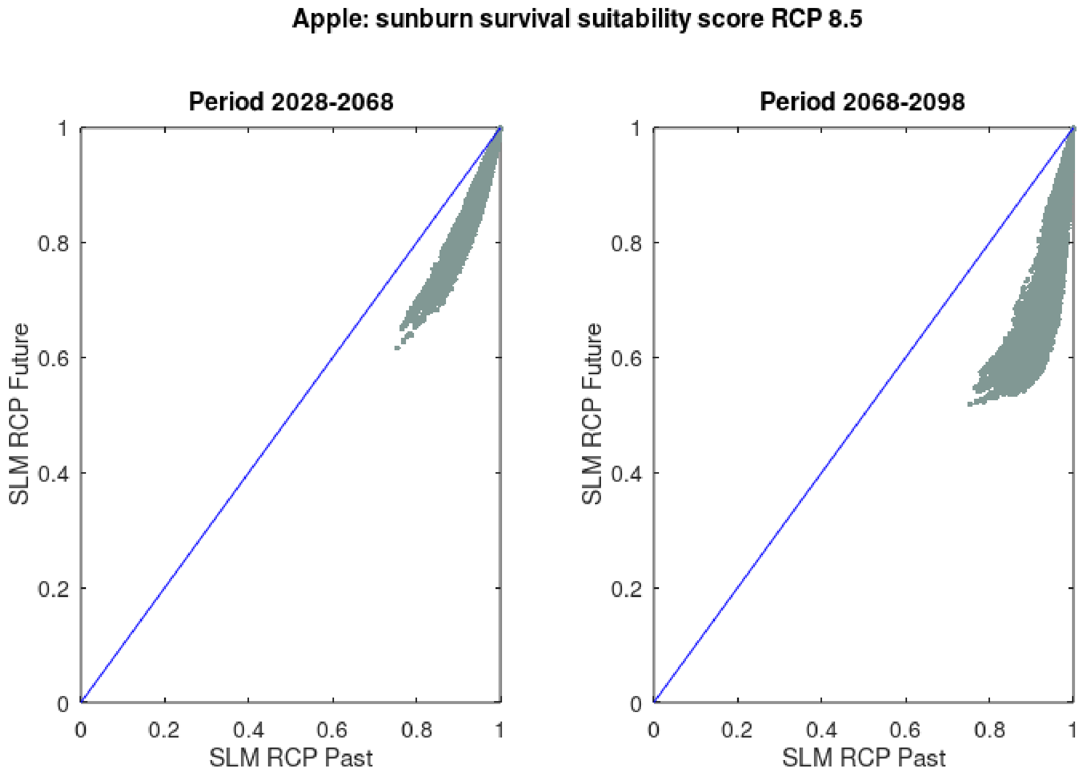
Apple: sunburn survival suitability score RCP 8.5
Period 2028-2068
Period 2068-2098
SLM RCP Future
SLM RCP Past
0
0.2
0.4
0.6
0.8
1

5 Kiwifruit RCP 2.6

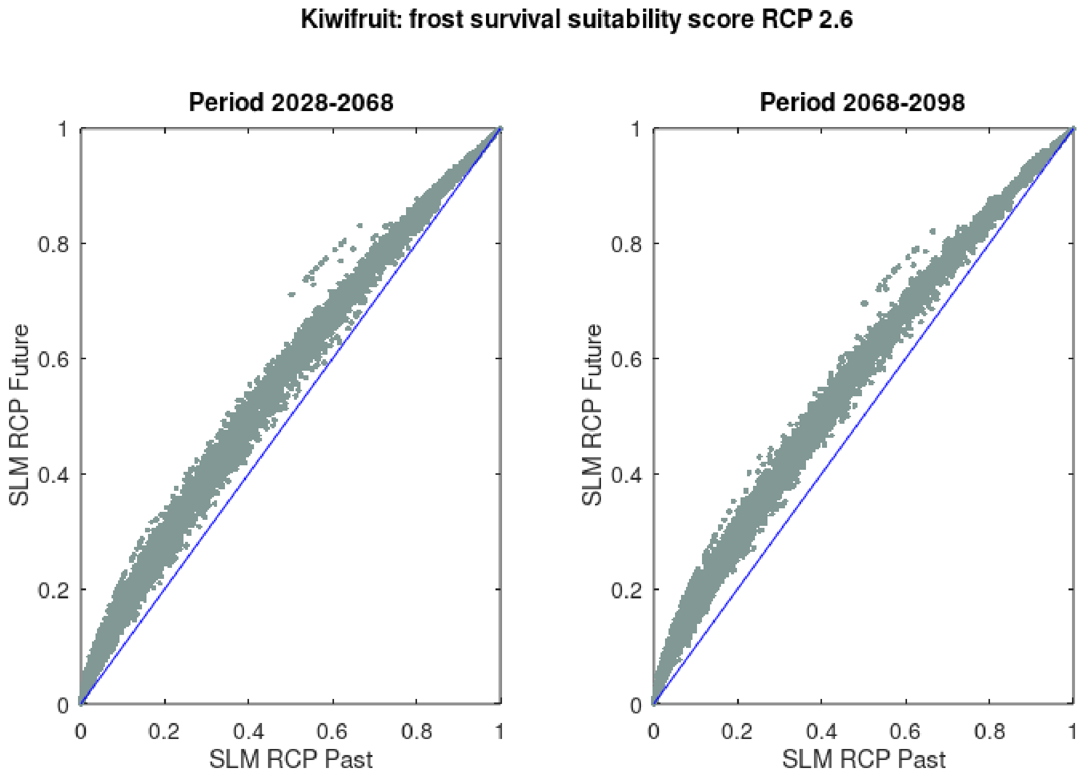

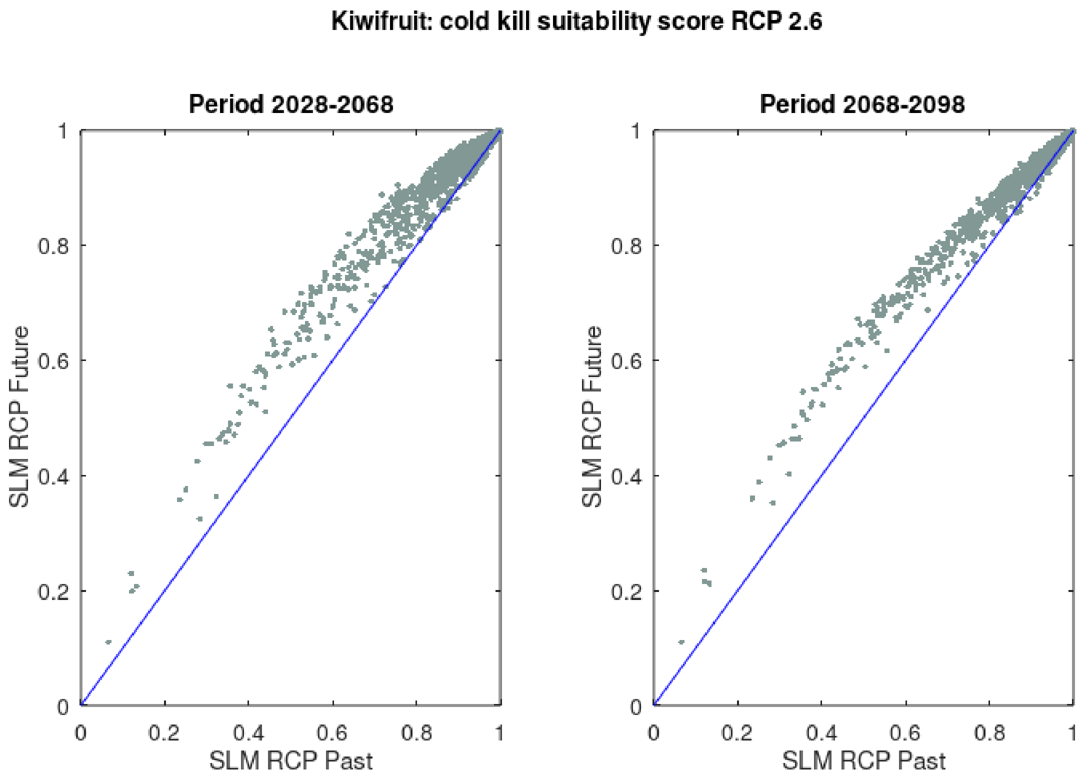

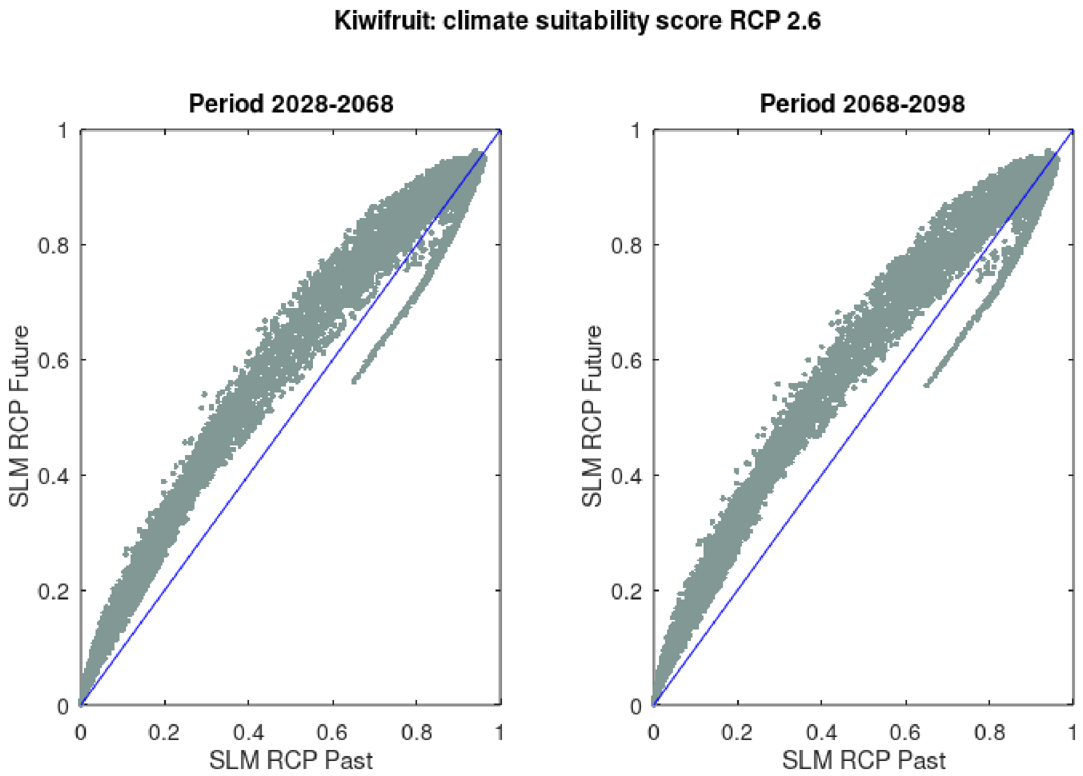
Kiwifruit: climate suitability score RCP 2.6
Period 2028-2068
Period 2068-2098
SLM RCP Future
SLM RCP Past
0
0.2
0.4
0.6
0.8
1

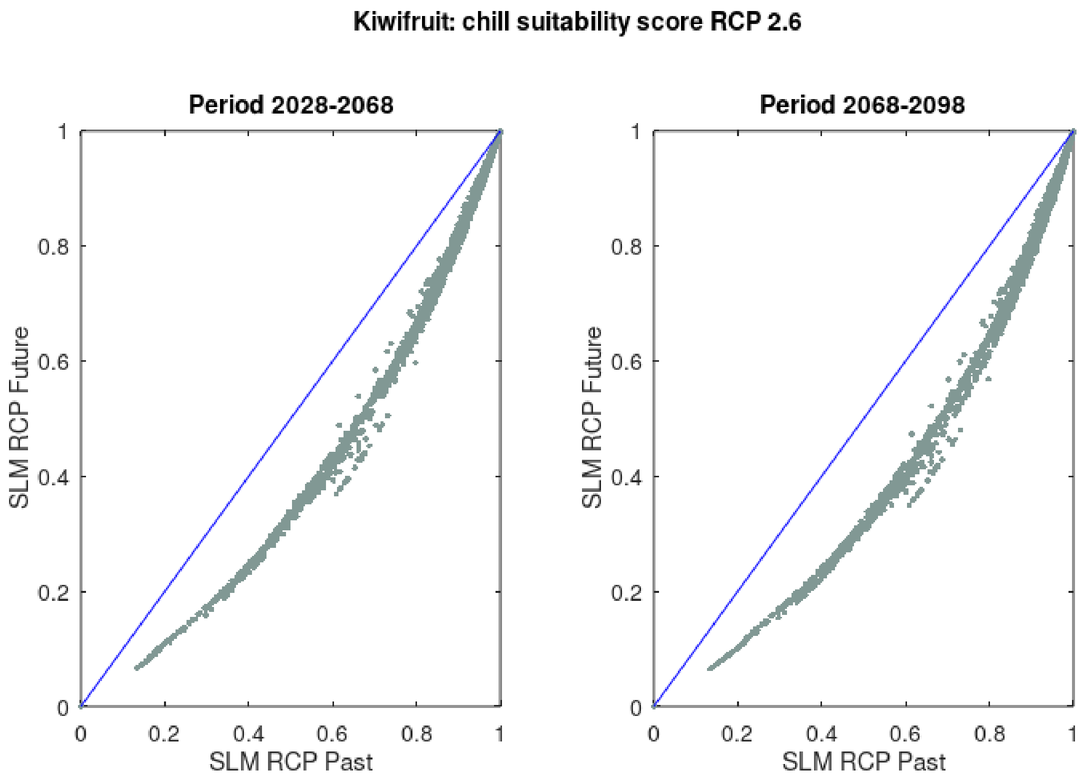
Kiwifruit: chill suitability score RCP 2.6
Period 2028-2068
Period 2068-2098
SLM RCP Future
SLM RCP Past
0
0.2
0.4
0.6
0.8
1

Kiwifruit: GDD suitability score RCP 2.6

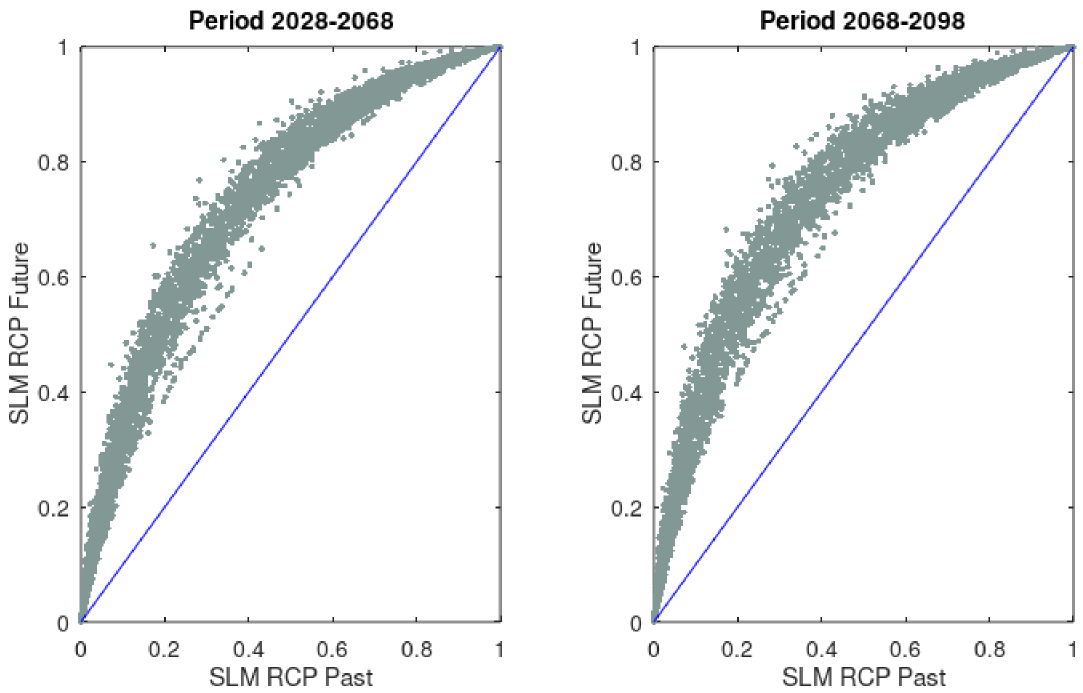

6 Kiwifruit RCP 4.5

Kiwifruit: frost survival suitability score RCP 4.5

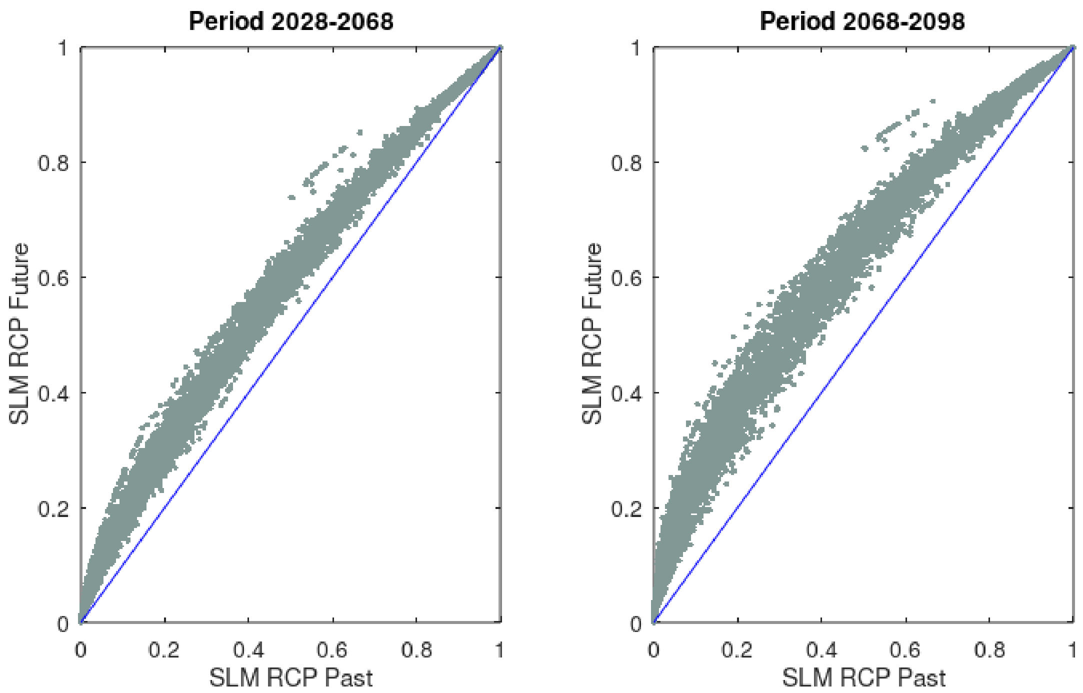

Kiwifruit: cold kill suitability score RCP 4.5

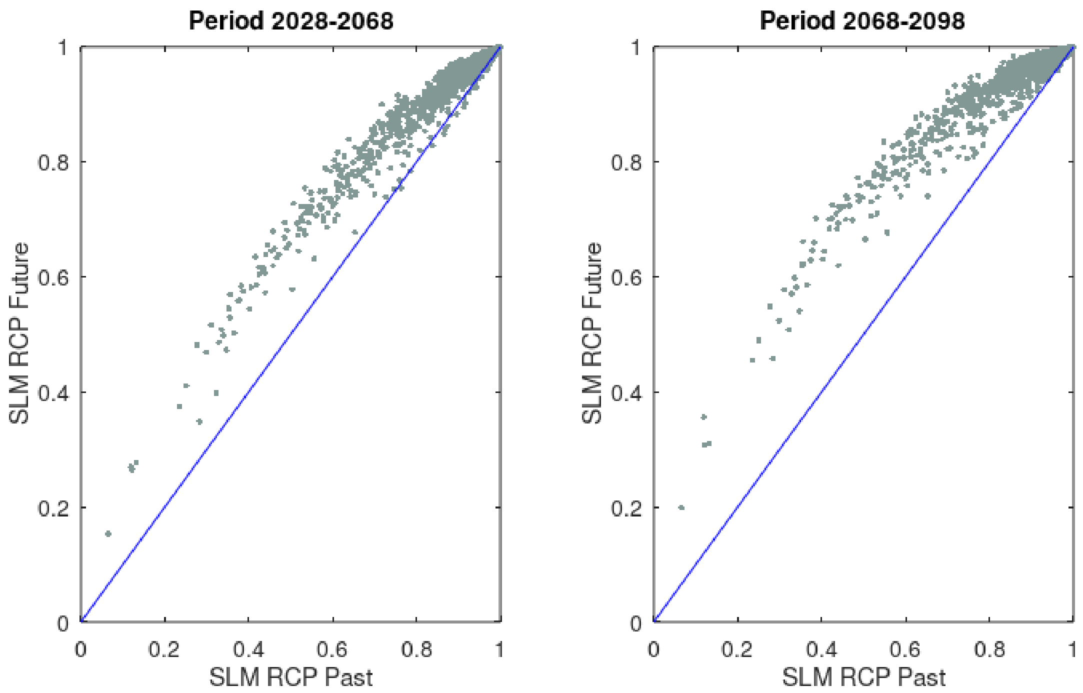

Kiwifruit: climate suitability score RCP 4.5

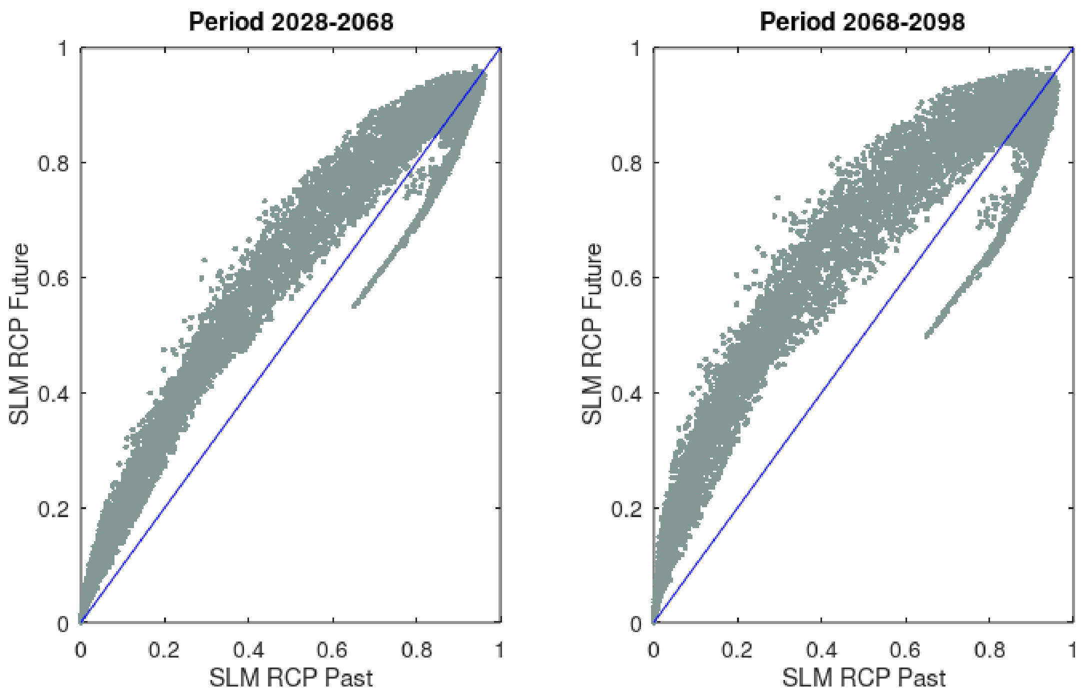

Kiwifruit: chill suitability score RCP 4.5

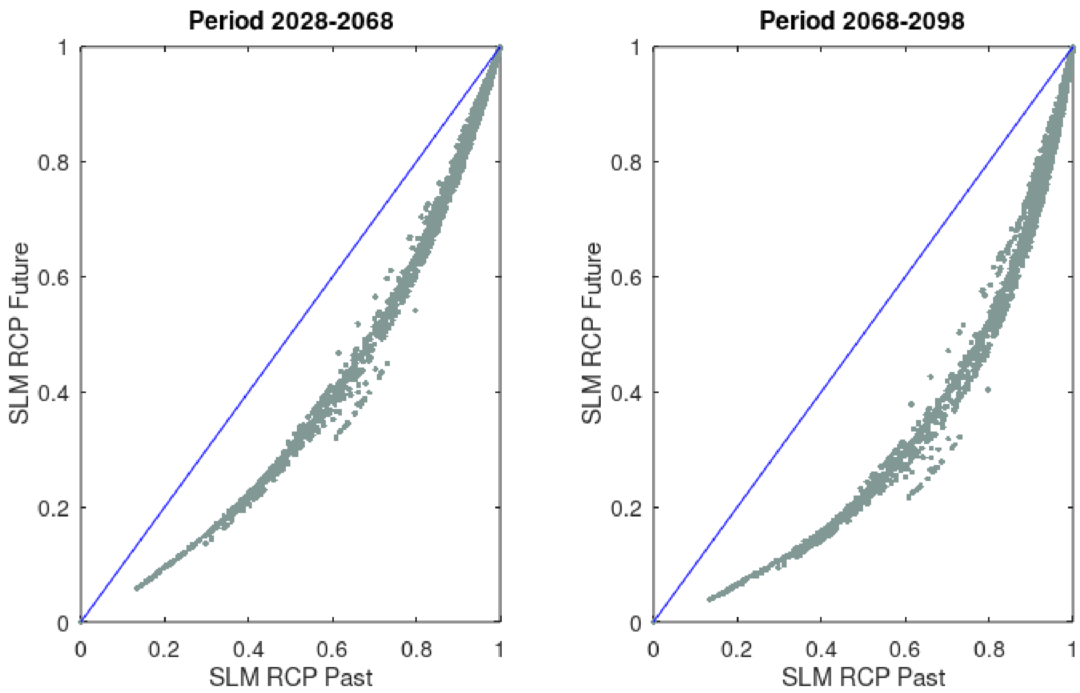

Kiwifruit: GDD suitability score RCP 4.5

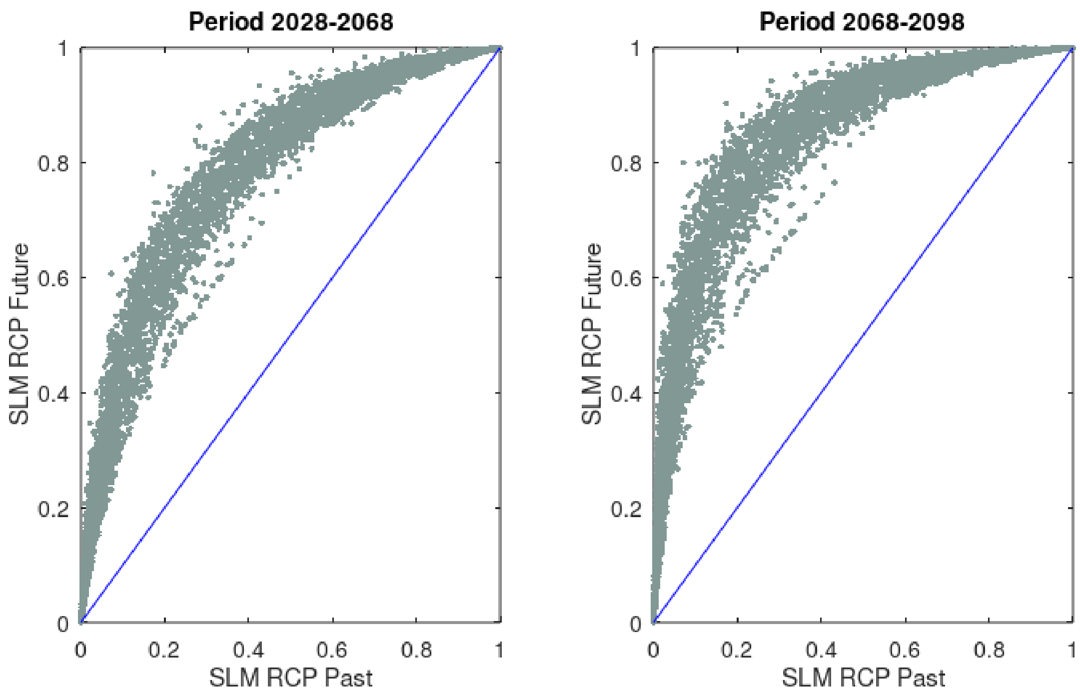

7 Kiwifruit RCP 6.0

Kiwifruit: cold kill suitability score RCP 6.0

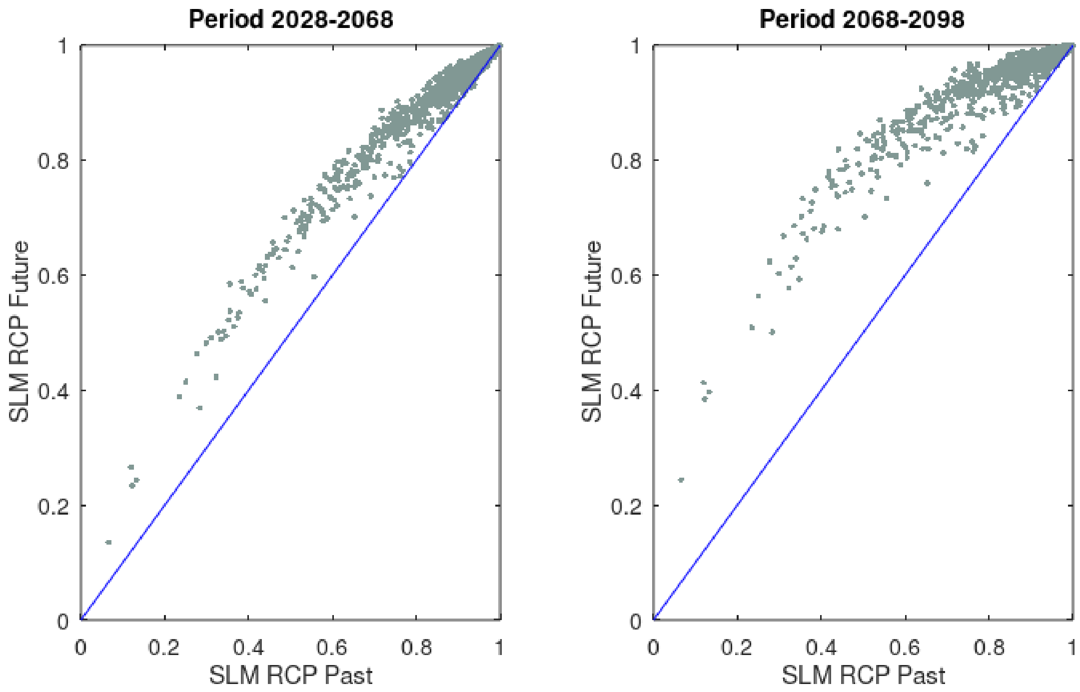

Kiwifruit: climate suitability score RCP 6.0

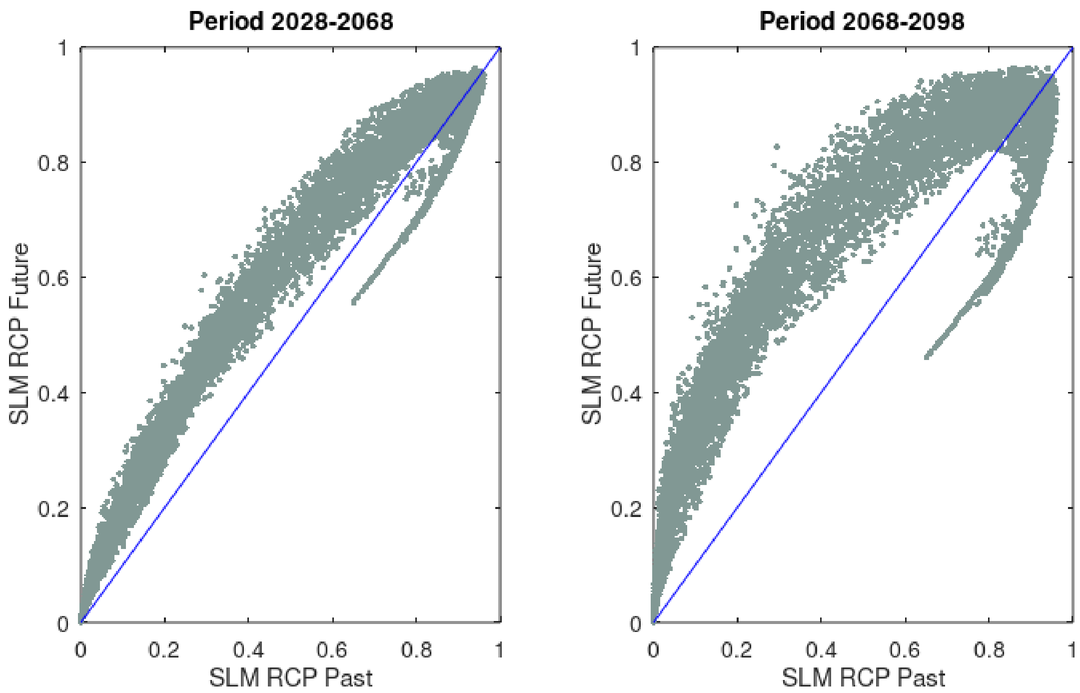

Kiwifruit: chill suitability score RCP 6.0

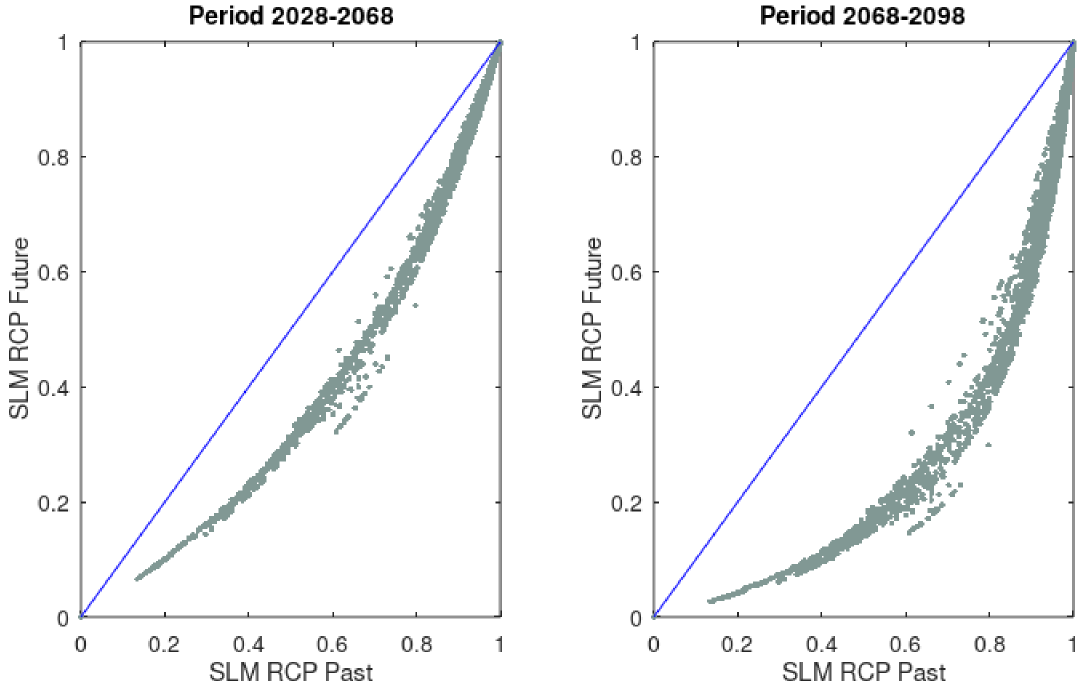

Kiwifruit: GDD suitability score RCP 6.0

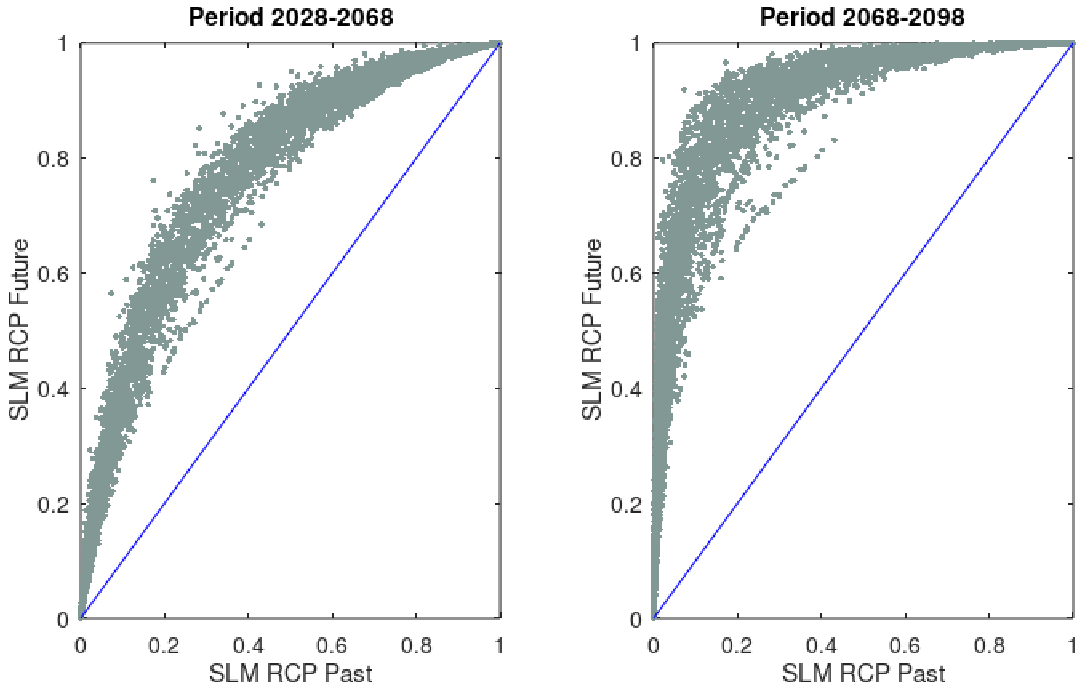

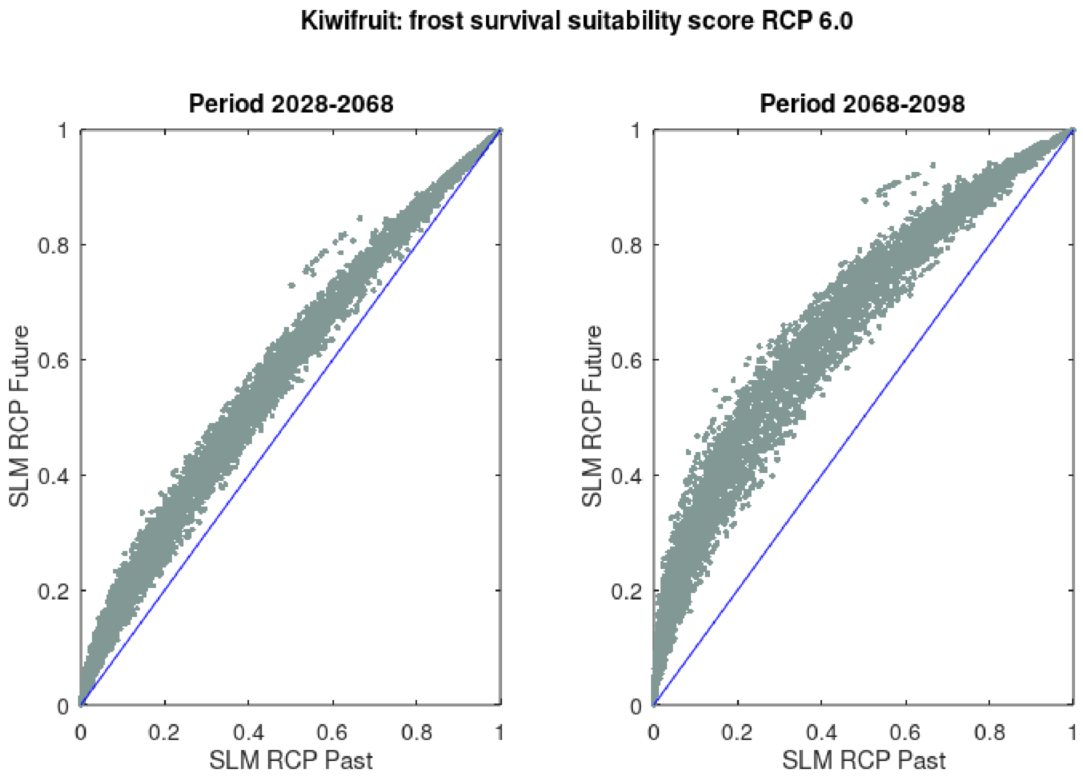

8 Kiwifruit RCP 8.5

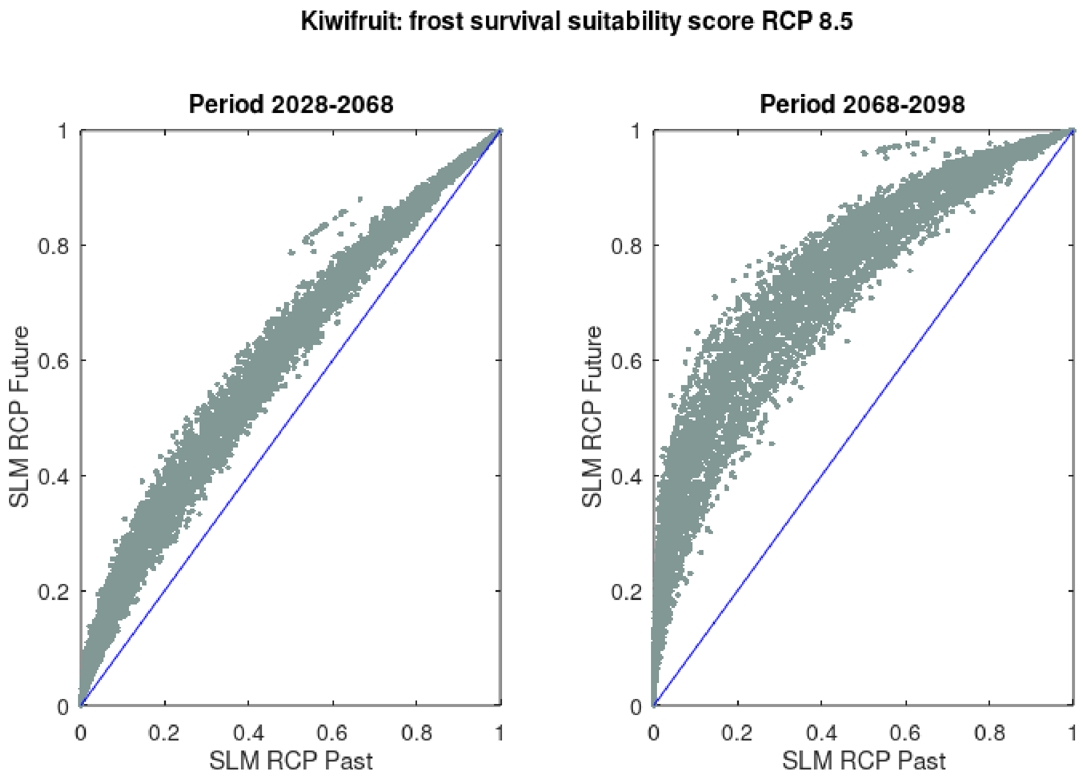

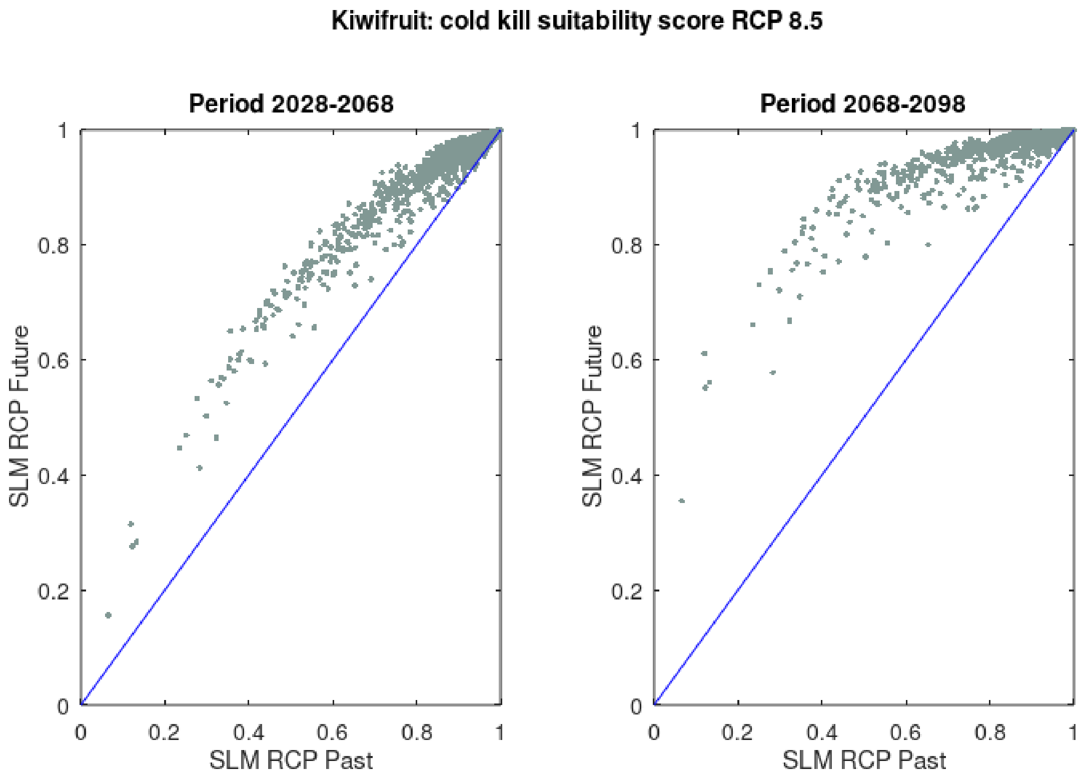
Kiwifruit: cold kill suitability score RCP 8.5
Period 2028-2068
Period 2068-2098
SLM RCP Future
SLM RCP Past
0
0.2
0.4
0.6
0.8
1

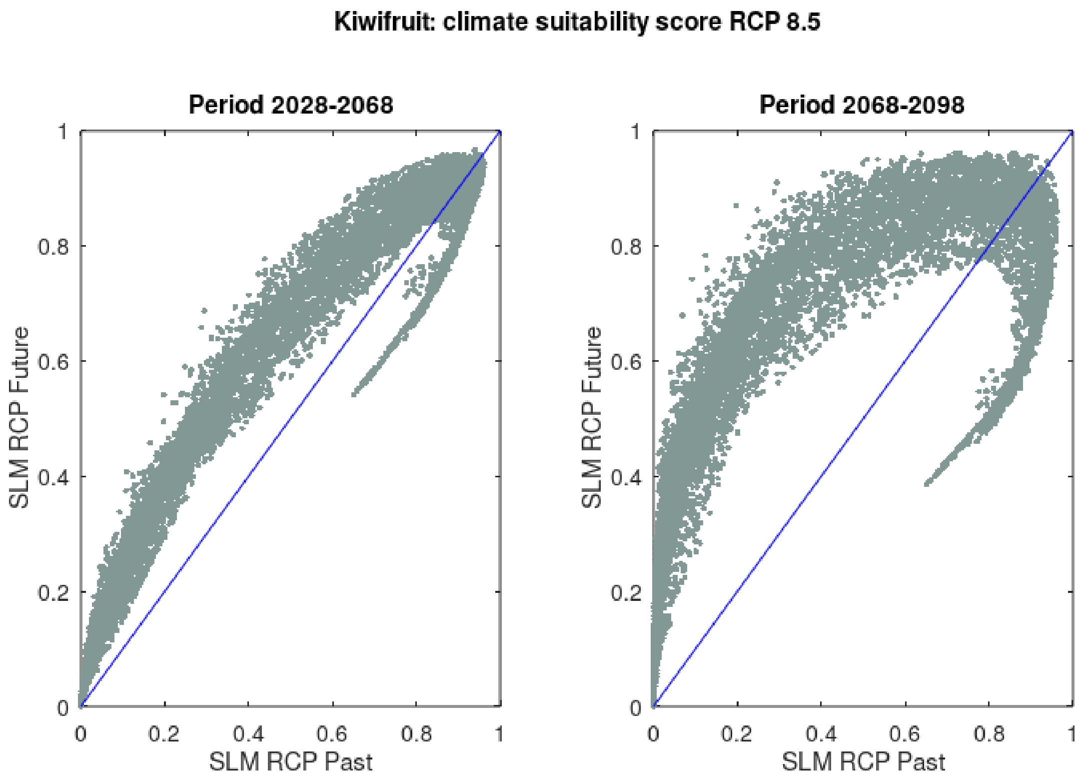
Kiwifruit: climate suitability score RCP 8.5
Period 2028-2068
Period 2068-2098
SLM RCP Future
SLM RCP Past
0
0.2
0.4
0.6
0.8
1

Kiwifruit: chill suitability score RCP 8.5

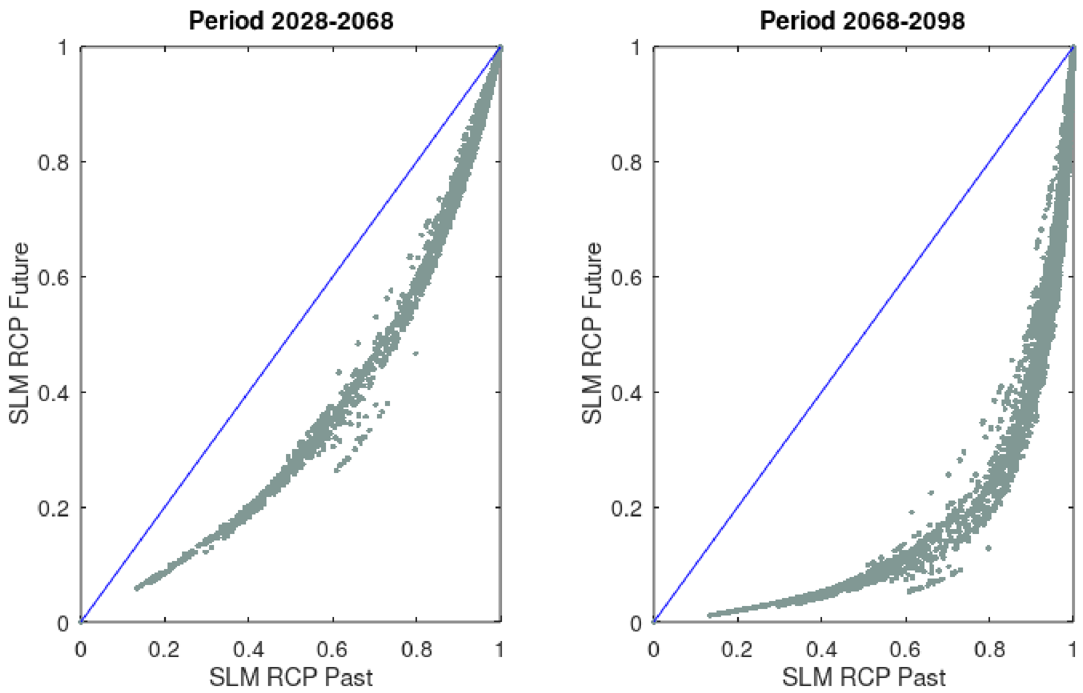

Kiwifruit: GDD suitability score RCP 8.5

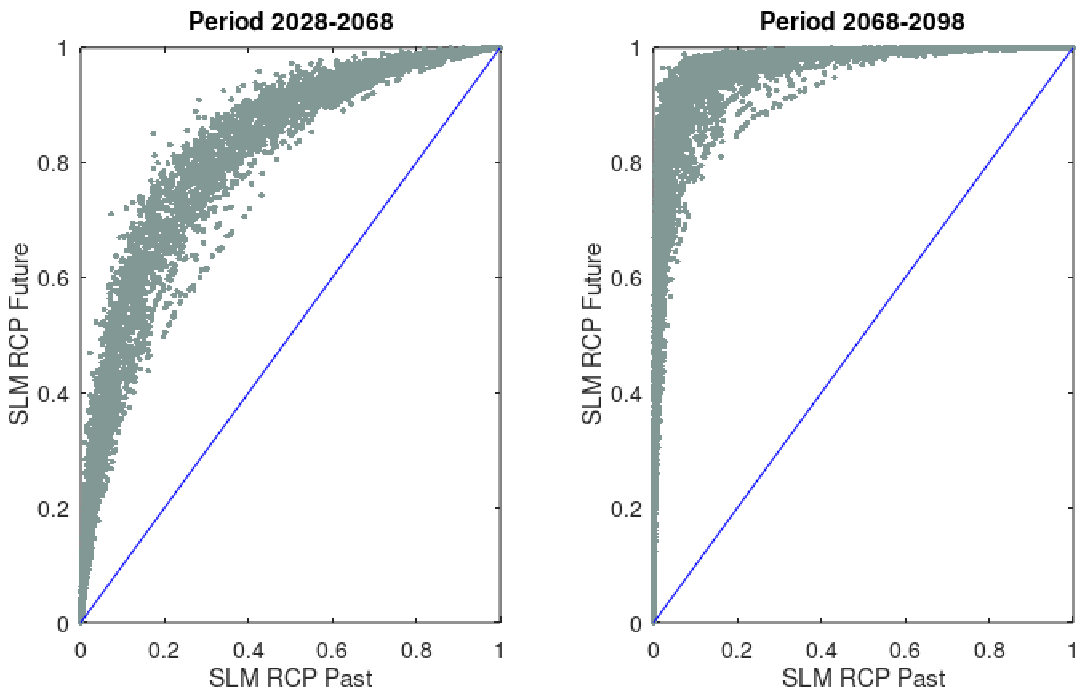

9 Avocado RCP 2.6

Avocado: frost survival suitability score RCP 2.6

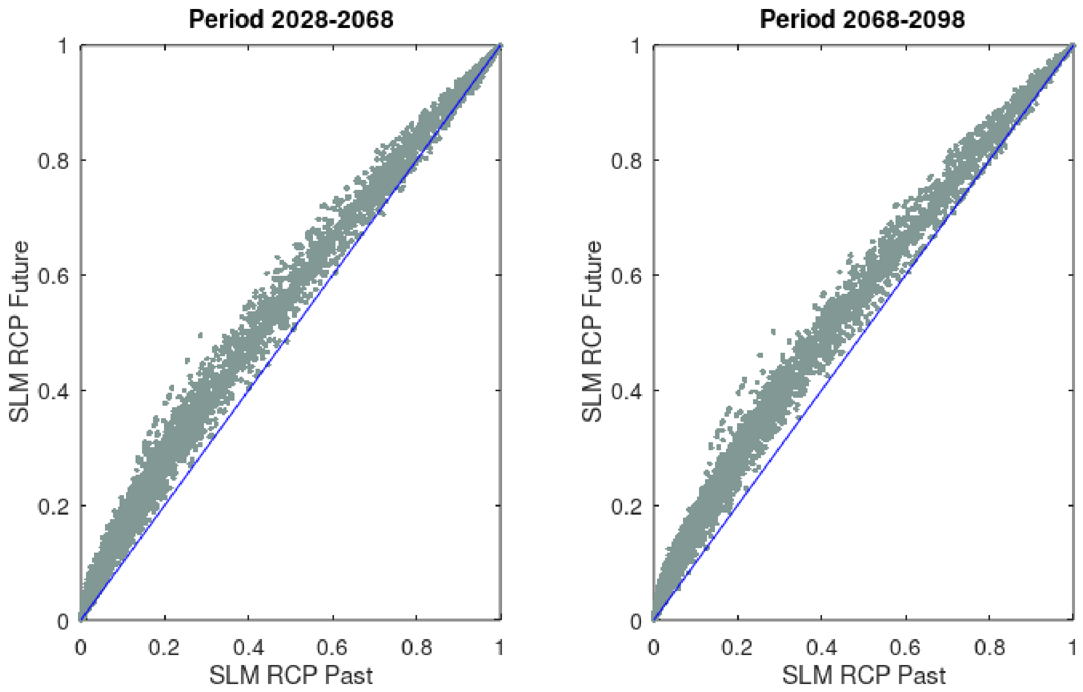

Avocado: climate suitability score RCP 2.6

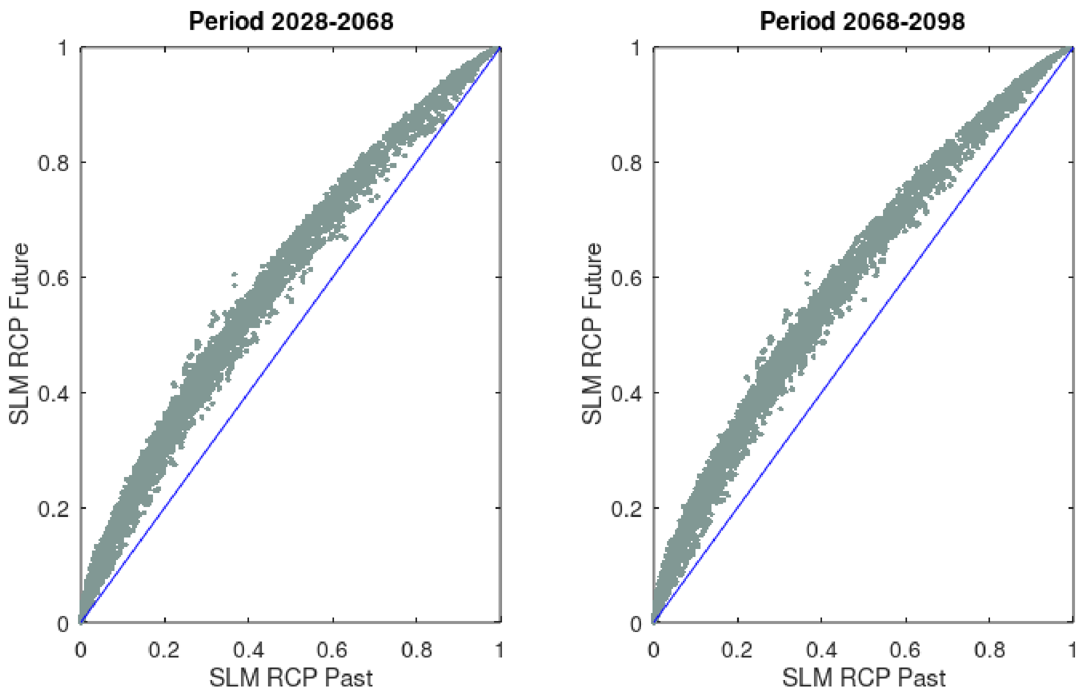

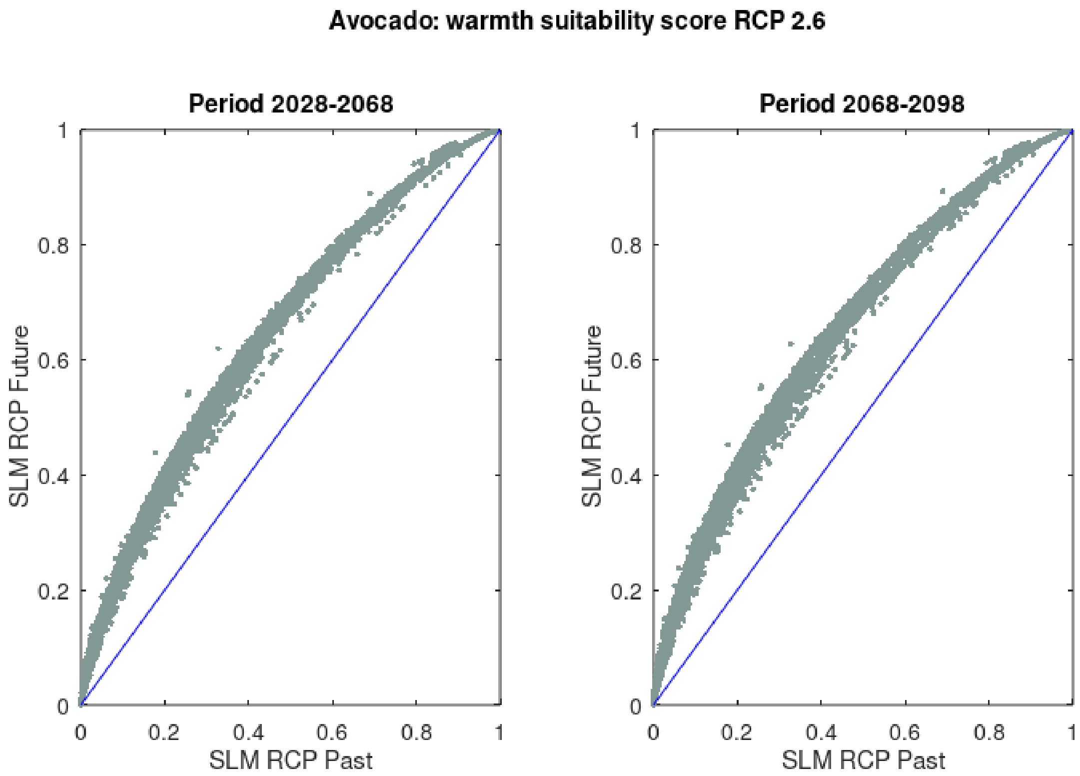

10 Avocado RCP 4.5

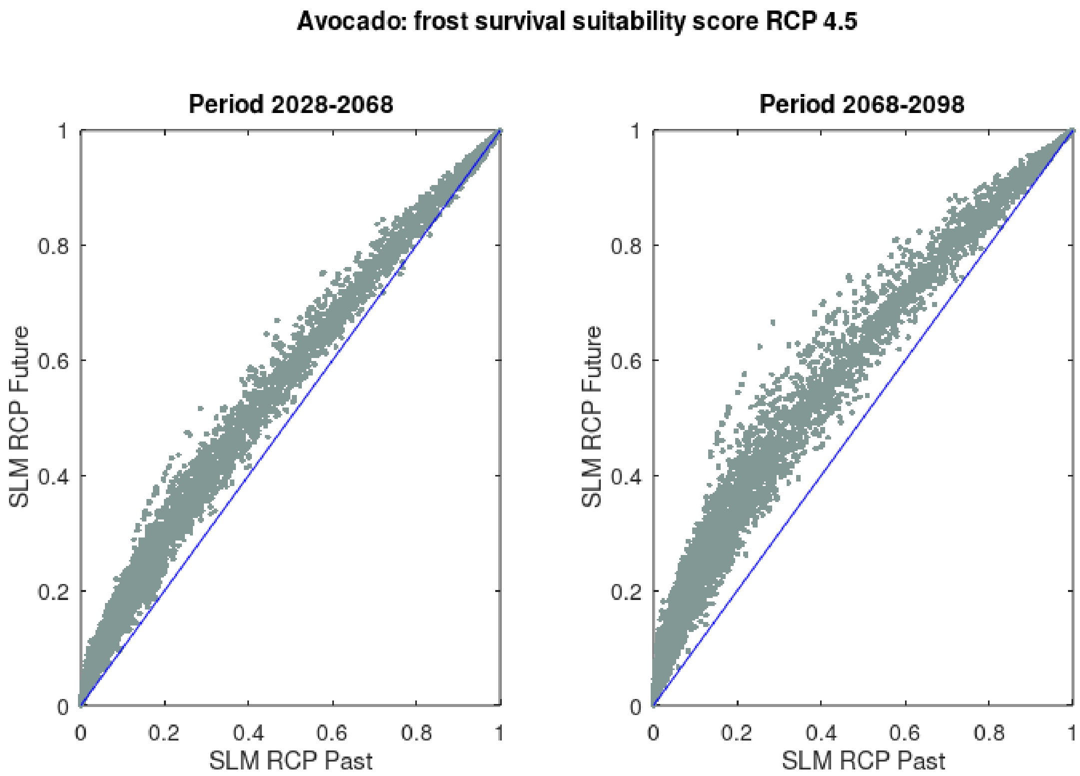

Avocado: climate suitability score RCP 4.5

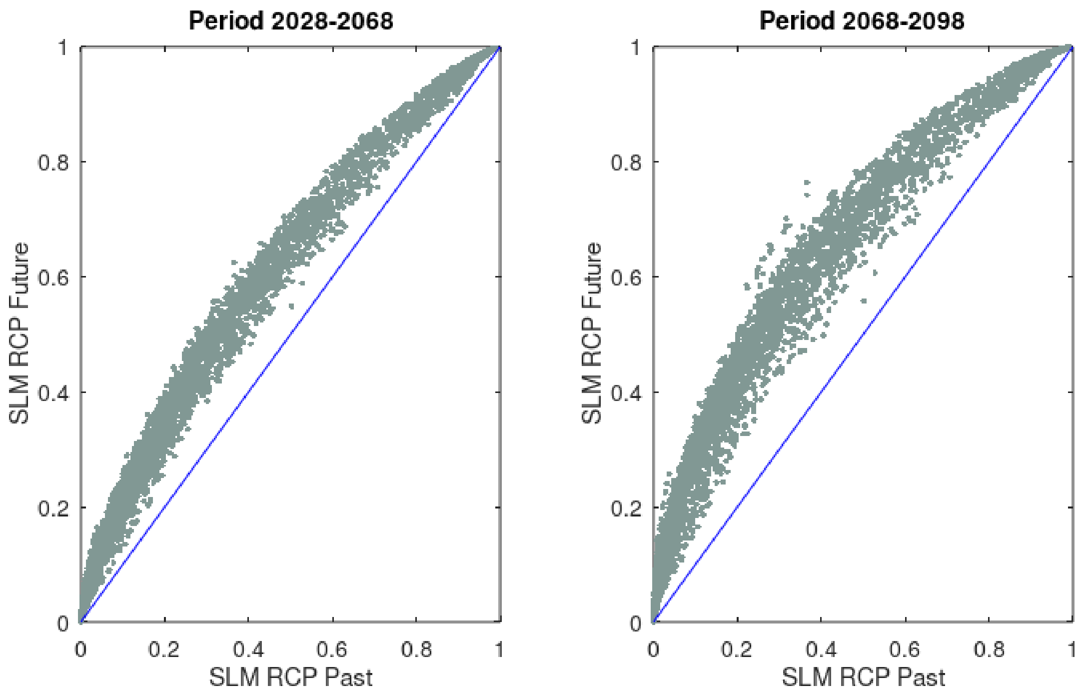

Avocado: warmth suitability score RCP 4.5

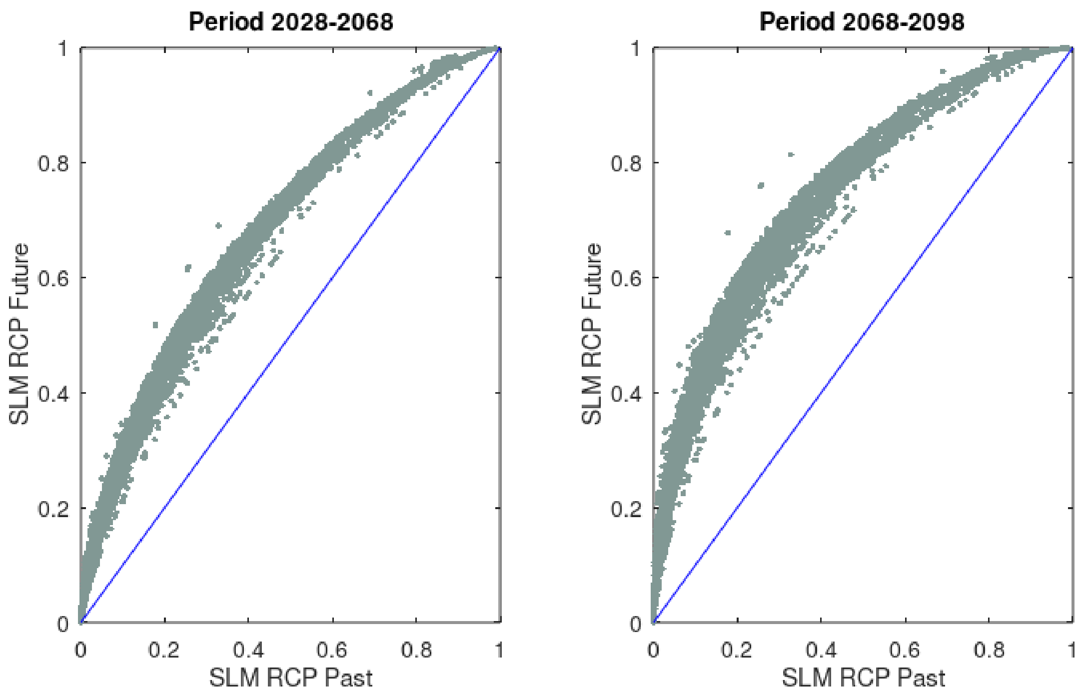

11 Avocado RCP 6.0

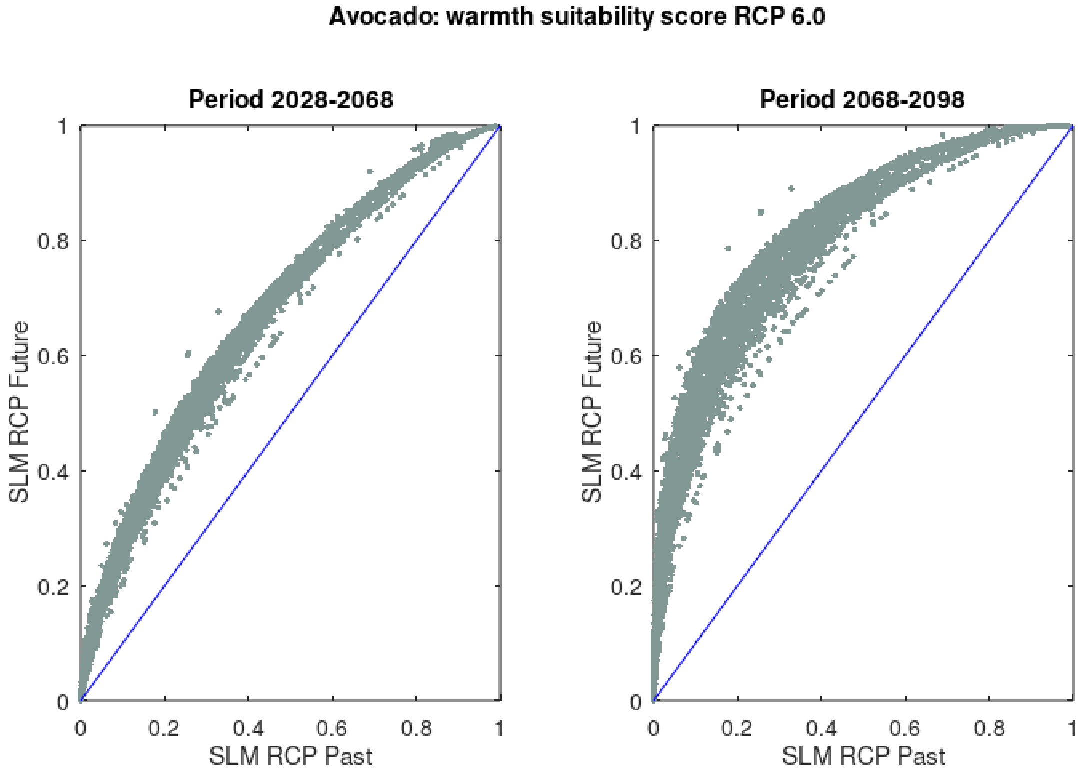

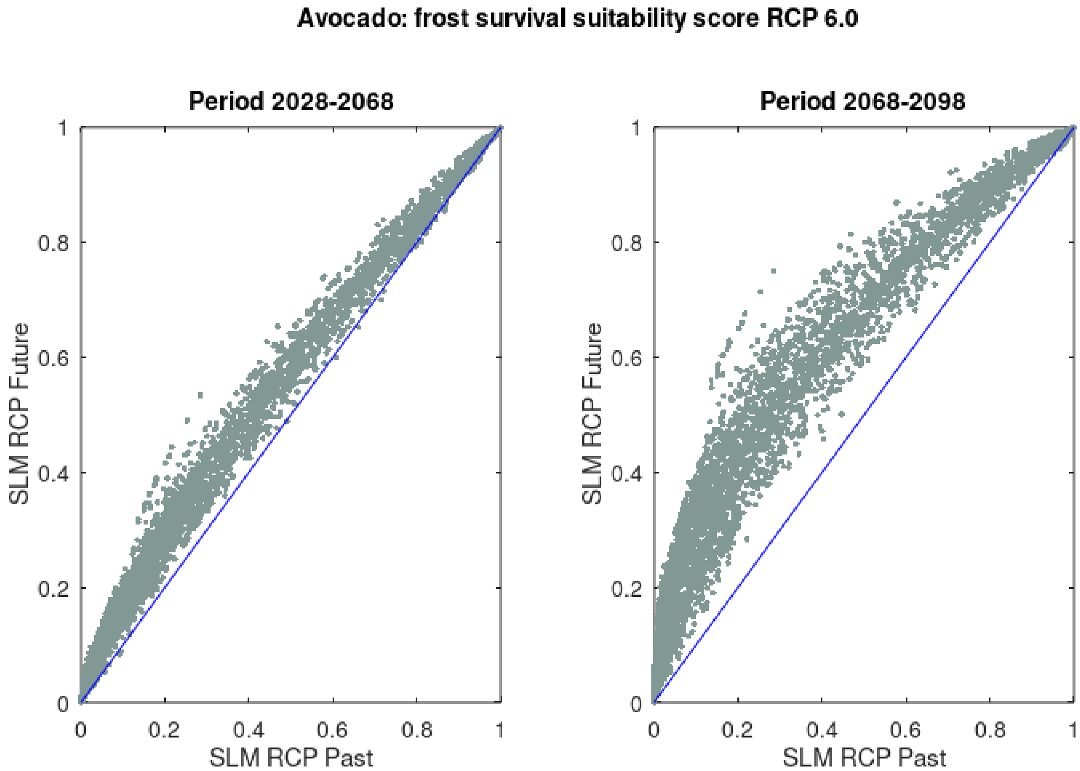

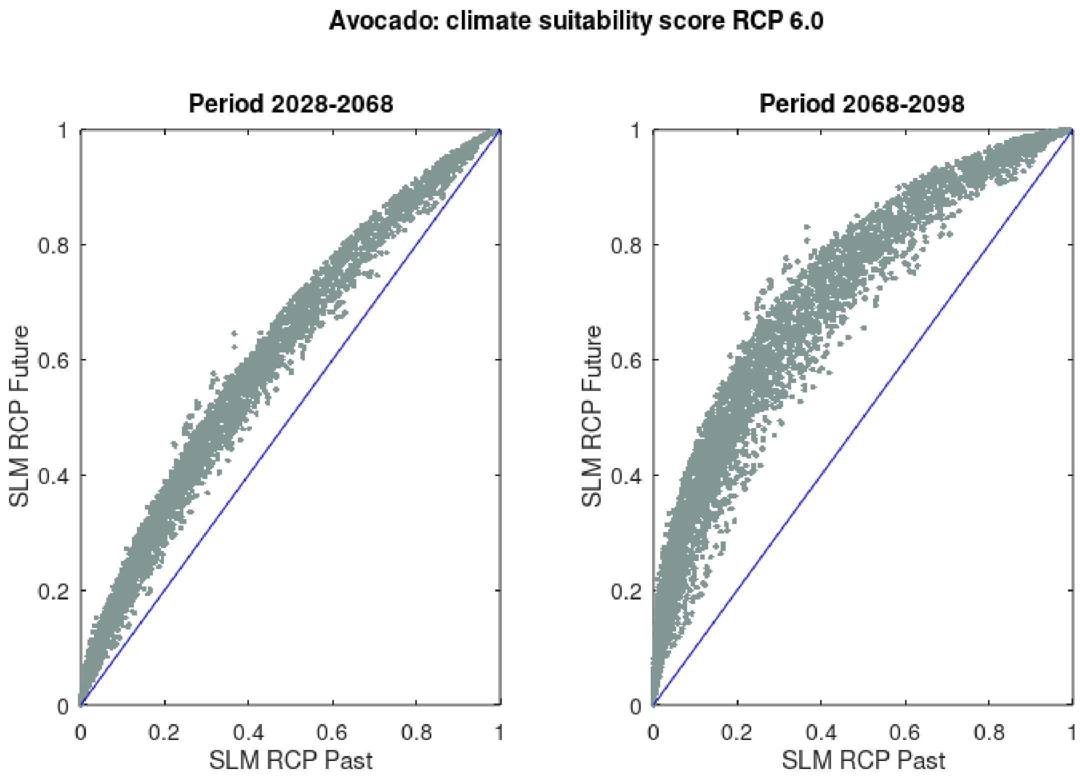

12 Avocado RCP 8.5

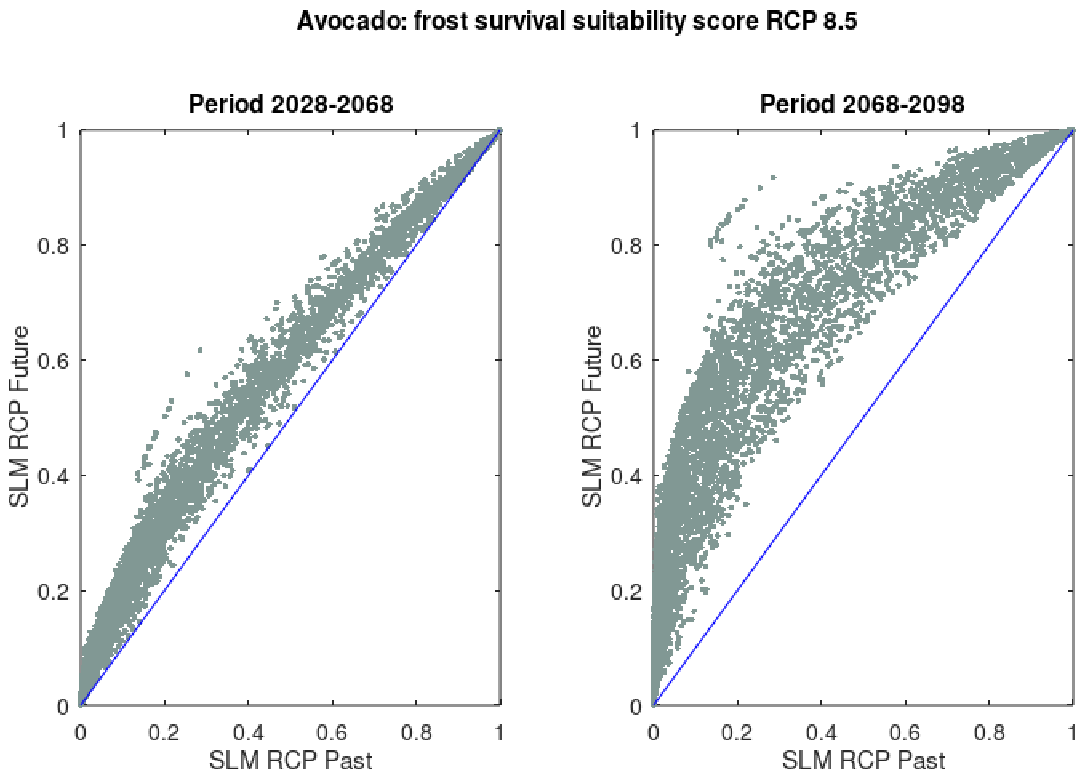

Avocado: climate suitability score RCP 8.5

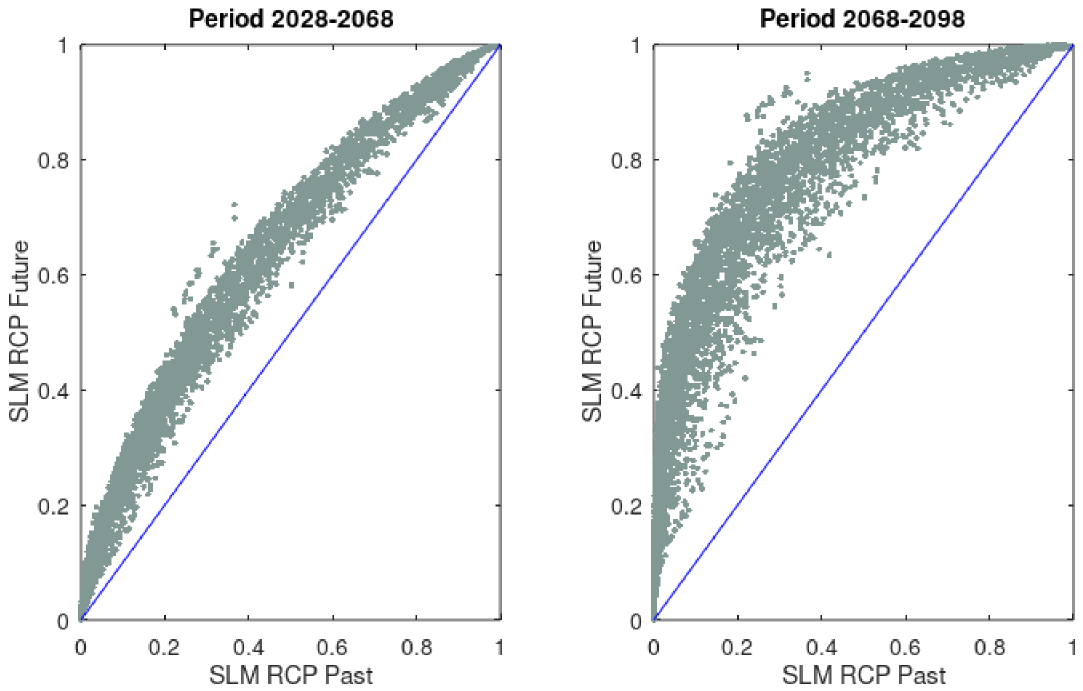

Avocado: warmth suitability score RCP 8.5

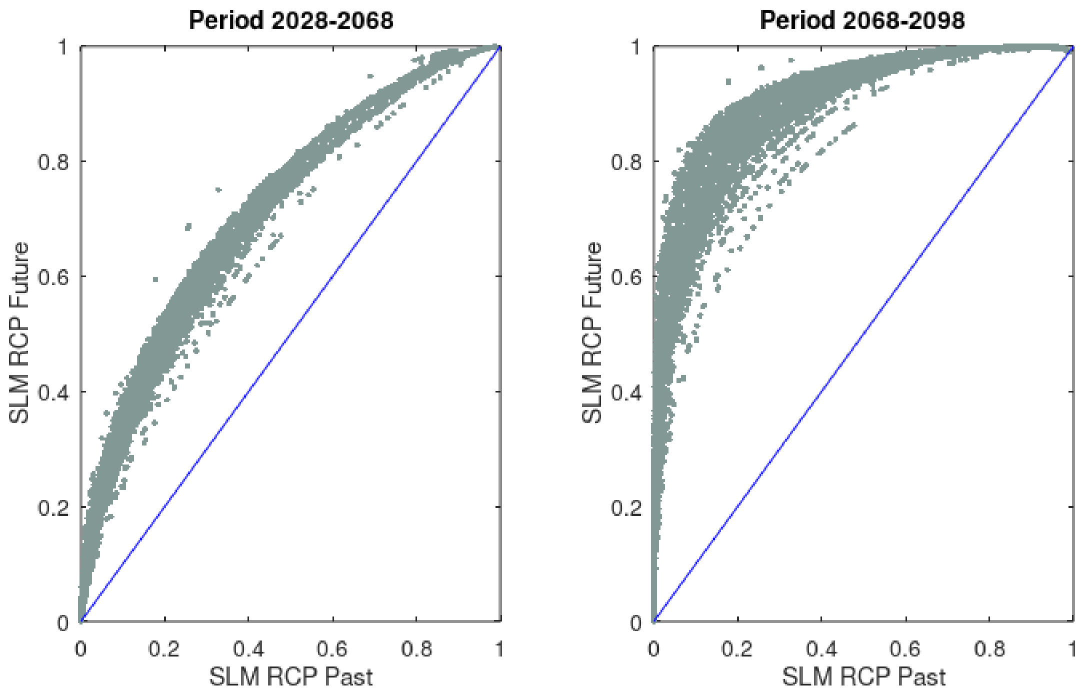

13 Blueberry RCP 2.6

Blueberry: climate suitability score RCP 2.6

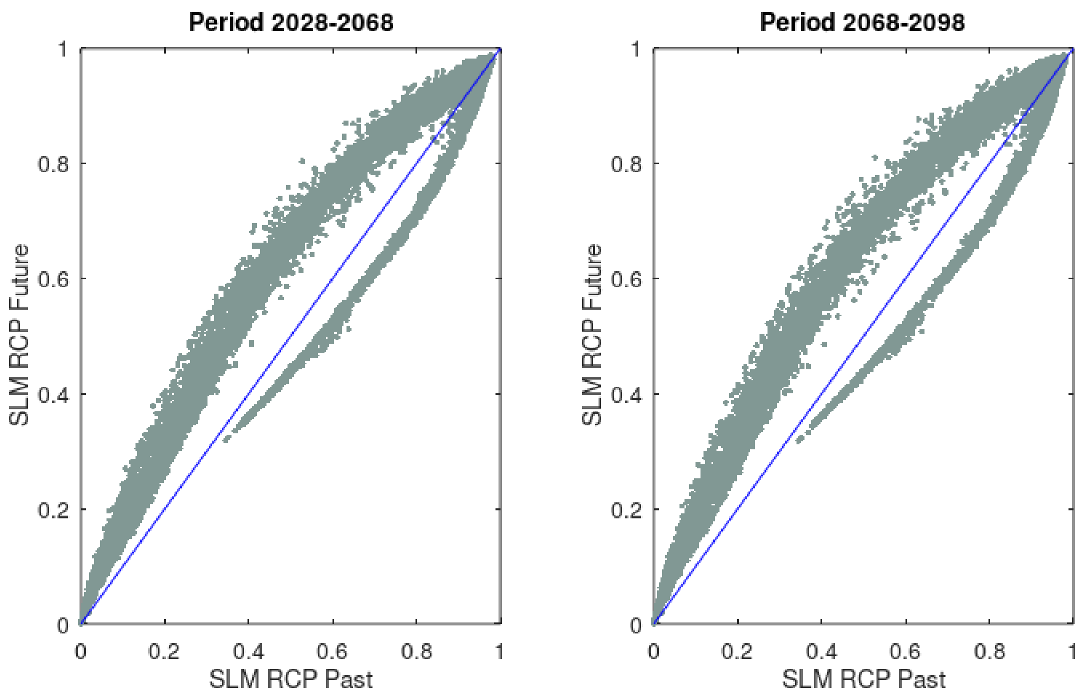

Blueberry: chill suitability score RCP 2.6

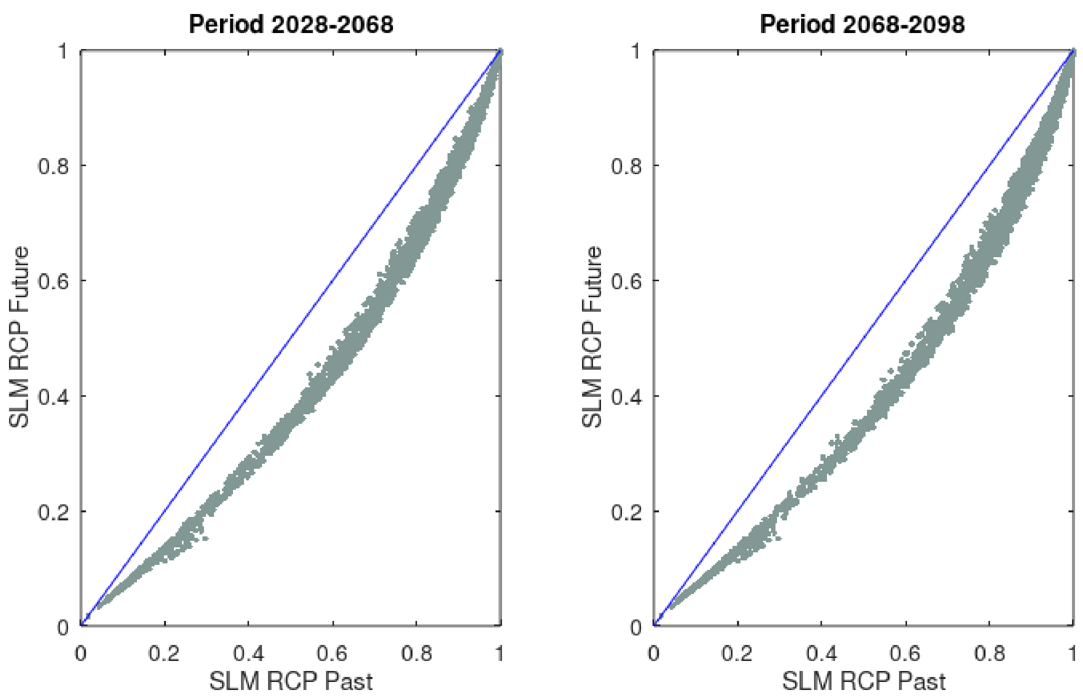

Blueberry: GDD suitability score RCP 2.6

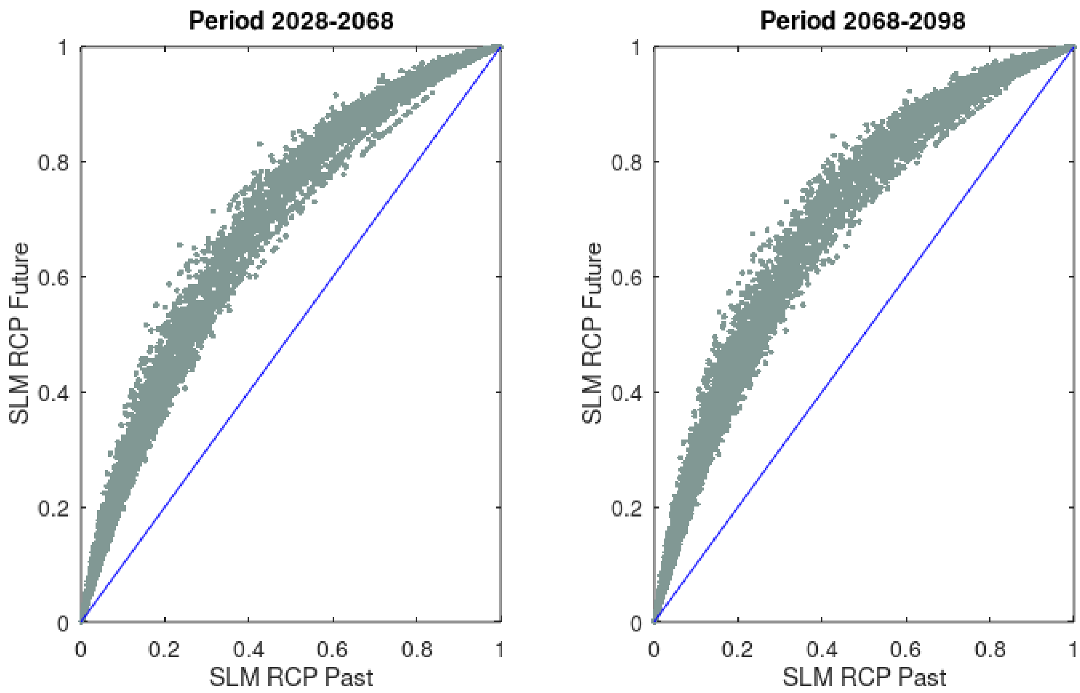

Blueberry: frost survival suitability score RCP 2.6

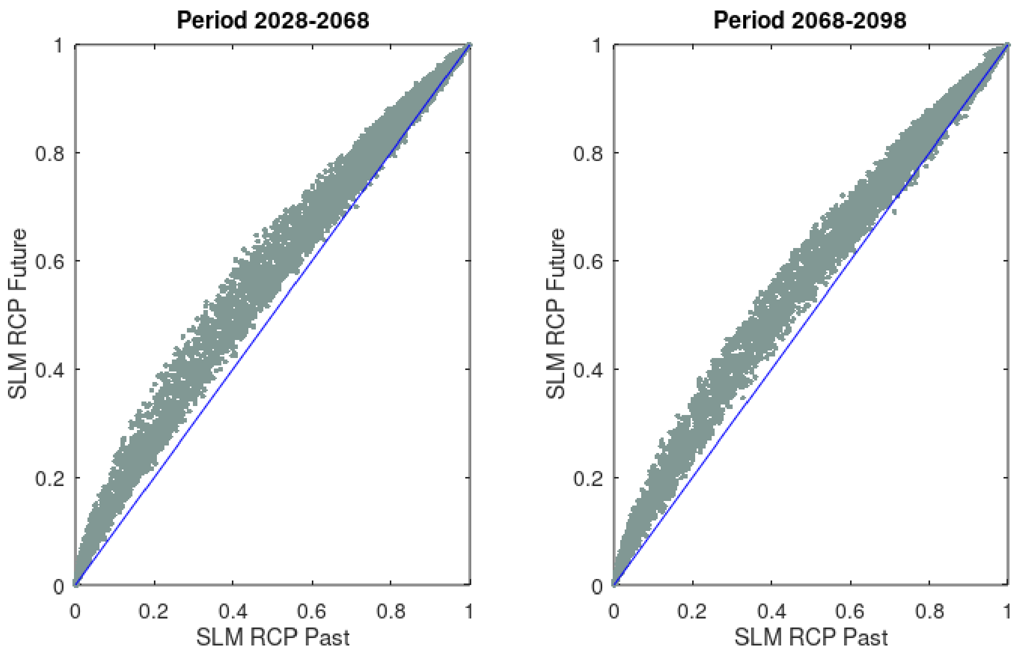

14 Blueberry RCP 4.5

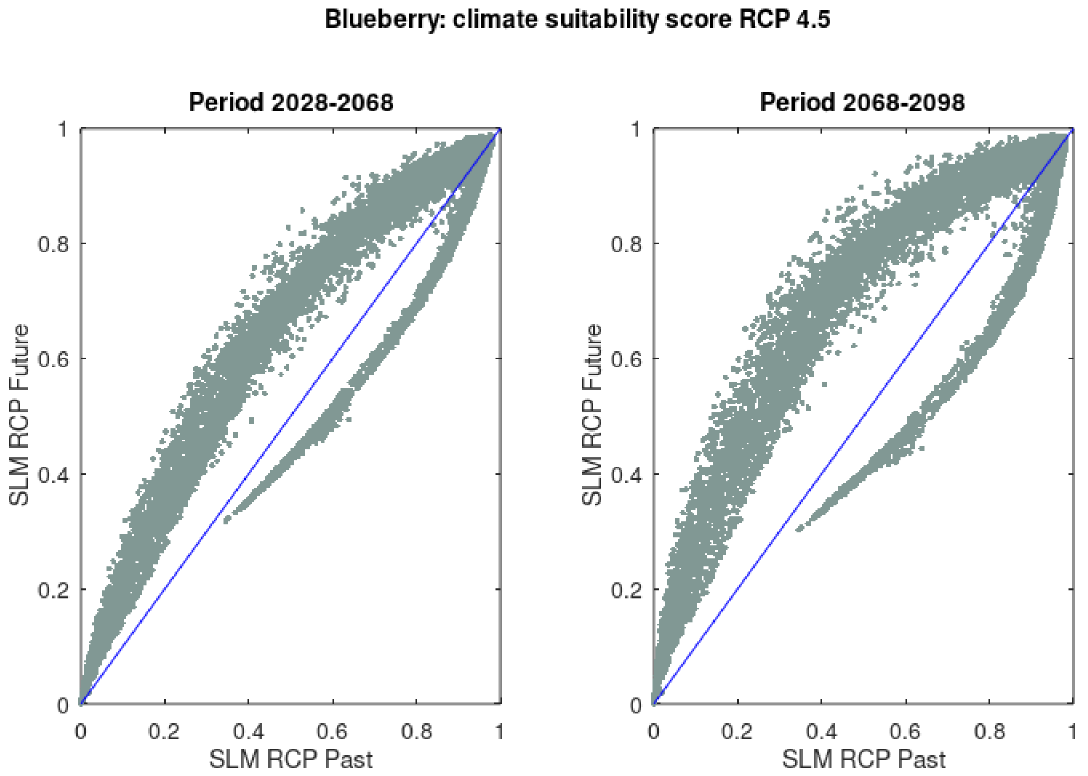

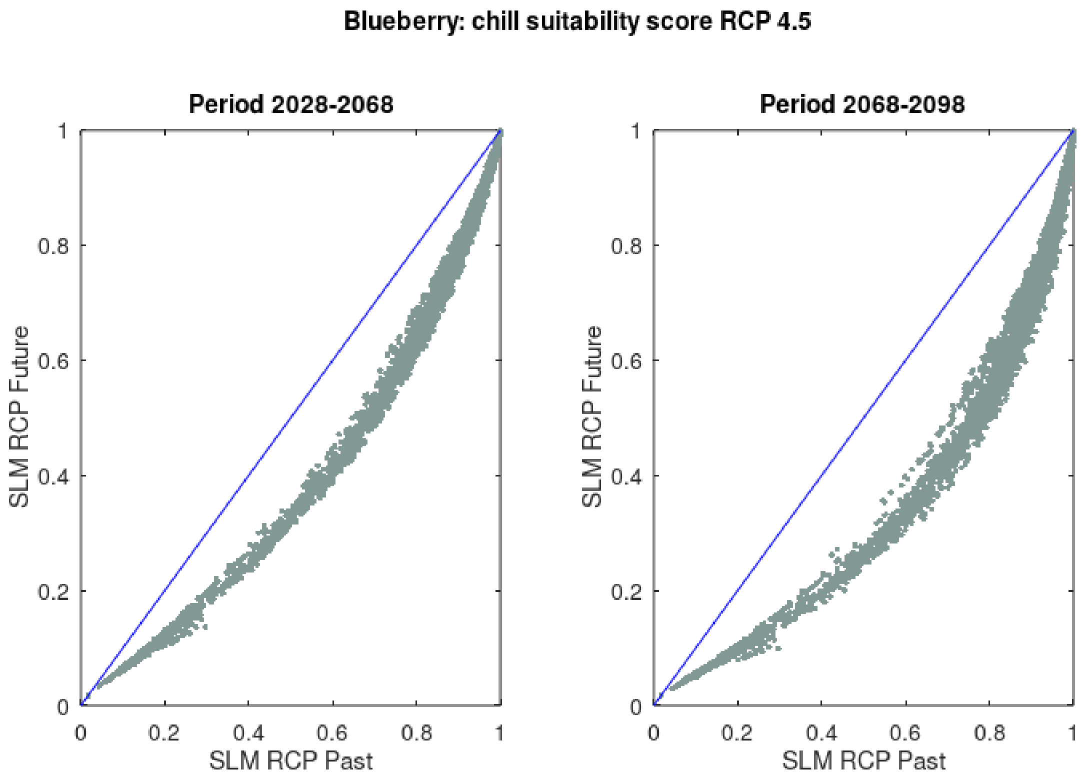

Blueberry: GDD suitability score RCP 4.5

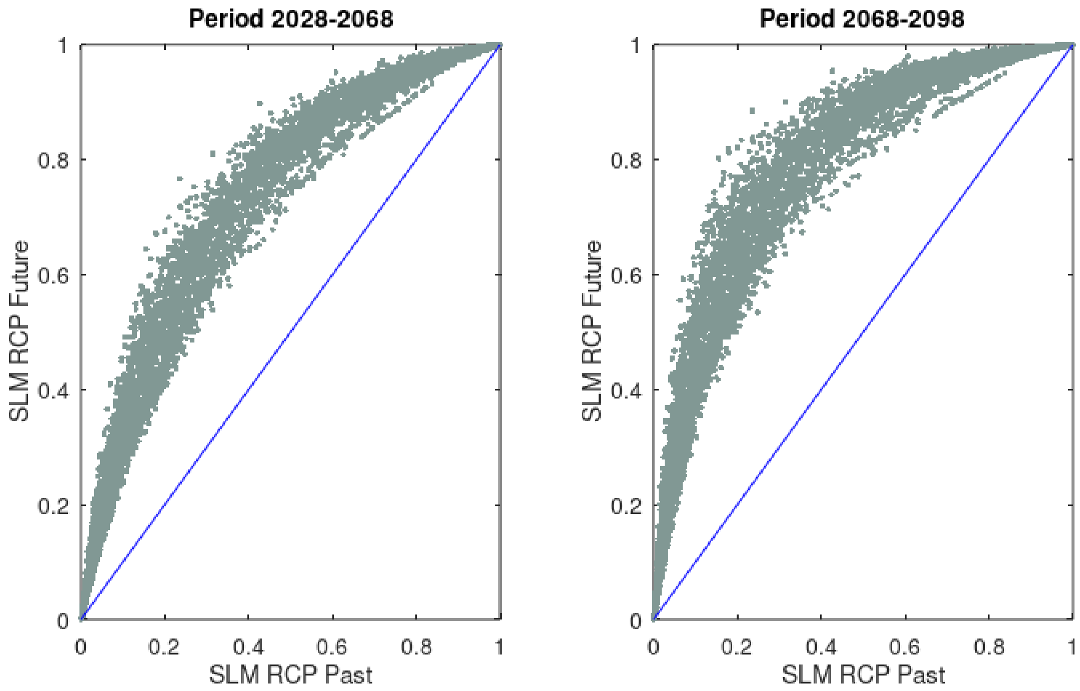

Blueberry: frost survival suitability score RCP 4.5

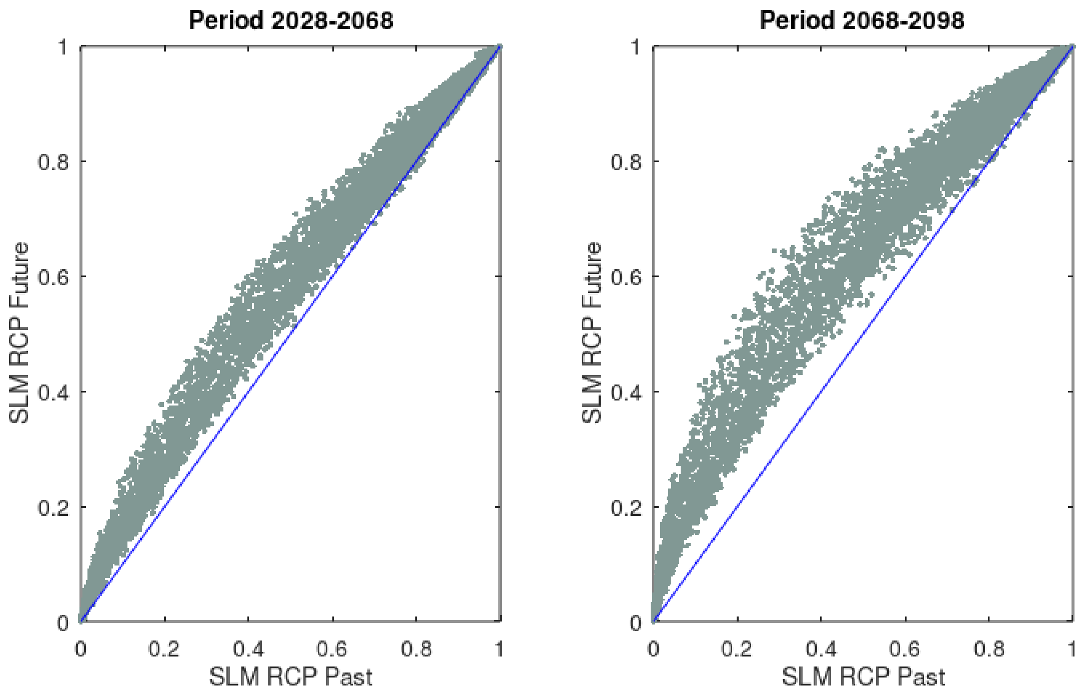

15 Blueberry RCP 6.0

Blueberry: climate suitability score RCP 6.0

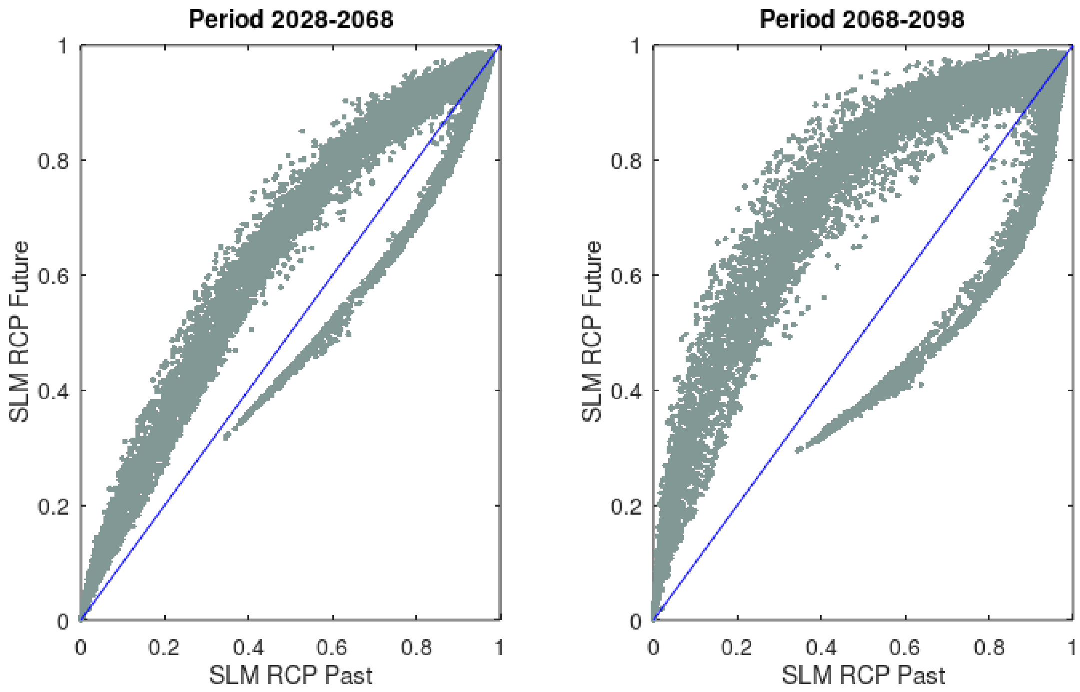

Blueberry: chill suitability score RCP 6.0

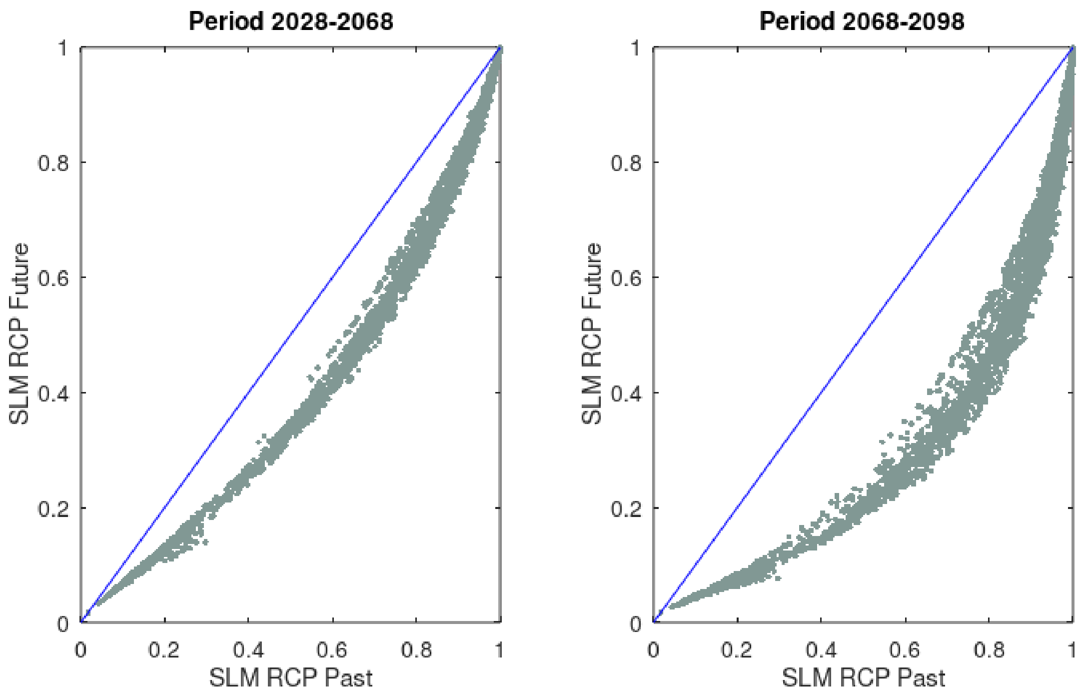

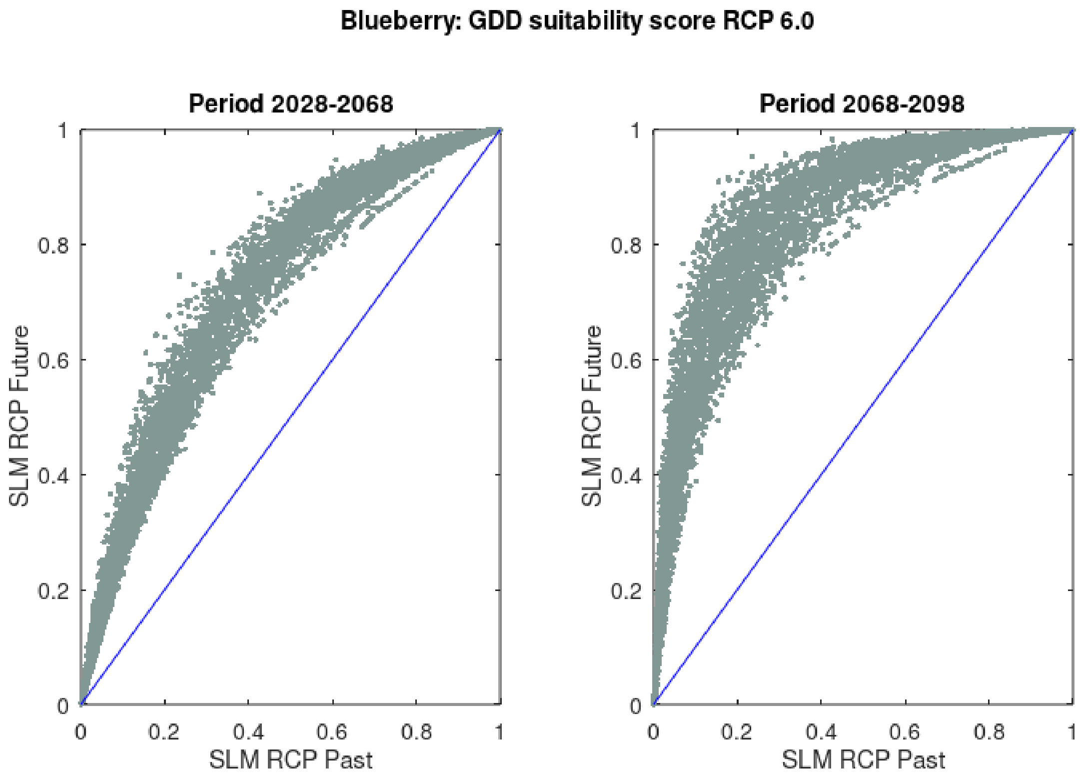
Blueberry: GDD suitability score RCP 6.0
Period 2028-2068
Period 2068-2098
SLM RCP Future
SLM RCP Past
0
0.2
0.4
0.6
0.8
1

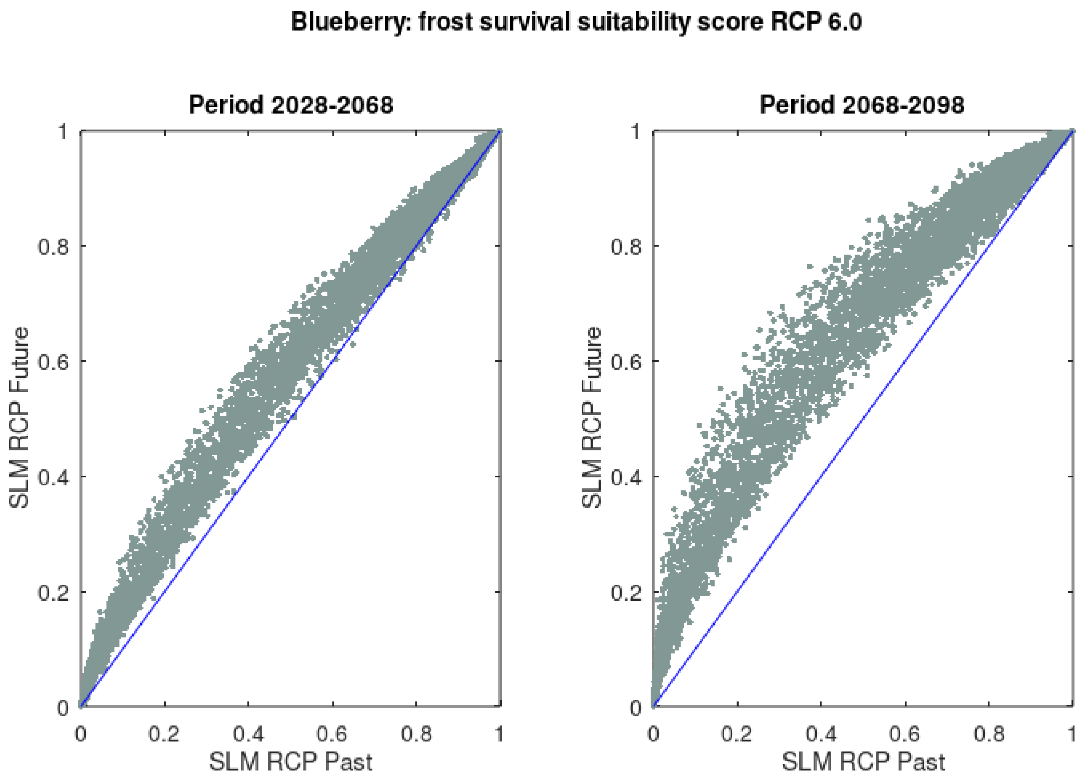
Blueberry: frost survival suitability score RCP 6.0
Period 2028-2068
Period 2068-2098
SLM RCP Future
SLM RCP Past
0
0.2
0.4
0.6
0.8
1

16 Blueberry RCP 8.5

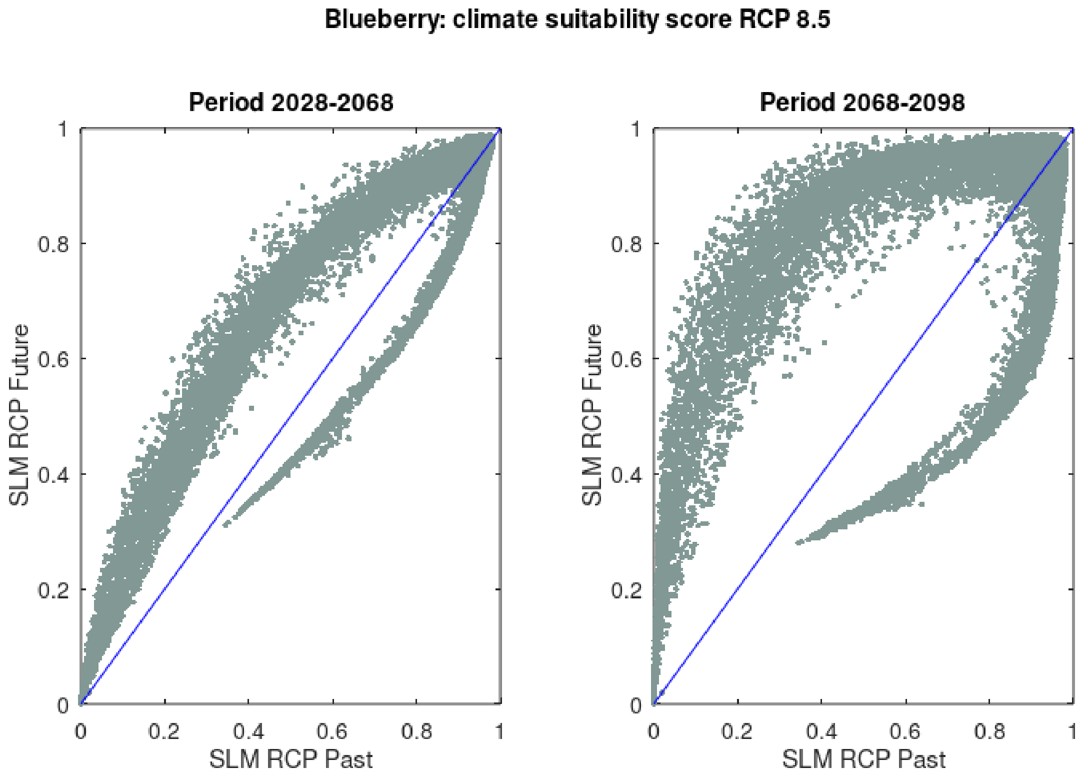

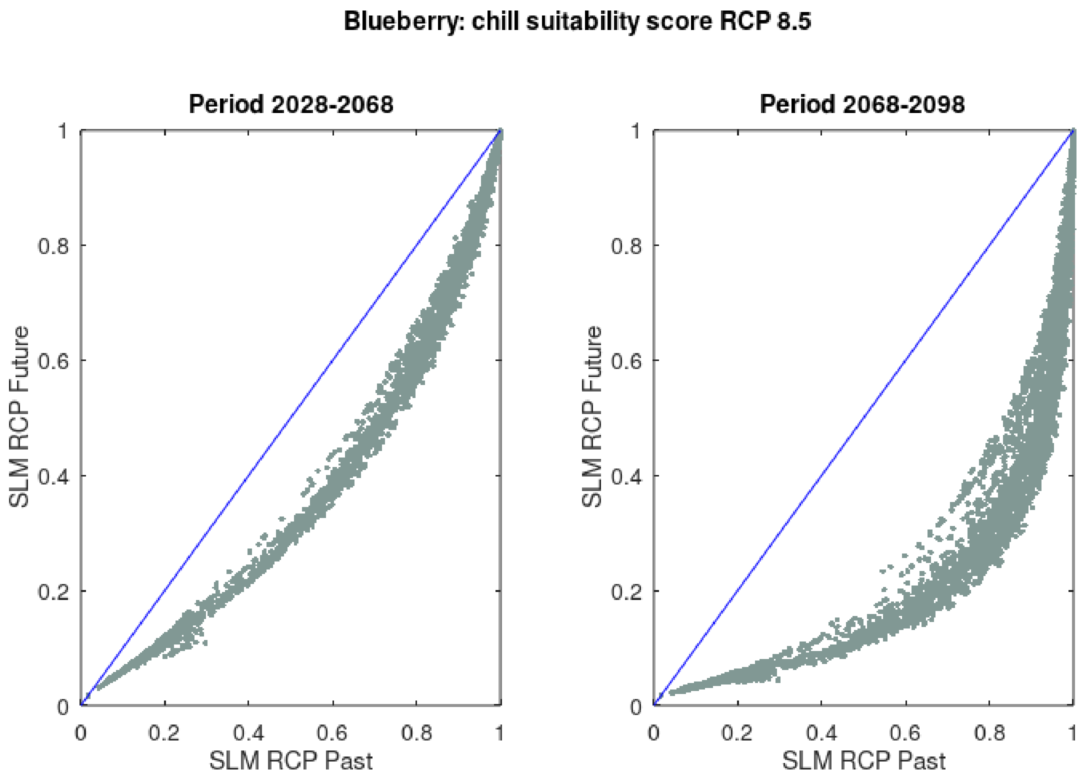

Blueberry: GDD suitability score RCP 8.5

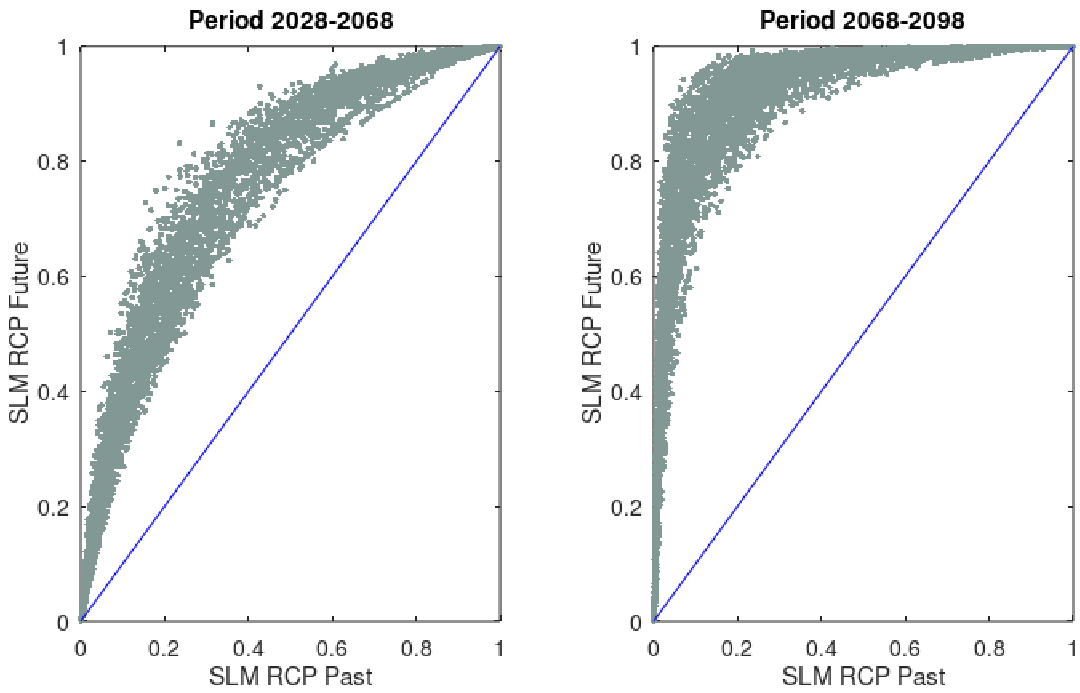

Blueberry: frost survival suitability score RCP 8.5

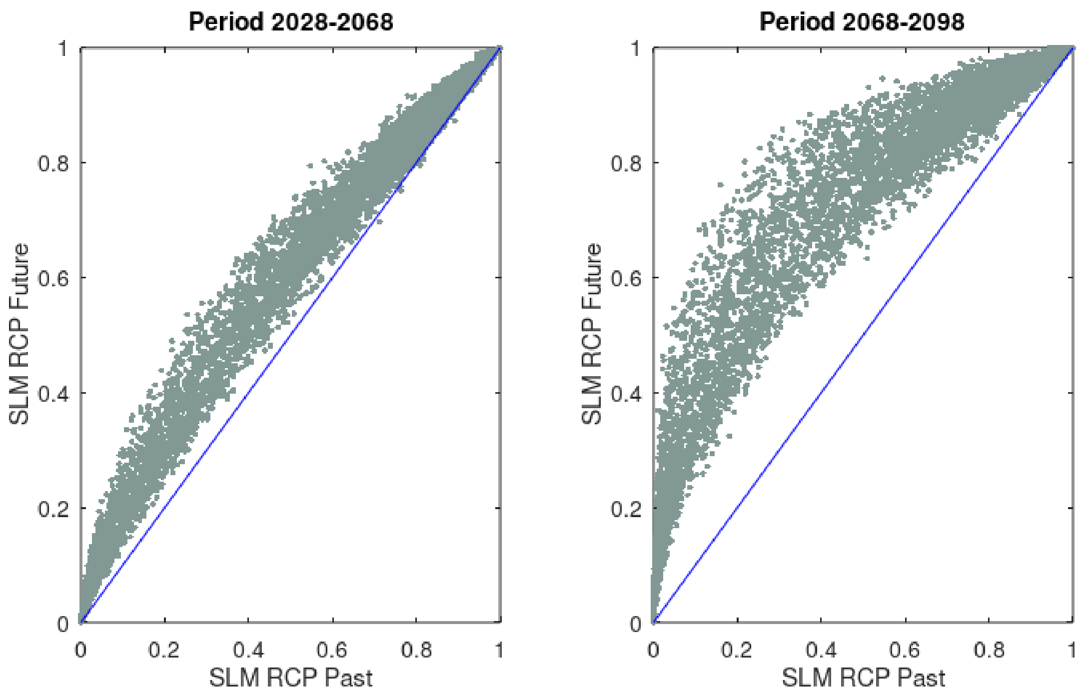

17 Cherry RCP 2.6

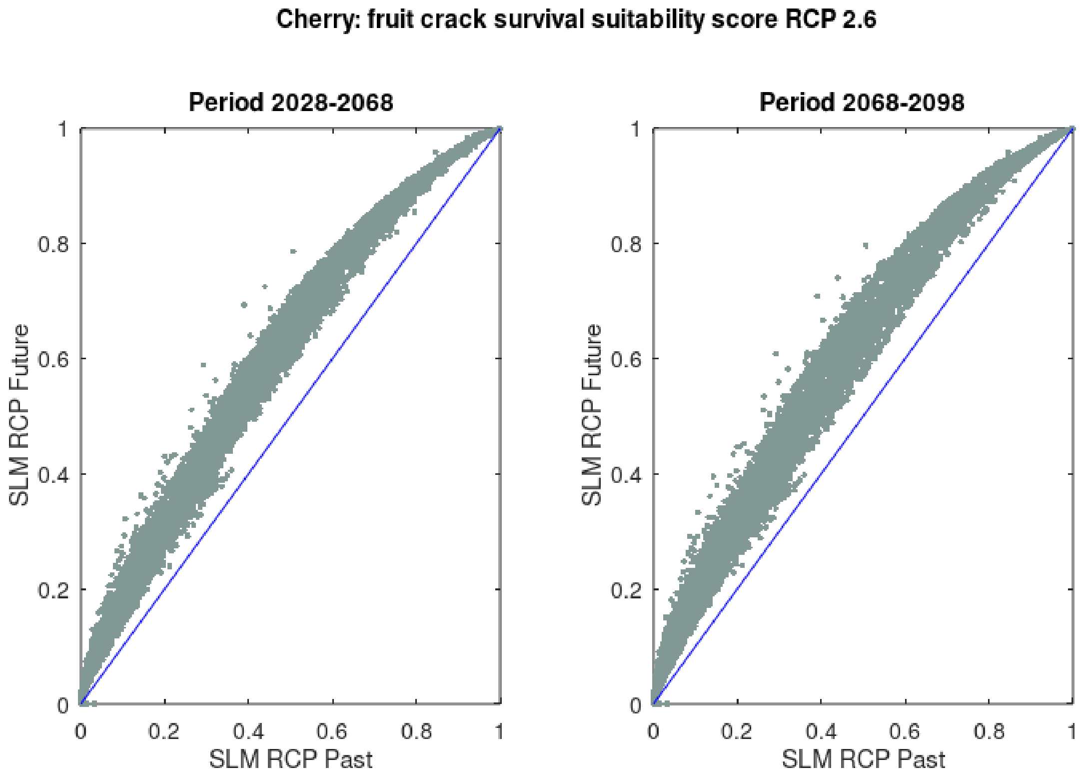

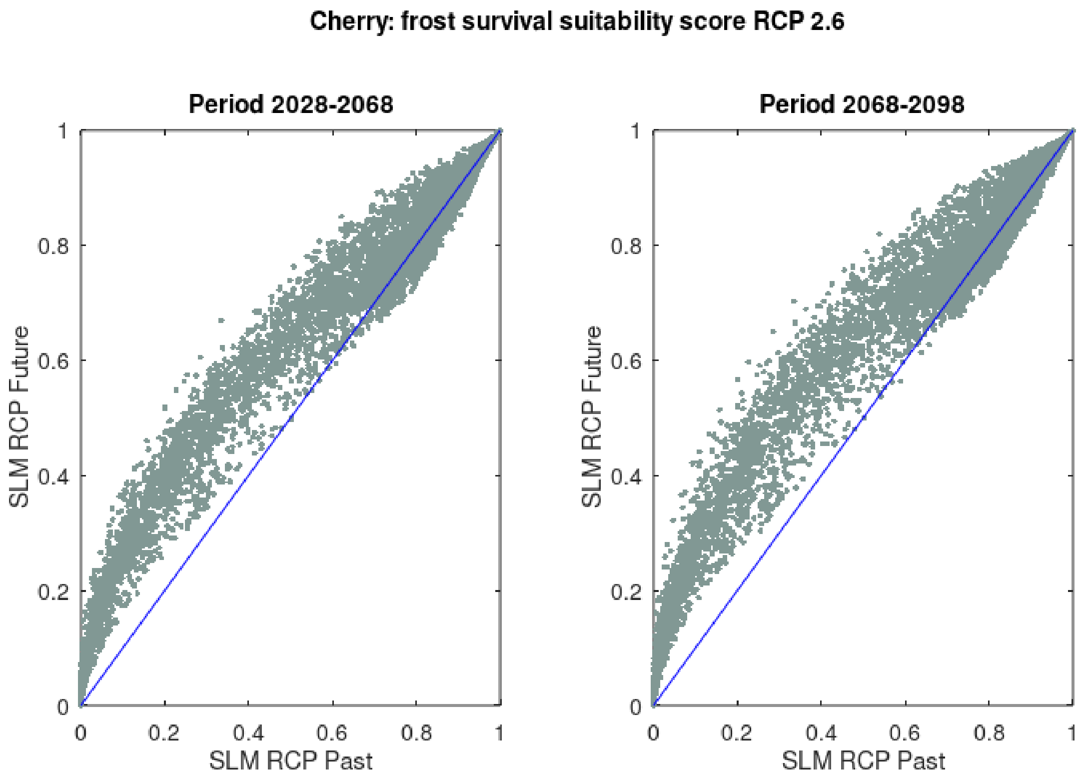

Cherry: climate suitability score RCP 2.6

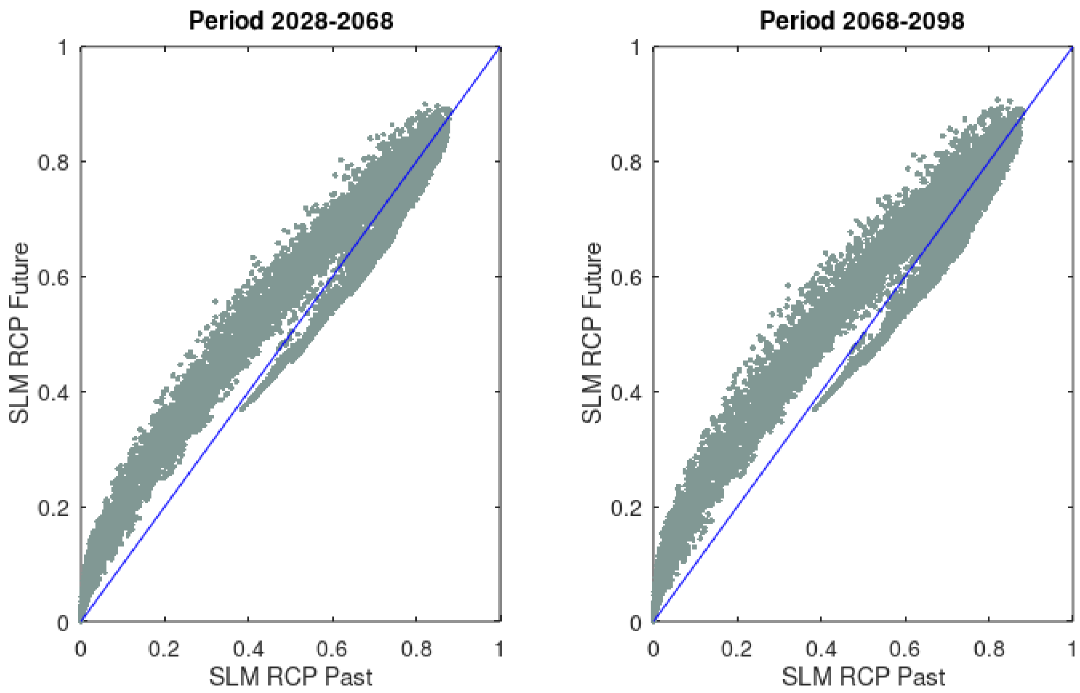

Cherry: chill suitability score RCP 2.6

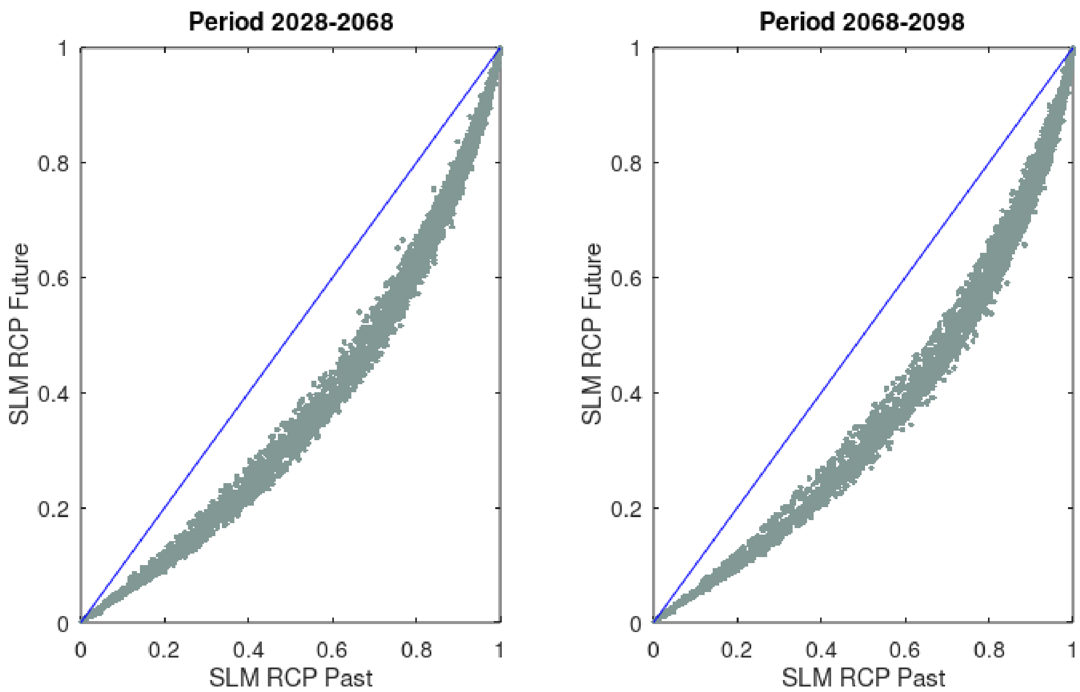

Cherry: GDD suitability score RCP 2.6

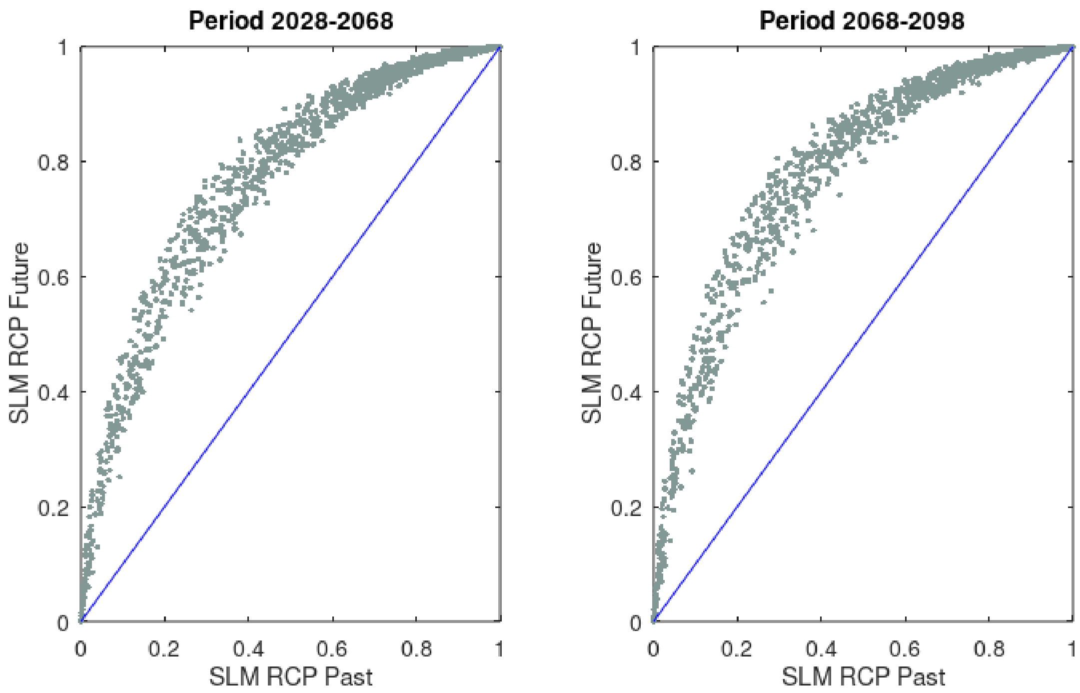

18 Cherry RCP 4.5

Cherry: frost survival suitability score RCP 4.5

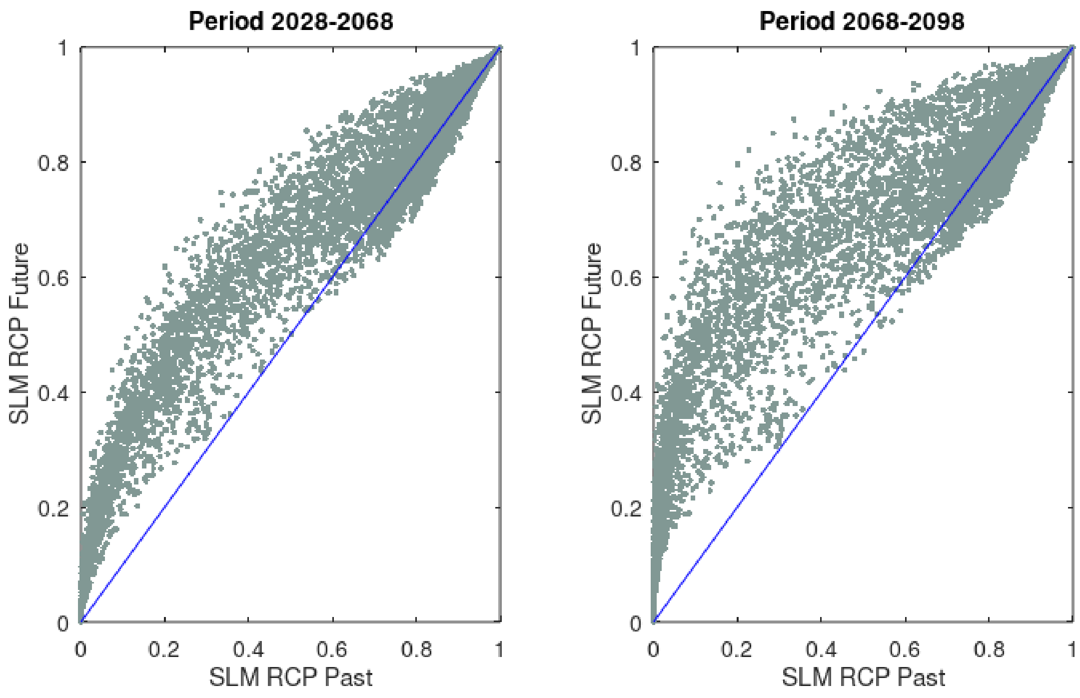

Cherry: climate suitability score RCP 4.5

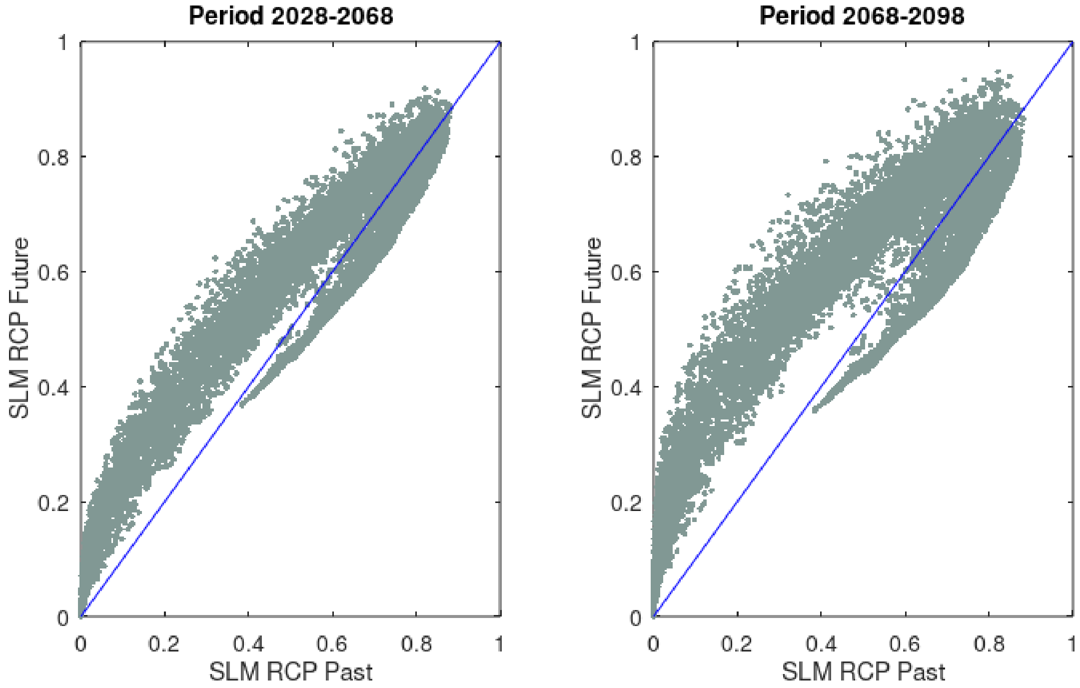

Cherry: chill suitability score RCP 4.5

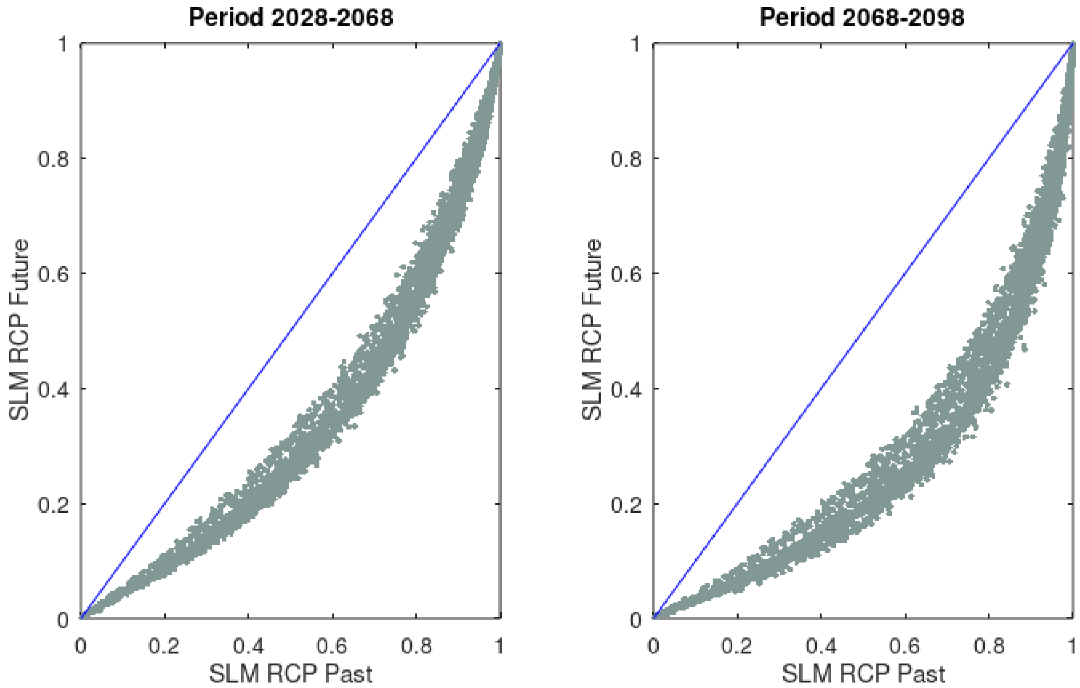

Cherry: GDD suitability score RCP 4.5

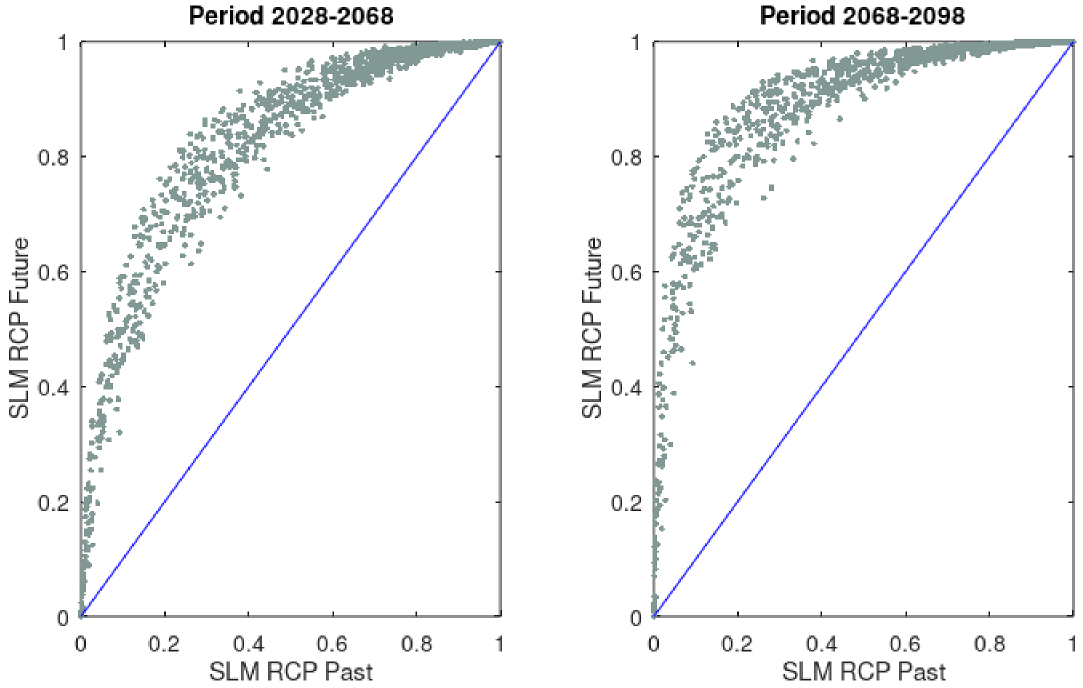

Cherry: fruit crack survival suitability score RCP 4.5

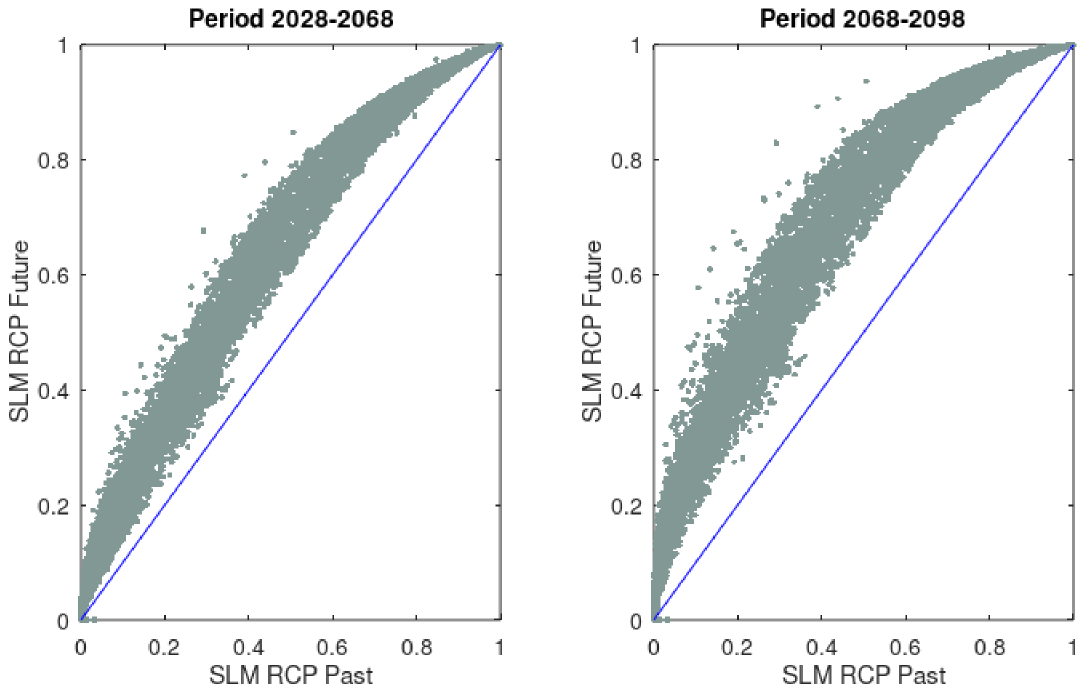

19 Cherry RCP 6.0

Cherry: fruit crack survival suitability score RCP 6.0

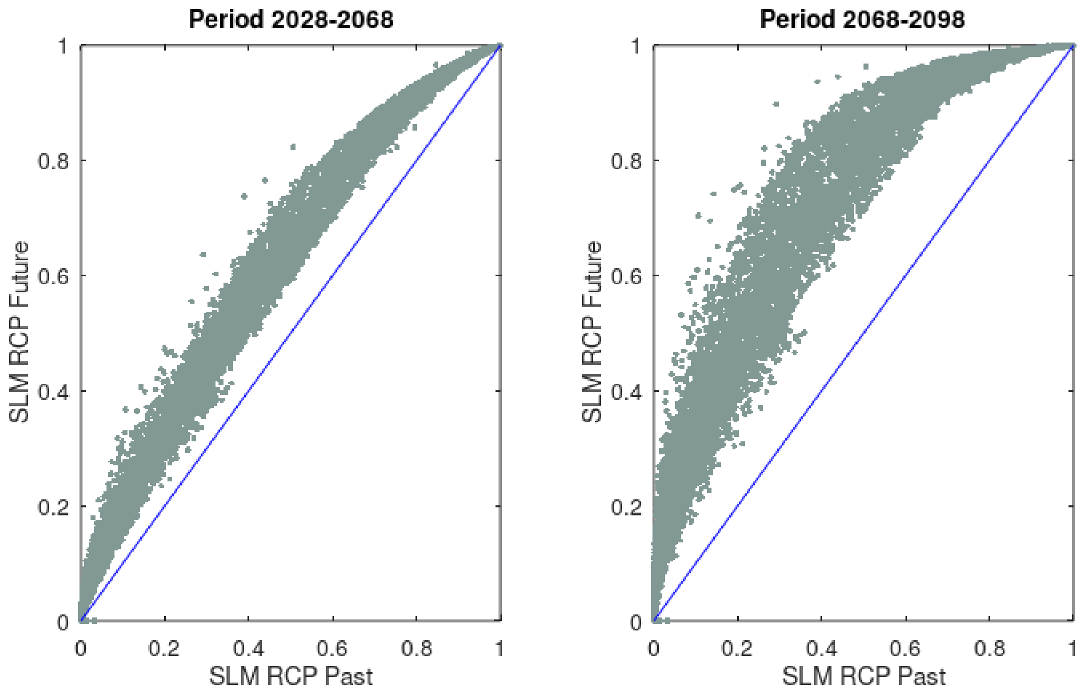

Cherry: frost survival suitability score RCP 6.0

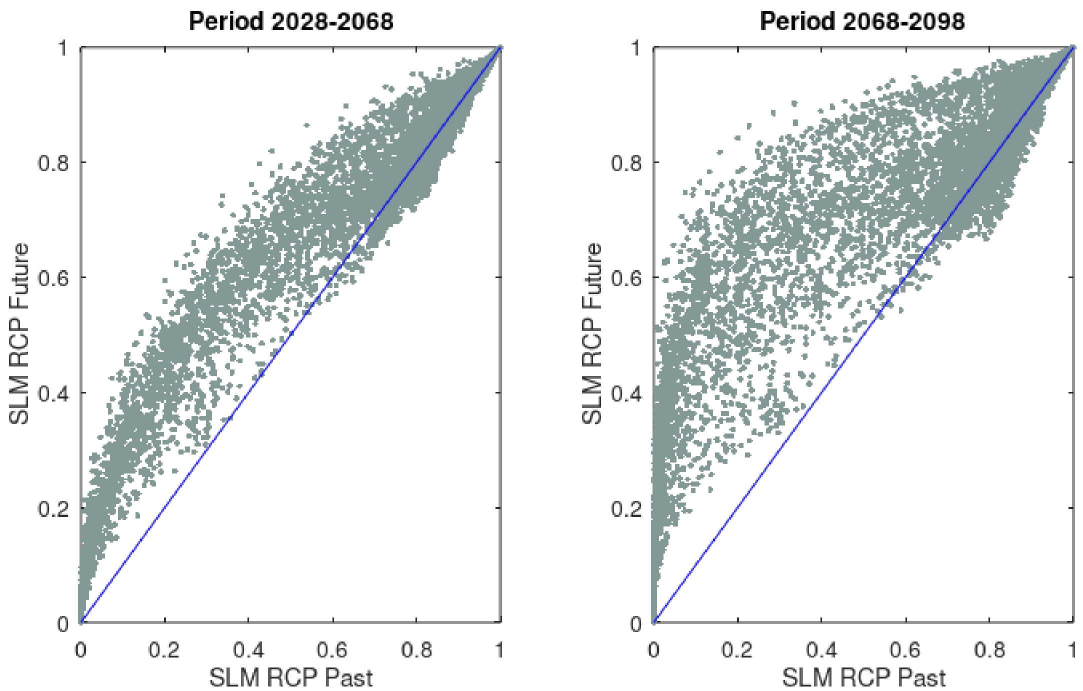

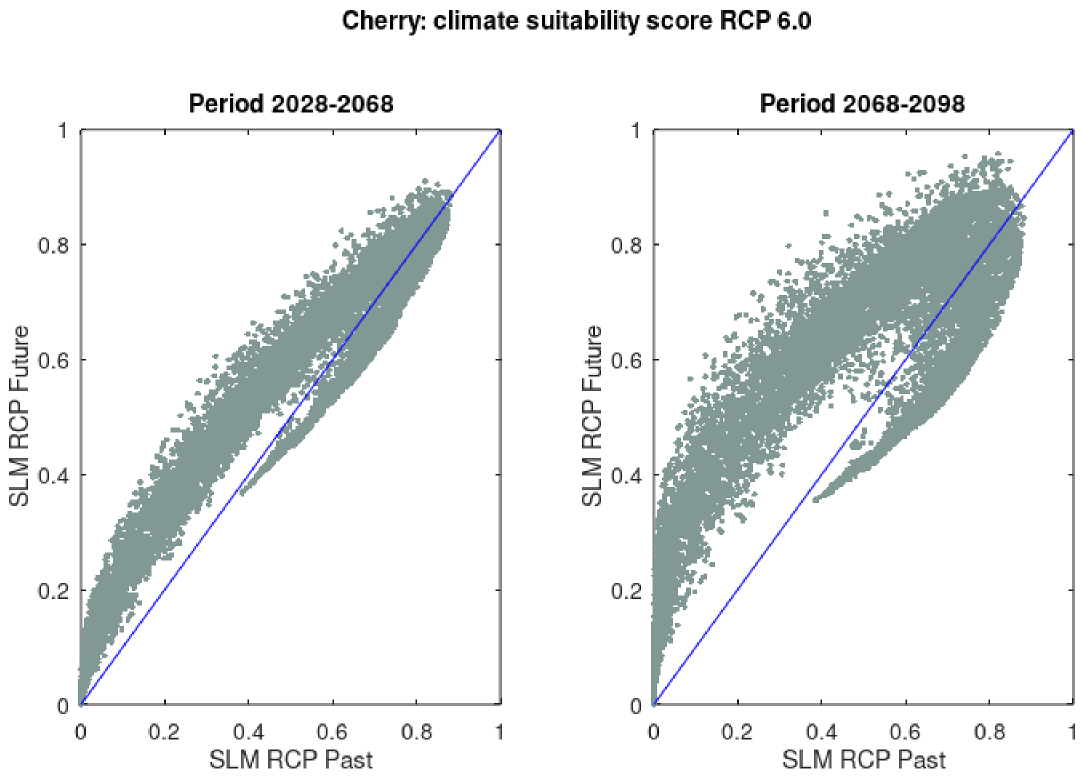
Cherry: climate suitability score RCP 6.0
Period 2028-2068
Period 2068-2098
SLM RCP Future
SLM RCP Past
0
0.2
0.4
0.6
0.8
1

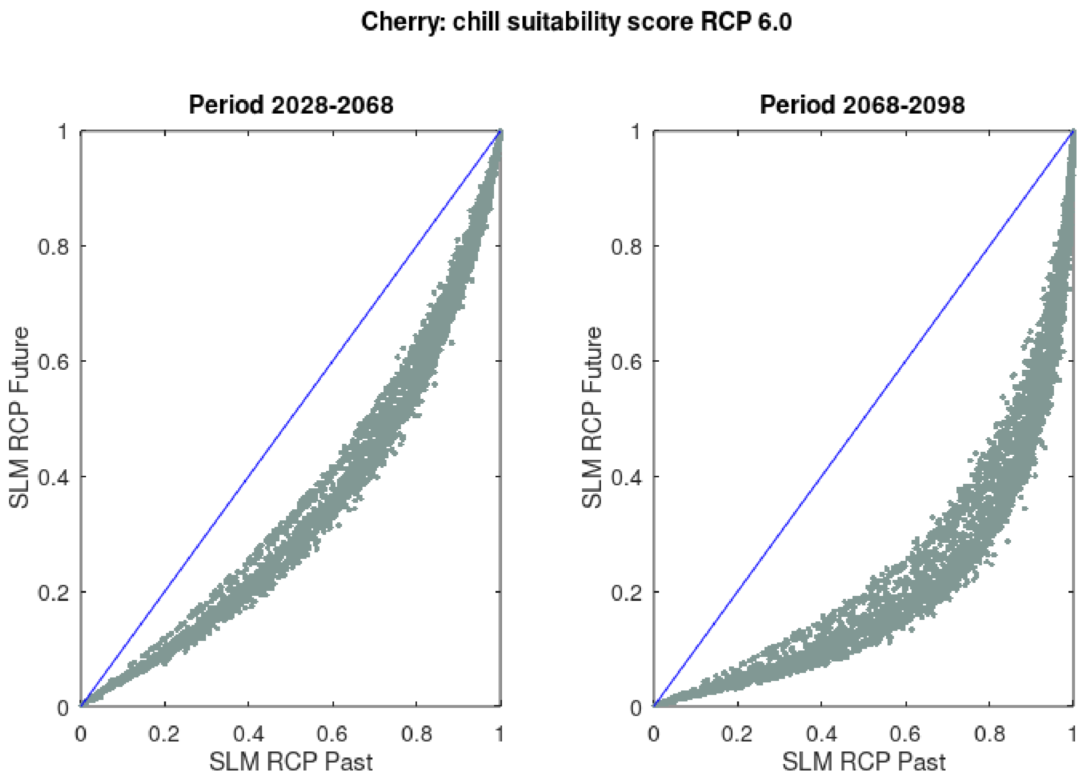
Cherry: chill suitability score RCP 6.0
Period 2028-2068
Period 2068-2098
SLM RCP Future
SLM RCP Past
0
0.2
0.4
0.6
0.8
1

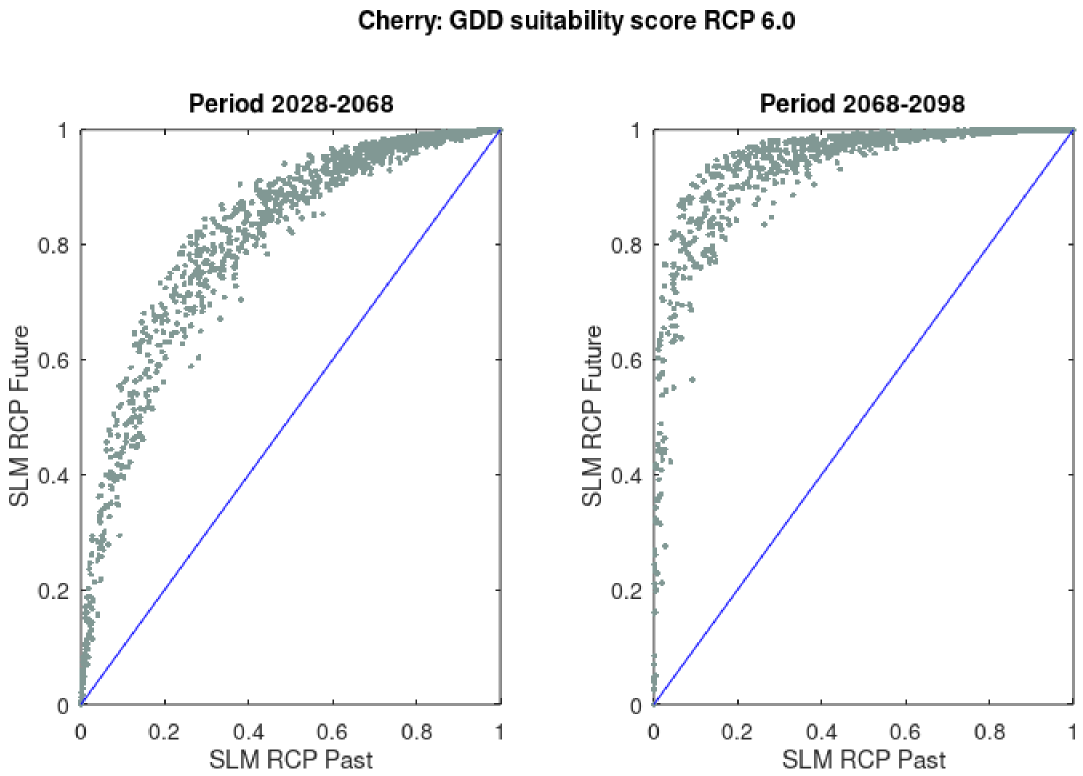

20 Cherry RCP 8.5

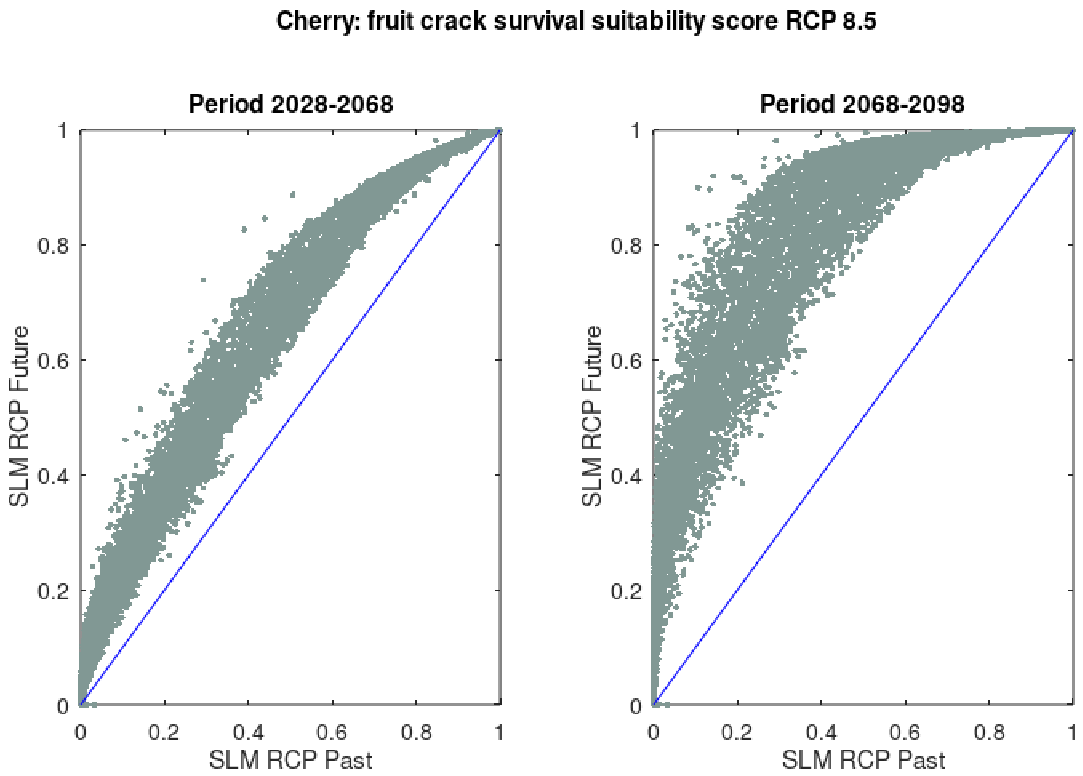

Cherry: frost survival suitability score RCP 8.5

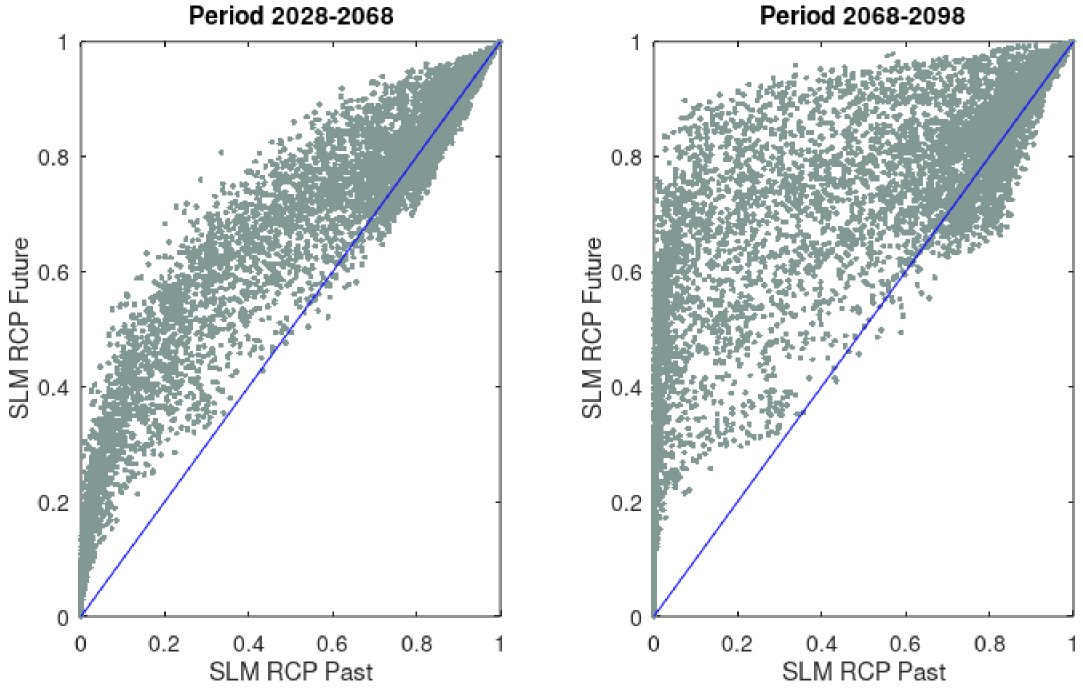

Cherry: climate suitability score RCP 8.5

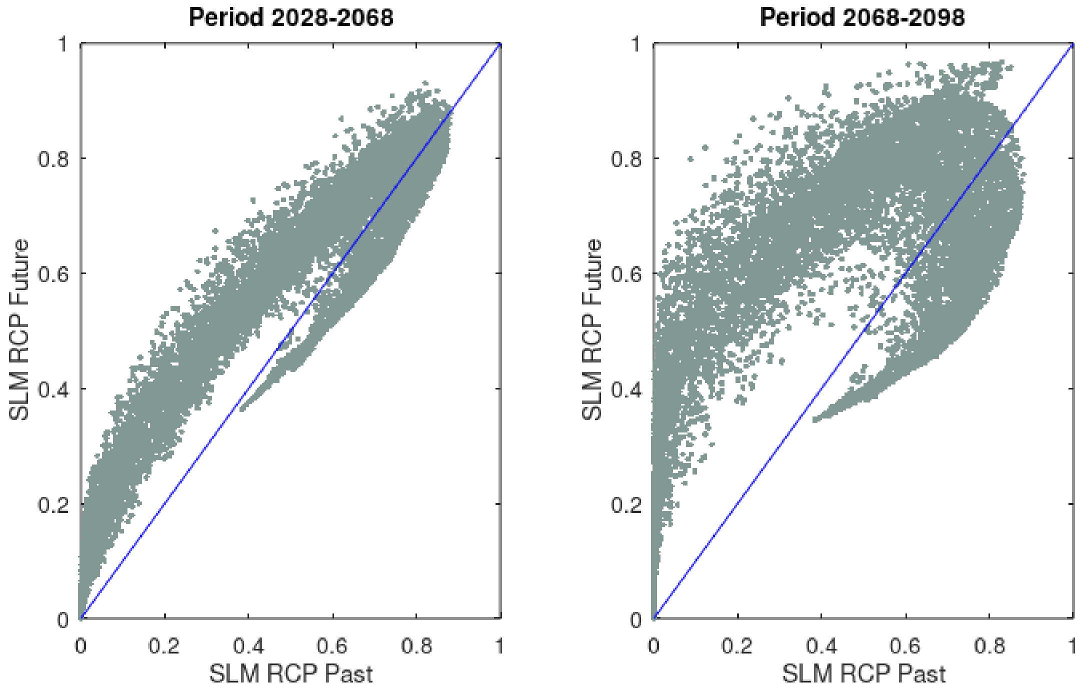

Cherry: chill suitability score RCP 8.5

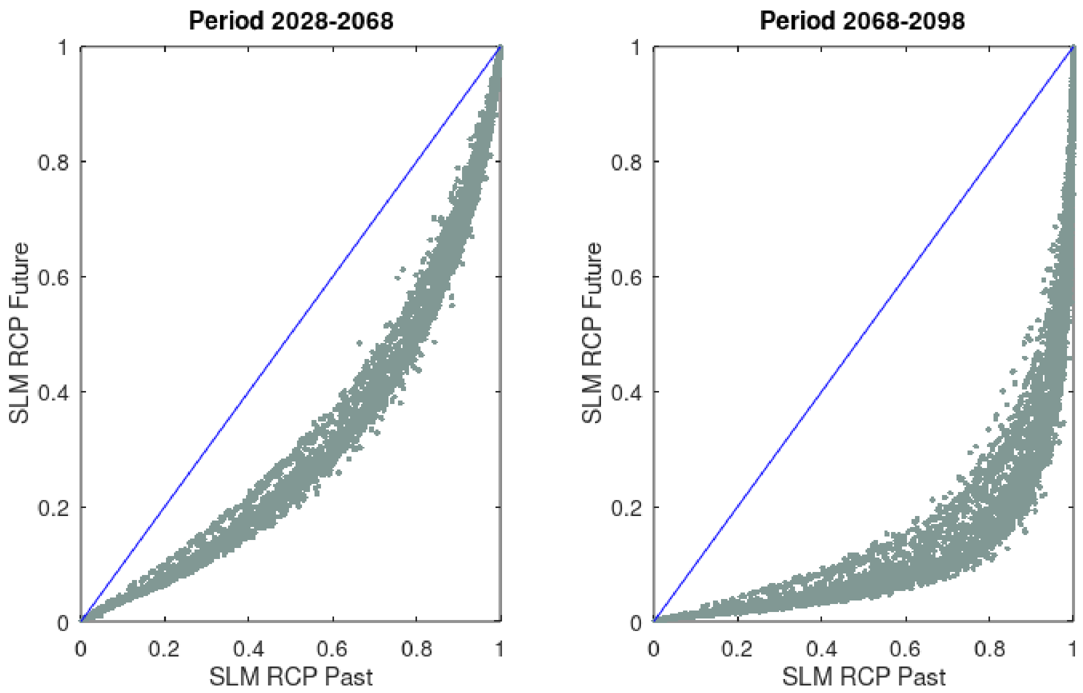

Cherry: GDD suitability score RCP 8.5

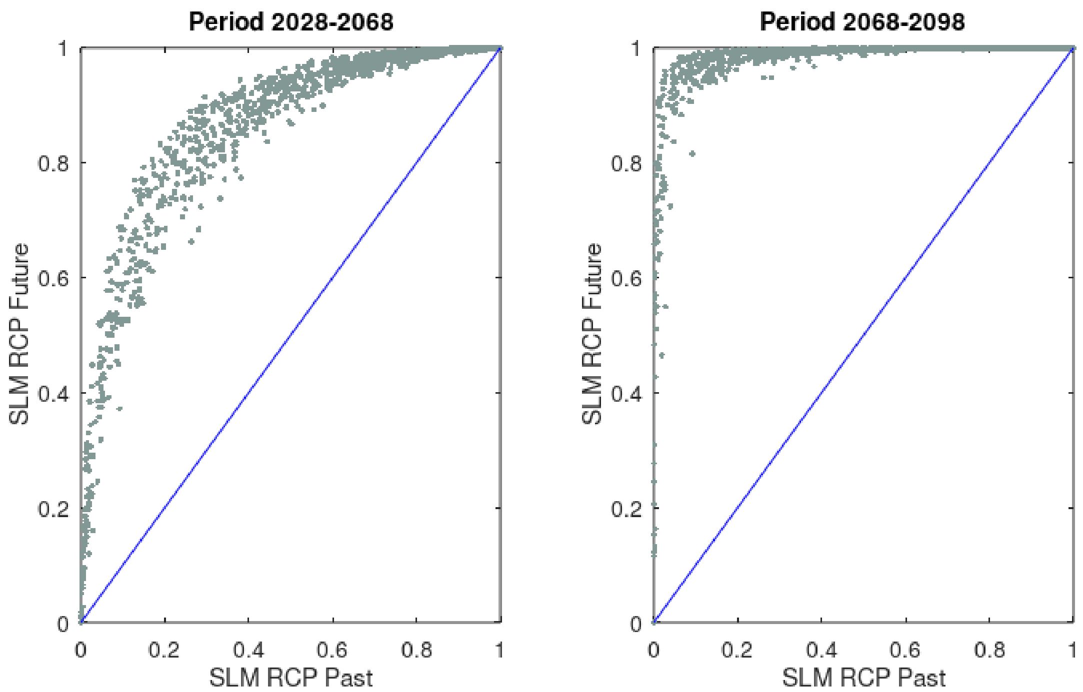

21 Wine grape common to both Pinot noir and Sauvignon blanc RCP 2.6

Wine grape: botrytis rain suitability score RCP 2.6

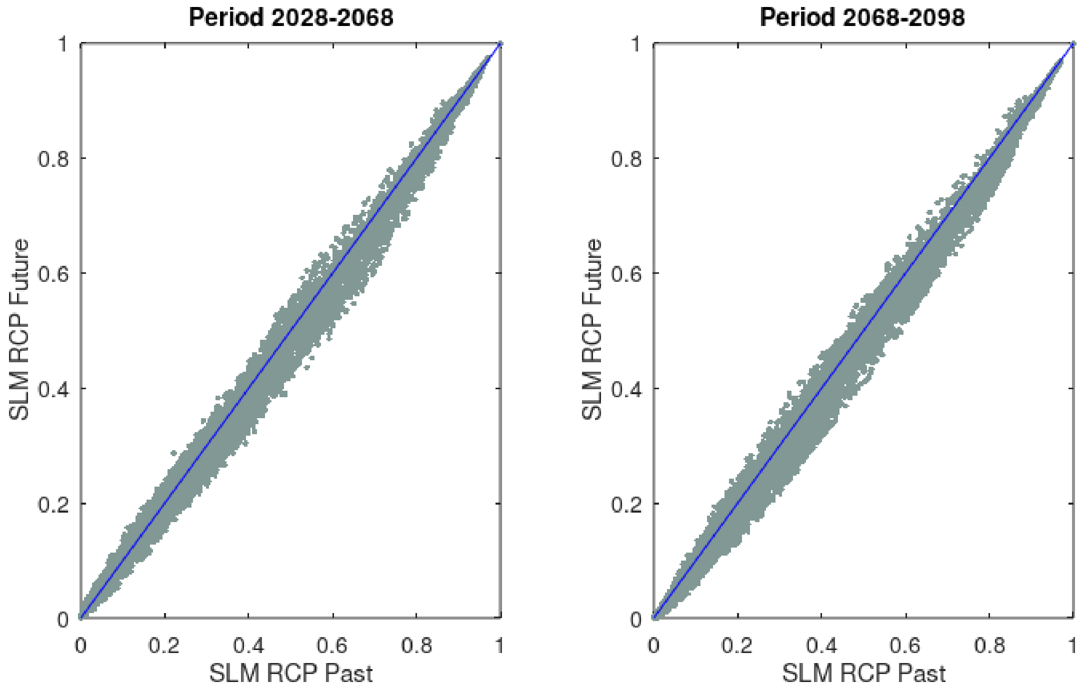

Wine grape: chill suitability score RCP 2.6

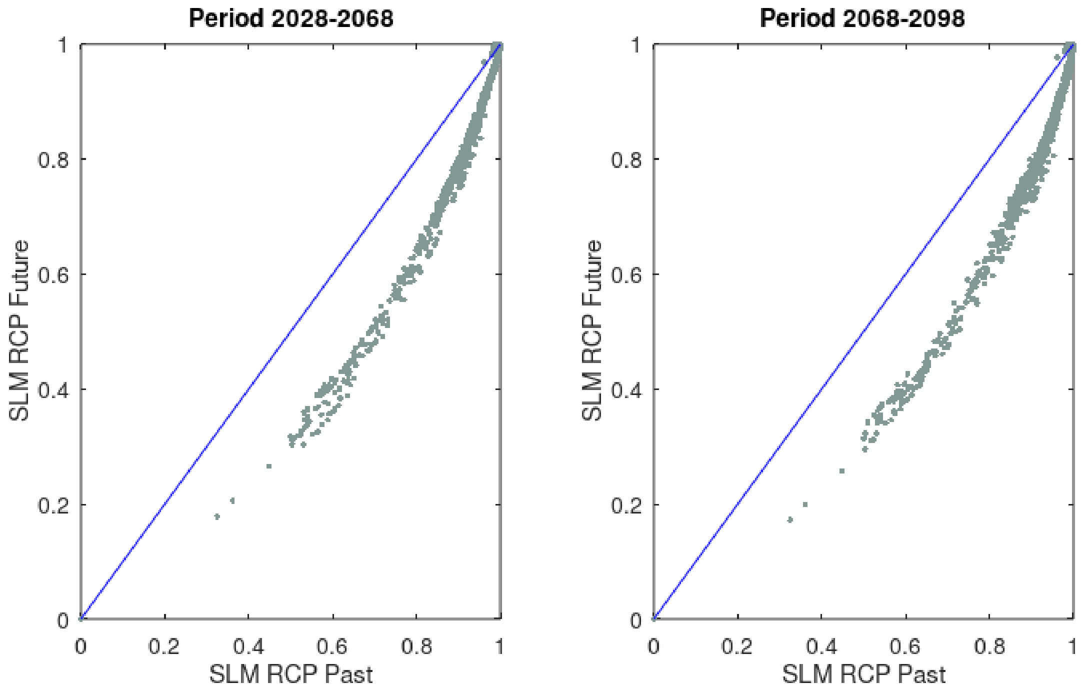

22 Wine grape common to both Pinot noir and Sauvignon blanc RCP 4.5

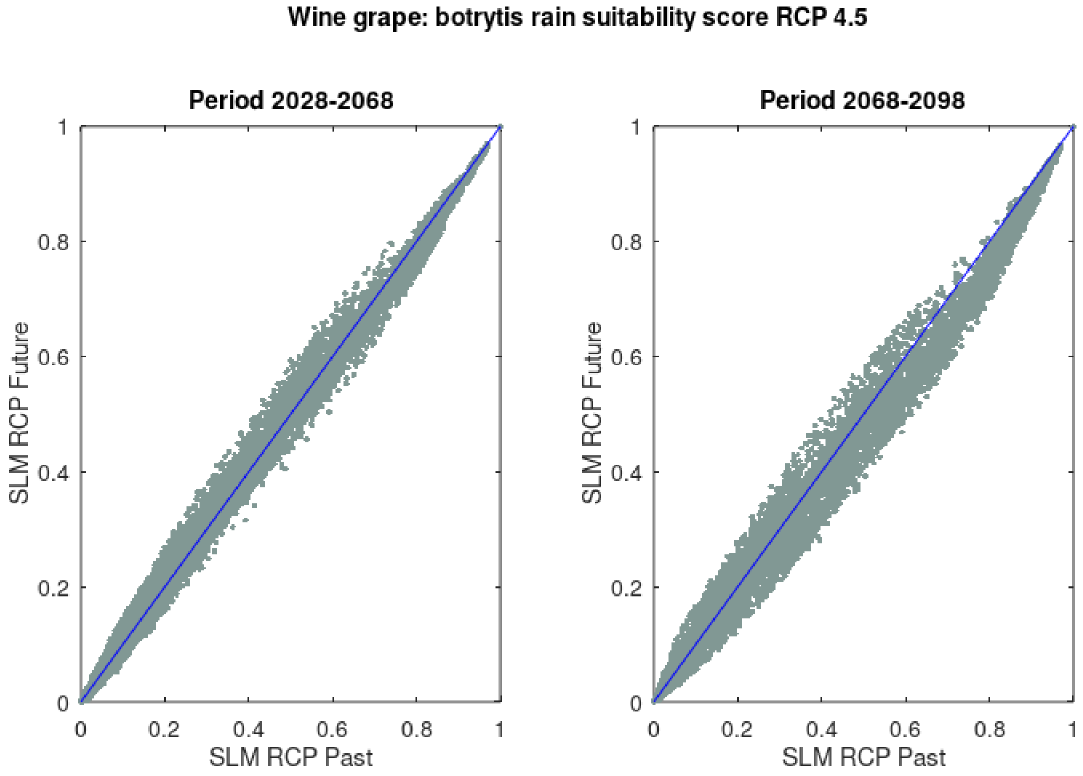

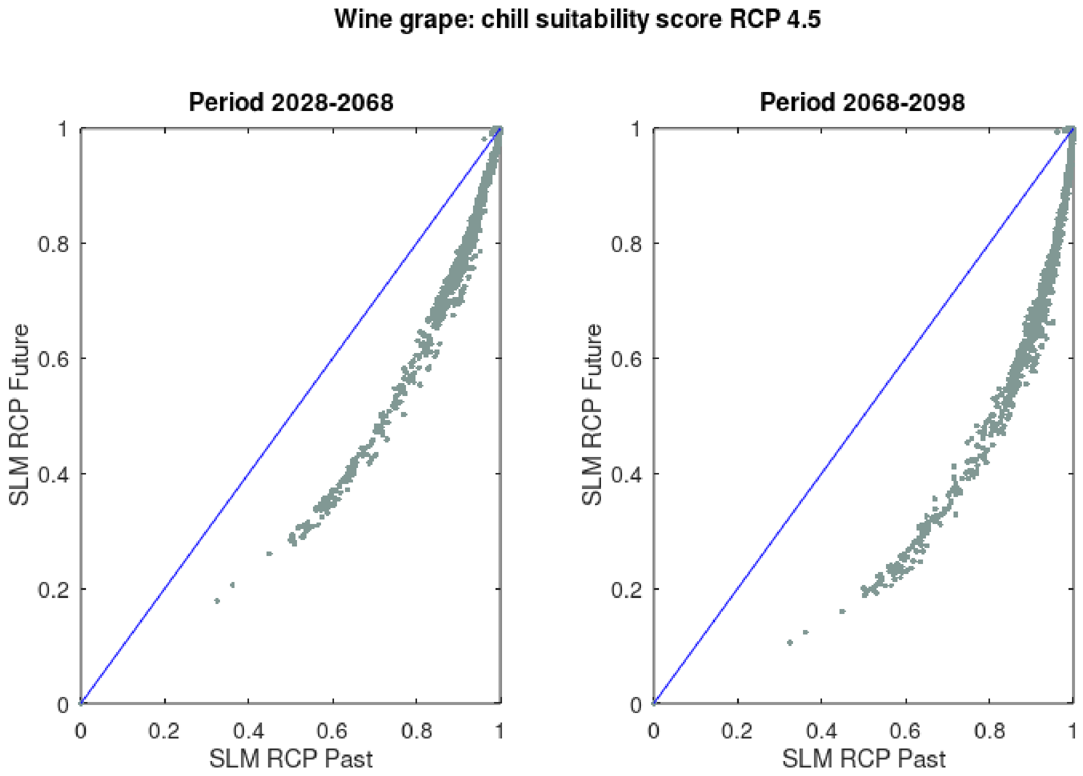

23 Wine grape common to both Pinot noir and Sauvignon blanc RCP 6.0

Wine grape: botrytis rain suitability score RCP 6.0

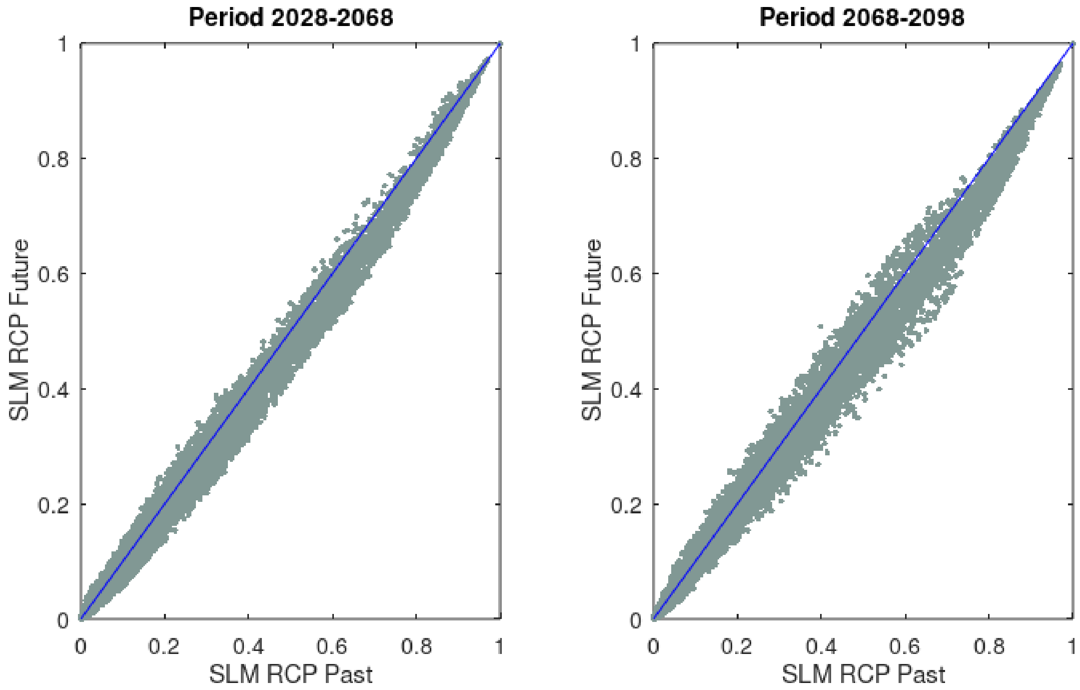

Wine grape: chill suitability score RCP 6.0

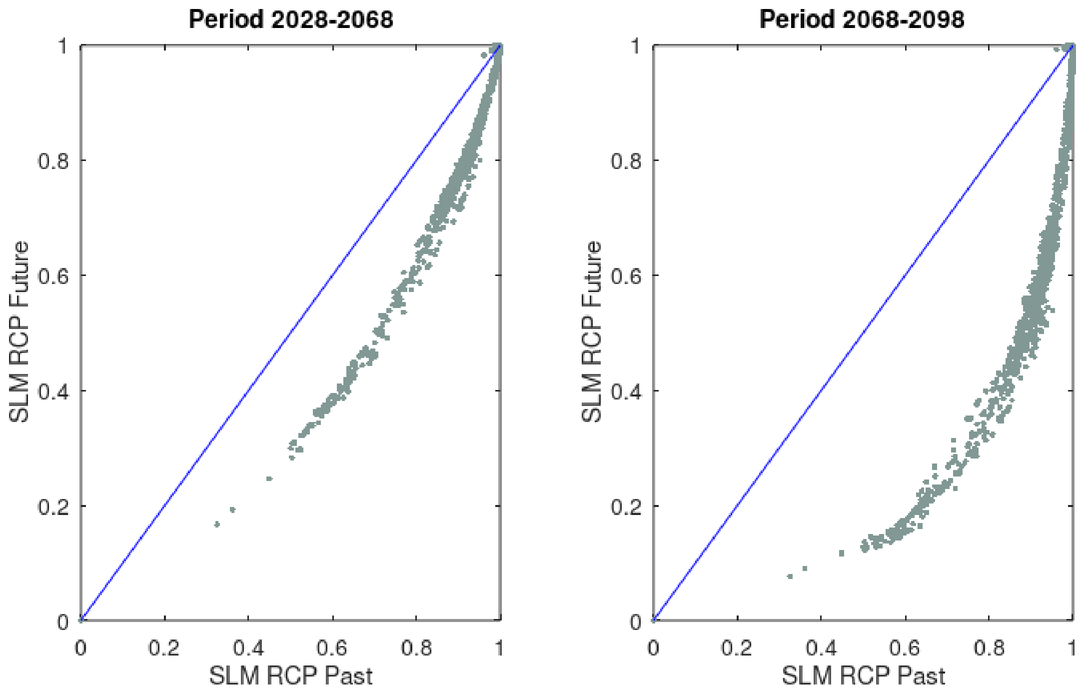

24 Wine grape common to both Pinot noir and Sauvignon blanc RCP 8.5

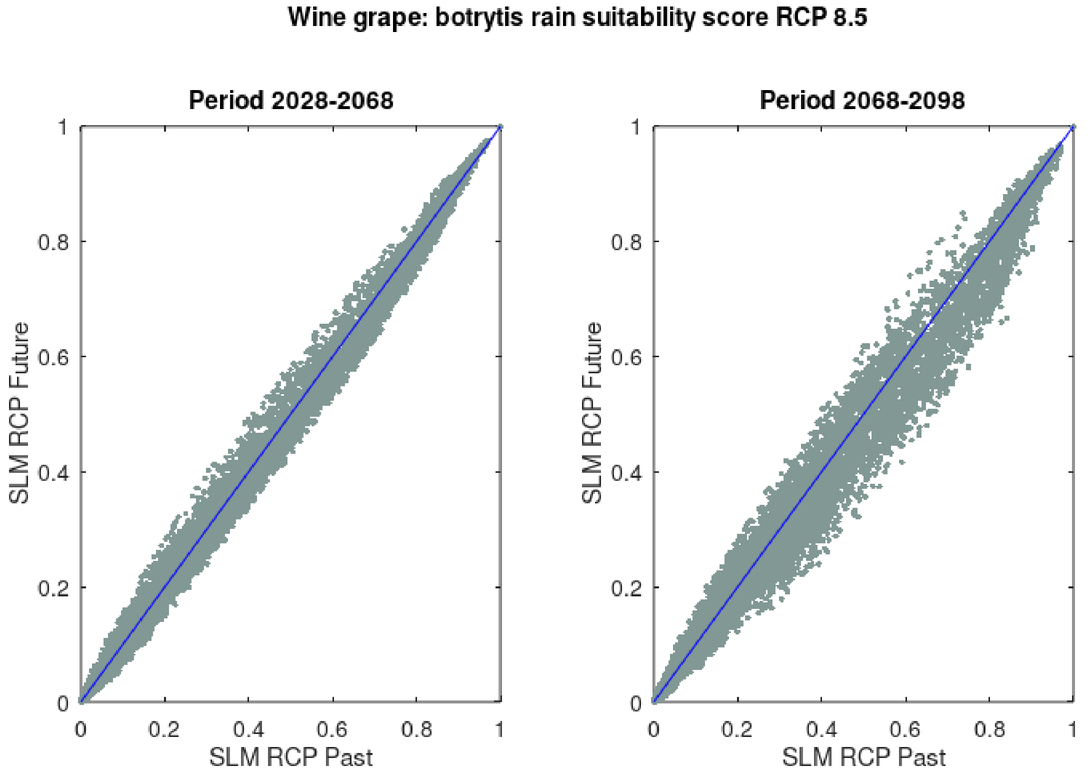

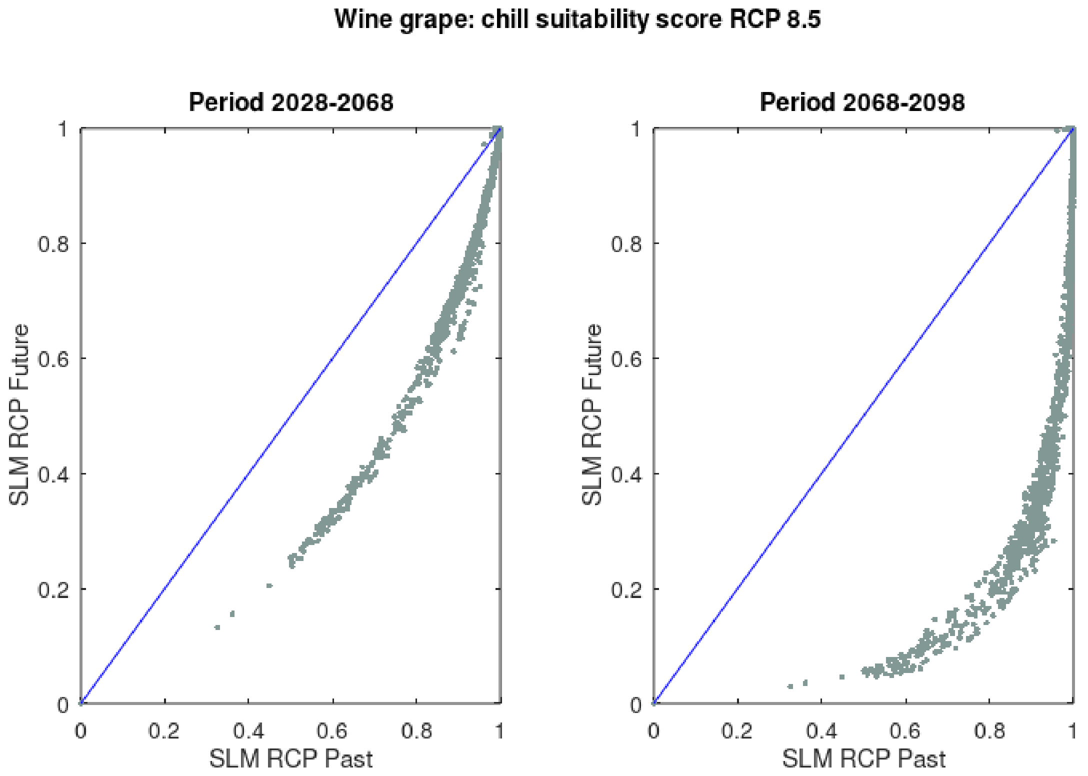

25 Pinot noir RCP 2.6

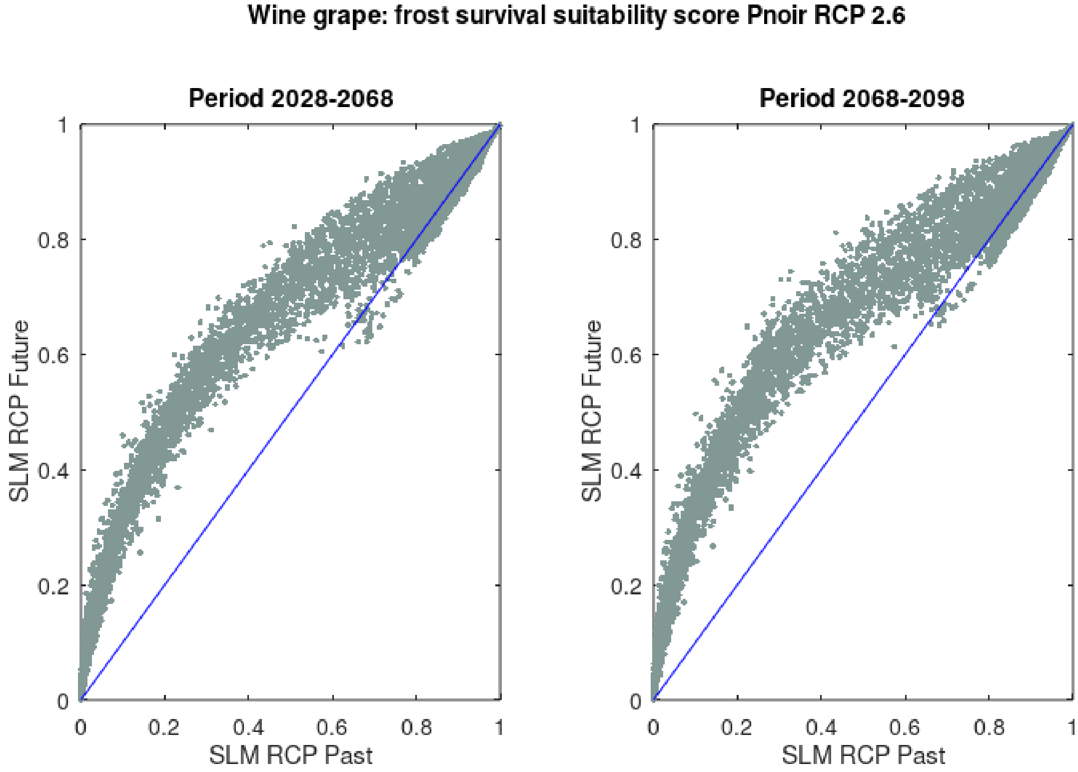

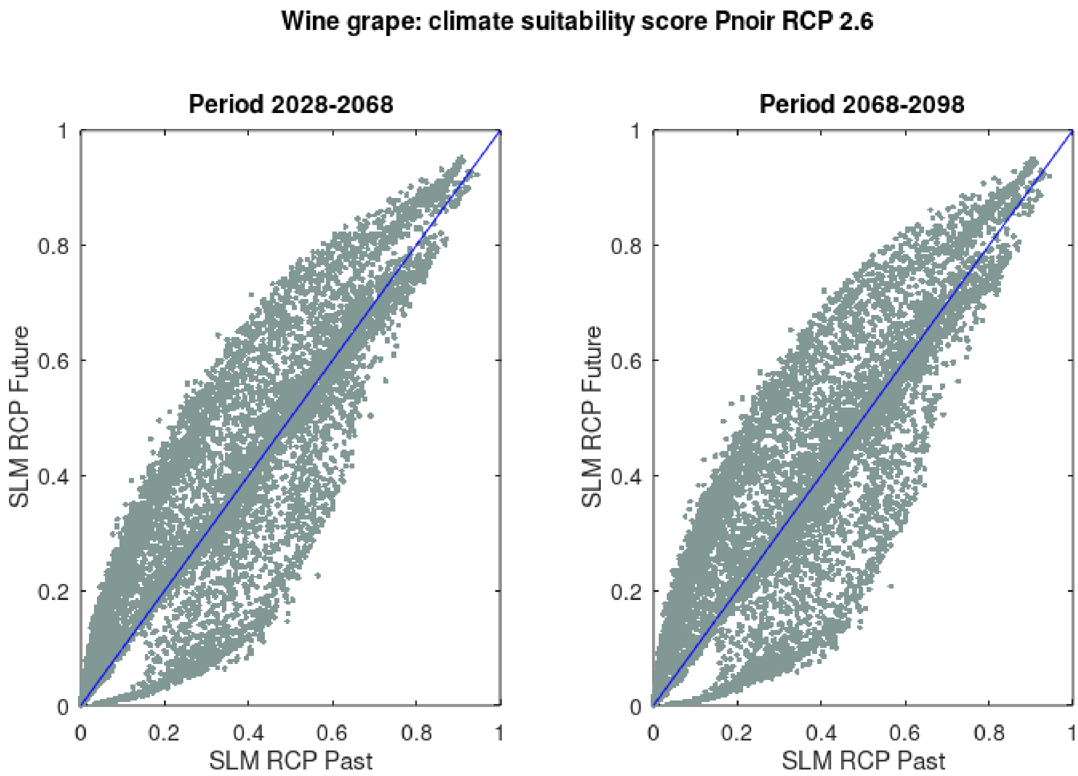

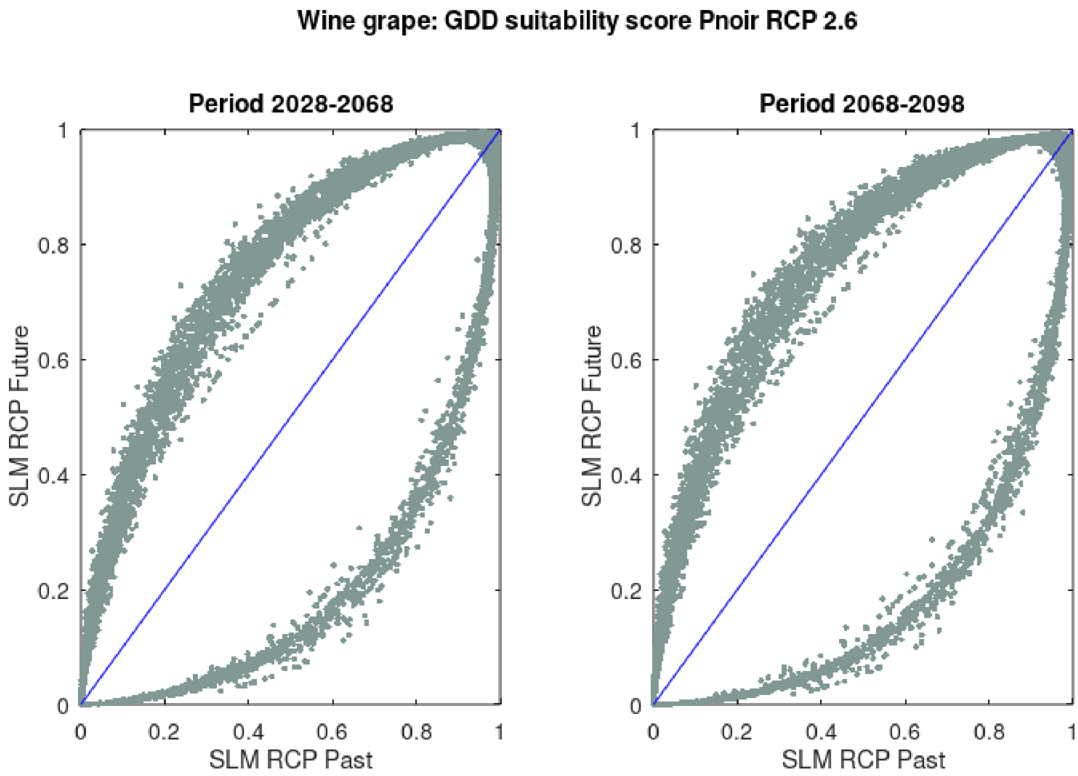
Wine grape: GDD suitability score Pnoir RCP 2.6
Period 2028-2068
Period 2068-2098
SLM RCP Future
SLM RCP Past
0
0.2
0.4
0.6
0.8
1

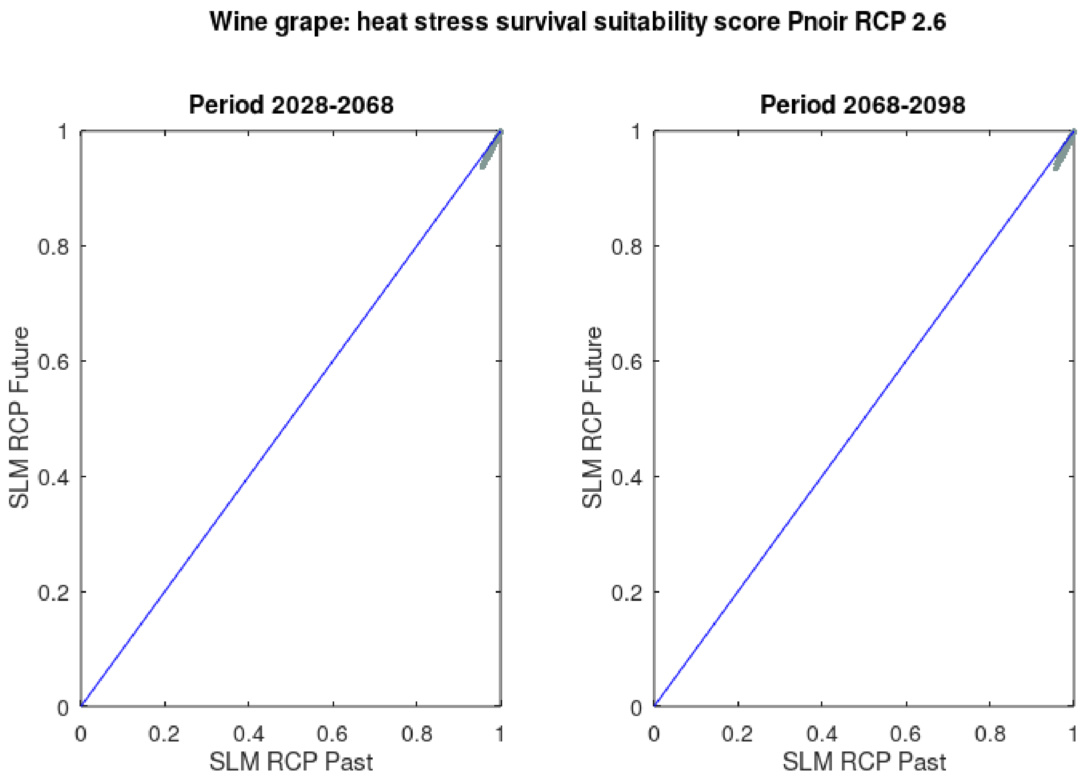
Wine grape: heat stress survival suitability score Pnoir RCP 2.6
Period 2028-2068
Period 2068-2098
SLM RCP Future
SLM RCP Past
0
0.2
0.4
0.6
0.8
1

26 Pinot noir RCP 4.5

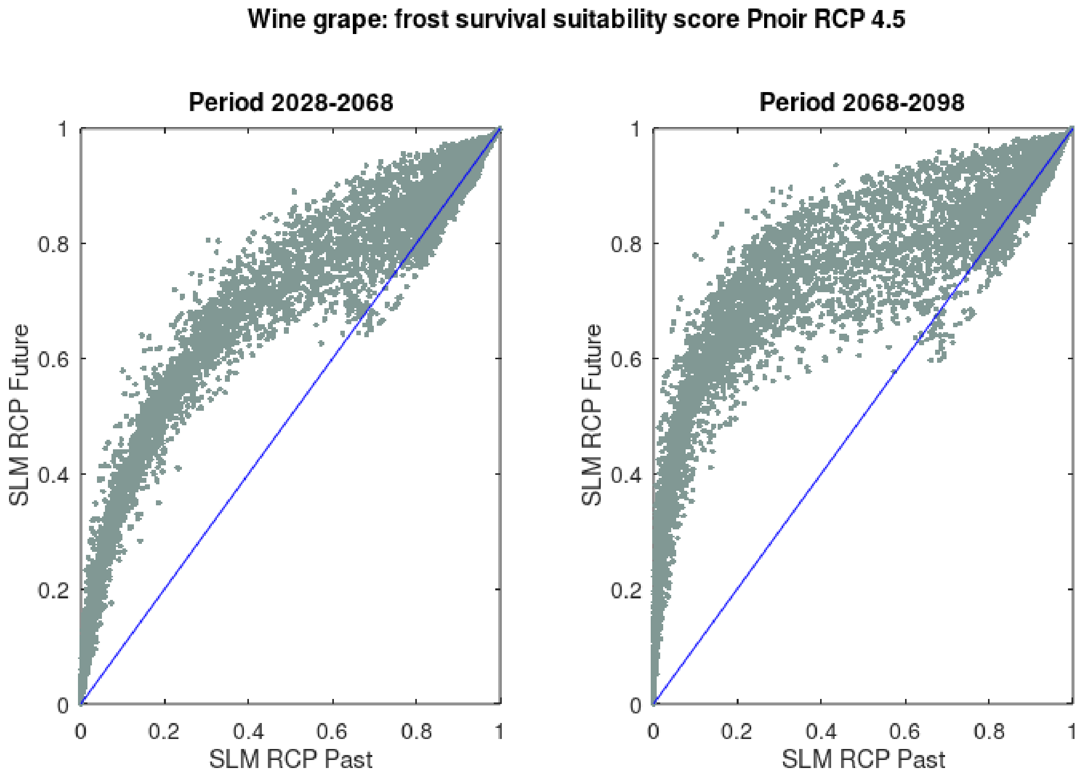

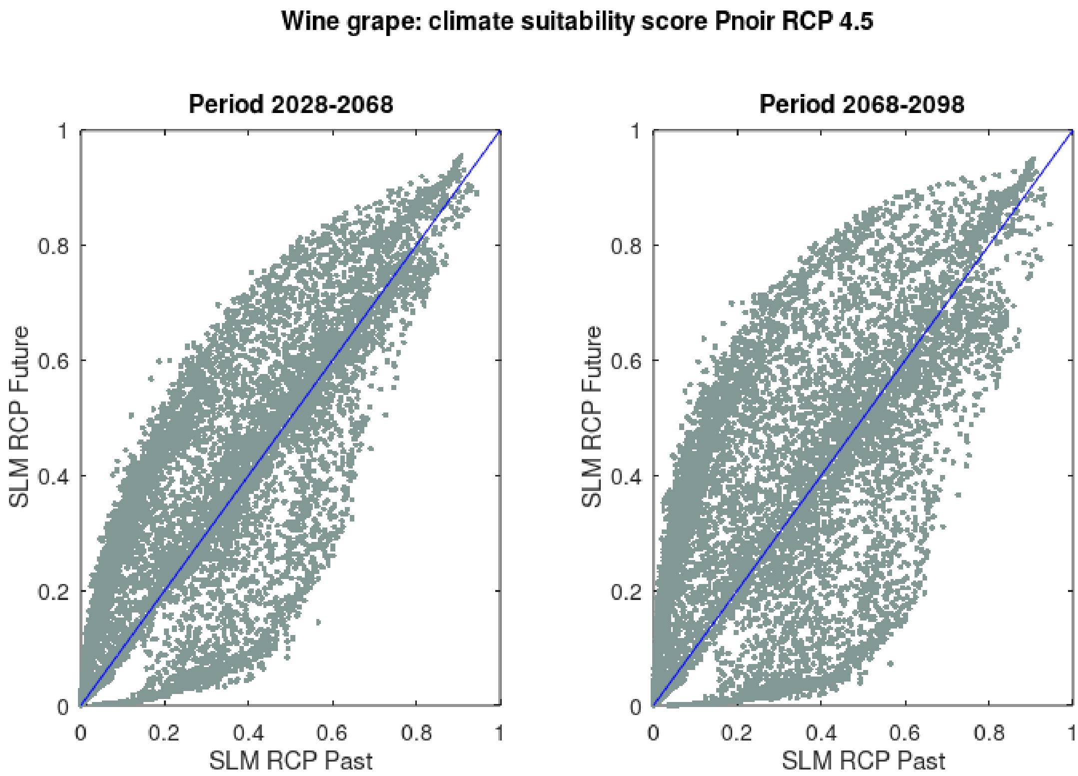

Wine grape: GDD suitability score Pnoir RCP 4.5

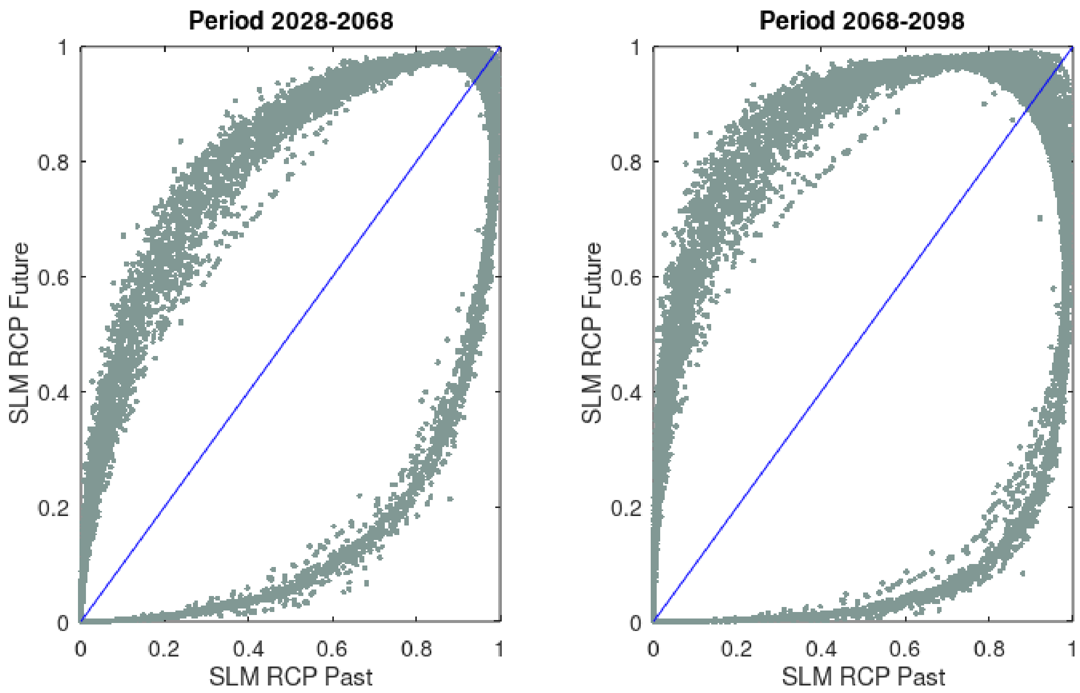

Wine grape: heat stress survival suitability score Pnoir RCP 4.5

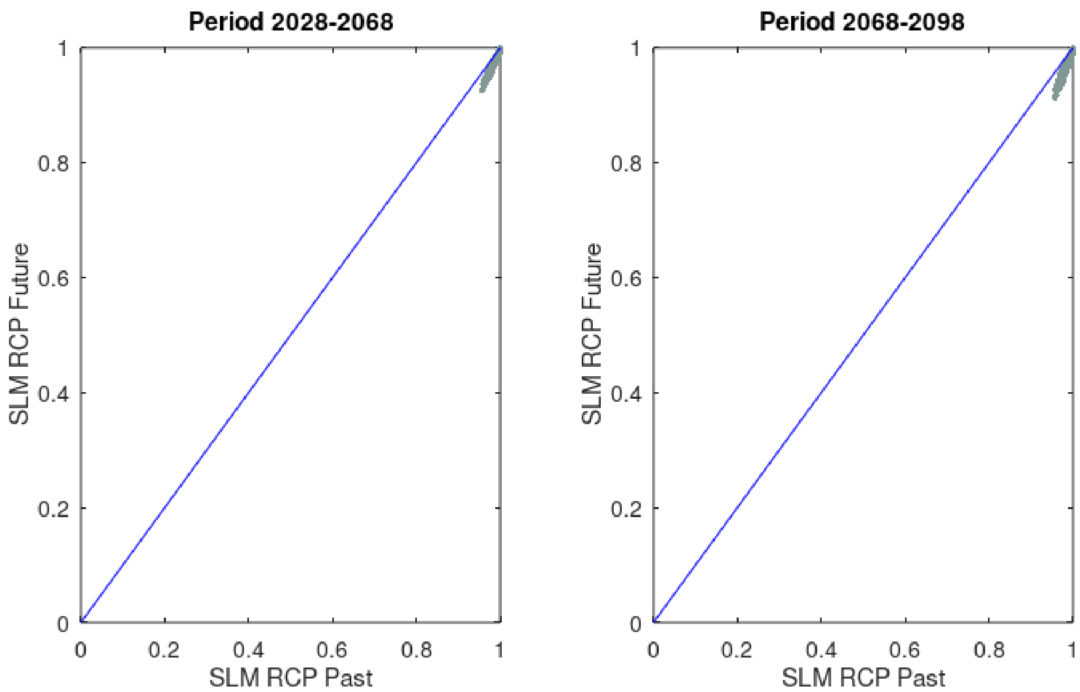

27 Pinot noir RCP 6.0

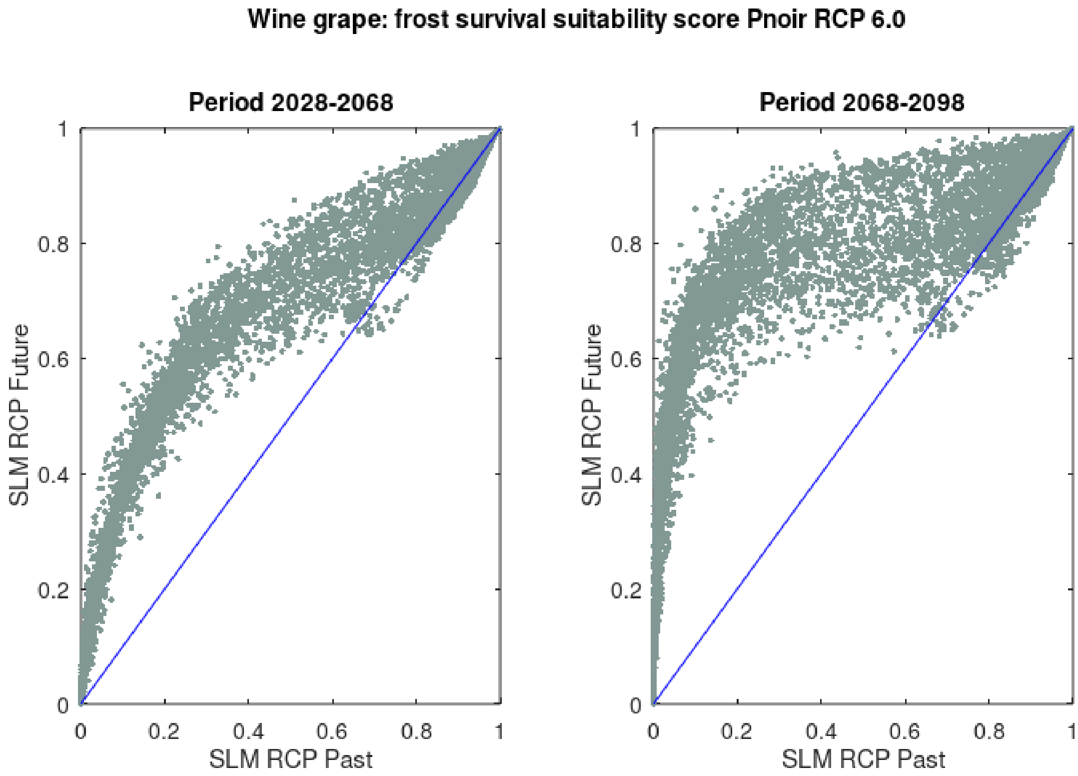

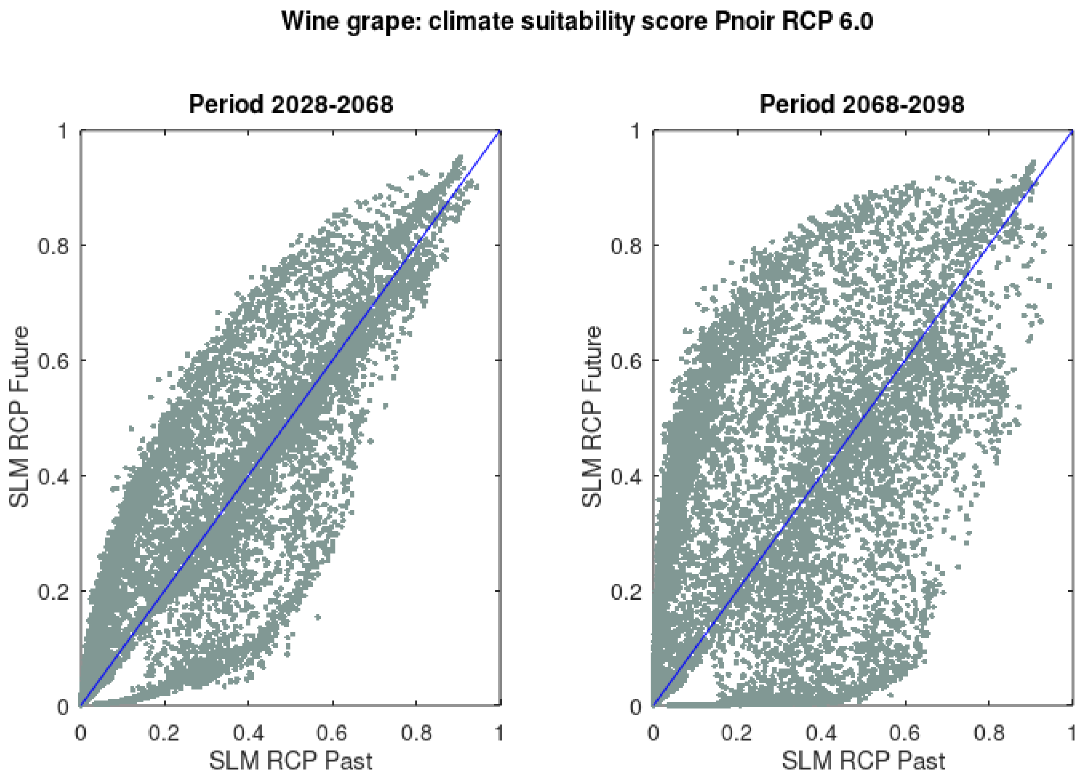

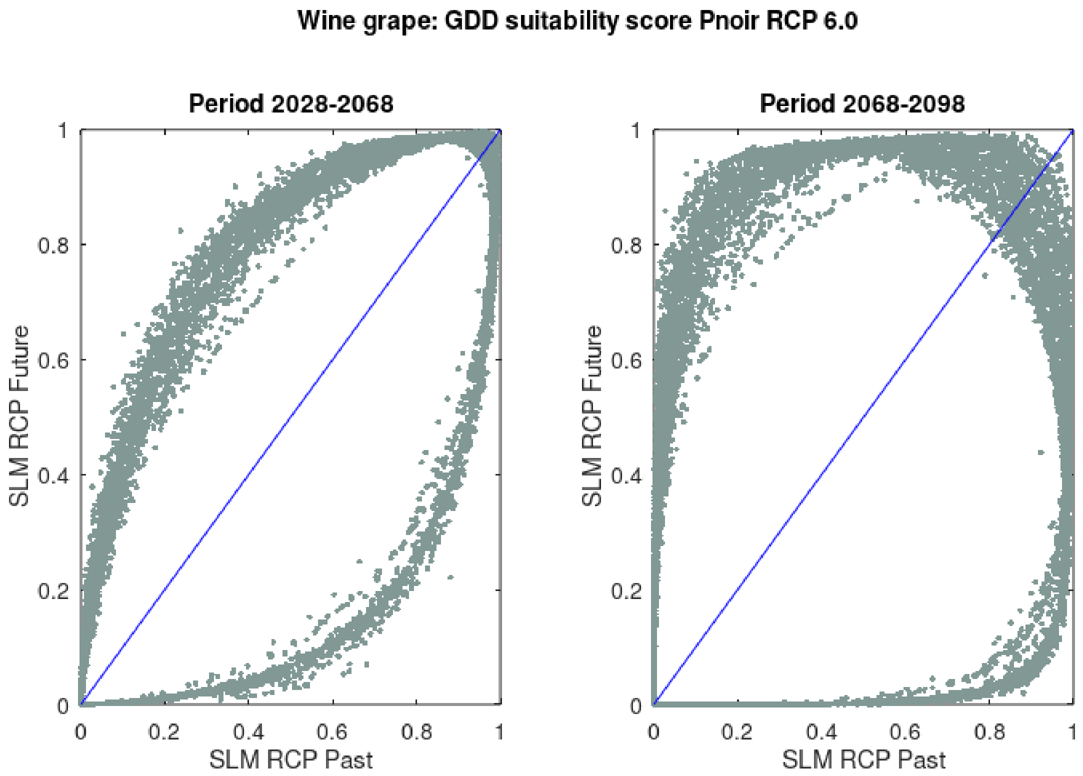
Wine grape: GDD suitability score Pnoir RCP 6.0
Period 2028-2068
Period 2068-2098
SLM RCP Future
SLM RCP Past
0
0.2
0.4
0.6
0.8
1

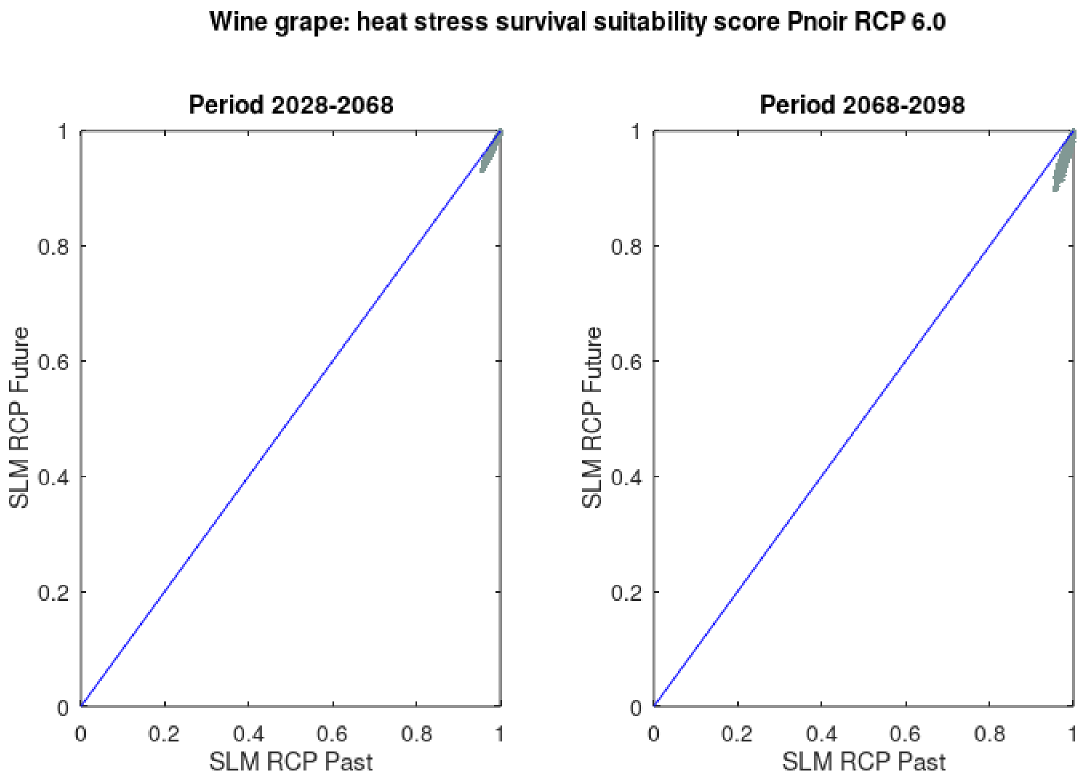
Wine grape: heat stress survival suitability score Pnoir RCP 6.0
Period 2028-2068
Period 2068-2098
SLM RCP Future
SLM RCP Past
0
0.2
0.4
0.6
0.8
1

28 Pinot noir RCP 8.5

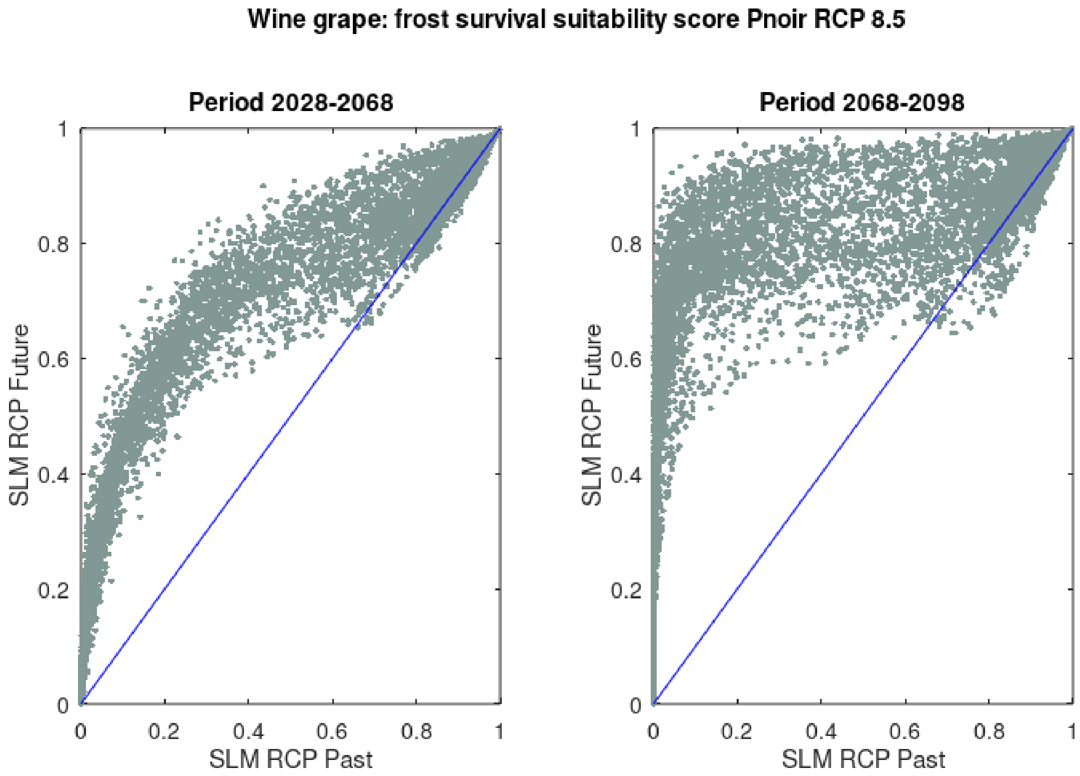

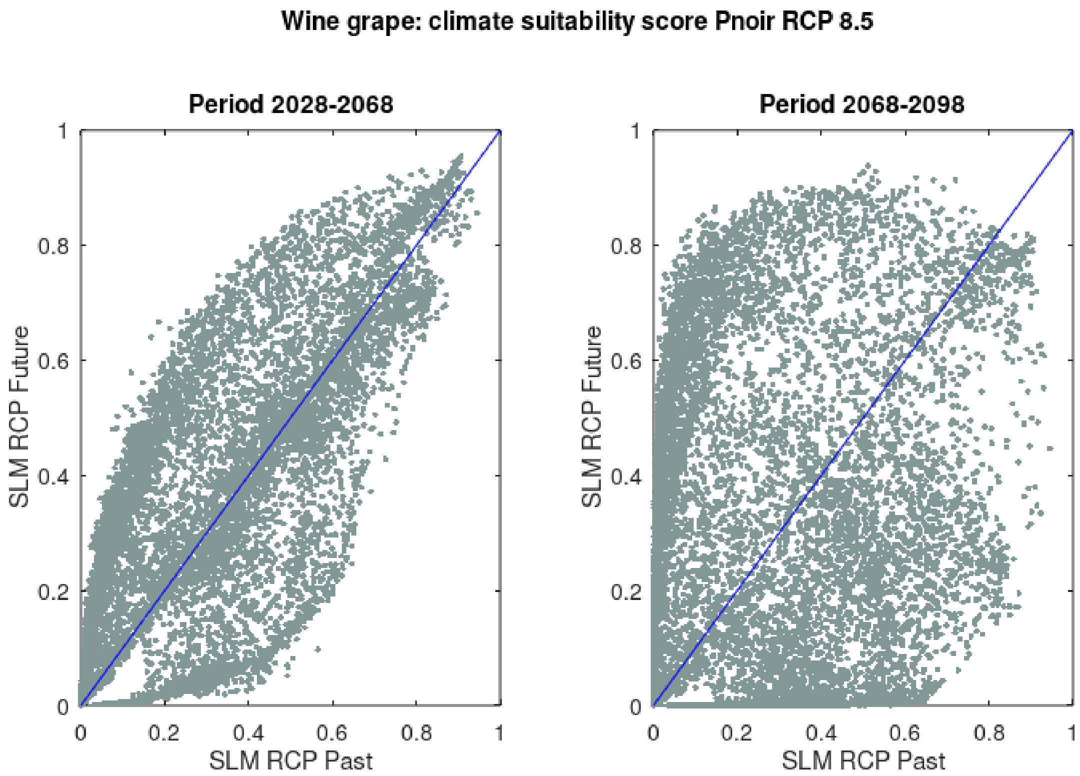

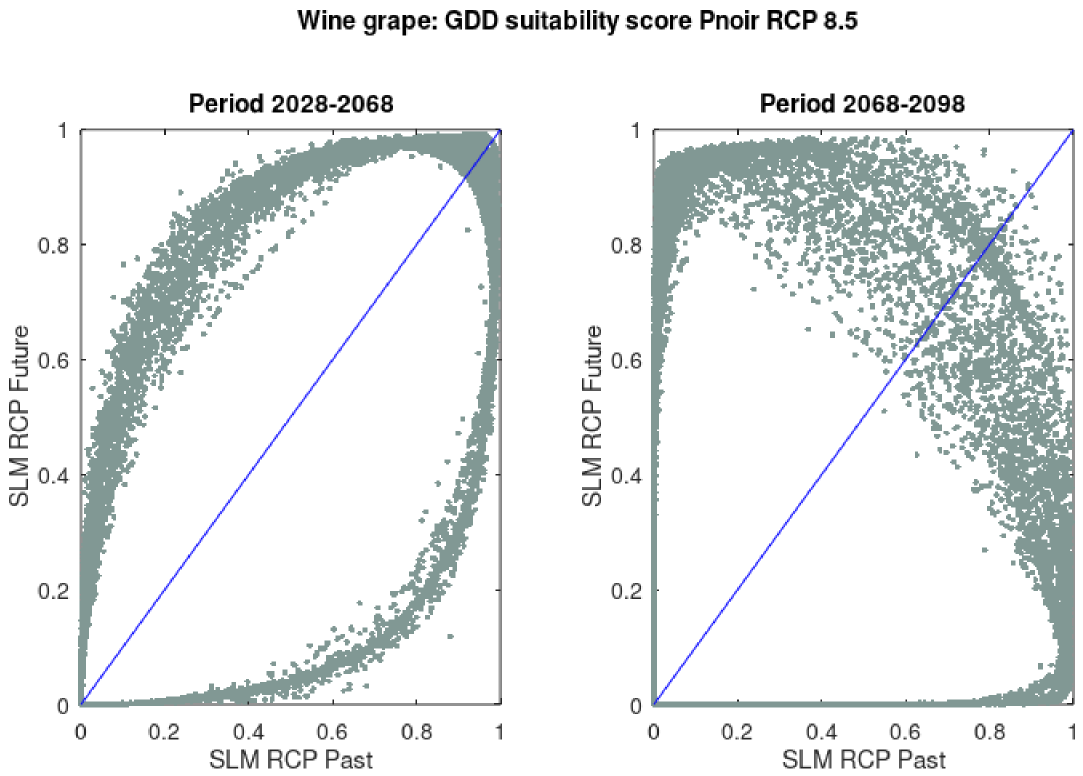
Wine grape: GDD suitability score Pnoir RCP 8.5
Period 2028-2068
Period 2068-2098
SLM RCP Future
SLM RCP Past
0
0.2
0.4
0.6
0.8
1

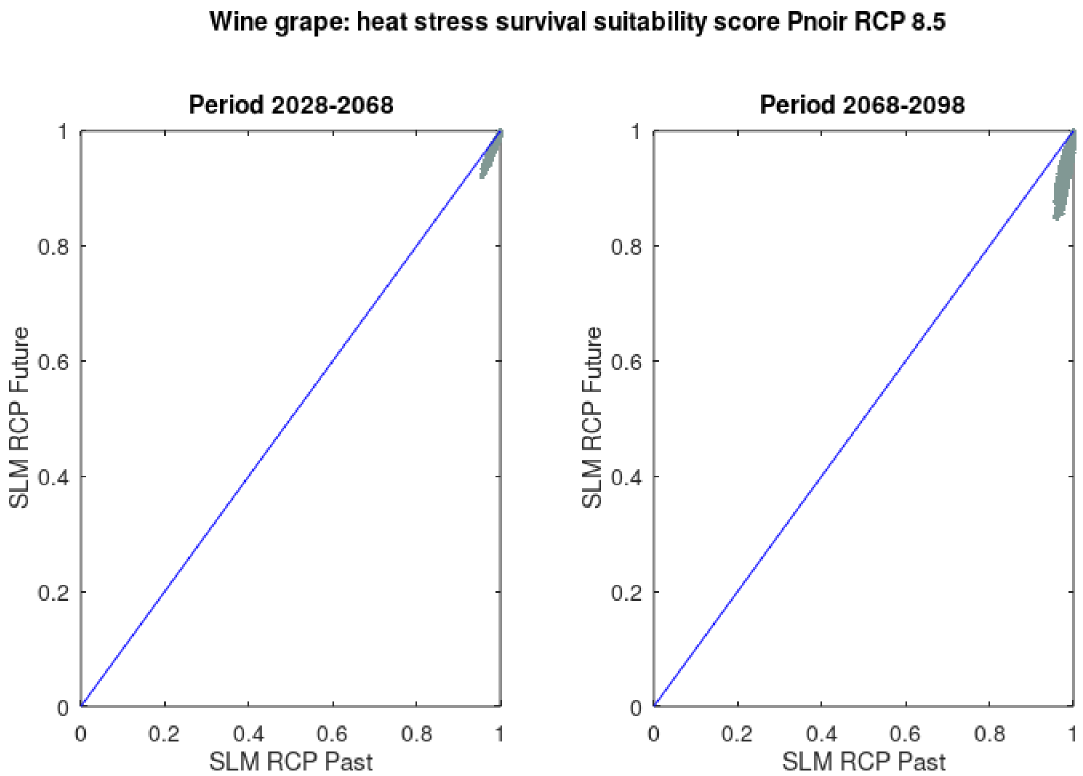
Wine grape: heat stress survival suitability score Pnoir RCP 8.5
Period 2028-2068
Period 2068-2098
SLM RCP Future
SLM RCP Past
0
0.2
0.4
0.6
0.8
1

29 Sauvignon blanc RCP 2.6

Wine grape: frost survival suitability score Sblanc RCP 2.6

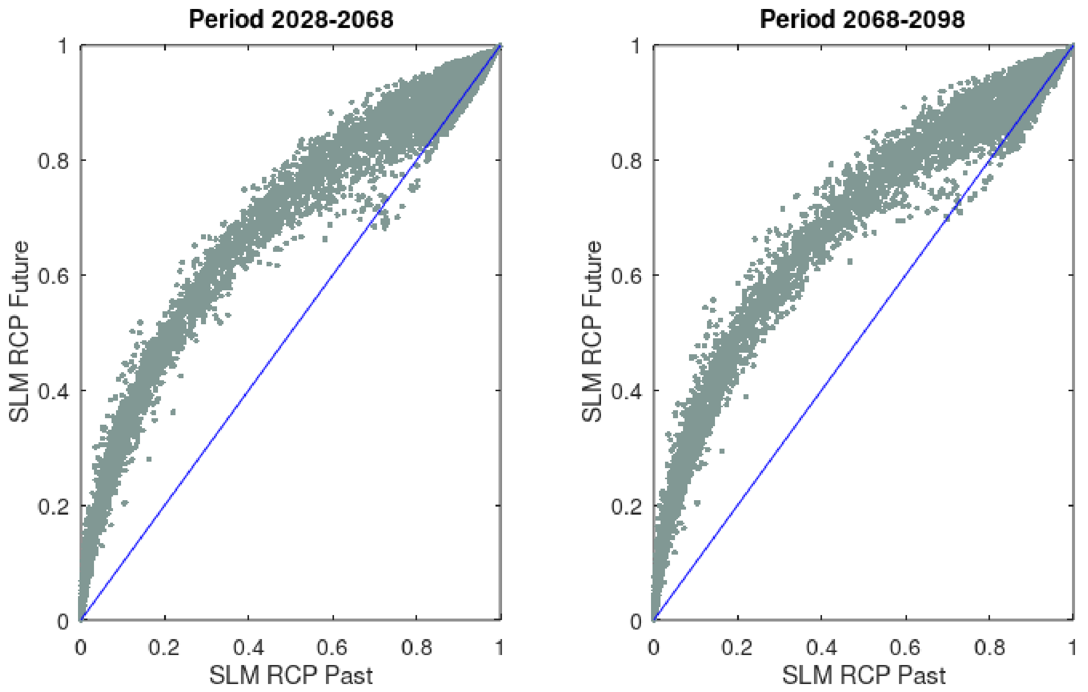

Wine grape: climate suitability score Sblanc RCP 2.6

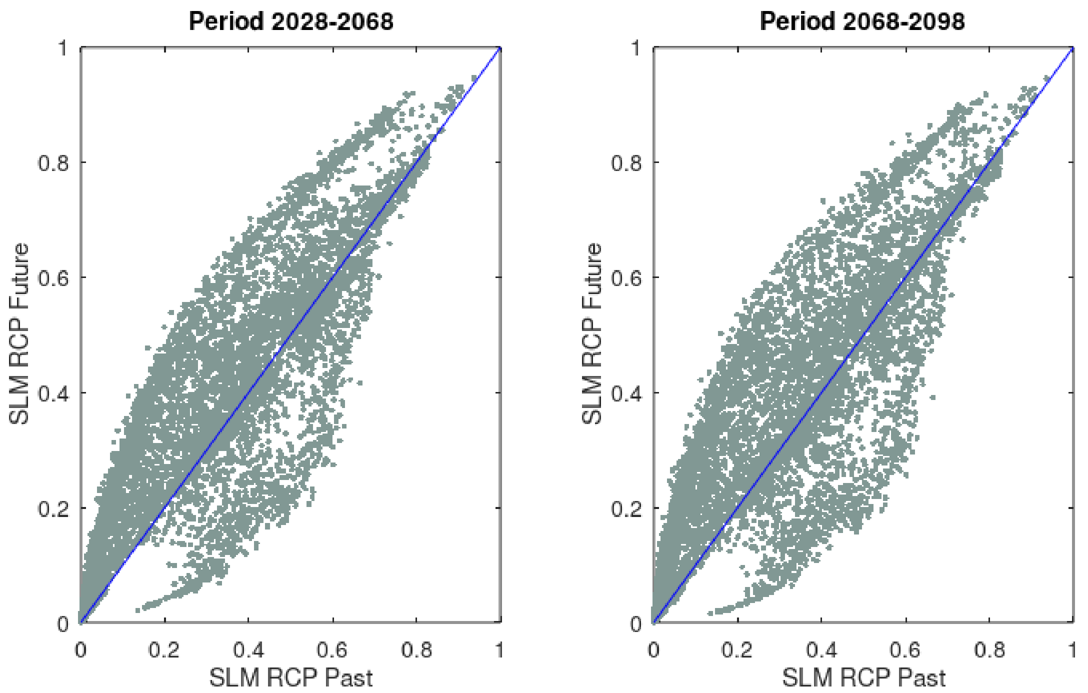

Wine grape: GDD suitability score Sblanc RCP 2.6

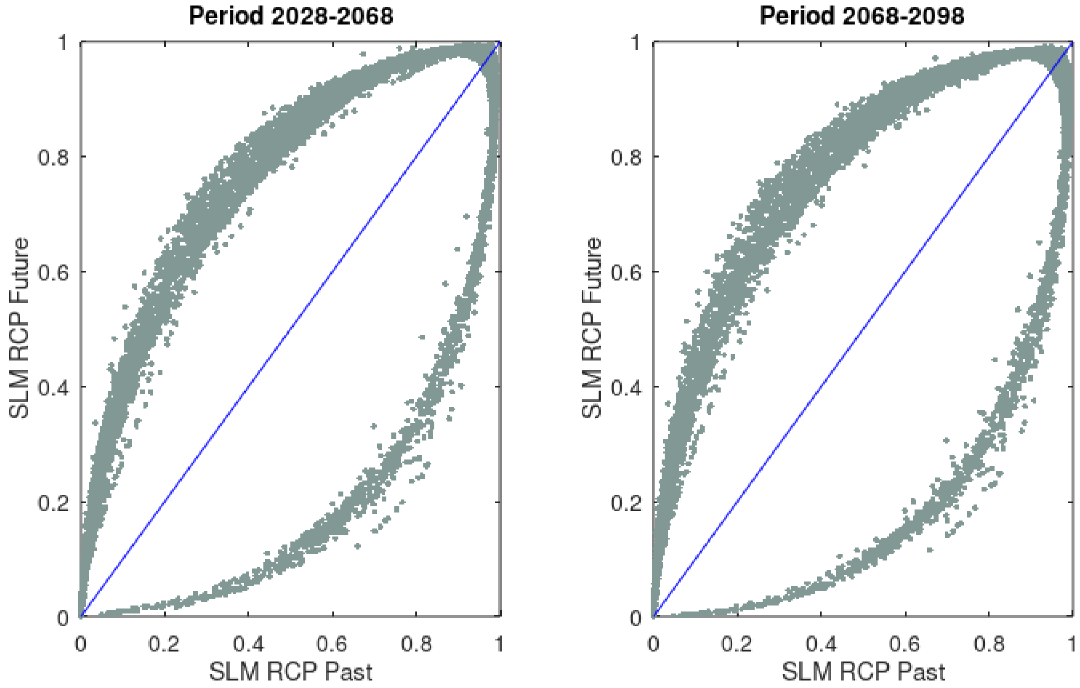

Wine grape: heat stress survival suitability score Sblanc RCP 2.6

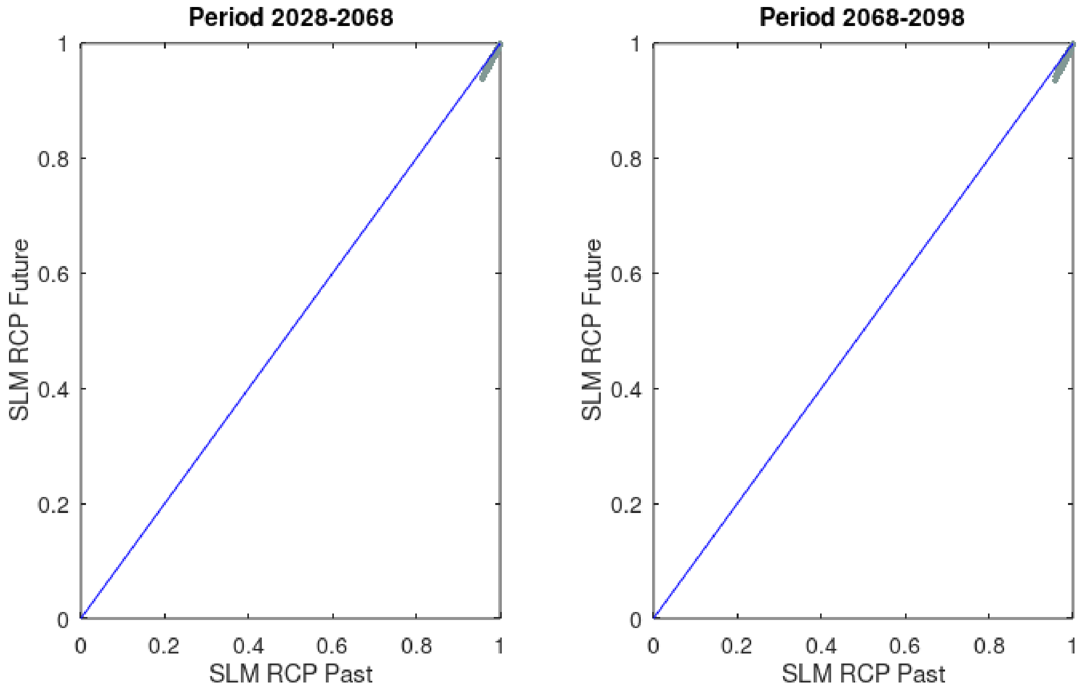

30 Sauvignon blanc RCP 4.5

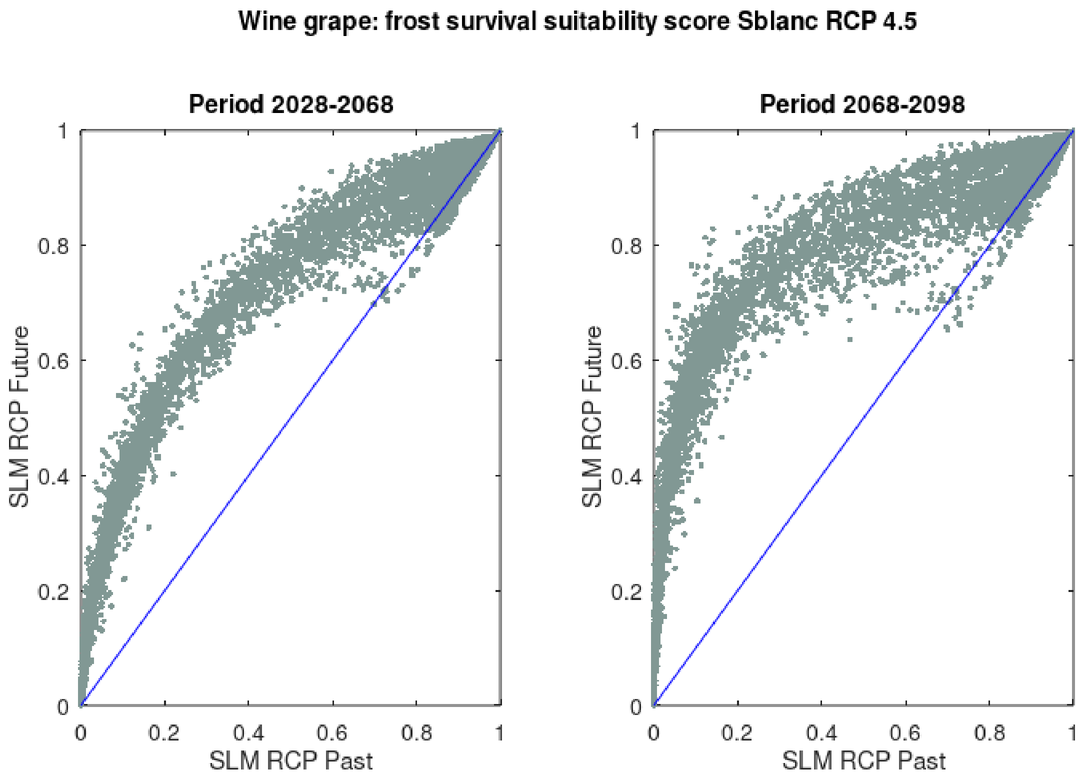

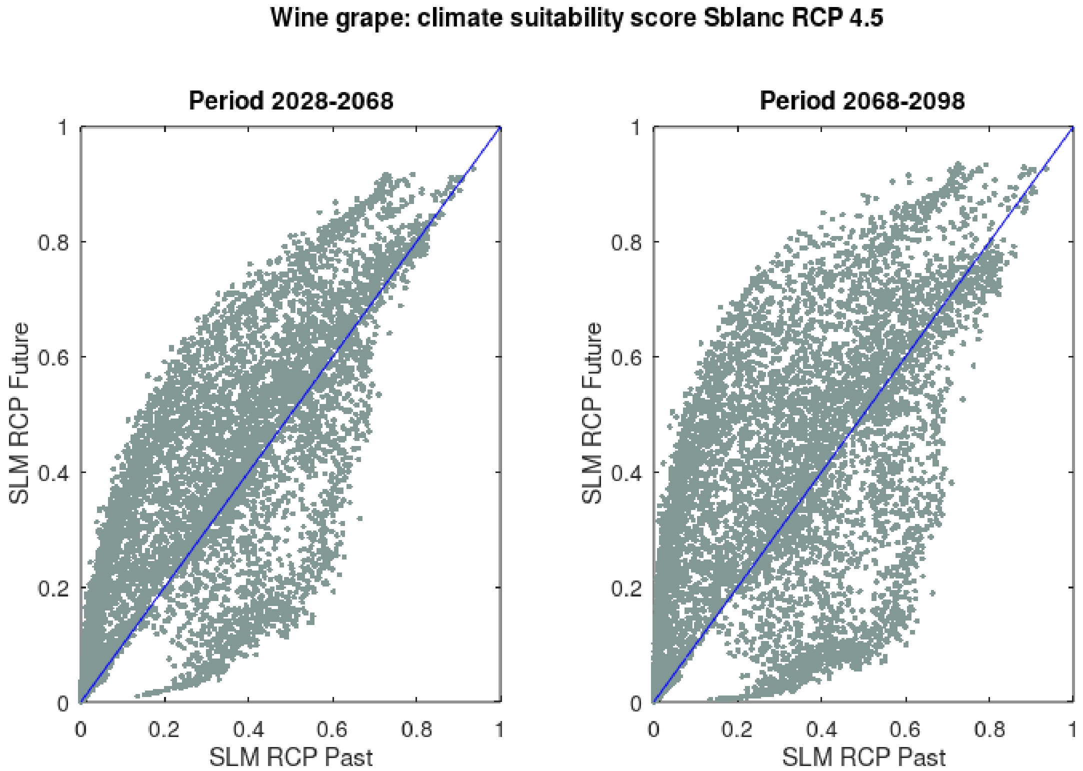

Wine grape: GDD suitability score Sblanc RCP 4.5

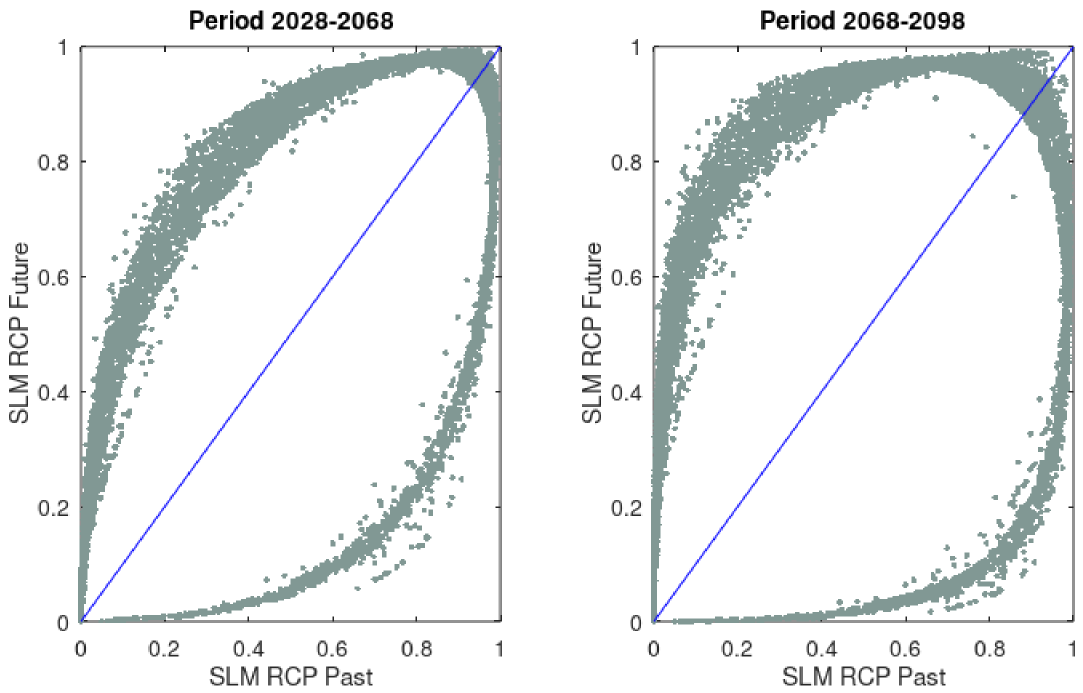

Wine grape: heat stress survival suitability score Sblanc RCP 4.5

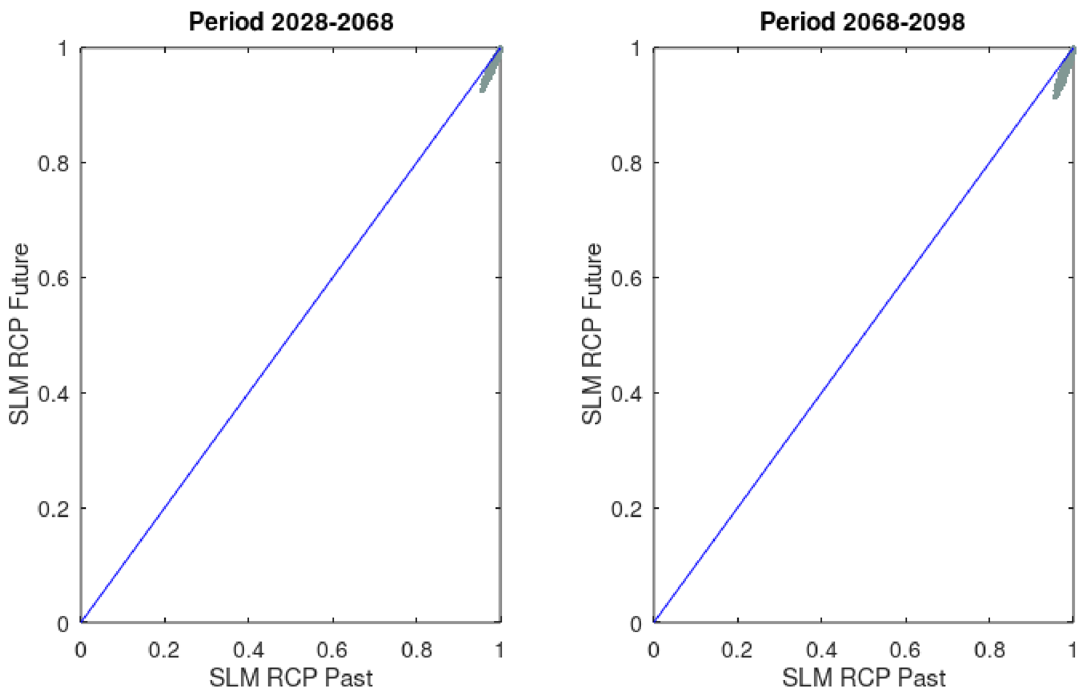

31 Sauvignon blanc RCP 6.0

Wine grape: frost survival suitability score Sblanc RCP 6.0

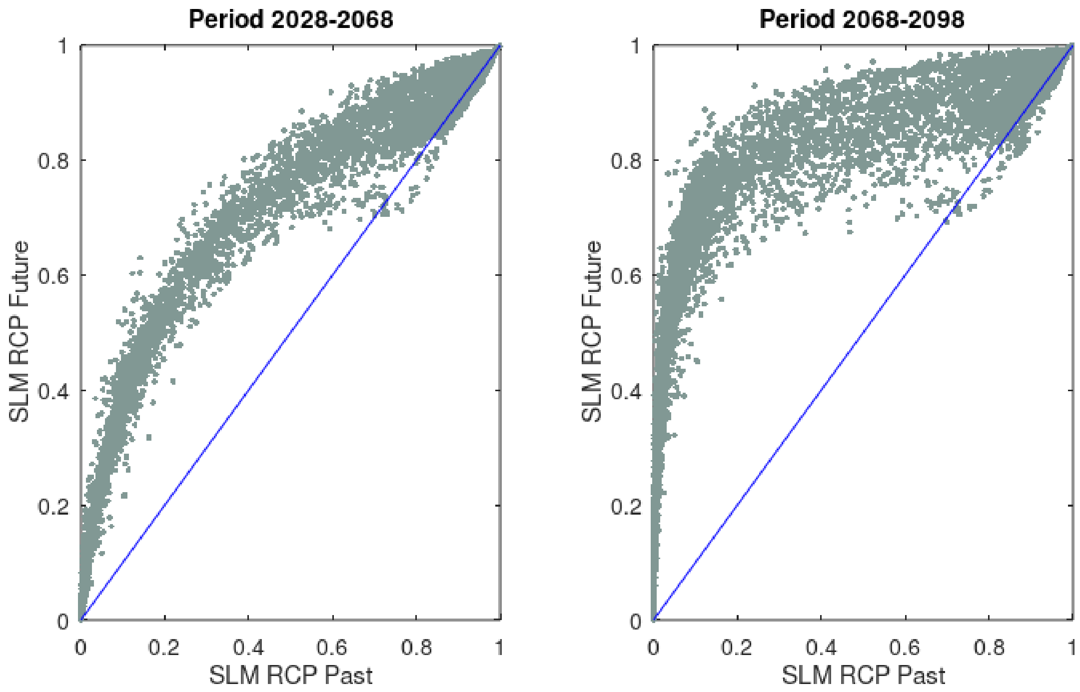

Wine grape: climate suitability score Sblanc RCP 6.0

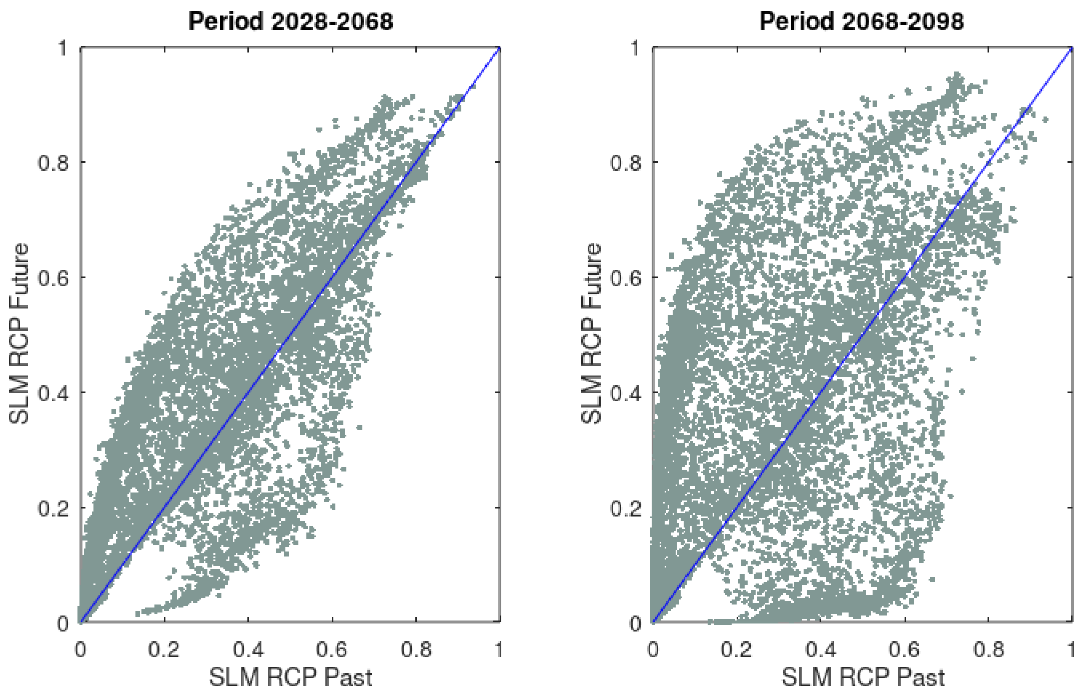

Wine grape: GDD suitability score Sblanc RCP 6.0

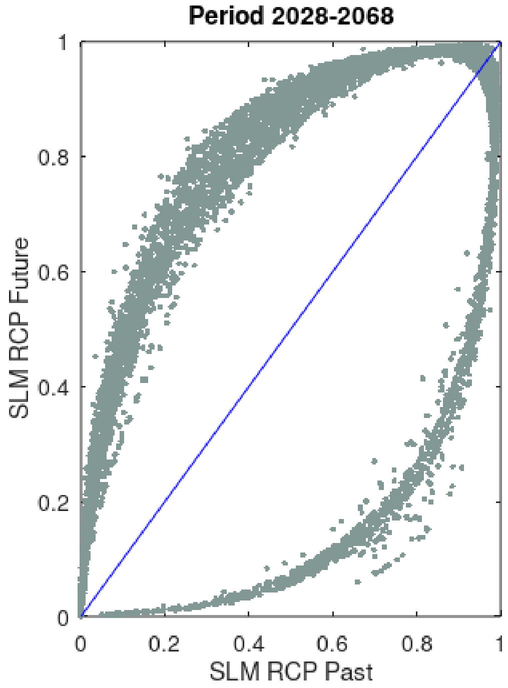

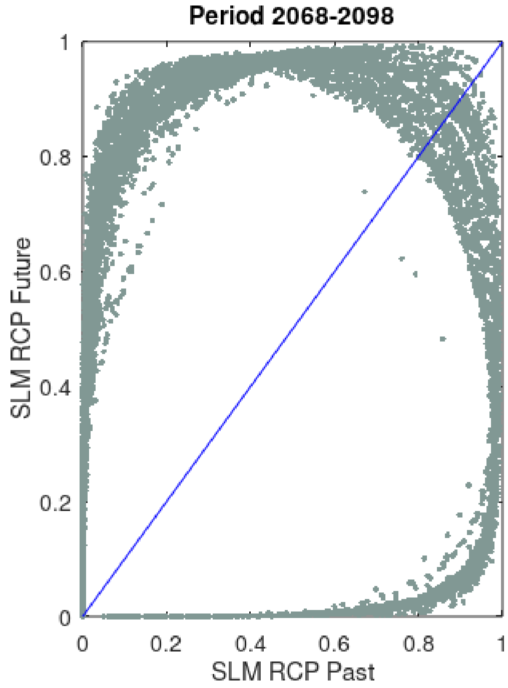

Wine grape: heat stress survival suitability score Sblanc RCP 6.0

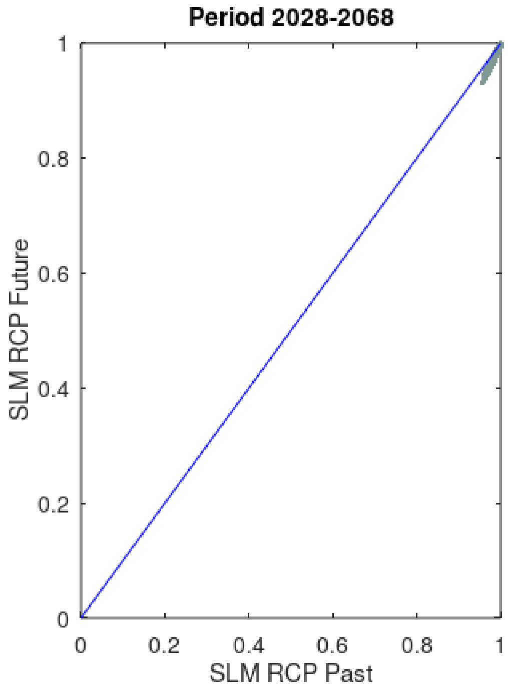

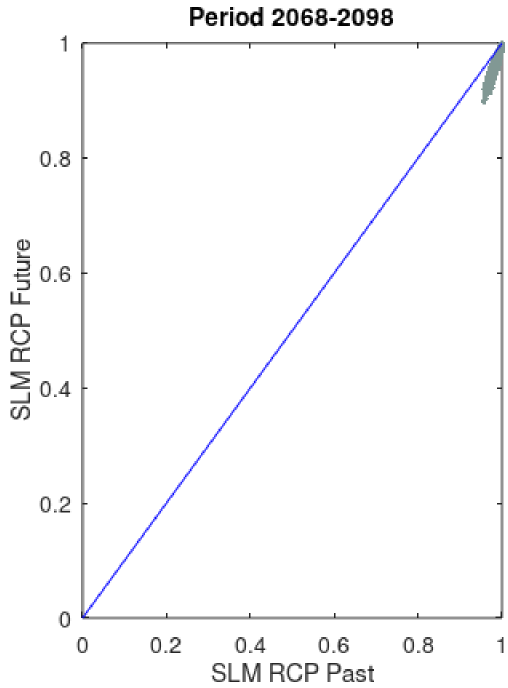

32 Sauvignon blanc RCP 8.5

Wine grape: frost survival suitability score Sblanc RCP 8.5

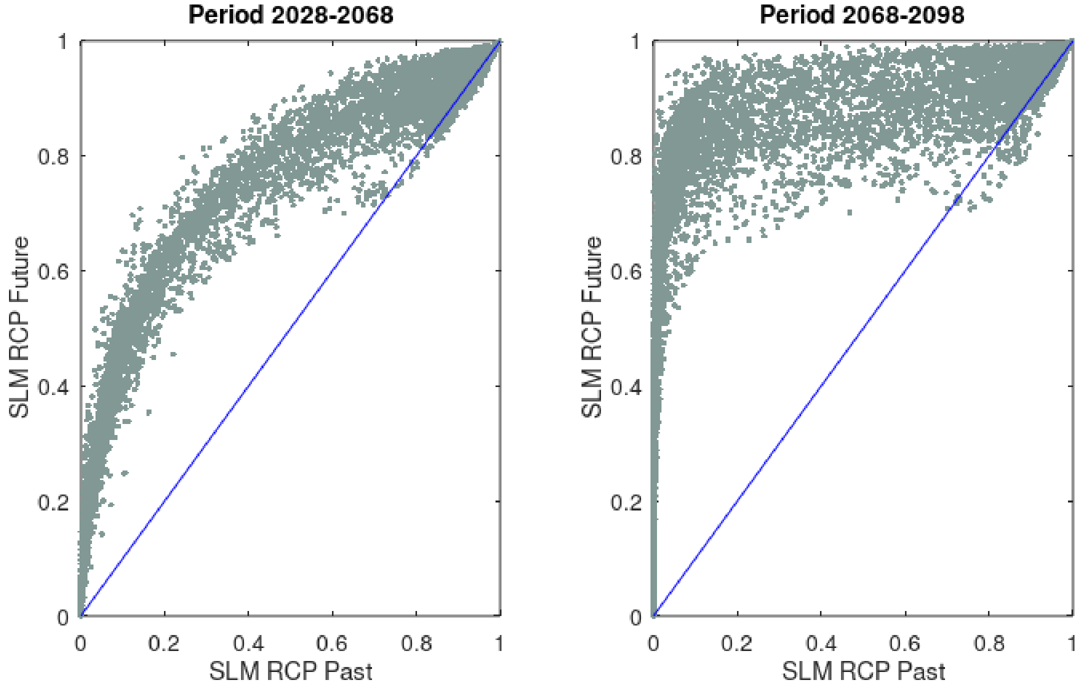

Wine grape: climate suitability score Sblanc RCP 8.5

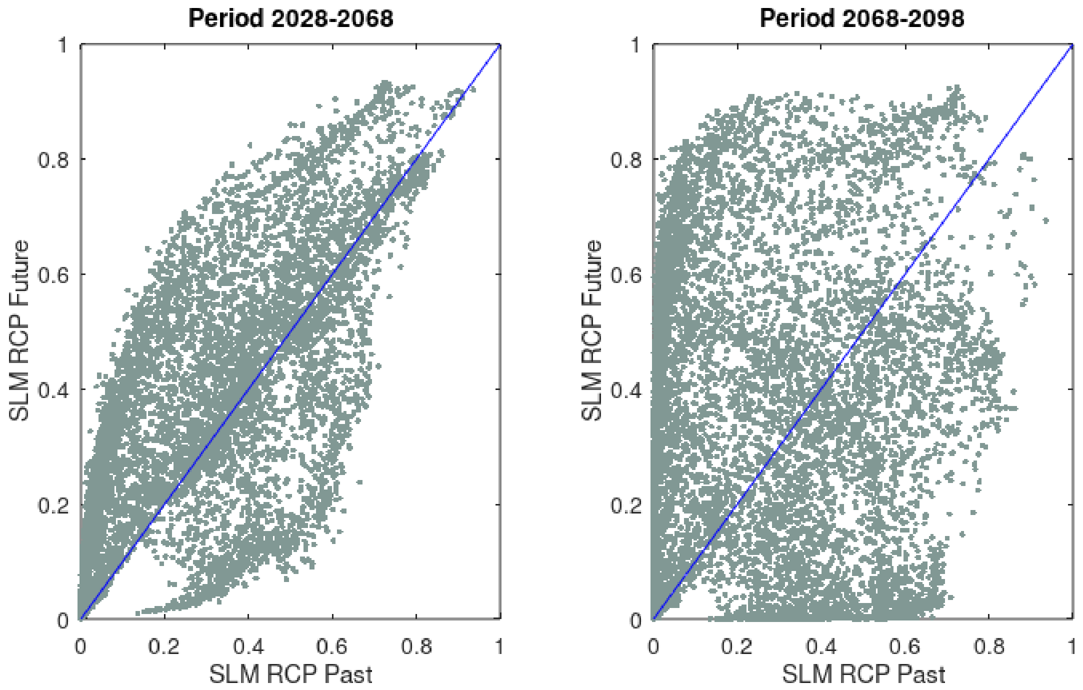

Wine grape: GDD suitability score Sblanc RCP 8.5

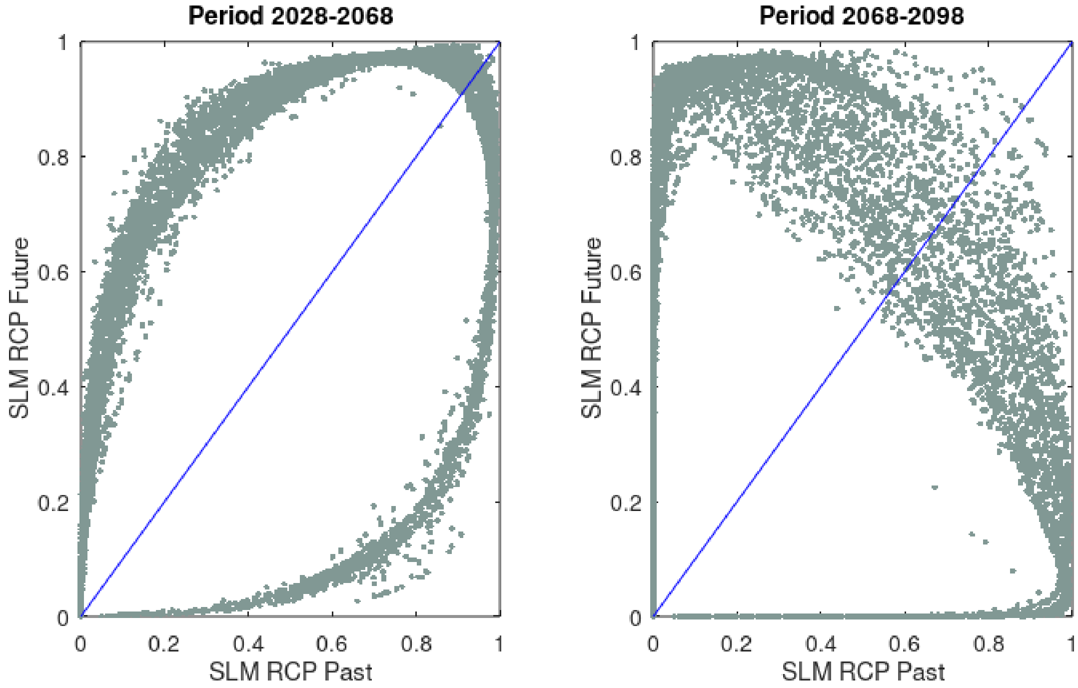

Wine grape: heat stress survival suitability score Sblanc RCP 8.5

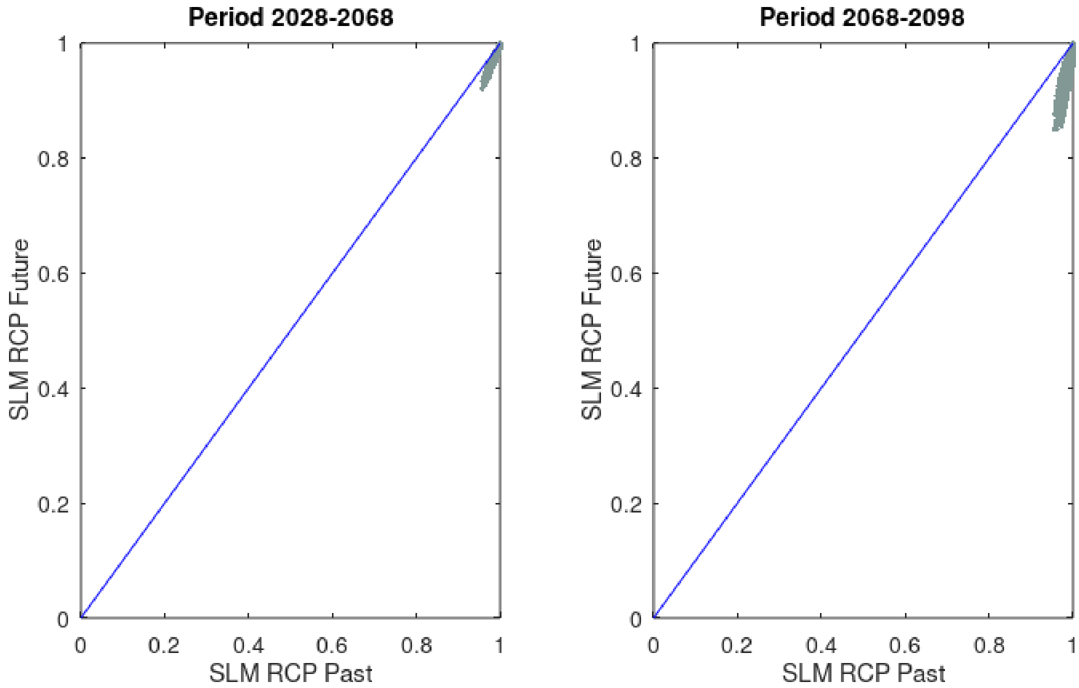

33 Impact of bias corrections on climate change signals

Climate change signals were calculated by comparing how the statistics of variables changed from the 1986–2005 period to both the 2031–2050 and the 2080–2099 periods, for each individual grid location. Change signals for minimum, maximum and mean annual temperature, and for relative humidity (RH) were obtained by calculating the difference between means for the periods. Change signals for the variance of minimum and maximum temperatures were calculated by taking variance ratios. Change signals for rainfall were calculated in terms of percent change.

These calculations were done separately for the 24 combinations of six GCMs × four RCP scenarios, for both the original RCP datasets and the new SLM datasets. The impact of the bias corrections on the climate change signal was obtained by looking at the differences in change signals between the RCP and SLM RCP datasets.

Results indicate that the impacts on change signals were slight to small, and further reduced by considering an ensemble of all six GCMs in an RCP scenario. The impacts on the change signal for minimum and maximum tended to have opposing signs with similar magnitude which cancelled each other when mean temperatures were calculated. Thus the change signal for mean temperature was much less affected by the bias corrections.

Impacts of the bias corrections are presented below for ensembles and then for individual GCMS.

33.1 Impact of bias corrections on ensemble climate change signals under RCP 2.6

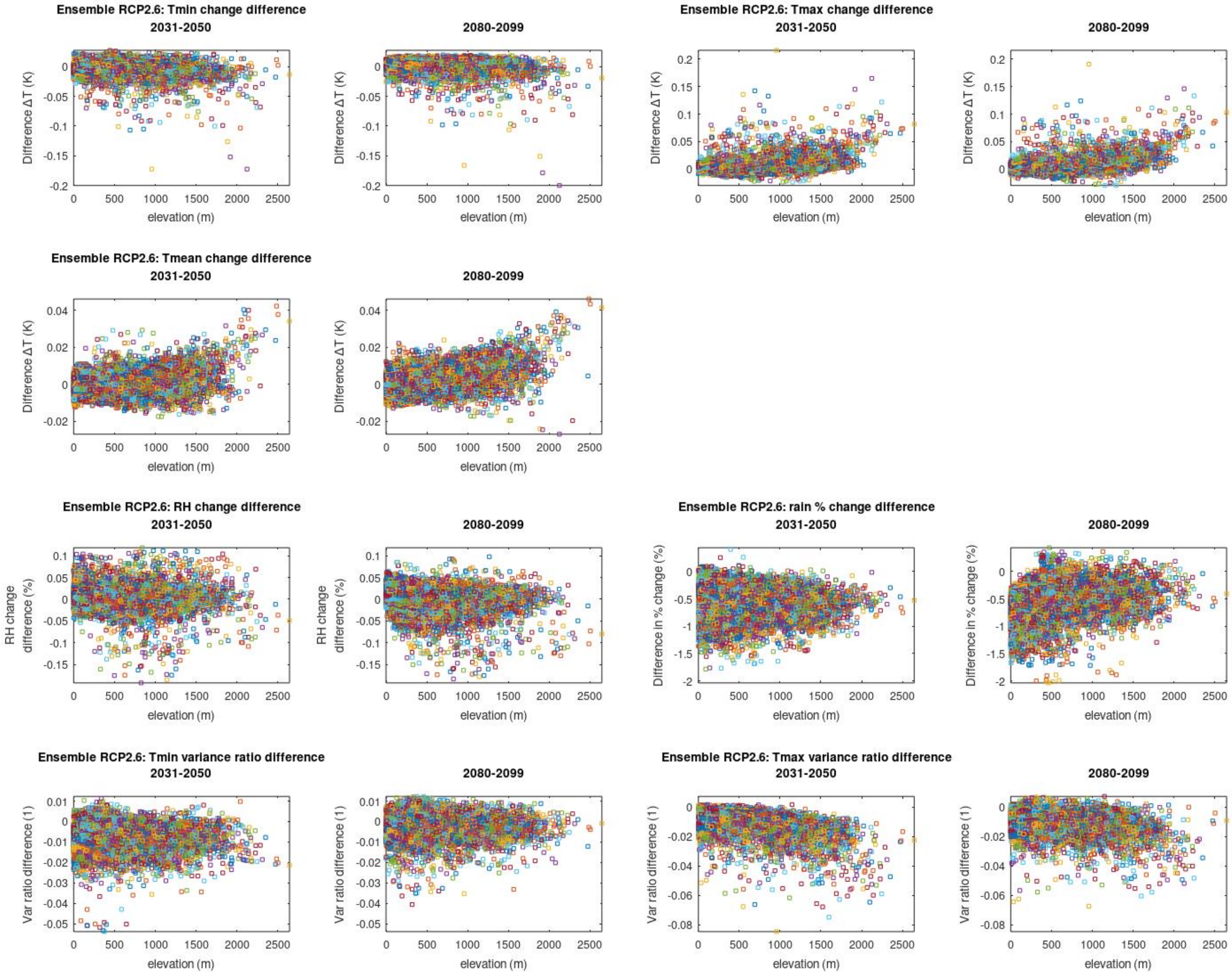

33.2 Impact of bias corrections on ensemble climate change signals under RCP 4.5

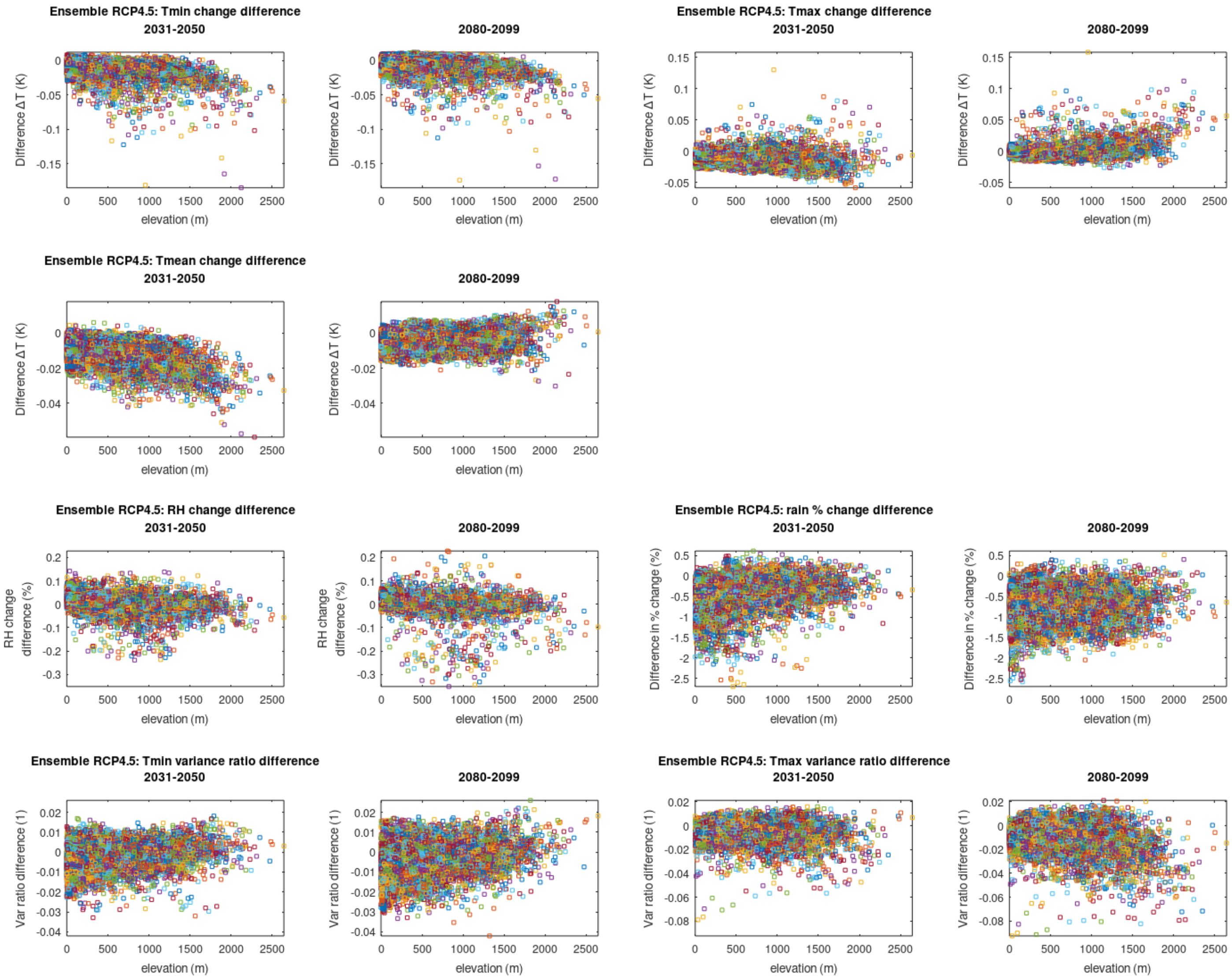

33.3 Impact of bias corrections on ensemble climate change signals under RCP 6.0

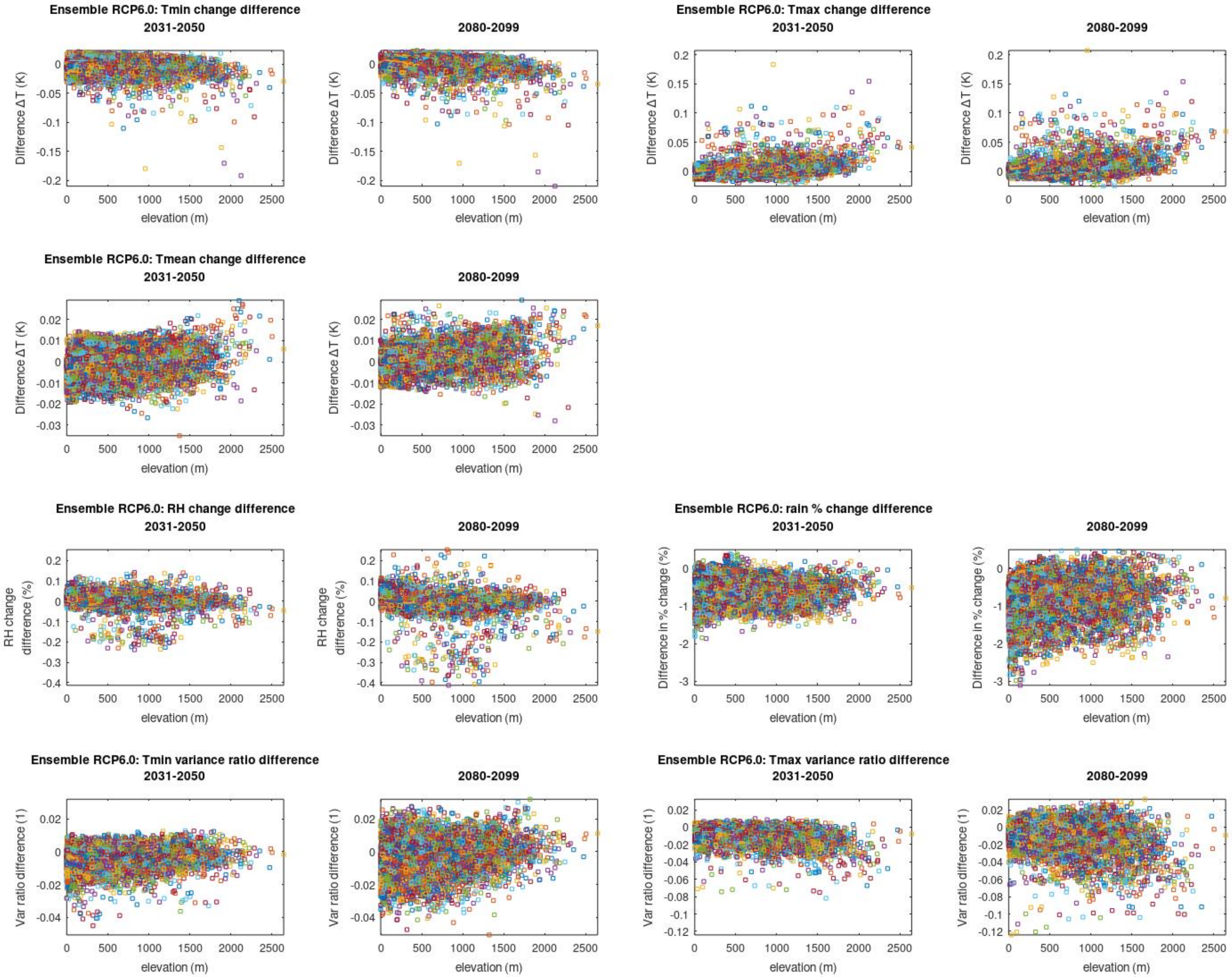

33.4 Impact of bias corrections on ensemble climate change signals under RCP 8.5

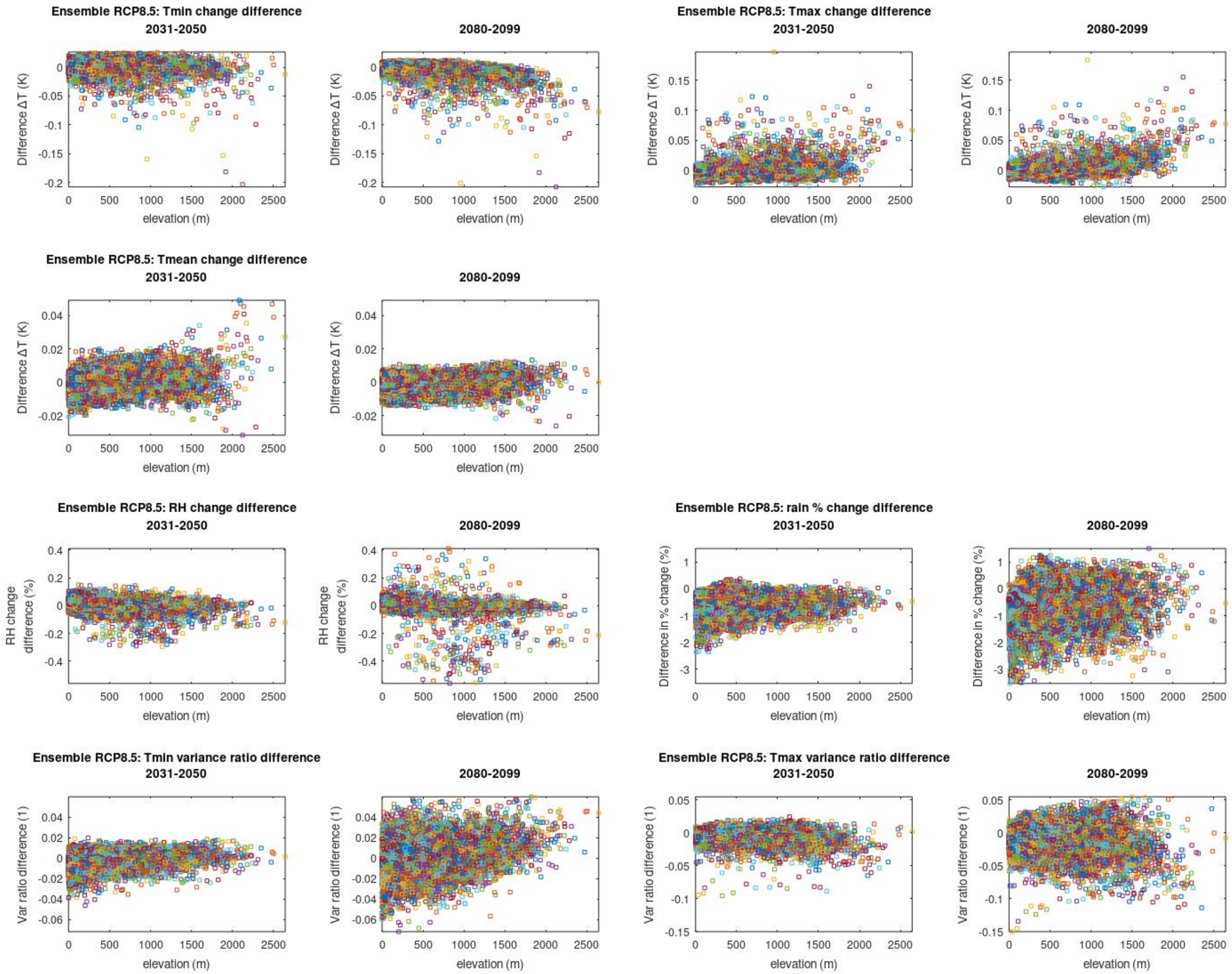

33.5 Impact of bias corrections on individual GCM climate change signals under RCP 2.6

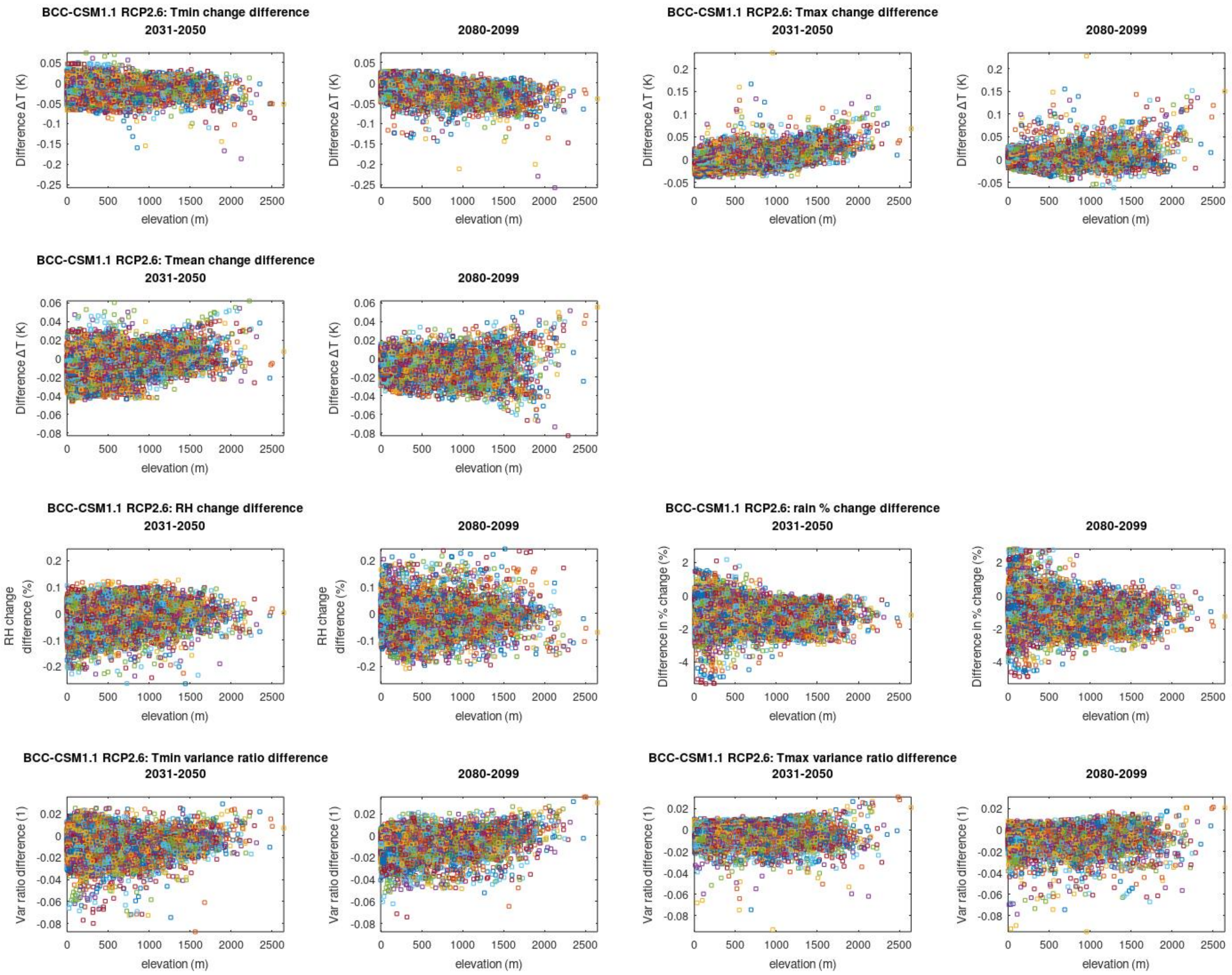

CESM1-CAM5 RCP2.6: Tmin change difference

2031-2050

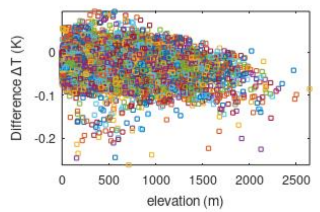

2080-2099

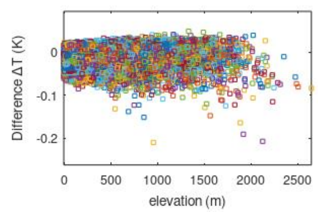

CESM1-CAM5 RCP2.6: Tmax change difference

2031-2050

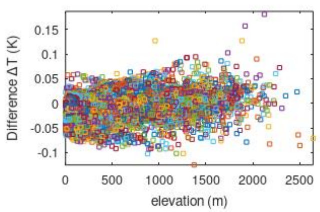

2080-2099

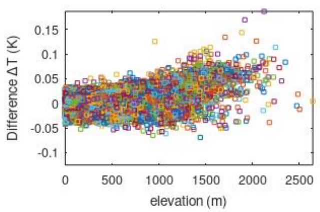

CESM1-CAM5 RCP2.6: Tmean change difference

2031-2050

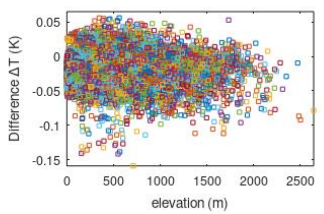

2080-2099

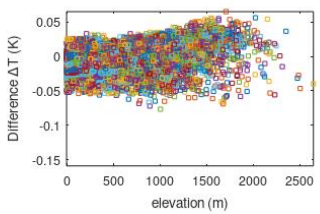

CESM1-CAM5 RCP2.6: RH change difference

2031-2050

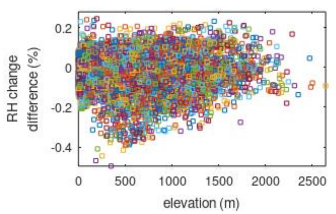

2080-2099

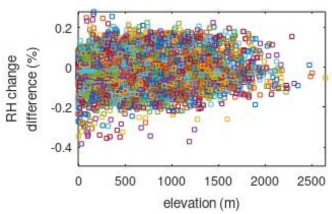

CESM1-CAM5 RCP2.6: rain % change difference

2031-2050

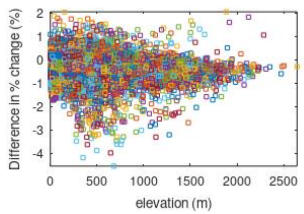

2080-2099

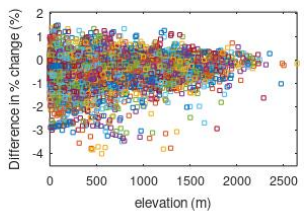

CESM1-CAM5 RCP2.6: Tmin variance ratio difference

2031-2050

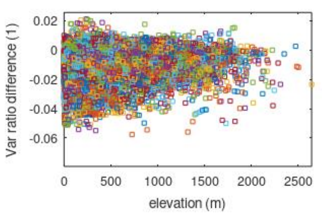

2080-2099

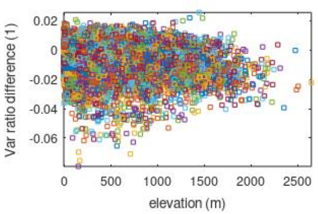

CESM1-CAM5 RCP2.6: Tmax variance ratio difference

2031-2050

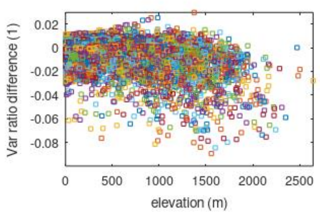

2080-2099

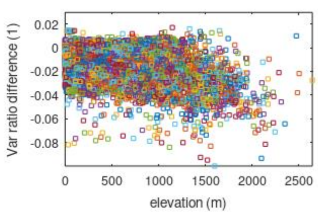

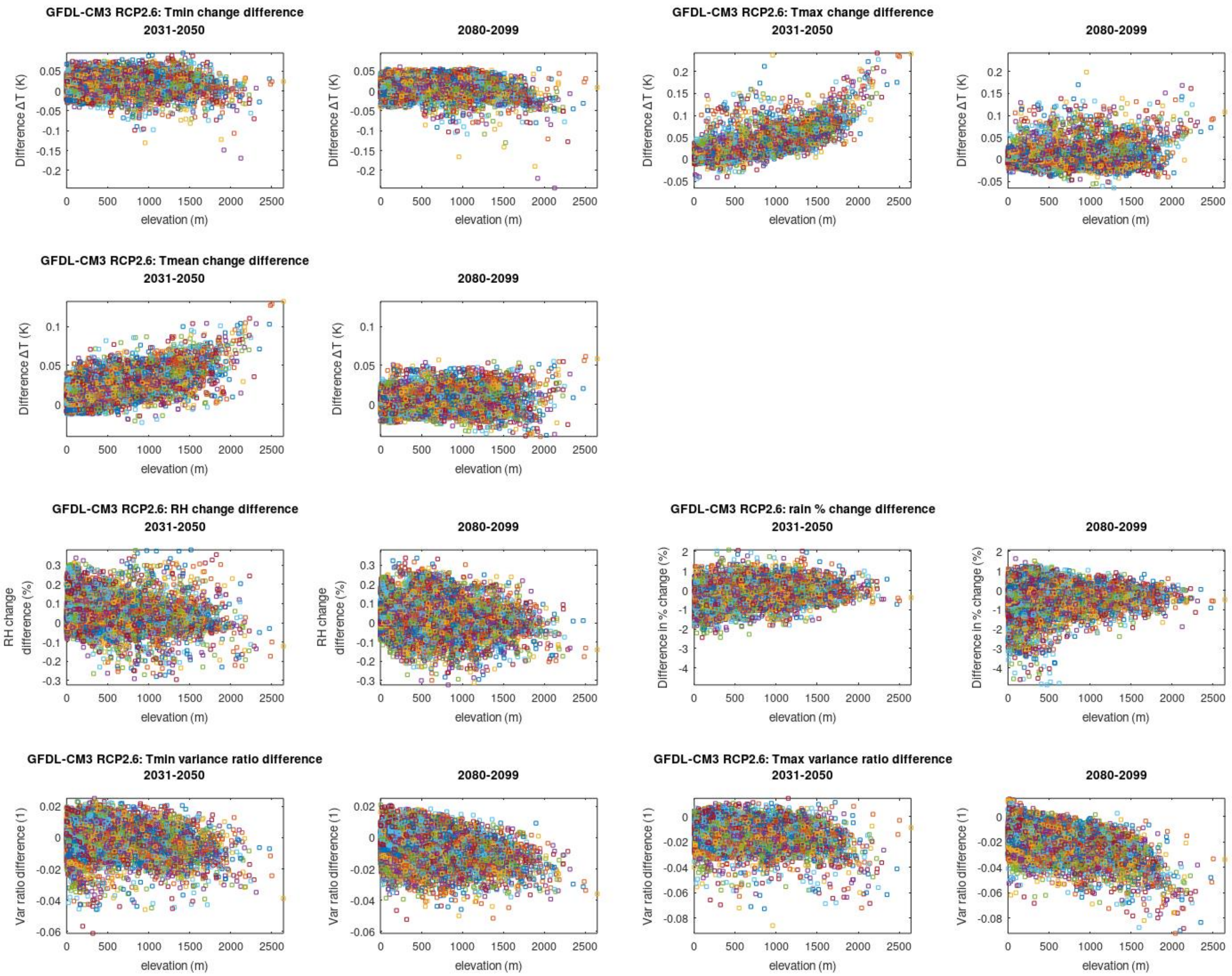
GFDL-CM3 RCP2.6: Tmin change difference
2031-2050
2080-2099
GFDL-CM3 RCP2.6: Tmax change difference
2031-2050
2080-2099
GFDL-CM3 RCP2.6: Tmean change difference
2031-2050
2080-2099
GFDL-CM3 RCP2.6: RH change difference
2031-2050
2080-2099
GFDL-CM3 RCP2.6: rain % change difference
2031-2050
2080-2099
GFDL-CM3 RCP2.6: Tmin variance ratio difference
2031-2050
2080-2099
GFDL-CM3 RCP2.6: Tmax variance ratio difference
2031-2050
2080-2099
Difference ΔT (K)
RH change difference (%)
Difference in % change (%)
Var ratio difference (1)
elevation (m)

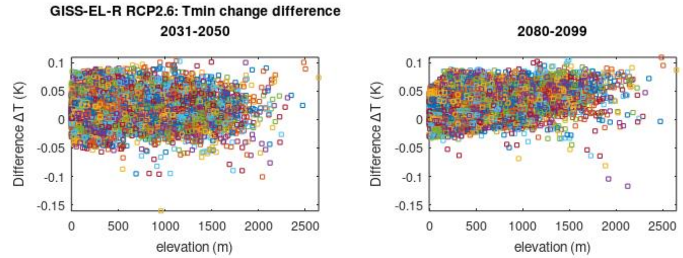
GISS-EL-R RCP2.6: Tmin change difference
2031-2050
2080-2099
Difference ΔT (K)
elevation (m)

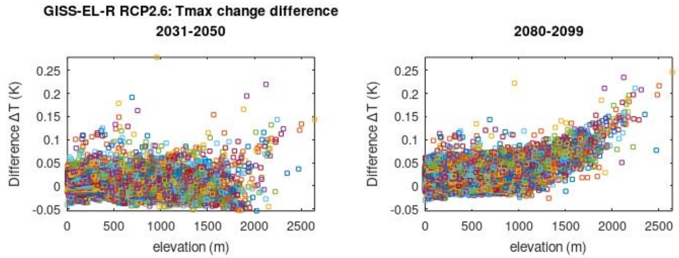
GISS-EL-R RCP2.6: Tmax change difference
2031-2050
2080-2099
Difference ΔT (K)
elevation (m)

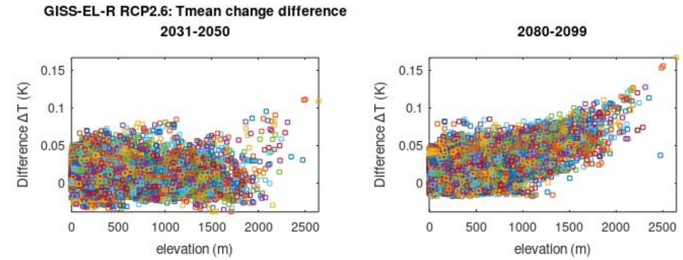
GISS-EL-R RCP2.6: Tmean change difference
2031-2050
2080-2099
Difference ΔT (K)
elevation (m)

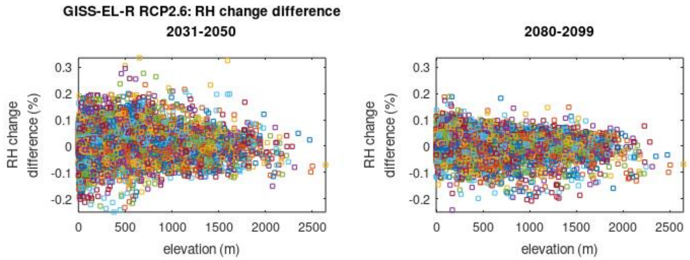
GISS-EL-R RCP2.6: RH change difference
2031-2050
2080-2099
RH change difference (%)
elevation (m)

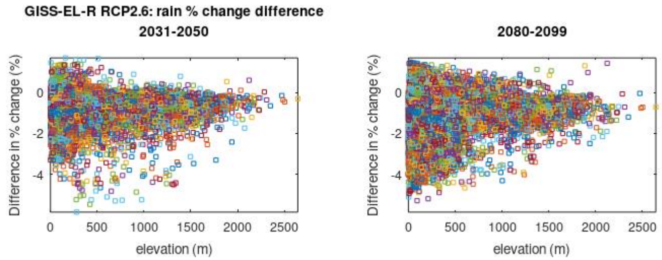
GISS-EL-R RCP2.6: rain % change difference
2031-2050
2080-2099
Difference in % change (%)
elevation (m)

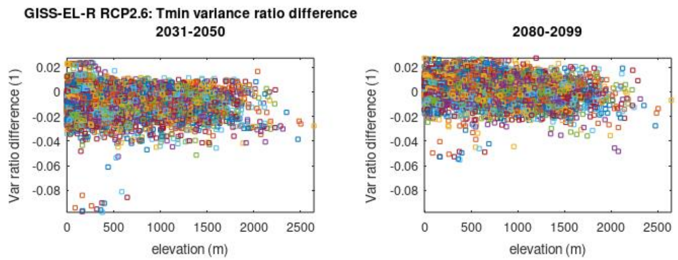
GISS-EL-R RCP2.6: Tmin variance ratio difference
2031-2050
2080-2099
Var ratio difference (1)
elevation (m)

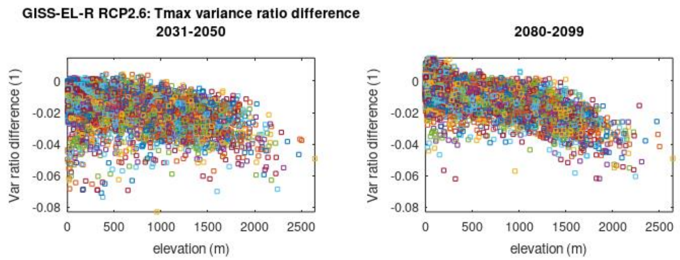
GISS-EL-R RCP2.6: Tmax variance ratio difference
2031-2050
2080-2099
Var ratio difference (1)
elevation (m)

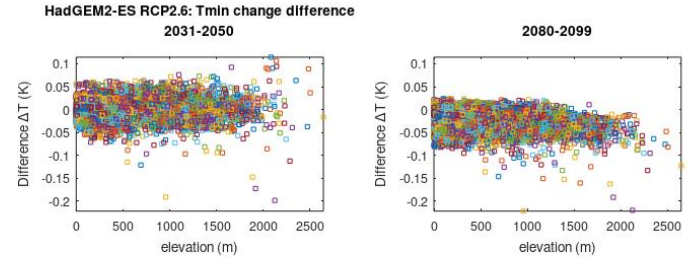
HadGEM2-ES RCP2.6: Tmin change difference
2031-2050
2080-2099
Difference ΔT (K)
elevation (m)

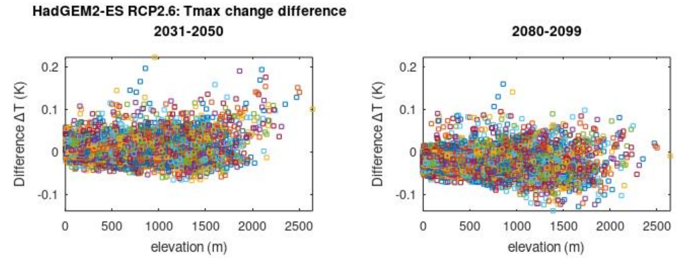
HadGEM2-ES RCP2.6: Tmax change difference
2031-2050
2080-2099
Difference ΔT (K)
elevation (m)

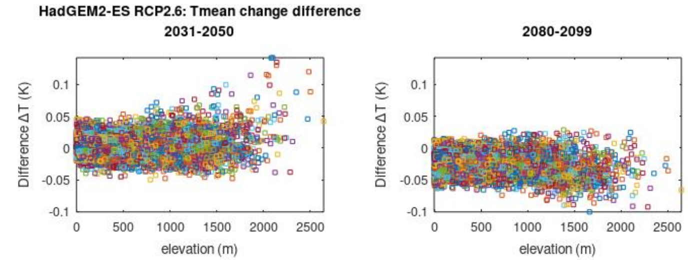
HadGEM2-ES RCP2.6: Tmean change difference
2031-2050
2080-2099
Difference ΔT (K)
elevation (m)

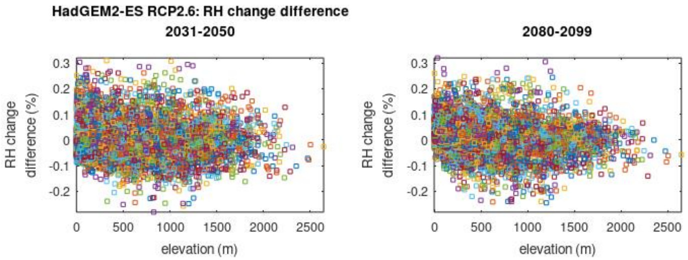
HadGEM2-ES RCP2.6: RH change difference
2031-2050
2080-2099
RH change difference (%)
elevation (m)

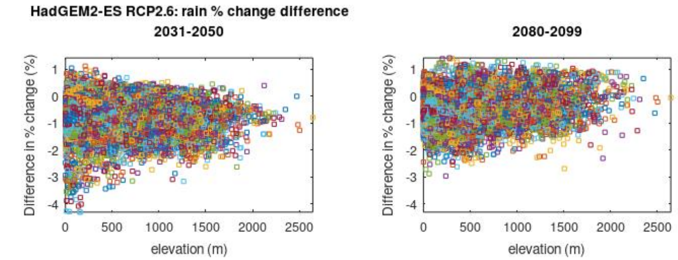
HadGEM2-ES RCP2.6: rain % change difference
2031-2050
2080-2099
Difference in % change (%)
elevation (m)

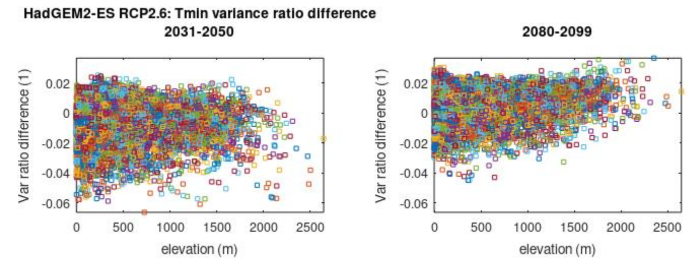
HadGEM2-ES RCP2.6: Tmin variance ratio difference
2031-2050
2080-2099
Var ratio difference (1)
elevation (m)

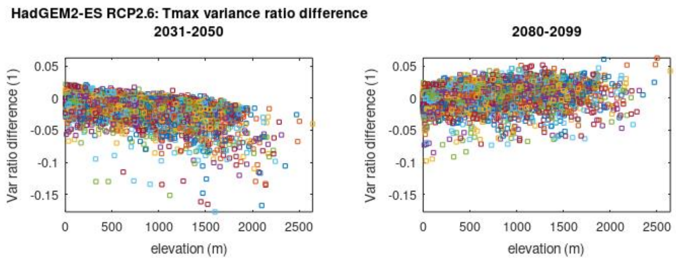
HadGEM2-ES RCP2.6: Tmax variance ratio difference
2031-2050
2080-2099
Var ratio difference (1)
elevation (m)

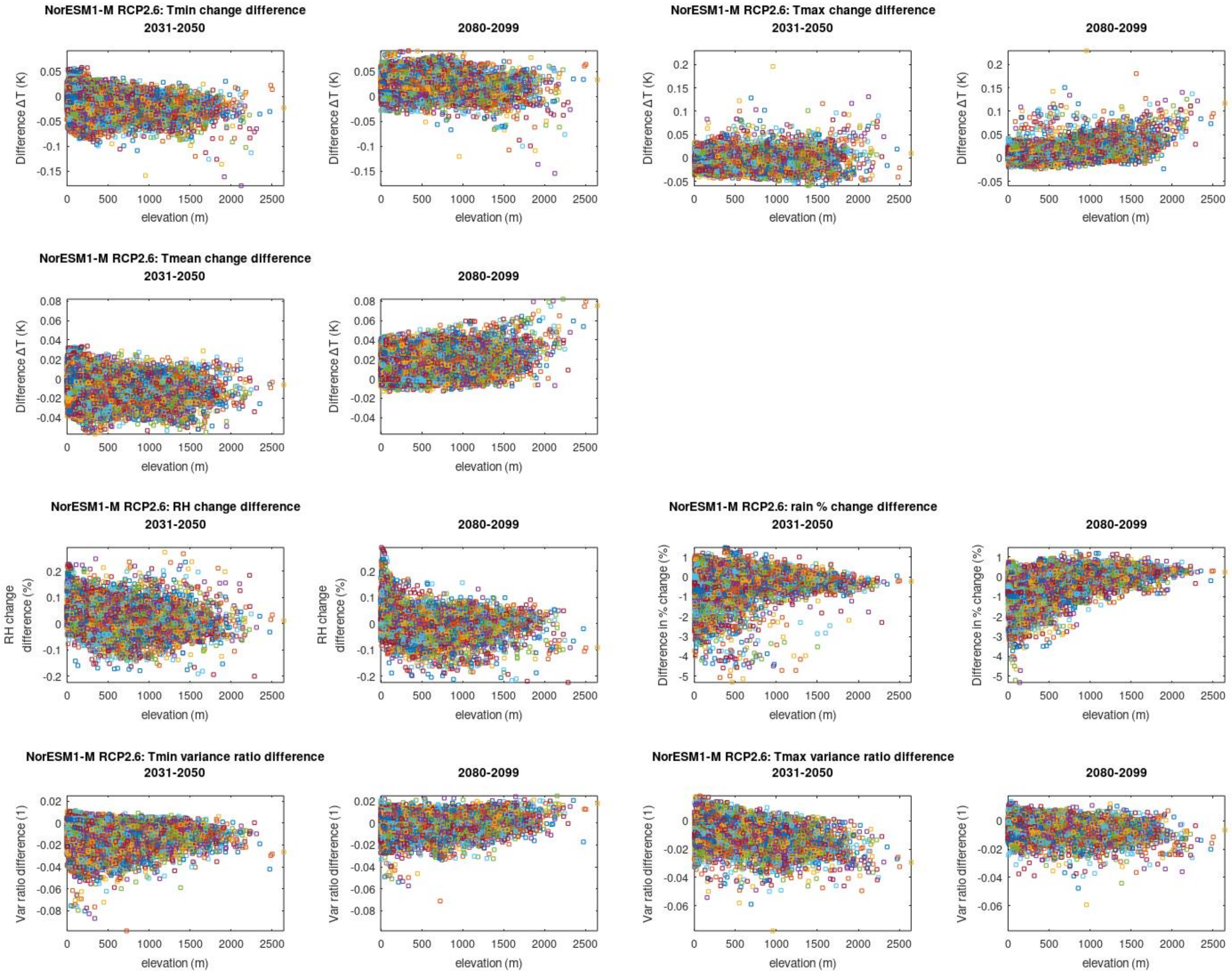
NorESM1-M RCP2.6: Tmin change difference
2031-2050
2080-2099
NorESM1-M RCP2.6: Tmax change difference
2031-2050
2080-2099
NorESM1-M RCP2.6: Tmean change difference
2031-2050
2080-2099
NorESM1-M RCP2.6: RH change difference
2031-2050
2080-2099
NorESM1-M RCP2.6: rain % change difference
2031-2050
2080-2099
NorESM1-M RCP2.6: Tmin variance ratio difference
2031-2050
2080-2099
NorESM1-M RCP2.6: Tmax variance ratio difference
2031-2050
2080-2099
Difference ΔT (K)
RH change difference (%)
Difference in % change (%)
Var ratio difference (1)
elevation (m)

33.6 Impact of bias corrections on individual GCM climate change signals under RCP 4.5

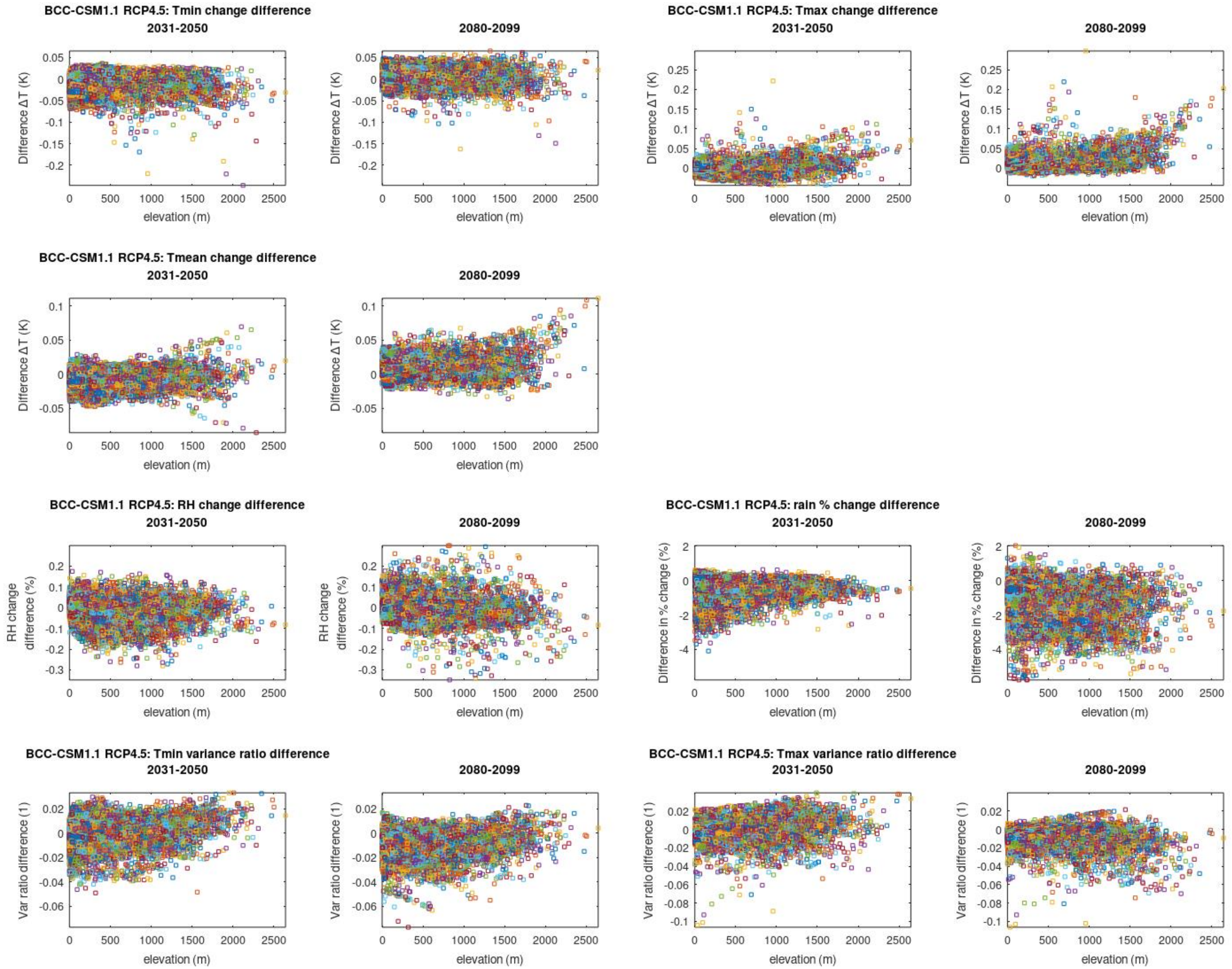

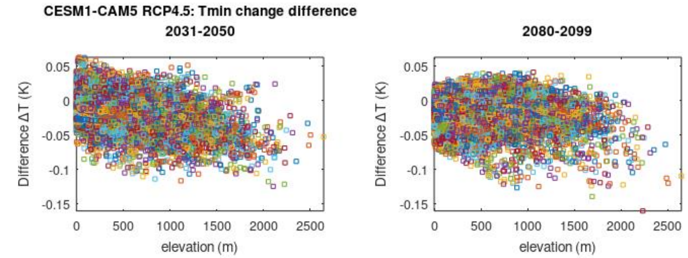
CESM1-CAM5 RCP4.5: Tmin change difference
2031-2050
2080-2099
Difference ΔT (K)
elevation (m)

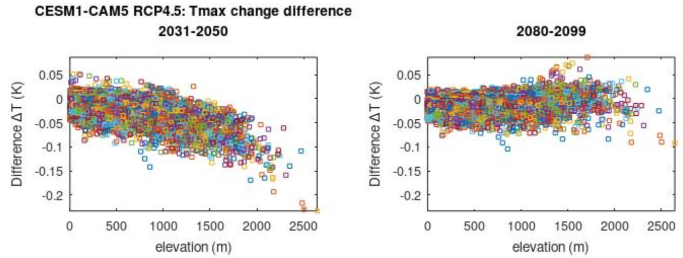
CESM1-CAM5 RCP4.5: Tmax change difference
2031-2050
2080-2099
Difference ΔT (K)
elevation (m)

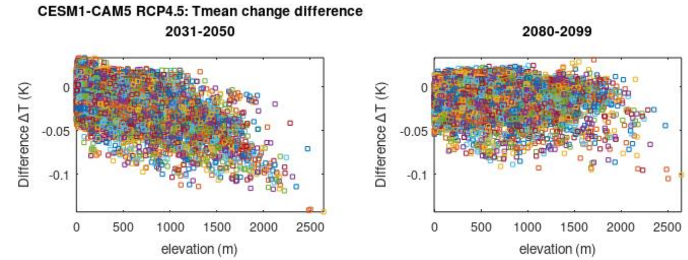
CESM1-CAM5 RCP4.5: Tmean change difference
2031-2050
2080-2099
Difference ΔT (K)
elevation (m)

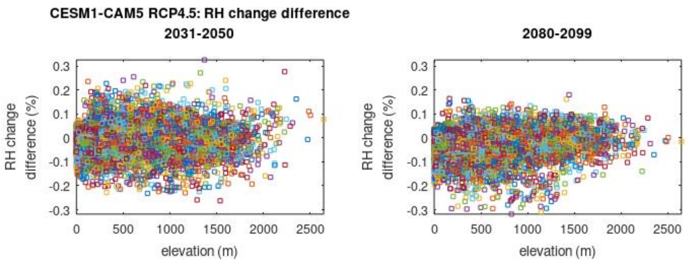
CESM1-CAM5 RCP4.5: RH change difference
2031-2050
2080-2099
RH change difference (%)
elevation (m)

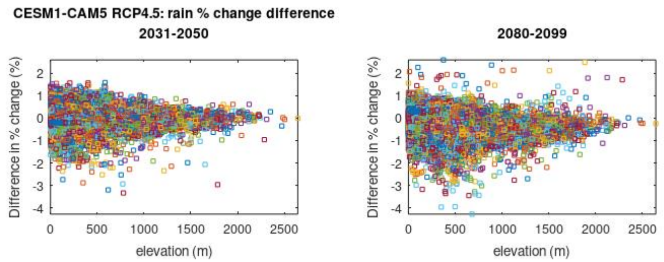
CESM1-CAM5 RCP4.5: rain % change difference
2031-2050
2080-2099
Difference in % change (%)
elevation (m)

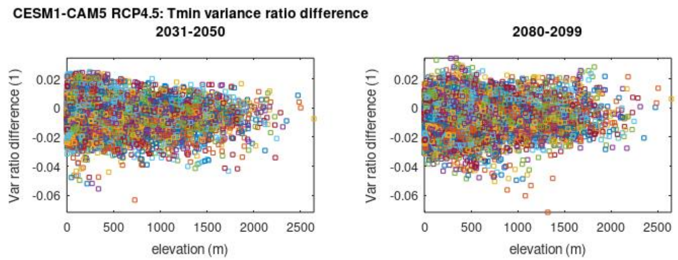
CESM1-CAM5 RCP4.5: Tmin variance ratio difference
2031-2050
2080-2099
Var ratio difference (1)
elevation (m)

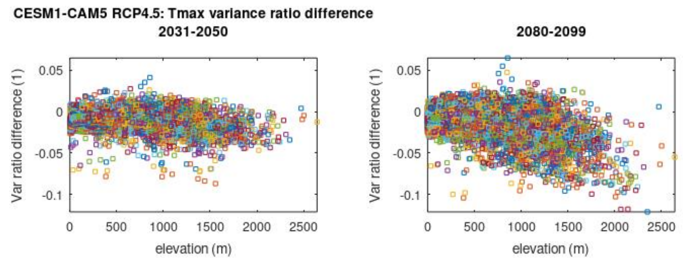
CESM1-CAM5 RCP4.5: Tmax variance ratio difference
2031-2050
2080-2099
Var ratio difference (1)
elevation (m)

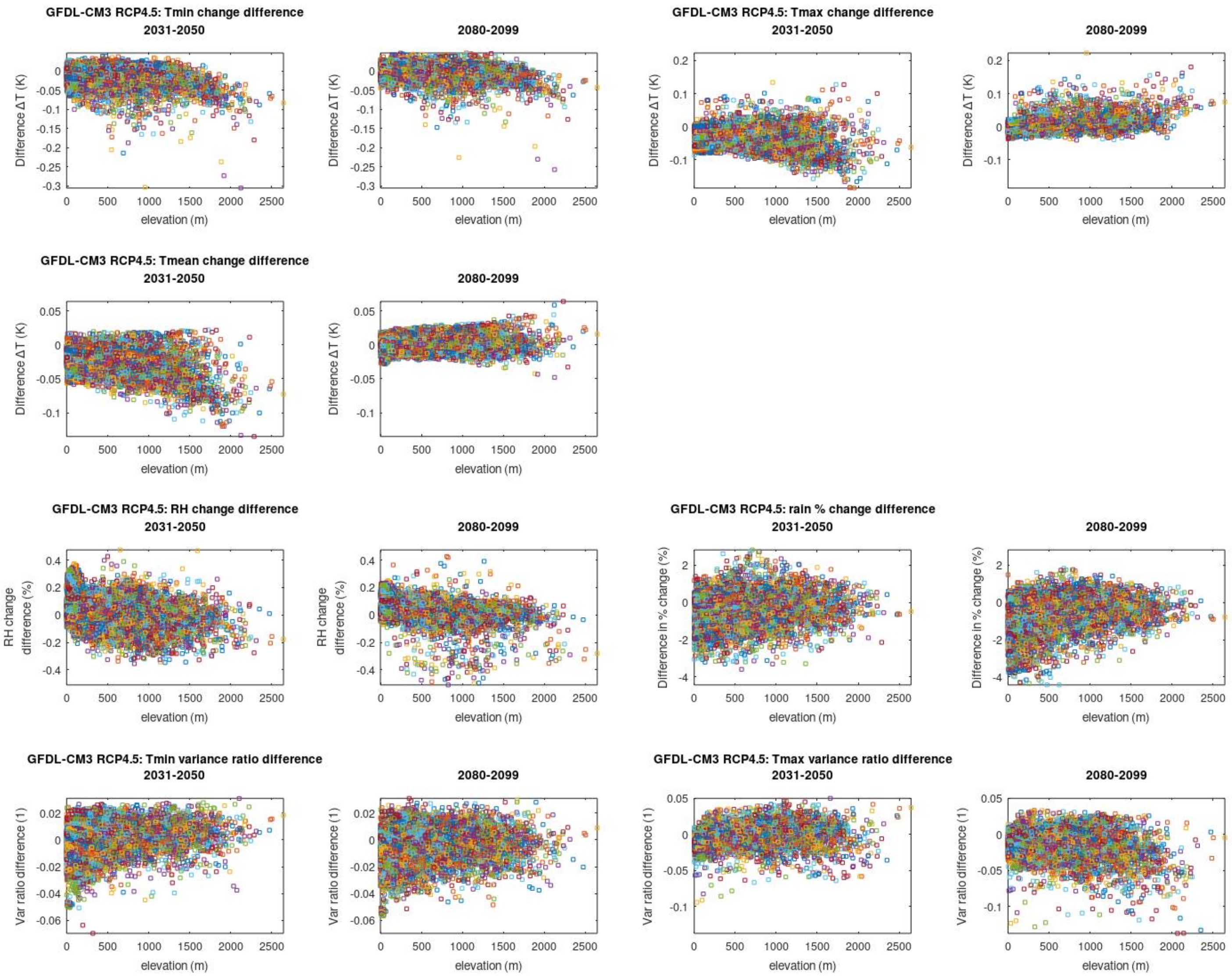
GFDL-CM3 RCP4.5: Tmin change difference
2031-2050
2080-2099
Difference ΔT (K)
elevation (m)
GFDL-CM3 RCP4.5: Tmax change difference
2031-2050
2080-2099
Difference ΔT (K)
elevation (m)
GFDL-CM3 RCP4.5: Tmean change difference
2031-2050
2080-2099
Difference ΔT (K)
elevation (m)
GFDL-CM3 RCP4.5: RH change difference
2031-2050
2080-2099
RH change difference (%)
elevation (m)
GFDL-CM3 RCP4.5: rain % change difference
2031-2050
2080-2099
Difference in % change (%)
elevation (m)
GFDL-CM3 RCP4.5: Tmin variance ratio difference
2031-2050
2080-2099
Var ratio difference (1)
elevation (m)
GFDL-CM3 RCP4.5: Tmax variance ratio difference
2031-2050
2080-2099
Var ratio difference (1)
elevation (m)

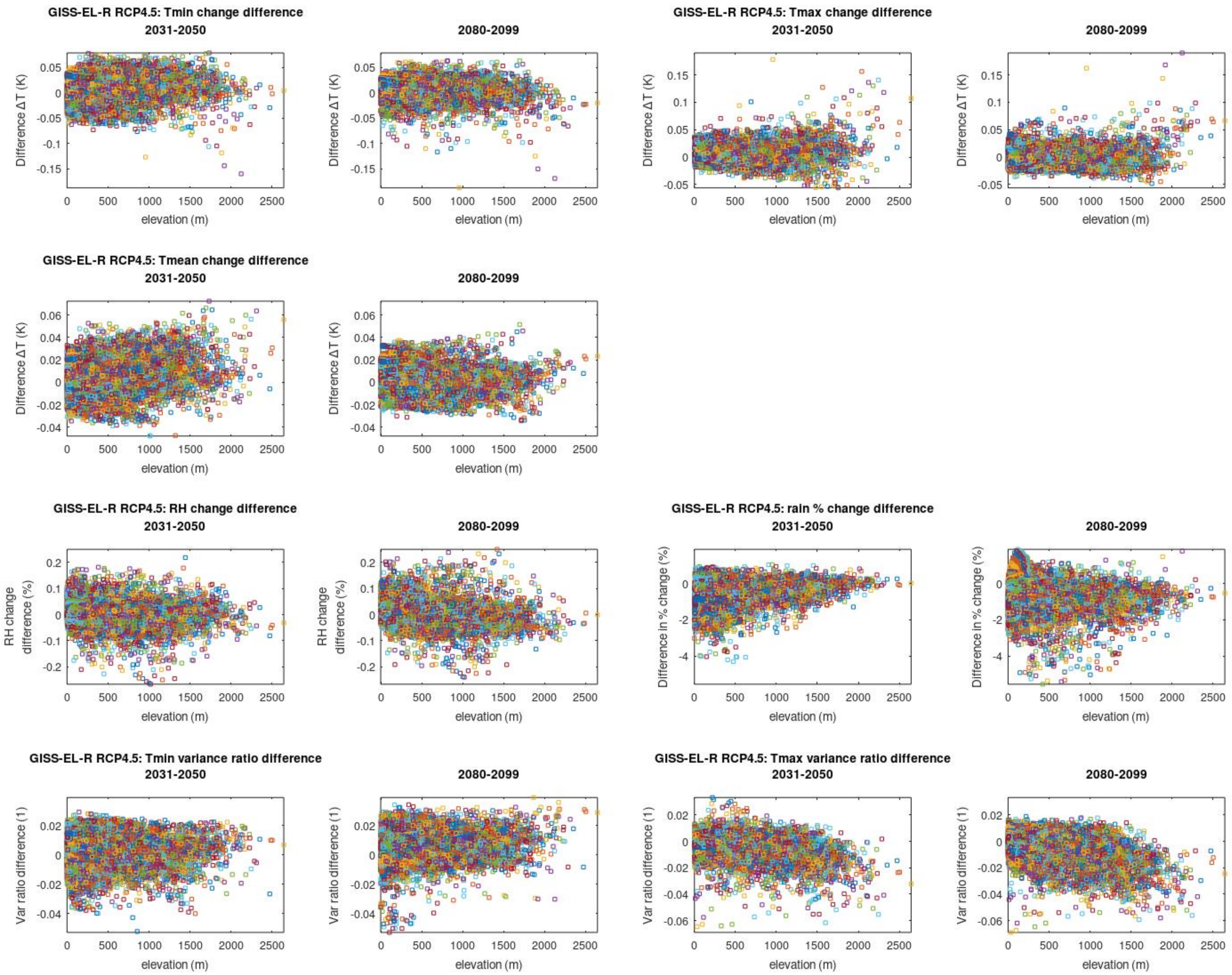
GISS-EL-R RCP4.5: Tmin change difference
2031-2050
2080-2099
GISS-EL-R RCP4.5: Tmax change difference
2031-2050
2080-2099
GISS-EL-R RCP4.5: Tmean change difference
2031-2050
2080-2099
GISS-EL-R RCP4.5: RH change difference
2031-2050
2080-2099
GISS-EL-R RCP4.5: rain % change difference
2031-2050
2080-2099
GISS-EL-R RCP4.5: Tmin variance ratio difference
2031-2050
2080-2099
GISS-EL-R RCP4.5: Tmax variance ratio difference
2031-2050
2080-2099
Difference ΔT (K)
RH change difference (%)
Difference in % change (%)
Var ratio difference (1)
elevation (m)

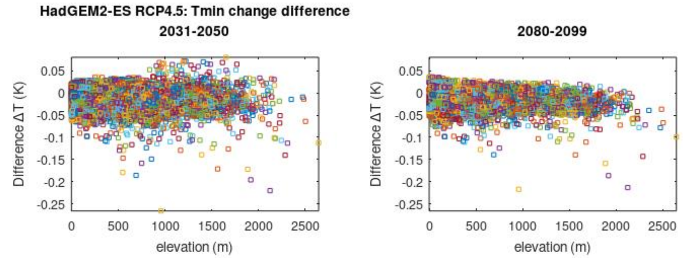
HadGEM2-ES RCP4.5: Tmin change difference
2031-2050
2080-2099
Difference ΔT (K)
elevation (m)

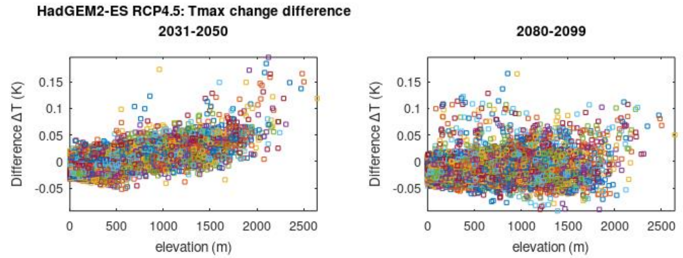
HadGEM2-ES RCP4.5: Tmax change difference
2031-2050
2080-2099
Difference ΔT (K)
elevation (m)

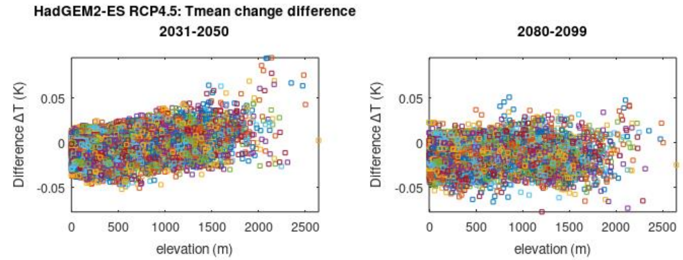
HadGEM2-ES RCP4.5: Tmean change difference
2031-2050
2080-2099
Difference ΔT (K)
elevation (m)

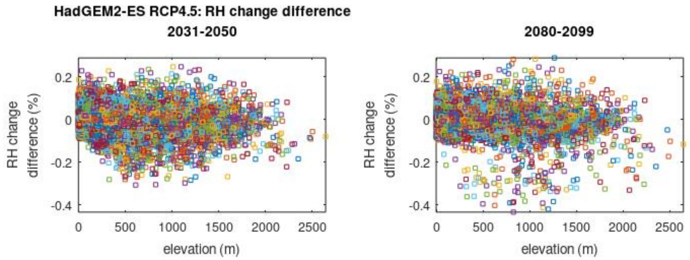
HadGEM2-ES RCP4.5: RH change difference
2031-2050
2080-2099
RH change difference (%)
elevation (m)

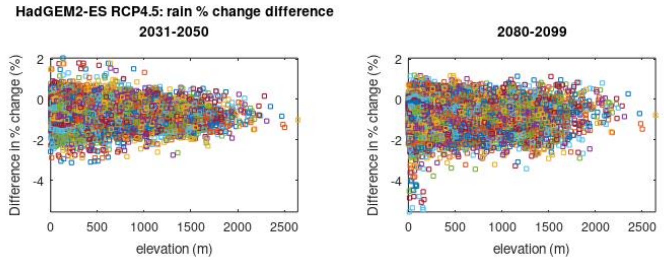
HadGEM2-ES RCP4.5: rain % change difference
2031-2050
2080-2099
Difference in % change (%)
elevation (m)

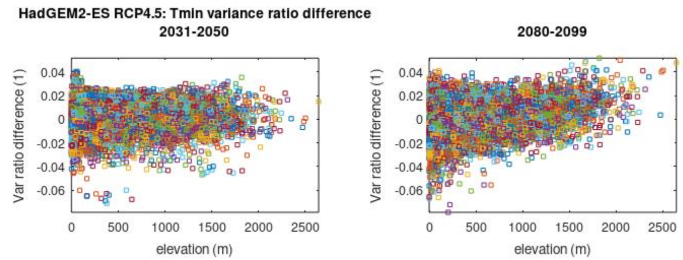
HadGEM2-ES RCP4.5: Tmin variance ratio difference
2031-2050
2080-2099
Var ratio difference (1)
elevation (m)

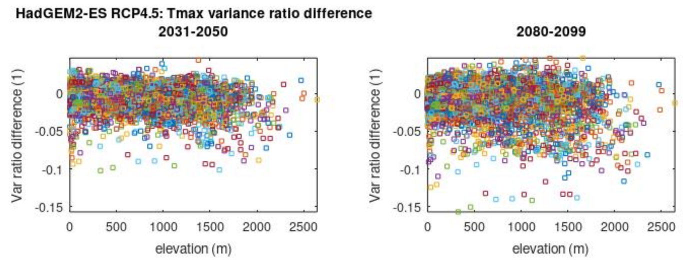
HadGEM2-ES RCP4.5: Tmax variance ratio difference
2031-2050
2080-2099
Var ratio difference (1)
elevation (m)

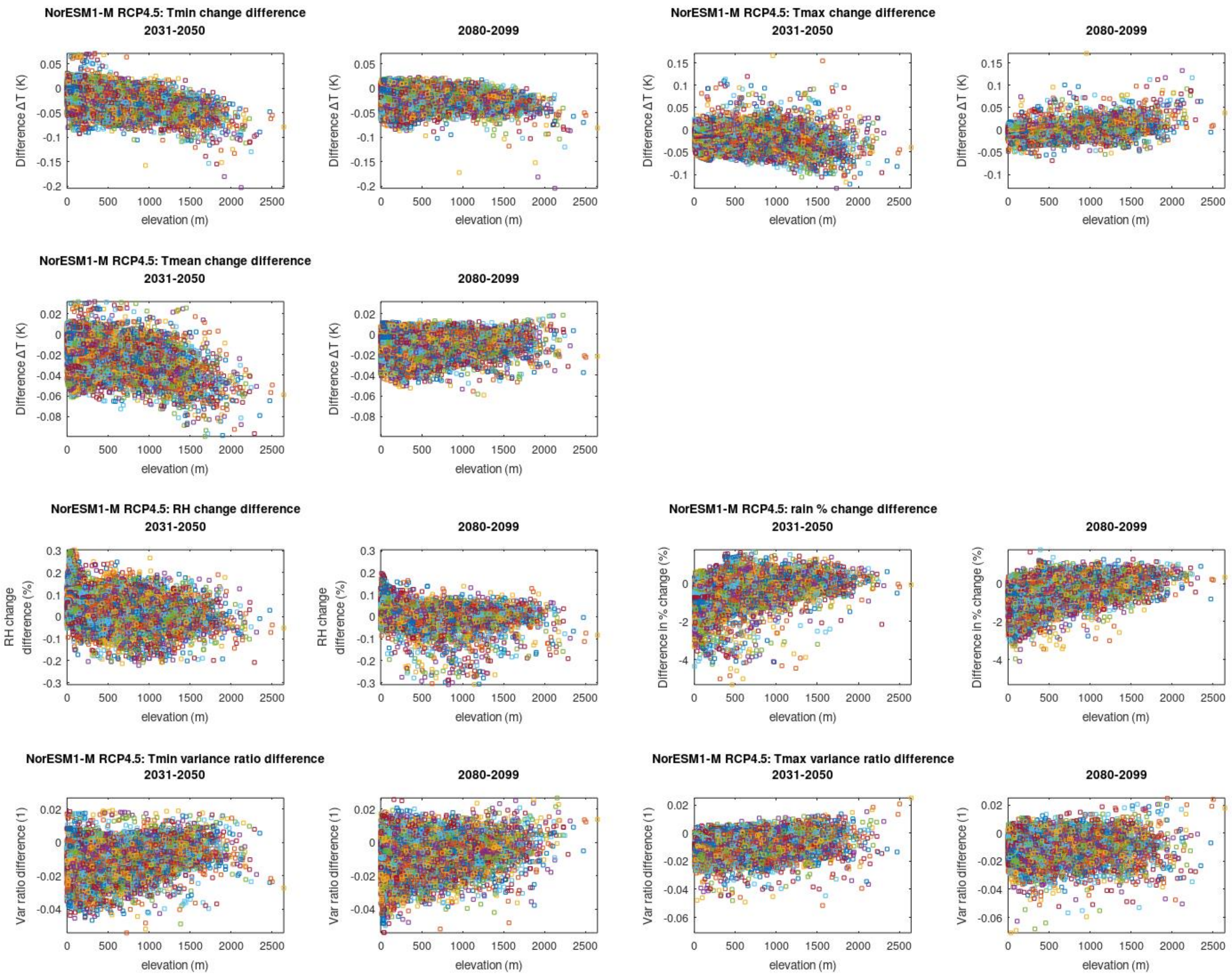
NorESM1-M RCP4.5: Tmin change difference
2031-2050
2080-2099
NorESM1-M RCP4.5: Tmax change difference
2031-2050
2080-2099
NorESM1-M RCP4.5: Tmean change difference
2031-2050
2080-2099
NorESM1-M RCP4.5: RH change difference
2031-2050
2080-2099
NorESM1-M RCP4.5: rain % change difference
2031-2050
2080-2099
NorESM1-M RCP4.5: Tmin variance ratio difference
2031-2050
2080-2099
NorESM1-M RCP4.5: Tmax variance ratio difference
2031-2050
2080-2099
Difference ΔT (K)
RH change difference (%)
Difference in % change (%)
Var ratio difference (1)
elevation (m)

33.7 Impact of bias corrections on individual GCM climate change signals under RCP 6.0

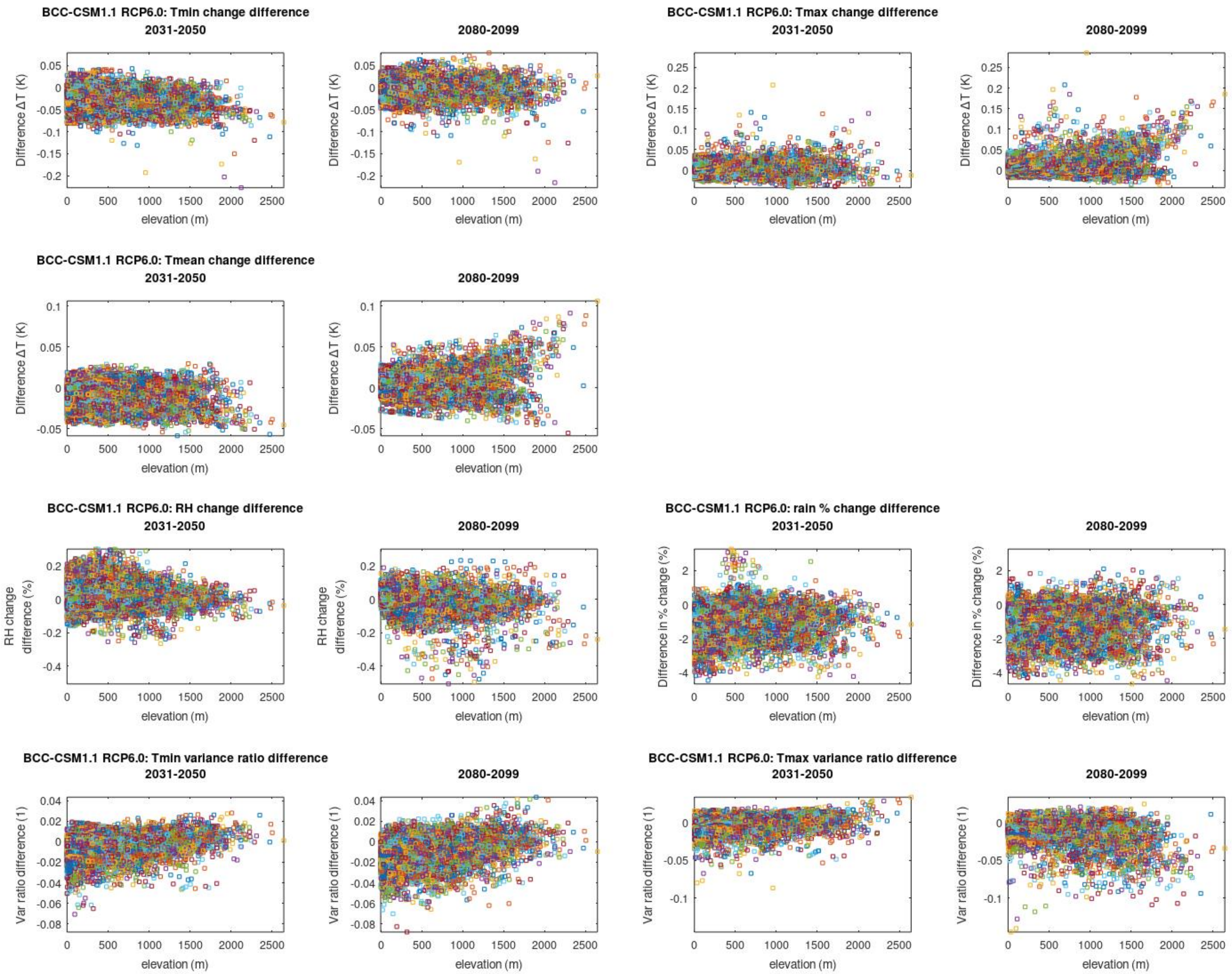

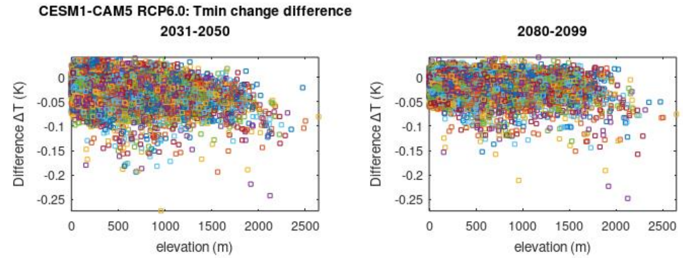
CESM1-CAM5 RCP6.0: Tmin change difference
2031-2050
2080-2099
Difference ΔT (K)
elevation (m)

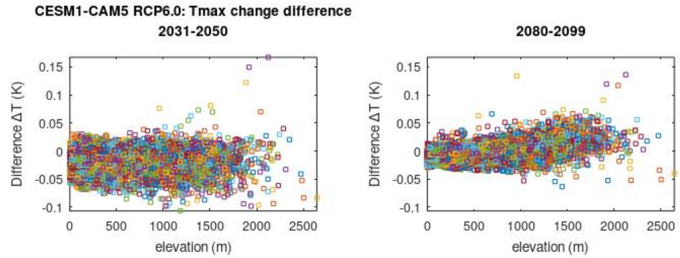
CESM1-CAM5 RCP6.0: Tmax change difference
2031-2050
2080-2099
Difference ΔT (K)
elevation (m)

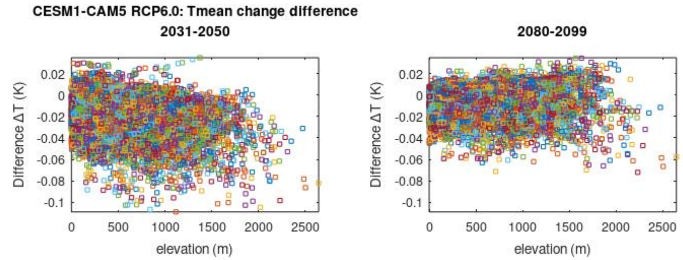
CESM1-CAM5 RCP6.0: Tmean change difference
2031-2050
2080-2099
Difference ΔT (K)
elevation (m)

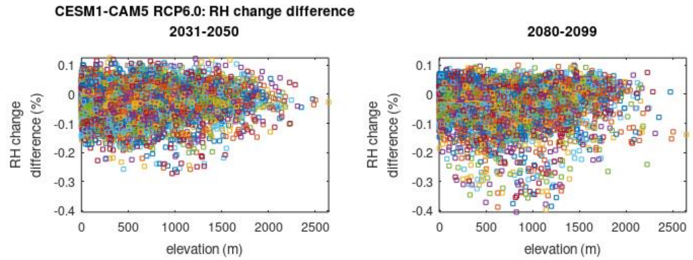
CESM1-CAM5 RCP6.0: RH change difference
2031-2050
2080-2099
RH change difference (%)
elevation (m)

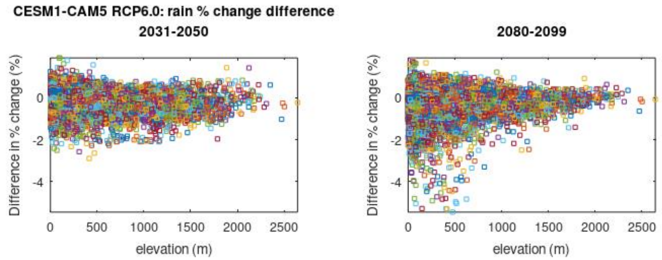
CESM1-CAM5 RCP6.0: rain % change difference
2031-2050
2080-2099
Difference in % change (%)
elevation (m)

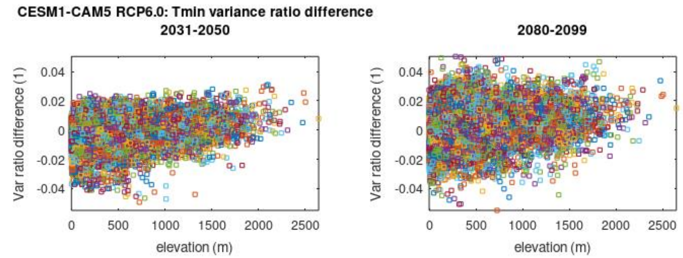
CESM1-CAM5 RCP6.0: Tmin variance ratio difference
2031-2050
2080-2099
Var ratio difference (1)
elevation (m)

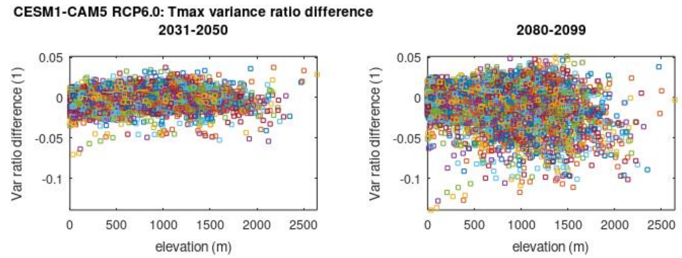
CESM1-CAM5 RCP6.0: Tmax variance ratio difference
2031-2050
2080-2099
Var ratio difference (1)
elevation (m)

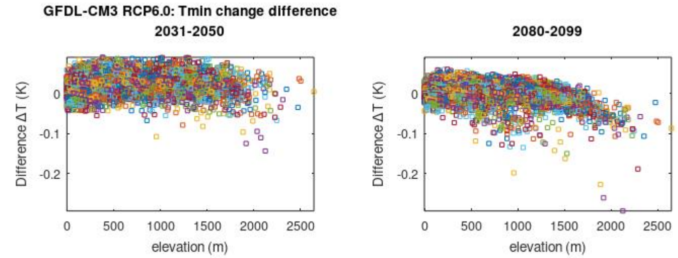
GFDL-CM3 RCP6.0: Tmin change difference
2031-2050
2080-2099
Difference ΔT (K)
elevation (m)

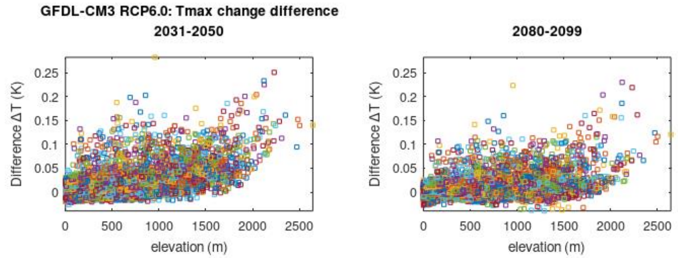
GFDL-CM3 RCP6.0: Tmax change difference
2031-2050
2080-2099
Difference ΔT (K)
elevation (m)

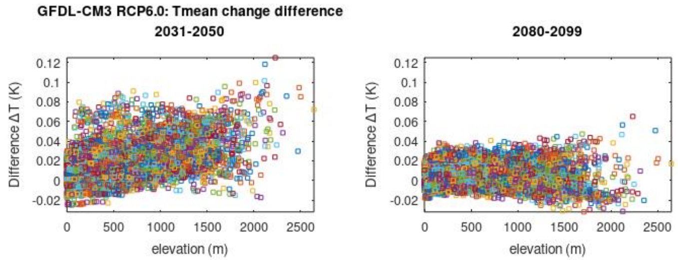
GFDL-CM3 RCP6.0: Tmean change difference
2031-2050
2080-2099
Difference ΔT (K)
elevation (m)

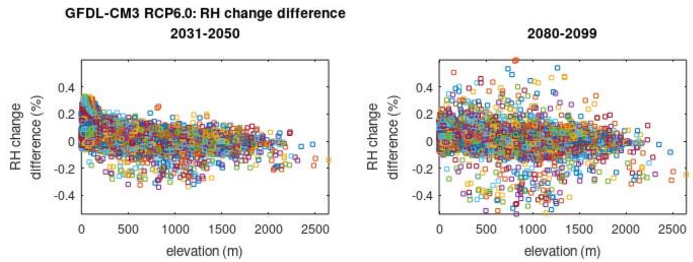
GFDL-CM3 RCP6.0: RH change difference
2031-2050
2080-2099
RH change difference (%)
elevation (m)

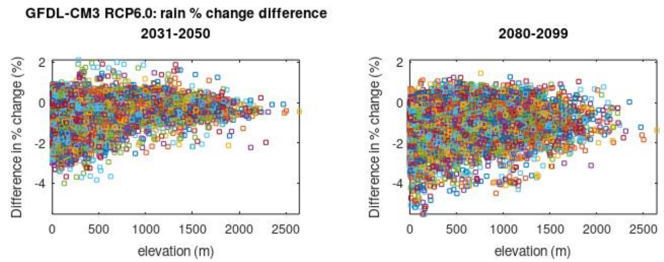
GFDL-CM3 RCP6.0: rain % change difference
2031-2050
2080-2099
Difference in % change (%)
elevation (m)

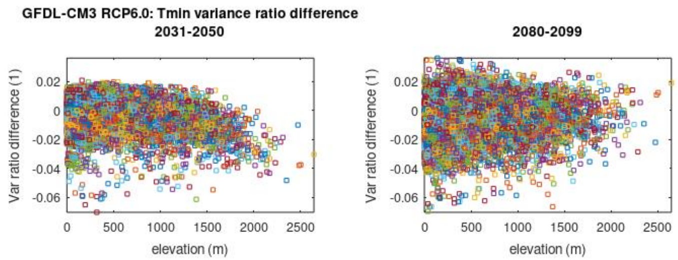
GFDL-CM3 RCP6.0: Tmin variance ratio difference
2031-2050
2080-2099
Var ratio difference (1)
elevation (m)

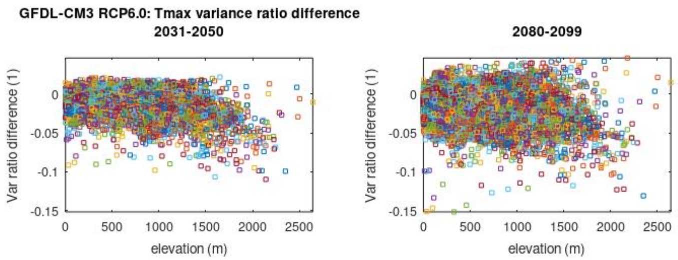
GFDL-CM3 RCP6.0: Tmax variance ratio difference
2031-2050
2080-2099
Var ratio difference (1)
elevation (m)

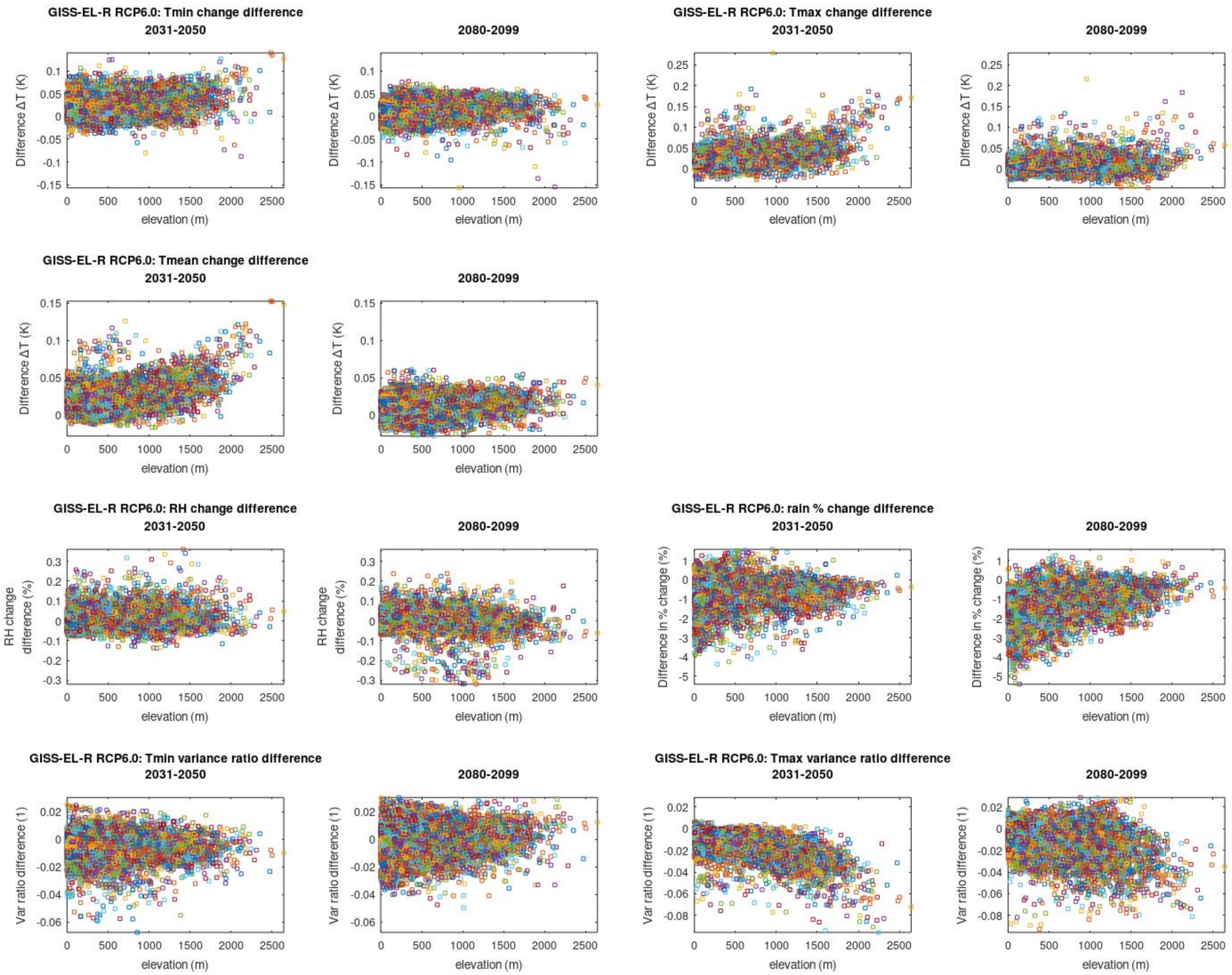
GISS-EL-R RCP6.0: Tmin change difference
2031-2050
2080-2099
GISS-EL-R RCP6.0: Tmax change difference
2031-2050
2080-2099
GISS-EL-R RCP6.0: Tmean change difference
2031-2050
2080-2099
GISS-EL-R RCP6.0: RH change difference
2031-2050
2080-2099
GISS-EL-R RCP6.0: rain % change difference
2031-2050
2080-2099
GISS-EL-R RCP6.0: Tmin variance ratio difference
2031-2050
2080-2099
GISS-EL-R RCP6.0: Tmax variance ratio difference
2031-2050
2080-2099
Difference ΔT (K)
RH change difference (%)
Difference in % change (%)
Var ratio difference (1)
elevation (m)

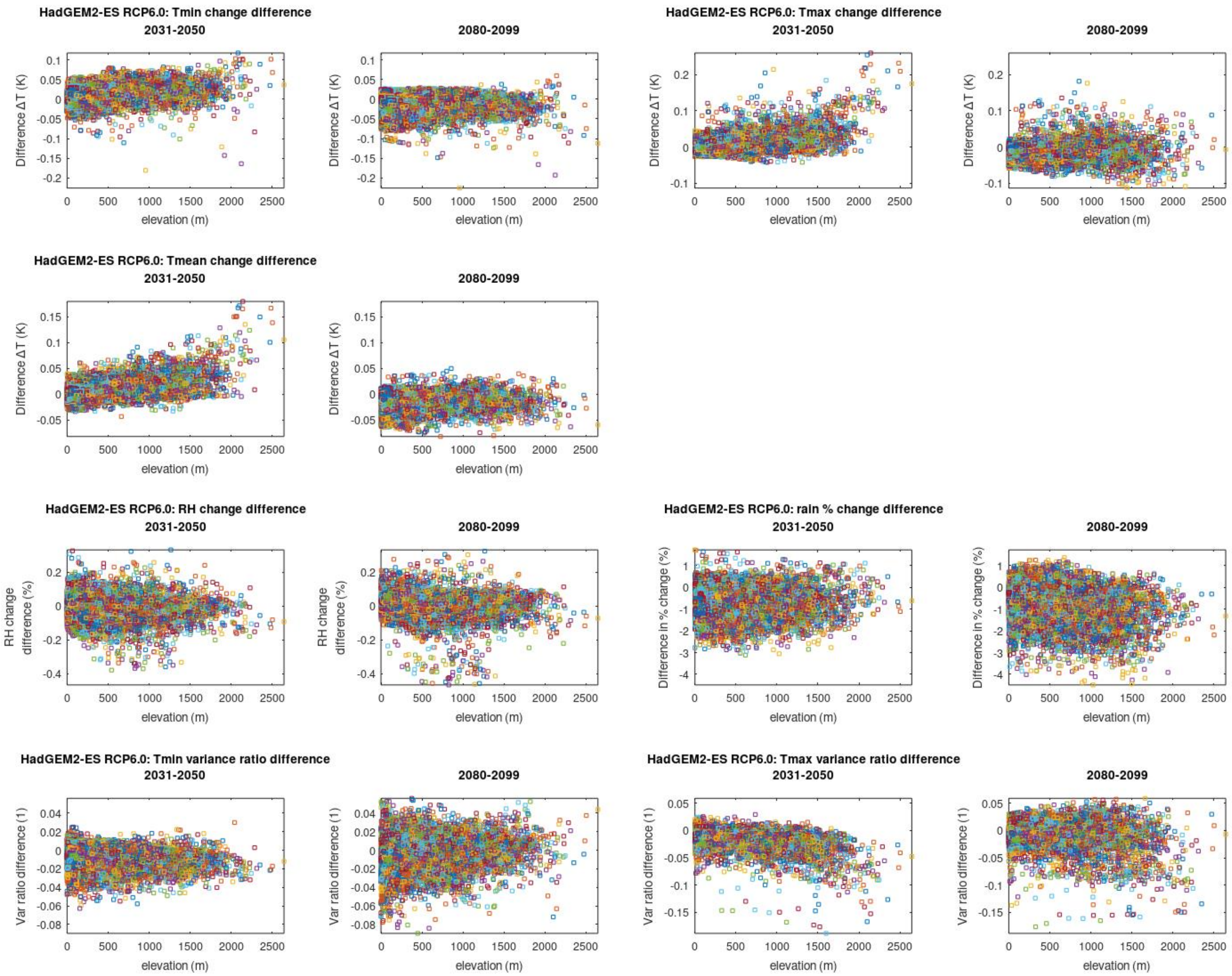
HadGEM2-ES RCP6.0: Tmin change difference
2031-2050
2080-2099
HadGEM2-ES RCP6.0: Tmax change difference
2031-2050
2080-2099
HadGEM2-ES RCP6.0: Tmean change difference
2031-2050
2080-2099
HadGEM2-ES RCP6.0: RH change difference
2031-2050
2080-2099
HadGEM2-ES RCP6.0: rain % change difference
2031-2050
2080-2099
HadGEM2-ES RCP6.0: Tmin variance ratio difference
2031-2050
2080-2099
HadGEM2-ES RCP6.0: Tmax variance ratio difference
2031-2050
2080-2099
Difference ΔT (K)
RH change difference (%)
Difference in % change (%)
Var ratio difference (1)
elevation (m)

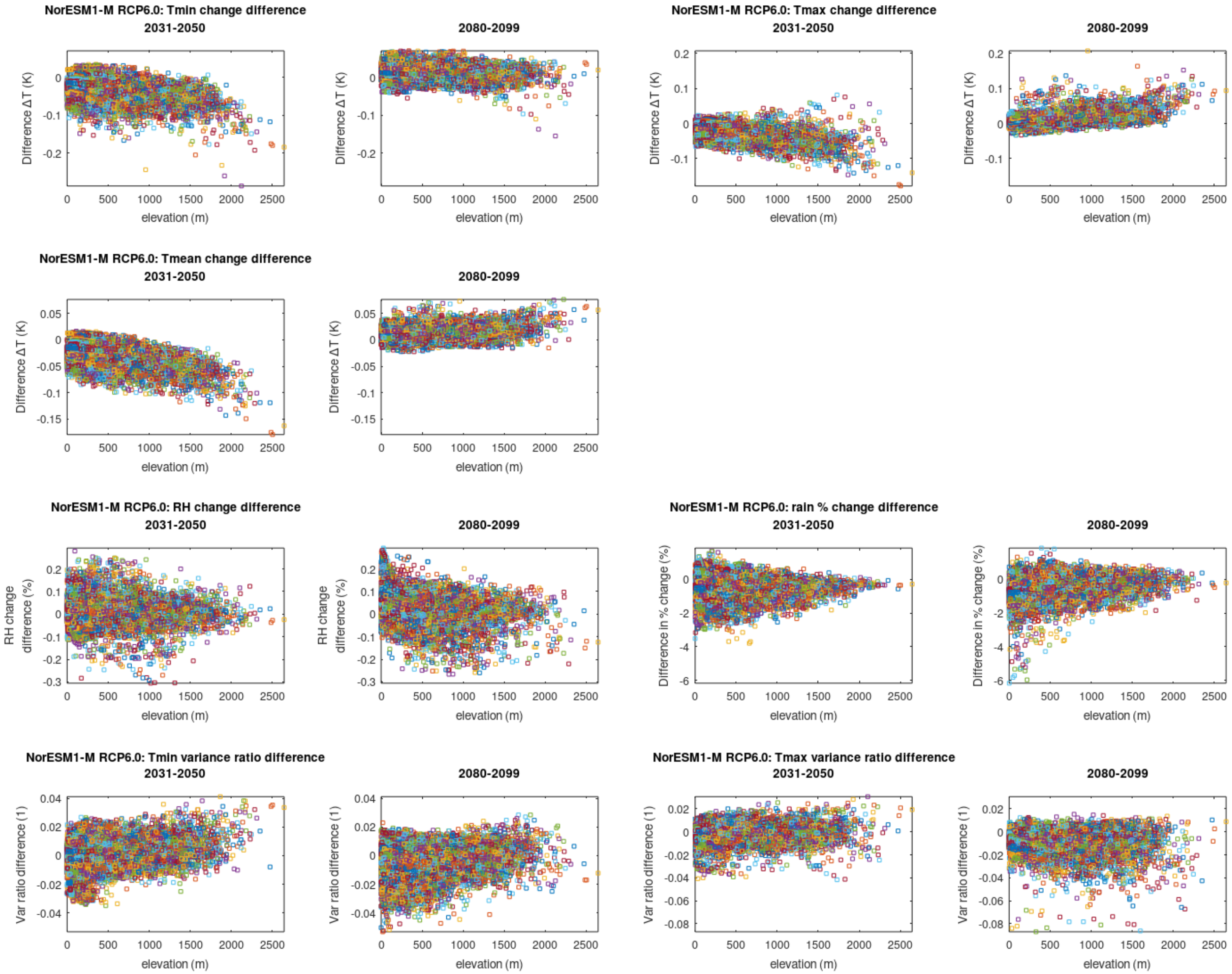

NorESM1-M RCP6.0: Tmin change difference
2031-2050
2080-2099
Difference ΔT (K)
elevation (m)
NorESM1-M RCP6.0: Tmax change difference
2031-2050
2080-2099
Difference ΔT (K)
elevation (m)
NorESM1-M RCP6.0: Tmean change difference
2031-2050
2080-2099
Difference ΔT (K)
elevation (m)
NorESM1-M RCP6.0: RH change difference
2031-2050
2080-2099
RH change difference (%)
elevation (m)
NorESM1-M RCP6.0: rain % change difference
2031-2050
2080-2099
Difference in % change (%)
elevation (m)
NorESM1-M RCP6.0: Tmin variance ratio difference
2031-2050
2080-2099
Var ratio difference (1)
elevation (m)
NorESM1-M RCP6.0: Tmax variance ratio difference
2031-2050
2080-2099
Var ratio difference (1)
elevation (m)

33.8 Impact of bias corrections on individual GCM climate change signals under RCP 8.5

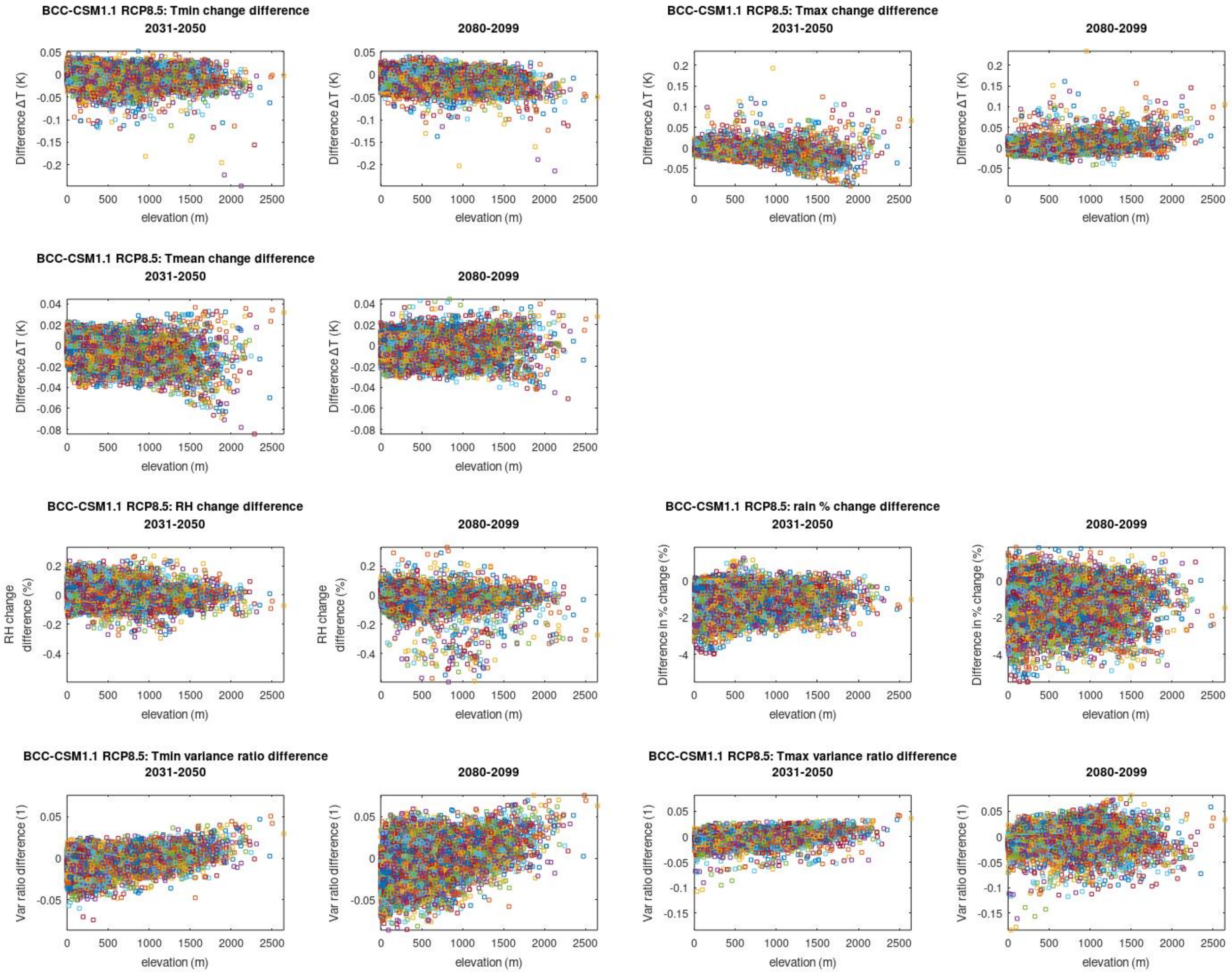

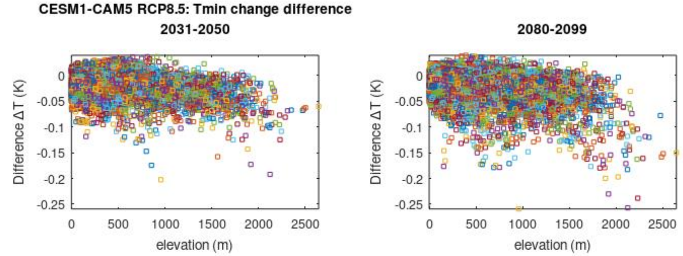
CESM1-CAM5 RCP8.5: Tmin change difference
2031-2050
2080-2099
Difference ΔT (K)
elevation (m)

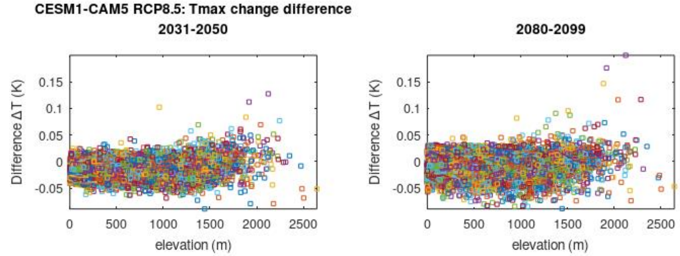
CESM1-CAM5 RCP8.5: Tmax change difference
2031-2050
2080-2099
Difference ΔT (K)
elevation (m)

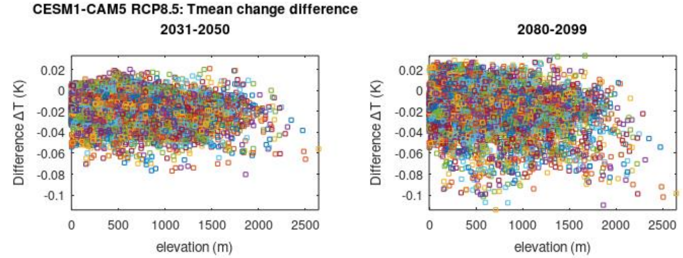
CESM1-CAM5 RCP8.5: Tmean change difference
2031-2050
2080-2099
Difference ΔT (K)
elevation (m)

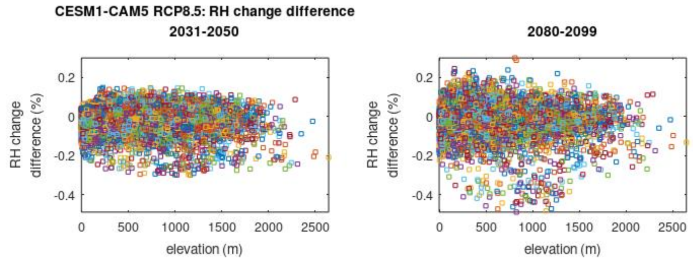
CESM1-CAM5 RCP8.5: RH change difference
2031-2050
2080-2099
RH change difference (%)
elevation (m)

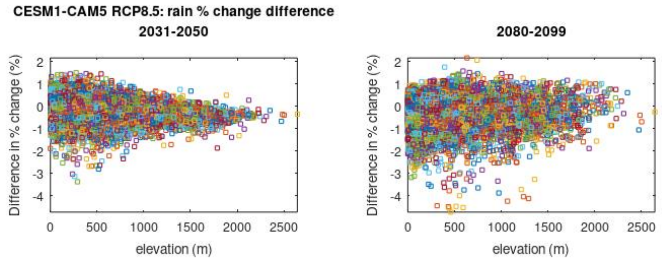
CESM1-CAM5 RCP8.5: rain % change difference
2031-2050
2080-2099
Difference in % change (%)
elevation (m)

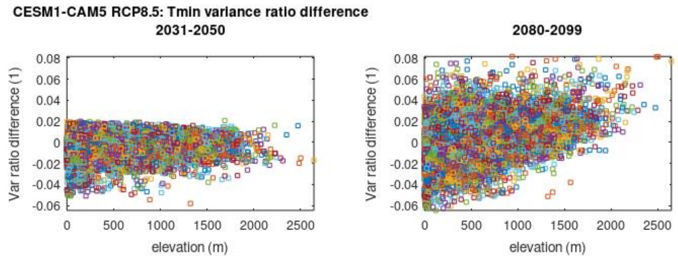
CESM1-CAM5 RCP8.5: Tmin variance ratio difference
2031-2050
2080-2099
Var ratio difference (1)
elevation (m)

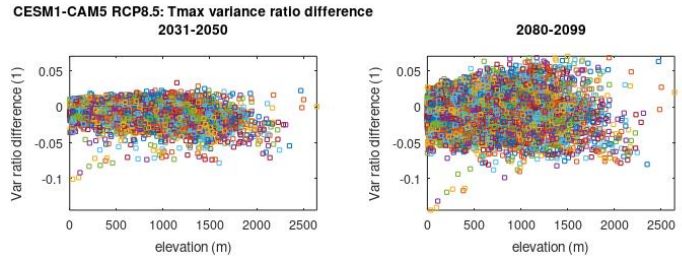
CESM1-CAM5 RCP8.5: Tmax variance ratio difference
2031-2050
2080-2099
Var ratio difference (1)
elevation (m)

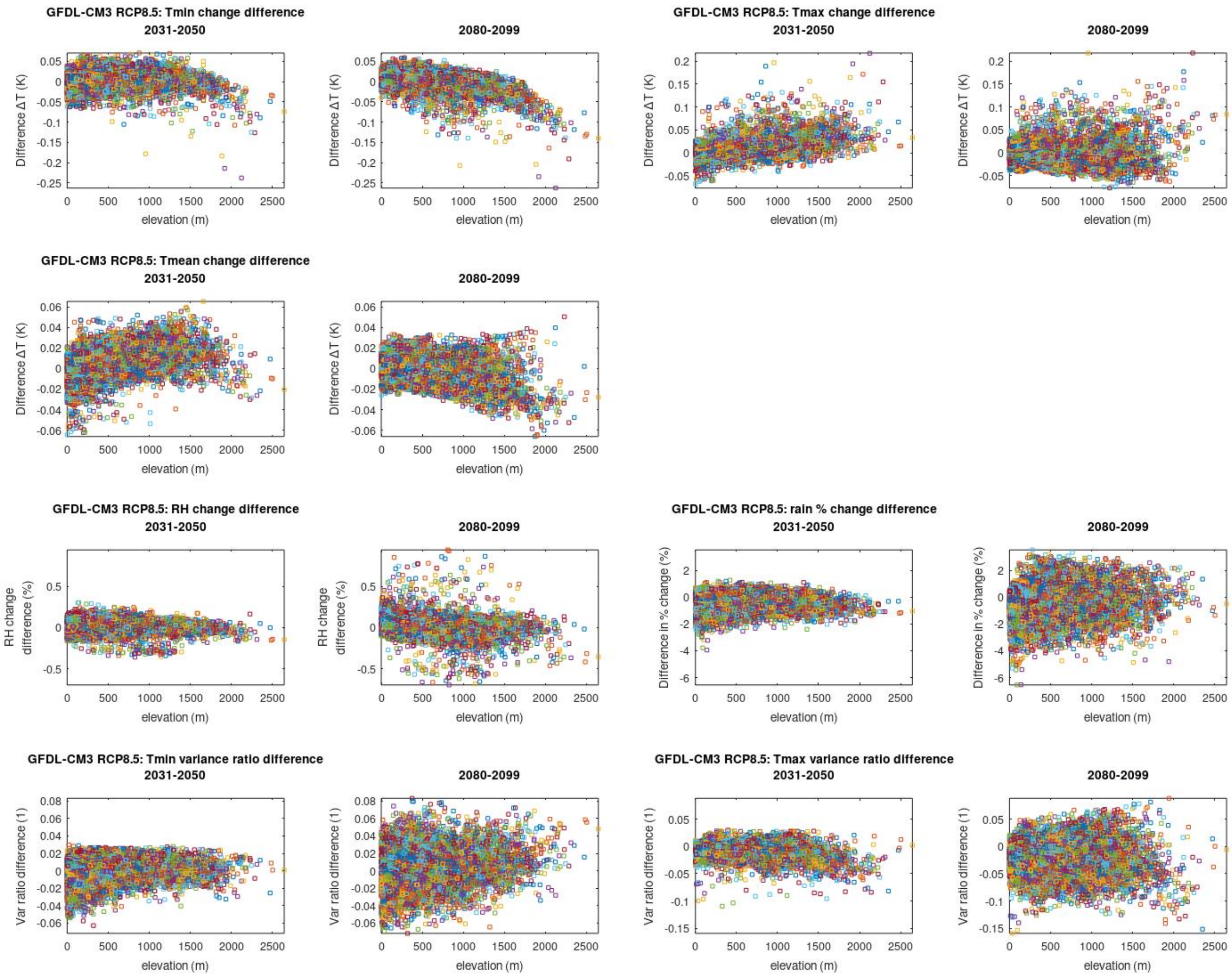
GFDL-CM3 RCP8.5: Tmin change difference
2031-2050
2080-2099
GFDL-CM3 RCP8.5: Tmax change difference
2031-2050
2080-2099
GFDL-CM3 RCP8.5: Tmean change difference
2031-2050
2080-2099
GFDL-CM3 RCP8.5: RH change difference
2031-2050
2080-2099
GFDL-CM3 RCP8.5: rain % change difference
2031-2050
2080-2099
GFDL-CM3 RCP8.5: Tmin variance ratio difference
2031-2050
2080-2099
GFDL-CM3 RCP8.5: Tmax variance ratio difference
2031-2050
2080-2099
Difference ΔT (K)
RH change difference (%)
Difference in % change (%)
Var ratio difference (1)
elevation (m)

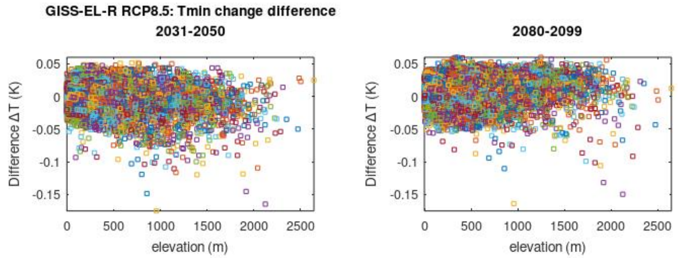
GISS-EL-R RCP8.5: Tmin change difference
2031-2050
2080-2099
Difference ΔT (K)
elevation (m)

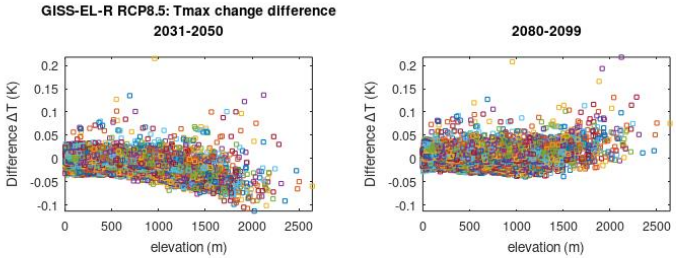
GISS-EL-R RCP8.5: Tmax change difference
2031-2050
2080-2099
Difference ΔT (K)
elevation (m)

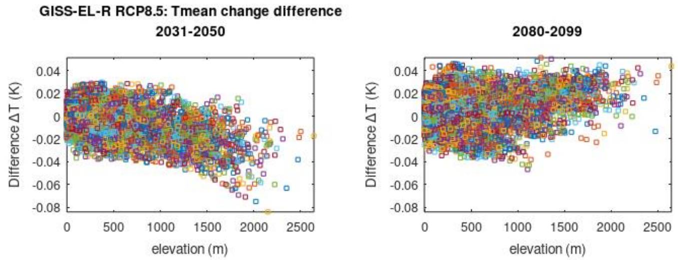
GISS-EL-R RCP8.5: Tmean change difference
2031-2050
2080-2099
Difference ΔT (K)
elevation (m)

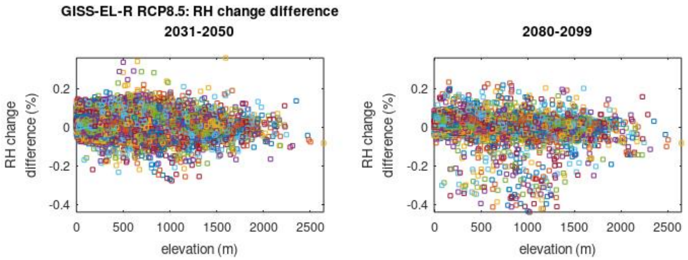
GISS-EL-R RCP8.5: RH change difference
2031-2050
2080-2099
RH change difference (%)
elevation (m)

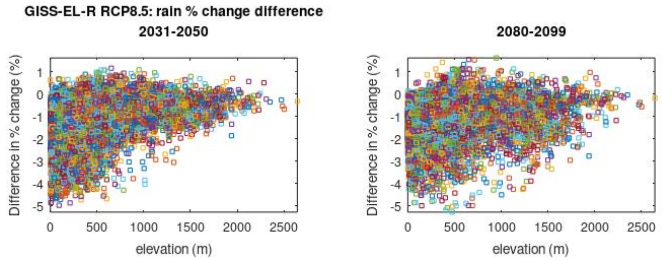
GISS-EL-R RCP8.5: rain % change difference
2031-2050
2080-2099
Difference in % change (%)
elevation (m)

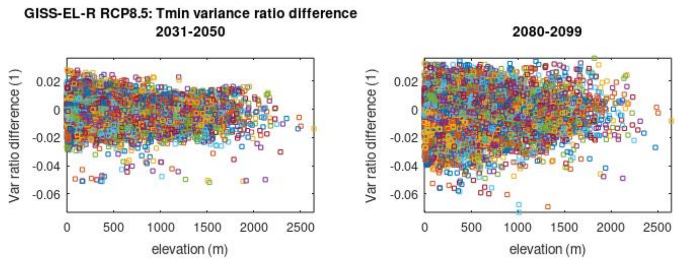
GISS-EL-R RCP8.5: Tmin variance ratio difference
2031-2050
2080-2099
Var ratio difference (1)
elevation (m)

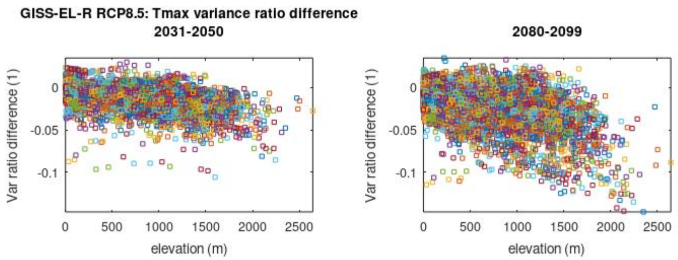
GISS-EL-R RCP8.5: Tmax variance ratio difference
2031-2050
2080-2099
Var ratio difference (1)
elevation (m)

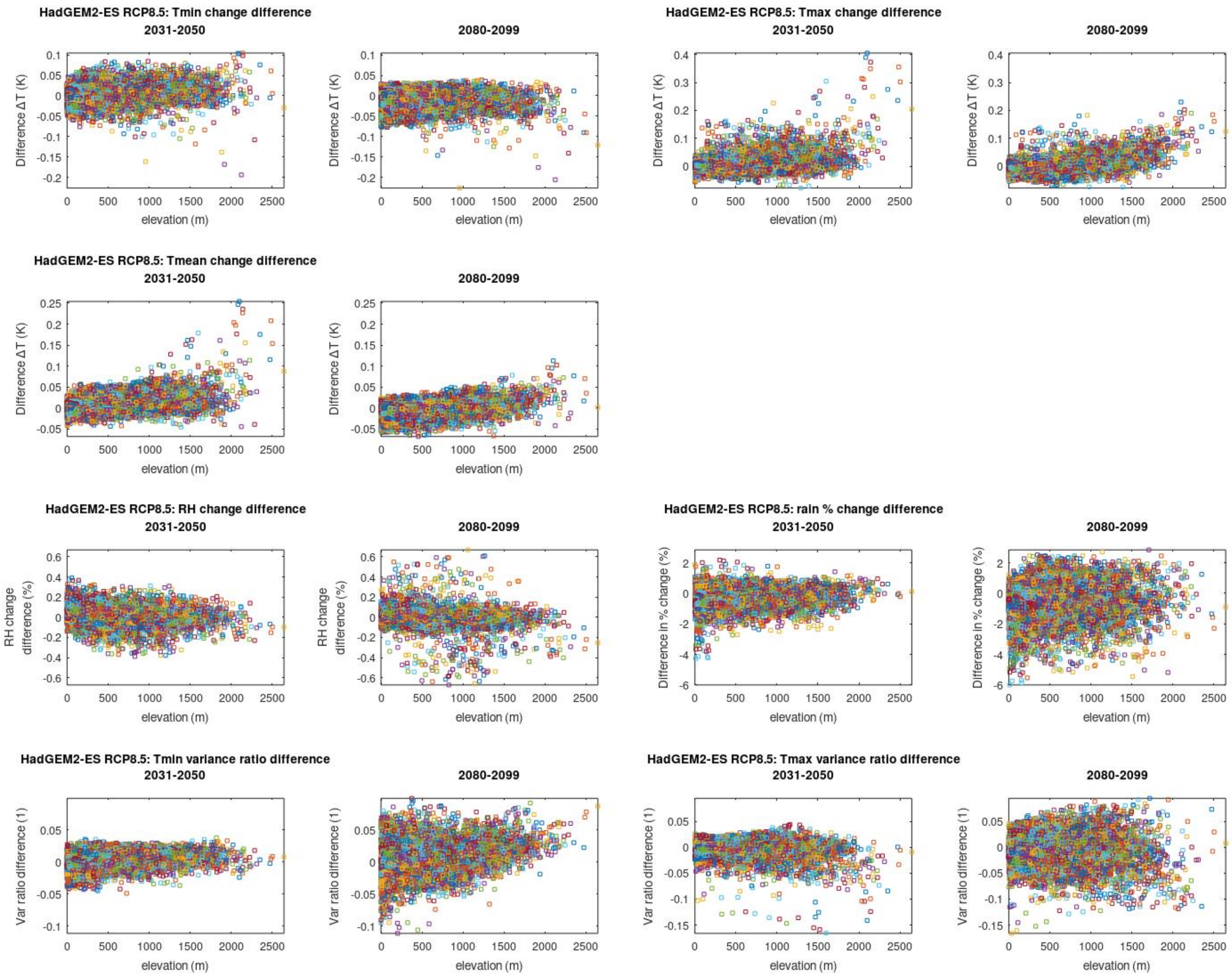
HadGEM2-ES RCP8.5: Tmin change difference
2031-2050
2080-2099
HadGEM2-ES RCP8.5: Tmax change difference
2031-2050
2080-2099
HadGEM2-ES RCP8.5: Tmean change difference
2031-2050
2080-2099
HadGEM2-ES RCP8.5: RH change difference
2031-2050
2080-2099
HadGEM2-ES RCP8.5: rain % change difference
2031-2050
2080-2099
HadGEM2-ES RCP8.5: Tmin variance ratio difference
2031-2050
2080-2099
HadGEM2-ES RCP8.5: Tmax variance ratio difference
2031-2050
2080-2099
Difference ΔT (K)
RH change difference (%)
Difference in % change (%)
Var ratio difference (1)
elevation (m)

NorESM1-M RCP8.5: Tmin change difference

2031-2050 2080-2099

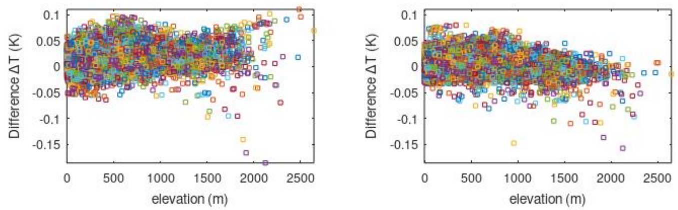

NorESM1-M RCP8.5: Tmax change difference

2031-2050 2080-2099

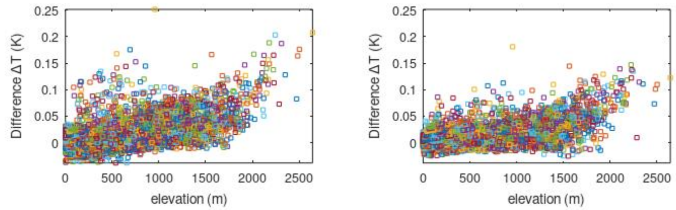

NorESM1-M RCP8.5: Tmean change difference

2031-2050 2080-2099

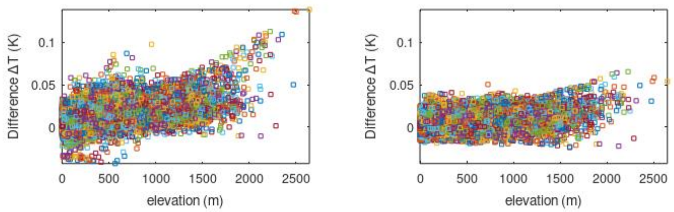

NorESM1-M RCP8.5: RH change difference

2031-2050 2080-2099

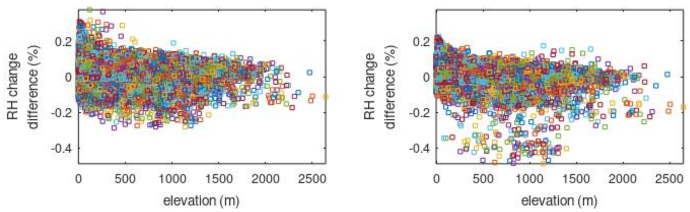

NorESM1-M RCP8.5: rain % change difference

2031-2050 2080-2099

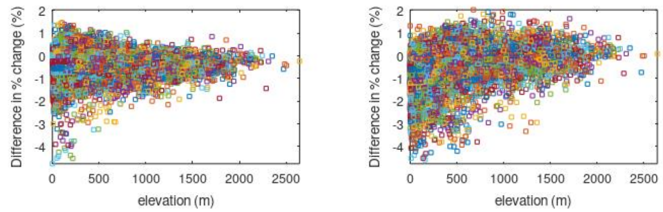

NorESM1-M RCP8.5: Tmin variance ratio difference

2031-2050 2080-2099

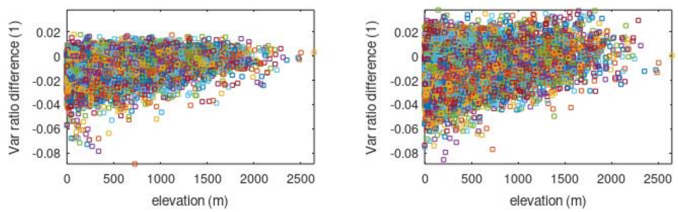

NorESM1-M RCP8.5: Tmax variance ratio difference

2031-2050 2080-2099